Study of Surface Roughness Effects on Deposition of Atmospheric Aerosols using ^{210}Pb Soil Inventories

Thesis

Submitted by

Masoud Vahabi-Moghaddam

for the degree of

Doctor of Philosophy

Department of Physics and Astronomy
University of Edinburgh
1998

Abstract

Inventories of atmospherically derived ^{210}Pb in soil are used to determine deposition patterns of atmospheric aerosols averaged over decades (physical half-life of ^{210}Pb is 22.3 years). The method has been applied to quantify the long-term average enhancement in aerosol and cloud water deposition as a consequence of aerodynamic roughness effects of forest canopies in Scotland and Sweden.

Split-level sampling techniques were applied to determine the depth profiles of ^{210}Pb from the surface to 20-30 cm at selected locations from within the canopy as well as the adjacent open land at each site. The specific activities of ^{210}Pb in dried soil samples were determined by non-destructive γ-spectrometry using high resolution HPGe detectors, one of which is fitted with a Compton suppression system.

Initial sampling was conducted at Dunslair Heights beneath a Norway spruce (Picea abies) canopy and in the adjacent open grassland at an elevation of 450 m asl in the Scottish Southern Uplands. The average enhancement in the ^{210}Pb inventory under the forest canopy of 37% is found to be consistent with deposition estimates obtained from a continuous record of cloud frequency and meteorological variables, and is also in good agreement with the UK model deposition estimates for the site. Measurement of atmospheric ^{210}Pb inventories at the second site, an old plantation of Scots pine (Pinus sylvestris) at 420 m asl near the summit of Dun Coillich in the Scottish Highlands, revealed an average canopy enhancement in deposition of approximately 36% relative to the open heathland in close correspondence with independent estimates of cloud droplet deposition at the site. Deposition at the exposed edge of stand, however, exceeds that in the open by approximately 56%.

The method was then applied to measure the pattern of total aerosol deposition (dry plus wet and occult deposition) at ten sites in south-west Sweden, along a transect from Hallands Vadero Island at the coast to the southern Swedish uplands. The soil inventory of ^{210}Pb increases with distance from the west coast and generally follows the trend in the long-term average precipitation field. However, the canopy enhancement in deposition was found to be relatively high for quite modest elevations of a few hundred meters at 20-30 km from the coast, with almost no enhancement in the coastal region, suggesting that the significant

difference is mainly due to cloud/fog deposition at elevated sites inland. The increased input to exposed forests on elevated hills inland is up to 100% relative to that in open fields covered by short vegetation in the coastal area. Finally, a series of measurements were made at four sites in the Transtrand Mountains in central Sweden. These data revealed a significant increase in deposition on the summit of Gammalsaters, 870 m asl, relative to the valley at 540 m asl. A higher rate of increase with elevation was observed for ^{210}Pb inventories under forest canopies sampled in these mountains relative to the open fields. The mean atmospheric ^{210}Pb inventory at the exposed edge of a forest canopy at 620 m asl exceeds that of open grassland at an elevation of 540 m asl by approximately 90%.

Based on measured soil inventories, the average flux of ^{210}Pb to forests in Dunslair Heights, Dun Coillich, SW Sweden, and central Sweden sites are approximately 100, 130, 130, and 140 Bq m^{-2} y^{-1}, respectively; the mean flux to the open field for Scottish sites is 85 Bq m^{-2} y^{-1}, and for Swedish sites is approximately 100 Bq m^{-2} y^{-1}. These latter figures correspond to a mean concentration of ^{210}Pb in rainfall of 70 mBq l^{-1} and 90 mBq l^{-1}, respectively. The data clearly indicate the importance of land use in controlling input to catchments, especially in upland regions.

The direct γ-spectrometry technique allowed measurements on the same sample for radionuclides ^{137}Cs and ^{214}Pb. However, the value of using the former as a confirmatory tracer is diminished due to heterogeneous deposition of the Chernobyl-derived fraction, and its relative mobility in the acidic and highly organic soils within coniferous forests in this study. The ^{137}Cs soil inventories in the open fields range approximately from 1800 to 8050 Bq m^{-2} for sites in Scotland, 2590-5720 Bq m^{-2} in SW Sweden, and 2320-2950 Bq m^{-2} in central Sweden. The measured inventories of ^{214}Pb were used to correct the supported ^{210}Pb due to in situ decay of ^{222}Rn.

It is concluded that the soil inventories of ^{210}Pb provide a measure of long-term spatial variation in deposition rate of atmospheric aerosols as particles and/or droplets that is operationally easier to carry out than the direct measurement by artificial collectors over extended period of time. It is well suited for measurements at a large number of sites, and appears to be particularly valuable in quantifying aerosol and wet deposition processes at sites where conventional methods are not applicable.

Acknowledgement

This study was begun while the author was in receipt of a 4 year scholarship from the University of Guilan and the Iranian Ministry of Culture and Higher Education. The Institute of Terrestrial Ecology provided the funds for travel between Edinburgh and the fieldwork sites in Sweden.

I would like to express my gratitude to David Fowler and Derek Branford for their invaluable assistance and enthusiasm in the completion of this study and their advice in the preparation of this thesis.

I am grateful to Tom Davinson for his efficient management and development of the computer facilities. Likewise, to Gordon Turnbull for his assistance in constructing sample holders and surface-frame samplers.

Thanks to Harry Napier for his assistance in preparing spiked matrices, and to Bob Galloway for giving the permission of using the facilities in his laboratory.

Thanks are also due to Alan Shotter for his support, and for keeping a nice and friendly working environment in the Nuclear Physics Group.

The fieldwork in Sweden could not have been performed without the valuable assistance of Lennart Granat from Arrhenius Laboratory at Stockholm University.

I wish to thank all persons who assisted with the fieldwork, in particular Richard Mourne, Ian Leith, Alan Crossley and Kerstin Nordstrom.

This project would not have been completed without the encouragement and support of my wife, Navid, to whom this document is dedicated.

'God will not seek thy race,

nor will He ask thy birth.

Alone,

He will demand of thee

"What hast thou done with the land

that I gave thee?"'

Old Persian proverb

Contents

Chapter 1

Introduction and Background

This thesis reports an experimental investigation into the effects of aerodynamic roughness of terrestrial surfaces on deposition of atmospheric aerosols using ^{210}Pb soil inventories. The present chapter continues with an overview of acid deposition issue with a European and global perspective followed by a description of aims of this study. Then, a background is presented on acidic pollutants in the environment including their emission, transformation, transport, and deposition. The first chapter ends with a brief review on the application of radioactive tracers to aerosol deposition study including properties of the radionuclides of concern and their fate in the atmosphere and soil environments. Chapter 2 describes the sampling programme and procedure, sample preparation, and γ-ray analysis technique for measuring the radionuclides present in a sample. The results of the γ-ray analyses on the collected soil samples are presented in Chapter 3, and in Chapter 4 the results of all measurements are discussed and compared with the published literature.

1.1 Overview

Since the beginning of this century, accelerated rates of anthropogenic emissions of pollutants have led to a substantial increase in acidity of aerosol particles, cloud droplets, and precipitation in and around industrialised regions, particularly in Europe and North America (Rodhe et al., 1995). Enhanced

acidification of soil and water as well as eutrophication (over-enrichment through the deposition of nitrogen compounds) are environmental threats which have had significant adverse effects on many elements of both terrestrial and aquatic ecosystems. The impact on human health and material corrosion (predominantly stone decay which has been affecting Europe's heritage buildings and monuments) are other areas of concern.

The major pollutants involved are sulphur dioxide (SO_2), nitrogen oxides (NO_X) and ammonia (NH_3). However, the full range would include sulphur species (SO_X), oxidised nitrogen species (NO_Y), volatile organic compounds (VOCs), and ozone as well. *'Acid deposition'* is the term used for the removal of the atmospheric pollutants of an acidic, or potentially acidic, nature whether they be deposited in rain or snow (wet deposition), as gases and aerosol particles (dry deposition) or in cloud droplet interception (occult deposition). The phenomenon of acid deposition (the commonly identified term for which is *acid rain*) appears to have been discovered first by an English chemist, Robert Angus Smith, in the middle of the nineteenth century in Manchester (Cowling, 1982).

Rainfall acidity measurements have revealed that precipitation is more acidic in industrialised regions of the world. Figure 1.1 shows the global pattern of rainfall acidity with a range of pH values from 4.0 in central Europe and eastern North America to 6.3 in Australia and India.

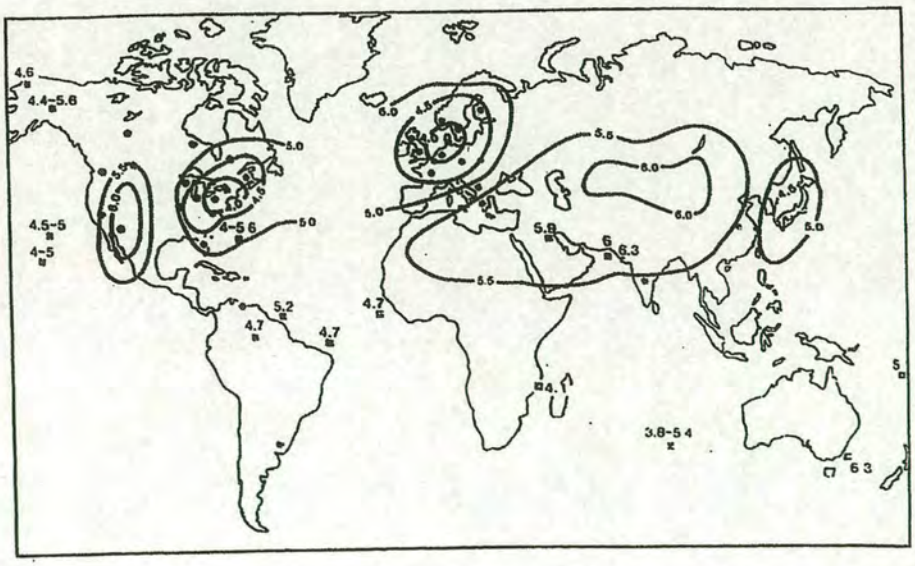

Fig. 1.1: Global pattern of rainfall acidity (WMO, 1989).

Diatom analyses of sediment cores obtained from numerous lakes provided clear and quite dramatic evidence of marked acidification of surface waters in the early decades of the 20th century. The diatoms found in sediments can be used as a biological pH indicator, indicating changes in the acidity of a lake over time. Furthermore, the sediment studies also reveal that this modern-day acidification coincides in time with rising sediment levels of substances like heavy metals and soot particles which are indicative of deposited pollution from the combustion of fossil fuels and from industrial emissions. Renberg and Hellberg (1982), for example, analysed diatom assemblages in Lake Gardsjon sediment cores and found that the pH of the lake had decreased from about 7 to about 6 in the period of 12500 BC to 1950s due to natural long-term acidification. However, a more marked decrease in pH values from 6 to around 4.5 occurred in the period of 1950s to late 1970s (Figure 1.2). Similar investigations in the UK (Battarbee et al., 1985), Norway (Berge et al., 1991), Sweden (Renberg et al., 1991) and North America (Charles, 1991) have revealed temporal trends in lake water pH in the post-1850 period in response to industrialisation and increasing use of fossil fuels.

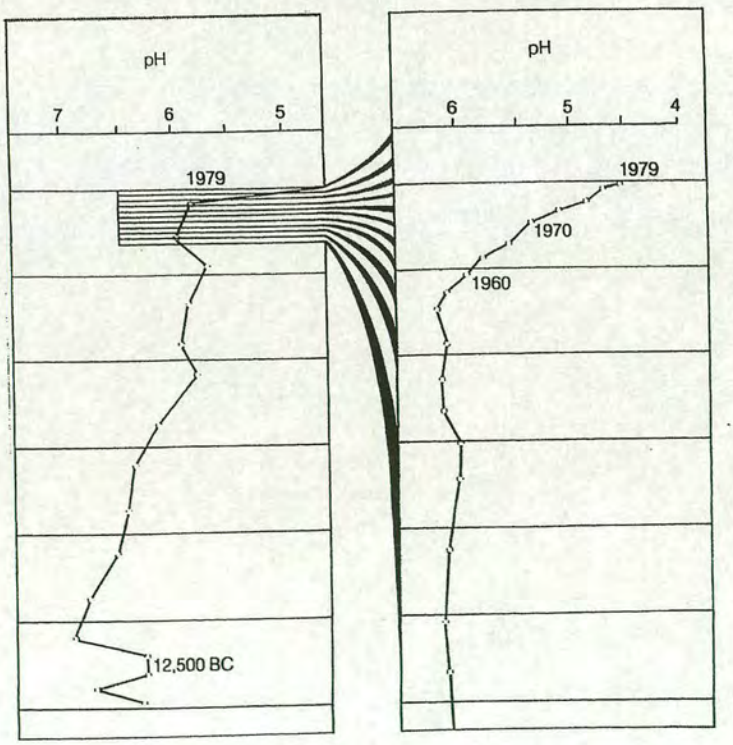

Fig. 1.2: The pH of Lake Gardsjon, SW Sweden, over a time-scale from 12500 BC to 1979 AD (taken from Elsom, 1987).

It is well established that the recent enhanced acidification is due almost entirely to anthropogenic activity, and their effects on freshwater ecosystems in the acidic bedrock regions of the northern hemisphere (AWRG, 1986; Brodin and Kuylenstienna, 1992; Havas and Rosseland, 1995) are among the most important ecological effects. On the other hand, the impact of acidification on terrestrial ecosystems is more controversial. The potential of acidic deposition to change the soil environment of trees is obvious, but, one characteristic feature of the health condition of forest areas is the complex nature of pathological phenomena and the positive feedback of the negative results of action of many simultaneously occurring factors, both natural (droughts, winds, frosts, fires, insects, fungi etc.) and paranatural, the latter including chiefly emissions of environment-polluting substances that cause acidification and eutrophication of sites, toxic deposition of heavy metals and high concentration of tropospheric ozone (Tamm, 1989; Roberts et al., 1989; Aamid et al., 1992; Matzner and Murach, 1995). Where the concentrations of air pollutants are very large, the connection is clear. The Europe-wide survey of leaf and needle losses in 1995 and 1996 revealed that 25% of the sample trees could be classified as damaged with a defoliation of more than 25 per cent. The highest degree of damage has been found in Central Europe, namely in Poland, Czech Republic, Slovakia and eastern Germany, where local emissions of pollutants are substantial (Cerny and Paces, 1995; Elvinsen, 1996; UN ECE, 1997). Figure 1.3 shows the pattern of defoliation intensity of trees in Europe in 1996.

Fig. 1.3: Intensity of defoliation in Europe in 1996. Figures represent percentage of trees with defoliation more than 25%. For all species, unless marked * for conifers only (UN ECE, 1997).

It is quite likely that even relatively small concentrations of air pollutants or prolonged acidification of the soil will increase the degree of stress the trees are subject to and make them more susceptible to damage from drought, frost, insect attack, etc. Where, however, acidic emissions have been reduced and where mitigation measures have been employed, there is evidence that ecosystems can recover (Aamlid et al., 1992; Rasmussen et al., 1995; Visser, 1995; Elingson, 1996).

In late 1960s, a Swedish soil scientist named Svante Oden hypothesised the broad ecological consequences of long-range transport of acidifying air pollutants on the basis of measurements through Scandinavian network of surface water chemistry (Oden, 1968). The international perspective of his findings and hypotheses had an important role in drawing the world's attention to the phenomena and stimulation of further national and international research on identifying emission sources, pollutant deposition processes and patterns, acidification of ecosystems and source-effect relationships (OECD, 1977; Overrein et al., 1980; Cowling, 1982; Gorham, 1989; Cowling and Nelsson, 1995). Sulphur dioxide and nitrogen oxides are derived mainly from the combustion of fossil fuels (coal and oil products) in power stations, industrial boilers and motor vehicles. The major sources of ammonia, by contrast, are animal wastes and the application of fertilisers. These pollutants and their transformation products have long atmospheric lifetimes and can be carried by weather systems distances of up to a few thousand kilometres from their point of emission. This causes acid deposition far from the primary source of pollution, thus making it a regional problem and an international transboundary issue (Howells, 1990; Mason, 1992).

Following the historical United Nation Conference in Stockholm in 1972, concerned with *Human Environment* and *Air Pollution Across National Boundaries* , a series of co-ordinated international conferences on the issue were held every fifth year in Columbus, USA(1975), Sandefjord, Norway(1980), Muskoka, Canada(1985), Glasgow, UK(1990) and Goteborg, Sweden(1995). The essential outcome of the Goteborg conference is that acid deposition remains an important environmental issue in the western world (Rodhe et al., 1995). Although the emissions of sulphur dioxide have declined generally both in Europe and North America and reduced deposition has been recorded even in the so-called Black Triangle (the area of Central Europe

where Germany, Poland and the Czech Republic converge), in many areas the deposition is still five or ten times greater than nature can withstand. There are as yet no signs of any decline in the emissions of nitrogen oxides and ammonia; the same can be said of the concentrations of low-level ozone, which is formed from nitrogen oxides and VOCs (Rodhe et al., 1995; Cerny and Paces, 1995). Furthermore, in some areas of the developing world, such as east and south-east Asia, southern Africa and South America, recent industrialisation has created major increases in pollutant emissions and acidity (Zhao and Sun, 1986; Foell and Green, 1990; Galloway, 1995). Figure 1.4 represents the continental emissions of SO_2, NO_X and NH_3 projected for the year 2020. Ammonia has been also considered here because it may cause acidification of soils and surface waters even though in the gaseous phase it is alkaline and, thus neutralises airborne acids. In addition, ammonia and nitrogen oxides may act as fertilisers as well and cause eutrophication in aquatic ecosystems.

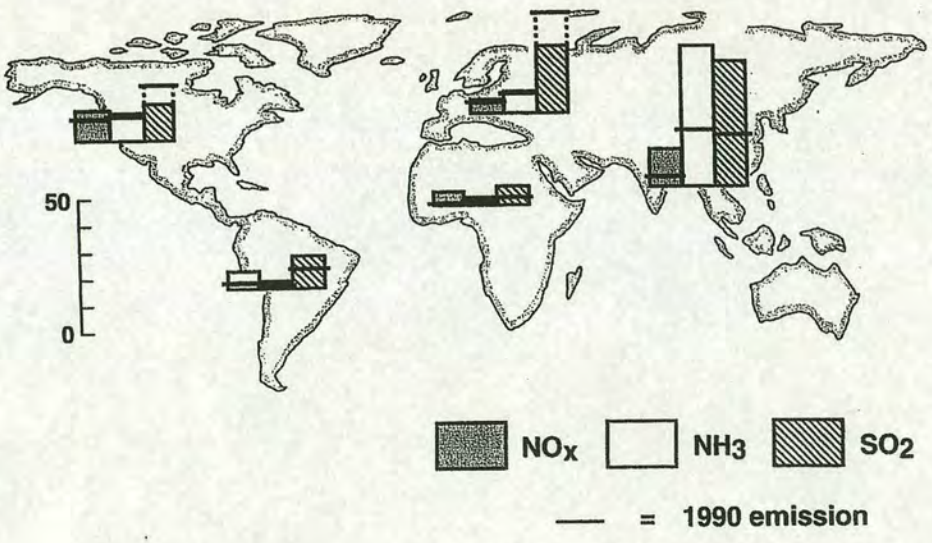

Fig. 1.4: Map of projected 2020 emissions by continent of SO_2, NO_X and NH_3 in Tg S yr^{-1}, Tg S yr^{-1}, and Tg N yr^{-1}, respectively; bar represents 1990 emissions (Galloway, 1995).

During the last few decades, considerable advances in the understanding of acidic emissions, transportation, deposition and consequent effects on ecosystems have allowed the development of the concept of *'Critical loads'*. These are

quantitative thresholds which help scientists and policy-makers in their assessments in identifying areas most at risk from continued deposition, while evaluating the impact of various pollution-reduction strategies. These thresholds are defined individually for particular pollutants and their receptors (i.e. water, soil, vegetation or materials) which, once exceeded, will cause chemical changes leading to long-term harmful effects on ecosystem structure and functioning (Brodin and Kuylenstierna, 1992; Sverdrup et al., 1992; Henriksen et al., 1992; CLAG, 1994). The definition of critical load adopted by UN ECE (1988) is: *'a quantitative estimate of exposure to one or more pollutants below which significant harmful effects on sensitive elements of the environment do not occur according to present knowledge'*. The term *'exposure'* refers to a dose of pollutant deposition to a defined area over a specified time period and is expressed as deposition per unit area; *'pollutants'* refers mainly to atmospheric emissions of sulphur and nitrogen compounds; *'harmful effects'* refers to biological aspects of ecosystems considering both direct or indirect responses; and finally, *'sensitive elements'* may be chosen by individual countries and entire ecosystems or single species may be selected (Sverdrup et al., 1990; Brodin and Kuylenstierna, 1992). *'Critical levels'* (the thresholds for gaseous concentration exposures) have been also defined in a similar way.

Critical loads/levels have become an integral part of international negotiations aimed at controlling emission levels within Europe, but not elsewhere (RGAR, 1997). Maps of critical loads for acidifying substances and the areas where the loads are exceeded play a vital part in deciding where and by how much, reductions need to be made. At a European scale, pollutants are mapped at 150 km x 150 km grid scale (the European Monitoring and Evaluation Programme (EMEP) network) and in conjunction with land use, geology and vegetation, maps of critical loads and exceedances have been developed and the cost benefits of abatement measures explored. As an example, European sulphur deposition on the basis of EMEP grid is illustrated in Figure 1.5, along with the critical load map and exceedance of critical load for sulphur in Europe in 1990 (Rodhe et al., 1995). The question at this stage is: How detailed should these maps be? Abatement strategies based on the critical load concept require adequate deposition data on both local and regional scales. At the large-scale, considering pollutant deposition over Europe, the EMEP model has been

a.

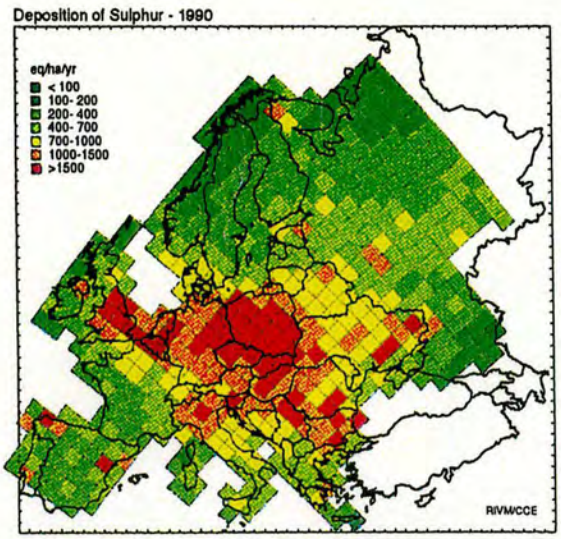

b.

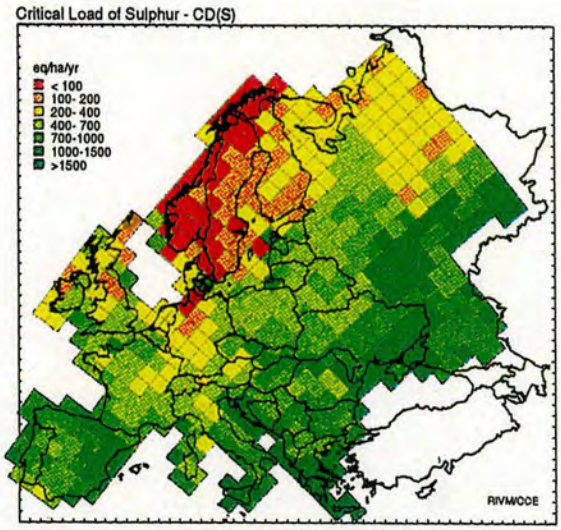

c.

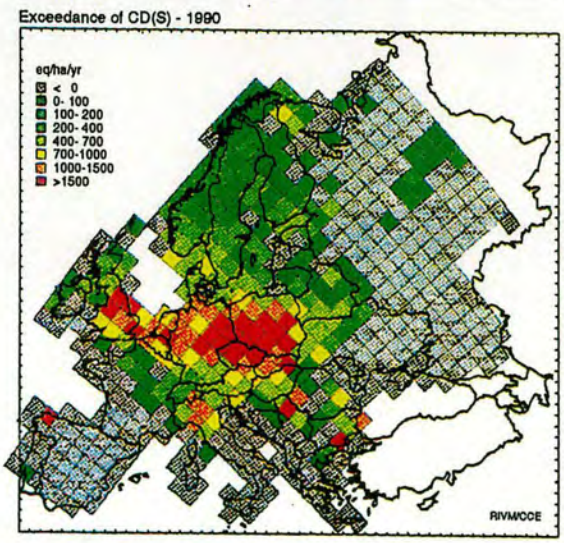

Fig. 1.5: a) Sulphur deposition in Europe in the year 1990. b) Critical load of sulphur deposition in Europe. c) Exceedance of critical load in Europe, i.e. 'map a' minus 'map b' (Rodhe et al., 1995).

considered as adequate for the quantification of transboundary exchange of pollutants (Lovblad et al., 1992). However, one problem of these large grids is that they mask a great degree of landscape heterogeneity. Within-grid square deposition variability could be high over different types of landscapes and within forested areas (see for instance Choularton et al., 1988, and Dore et al., 1992, for orographic enhancement; Bobbink et al., 1992, for heathland ecosystems; Godt and Mayer, 1988, and Draaijers et al., 1992, for high and low elevation forests, respectively; Fowler et al., 1991a, and Erisman and Draaijers, 1995, for different terrestrial surfaces). This is especially the case for coniferous forests where deposition may be much larger than to shorter vegetation. For forests growing near the ocean, or on mountain slopes which are frequently immersed in fog or clouds, interception deposition of droplets can remove significant quantities of water and pollutants from the atmosphere (Fowler, 1984; Lovett and Reiners, 1986; Fowler et al., 1989; Collett et al., 1991; Fowler et al., 1992). In upland areas, enhancement in deposition through this mechanism may influence the pollutant inputs to catchments (RGAR), 1997). Furthermore, forests are often grown on soils which are more sensitive to acidification and are thus the determining receptor areas for critical loads (Hultberg & Grennfelt, 1992).

Reducing the size of the grid can minimise the problem of within-grid variability as illustrated in Figure 1.6, where dry deposition of sulphur in Europe on a 150 km x 150 km scale using EMEP model is compared with a map of deposition on $1/6 \times 1/6^{o}$ (ca. 10 km x 20 km) scale constructed on the basis of a fine resolution roughness-length map and other relevant data (Erisman et al., 1994). The roughness length map itself has been provided from the land use map for Europe constructed from ground-based and satellite observations. Such small-scale approaches have also been applied in preparation of critical load maps for soils and freshwater in the UK (CLAG, 1994) and Sweden (Allard et al., 1994). However, even the small-grid approach masks considerable heterogeneity.

The pollutant deposition maps are provided by high density monitoring networks of precipitation collectors for rainfall amount in conjunction with relatively low density precipitation chemistry network, to account for wet deposition. Estimates of dry deposition loads are obtained from a process based model that uses air concentrations, meteorological parameters, surface resistances and surface roughness.

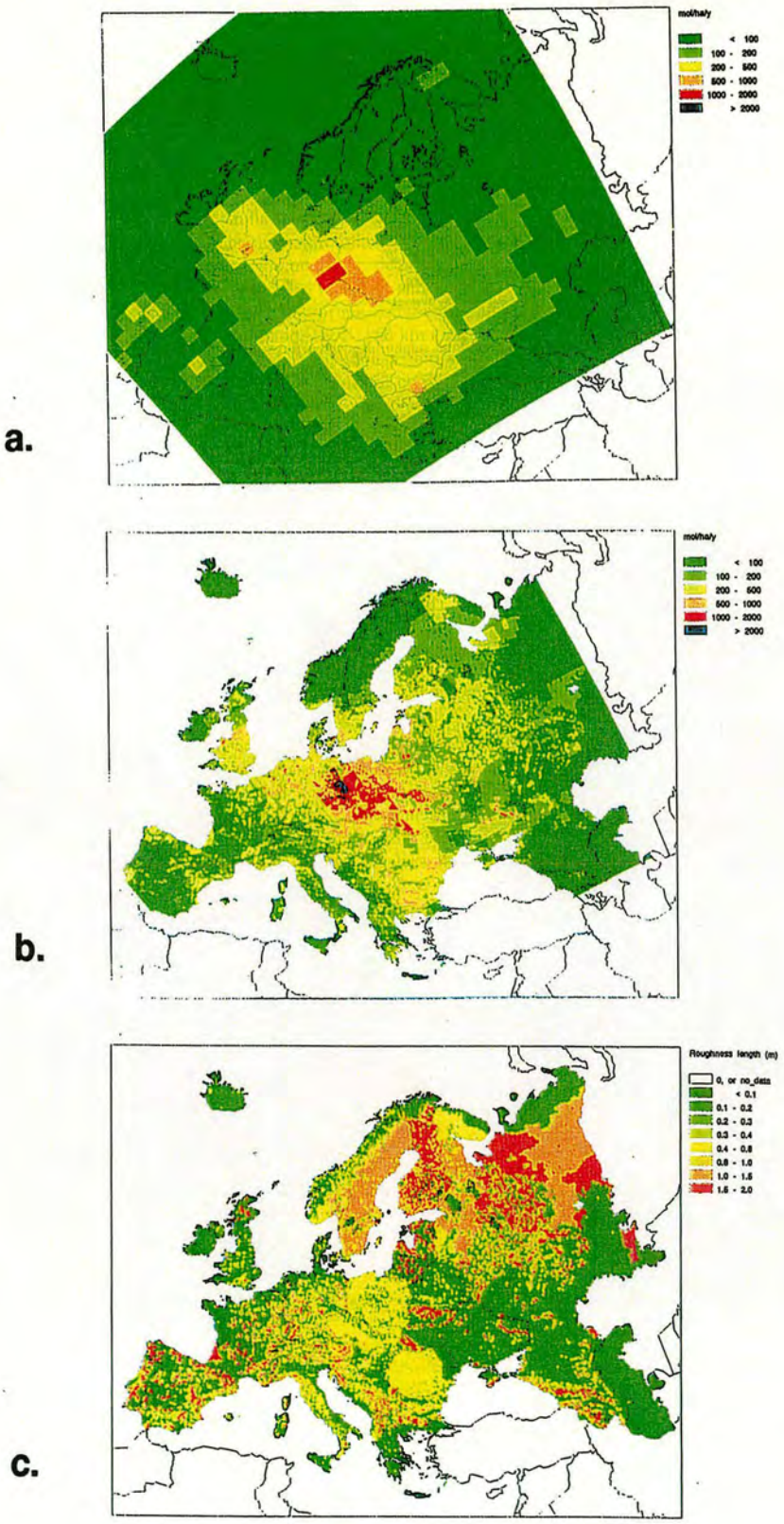

Fig. 1.6: Dry deposition of sulphur in Europe in the year 1989, in mol ha^{-1} yr^{-1}: a) on EMEP scale; b) on a 1/6x1/6° scale. c) Roughness length map (m) of Europe (1/6x1/6 °)(Erisman et al., 1994).

Forests cover a significant part of the landscape in many European countries (e.g. about 65% of the area of Sweden, and a total of 625000 km^2 in the Nordic countries). They are usually assumed to be uniform in these deposition models, with similar surface roughness. Although such homogeneous areas of forest exist, many forested areas are more accurately described as a complex spatial mosaic, often containing or surrounded by agricultural areas, bogs and heathland, and comprised of a variety of differing compositions, height and canopy structures (Lovett and Reiners, 1986; Draaijers et al., 1992; Lovblad et al., 1992).

The rates of both dry deposition of particles and occult deposition are largely dependent on surface properties and in the case of deposition to forests are currently very uncertain. (Ruijgrok, 1995; Erisman and Draaijers, 1995). Neither dry deposition nor cloud droplet interception is easily quantified and many studies have been devoted to an assessment of their contribution to total deposition to forests (e.g. Lovett and Lindberg, 1984; Fowler et al., 1989; Beier et al., 1992; Gallagher et al., 1992; Vermeulen et al., 1994; Erisman et al., 1995). However, there is a lack of large-scale, long-term measurements in this regard and there is a large gap between the results from field experiments, wind tunnel studies, and model estimates (Ruijgrok et al., 1995). In the process of establishing critical loads, soil acidification in forests as well as the influence of upland forests on pollutant inputs to catchments need to be quantified. Thus, it is important to be able to quantify the atmospheric input to forests mechanistically. The quantification is necessary at a local level to make a linkage between modelled deposition estimates and soil loads. Moreover, if the intent is to help protect sensitive areas then there is no substitute for good on-site data (Hicks, 1995).

Wet deposition is rather evenly distributed over large areas in flat or gently underlying terrain and its measurement is more straightforward than the measurement of dry and cloud droplet deposition by using precipitation collectors. However, to perform accurate measurements, special attention should be devoted to efficient collection of precipitation at windy sites, exclusion of dry deposition and contamination, and prevention of chemical changes in samples. The exception is of course in upland areas where orographic enhancement of rainfall occurs and an assessment of the extent of seeder-feeder effect has to be made (RGAR, 1997).

Several methods exist to estimate the dry and occult deposition to forests on small spatial scales. Those which are mostly applied in recent studies are: Micrometeorological methods, surface wash methods (mainly throughfall technique), watershed mass balance methods (i.e. outflow monitoring from small catchments) and inferential methods. These methods are reviewed by Hicks et al. (1989), Davidson and Wu (1990), Erisman and Draaijers (1995), Ruijgrok, W. et al. (1995) and RGAR (1997). Direct measurement of aerosols and cloud droplet deposition is difficult except by micrometeorological methods which suffer mainly from their limitation to certain terrain situations. The most important drawback of the throughfall method is the problem associated with canopy exchange processes which may modify throughfall results especially for nitrate, ammonia and base cations. The small catchment method is only applicable to elements which are transported through the system without any large losses and is limited to those areas where necessary assumptions are valid. And finally, the inferential method relies basically on site specific data and the outcome could be subject to large uncertainty.

In summary, acid deposition remains an important environmental issue, now with a global perspective. Considering the large variation in pollutant deposition to various ecosystems, receptor specific estimates are required to determine the relation between effects and deposition. Our present knowledge on cloud droplet deposition and dry deposition of aerosols to forests is still insufficient and there is a need for the clarification of the present large gap between measured values in field experiments and results from model and wind tunnel work. However, collection of more reliable field data using conventional methods, especially over extended period of time, requires extensive field and/or laboratory work which could be very costly.

1.2 Aims of Study

Natural and artificial radionuclides present in the atmosphere (radon and its daughters, cosmogenic origin ^{7}Be, fission products) have long been used as atmospheric tracers (Rama, 1963; Bhandari et al., 1970; Poet et al., 1972; Dibb et al.,

1992; Graustein and Turekian, 1996). These radionuclides are associated with nonradioactive aerosols and hence can serve to trace the fluxes of aerosols to various surfaces. Lead-210 and ^{137}Cs have been shown (Moore et al., 1973; Graustein and Turekian, 1986) to be particularly useful because they are associated mainly with submicron-sized aerosols which contain the bulk of the pollutant sulphur and nitrogen. When scavenged from the atmosphere along with carrier aerosols, ^{210}Pb is retained by the organic-rich surface horizons of soil which acts as an efficient integrating collector (Lewis, 1977). The ^{210}Pb isotope (half-life: 22.3 years) is the decay product of ^{222}Rn, a water-insoluble inert gas which belongs to the natural uranium ^{238}U decay series and readily diffuses from soil into the atmosphere. Its total inventory (less the supported fraction by the in situ decay of ^{222}Rn) in undisturbed soils may be used as a measure of total aerosol deposition (dry plus wet and occult deposition) averaged over about 30 years, approximately the mean nuclear lifetime. Measurement of deposition fluxes of ^{210}Pb through studies of soils have been developed by Benninger et al. (1975), Moore and Poet (1976), Volchok (1980), and Graustein and Turekian (1986). More recently, the technique has been applied to quantify the wet deposition of pollutants in areas of complex topography (Mourne, 1993; Fowler et al., 1995a; Branford et al., 1998).

The overall aim of this experimental study is to use the soil inventory of atmospherically derived ^{210}Pb to quantify the effects of aerodynamic roughness on the deposition of atmospheric aerosols as particles and/or droplets. Forest canopy enhancement and within canopy spatial variability in deposition should become evident through the observation of a ^{210}Pb soil inventory pattern. This independent technique may enable improved estimates of the effects of land use on long-term inputs of pollutants in precipitation, cloud droplets or as aerosol.

To assess the feasibility of determining long-term rates of total aerosol scavenging by forest canopies from ^{210}Pb inventories in soil, a series of measurements have been made at two sites in Scotland, Dunslair Heights in the Southern Uplands and Dun Coillich in the Highlands, ten sites in the south-west Sweden province of Hallands, from Hallands Vadero Island up to Southern Swedish Highland, and four sites in Transtrand Mountains in central Sweden. Soil samples were taken from within the canopy of conifers and the adjacent open land to each site. Dunslair

Heights was chosen initially to test the sampling and analysis technique as well as the hypothesis. Continuous meteorological observations as part of the DoE Air Quality Research programme (RGAR, 1997), and previous meteorological studies at the site (Crossley et al., 1988; Gallagher et al., 1992) provided means for a comparative study. The isolated rectangular plantation quite close to the timberline for Scotland and frequently exposed to orographic cloud in Dun Coillich was chosen later as a more suitable site to confirm the findings in Dunslair Heights. The technique was then applied to south-west Sweden sites situated almost along a transect from the Kattegatt seashore to Bolman lake about 60 km inland. The primary objectives were to check if the measurements could also reflect the trend in long-term average precipitation pattern in the area, and to investigate the claim that large input by dry deposition in south-west Sweden is the cause for the significant difference in pollutant deposition due to landuse and ecosystem structures (Hultberg and Grennfelt, 1991; Lovblad et al., 1994). The final series of measurements were conducted on Transtrand mountains in central Sweden, where they are mainly screened from the west by the high elevation mountains of Norway and could be considered as more continental in nature.

The non-destructive determination of ^{210}Pb by γ-spectrometry method, as applied in this study, allows measurements on the same sample for other radionulides. Although ^{137}Cs is not expected to be immobilised in the acidic and highly organic soils within coniferous forests in Northern Europe (Liven et al., 1991), measurements were made of its soil inventory for all collected samples. Measurement of ^{214}Pb inventories were also conducted for each sub-section of a core, in order to make corrections for *supported* ^{210}Pb due to *in situ* decay of ^{222}Rn.

There has been an increasing interest in airborne ^{210}Pb as a tracer of atmospheric circulation to validate global model simulations for a better understanding of atmospheric processes that control global climate changes (Lee and Feichter, 1995; Rehfeld and Heiman, 1995; Guelle et al., 1998). This has led to the construction of a database on ^{210}Pb measured concentrations in surface air and deposition fluxes by Preiss et al. (1996, 1997) which aims at representative spatial distribution over the world. However, the spatial coverage of the database is only very partial. Hence a significant number of the ^{210}Pb deposition flux values given in the

present study might also serve to improve such databases and consequently zonal averages on deposition data.

1.3 Acidity Precursors in the Environment

The acidity of an atmospheric system is well described by Beilke, 1982, as: *Acidity is the capability of a single substance or a system of substances to produce protons by reacting with water, and the acidity of an atmospheric system is determined by its ability to transfer protons directly to or to cause the formation of protons within a receptor system.* Cloud droplets, snowflakes and aerosol particles transfer atmospheric acidity onto the ground as bulk H^+-carriers. Natural rainwater is slightly acidic with a pH of approximately 5.6, as a result of carbon dioxide (CO_2) dissolving in it to produce carbonic acid (H_2CO_3) (Howells, 1990). However, as a result of SO_2 and NO_X emissions, rain with a pH of approximately 4.0 regularly falls in many areas of the world (Figure 1.1; Smith, 1991). The pH as a measure of acidity is defined as the negative logarithm of the molar hydrogen ion concentration:

$$pH = -\log_{10} [H^+] = 6.0 - \log (\mu Eq\ H^+\ l^{-1})$$

The scale ranges from 1.0 (very strongly acidic) to 14.0 (very strongly basic). A dual scale of pH and H+ concentration is shown in Figure 1.7 (Howells, 1990).

In order to understand the problem of acid deposition, knowledge of the distribution in space and time for acidity pollutants, their chemical transformation in the atmosphere, and their deposition back to the Earth's surface is required. This involves both primary pollutants SO_2, NO, HCl and secondary pollutants NO_2, sulphuric acid, nitric acid and sulphate and nitrate aerosols as well as aerosols of natural origin from sea spray. However, sulphur dioxide (SO_2), oxides of nitrogen (NO_X), and ammonia (NH_3) are considered as the major precursors of acidic deposition. Ammonia is included due to its important role in neutralising acids in rainwater and its potential for being converted into nitrate by nitrifying bacteria in the

soil system. It may act as a fertiliser as well and cause eutrophication in aquatic ecosystems (Liu et al., 1992; Galloway, 1995).

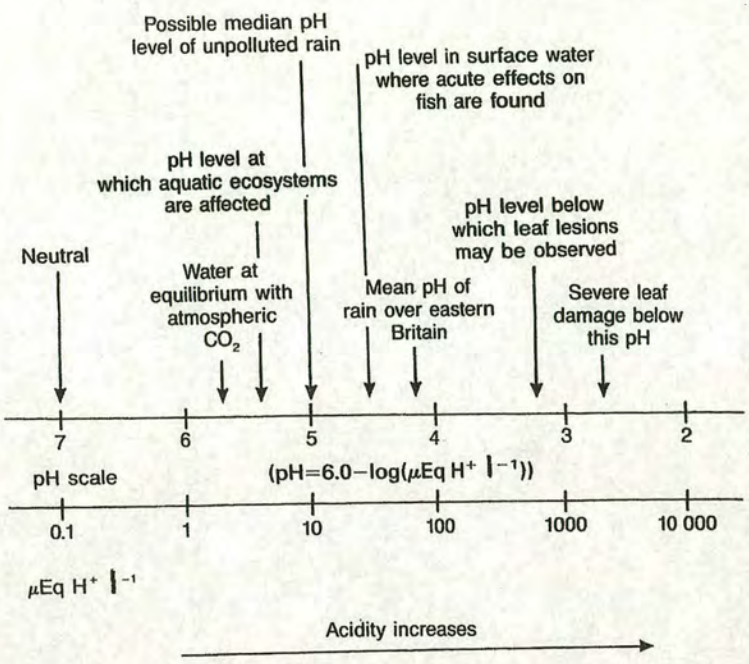

Fig. 1.7: Scale of pH and H^+ concentration.

The emitted acidifying pollutants remain in the atmosphere for different periods of time, depending on the height of the source, wind condition and other climatic and meteorological influences. They can thus be transported by weather systems over both short and long distances (up to a few thousand kilometres) before being deposited onto vegetation, surface waters and soils. Their removal from the atmosphere may be either directly in gaseous or particulate form (dry deposition), or after incorporation into cloud droplets and being consequently deposited by precipitation (wet deposition) or by cloud droplet interception (occult deposition). Spatial dispersion of emissions and deposition of pollutants is illustrated in Figure 1.8 (Krahl-Urban, 1990). The term Filter Effect in this diagram refers to the enhanced droplet and dry deposition onto foliage in forested areas (Kamari, 1986). It is well known that closer to the source regions of gaseous pollutants, dry deposition is the major mechanism for the transfer of such pollutants from the atmosphere to the

surfaces and further away from the source regions, wet deposition plays the dominant role.

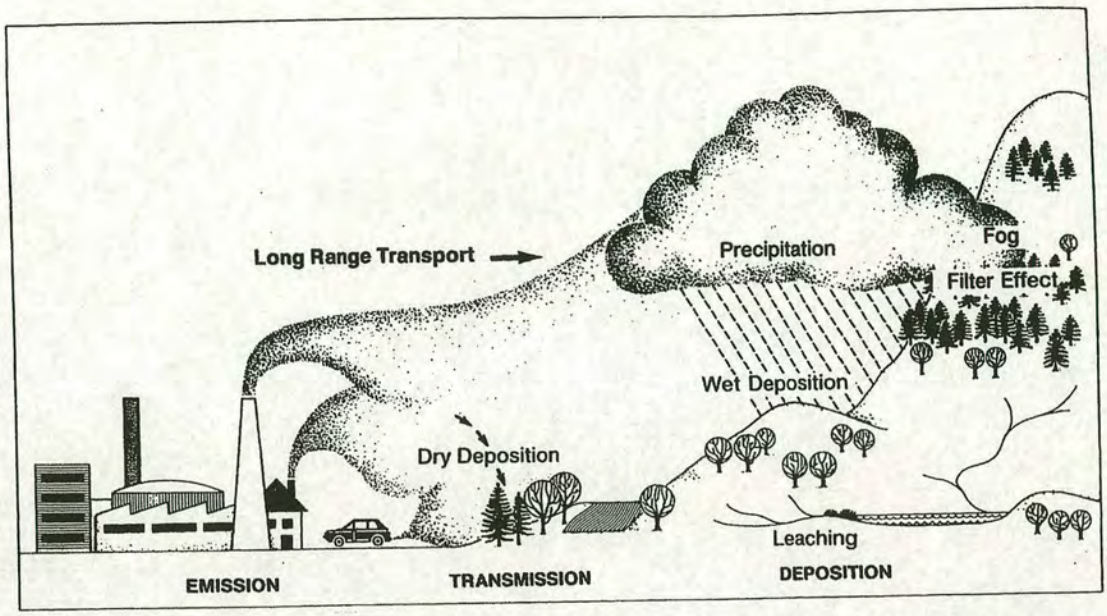

Fig. 1.8: Spatial dispersion of emissions and deposition of pollutants.

Removal mechanisms for gaseous pollutants are strongly influenced by their chemical properties, whereas for particulates the size is the predominant factor to be considered. Size distribution studies of aerosol sulphate, nitrate and ammonium have revealed a range of roughly 0.1 to 1.0 μm for these particles (e.g. Twomey, 1977; Charlson et al., 1978; Whitby, 1978; Brimblecombe, 1996). However, many of the pollutant derived aerosols are hygroscopic and at the common climatic condition over Western Europe, these particulate pollutants are mainly present as larger size droplets (Fowler, 1986).

The following sections describe the emission of pollutants into the atmosphere and their fate through transformation, transport, and deposition.

1.3.1 Emission

Anthropogenic emissions of acidic precursors, as products of the post-Industrial Revolution period, have increased considerably during the past century. The major pollutants involved are the oxides of sulphur and nitrogen as well as ammonia.

The emission inventories of these pollutants on a spatial and time resolution basis are needed as an important input to both long-term and episodic transport models which try to establish source-receptor relationships in acid deposition (Amann, 1990).

Sulphur dioxide (SO_2) in the atmosphere is derived either from direct emission of both anthropogenic and natural sources (mainly volcanoes and biomass burning) or from the secondary products of natural emissions such as dimethyl sulphide (DMS) and hydrogen sulphide (H_2S) (RGAR, 1997). The anthropogenic fraction is mainly generated by the oxidation of sulphur in the course of combustion of fossil fuels, or smelting of ores. DMS is primarily emitted from oceans (Erisman and Draaijers, 1995), whereas H_2S is formed primarily from the natural decay of vegetation either on land or in the oceans (Whelpdale, 1987). Nitrogen oxides (nitric oxide, NO, and nitrogen dioxide, NO_2, collectively termed NO_X) are emitted into the atmosphere manly during the process of combustion, by oxidation of the nitrogen present in the air and also nitrogen in fossil fuels. The contribution of natural sources is from soils, lightning, and biomass burning (Howells, 1990; RGAR, 1997). Ammonia (NH_3), on the other hand, is primarily emitted in the process of livestock and fertiliser volatilisation. Other major sources include oceans and biomass burning (Erisman and Draaijers, 1995; RGAR, 1997). The source contribution of anthropogenic sulphur dioxide, nitrogen oxides, and ammonia to anthropogenic emissions in Europe is illustrated in Figure 1.9 based on data provided by Hov et al., 1987 and Asman, 1992. Figure 1.10 shows the spatial distribution of major pollutant emissions in Europe. The data are for 1986 on a 150 km x 150 km grid. There are extensive emissions of SO_2 in Central and Eastern Europe, where large quantities of high sulphur content fuel are burnt; The NO_X emissions are more geographically dispersed though their concentration are somewhat farther westwards, mainly owing to the more intensive road traffic in Western Europe; and major sources of ammonia are situated where cattle farming is intensive, as in the Netherlands (Bernes, 1992).

The emissions into the global atmosphere of gaseous sulphur and nitrogen compounds have been estimated as follows:

- Anthropogenic and natural sulphur dioxide account for 65-85 and 15-25 Mtonnes S yr^{-1}, respectively (Whelpdale, 1987; Spiro et al., 1992; IPCC,

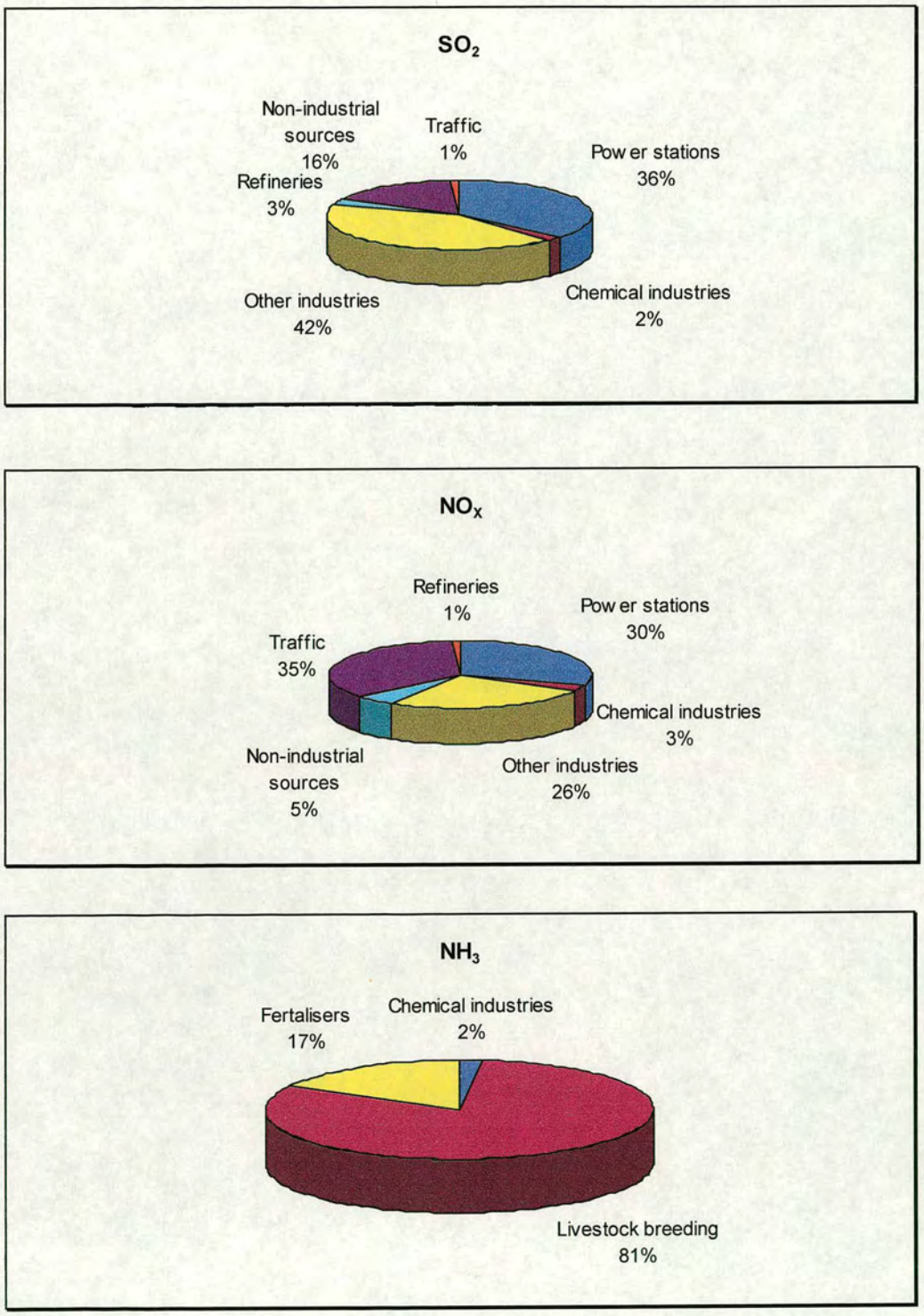

Fig. 1.9: Source contribution of anthropogenic sulphur dioxide, nitrogen oxides, and ammonia to anthropogenic emissions in Europe.

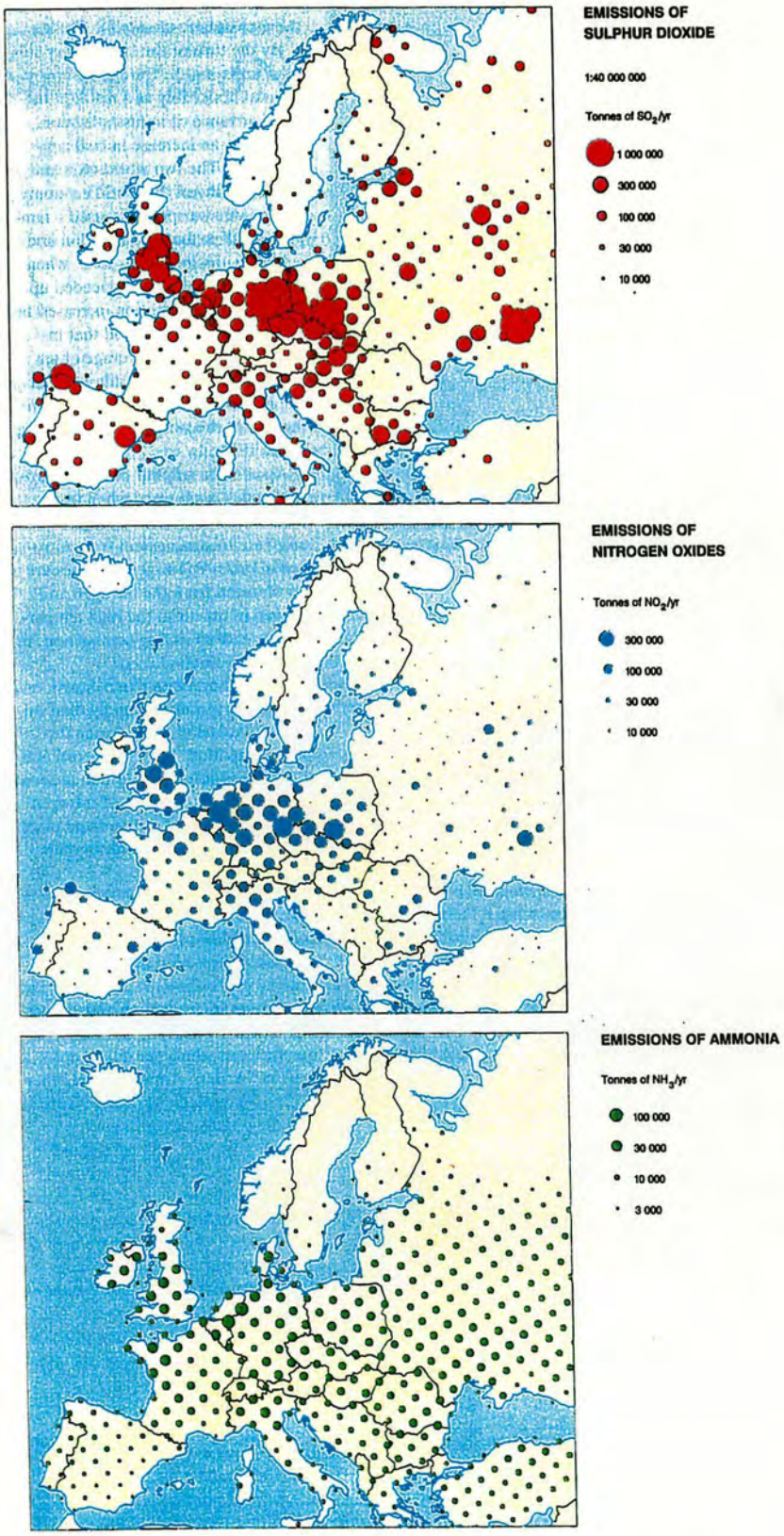

Fig. 1.10: Europe emissions of SO_2, NO_X and NH_3 on a 150 km x 150 km grid.

1992; Dentener & Crutzen, 1993; Graedel et al., 1995; Benkovitz et al., 1996);

- Anthropogenic nitrogen oxides 21-22 Mtonnes N yr^{-1} (Graedel et al., 1995; Benkovitz et al., 1996; RGAR, 1997), natural nitrogen oxides 15-20 Mtonnes N yr^{-1} (Whelpdale, 1987; Graedel et al., 1995; Lee et al., 1997);
- Total ammonia 45-75 Mtonnes N yr^{-1} (Graedel et al., 1995; RGAR, 1997). The estimates for anthropogenic and natural contributions are 31 and 23 Mtonnes N yr^{-1}, respectively (Bouwman et al., cited in RGAR, 1997).

The substantial quantity of emitted sulphate as sea spray and soil dust occur in neutralised form, and hence does not contribute to acidic deposition (Rodhe et al., 1995).

The European contribution to the global emissions of sulphur and nitrogen compounds have been estimated as :

- Anthropogenic sulphur dioxide from 26 Mtonnes S yr^{-1} (Whelpdale, 1987) to 13 Mtonnes S yr^{-1} in 1993 (RGAR, 1997); natural sulphur dioxide 2 Mtonnes S yr^{-1} in (Whelpdale, 1987);
- Anthropogenic and natural oxides of nitrogen 6 and 0.5 Mtonnes N yr^{-1}, respectively (Whelpdale, 1987).

The trend in total European emissions of SO_2 and NO_X in the period of 1880-1993 is shown in Figure 1.11 (taken from RGAR, 1997). Note that sulphur dioxide emissions peaked at more than 21 Mtonnes S in the 1970s and have fallen to 13 Mtonnes S in 1993, mainly due to abatement strategies adapted under the UN ECE (United Nations Economic Commission for Europe) Convention on Long Range Transboundary Air Pollution. On the other hand, there have been little changes in nitrogen oxides emissions over the period of 1980-1993. In the case of ammonia, global emission is expected to increase with the rise in intensive livestock farming and fertiliser application to crops as a consequence of human population growth especially in developing regions of the World (Figure 1.4; Galloway, 1995).

Variation in the European emissions of SO_2 and NO_X with respect to their spatial distribution may be examined by comparing their 1986 emissions illustrated in Figures 1.5 & 1.6 with those of 1993, demonstrated in Figures 1.12 & 1.13 (RGAR, 1997). While there are no obvious changes in the extent and pattern of NO_X emissions

over a decade, it is clear that SO_2 emissions from the western European countries have been reduced more significantly than those from eastern Europe and Spain.

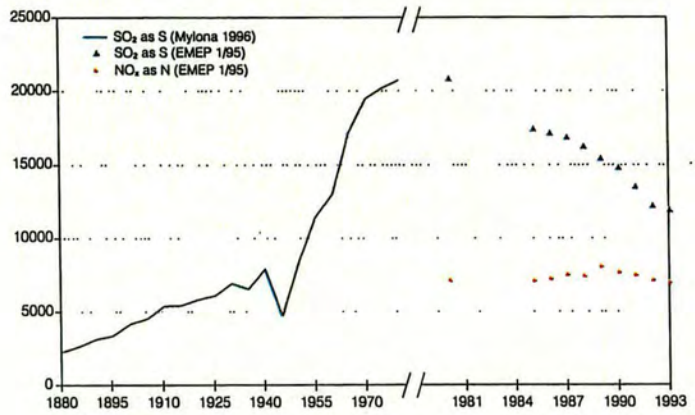

Fig. 1.11: Total European emissions of SO_2 (ktonnes S yr^{-1}) and NO_X (ktonnes N yr^{-1}) 1880-1993.

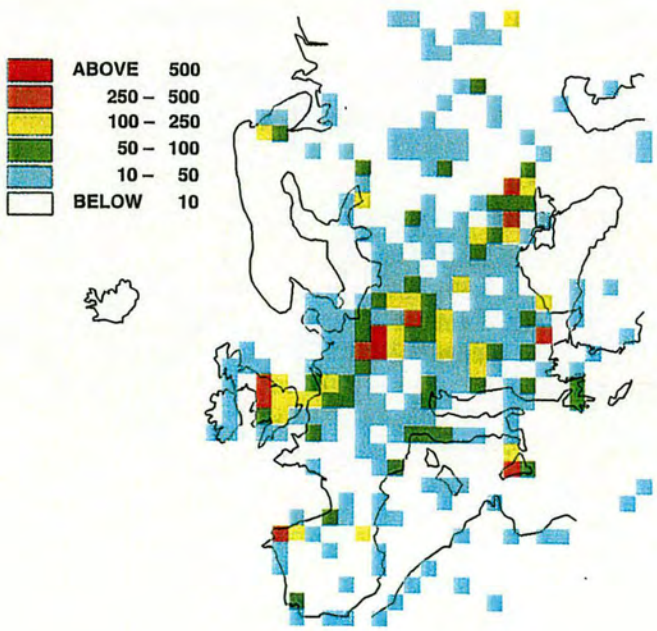

Fig. 1.12: Spatial distribution of European emissions of SO_2, 1993 (ktonnes S yr^{-1} per 150 km x 150 km grid square).

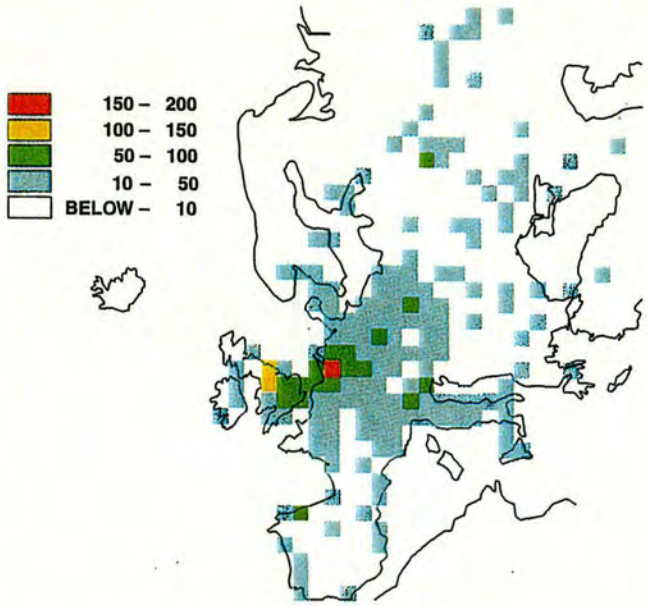

Fig. 1.13: Spatial distribution of European emissions of NO_X, 1993 (ktonnes N yr^{-1} per 150 km x 150 km grid square).

Monitoring figures on emissions of sulphur and nitrogen oxides in Europe are now published regularly as EMEP reports. The EMEP (European Monitoring and Evaluation Programme) figures are based on data supplied by each of the countries participating in the programme. The most recent report (EMEP, 1997) shows the continuing fall in emissions of sulphur and nitrogen oxides. In 1995 the European emissions of SO_2 were 30.7 Mtonnes, as against 41.8 in 1990 and 59.3 in 1980. Emission of nitrogen oxides are also declining from a peak in the later eighties, now being approximately 10% lower than they were in 1980 (see Table 1.1).

1.3.2 Transformation and Transport

Once emitted into the atmosphere, natural and anthropogenic acidifying pollutants are carried, dispersed, and diluted downwind of the source, the extent of which depends on atmospheric motions with a wide range of scales. However, since the atmosphere is an oxidising environment (Cox & Penkett, 1983), chemical oxidation of the primary pollutants occurs as they are dispersed. It appears that a

Table 1.1: Emissions of SO_2 and NO_X (ktonnes yr^{-1}).

		Sulphur dioxide			Nitrogen oxides (as NO_2)		
		1980	1990	1995	1980	1990	1995
Albania	AL	[72]	[72]	[72]	[24]	[24]	[24]
Austria	AT	397	90	74*	246	222	177*
Belarus	BY	740	637	275	234	285	195
Belgium	BE	828	317	253*	442	352	345*
Bosnia & Herzegov.	BA	[480]	480	[480]	[80]	[80]	[80]
Bulgaria	BG	2050	2020	1497	[416]	376	266
Croatia	HR	150	180	63	[83]	83	55
Czech Republic	CS	2257	1876	1091	937	742	412
Denmark	DK	450	184	150	282	279	250
Estonia	EE	[239]	239	110	[93]	93	50*
Finland	FI	584	260	96	295	300	259
France	FR	3338	1298	989	1823	1585	1666
Georgia		[162]	[162]	[162]	[188]	[188]	[188]
Germany[1]	DE	7514	5326	2995*	3334	2640	2210*
Greece	GR	400	510	[556]	[306]	[392]	[357]
Hungary	HU	1633	1010	699	273	238	171
Iceland	IS	18	24	24	[18]	20	23
Ireland	IE	222	178	166	73	115	116
Italy	IT	3800	1678	[1437]	1480	2047	[2157]
Kazakstan[2]		[140]	[140]	[140]	[76]	[76]	[76]
Latvia	LV	[57]	57	38	[90]	90	29
Lithuania	LT	311	222	107	152	158	67
Luxembourg	LU	24	14	8	23	23	20
Macedonia	FYM	[106]	[106]	[106]	[39]	[39]	[39]
Moldova	MD	308	231	59	58	39	25
Netherlands	NL	490	205	147	583	575	518
Norway	NO	140	53	35	192	227	222
Poland	PL	4100	3210	2337	1229	1279	1120
Portugal	PT	266	283	272*	[96]	221	254*
Romania	RO	1055	1311	912*	523	546	319*
Russian Federation[2]	RU	7161	4460	2983*	1734	2675	1995*
Slovakia	SK	780	543	238*	[197]	227	173*
Slovenia	SI	234	195	119	51	57	67
Spain	ES	3319	2266	[2061]	950	1178	1223*
Sweden	SE	508	136	94	448	411	362
Switzerland	CH	116	43	34	170	165	136
Turkey[2]	TR	860	[354]	[354]	[175]	[175]	[175]
Ukraine	UA	3849	2782	1639	1145	1097	530
United Kingdom	GB	4913	3756	2365	2416	2897	2295
Yugoslavia[3]	YU	406	508	462	47	66	59
Baltic Sea	BAS	[72]	[72]	[72]	[80]	[80]	[80]
North Sea	NOS	[475]	[475]	[475]	[710]	[710]	[710]
Remaining NE Atl.	ATL	[891]	[891]	[891]	[1275]	[1275]	[1275]
Mediterranean Sea[2]	MED	[12]	[12]	[12]	[13]	[13]	[13]
Natural oceanic	NAT	[724]	[724]	[724]	[0]	[0]	[0]
Volcanic[4]		[2144]	1645	[2235]	[0]	[0]	[0]
Sum		**59,345**	**41,804**	**30,724**	**23,215**	**24,480**	**20,903**

The table shows national official data received at the ECE secretariat. Data estimated by MSC-W/CCC are given in square brackets. * 1994 figures. [1]Including East Germany in 1980 and 1990 figures. [2]Part within the EMEP area of calculation. [3]The Federal Republic of Yugoslavia (Serbia and Montenegro). [4]Natural emissions reported by Italy.

variety of mechanisms can cause acids to form and that the dominant chemical reactions depend on the location and weather conditions as well as on the chemical composition of the local atmosphere (Goldsmith et al., 1984; Seinfeld, 1986; Wellburn, 1988; Smith, 1991; RGAR, 1997). Transformation (oxidation) of atmospheric pollutants (e.g. SO_2, NO_X) occurs via chemical processes taking place in both the gaseous and aqueous phases of clouds and results in acidic deposition. Major oxidants involved are ozone, hydroxyl radicals and hydrogen peroxide. These oxidants occur naturally, being formed in the stratosphere by ultraviolet light or

produced within the lower, polluted layers of the atmosphere in the presence of sunlight, hydrocarbons, nitrogen compounds and water (Smith, 1991). The main chemical reactions that convert SO_2 to sulphuric acid and NO_X to nitric acid can be summarised as follows (Mannion & Bowlby, 1992):

Sulphuric acid

- In the aqueous phase, sulphur dioxide disolves in atmospheric water droplets to form bisulphite, the oxidation of which yields sulphate,

$$SO_2 + H_2O \longrightarrow H_2SO_3 \rightleftharpoons H^+ + HSO_3^-$$

- in gas or aqueous phase, sulphur dioxide can be oxidised by various oxidants,

$$SO_2 \xrightarrow{\text{oxidant}} SO_3$$

- aqueous sulphur trioxide forms sulphuric acid,

$$SO_3 + H_2O \longrightarrow H_2SO_4 \rightleftharpoons H^+ + HSO_4^- \rightleftharpoons 2H^+ + SO_4^{2-}$$

Nitric acid

- In the presence of O_3 or a reactive hydrocarbon (RH), NO is converted rapidly into NO_2,

$$O_3 + NO \longrightarrow NO_2 + O_2$$

- NO_2 can be oxidised to HNO_3 either by direct reaction with OH, or by reaction with ozone and through formation of NO_3 and N_2O_5,

$$2NO_2 + H_2O \longrightarrow HNO_3 + HNO_2$$

The oxidisation processes of nitrogen compounds are complicated because they may be governed by differnt mechanisms during the day, or at night-time. These chemical transformation of sulphur dioxide and nitrogen oxides eventually lead to the formation of sulphates and nitrates, respectively.

The atmospheric paths leading to acid deposition are depicted in a diagram by Seinfeld (1986) shown in Figure 1.14. The major pathways by which primary and secondary acidic precursors can be incorporated into precipitation are described as:

- nucleation scavenging of sulphate or nitrate-containing aerosol particles in cloud formation;
- aqeous-phase formation of sulphate from absorbed SO_2 in cloud droplets, and absorption of gaseous nitric acid by cloud droplets;
- below-cloud scavenging of sulphate and nitrate-containing aerosols by rain.

Note that the chart does not show a path for the conversion of gaseous NO_X to nitrate in cloud because aqueous-phase formation of nitrate from absorbed NO and NO_2 is found to be too slow to be of atmospheric importance. Recent studies at Great Dun Fell, however, have revealed an important role of clouds as chemical reactors in transforming NO_X into other gaseous nitrogen compounds, and particulate nitrate (Cape et al., 1997; Choularton et al., 1997; RGAR, 1997).

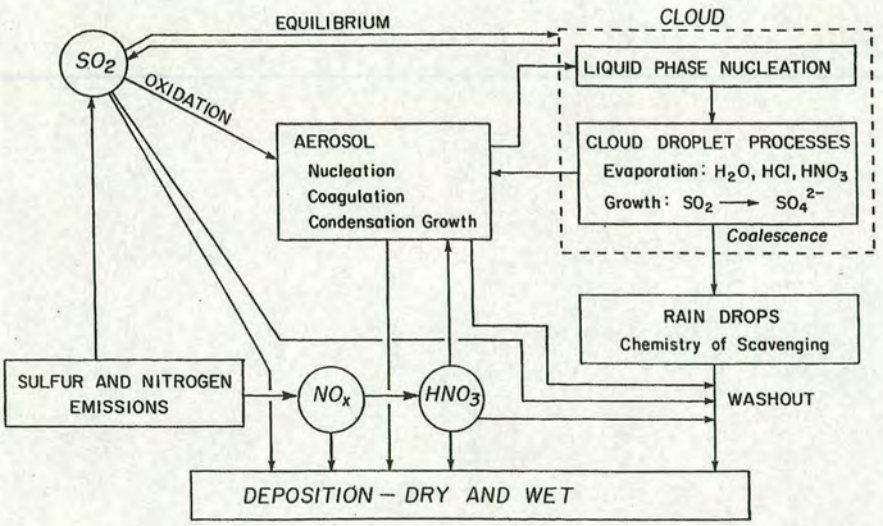

Fig. 1.14: Atmospheric paths leading to acid deposition.

Most natural (apart from volcanoes) and some anthropogenic emissions (e.g. mobile sources) originate at ground level whilst others are emitted from the tall stacks often over a hundred metres high. The extent of pollutant dispersion depends on source height, local topography as well as the mixing characteristics of the atmosphere prevailing at the time of release, but essentially the wind carry them along

trajectories determined by large scale weather system (Hov et al., 1987; Wellburn, 1988; RGAR, 1997). The primary pollutants and their trnsformation products have atmospheric lifetimes in the order of days, a time-scale over which they can be carried by weather systems over continental distances of a few thousand kilometers. In the case of SO_2, for instance, the transformation from gas to sulphate particles is gradual, taking a matter of days. During that time, sulphur pollution may be deposited back onto the earth's surface, either in the form of sulphur dioxide or sulphate. In either form, sulphur pollution can be deposited by wet or by dry deposition processes, where dry deposition dominates closer to the source, and wet deposition increases with oxidation downwind (Howells, 1990). Figure 1.15 suggests the effects of time and distance on the conversion and deposition of sulphur (OTA, 1984).

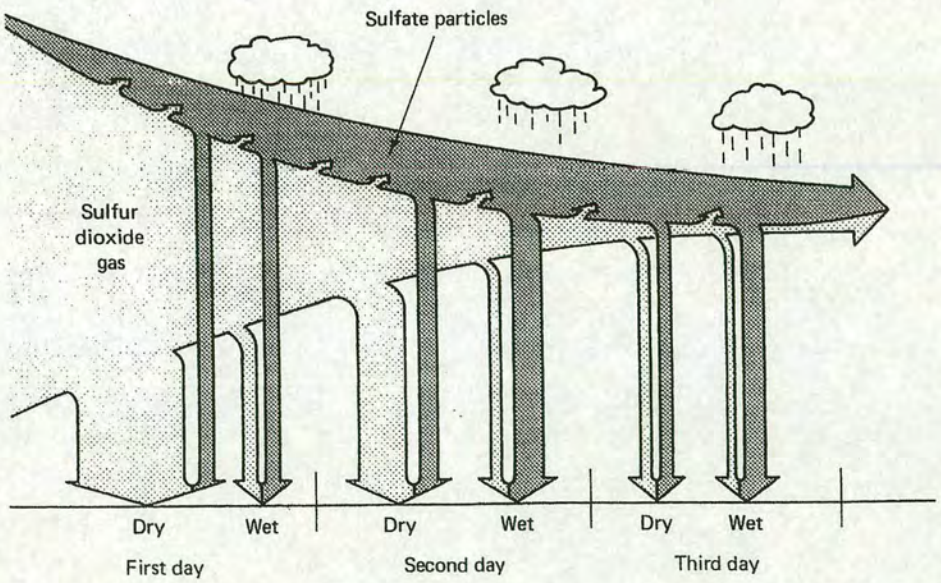

Fig. 1.15: The effects of time and distance on conversion and deposition of sulphur pollution.

1.3.3 Deposition

Atmospheric aerosols and gases are transferred onto terrestrial surfaces by a variety of processes which may be placed into three categories: *Dry deposition*, which

includes the direct take-up of airborne substances to the surface or to vegetation by processes of absoption, impaction or sedimentation; *wet deposition*, which includes the indirect transfer of airborne gaseous or particulate material to the ground via hydrometeors (i.e. raindrops, snowflakes, hailstones); and *cloud droplet interception* (often referred to as 'occult' deposition), the process by which cloud and fog droplets are directly intercepted by the earth's surface. The partition of total deposition into these different fractions is presented in a chart (Figure 1.16) adapted from Bredemeier (1988) and Godt & Mayer (1988). These deposition mechanisms are described in the following sections along with an outline on total deposition of major acidic pollutants in the UK and Europe.

1.3.3.1 Wet deposition

Wet deposition is usually determined from the composition and amount of rainfall and is relatively well known. It is defined as the process by which atmospheric pollutants are attached to and dissolved in cloud and precipitation droplets (or particles) and concequently delivered to the earth's surface during precipitation. This tends to be an efficient pathway for removing most acidic species from the atmosphere, the amount of which is strongly dependent on the amount of rain and the location of the receptor with respect to sources (Erisman & Draaijers, 1995). The pollutant content of wet deposition is the result of physico-chemical processes within clouds (often called "rain-out" or "in cloud scavenging"), and those transferring material to falling raindrops below cloud base (often called "wash-out" or "below cloud scavenging")(Beilke, 1982). Aerosols and particles may be incorporated into cloud or precipitation elements by any of the following processes (Smith. 1991):

- being swept out as the element falls through the air;
- becoming cloud condensation nuclie for developing cloud droplets which subsequently turn into precipitation elements by coalescence;
- through phoretic effects where various forces (e.g. electrical, thermal) act on the particles pushing them towards the droplet; or

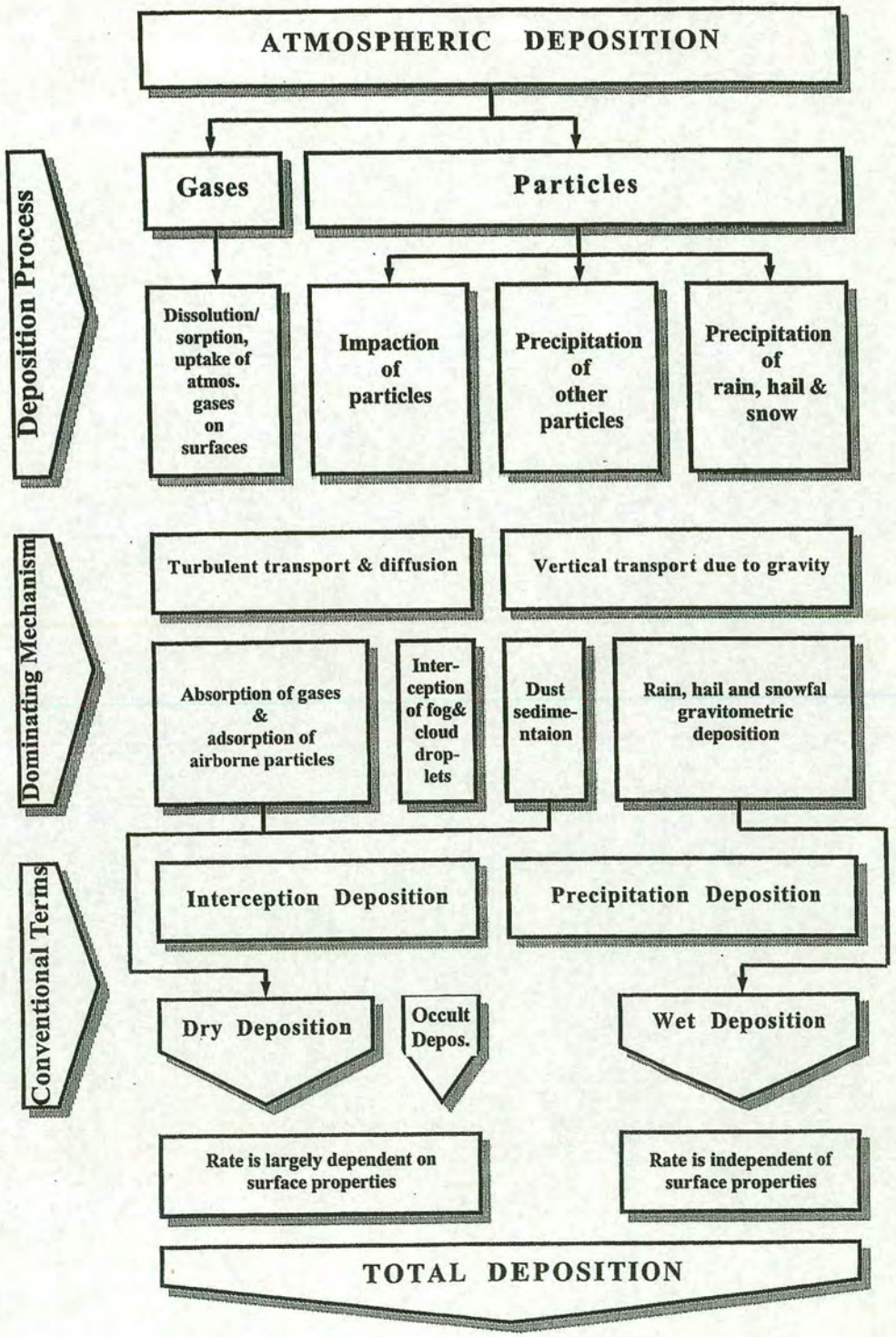

Fig. 1.16: Partition of total deposition.

- by so-called Brownian capture in which sufficiently small particles (<< 0.1 μm) are moved by molecular bombardment and may collide with, and be captured by, larger cloud droplets.

The first two are major mechanisms involved in wet scavenging of acidic particles. Gaseous pollutants are removed differently through solution and oxidation in cloud and rain water. The uptake and oxidation of sulphur dioxide in cloud water is quite efficient (Cox & Penkett, 1983), and this mechanism is considered to be an important pathway for scavenging SO_2 in orographic cloud (Dollard et al., 1988; Gevat et al., 1988).

The rates of wet deposition (D_w) do not depend on the underlying surface characteristics but on the precipitation rate (R), the wash-out/rain-out ratio (ω) and the ambient air concentration (C_a); where ω is the concentration of dissolved pollutant per unit mass of cloudwater (C_c) or rain (C_r) divided by the concentration of the same pollutant or precursor per unit mass of air (C_a)(Wellburn, 1988; Smith, 1991):

D_w	=	C_r	x	R	=	ω	x	C_a	x	R
$g\ m^{-2}$		$g\ l^{-1}$		mm		100		$g\ l^{-1}$		mm

If C_a and C_r (or C_c) are expressed in $g\ l^{-1}$ then ω is usually of the order of 100 for wash-out and 500 for rain-out. The quoted value for $\omega_{\text{wash-out}}$ refer to a depth of 1000 meters of the polluted column through which the rain falls.

Though wet deposition is not directly influenced by land use but its spatial patterns depend on the topography. Rainfall tends to increase with ground elevation. For instance, the rainfall map of the UK, when viewed on a large scale, is qualitatively very similar to the physical map showing contours of height above mean sea level (Smith, 1991). In mountainous regions, however, orographic effects increase not only the rainfall rate but also the concentration of the major ions in precipitation through "seeder-feeder" mechanism (Choularton et al., 1988; Fowler et al.1991). The precipitation from higher level cloud (called 'seeder') *washes* out more polluted cloudwater from the lower level orographic (called 'feeder') cloud (Fowler, 1994). Detailed studies of the mechanisms of orographic enhancement have led to the modification of wet deposition maps of the UK (Carruters & Choularton, 1984; Fowler et al., 1988; Dore et al., 1992).

Wet deposition measurement is rather simple to perform by placing collectors in the open field (usually 1.5 to 2 m above the ground) for a certain duration of time, and a routine analysis of the collected samples for their chemical composition. The product of precipitation amount and the concentration of individual chemical species provide their wet deposition estimate at the site. A decision has to be made of course whether to use a wet-only collector or a bulk collector, which depends on the relative proportion of wet to dry deposition at the monitoring site as well as the objectives of the monitoring programme. To perform an accurate measurement, however, special attention should be devoted to efficient collection of precipitation at windy sites, exclusion of dry deposition and contaminations, and prevention of chemical changes in samples (RGAR, 1997). On a large scale, the wet deposition estimates for relatively simple terrain are easily made by combining the *precipitation field* with the *concentration field* for individual chemical species. The difficulty lies with the estimation of input to complex terrain, where orographic effects (e.g. seeder-feeder effects) lead to marked increase in wet deposition. The problem has been resolved in the UK by developing parameterization schemes to modify wet deposition maps for this effect (Fowler, 1995b).

1.3.3.2 Dry deposition

The direct sorption of gases by vegetation, soil or water surfaces and the impaction and gravitational settling of particles are collectively known as dry deposition (see Figure 1.16). The transfer of trace substances by this mechanism is commonly expressed as:

F	=	v_d	x	C(z)
$g\ m^{-2}\ s^{-1}$		$m\ s^{-1}$		$g\ m^{-3}$

where F is the flux of pollutant to unit area of the earth's surface, and is considered to be proportional to pollutant concentration in air, C(z), at height z. The coefficient v_d has the dimensions of a velocity so that is called the deposition velocity. Dry

deposition is governed by processes which are usually treated in three stages for convenience:

1. transport of gases and particles from the free atmosphere down to the viscous sublayer that envelops all surfaces;
2. transport by Brownian diffusion, phoretic effects, interception, impaction, and sedimentation through the viscous sublayer; and finally,
3. interaction of gases and particles with the surface: they may be absorbed, adhered, or they may bounce off.

These stages are illustrated for the transport of gases and small particles to vegetation in Figure 1.17, taken from Fowler et al. (1989).

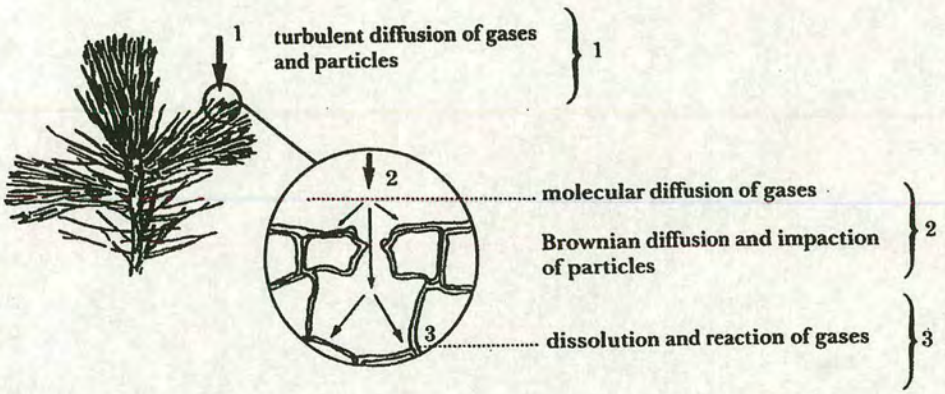

Fig. 1.17: Transport processes of gases and small particles to vegetation.

The deposition velocity is usually described as a function of different resistance's representing the deposition process as an analogue to electrical current flow through resistance's in parallel and series (Thom, 1975; Garland, 1977; Fowler, 1978). The framework is demonstrated in Figure 1.18, taken from RGAR (1997). The total resistance to deposition, R with dimensions of s cm^{-1}, is the reciprocal of the

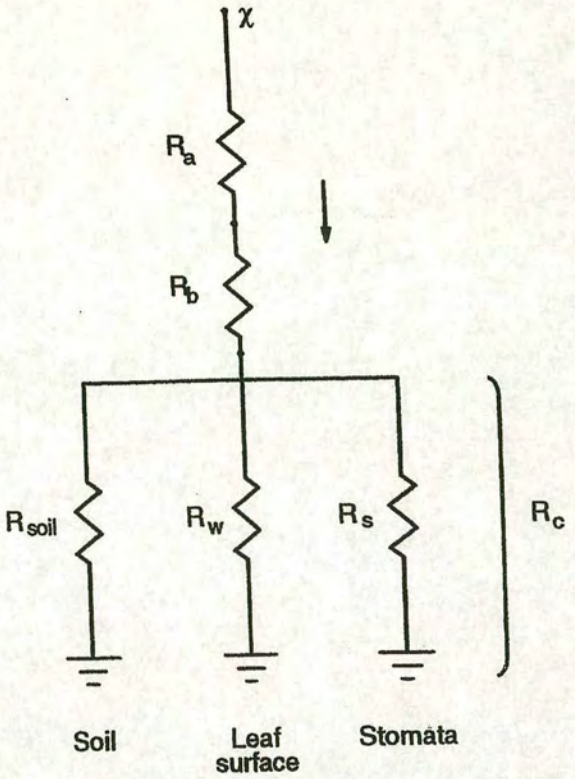

Fig. 1.18: Schematic showing the factors controlling the dry deposition rate using the resistance analogy

deposition velocity vd, is expressed as the sum of the resistance's for each stage of the transfer:

$$R = R_a + R_b + R_c = R_{air} + R_c = v_d^{-1}$$

where R_a represents the resistance to turbulent transport from the height (z) above the surface to the leaf boundary layer; R_b represents the transport to foliar surfaces; and Rc, the canopy resistance, accounts for the component surface resistance's including stomata resistance (R_s), leaf surface resistance (R_w), and soil resistance (R_{soil}):

$$R_c^{-1} = R_s^{-1} + R_w^{-1} + R_{soil}^{-1}$$

R_a and R_b may be combined to represent the resistance to transport through the air (R_{air}):

$$R_{air} = R_a + R_b$$

The deposition velocity of particles is highly dependent on particle size with different removal processes at work in different size regions as demonstrated by the particle size distribution velocity relationship in Figure 1.19.

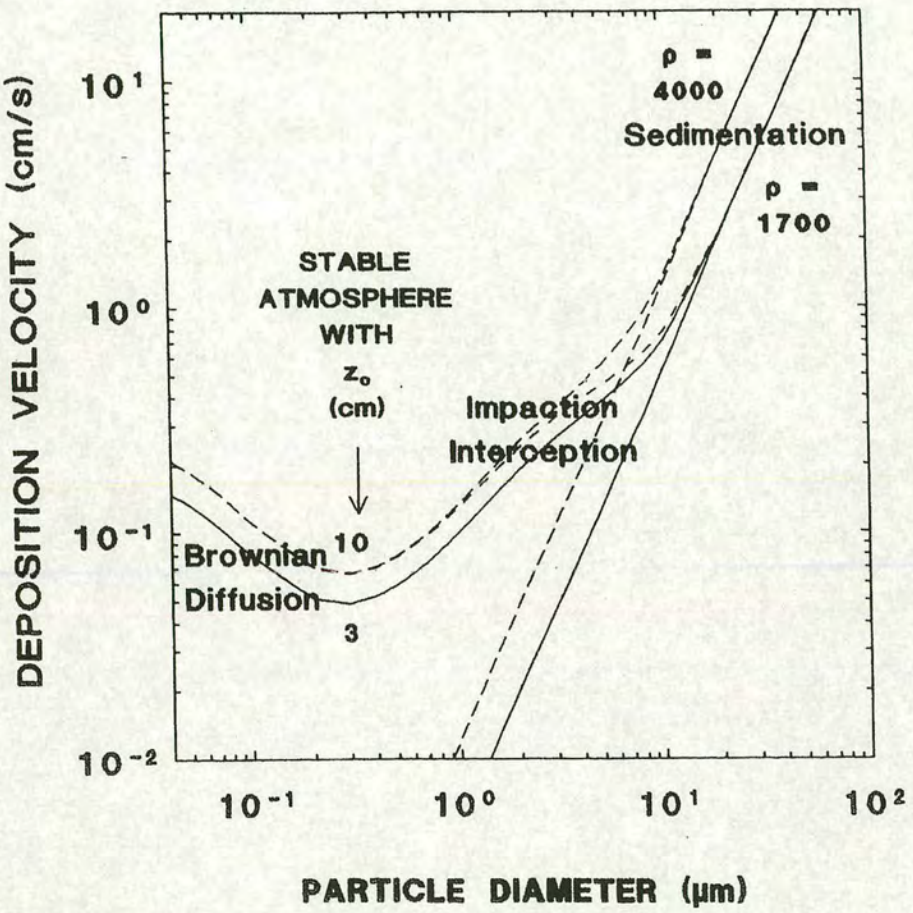

Fig. 1.19: Typical curves for the deposition velocity of particles as a function of size in a stable atmosphere for two different roughness lengths (z_0 in cm) and particle densities (ρ in kg m^{-3}). The curves were calculated with u = 5 m s^{-1} (Ruijgrok, 1995).

The curves in Figure 1.19 were calculated using the deposition model described by Sehmel & Hodgson (1980). It should be noted, however, that there is a wide variation in calculated and measured values of v_d for particles in literature. For instance, the values of vd predicted by Wiman & Agren (1985) are about a factor of 5 larger than those given by the model of Slinn (1982). The range of measured values is from

negative values to several cm s^{-1} (Ruijgrok, 1995). The discrepancy has not yet been adequately explained (Fowler et al., 1991).

Methods used to quantify the dry deposition can be grouped into the following categories (Fowler, 1986; Erisman et al., 1994b; Ruijgrok, 1995):

Micrometeorological methods. 'Eddy correlation' and 'flux gradiant' (or profile) methods are the two most widely used micrometeorological methods. Both require a considerable monitoring effort, but are very useful for the study of deposition processes and for validating models. Fluxes, however, can not be estimated in complex terrain or near to sources.

Surface accumulation methods. Measurements of dry deposition are made by measuring the deposition at the surface either directly (e.g. 'throughfall' method, electron microscope counting of accumulated material, wind-tunnel studies, and chamber studies) or indirectly (measuring deposition to different surrogate surfaces intended to approximate natural surfaces). Throughfall method has been widely used, at least for sulphur deposition study, despite criticism on possible interference by vegetation (due to canopy exchange processes). The main question concerned in using surrogate surfaces is to what extent these devices are representative of natural surfaces. Their application may lead to either the overcollection or undercollection of depositing particles.

Watershed mass balance method. This method estimates the dry deposition by measuring the outflow from a catchment with the assumption that it is equal to the sum of wet+dry deposition. The limitation is that the weathering release and net change in storage in biomass and soil are not always negligible, and it may not be easy to quantify them.

Inferential technique. The dry deposition fluxes are inferred as the products of ambient concentrations of chemicals of interest and their dry deposition velocities. For each substance, v_d is either measured or derived from a transfer model based on the resistance framework for coupling individual processes involved (e.g. Hicks et al., 1987). The technique relies on the availability and quality of data as well as the adequate description of the resistance's. However, it has been used widely in the UK (RGAR, 1997), Sweden (Lovblad et al., 1992), the Netherlands (Erisman, 1993), USA (Clarke, 1992), and Canada (Eder & Dennis, 1990).

None of the available techniques provide a measure of dry deposition for individual ecosystems with sufficient accuracy (Erisman et al., 1994b).

1.3.3.3 Cloud droplet interception

The third pathway for the deposition of atmospheric substances is by interception of cloud or fog droplets onto terrestrial surfaces. This process has been widely referred to by the often misunderstood term "occult deposition" to illustrate the fact that the input is largely 'hidden' from standard precipitation collectors (RGAR, 1997) (see also Figure 1.16). The input via this pathway in coastal areas and high altitudes, where low cloud is common, can lead to a significant contribution to the annual deposition budget especially where the surface vegetation is efficient at capturing cloudwater, i.e. forests (Dollard et al., 1983; Neal et al., 1986; Lovett & Reiners, 1986; Fowler et al., 1989; Unsworth & Wilshaw, 1989; Gallagher et al., 1992; Crossley et al., 1992; Fowler et al., 1998).

The interception of wind-blown cloud or fog droplets by vegetation has long been recognised as a significant hydrological input to forests frequently immersed in fog or clouds (e.g. Linke, 1916; Descombes, 1919; Schubert, 1927; Geiger, 1950; Sauberer, 1952; Hori, 1953; Friedrich, 1954; Delfs, 1955; and Grunow, 1955, all quoted in an excellent review of mist precipitation on vegetation by Kerfoot, 1968). One of the earliest observed evidences is described by Scottish mariner George Glas in his 1764 book on the history of Canary Ilands as a tree that stand in the path of early morning mists and delivered fresh water to island residents (Kerfoot, 1968). In a recent project, giant polypropylene mesh collectors on the summit of El Tofo, a 1033 m asl coastal mountain in southern Atacama Desert in Chile, capture enough fog droplets to provide the community's water supply for a fishing village of 330 inhabitants at the foot of mountain. Banks of fog roll in from the pacific 300 days a year onto 75 passive cloudwater collectors (nets with an area of about 47 m^2 each) which draw a daily average of approximately 10000 litres of water from them. This rate increases by as much as an order of magnitude in the wetter summer season (Pfeiff, 1997).

Because of the large specific surface area provided by foliage, vegetations particularly forests represent a significant potential sink for atmospheric substances incorporated into hill cloud and lowland fog droplets, which are typically in the size range of 5-50 μm (Lovett & Reiners, 1986). The total amount of vegetative surface area available for deposition may well exceed the total land area. The leaf area index L, defined as m^2 of leaf area per m^2 of subtended land surface is in the range of 3-10 (Evans, 1972). Numerous studies of turbulent deposition of droplets onto natural surfaces (e.g. Dollard et al., 1983; Lovett & Reiners, 1986; Gallagher et al., 1988; Fowler et al., 1989; Kroll & Winkler, 1989; Collett et al., 1991; Fowler et al., 1991; Lindberg, 1992) have revealed that the rate of cloudwater deposition is mainly controlled by the following parameters:

- droplet size distribution;
- ambient windspeed;
- cloud/fog frequency;
- cloud/fog liquid water content (LWC);
- aerodynamic characteristics of the forest canopy; and
- the concentration of pollutants in cloud/fog water.

Size dependence of cloud droplet deposition is illustrated in Figure 1.20, from measurements by Gallagher et al. (1992), which shows the similarity between cloudwater and momentum deposition rates. Based on this similarity within the range of droplet radius 4-20 μm which includes the bulk of the liquid water in orographic cloud on windy uplands of Northern Europe, it has been suggested that cloud droplet interception can be modelled from the relatively well known (and monitored) data on wind and roughness length (Fowler et al., 1991; Beswick et al., 1991; Fowler, 1995b).

The aerodynamic roughness length, z_o, as a surface length scale is the height where the wind speed becomes zero, best defined by the standard wind profile equation (Thom, 1975; Stull, 1988; Monteith & Unsworth, 1991):

$$U_{(z)} = (U_*/k)\ ln(z/z_o)$$

in which U is the average wind speed at any height z, U_* is friction velocity, and k is

the von Karman's constant. Even though z_o is not exactly equal to the height of roughness found on the earth's surface and encountered in the air mass's flow, a

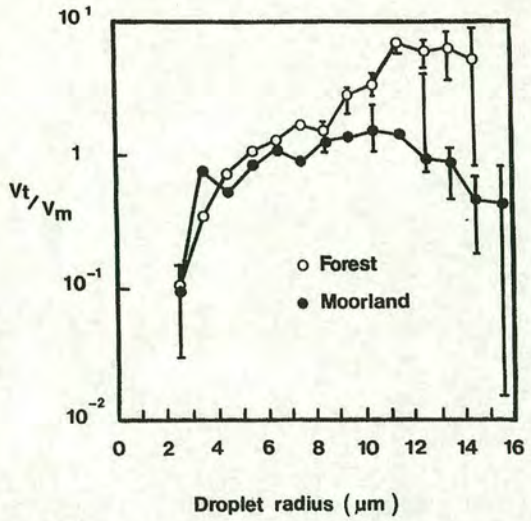

Fig. 1.20: Effects of droplet size in the range 2-15 μm on the ratio of turbulent deposition velocity (V_t) to that of momentum (V_m) (where $V_m = r_{am}^{-1}$ for forest and moorland from measurements by Gallagher et al., 1992, taken from Fowler, 1995b).

bi-univocal relation does exist between the two. Typical values of this parameter are indicated in Table 1.2, taken from Stull (1988). It shows that higher roughness elements are associated with larger aerodynamic roughness lengths. However, the aerodynamic roughness length is always smaller (typically an order of magnitude) than the physical height of the surface roughness element (Thom, 1975).

If roughness elements are grouped close together, as, for example, in the presence of a forest (or urban area), this parameter is no longer sufficient to describe boundary-layer surface interactions. The so-called zero-plain displacement height d is then necessary, which is defined as the altitude above which the wind profile is again described by the logarithmic wind profile equation. In this case for every height z greater than d, the previous equation is modified as follows:

$$U_{(z)} = (U*/k)\ ln\{(z-d)/z_o\}$$

Above the canopy top, the wind profile increases logarithmically with height, as shown in Figure 1.21 (Stull, 1988). Maps of land use and wind velocity provide the

required data to calculate the deposition velocity $V_{d(z)}$ as $V_{d(z)} = U_*^2/U_z$ at reference height z above the canopy (Fowler et al., 1991).

Table 1.2: Aerodynamic roughness lengths for typical terrain types from Stull (1988).

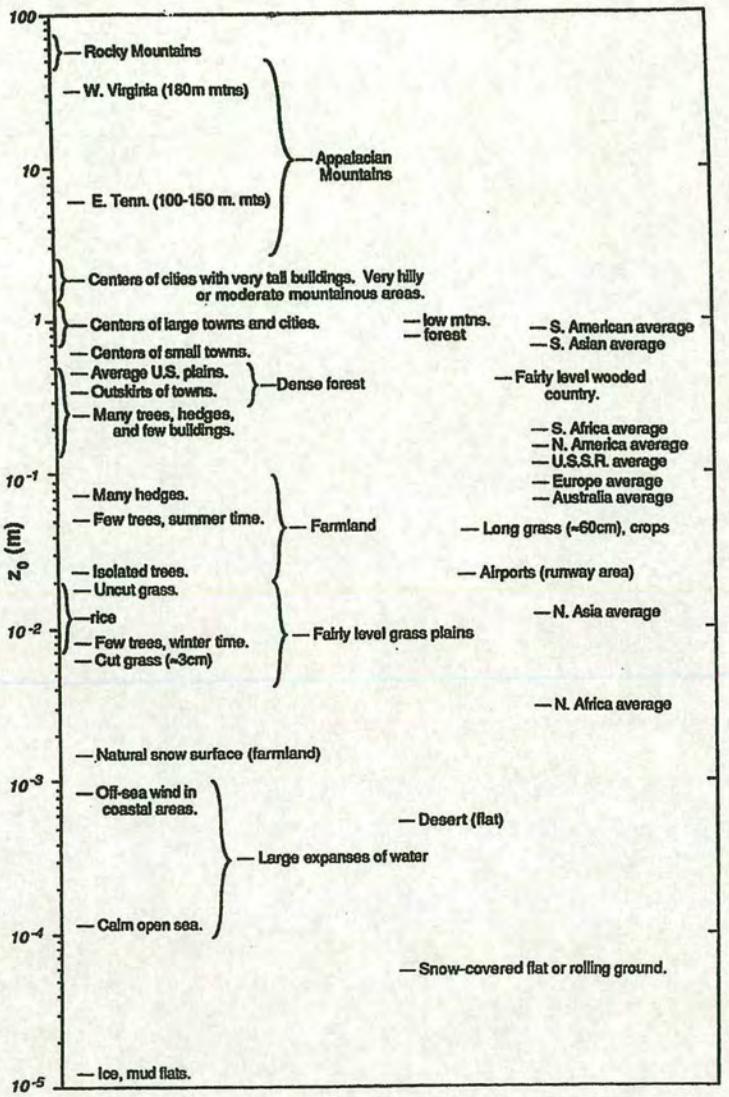

To estimate the cloud interception inputs of major pollutants, the quantification of the spatial variability in cloud frequency and the ion concentrations in cloudwater are also needed. Cloud immersion frequencies for the UK are available through the 3 dimensional frequency fields of cloud cover developed by Weston (1992). Measurements at several sites in the UK and Germany have demonstrated a consistent height dependence of the concentrations of major ions as illustrated in Figure 1.22, taken from Fowler et al. (1991). The concentration field may be taken

from network measurement data by interpolation. The average enhancement in ion concentration in orographic cloud relative to that in rain is then incorporated in the calculation.

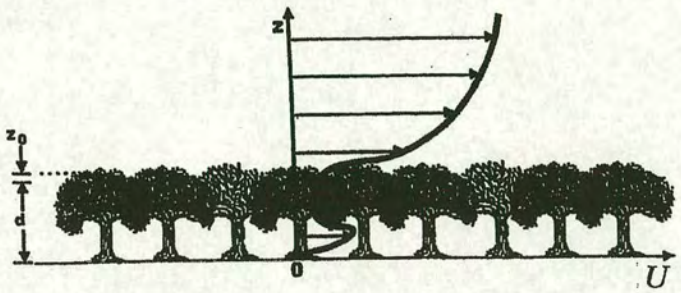

Fig. 1.21: Flow over forest canopy showing wind speed, U, as a function of height, z. The thick canopy layer acts like a surface displaced a distance, d, above the true surface. z_o = roughness length.

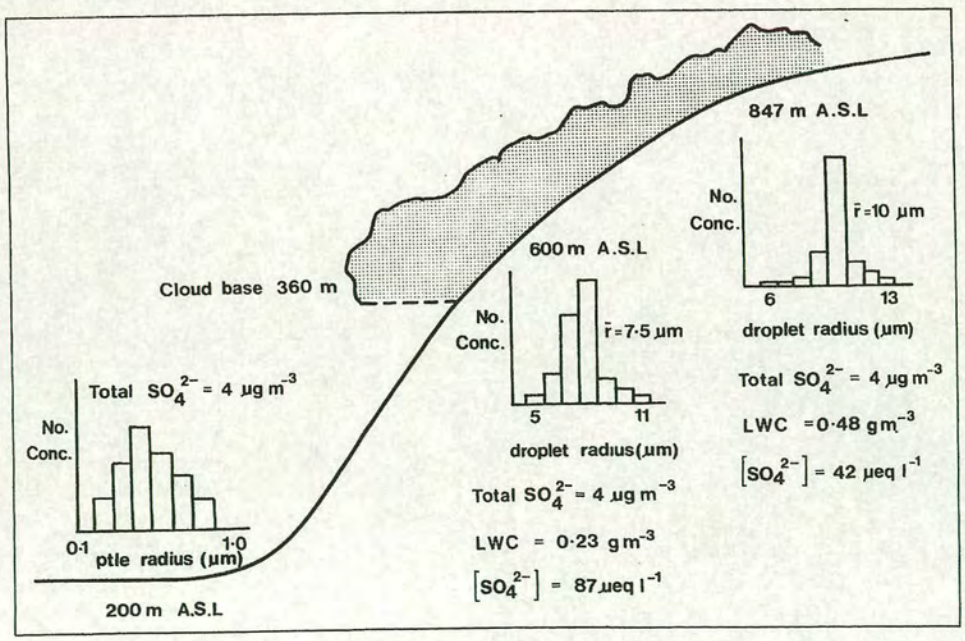

Fig. 1.22: An illustration of the changes that occur at Great Dun Fell in the sizes of particle cloud droplets as they are advected up the hillside (from Fowler et al., 1991).

The annual input of cloud water in the UK determined by this procedure shows that the absolute magnitude of the input is small and contributes little to the total deposition for the UK as illustrated in Figure 1.23 taken from CLAG (1997). However, it should be noted that the input through this pathway is concentrated in forested upland areas where some of the most sensitive ecosystems are located (RGAR).

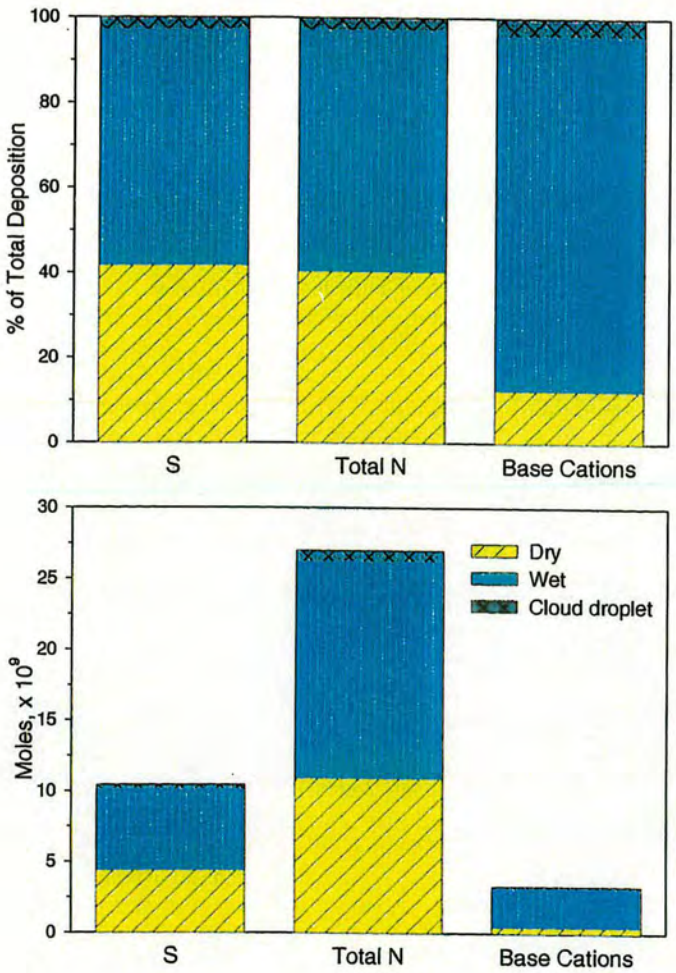

Fig. 1.23: Contribution of the deposition pathways to mean annual total deposition of non-marine sulphur, nitrogen and base cations in the UK during 1992-94 as (a) a percentage of the total, and (b) mols x 10^9.

In addition to the inferential method just mentioned, other techniques have also been applied to determine atmospheric deposition through this pathway. These are reviewed by Erisman et al. (1994b) and include mainly:

- collection of droplets using passive cloudwater monitoring systems, e.g. fog samplers (Collett et al., 1991). Because of the strong acceptor-dependency, they provide at best only relative results (Prinz, 1989);
- micrometeorological measurements of droplet deposition to short vegetation and forests (e.g. Gallagher et al., 1988; Vermeulen et al., 1995). Micro. met. techniques suffer mainly from their limitation to certain terrain situations (Erisman et al., 1994b);
- throughfall measurements together with cloud occurrence detection and cloud water measurement (Joslin & Wolfe, 1992). Throughfall techniques generally require the use of large number of samplers for a reasonable overall estimate of deposition and are only applicable where canopy exchange of the concerned chemical is negligible (RGAR, 1997).

1.3.3.4. Sulphur and nitrogen budgets

The purpose of this section is to provide an overall view of the total emission and deposition of acidic substances in the UK and Europe by presenting budgets for the major pollutants involved. The UK budgets for sulphur, oxidised nitrogen, and reduced nitrogen during 1992-94 is illustrated schematically in Figure 1.24, and is briefly described here (RGAR, 1997):

- *Sulphur*. Total input of sulphur to the UK atmosphere is estimated as 1760 kT, where UK's contribution is 1600 kT (91%). The annual deposition is 350 kT (20%) which is partitioned between wet and dry deposition by 60% and 40%, respectively. Cloud deposition is less than 5% and is included in with wet deposition.
- *Oxidised nitrogen*. The total atmospheric input of oxidised nitrogen is estimated as 840 kT. The UK's contribution to this total is 780 kT (93%). Total deposition is 18% (150 kT) of the input to the atmosphere. Wet deposition is the predominant fraction at 75% of the total deposition.

Reduced nitrogen. The budget for reduced nitrogen shows quite a different picture. From the total input of 290 kT, nearly 80% (230 kT) is deposited onto

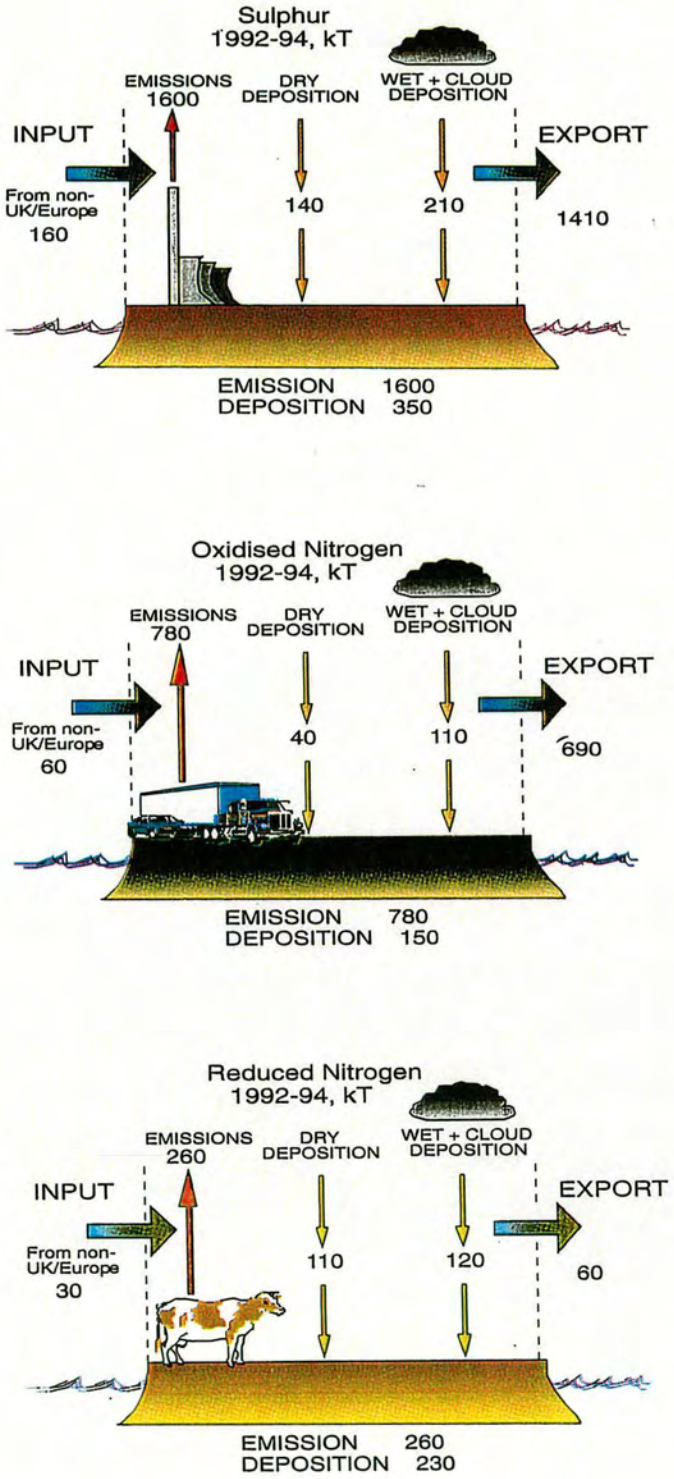

Fig. 1.24: Schematic representation of the UK sulphur, oxidised nitrogen, and reduced nitrogen budgets 1992-94 (from RGAR, 1997).

UK's terrestrial surfaces. Dry deposition represent approximately 50% of the total deposition.

To extend the view on a European scale, the 10 years average budget of sulphur and oxidised nitrogen for European countries are presented in Tables 1.3 and 1.4. These EMEP figures are based on data supplied by each of the countries participating in the programme (MSC-W, 1997). These in turn form, together with meteorological data, the basis for calculation in a computer model describing the transformation and deposition of pollutants as they move about over Europe (Alcamo et al., 1990). The two tables clearly demonstrate the transboundary nature of acidic deposition. Note that the EMEP procedure does not consider the enhancements in deposition due to orographic effects and full account of cloud droplet deposition whereas both these enhancements are incorporated in the UK national estimates. It should be also noted that EMEP results are based on a lower resolution mapping system which masks a great degree of landscape heterogenity.

For country/area codes, see Table 1.1. To find the contribution from other countries to a certain country, follow the horizontal row starting from the relevant country code on the far left. To find the contribution from a certain country to other countries, follow the vertical column starting from the relevant country code at the top. All figures represent the percentage of total deposition received by each country/area, except for the SUM column, which denotes the totals in the unit 1000 tonnes S or N per year. Since some of the depositions cannot be traced to any specific country, they have to be assigned to indetermined sources (IND) in the table, two-thirds of which are though to emanate from within Europe, the rest being carried in by the winds from North America and Asia. Besides the country figures, the tables also include estimates of the natural emissions of sulphur from the seas (production of dimethyl sulphide by phytoplankton). Taking into the consideration the fact that transport of pollutants may vary considerably, on account of the weather and atmospheric currents, the values in the tables represent an average for the period from 1985 to 1995.

Table 1.3: Sulphur budget for Europe. Average for 1985-1995.

See text for descriptions (MSC-W, 1997).

	AL	AT	BE	BG	DK	FI	FR	DE	GR	HU	IS	IE	IT	LU	NL	NO	PL	PT	RO	ES	SE	CH	TR	GB	BY	UA	MD	RU	EE	LV	LT	SI	HR	BA	YU	FYM	CS	SK	REM	BAS	NOS	ATL	NAT	IND	SUM
AL	13	0	0	9	0	0	1	3	9	3	0	0	10	0	0	0	2	0	2	1	0	0	0	1	0	1	0	0	0	0	0	0	1	5	5	3	2	1	10	0	0	0	0	20	34
AT	0	6	1	1	0	0	4	25	0	5	0	0	8	0	0	0	7	0	1	1	0	1	0	3	0	1	0	0	0	0	0	5	1	1	1	0	13	3	1	0	1	0	0	13	150
BE	0	0	27	0	0	0	17	19	0	0	0	0	0	0	4	0	1	0	0	1	0	0	0	15	0	0	0	0	0	0	0	1	0	0	0	0	2	0	0	0	5	1	0	7	72
BG	0	0	0	55	0	0	0	3	1	3	0	0	1	0	0	0	2	0	10	0	0	0	0	0	0	3	2	0	0	0	0	0	0	1	4	1	1	1	1	0	0	0	0	9	225
DK	0	0	0	0	17	1	9	0	1	0	0	0	0	0	0	8	0	1	0	2	0	0	3	2	2	0	21	4	1	1	0	0	0	0	0	3	1	0	1	1	0	1	19	181
FI	0	0	0	0	0	33	12	0	1	0	0	4	0	1	0	2	0	0	0	9	0	0	0	9	0	0	0	0	0	0	0	0	0	0	0	0	2	0	1	0	3	2	1	16	469
FR	0	0	3	0	0	0	33	12	0	1	0	0	4	0	1	0	2	0	0	9	0	0	0	9	0	0	0	0	0	0	0	0	0	0	0	0	9	0	0	0	2	0	0	8	984
DE	0	0	3	0	1	0	5	59	0	1	0	0	1	0	4	0	1	0	0	1	0	0	0	6	0	0	0	0	0	0	0	0	0	0	0	0	2	0	1	0	3	2	1	16	469
GR	1	0	0	30	0	0	1	2	18	2	0	0	3	0	0	0	2	0	4	0	0	0	1	0	0	2	1	0	0	0	0	0	0	2	3	2	1	1	5	0	0	0	0	18	119
HU	0	1	0	1	0	0	1	9	0	41	0	0	3	0	0	0	8	0	5	0	0	0	0	1	0	1	0	0	0	0	0	0	1	1	2	3	0	6	7	1	0	0	0	7	210
IS	0	0	0	0	0	0	1	4	0	0	12	1	0	0	0	0	1	0	0	1	0	0	0	13	0	0	0	1	0	0	0	0	0	0	0	0	1	0	0	0	1	2	15	45	10
IE	0	0	1	0	0	0	2	5	0	0	0	28	0	0	0	0	1	0	0	1	0	0	0	31	0	0	0	0	0	0	0	0	0	0	0	0	1	0	0	0	2	7	4	16	41
IT	0	1	0	1	0	0	4	5	0	2	0	0	40	0	0	0	2	0	1	2	0	1	0	1	0	0	0	0	0	0	0	2	1	2	1	0	2	1	16	0	0	0	0	16	376
LU	0	0	6	0	0	0	30	24	0	0	0	0	1	7	2	0	0	0	0	1	0	0	0	23	0	0	0	0	0	0	0	0	0	0	0	0	2	0	0	0	7	1	0	6	85
NL	0	0	9	0	0	0	7	25	0	0	0	0	0	0	15	0	2	0	0	1	0	0	0	18	0	1	0	7	0	0	0	0	0	0	0	0	3	0	0	0	3	1	2	27	135
NO	0	0	1	0	2	1	2	15	0	1	0	1	0	0	1	4	6	0	0	0	2	0	0	18	0	1	0	7	0	0	0	0	0	0	0	0	3	0	0	0	3	1	2	27	135
PL	0	0	0	0	1	0	1	28	0	2	0	0	0	0	0	43	0	1	0	0	0	0	2	0	1	0	0	0	0	0	0	0	0	0	0	0	0	10	2	0	0	1	0	0	5	1008
PT	0	0	0	0	0	0	1	1	0	2	0	0	0	0	0	0	39	0	28	0	0	0	1	0	0	0	0	0	0	0	0	0	0	0	0	0	0	0	0	0	1	0	0	1	41
RO	0	0	0	8	0	0	0	6	0	9	0	0	1	0	0	0	7	0	34	0	0	0	0	1	1	6	2	1	0	0	0	0	0	0	0	0	0	0	0	0	0	0	13	0	74
ES	0	0	0	0	0	0	3	2	0	0	0	0	1	0	0	0	4	0	67	0	0	0	2	0	0	0	0	0	0	0	0	0	0	0	0	0	0	0	0	0	2	0	0	4	282
SE	0	0	1	0	5	3	2	20	0	1	0	0	0	0	1	11	0	1	0	0	0	0	0	10	1	1	0	5	1	0	1	0	0	0	0	0	4	1	0	1	1	2	1	19	226
CH	0	1	1	0	0	0	15	14	0	1	0	0	23	0	1	0	2	0	0	3	0	0	0	3	0	0	0	0	0	0	0	0	0	0	0	0	4	1	0	1	1	1	0	19	226
TR	0	0	0	13	0	0	0	2	3	2	0	0	0	0	1	1	11	0	1	0	0	0	0	8	0	0	0	17	0	1	7	1	1	1	0	0	0	0	0	0	0	0	0	37	214
GB	0	0	1	0	0	0	2	4	0	0	0	1	0	0	1	0	1	0	0	1	0	0	0	78	0	0	0	0	0	0	0	0	0	0	0	0	3	0	0	0	0	0	0	12	297
BY	0	0	0	1	0	0	1	12	0	3	0	0	1	0	0	21	0	2	0	0	0	0	2	0	20	8	1	4	1	1	0	3	0	0	0	1	0	5	2	0	0	0	0	12	297
UA	0	0	0	3	0	0	0	7	0	4	0	0	1	0	0	0	13	0	4	0	0	0	0	1	2	40	2	4	0	0	0	0	0	0	0	0	3	2	0	0	0	0	0	12	45
MD	0	0	0	8	0	0	0	8	0	4	0	0	1	0	0	0	10	0	13	0	0	0	0	1	1	20	16	2	0	0	0	0	0	0	0	0	1	0	0	0	1	0	0	25	2088
HU	0	0	0	1	0	1	0	4	0	1	0	0	0	0	0	5	0	1	0	0	0	0	1	4	11	0	40	2	0	1	0	0	0	0	0	0	1	0	0	0	1	0	0	14	51
EE	0	0	0	0	1	5	1	12	0	1	0	0	0	0	0	12	0	1	0	2	0	0	3	3	3	0	7	22	2	3	0	0	0	0	0	0	4	1	0	1	1	0	0	14	74
LV	0	0	1	1	1	1	1	16	0	2	0	0	0	0	0	18	0	1	0	1	0	0	4	5	3	0	5	2	7	9	0	0	0	0	0	5	1	0	1	1	1	0	0	11	98
LT	0	0	1	1	1	0	1	16	0	2	0	0	0	0	0	23	0	1	0	1	0	0	3	3	3	0	4	1	1	20	0	0	0	0	0	5	1	0	1	1	1	0	0	11	98
SI	0	2	0	1	0	0	2	9	0	6	0	0	14	0	0	0	5	0	1	1	0	0	0	1	0	1	0	0	0	0	0	33	3	2	1	0	5	2	1	0	0	0	0	11	44
HR	0	1	0	2	0	0	2	9	0	12	0	0	0	0	0	7	0	2	1	0	0	0	1	0	1	0	0	0	0	0	0	3	10	9	4	0	6	3	2	0	0	0	0	13	85
BA	0	0	0	2	0	0	1	6	1	7	0	0	7	0	0	4	0	2	1	0	0	0	1	0	1	0	0	0	0	0	0	1	3	37	5	0	4	2	3	0	0	0	0	12	90
YU	1	0	0	6	0	0	1	6	1	9	0	0	4	0	0	4	0	5	0	0	0	0	1	0	1	0	0	0	0	0	0	1	1	12	25	2	3	2	3	0	0	0	0	12	161
FYM	4	0	0	21	0	0	1	3	8	4	0	0	4	0	0	0	2	0	4	0	0	0	0	0	0	1	0	0	0	0	0	0	1	4	8	10	2	1	4	0	0	0	0	18	28
CS	0	1	1	0	0	0	1	34	0	2	0	0	1	0	0	0	10	0	0	0	0	0	0	0	0	0	0	0	0	0	0	0	0	0	0	0	40	2	0	0	0	0	0	5	338
SK	0	1	0	1	0	0	1	13	0	17	0	0	2	0	0	0	18	0	2	0	0	0	0	1	0	1	0	0	0	0	0	1	1	1	1	0	11	21	0	0	0	0	0	8	138
BAS	0	0	1	0	5	4	2	25	0	1	0	0	1	0	1	0	17	0	1	0	3	0	0	7	1	2	0	4	2	1	2	0	0	0	0	0	5	1	0	3	2	0	1	11	436
NOS	0	0	2	0	1	0	5	13	0	0	0	1	0	0	3	0	3	0	0	1	0	0	0	48	0	0	0	0	0	0	0	0	0	0	0	0	2	0	0	0	7	1	2	9	858
ATL	0	0	1	0	0	0	3	4	0	0	0	2	0	0	1	1	1	0	11	0	0	0	0	15	0	0	0	7	0	0	0	0	0	0	0	0	1	0	0	0	1	11	10	30	1447
MED	0	0	0	6	0	0	4	4	4	2	0	0	15	0	0	0	2	0	2	5	0	0	1	1	0	1	0	0	0	0	0	0	0	1	2	1	0	2	1	20	0	0	0	1	21	1207

Table 1.4: Oxidised nitrogen budget for Europe. Average for 1985-1995.

See text for descriptions (MSC-W, 1997).

	AL	AT	BE	BG	DK	FI	FR	DE	GR	HU	IS	IE	IT	LU	NL	NO	PL	PT	RO	ES	SE	CH	TR	GB	BY	UA	MD	RU	EE	LV	LT	SI	HR	BA	YU	FYM	CS	SK	RES	BAS	NO	ATL	IND	SUM
AL	4	1	0	3	0	0	4	4	11	1	0	0	28	0	0	0	2	0	2	2	0	0	0	1	0	1	0	0	0	0	0	0	1	1	0	0	7	1	0	0	2	1	11	68
AT	0	6	2	0	0	0	10	26	0	1	0	0	14	0	2	0	4	0	1	1	0	3	0	4	0	0	0	0	0	0	0	0	0	0	0	0	1	0	0	0	0	0	0	3	32
BE	1	0	13	0	0	0	18	17	0	0	0	0	1	0	9	0	1	0	0	1	0	0	0	20	0	0	0	0	0	0	0	0	0	0	0	0	2	1	0	0	1	0	16	38
BG	0	1	0	22	0	0	1	7	5	3	0	0	5	0	1	0	5	0	15	0	0	0	1	1	1	5	1	2	0	0	0	0	0	0	0	0	2	0	0	0	1	9	2	8	27
DK	0	0	3	0	10	0	5	18	0	0	0	1	0	0	7	1	4	0	0	0	2	0	0	28	0	0	0	0	0	0	0	0	0	0	0	0	2	0	0	2	3	1	17	7
FI	0	0	1	0	3	16	2	10	0	0	0	0	0	0	2	3	7	0	0	0	9	0	0	7	2	2	0	7	2	1	2	0	0	0	0	0	2	0	0	2	3	1	17	7
FR	0	0	3	0	0	0	33	11	0	0	0	0	5	0	3	0	1	1	0	6	0	1	0	11	0	0	0	0	0	0	0	0	0	0	0	0	5	0	0	0	5	1	7	346
DE	0	1	5	0	1	0	11	39	0	0	0	0	2	0	7	0	3	0	0	1	0	0	1	11	0	0	0	0	0	0	0	0	0	0	1	1	2	1	0	0	0	0	25	28
GR	1	1	0	10	0	0	3	4	21	1	0	0	11	0	1	0	3	0	5	1	0	0	2	1	0	3	0	1	0	0	0	0	1	2	1	1	8	6	0	0	1	0	11	50
HU	0	4	1	1	0	0	4	14	0	12	0	0	11	0	1	0	9	0	5	0	0	1	0	2	0	1	0	0	0	0	0	0	0	0	0	0	0	0	0	0	0	4	6	47	7
IS	0	3	1	0	1	0	3	5	0	0	5	1	0	0	3	1	1	0	0	0	1	0	0	19	0	0	0	0	0	0	0	0	0	0	0	0	1	0	0	0	5	14	20	20
IE	0	0	2	0	0	0	6	6	0	0	0	11	0	0	3	0	1	0	0	1	0	0	0	31	0	0	0	0	0	0	0	0	0	0	0	0	1	0	0	0	2	1	1	14	149
IT	0	1	1	0	0	0	11	7	1	1	0	0	50	0	1	0	2	0	1	2	0	2	0	2	0	2	0	0	0	0	0	0	0	1	0	0	0	0	0	0	4	4	8	3
LU	0	0	8	0	0	0	28	21	0	0	0	0	0	4	4	0	0	0	0	3	0	0	0	11	0	0	0	0	0	0	0	0	0	0	0	0	0	0	0	0	1	0	0	6	38
NL	0	0	7	0	1	0	8	19	0	0	0	0	1	0	16	0	1	0	0	1	0	0	0	27	0	0	0	0	0	0	0	0	0	0	0	0	2	0	0	1	8	3	20	82
NO	0	0	2	0	4	1	3	12	0	0	0	1	0	0	4	9	3	0	0	0	5	0	0	22	0	0	0	1	0	0	0	0	0	0	0	0	9	2	0	1	3	1	8	229
PL	0	1	2	0	2	0	4	25	0	1	0	0	2	0	3	0	24	0	1	0	1	0	0	6	1	1	0	1	0	0	0	0	1	0	0	0	0	0	0	0	1	25	26	21
PT	0	0	0	0	0	0	2	1	0	0	0	0	0	0	0	0	0	23	0	19	0	0	0	2	0	0	0	1	0	0	0	0	0	0	0	0	0	0	0	0	1	0	13	87
RO	0	1	1	5	0	0	2	8	1	5	0	0	5	0	1	0	9	0	23	0	0	0	0	2	1	6	1	2	0	0	0	0	1	1	1	0	0	0	0	0	1	10	19	113
ES	0	0	1	0	0	0	8	3	0	0	0	0	2	0	1	0	6	0	0	45	0	0	0	4	0	0	0	0	0	0	0	0	0	0	0	0	2	0	0	1	5	1	14	126
SE	0	0	2	0	6	4	3	14	0	0	0	0	0	0	4	5	6	0	0	0	12	0	0	13	1	1	0	2	1	1	1	0	0	0	0	0	2	0	0	2	2	2	12	30
CH	0	1	2	0	0	0	24	14	0	0	0	0	20	0	2	0	1	0	0	2	0	11	0	5	0	0	0	0	0	0	0	0	0	0	0	0	2	1	0	0	0	0	41	63
TR	0	0	0	5	0	0	1	4	6	1	0	0	3	0	0	0	3	0	1	0	0	0	0	57	0	0	0	0	0	0	0	0	0	0	0	0	0	0	0	0	0	7	6	9	138
GB	0	0	2	0	1	0	5	6	0	0	0	2	0	0	3	0	1	0	0	1	0	0	0	1	0	0	0	4	9	6	0	5	1	1	3	0	0	0	5	1	0	1	2	12	89
BY	0	1	1	1	2	1	3	14	0	1	0	0	2	0	2	1	18	0	2	0	2	0	0	2	0	0	0	11	0	0	0	0	0	0	0	0	0	0	0	0	0	4	2	20	212
UA	0	1	1	2	1	0	2	9	0	2	0	0	2	0	2	0	14	0	4	0	1	0	0	2	3	23	1	7	0	0	1	0	0	0	0	0	4	2	0	0	1	0	15	10
MD	0	1	1	3	1	0	2	8	1	3	0	0	3	0	1	0	12	0	11	0	1	0	0	2	2	17	4	4	0	0	1	0	0	0	0	0	4	2	0	0	1	0	0	24	668
RU	0	0	0	0	1	3	1	5	0	1	0	0	1	0	1	1	6	0	1	0	2	0	0	2	3	8	0	32	1	1	1	0	0	0	0	0	2	1	1	1	0	0	16	24
EE	0	1	1	0	4	8	2	13	0	1	0	0	1	0	1	2	10	0	0	0	8	0	0	8	2	2	0	5	5	3	3	0	0	0	0	0	3	1	0	2	3	1	13	19
LV	0	1	1	0	4	3	3	14	0	1	0	0	1	0	1	2	10	0	1	0	8	0	0	8	3	2	0	3	2	4	5	0	0	0	0	0	4	1	0	1	3	1	11	33
LT	0	1	1	0	4	1	3	16	0	1	0	0	1	0	1	3	16	0	1	0	4	0	0	7	3	2	0	3	1	2	8	0	0	0	0	0	4	1	0	1	3	1	11	33
SI	0	6	1	0	0	0	6	13	0	2	0	0	32	0	1	0	6	0	2	1	0	1	0	2	0	1	0	0	0	0	0	0	1	4	3	1	0	5	2	0	0	1	0	13	28
RR	0	4	1	1	0	0	8	11	1	4	0	0	28	0	1	0	6	0	2	1	0	1	0	2	0	1	0	0	0	0	0	0	0	1	3	6	2	0	5	2	0	0	1	16	24
BA	0	2	1	1	0	0	5	9	1	4	0	0	27	0	1	0	5	0	1	0	1	0	0	2	0	1	0	0	0	0	0	0	0	2	3	5	2	5	2	0	0	1	0	17	38
YU	1	2	1	4	0	0	3	9	3	5	0	0	17	0	1	0	5	0	6	1	0	1	0	2	0	1	0	0	0	0	0	0	0	1	2	3	5	2	2	0	0	0	0	22	7
FYM	3	1	0	10	0	0	2	5	14	2	0	0	14	0	0	0	3	0	5	0	0	0	1	0	0	0	0	0	0	0	0	0	0	0	0	0	0	20	1	0	0	2	1	8	73
CS	0	2	2	0	1	0	7	32	0	1	0	0	3	0	3	0	8	0	1	0	0	0	0	3	0	1	0	0	0	0	0	0	0	1	1	0	0	12	9	0	0	1	0	9	34
SK	0	4	1	1	1	0	4	17	0	7	0	0	6	0	2	0	16	0	2	0	0	0	1	3	0	1	0	0	2	1	1	1	0	0	0	0	3	1	0	2	5	1	10	167
BAS	0	0	2	0	6	3	4	19	0	0	0	0	1	0	4	2	9	0	0	0	8	0	0	12	1	1	0	2	1	1	1	0	0	0	0	0	3	1	0	2	5	1	10	318
NOS	0	0	3	0	2	0	7	12	0	0	0	1	0	0	6	1	2	0	0	1	1	0	0	39	0	0	0	0	0	0	0	0	0	0	0	0	1	0	0	0	4	15	38	668
ATL	0	1	1	0	1	1	5	5	0	0	0	1	0	0	2	1	1	0	3	1	0	0	0	17	0	0	0	1	0	0	0	0	0	0	0	0	1	0	0	0	1	1	24	335
MED	0	1	1	2	0	0	11	6	4	1	0	0	28	0	1	0	2	0	1	7	0	1	1	2	0	1	0	0	0	0	0	0	0	1	1	0

1.4 Radioactive Tracers

The radioactive tracers used in the atmospheric studies may be divided into three groups:

- natural radionuclides from emissions out of the Earth's surface;
- natural radionuclides produced by cosmic radiation; and
- artificial radionuclides introduced by nuclear weapons tests or nuclear installations accidents.

The first experiments with radioactive tracers were conducted in 1913 by de Hevesy and Paneth (cited in Choppin et al., 1995) who determined the solubility of lead salts by using the naturally occurring radioactive isotopes of lead. However, the radioactive tracer technique did not come into common use until after World War II when relatively large amounts of radionuclides became available through the use of nuclear reactors. The world-wide fallout of fission products from bomb tests in the mid-1950's, had an important role in drawing particular attention to radioactive aerosols. In the same decade, a considerable amount of fission products were released as a consequence of the Windscale reactor accident in 1957, which were tracked over much of Europe. The event repeated on a much larger scale after the Chernobyl accident in 1986.

The fission products presented to the atmosphere, as well as the airborne natural radionuclides such as radon and its progeny, and cosmogenic ^{7}Be have been widely applied in atmospheric research in the last decades (e.g. Rama, 1963; Bhandari et al., 1970; Poet et al., 1972; Dibb et al., 1992; Graustein & Turekian, 1996). These radionuclides are associated with nonradioactive aerosols and hence can serve to trace the fluxes of aerosols to terrestrial surfaces. The natural radionuclide ^{210}Pb and the fission product ^{137}Cs have been shown (Moore et al., 1973; Graustein & Turekian, 1986) to be particularly useful in acidic deposition studies because they become attached mainly to submicron-sized aerosols which contain the bulk of the pollutant sulphur and nitrogen.

Among the advantages of using radiotracers, the following can be listed (Chamberlain, 1991; Choppin et al., 1995):

- radiotracers are easy to detect and measure with high precision using very sensitive methods;
- the radioactivity is independent of pressure, temperature, chemical and physical state; and

- nondestrutive methods are available which allow measurements on the same sample for numerous radionuclides and /or repeated measurements.

1.4.1 Lead 210 in the Environment

Lead 210 is an intermediate product in a naturally occurring decay chain that starts with uranium 238 and ends with a stable isotope of lead. Figure 1.25 diagrams this radioactive series. The physical half-life of ^{210}Pb is 22.3 years and it decays to ^{210}Bi by beta emission [*Principle Modes of Decay (keV):* β 15 (81%), 61 (19%); γ 46.5 (3.86%); Bi X-rays ¬ 13 av. (23.35%), Eisenbud (1987)]. The major source of ^{210}Pb is in the troposphere, where ^{222}Rn emanates from the Earth's crust as a result of the following series of events. Radium 226 in the soil (a breakdown product of ^{238}U found in minute quantities in most soils) decays to the rare gas ^{222}Rn (half-life of 3.8 days). Since radon is an inert gas, it does not react with the soil, which merely serves as a channel through which the gas moves. Radon 222 may escape to the atmosphere, where it decays via a series of relatively short-lived intermediates to ^{210}Pb. Molecular diffusion is considered to be the main mechanism to explain the Rn flux to the atmosphere, though other mechanisms (e.g. atmospheric pumping) have also been proposed (Clement & Wilkening, 1974). As radon is quite soluble in water, Pearson & Jones (1965) suggest that the transpiration by vegetation should also be considered as another pathway. The estimated ^{222}Rn flux from land ranges from 7000 to 12000 atoms m^{-2} s^{-1} (Junge, 1963; Wilkening et al., 1975; Turekian et al., 1977; Eakins et al., 1984).

Unlike the noble gas Rn, ^{210}Pb (and all of the intermediate daughters) is metallic, electrically charged when formed, and reacts rapidly with trace gases and vapours forming clusters or attaches to existing aerosol surfaces within 1-100 s (Eisenbud, 1987; Turekian et al., 1977; Porstendorfer, 1994). The attachment rate is a function of particle size. The reported diameter of ^{210}Pb containing aerosols ranges from 0.1 to 1.2 μm (Junge, 1963; Knuth et al., 1983; Graustein & Turekian, 1996).

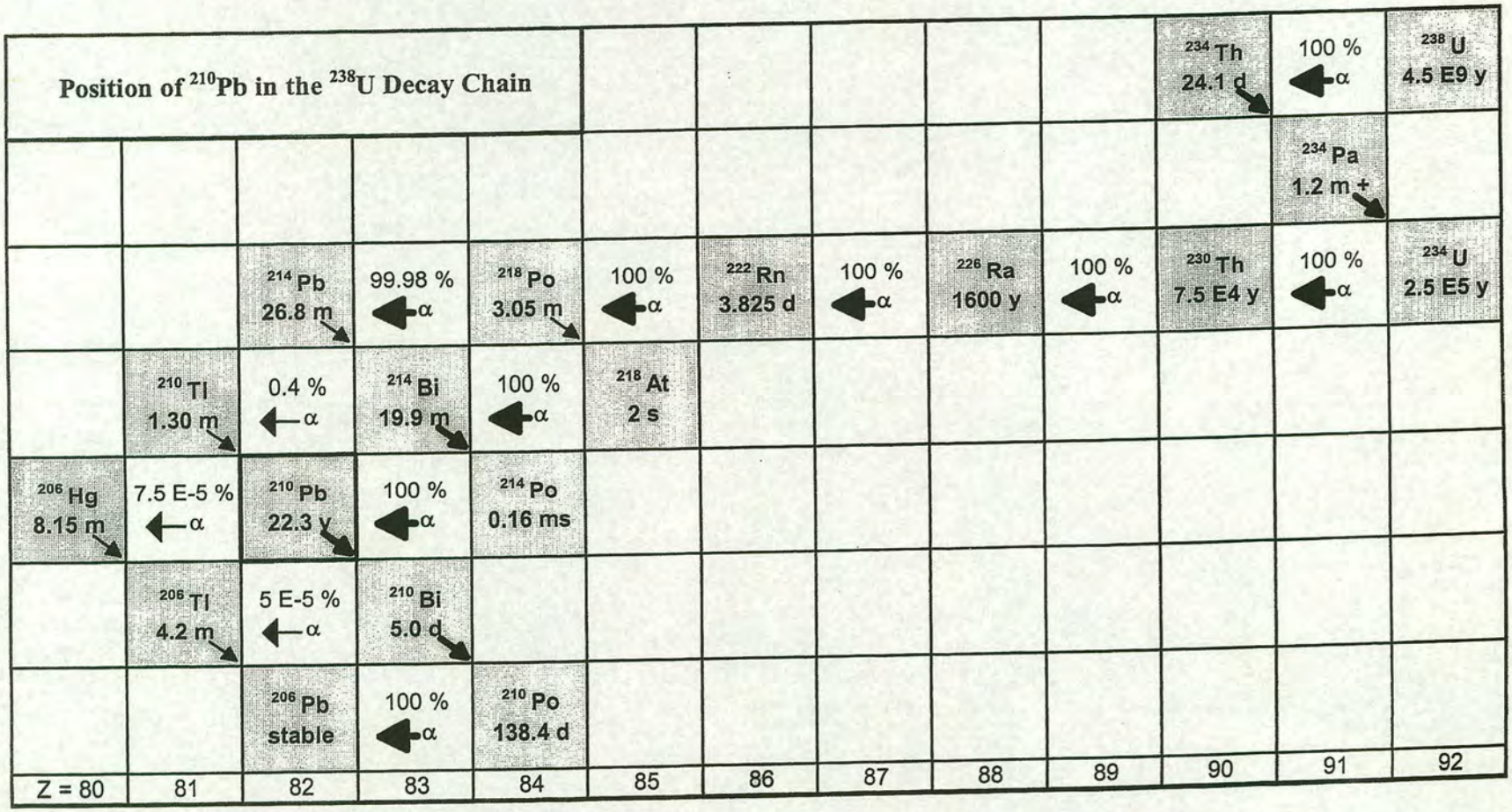

Fig. 1.25: The ^{238}U natural radioactive decay chain. Arrows to the left indicate α-decay with the intensity in percent per decay of the emitting nuclide, arrows down-right indicate β-decay. The half-life of the nuclides is given below their symbols. Thick arrows show the main decay path (adapted from Friedmann, 1977).

Most atmospheric ^{210}Pb (~ 90%), however, is concentrated on submicron aerosols in the diameter range of 0.1-1.0 μm with a modal value of ~ 0.2 μm (Robins, 1978).

The production of ^{210}Pb from the oceans is small compared to that produced from the land, since ^{226}Ra concentration in seawater is much less than that in the Earth's crust (Nijampurkar & Clausen, 1990). The contribution of other possible sources, both natural and artificial, to the ^{210}Pb content of the atmosphere are either small or insignificant (Peirson et al., 1966; Jaworowski, 1969; Turekian et al., 1977; Nijampukar & Clausen, 1990). Table 1.5 presents various natural and artificial sources of ^{210}Pb in the atmosphere.

Table 1.5: Sources of ^{210}Pb in the atmosphere (adapted from Nijampurkar & Clausen, 1990)

Source	Amount (T Bq y^{-1})
^{222}Rn exhalation from lands	25530
^{222}Rn exhalation from oceans	925
tetraethyl lead	85
radium-rich phosphate fertilisers	4-22
burned coal	0.015
volcanoes	insignificant
atmospheric thermonuclear bomb tests	insignificant

The measured concentration of ^{210}Pb in ground level air ranges from 0.23 to 0.5 mBq m^{-3} in Europe (Peirson et al., 1966; Kavranen & Meittinen, 1974), 0.5-1.0 mBq m^{-3} in eastern USA (Graustein & Turekian, 1986), 0.033-0.27 mBq m^{-3} in the Pacific Ocean (Graustein & Turekian, 1996), and 0.16 mBq m^{-3} in Australia (Bonnyman et al., 1972). These measured values satisfy the expectation of greater concentrations in the continental climate relative to the oceanic, and reduced concentrations in the southern hemisphere due to the smaller land area. Peirson et al. (1966) found an increase in ^{210}Pb concentration with height in the atmosphere of the UK from 0.21 mBq kg^{-1} of air at ground level to 0.26 mBq kg^{-1} at 7.6 km and 0.36 mBq kg^{-1} in the stratosphere. Moore et al. (1973) found a different profile in the US, where the concentration decreasing with height to 0.04 mBq kg^{-1} at the tropopause

but increasing again to 0.28 mBq kg^{-1} in the stratosphere. The different profile over the UK is suggested to be due to the depletion of the lower part by deposition during passage of air over the Atlantic (Chamberlain, 1991).

Considering the relatively long half-life of ^{210}Pb, it is principally removed from the atmosphere not by radioactive decay but by the deposition of its carrier aerosols. The mean residence time of these aerosols in the troposphere is a few days to a few weeks depending on altitude and regional climatology (Peirson et al., 1966; Moore et al., 1973; Fukuda & Tsunogai, 1975; Graustein & Turekian, 1986 & 1996). Wet deposition is the predominant mechanism of ^{210}Pb removal from the atmosphere. The contribution of dry deposition is considered to be less than 10% to lowlands, and is expected to increase with altitude due to the greater mean wind speeds at higher elevations (Knuth et al., 1983; Graustein & Turekian, 1986; Todd et al, 1989). Cloud droplet interception in coastal areas and high altitudes, where ground-level cloud is common, can lead to a significant contribution to the total ^{210}Pb scavenging from the atmosphere (Graustein & Turekian, 1989).

The mean concentration of ^{210}Pb in rain, measured at several locations in the UK, ranges from 62 to 84 mBq l^{-1} (Burton & Stewart, 1960; Peirson et al., 1966; Eakins & Morrison, 1976; Eakins et al., 1984; Clifton, 1991). Larger concentration values of 133 mBq l^{-1} and 222-300 mBq l^{-1} have been observed by Knuth et al. (1983) in the USA, and Fukuda & Tsunogai (1975) in Japan, respectively.

Following deposition to terrestrial surfaces, ^{210}Pb becomes readily attached to organic matter in soils, primarily in the surface layer, and is not readily leached (Fisenne, 1968; Lewis, 1977; Graustein & Turekian, 1982). It is considered that the organic matter in soil is almost 100% efficient at scavenging and retaining of ^{210}Pb, and soil erosion is the only significant removal process (Lewis, 1977). The mean residence time of ^{210}Pb in organic soils is estimated to be in the order of 2000-5000 years (Benninger et al., 1975; Lewis, 1977) which is much longer than its physical half-life of 22.3 years.

In a study of ^{210}Pb mobility in peat, Urban et al. (1990) found some evidence that ^{210}Pb is mobilised by the organic-rich waters of peatlands in north-east USA where inventories of ^{210}Pb were found depleted in peatland hollows relative to

hummocks. Pulford et al. (1995) in their study of ^{210}Pb and ^{137}Cs mobility in Scottish peatlands, however, found that the inventories for ^{210}Pb suggested little, if any, downslope movement at a hillside. They also used IR spectroscopy to identify the type of bonding mechanisms holding Cs and Pb on humic substances, which showed that Cs is held as a simple metal-humate salt by ionic bonding, whereas Pb is held by more complex bonding, possibly involving the formation of conjugated ketonic structures. The difference in bond strength is also shown by the difference in stability constants for complexes of Cs and Pb with humic acid, measured by the potentiometric titration method. According to their measurements at about pH5, Cs complexes had a logK of 1.43, whereas Pb complexes had a logK of 6.53. On the basis of these evidences as well as field measurements, they conclude a relatively very low mobility of ^{210}Pb in organic soils. Wild (1993) suggests that the low mobility of ^{210}Pb in soil is due to adsorption on the surfaces of iron and manganese oxides and clay aluminosilicates. He also states that lead reacts with organic matter to form a complex of low solubility. Experiments by Godt et al. (1986) have revealed that plant uptake and thereby leaching (elemental turnover by internal fluxes in a canopy of tree stands) of Pb is negligible. The concentration of lead in soil solutions is also found to be low. These findings support the use of atmospheric ^{210}Pb soil inventories in the study of aerosol deposition onto forests where soils beneath the canopies are usually very organic.

1.4.2 Caesium 137 in the Environment

Caesium 137 is an artificial radionuclide, a product of nuclear fission reaction with a half-life of 30.2 years which decays to ^{137}Ba by beta emission [*Principle Modes of Decay (keV):* β 510 (94%), 1180 (6%); γ 661 (85%), Eisenbud (1987)]. The atmospheric ^{137}Cs is derived from two principle sources:

- atmospheric testing of nuclear weapons; and
- nuclear reactor/plant accidents.

Weapons tests in the northern hemisphere commenced around 1954, peaked in 1963 and the corresponding fallout fell to insignificant levels by 1986 (Smith et al, 1997). Two major nuclear accidents released significant quantities of ^{137}Cs into the atmosphere in 1957: Windscale reactor melt-down in the UK, and a chemical explosion in a Soviet plant treating active wastes, situated in the Urals (Chamberlain, 1991). On 26 April 1986, however, a massive release of ^{137}Cs and other radionuclides occurred as a result of the reactor melt-down accident at Chernobyl in the Ukraine. Winds initially carried the greater part of the radioactive cloud towards the north-west. When, three days after the disaster, the cloud drifted in over Sweden, a considerable part of its contents deposited onto the ground by precipitation. Around Gavle, over 1300 km away from Chernobyl, the fallout was larger than Kiev, which lies hardly 100 km from the reactor (Bernes, 1992). Figure 1.26 shows the pattern of ^{137}Cs deposition in Scandinavia.

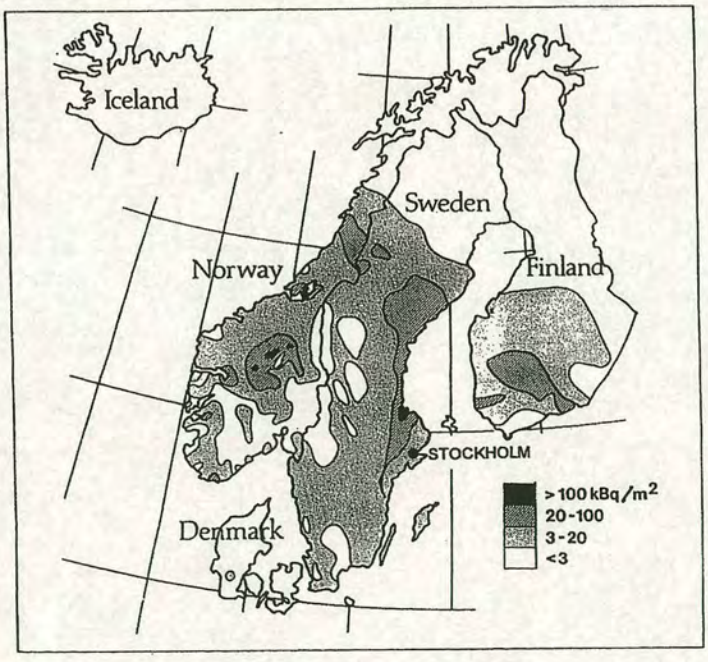

Fig. 1.26: Deposition of ^{137}Cs in Scandinavia from the Chernobyl accident (Choppin et al., 1995).

The atmospheric plume of radioactivity reached the UK on 2 May 1986. Parts of the UK received a total radionuclide deposition of more than 200 kBq m^{-2}, with levels of ^{137}Cs being particularly high (Cambray et al., 1987; Clark & Smith, 1988).

The deposition pattern of Chernobyl ^{137}Cs over the UK is illustrated in Figure 4.4 in section 4.1.2. Note the patchy nature of deposition in both Figures 1.26 & 4.4. See also Table 1.6 which summarises the extent of ^{137}Cs releases in weapons tests and nuclear accidents.

Table 1.6: Release of ^{137}Cs in weapons tests and nuclear accidents (Chamberlain, 1991).

Source	^{137}Cs (T Bq)
Nevada atmospheric tests (total yield 1 MT)	6×10^3
All H-tests (200 MT)	1×10^6
Windscale accident	80
Chemical explosion in the Urals	30
Chernobyl accident	4×10^4

The ^{137}Cs from nuclear accidents and a fraction of ^{137}Cs from weapons tests were dispersed in the troposphere and became associated with the ambient tropospheric aerosols in the size range of 0.3-1.0 μm. These carrier aerosols were subject to the same scavenging processes as other atmospheric aerosols and deposited on a timescale of days (Cambray et al., 1987). Most of weapons tests ^{137}Cs (particularly in the case of high altitude and high yield H-bombs) were injected into the stratosphere, and subsequently deposited world-wide over a period of many months (Eisenbud, 1987). In return to troposphere, this fraction of ^{137}Cs also attaches to the same size (0.3-1.0 μm) tropospheric aerosols (Lockhart et al., 1965). Therefore, like ^{210}Pb, ^{137}Cs is carried by sub-micrometer aerosols and delivered to the Earth's surfaces (Volchok, 1980). The different sources of these isotopes lead to differing vertical distributions in the atmosphere. Caesium 137 concentration in air does not change systematically with altitude (Graustein & Turekian, 1989).

When scavenged from the atmosphere, caesium ions (Cs^+) are adsorbed by soils. They displace more hydrated ions, e.g. Na^+, Ca^{2+}, Mg^{2+}, from the interlayer spaces of clay minerals like smectits and illite, the layers collapse and trap the caesium ions in cavities. The adsorption of small amounts of Cs^+ by these clay minerals and especially by illite is difficult to reverse (Cremers et al., 1988). This is

actually the behaviour of Cs in fertile soils, intensively used for agriculture, with relative abundance of clay and mica minerals, particularly illite. However, the mechanisms controlling Cs availability in soil-plant systems typical of upland areas of Northern Europe are not well known (Frederiksson et al., 1966). These ecosystems characteristically comprise bog, heathland, or coniferous forest, with highly organic soils. In many of these soils, clays are scarce and their behaviour may be modified by extensive interaction with organic matter (Livens et al., 1991). Based on their field measurements, Livens et al. (1991) claim that in the condition encountered in these soils , extensive sorption to clays does not occur. They suggest this may be due to recycling of radiocesium in the uppermost organic horizons, which prevents it reaching the clay-rich, deeper horizons, or it could be due to the prevention of Cs-clay interaction by organic matter. In other words, the organics can either take up radiocesium in competition with the minerals or they may react with the minerals and block the Cs uptake sites. In a study of ^{137}Cs and ^{210}Pb mobility in Scottish peatlands, Pulford et al. (1995) found evidences that suggest Cs is much more mobile than Pb in organic soils. Their field experiments revealed vertical movement of ^{137}Cs down the cores as well as considerable lateral movement downhill in the water flow. Using potentiometric titration method, they also found a very low stability constant for complexes of Cs with humic acid (see previous section). Being analogue to potassium, caesium is highly 'bioactive' and is readily taken up by components of the soil biota, particularly if they are limited by these nutrients. Uptake will tend to be greater in peaty rather than mineral soils. Uptake will also tend to decrease as the clay content of the soil increases, as the capacity for clay fixation of radionuclide increases (Killham, 1994).

The mean fallout per unit area in the northern hemisphere is estimated to be 1429 Bq m^{-2} (decay corrected to 1993 from the value for 1986; Smith et al., 1997). This value is considerably smaller than the mean UK inventory of 2740 Bq m^{-2} per 1000 mm y^{-1} rainfall, to 30 cm depth (decay corrected to 1993 from the value for 1980; Bonnet & Camberly, 1991). None of these values include the contribution of ^{137}Cs from Chernobyl accident. The larger value of the UK mean inventory may be attributed to the contribution of very high deposition values for high rainfall areas of

the western England, Wales and north-west Scotland. Indeed, a significant correlation has been found between total ^{137}Cs deposition in soils and mean annual precipitation (Peirson & Salmon, 1959; Cawse & Horril, 1986; Cawse et al., 1988; Bunzl & Kracke, 1988).

1.4.3 The Tracer Technique

The ambient-borne ^{210}Pb isotope has been widely applied in environmental research, more commonly for dating purposes of lake sediments (Krishnaswamy et al., 1971; Koide et al., 1972; Robins, 1978; Joshi & Mudroch, 1988).

The ^{210}Pb ions produced by the decay of ^{222}Rn are quickly scavenged by submicron-sized aerosols which contain the bulk of the pollutant sulphur and nitrogen. They become instantaneously and irreversibly bound to these aerosol particles (Robins, 1978). The ^{210}Pb 'tags' the aerosols and can therefore be used as a tracer for atmospheric processes, in general, and deposition of acidic pollutants, in particular. The half-life of ^{210}Pb is 22.3 years, far longer than the residence time of tropospheric aerosols, so scavenging of the carrier aerosols is the primary mechanism of removal of ^{210}Pb from the atmosphere. When scavenged from the atmosphere along with carrier aerosols, ^{210}Pb is retained by surface horizons of soil (Lewis, 1977) as a unique long-term collector. The residence time of ^{210}Pb in soils is far longer than its half-life (Benninger et al., 1975), so in soils that are not physically disturbed for at least several decades, the inventory of ^{210}Pb is at steady state, with its decay rate equalling the mean deposition rate. However, an important correction has to be made to the inventory to compensate for any ^{210}Pb which is produced by the *in situ* decay of ^{222}Ra. This fraction, termed the *supported* fraction may be calculated by measuring the parent ^{214}Pb activity in soil.

While the absolute value for the ^{210}Pb inventory is influenced by larger-scale processes, and by the sources of air scavenged by precipitation (continental air is richer in ^{210}Pb than oceanic air), however, at a local scale, and to some extent over small regions, the long-term average ^{210}Pb concentration in the atmosphere may be

considered reasonably constant (Nijampurkar & Clausen, 1990). Thus, variability in the soil inventory of ^{210}Pb provides a direct measure of the local variability in deposition of aerosols (by wet, dry and cloud deposition). The method is not applicable for the dry deposition of gases.

When a steady state between atmospheric supply and radioactive decay exists, the flux of ^{210}Pb from the atmosphere (F_{pb}) may be obtained as the product of the decay constant (λ) for ^{210}Pb and the inventory of unsupported (atmospheric) ^{210}Pb in the soil profile (I):

F_{pb}	=	λ	x	I
Bq m^{-2} y^{-1}		y^{-1}		Bq m^{-2}

Measurement of deposition fluxes of ^{210}Pb through studies of soils have been developed by Benninger et al. (1975), Moore et al. (1976), Volchok (1980), and Graustein & Turekian (1986). More recently, the technique has been applied to quantify the wet deposition of pollutants in areas of complex topography (Mourne, 1993; Fowler et al., 1995a; Branford et al., 1998).

The mean atmospheric ^{210}Pb flux for the UK is estimated as 77±14 Bq m^{-2} y^{-1} per meter of rainfall by Smith et al. (1977) based on several UK measurements. The corresponding measured fluxes for south-west and central Sweden are 93 and 100 Bq m^{-2} y^{-1}, respectively (Al-Doushy, 1986).

Chapter 2

Experimental Methods & Techniques

The method is based on the spacial variability of atmospherically derived radionuclides in undisturbed soils. When scavenged from the atmosphere along with carrier aerosols, ^{210}Pb is retained by surface horizons of soil as a unique long-term collector (Lewis, 1977). In the course of this study, the inventories of this radionuclide has been used to investigate the effects of aerodynamic roughness of the surface (see section 1.3.3) on the deposition of atmospheric aerosols as particles and droplets (see also section 1.4.3). The direct γ-spectrometry technique applied in this study (section 2.2) allows measurements on the same sumple for other radionuclides. Measurements were also made of ^{137}Cs and ^{214}Pb inventories for all collected samples in order to verify the value of the former as a confirmatory tracer, and to use the activities of the latter to make corrections for the *supported* ^{210}Pb due to the in situ decay of ^{222}Rn.

Soil samples were collected from inside coniferous forest stands as well as the adjacent open fields in four different regions of the United Kingdom and Sweden. The preparation of all the samples were carried out at the Scottish Agricultural College (SAC). They have been subsequently analysed, at Edinburgh University, for their radionuclide content (^{210}Pb, ^{214}Pb and ^{137}Cs) by gamma-ray spectrometry.

This chapter describes the details of the sampling programme including sampling sites and sampling procedures together with a description of the gamma-ray analysis techniques for measuring the radionuclides present in a sample.

2.1 The Sampling Programme

The feasibility of using ^{210}Pb as a tracer for investigating surface roughness effects on aerosol deposition was first put in a test at Dunslair Heights, a site in the Southern Uplands of southeast Scotland. Continuous meteorological observations as part of the DoE Air Quality Research programme (RGAR, 1997), and previous studies at the site (e.g. Crossley et al., 1988; Gallagher et al., 1992) provided means for a comparative study. The findings at Dunslair Heights were then confirmed in a more suitable site, an isolated rectangular plantation quite close to treeline in Scotland and frequently exposed to orographic cloud on Dun Coillich, in the Highlands of Scotland. The technique was subsequently applied to 10 sites located from Kattegatt seashore to 60 km inland, in south-west Sweden to investigate the mechanisms which cause the increase in deposition along the tnansect from the coastal region to Swedish southern uplands described in section 2.1.1.2. Four sites on the two adjacent mountains, Gammalsaters and Skaftasen, from the Transtrands range in central Sweden were the last sites sampled in this study. The mountains are screened from the west by the high elevation mountains of Norway and could be considered as more continental in nature. The geographic distribution and brief descriptions of the mentioned sites are illustrated in Figure 2.1.

Care was taken in the selection of suitable sites. Coniferous forest stands were selected for their higher efficiency in capturing aerosols. The sampling sites were chosen to conform to the following criteria:

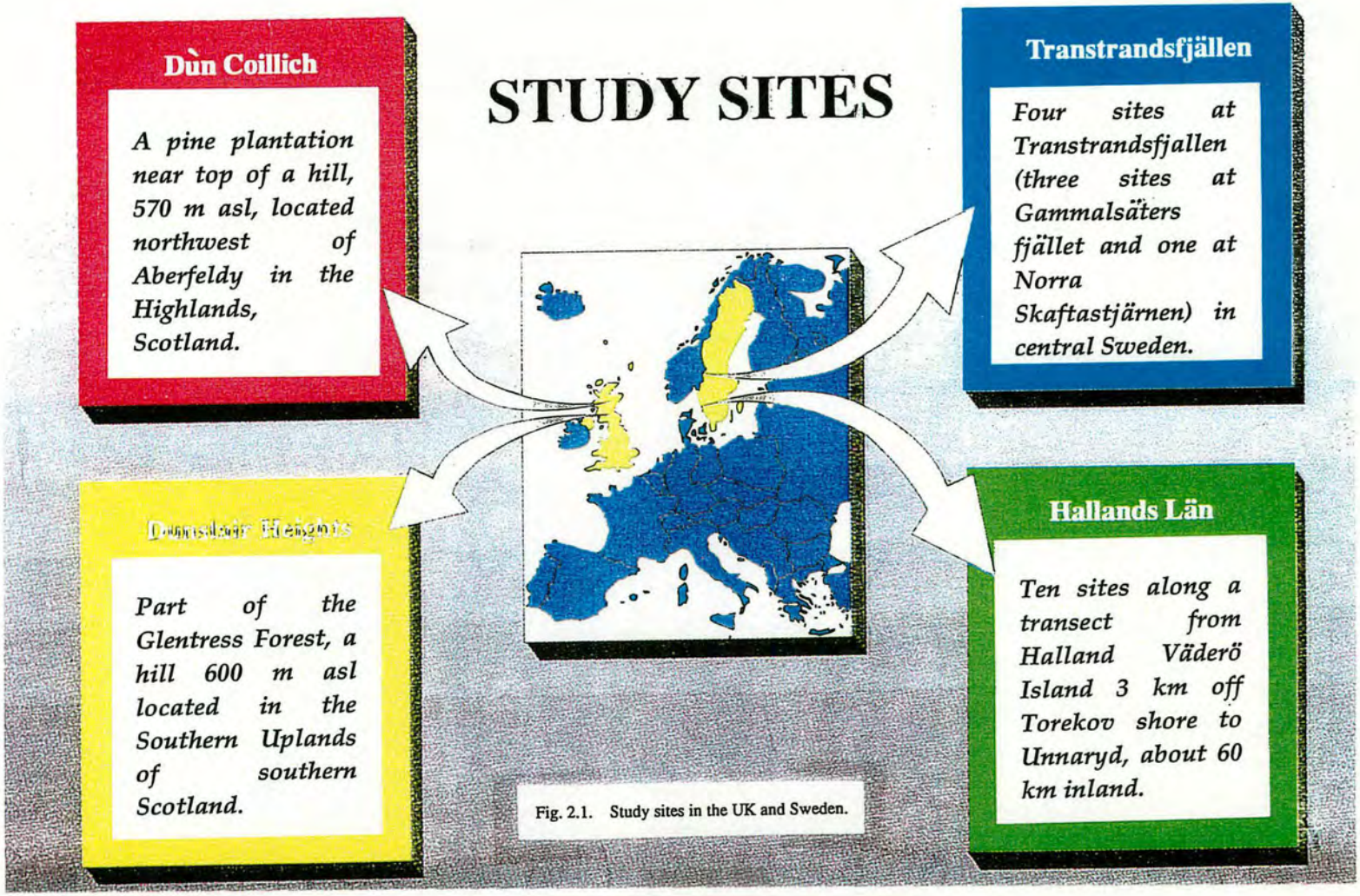

Fig. 2.1. Study sites in the UK and Sweden.

I. Sites were situated on land that had remained without major natural or man-made disturbances for about a century or at least several decades, to ensure that soil is in steady state with respect to the input of ^{210}Pb;

II. In each individual site, sampling was possible inside the canopy as well as in a suitable adjacent open field;

III. The sampling sites were on level ground (preferably), or sloping ground not subject to intensive erosion or movement of surface water. Land with any history or liklihood of flooding or heavy sedimentation was avoided.

Overall, 159 individual locations at the following mentioned 16 sites were sampled, from which a total of 531 samples of soil and vegetation were analysed. Brief details of the site characteristics are given in Table 2.1.

2.1.1 Sampling sites

2.1.1.1 Scottish sites

Two Scottish sites, Dunslair Heights and Dun Coillich, are situated in the Southern Uplands and Southern Highlands which are defined as the hill country to south and north of Scotland's lowland waist (see Figures 2.2 &2.3 and Table 2.1).

The Southern Uplands are a hill range lying across the country with well-defined boundaries: to the east and west, the sea; to the south, the Cheviot Hills along the English Border; and to the north, the Southern Uplands Boundary Fault (Figure 2.4). For most part the hills lift boldly above the Lowland fields or moorland in seven principal hill-groups with the five tops rising above 800 meters. Dunslair Heights is part of the Moorfoots of Midlothian group which stretch from Peebles to the upper reach of Gala Water with six tops rising above 610 meters in the southern half. Their south boundary is the Tweed and the Gala Water, and their north the Uplands'

Table 2.1 Site characteristics

Region	Site	Altitude (m asl)	Latitude	Longitude
South-east Scotland	Dunslair Heights	450	55o 41' N	03o 08' W
Highlands Scotland	Dun Coillich	420	56o 39' N	04o 01' W
Southwest Sweden	Hallands Vadero island	10	56o 26' N	12o 34' E
	Haverdals naturreservat	5-10	56o 42' N	12o 42' E
	Bjorketrop (Haverdal)	20	56o 44' N	12o 41' E
	Harplinge	50-80	56o 45' N	12o 44' E
	Kvibille	100	56o 47' N	12o 51' E
	Ovraboke	160	56o 55' N	12o 55' E
	Stammilt	180	56o 55' N	12o 57' E
	Normanstorp	125-130	57o 06' N	12o 46' E
	Broda	130	56o 44' N	13o 10' E
	Hasslehult	160	57o 01' N	13o 31' E
	Hassleberg	160	57o 00' N	13o 31' E
Central Sweden	Gammalsaters fjallet	530-870	61o 05' N	13o 11' E
	Skaftasen fjallet	620	61o 04' N	13o 16' E

Boundary Fault (Figures 2.4 and 2.5). These are hills with simple convex strong and steep slopes (Bown and Shipley, 1982; Murray, 1993).

The Southern Highlands region is bounded by the Highland Boundary Fault in the south to Loch Rannoch, Rannoch Moor and Loch Tummel in the north. Its west boundary is the Atlantic; Its east, the road from Perth to Pitlochry. Southern Highland are divided by the sea and the glens into fourteen distinct mountain groups. The Lyon group has seven Munros (separate mountains, named after H.T. Munro) with at least two dozen tops above 600 meters. Six of these tops are above 914 meters, all to the north of Glen Lyon and south of Loch Rannoch, the highest Schihallion, 1083 meters. These are mainly rugged hills with strong and steep slopes and very rocky (Walker et al., 1982; Murray, 1993). Dun Coillich, 569 m asl, is situated just to the south-east of Schihallion over looking Keltney Burn (Figures 2.6 & 2.7).

Fig. 2.2: Map of Scotland showing the position of different regions.

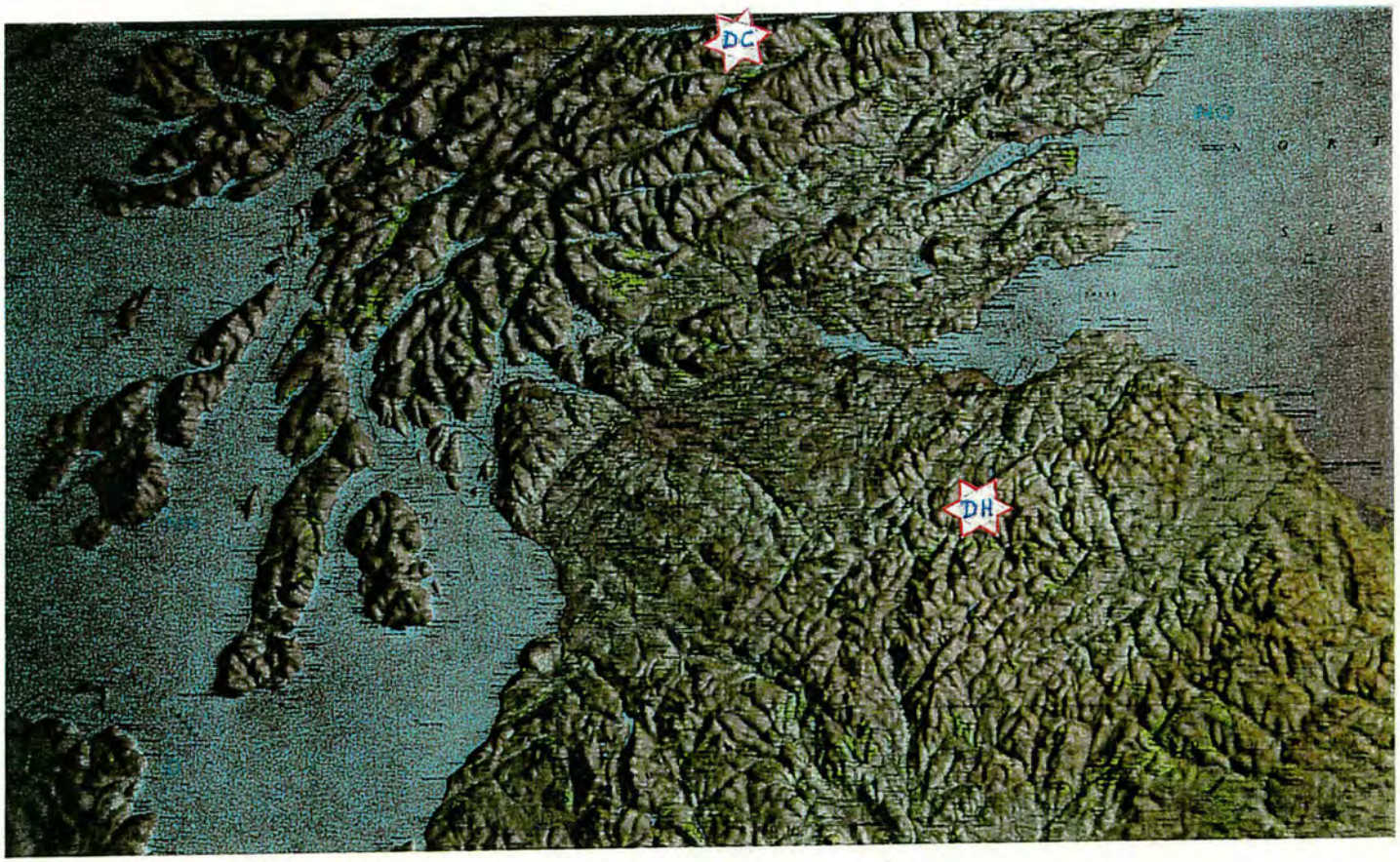

Fig. 2.3: Position of sampling sites (shown by white stars) in the hill country to south and north of Scotland's lowland waist.

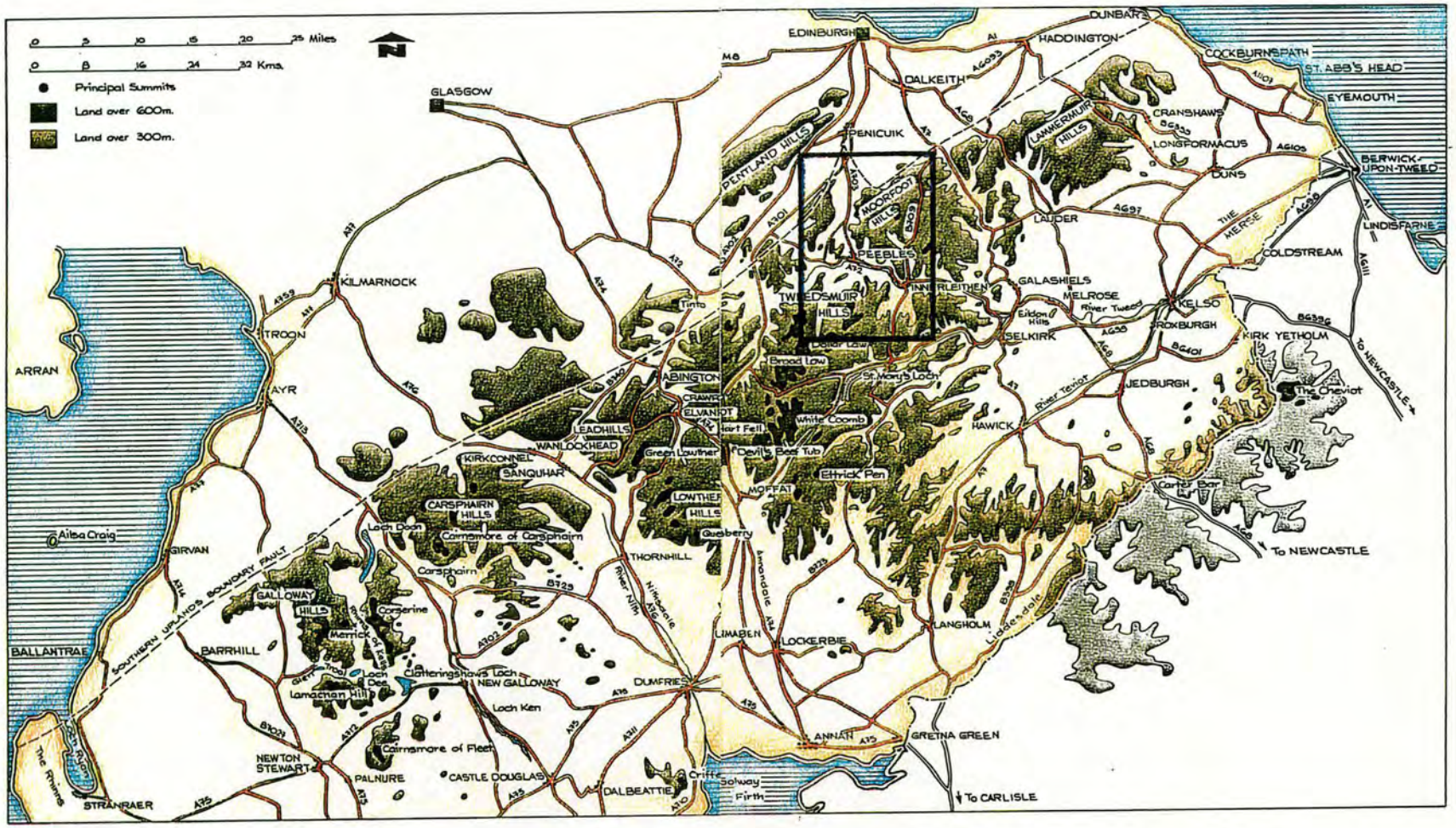
0 5 10 15 20 25 Miles
0 8 16 24 32 Kms.
Principal Summits
Land over 600m.
Land over 300m.
EDINBURGH
GLASGOW
DUNBAR
HADDINGTON
COCKBURNSPATH
ST. ABB'S HEAD
EYEMOUTH
BERWICK-UPON-TWEED
LINDISFARNE
DALKEITH
PENICUIK
PENTLAND HILLS
LAMMERMUIR HILLS
CRANSHAWS
LONGFORMACUS
DUNS
MOORFOOT HILLS
PEEBLES
LAUDER
COLDSTREAM
GALASHIELS
MELROSE
KELSO
ROXBURGH
KIRK YETHOLM
The Cheviot
TWEEDSMUIR HILLS
INNERLEITHEN
SELKIRK
Eildon Hills
River Tweed
Broad Law
Dollar Law
St. Mary's Loch
JEDBURGH
River Teviot
HAWICK
White Coomb
Hart Fell
Devil's Beef Tub
Ettrick Pen
Carter Bar
To NEWCASTLE
KILMARNOCK
TROON
AYR
ARRAN
Tinto
ABINGTON
CRAWFORD
ELVANFOOT
LEADHILLS
WANLOCKHEAD
Green Lowther
KIRKCONNEL
SANQUHAR
CARSPHAIRN HILLS
Loch Doon
Commore of Carsphairn
Carsphairn
Queensberry
LOWTHER HILLS
MOFFAT
THORNHILL
River Nith
Nithsdale
Ailsa Craig
GIRVAN
SOUTHERN UPLANDS BOUNDARY FAULT
GALLOWAY HILLS
Corserine
Merrick
Rhinns of Kells
BALLANTRAE
BARRHILL
Glen Trool
Loch Dee
Clatteringshaws Loch
NEW GALLOWAY
Lamachan Hill
Loch Ken
DUMFRIES
LIMEKILNS
LOCKERBIE
Ae Forest
Ettrick
Yarrow
Ettrick Water
Lauderdale
LANGHOLM
Ewes Water
Esk
Liddesdale
Ale Water
Jed Water
Teviot
Kale Water
Bowmont Water
Glen
Kale
Till
Tweed
Whitadder Water
Eye Water
Leet Water
Dye Water
Blackadder Water
Dunse Burn
Whiteadder Water
Eye
Leet
Dye
Blackadder
Dunse
Whiteadder
Ale
Jed
Kale
Bowmont
Till
Tweed
Whitadder

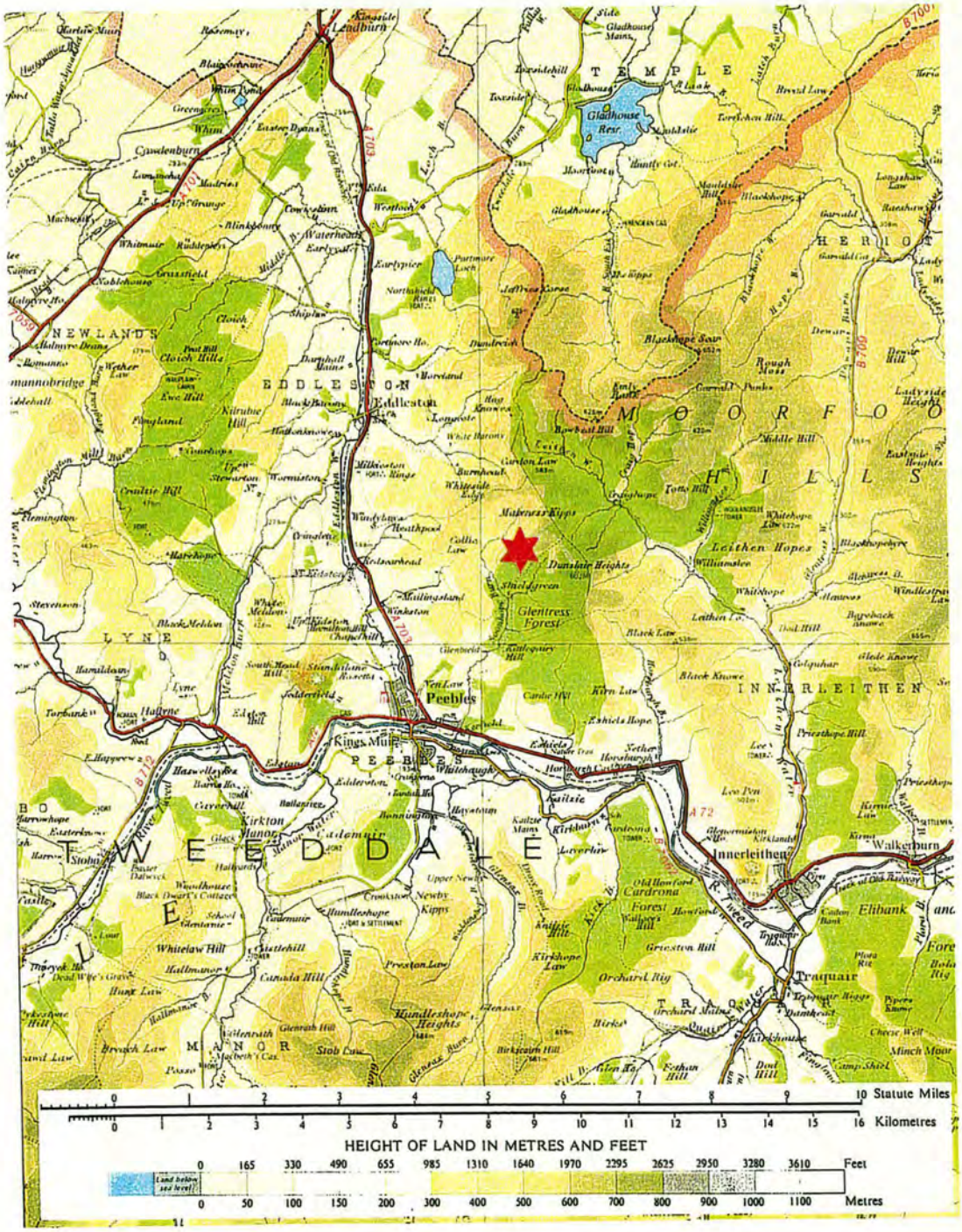

Fig. 2.5: The inset in Figure 2.4 showing the position of site at Dunslair Heights.

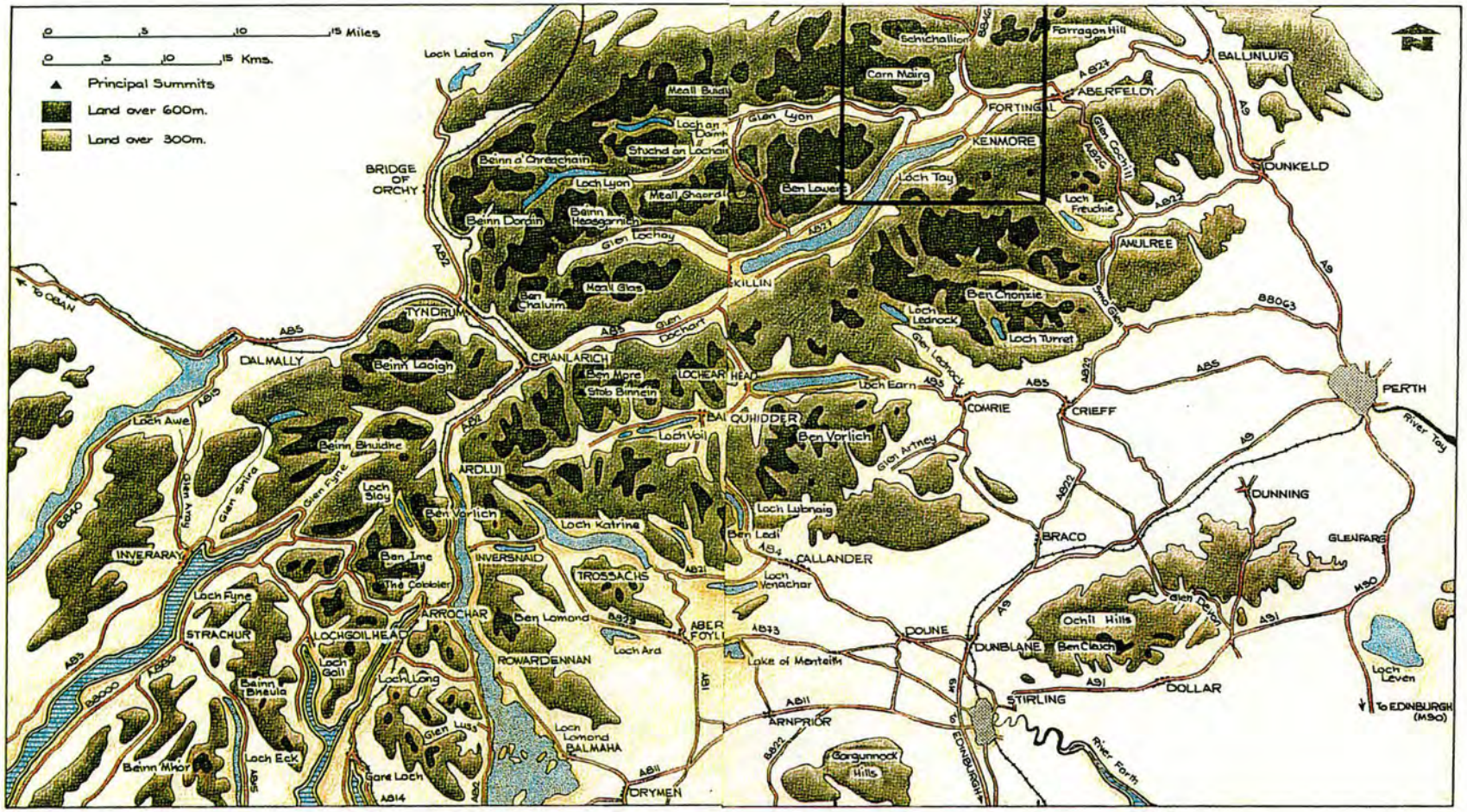

Fig. 2.6: The Scottish Southern Highlands. Schihallion and surrounding are situated in the northern part of the region, shown more clearly in Figure 2.7.

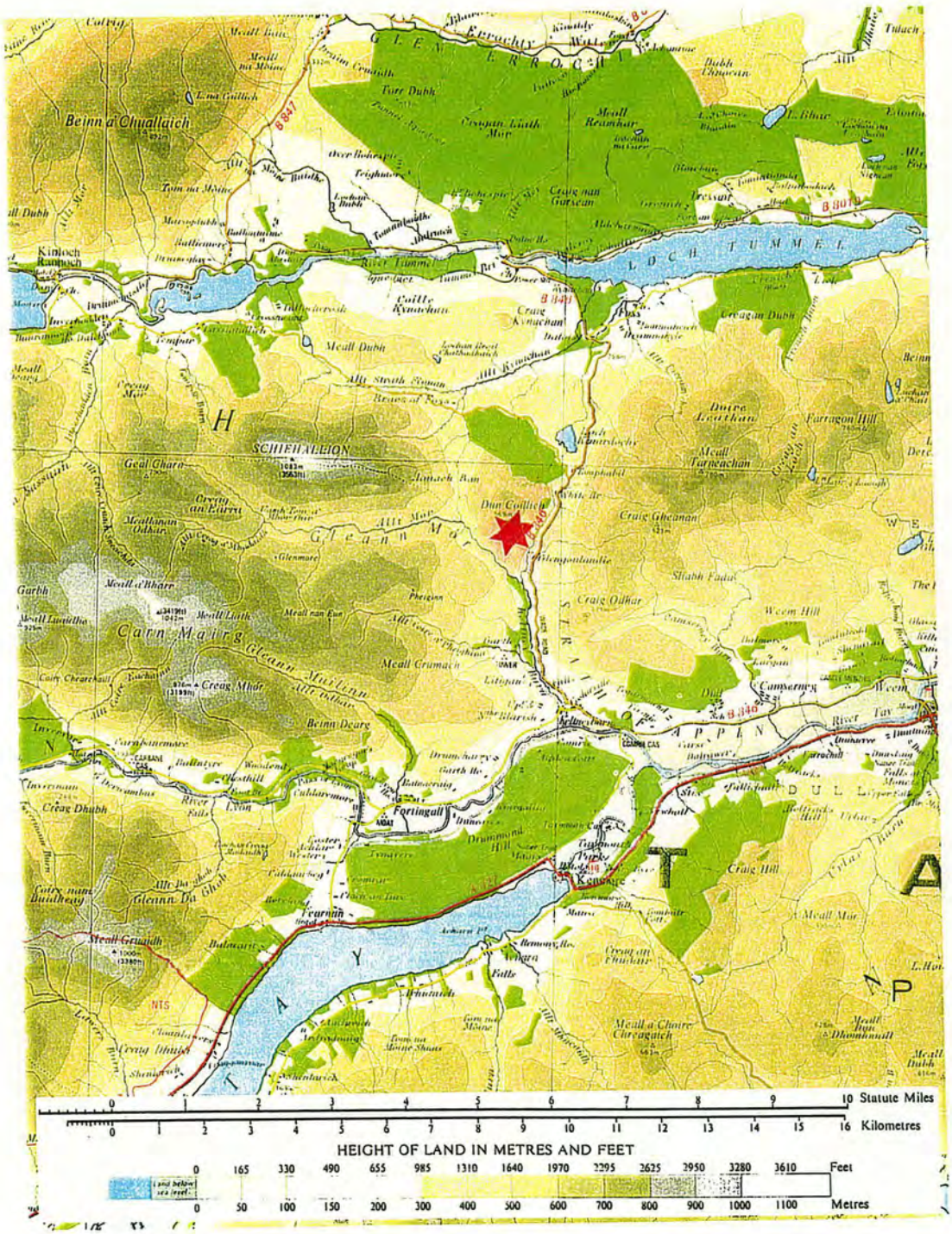

Fig. 2.7: The inset in Figure 2.6 showing the position of site at Dun Coillich.

Dunslair Heights

Dunslair Heights with a summit at 602 m asl is part of the south Moorfoot Hills located 5 km north-east of Peebles in south-east Scotland (Figure 2.6, Table 2.1). The chosen site is at an altitude of 460 m asl, on the north-west slope of Makeness Hill. The hill is partly covered by a conifer forest (*Picea abies*) with an age of approximately 60 years and canopy height of 10-12 metres; the rest, a grass-covered moorland with a canopy height of about 0.2 meter. The soil type is mainly brown forest soils, peaty podzols and some humus-iron podzols. Prevailing winds are south-westerly and the edge of stand faces north-west.

Dun Coillich

Dun Coillich is a 569 m asl hill of the Grampian Mountains situated between Loch Tay and Loch Tummel, about 11 km north-west of Aberfeldy in the Southern Highland region of Scotland (Figure 2.7, Table 2.1). The selected site is at an altitude of 420 m asl on the south slope of the hill. The forest is a fenced 80 years old rectangular plantation quite close to the tree line for Scotland and frequently exposed to orographic cloud (~ 13% of the time). The airflow at the edge presented with a sharp boundary in surface aerodynamic roughness from the grass and heathland to a 15-18 m canopy of Scots pine (*Pinus sylvestris*). The soil type is mainly peaty podzols, some humus-iron podzols and peaty gleys. The edge of stand is exposed to the prevailing south-westerly winds.

2.1.1.2 Swedish sites

The sampling in Sweden were carried out in the south-western province of Hallands and in the central Sweden mountain range of Transtrands. These sites are situated in SW regions No. 10 & 11 and central region No. 33 shown in Figure 2.8

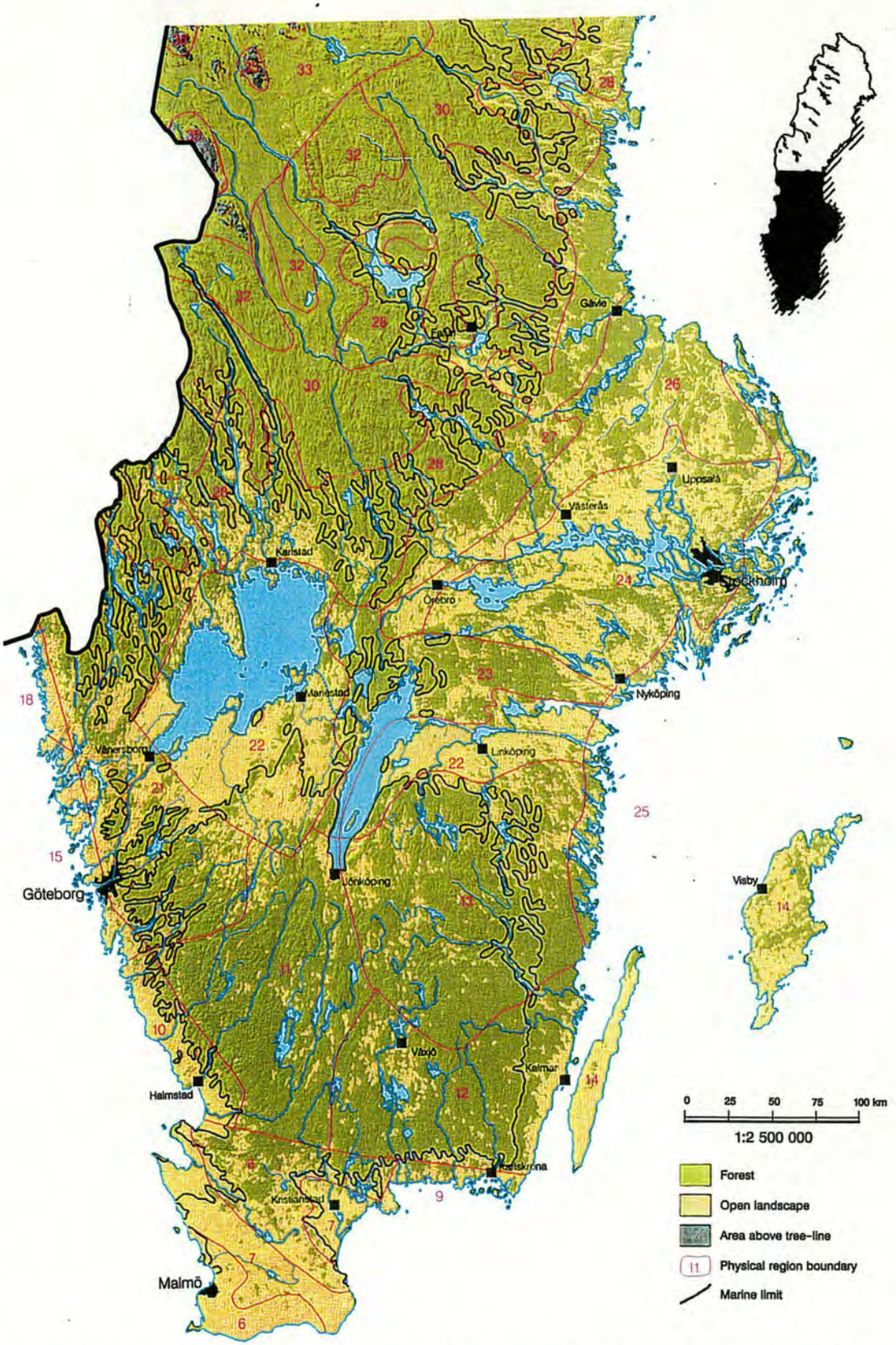

Fig. 2.8: Map of centrl and southern Sweden with designated physical regions (Grundsten, 1992). The Swedish sampling sites were selected in regions No. 10&11, and in the southern part of region 33.

(see also Table 2.1). The Nordic council of Ministers has devided Scandinavia into 76 physical regions, twenty-nine of which are in Sweden. The Halland's coastland consists of mainly sandy beaches, much arable land, large broad-leaved forests, and small pine forests. The southern Swedish uplands consists of rocky outcrops, coniferous forests (mostly spruce), large mires, and large deciduous forests. The landscape in the central is dominated by sub-mountainous terrain with sparce coniferous forests, mountain birch forests, plateus, and isolated mountain massifs with high vegetation limits (Grundsten, 1992).

South-west Sweden

Soil samples were taken from a total of 10 sites (code named A to J) in southwest Sweden; one site (A) located in Hallands Vadero island, about 3 km off Torekov shore, and the rest all located in the Hallands province (Figures 2.9, 2.10 & 2.11). From these ten sites, eight of them, A-G & J, lie along a transect leading NE to about 60 km inland from the coast. The other two, H & I, form a parallel line to the shoreline which includes site G as well. These three sites were chosen from an area with maximum precipitation field (see Figures 2.9 - 2.12). The three coastal sites A, B and C have got the lowest average annual precipitation among the selected sites.

The primary objectives in site selection were to check if the ^{210}Pb measurements could also reflect the trend in long term average precipitation pattern in the area and to investigate the mechanisms which cause the significant enhancement in pollutant deposition due to landscape and ecosystem structures. The specification of the sampling sites in SW Sweden are summarised in Table 2.2. The forest canopies sampled were Norway spruce (Picea abias) except at coastal region, where they were composed of thin Scots pine (Pinus sylvestris). Open fields were

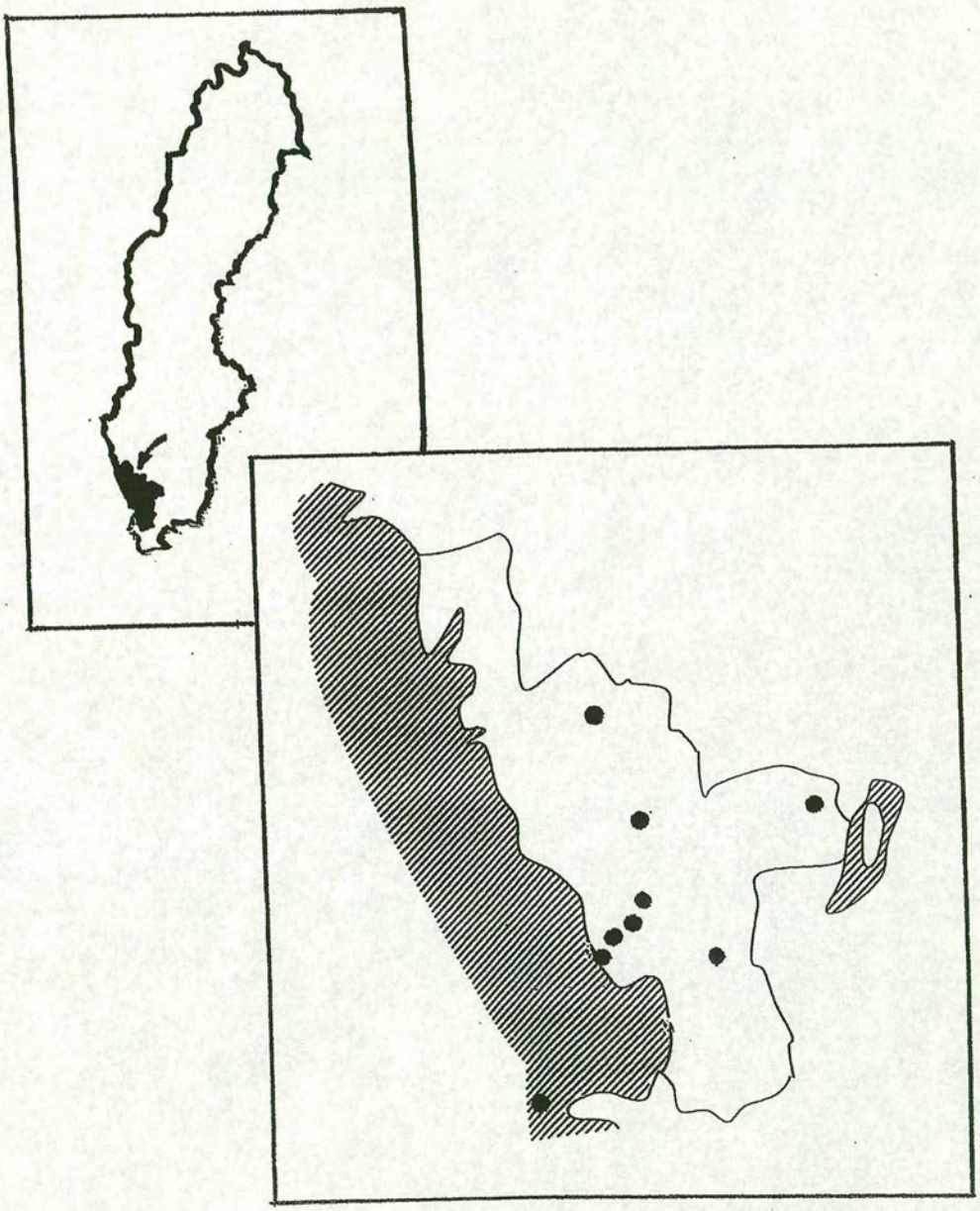

Fig. 2.9: Map of Sweden showing the position of Hallands province and, distribution of sites in the region.

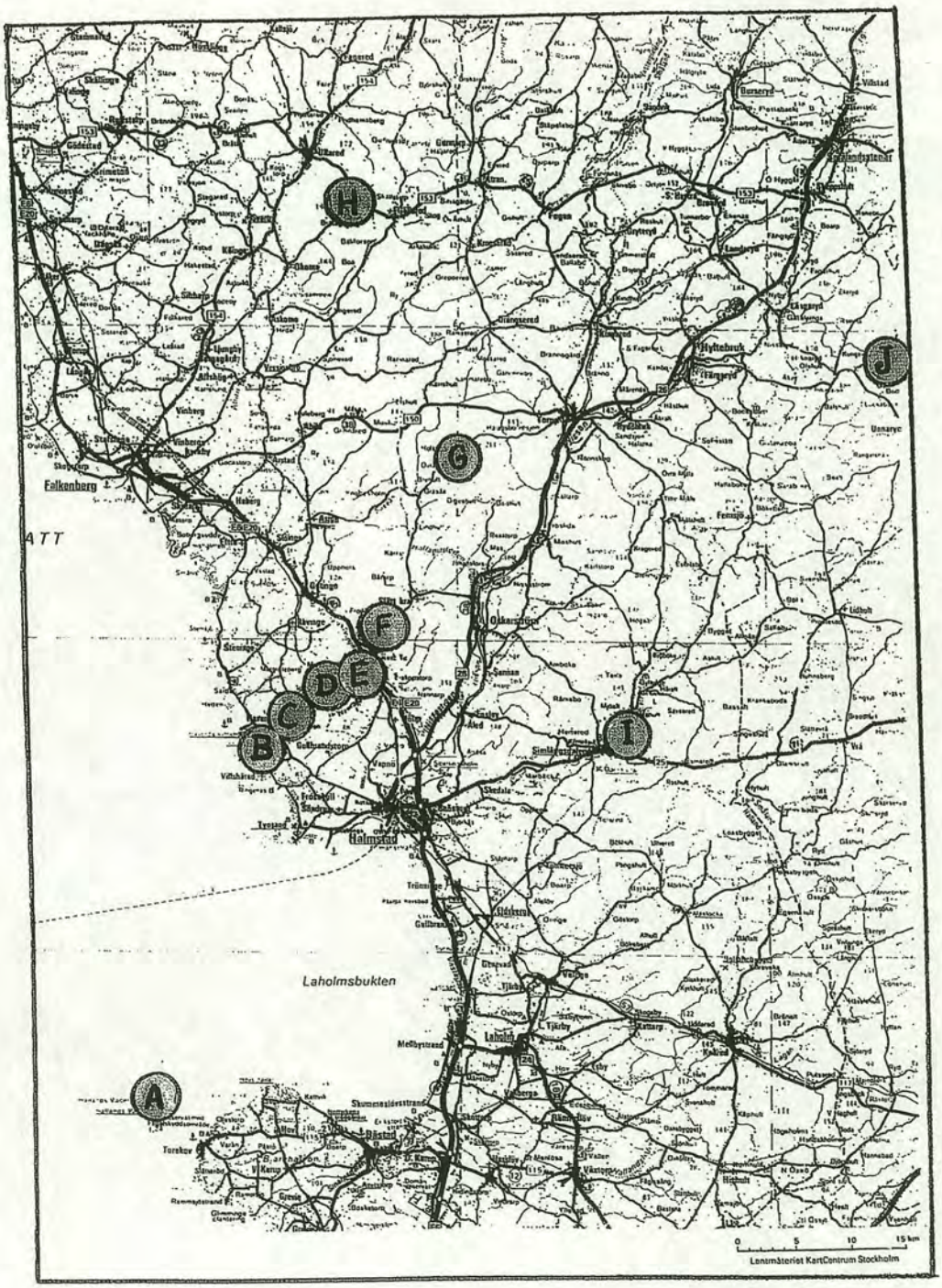

Fig. 2.10: Map of southwest Sweden showing the position of sampling sites A to J and major cities.

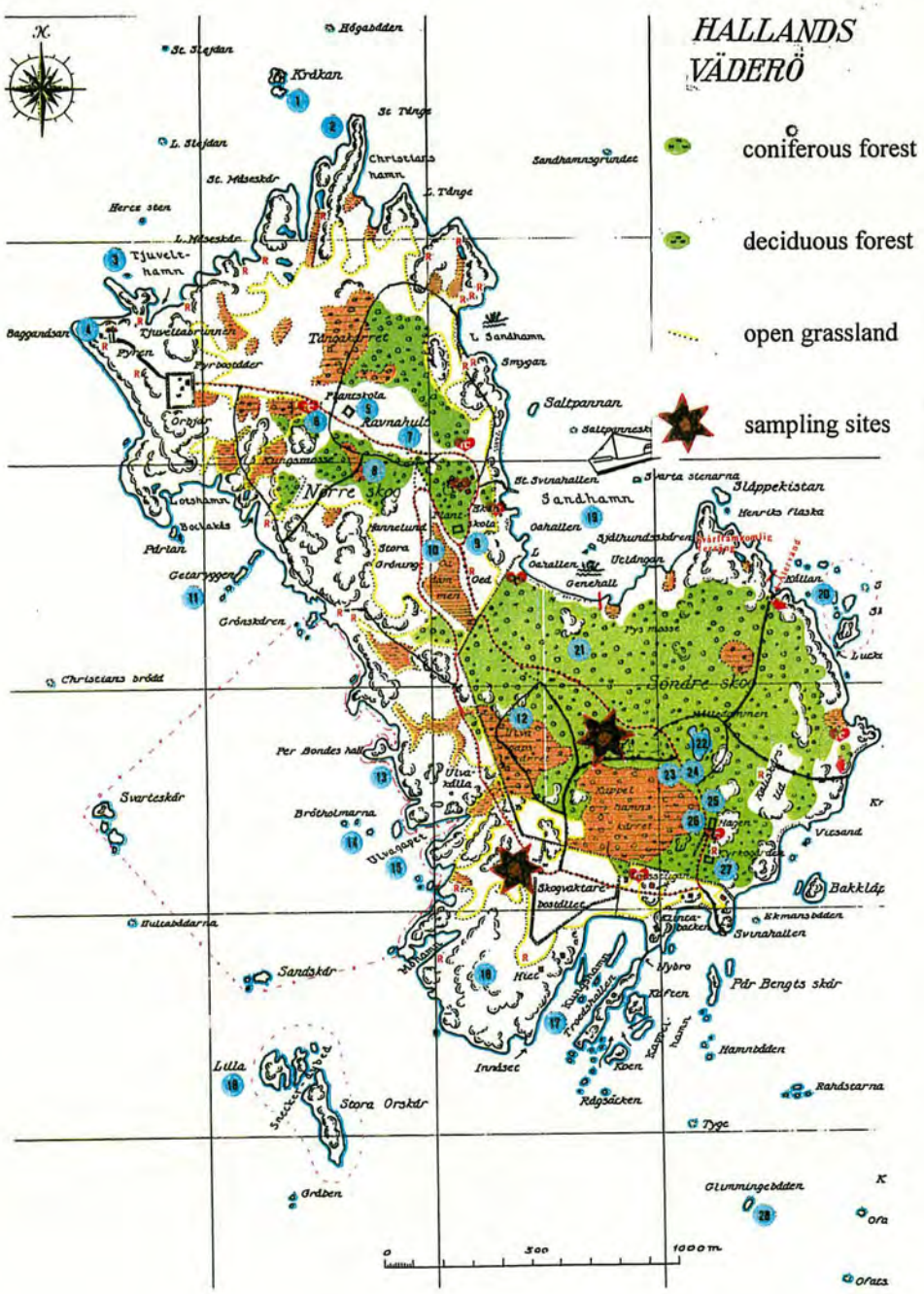

Fig. 2.11: Map of Hallands Vadero island showing the position of sampling sites inside the canopy and in the open field.

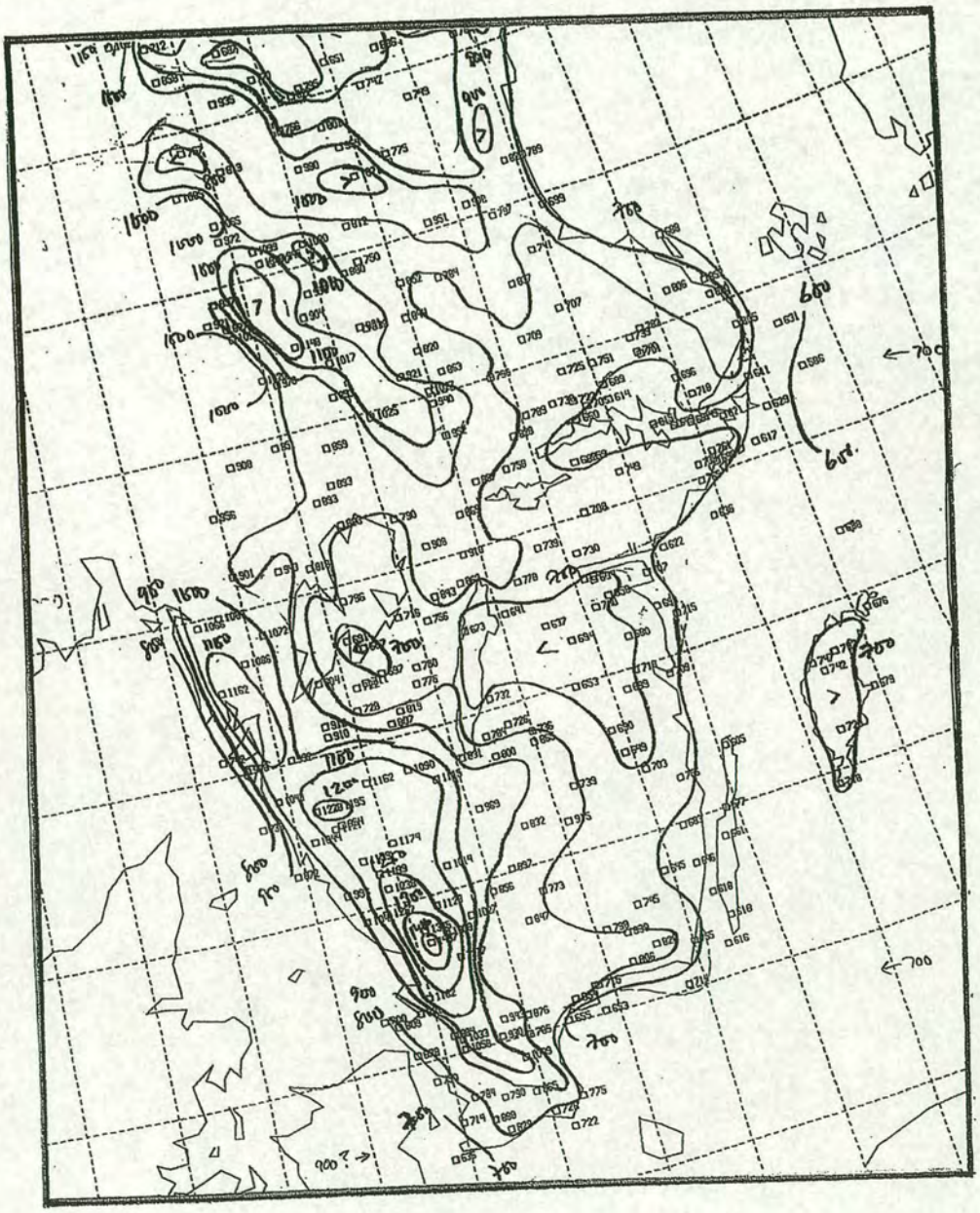

Fig. 2.12: Precipitation contours for south & central Sweden

on the basis of 1983-90 records (Granat, 1995).

mostly covered by short grass (less than 10 cm height), moss and wild flowers. The soil was peaty humus on top with a sandy layer at the bottom of the profile at the coastal region, but highly organic and peaty with too many stones in-land. The prevailing wind in the area is south-westerly.

Table 2.2: Specification of the sampling sites in south-west Sweden.

Site	code	Location of sampling points				Altitude (m asl)	distance inland (km)
		open field	forest canopy				
			spruce	pine	age, y		
Hallands Vadero island	A	●		●	60	10	-3
Haverdals naturreservat	B	●		●	90	5-10	0.5
Bjorktrop	C	●				20	1.5
Harplinge	D	●	●		70	50-80	6
Harplinge	E		●		70	60	6
Kvibille	F		●		70	100	13
Ovraboke/Stammilt	G	●	●		70	160/180	22/25
Normanstorp	H	●	●		70	120-130	31
Broda	I	●	●		60	130	19
Hasslehult/ Hassleberg	J	●	●		70	160	61/60

Central Sweden

In central Sweden, samples were collected at four sites on two adjacent mountains, Gammalsaters (870 m asl) and Skaftasen (660 m asl), from the Transtrand range. Coming from the south, Transtrands is the first isolated mountain massif on plateaus in west Kopparberg close to the Norwegian border (Figure 2.13, Table 2.1). These rounded mountains are mainly screened from the west by the high mountainous regions of Norwey and could be considered as more continental in nature. The first 3 sites (A to C) were selected at Gammalsaters, on its summit at 870 m asl (open field, A), at 720 & 740 m asl (under canopy & open heathland, B), and at its base at 430 & 440 m asl (under canopy & open grassland, C). Figure 2.14 shows a contour plot of Gammalsaters and Skaftasen. A schematic representation of Gammalsaters showing the position of the sampling sites is illustrated in Figure 2.15. The forests at Gammalsaters composed of mainly Norwey spruse (Picea abies), very dense at site C (>100 years old, ~20-25 m height), but almost thin at site B (>100 years old, ~20 m height). Site A is well above the timberline, an exposed site with sparce vegetation, covered partly by lickens and mosses. The open field at site B was covered by old, dense, and undisturbed heather. The soil at this site was extremely peaty and very wet. At site C, the soil was peaty humus on top at the open grass meadow with a large sandy layer at the botom of profile, but under canopy soil was peaty in most parts. The 4th site (D) was chosen on an adjacent mountain, Skaftasen. A relatively thin mixed spruse/pine canopy (~100 years old, 15-20 m height) beside Norra Skaftastjarnen lake at 620 m asl (Figure 2.14). The forest edge investigated is facing the lake and is very exposed to the prevailing south-westerly winds in the region.

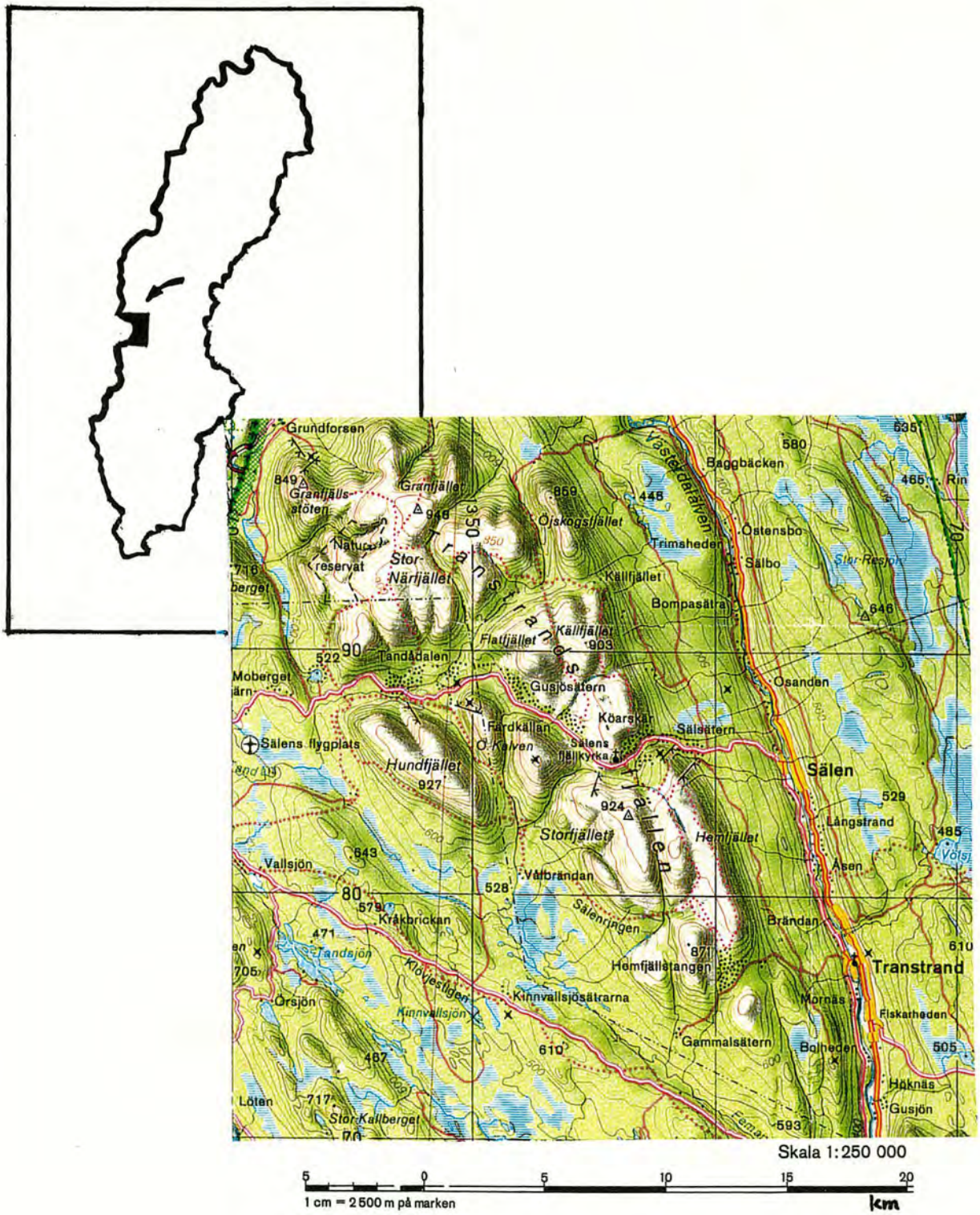

Fig. 2.13: Location of Transtrands Mountains in Sweden, and the map of Transtrands massif showing Gammalsaters and Skaftasen.

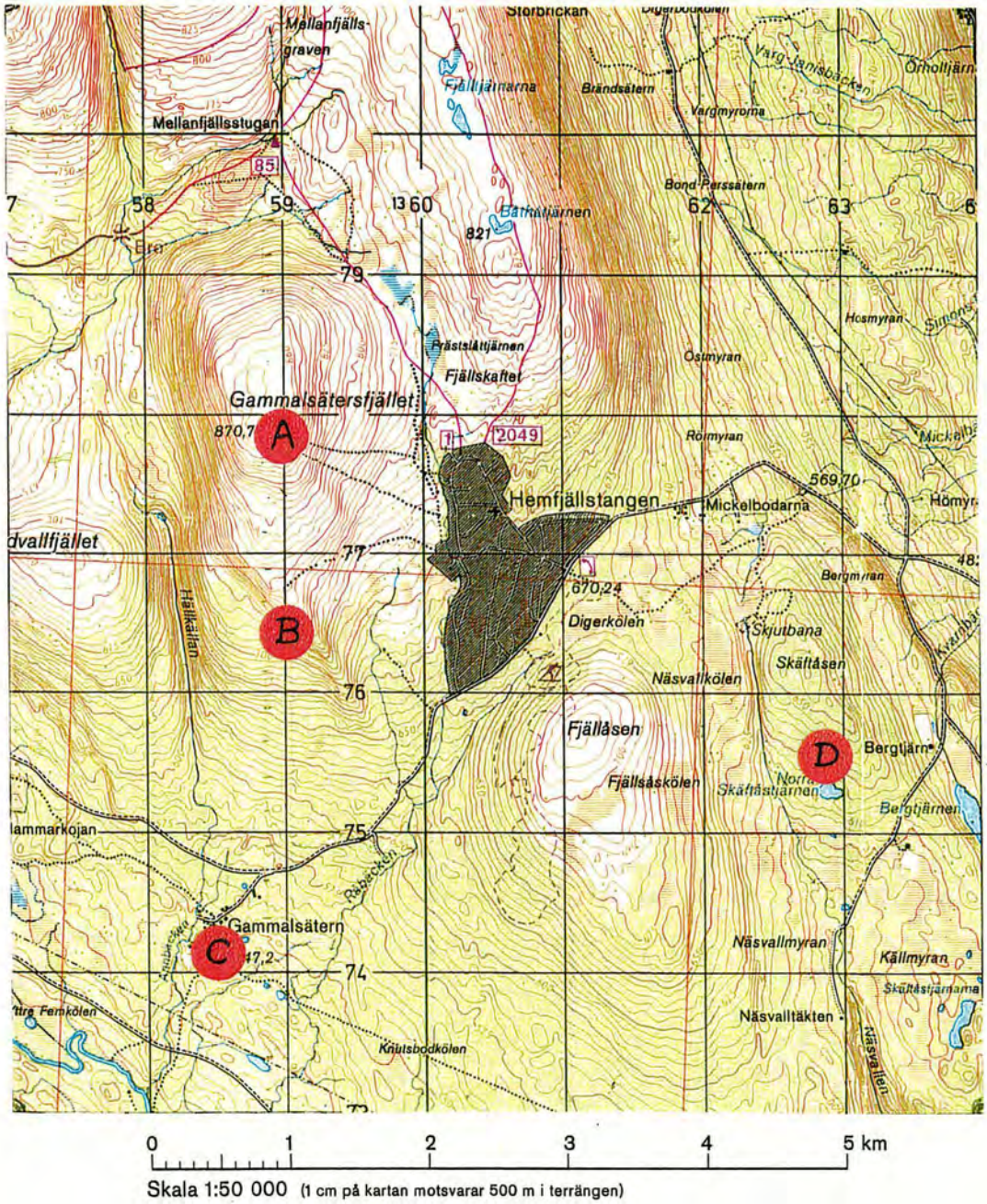

Fig. 2.14: A contour plot of Gammalsaters and Skatasen terrain (25 m contour intervals) showing the position of sampling sites.

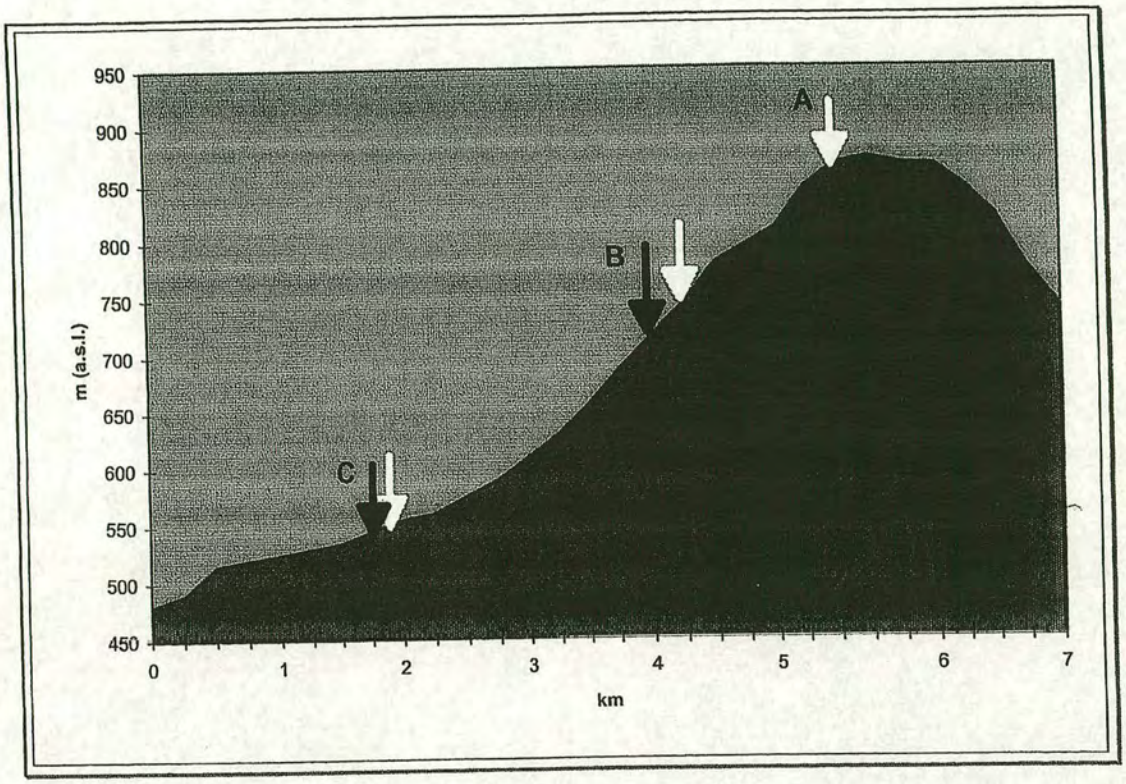

Fig. 2.15: Schematic representation of Gammalsatersfiallet showing the location of sampling sites.

2.1.2 Sampling Procedure

The method of split-level sampling of soil, mostly to a depth of 30 cm, was applied. Since information was required on the concentration of radioactivity per unit area, as well as dry weight of soil, samples were taken in the following ways:

- Using hand-driven brass pipe corers of either 5 cm internal diameter x 20 cm in lenght, or 6.4 cm internal diameter x 15 cm in length;
- Using a metal surface frame measuring 14 x 14 x 5 cm to take samples with the help of a sharp knife;
- Collecting pit samples with a specified area using a flat spade and/or a long sharp knife.

Figure 2.16 shows a sketch of the surface frame as well as core samplers used in this study. The surface frame was specially designed to overcome the difficulty of collecting samples of a constant thickness due to variable compaction of the highly organic horizons within forest canopies. Its application is through digging a pit, holding the frame in place on one side while the sample is cut out using a large knife guided by the frame perimeter.

Cores were subdivided into sections (usually 0-5, 5-10, 10-20 and 20-30 cm depth intervals) before being transported to the laboratory in plastic bags. Whenever sampling was only performed with the pipe corers, sections at each depth were bulked to form separate composite samples. The top 5 cm section included the organic mat layers for grassland samples, and the litter layer was also incorporated in the woodland soils. However, coarse twigs, but not needles, were removed from the woodland soils before sampling. Under canopy samples were taken in each case from the interior of the plantation, under the foliage and away from the base of trees.

To achieve an adequate site documentation, which is of obvious importance for unambigous correlation of final analytical results with the original sample and

satisfactory interpretation of data obtained from the sample, a record sheet was prepared and used in the field work (see Figure 2.17). At each site, details were recorded of the slope, altitude, and other charactristics of the sampling points.

Where possible, a pit was dug to examine the soil profile charactristics to a maximum depth of 50 cm (see Figure 2.18). At almost all sites, photograghs were taken to record the general charactristics of the forest canopy (e.g. Figures 2.19 and 2.20), the stand edge (e.g. Figure 2.21) and the open field (e.g. Figures 2.22, 2.23 and 2.24). This practice was extended to the sampling points as well inside the forest canopies in Sweden (e.g. Figures 2.25 and 2.26).

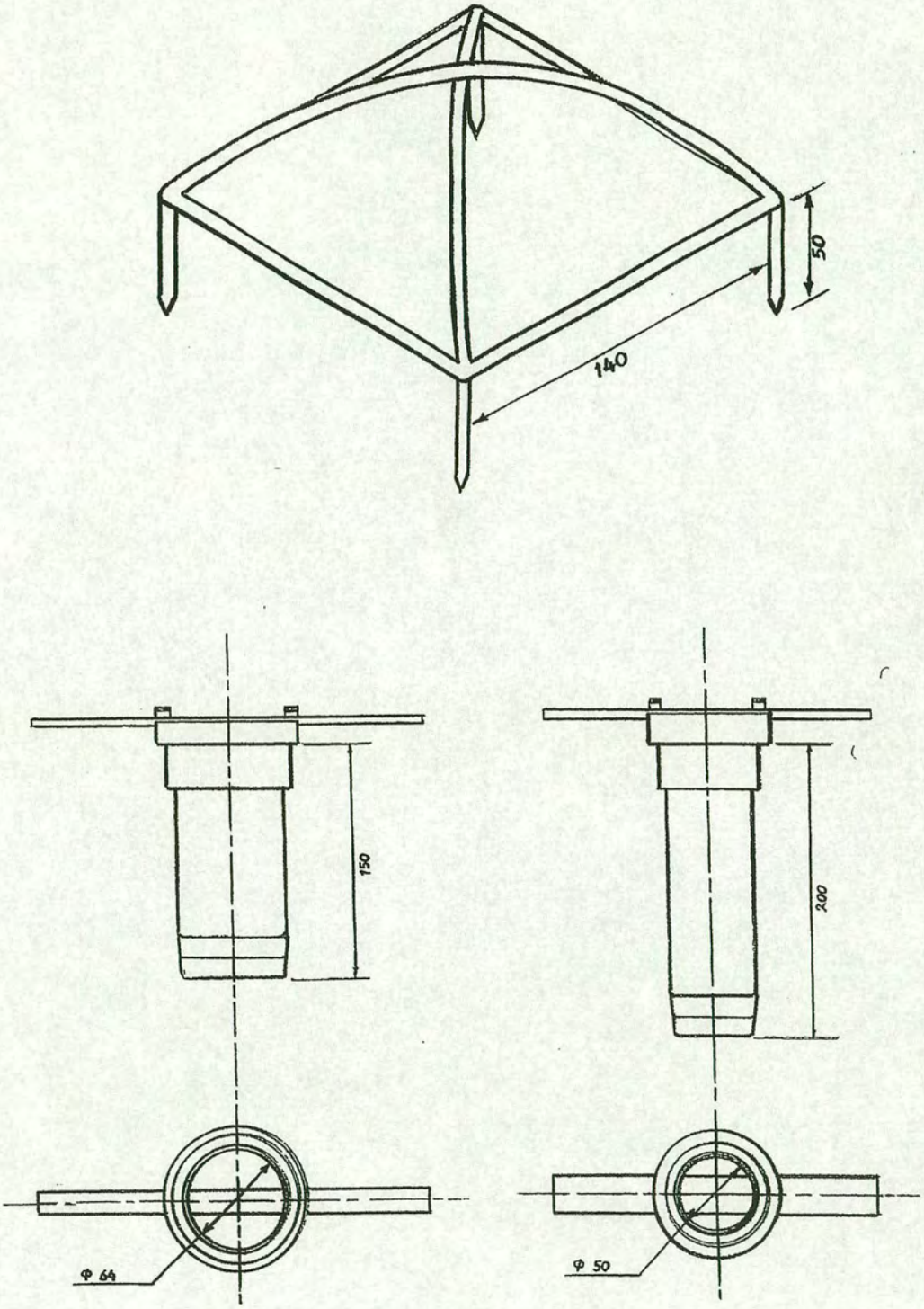

Fig. 2.16: The surface frame and cores used in field sampling.

RECORD OF AREA SAMPLED

1. Site: Hallands Väderö island (A)

2. Altitude (meters asl): ~10 m 3. Date: 3 May 94

4. Position:

☐ open field
undisturbed for .....yrs.

☑ inside forest canopy
composition: Tall Pines (20 m high)
Lower deciduous (2-3 m high)
age(yrs): 60
distance from edge of stand(m): 500

5. Wind direction (with respect to the edge of stand): ☑ ⊥ ☐ ∥ ☐ ∠ ..... °

6. Location No: A6

7. Slope: ☑ gentle ☐ moderate ☐ ridge ☐ valley

8. Sampling method: ☑ pipe corer ϕ [cm]= 5 depth[cm]= 20
☑ surface frame 2 x 5 cm
☐ pit area[cm^2]= ..... x .....

9. Depth of vegetation / litter (cm): 3

10. Maximum depth of sampling(cm): 30

11. Distance from the nearest tree(m): 1.8 ; it's size: ☐ S ☑ L

12. Avg. distance between trees(m): 3

13. Photograph No: 16

Fig. 2.17: Field data record-sheet

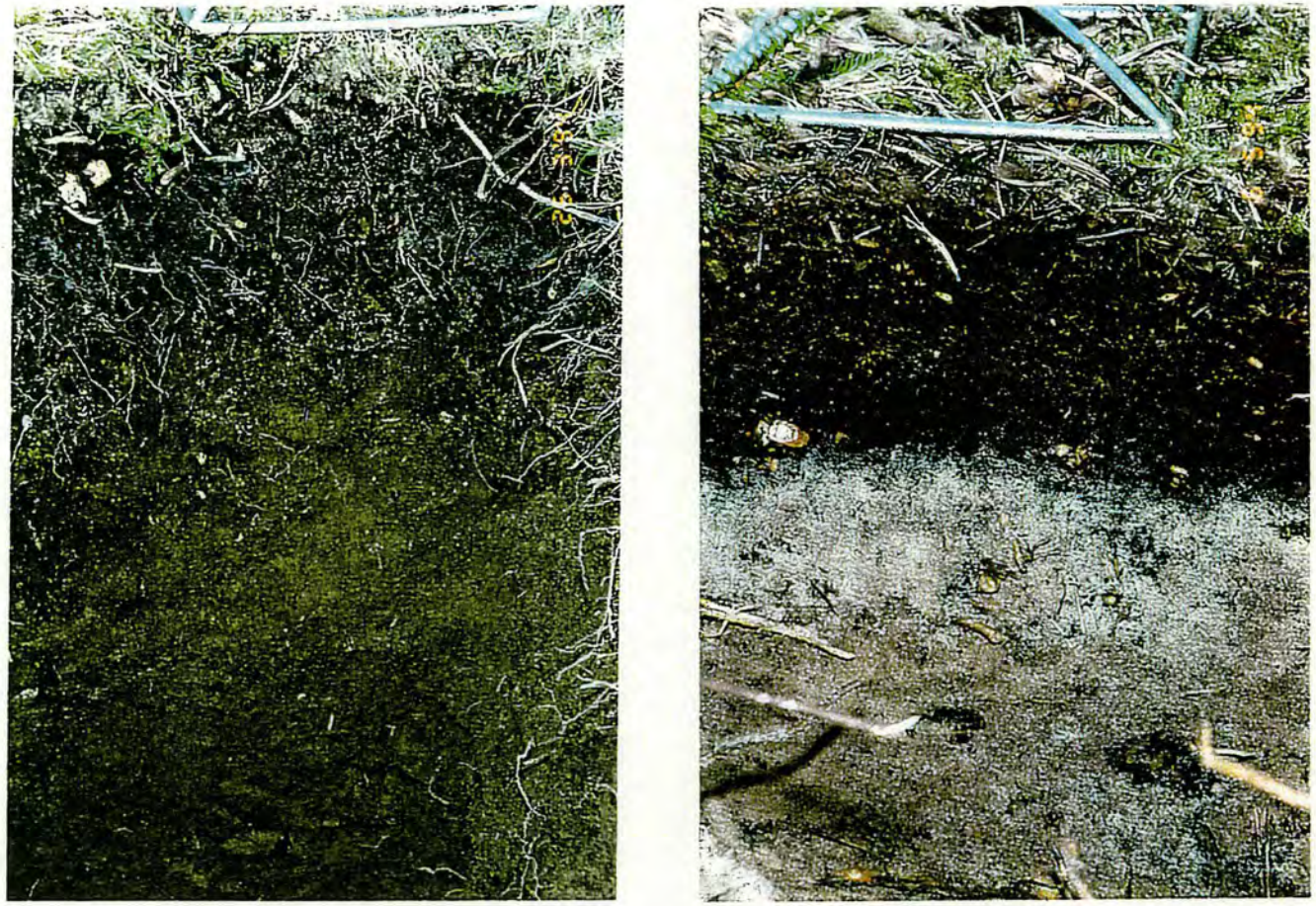

a b

Fig. 2.18: Soil profiles at a) Dun Coillich, and b) Haverdals naturreservat. The 14x14 cm surface sampler is shown as a reference scale.

Fig. 2.19: Highly exposed forest stand at high elevation,Dun Coillich in the Highlands, Scotland.

Fig. 2.20: Typical old forest sampled in central Sweden (Gammalsatern, site C).

a

b

Fig. 2.21: The edge of forest stands sampled at different sites:

a) Dun Coillich, 420 m asl,Highlands,Scotland; b) Normanstorp, 130 m asl, SW Sweden.

c

Fig. 2.21: c) The edge of forest stand at Nora Skaftastjarnen, 620 m asl, central Sweden .

a

b

Fig. 2.22: Open fields sampled at low elevation: a) Halland Vadero island, 10 m asl, SW Sweden; b) Bjorketrop, 20 m asl, SW Sweden.

Fig. 2.23: Open field sampled at medium elevation: Normanstorp, 125 m asl, southern Uplands, Sweden.

a

b

Fig. 2.24: Open fields sampled at high elevation:a) Dun Coillich, 420 m asl, Highlands, Scotland; b) Gammalsaters fjallet, 870 m asl, central Sweden.

a

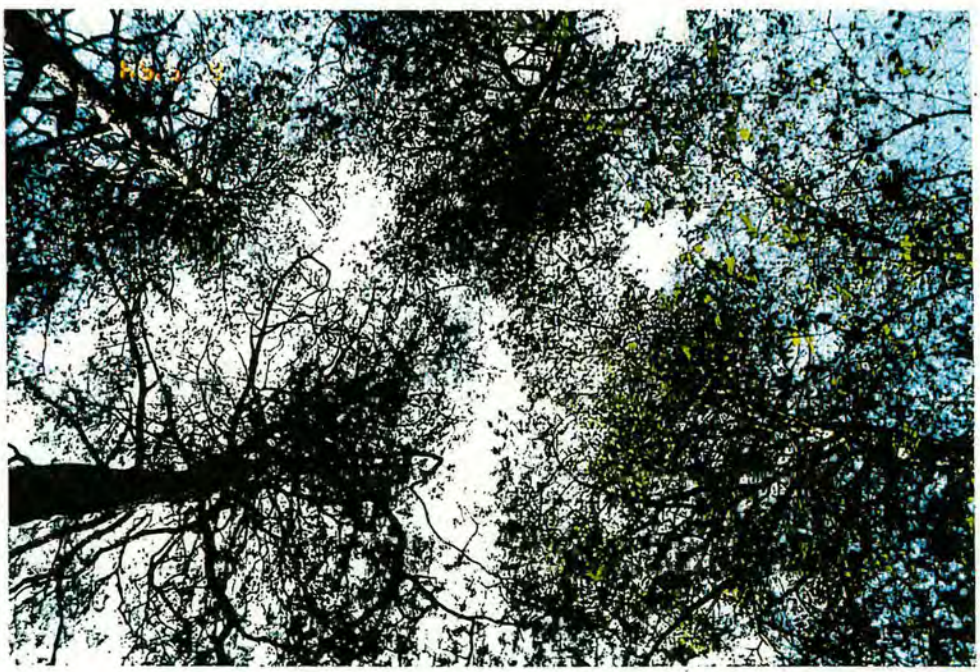

b

Fig. 2.25: Scots pine canopies, seen from the sampling points at: a) Halland Vadero island; b) Haverdals naturreservat; both in the coastal region, SW Sweden.

a

b

Fig. 2.26: Norway spruce canopies, seen from the sampling points at: a) Kvibille; b) Stammilt; both in the upland region, SW Sweden.

2.1.2.1 Dunslair Heights

Fieldwork at Dunslair Heights was carried out in February 1993. Soil samples were collected from four locations lying over a short transect (~80 m) across a boundary between open, grass-covered moorland and the spruce canopy. These locations include 20 points in 4 rows parallel to the edge of the stand, 3 inside the forest canopy (2, 15 and 40 m from the edge) and 1 in the adjacent open field (about 30-40 m from the edge). At 3 points in the open field , samples were taken by using the 6.4 cm diameter corer. Composite samples were obtained by combining subdivisions from 5 cores at each sampling point. At the other points, pit samples were collected from an area of either 10 x 20 cm^2 or 15 x 15 cm^2. Table 2.3 summarises the details of sampling at this site.

Table 2.3: Details of each sampling location at Dunslair Heights.

Sample ID	Location	Sample depth (cm)	Sub-divisions	Remarks
DH1A	open field,	16	5	5 cores
DH1B	20 m from	20	4	10 x 20 cm pit
DH1C	the edge of	20	5	10 x 20 cm pit
DH1D	stand.	16	5	5 cores
DH1E		16	5	5 cores
DH2A	1st row	20	5	15 x 15 cm pit
DH2B	under canopy,	20	5	15 x 15 cm pit
DH2C	2 m from	20	5	15 x 15 cm pit
DH2D	the edge.	20	5	15 x 15 cm pit
DH2E		20	5	15 x 15 cm pit
DH3A	2nd row	20	5	15 x 15 cm pit

DH3B	under canopy,	20	5	15 x 15 cm pit
DH3C	15 m from	20	5	15 x 15 cm pit
DH3D	the edge.	20	5	15 x 15 cm pit
DH3E		20	5	15 x 15 cm pit
DH4A	3rd row	20	5	15 x 15 cm pit
DH4B	under canopy,	20	5	15 x 15 cm pit
DH4C	40 m from	20	5	15 x 15 cm pit
DH4D	the edge.	20	5	15 x 15 cm pit
DH4E		20	5	15 x 15 cm pit

2.1.2.2 Dun Coillich

In late January 1994, a test sampling was performed at Dun Coillich. Surface soil samples measuring 14 x 14 x 10 cm were taken using a frame sampler from 6 locations, 3 inside the canopy and 3 in the adjacent open field. Encouraged by the results of radioanalysis of these initial samples, further fieldwork was carried out at Dun Coillich in the period of 26 March to 14 April 1994. Soil cores were taken mostly to a depth of 30 cm at four locations lying over a short transect (~100 m) across a boundary between open heathland and the pine canopy. Samples were collected from 5 points in the open field and 9 points in 3 rows inside the forest canopy, using 14 x 14 cm frame sampler. Details of sampling at Dun Coillich are summarised in Table 2. 4.

Table 2.4: Details of each sampling location at Dun Coillich.

Sample ID	Location	Sample depth (cm)	Sub-divisions	Remarks
DC1A	open field,	30	4	14 X14 cm
DC1B	30-50 m from	30	4	cores, using

DC1C	the edge of	30	4	frame
DC1D	stand.	30	4	sampler.
DC1E		50	6	
DC2A	1st row under	30	4	14 X14 cm
DC2B	canopy, 8 m	30	4	cores, using
DC2C	from the edge.	30	4	frame sampler.
DC3A	2nd row under	30	4	14 X14 cm
DC3B	canopy, 25 m	50	6	cores, using
DC3C	from the edge.	30	4	frame sampler.
DC4A	3rd row under	30	4	14 X14 cm
DC4B	canopy, 50 m	20	3	cores, using
DC4C	from the edge.	20	3	frame sampler.

2.1.2.3 Southwest Sweden

Sampling in south-west Sweden took place in early May 1994. Soil cores were obtained mostly to a depth of 30 cm at 10 locations at each site, 5 inside the forest canopy and 5 in the adjacent open field. At Normanstorp, however, sampling was performed at 15 locations inside the forest stand in order to be able to investigate the edge effect (enhancement in deposition at the edge of stand relative to the open field and inside the canopy due to the enhanced turbulence at the edge). Samples were taken with the help of 14 x 14 cm frame sampler to a depth of 10 cm (0-5 & 5-10), and by 5 cm diameter pipe corer further down to 30 cm (10-30). This method was

applied to overcome the difficulty of maintaining constant thickness of spongy, highly organic surface samples, and to get lower volume of deep mineral soil samples for the sake of easier transportation of too many samples. Table 2. 5 summarises the details of sampling at sites in southwest Sweden. All cores were subdivided into 3 sections (0-5, 5-10 and 10-20/30 cm) before being transported in plastic bags.

Table 2.5: Details of each sampling location at the sites in SW Sweden.

Site	Sample ID	Location	Sample depth (cm)	Remarks
Hallands Vadero island	SWSA1	open field, 200 m from the shore.	30	using 14 x 14 cm frame sampler & 5 cm corer
	SWSA2		30	
	SWSA3		30	
	SWSA4		30	
	SWSA5		30	
Hallands Vadero island	SWSA6	inside, the forest canopy	30	using 14 x 14 cm frame sampler & 5 cm corer
	SWSA7		30	
	SWSA8		30	
	SWSA9		30	
	SWSA10		30	
Haverdals naturreservat	SWSB1	open field, openning in the canopy.	30	using 14 x 14 cm frame sampler & 5 cm corer
	SWSB2		30	
	SWSB3		30	
	SWSB4		30	
	SWSB5		30	

Haverdals naturreservat	SWSB6	inside, the forest canopy	30	using 14 x 14 cm frame sampler & 5 cm corer
	SWSB7		30	
	SWSB8		30	
	SWSB9		30	
	SWSB10		30	
Bjorketrop (Haverdal)	SWSC1	open field	30	using 14 x 14 cm frame sampler & 5 cm corer
	SWSC2		30	
	SWSC3		30	
	SWSC4		30	
	SWSC5		30	
Harplinge	SWSD1	open field	20	using frame sampler (0-10 cm) & 7 x 14 cm pit (10-20 cm)
	SWSD2		20	
	SWSD3		20	
	SWSD4		20	
	SWSD5		20	
Harplinge	SWSD5	inside, the forest canopy	30	using 14 x 14 cm frame sampler & 5 cm corer
	SWSD6		28	
	SWSD7		20	
	SWSD4		30	
	SWSD5		30	
Harplinge	SWSE6	inside, the	30	using 14 x 14 cm
	SWSE7		30	

	SWSE8	forest	30	frame sampler
	SWSE9	canopy	30	&
	SWSE10		30	5 cm corer
Kvibille	SWSF6	inside,	20	using
	SWSF7	the	25	14 x 14 cm
	SWSF8	forest	25	frame sampler
	SWSF9	canopy	22	&
	SWSF10		20	5 cm corer
Ovraboke	SWSG1	open field	20	composite
	SWSG2		20	samples
	SWSG3		20	from
	SWSG4		20	3 or 2
	SWSG5		20	cores
Stammilt	SWSG6	inside,	30	using
	SWSG7	the	30	14 x 14 cm
	SWSG8	forest	30	frame sampler
	SWSG9	canopy	30	&
	SWSG10		30	5 cm corer
Normanstorp	SWSH1	open field	30	using
	SWSH2		30	14 x 14 cm
	SWSH3		30	frame sampler
	SWSH4		30	&
	SWSH5		30	5 cm corer

Normanstorp	SWSH6	inside	30	using
	SWSH7	the forest canopy,	30	14 x 14 cm
	SWSH8	5-10 m	30	frame sampler
	SWSH9	from	20	&
	SWSH10	the edge.	30	5 cm corer

Normanstorp	SWSH11	inside	30	using
	SWSH12	the forest canopy,	30	14 x 14 cm
	SWSH13	1-2 m	30	frame sampler
	SWSH14	from	30	&
	SWSH15	the edge.	30	5 cm corer

Normanstorp	SWSH16	inside	25	using
	SWSH17	the forest canopy,	30	14 x 14 cm
	SWSH18	100 m	30	frame sampler
	SWSH19	from	25	&
	SWSH20	the edge.	25	5 x 10 cm pit

Broda	SWSI1	open field	25	using
	SWSI2		30	14 x 14 cm
	SWSI3		30	frame sampler
	SWSI4		30	&
	SWSI5		30	5 cm corer

Broda	SWSI6	inside	30	using
	SWSI7	the	30	14 x 14 cm

	SWSI8	forest	30	frame sampler
	SWSI9	canopy.	30	&
	SWSI10		25	5 cm corer

Hasslehult	SWSJ1	open field	30	using
	SWSJ2		30	14 x 14 cm
	SWSJ3		30	frame sampler
	SWSJ4		30	&
	SWSJ5		30	5 cm corer

Hassleberg	SWSJ6	inside	35	using
	SWSJ7	the	30	14 x 14 cm
	SWSJ8	forest	30	frame sampler
	SWSJ9	canopy.	30	&
	SWSJ10		30	5 cm corer

2.1.2.4 Central Sweden

Sampling took place in central Sweden in early October 1994. Soil samples were taken mostly to a depth of 25 cm at 25 locations in Gammalsatern and 5locations at Skaftasen. They were obtained by either using 14 x 14 cm frame sampler to a depth of 5 cm and by 5 cm diameter pipe-corer further down to 25 cm (5-15 & 15-25 cm), or digging out a 7 x 14 cm pit to a depth of 25 cm and dividing it into 3 sections (0-5, 5-15 & 15-25 cm). Table 2.6 summarises the details of sampling at the 4 sites in central Sweden.

Table 2.6: Details of each sampling location at the sites in central Sweden.

Site	Sample ID	Location	Sample depth (cm)	Remarks
Gammalsaters fjallet	CSA1	open field, at the summit.	25	using 14 x 14 cm frame (0-5 cm), & & 5 cm corer (5-25 cm).
	CSA2		25	
	CSA3		25	
	CSA4		25	
	CSA5		25	
Gammalsaters fjallet	CSB1	open heathland at 740 m asl.	20	7 x 14 cm pit
	CSB2		25	
	CSB3		25	
	CSB4		25	
	CSB5		25	
Gammalsaters fjallet	CSB6	inside the forest canopy at 720 m asl.	25	using 14 x 14 cm frame (0-5 cm), & & 5 cm corer (5-25 cm).
	CSB7		25	
	CSB8		25	
	CSB9		25	
	CSB10		25	
Gammalsatern	CSC1	open grassland at 540 m asl.	25	7 x 14 cm pit.
	CSC2		25	
	CSC3		25	
	CSC4		25	

	CSC5		25	

Gammalsatern	CSC6	inside	20	7 x 14 cm pit.
	CSC7	the	17	
	CSC8	forest canopy at	17	
	CSC9	530 m asl.	20	
	CSC10		19	

Skaftasen	CSD6	at the	25	7 x 14 cm pit.
	CSD7	edge of	25	
	CSD8	forest canopy at	25	
	CSD9	620 m asl.	25	
	CSD10		25	

2.1.3 Sample Preparation

The sample preparation was carried out at the Scottish Agricultural College. They were weighed, air dried in plastic trays at 30 degrees centigrade, weighed again, ground (vegetal fragments) and sieved with 2-mm mesh screen. Stones above 2 mm were discarded on the basis of the assumption that such close systems are in radioactive equilibrium with respect to ^{226}Ra & ^{210}Pb, and do not contain any atmospheric ^{137}Cs. The remaining material was re-weighed and stored in plastic bags, ready for subsequent radioanalysis by gamma-ray spectrometry systems at the Nulear Physics Laboratory of Edinburgh University.

2.2 Radioactivity Measurement

A wide range of instruments and methods are available with which to monitor the presence and ecological behavior of radionuclides that are present in the environment (Tolgyessy, 1987; IAEA, 1989). The standard technique for the measurement of ^{210}Pb activity in soil, for many years, involved leaching or dissolution of the samples, followed by chemical purification and counting of either the beta particles emitted by the daughter, ^{210}Bi, or the alpha particles emitted by the granddaughter, ^{210}Po. Analysis of ^{226}Ra in soil or sediment samples has also been carried out in a similar manner by relying on the concentrations of ^{210}Po obtained in deeper sections of the soil/sediment core, or by alpha scintillation counting of ^{222}Rn (Tolgyessy, 1987; Cutshall, 1983).

This method of chemical processing is relatively complex, time consuming and destructive. It requires a considerable effort in the quantitative separation of these nuclides from soil and vegetation samples (Graustein & Turekian, 1982; Joshi, 1987). These difficulties led to the developement of a more convenient analytical technique for the activity measurement of ^{210}Pb, which has become the most common method in use today: *direct gamma-spectrometry*. It is a simple, relatively inexpensive and non-destructive analysis technique, which also permits simultaneous determination of ^{226}Ra and ^{137}Cs activities in soil samples (Gaggeler et al., 1976; Joshi & Mudroch, 1988; Monaghan, 1989). This eliminates the need for doing separate assays for these radionuclides of concern.

Details of the gamma analysis procedure employed in this study, will be presented in the following sections, together with a brief description of the detection mechanism.

2.2.1 Gamma-ray Spectrometers

The atomic nucleus is characterized by discrete energy levels. Transition between these levels (also called states) can be made by the emission (or absorption)

of electromagnetic radiation with an energy equal to the energy difference between the levels participating in the transition. In the process of alpha or beta-decay, daughter nuclei are often produced in their excited energy states. Gamma-decay is usually the most common mode of nuclear de-excitation. A nucleus emits one or more photons as it decays to its ground state or to lower-lying excited states.

The gamma-ray spectrum from a radionuclide is discrete. Just as optical spectra depend uniquely on the chemical elements that are exited, a gamma-ray spectrum depends uniquely on the particular radionuclides that are present. By techniques of gamma-ray spectroscopy, the intensities of photons at various energies can be measured to determine the distribution of radionuclides in a sample (see Figure 2.27).

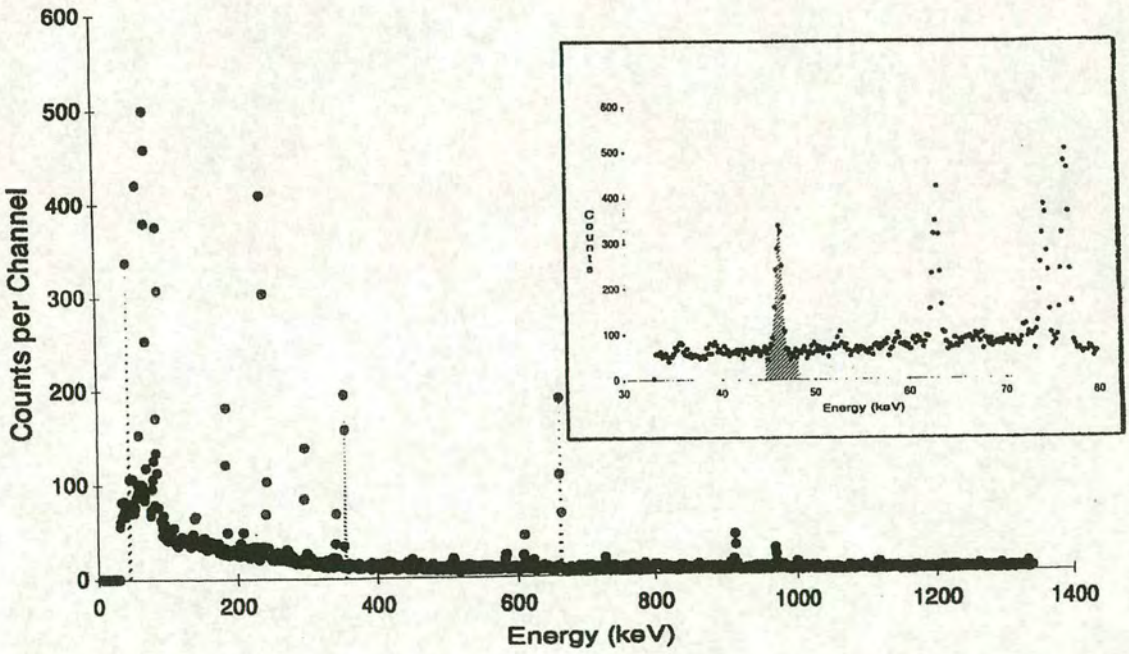

Fig. 2.27: A γ-ray spectrum of a soil sample recorded with the HPGe detector.
The ^{210}Pb peak is clearly shown in an expanded part of the spectrum inside the inset.

2.2.1.1 Detection mechanism and detectors

Gamma photons are detected by means of the electrons they produce when they interact with the material in a sensitive region of the detector. The main interactions of gamma-rays in matter, from the radiation measurement point of view, are: *photoelectric absorption, Compton scattering* and *pair production.* A beam of photons in its passage through a thickness of matter, is attenuated in intensity by these processes which remove photons from the beam entirely, either by absorption or scattering (Sutton, 1993).

Photoelectric Effect: This is an interaction between a photon and a bound atomic electron. As a result, the incident photon transmits its energy completely to the electron and, disappears. Subsequently, the electron, called the *photoelectron,* is ejected from the atom with a kinetic energy of

$$E_e = E_\gamma - \text{B.E.}$$

where B.E. is the binding energy of the electron. The energy of this electron as well as the energies of Auger electron and/or photoabsorbed characteristic X-rays due to absorber atom de-excitation are again transmitted completely to the detector through ionization. Photoelectric process is the predominant mode of interaction for low energy gamma-rays, and is also enhanced for high-Z materials. The probability of photoelectric absorption per atom varies as Z^n / E_γ^m, where m and n are constants with a value of 3 to 5 depending on E_γ (Evans, 1982). In the low energy region, it rises abruptly when the photon energy is sufficient to eject a photoelectron from the K shell of the atom which is known as the *K absorption edge* (see Figure 2.31). Similar absorption edges occure at lower energies for the other electron shells such as L, M, etc. (Knoll, 1989; Leo, 1987) Gamma-ray photons absorbed by this process will correspond to counts in the full-energy peak (FEP) of the spectrum (Figure 2.28).

Compton Scattering: In this case, the interaction is between a photon and a free electron. Of course, the electrons in matter are not free but loosely bound; however, if

the photon energy is high with respect to the binding energy, the electron may be considered free. The incident photon does not disappear but, is deflected through an angle with respect to its original direction (see sketch below).

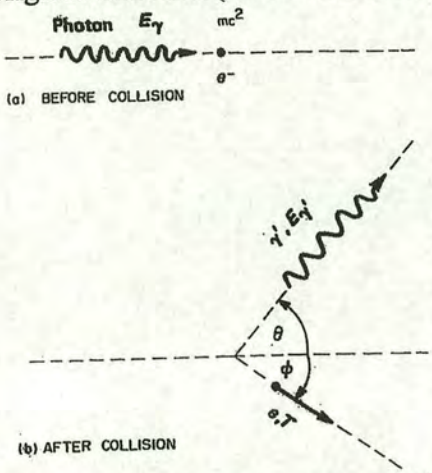

The photon energy is reduced by a certain amount that is given to the electron. Applying energy and momentum conservation, the following relations can be obtained for the energy of the scattered photon and the *recoil electron* (Evans, 1982):

$$E_{\gamma'} = \{1 / [1 + (E_\gamma / m_0c^2)(1 - \cos\theta)]\} E_\gamma$$

$$T = \{(E_\gamma / m_0c^2)(1 - \cos\theta) / [1 + (E_\gamma / m_0c^2)(1 - \cos\theta)]\} E_\gamma$$

The minimum energy of the scattered photon is obtained when $\theta = \pi$:

$$E_{\gamma', min} = \{1 / [1 + (2E_\gamma / m_0c^2)]\} E_\gamma$$

This corresponds to the maximum energy of the recoil electron:

$$T_{max} = \{(2E_\gamma / m_0c^2) / [1 + (2E_\gamma / m_0c^2)]\} E_\gamma$$

which is known as the *Compton edge*. The energy of the recoil electron is transmitted completely to the detector through ionization. The Compton electrons are responsible for the continuous part of the spectrum, extending from zero up to the Compton edge and called the *Compton continuum* (see Figure 2.28) (Tsoulfanidis, 1989; Leo, 1987). The probability of Compton scattering per atom of the absorber increases linearly with Z, and generally falls off gradually with increasing energy (Knoll, 1989).

Pair Prodution: This effect takes place between a photon and a nucleus. An energetic gamma photon, in the intence electric field close to a nucleus, transforms into an electron-positron pair. To create the pair, the photon must have at least an

energy of 1.022 MeV (twice the rest mass energy of an electron). Of the incident photon energy E_γ, the energy $E_\gamma - 2m_oc^2$ is transmitted to the detector. At the

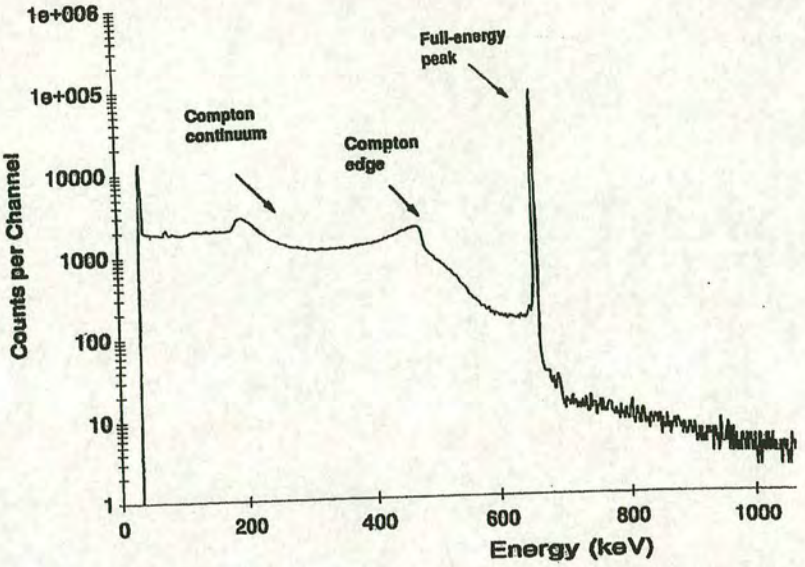

Fig. 2.28: A typical pulse height spectrum for the decay of ^{137}Cs obtained with the HPGe detector system.

end of the positron track, two photons of the energy m_oc^2 (0.511 MeV) are emitted in opposite directions as a result of positron-electron annihilation in the detector medium. The energy of these photons, as well as Compton scattered photons, may then be absorbed in the detector medium by successive Compton and photoelectric interactions.

The relative importance of the three interactions mentioned above, with respect to the photon energy and atomic number of absorbing material is well illustrated in Figure 2.29.

The attenuation suffered by a photon beam, as it passes through an absorbing medium, is exponential with respect to the thickness of the absorber, i.e.

$$I(x) = I_o \exp(-\mu x)$$

with I_o: incident beam intensity; x: thickness of absorber; μ: linear attenuation coefficient.

The attenuation coefficient is a quantity which is charactristic of the absorbing material, and is equal to the sum of three probabilities:

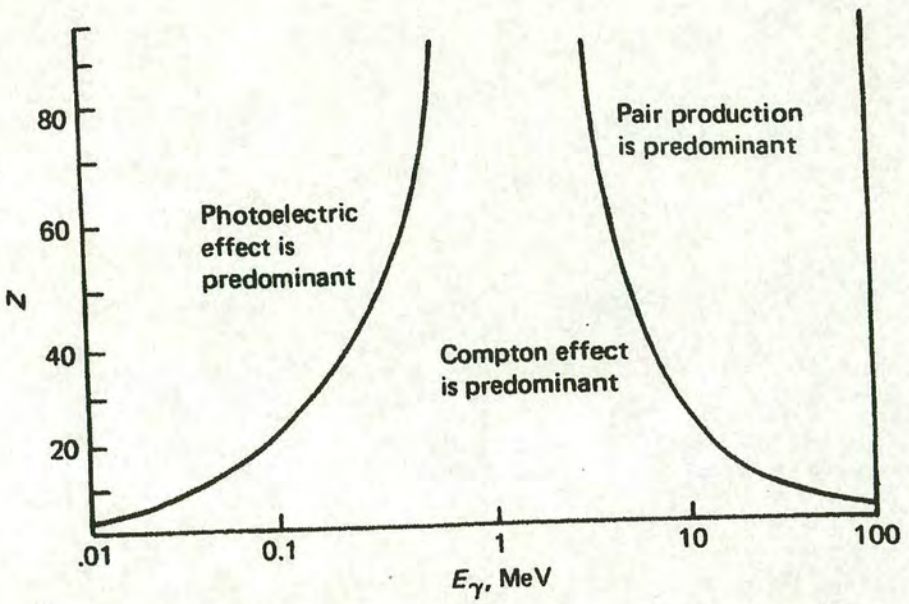

Fig. 2.29: The relative importance of the three major γ interactions (Evans, 1982).

$$\mu(m^{-1}) = \tau + \sigma + \kappa$$

where τ, σ, and κ are probabilities for photoelectric effect, Compton scattering, and pair production to occur per unit distance traveled by the photon. So, μ is the probability of interaction per unit distance (Tsoulfanidis, 1989; Leo, 1987). In the study of gamma attenuation in matter, the mass attenuation coefficient (μ_m) is mostly used rather than the linear attenuation coefficient. It is defined as:

$$\mu_m(m^2\ kg^{-1}) = \mu(m^{-1}) / \rho(kg\ m^{-3})$$

where ρ is density of the absorber. Figures 2.30 and 2.31 show the energy dependent attenuation coefficients for gammas in germanium and lead.

Direct quantitative measurement of many radionuclides in bulk environmental matrices is now possible by gamma-spectrometry using modern computer assisted spectral interpretation. The detector resolution becomes extremely valuable for the identification and precise measurement of radionuclides in these samples. Semiconductor germanium (Ge) detector systems are especially well suited in this respect because of their ability to resolve close lying peaks and to detect weak sources of discrete energies when superimposed on a broad continuum (Knoll, 1989).

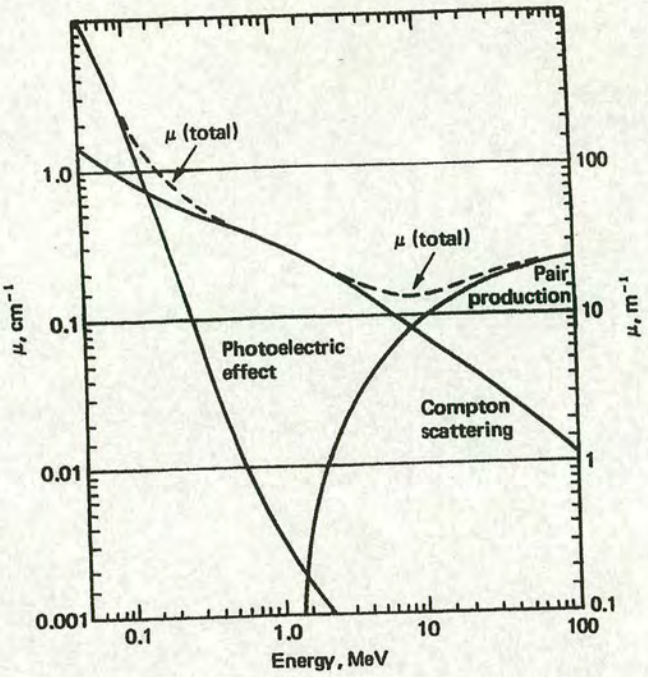

Fig. 2.30: Photon attenuation coefficients for germanium (Tsoulfanidis, 1989).

The usefulness of semiconductors for radiation measurements stems from the special properties created at a junction where *n*- and *p*-type semiconductors are brought into contact to form a single system with its own characteristics. The reverse-biased *n-p* junction constitutes an attractive radiation detector. The depletion region is the active volume of the detector. Electron-hole pairs produced there by radiation can be collected swiftly and efficiently (Tsoulfanidis, 1989; Knoll, 1989). Like ions in a gaseous ionization chamber, the number of electron-hole pairs, and consequently the electrical signal produced, is proportional to the energy deposited by radiation in the active volume. However, the conventional gas has been replaced in this case by a solid semiconductor material such as germanium or silicon. The W values (amount of energy required to create an electron-hole pair) for Ge and Si are, 2.98 eV and 3.81 eV at 77 K respectively; whereas, gases require about 30 eV of energy to produce an electron-ion pair. Thus, the amount of ionization produced for a given energy is an order of magnitude greater resulting in increased energy resolution and superior spectroscopic performance of semiconductor detectors (Muggleton,

1972; Leo, 1987). They have a greater stopping power due to their greater density; they are compact in size, and can have a fast response time. In comparison with scintillation detectors such as NaI(Tl), their outstanding energy resolution and enhanced peak to Compton ratios outweighs their relatively lower efficiency (Tsoulfanidis, 1989; Knoll, 1989).

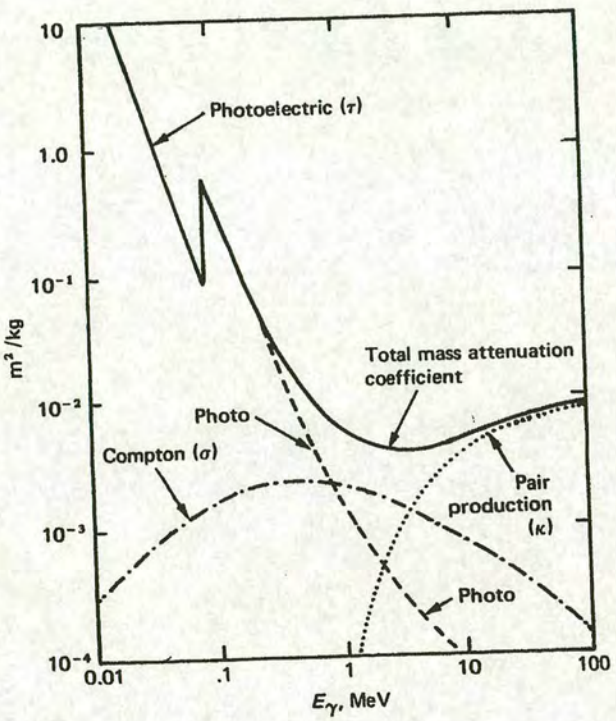

Fig. 2.31: Mass attenuation coefficients for lead ($\rho = 11.35 \times 10^3$ kg/m^3) (Tsoulfanidis, 1989).

The group IV elements Silicon and Germanium are by so far the most widely-used semiconductors. For gamma-ray detection, germanium is preferred over silicon because of its greater atomic number ($Z_{Si} = 14$, $Z_{Ge} = 32$), which results in a much greater photoelectric cross section. At the early stages of Ge-detector developement, there was a need for drifting lithium into germanium to compensate some p-type (acceptor) impurities normally present in pure materials which led to production of the so called *lithium-drifted germanium* [Ge(Li)] detectors. It is now possible to increase the purity of germanium to levels that correspond to impurity concentrations of less than 1 part in 10^{12} (compared to earlier 1 : 10^{11}) which makes lithium drifting unnecessary (Knoll, 1989). In addition, these *intrinsic* or *high purity germanium*

(HPGe) detectors make uninterrupted cooling less important; it is not required when storing the crystals, but should be used when measuring in order to improve resolution and prevent crystal overheating. HPGe crystals can be of either n- or p-type. The p-type detectors have usually a lower energy cutoff, beginning at about 100 keV, caused by the detector capsule wall and insensitive entrance layer. On the other hand n-type HPGe detectors can be made with a very thin entrance layer using ion-implantation technique and, when fitted with a Be-window, have a low energy cutoff beginning at about 6 keV. Intrinsic germanium detectors have to a large extent replaced the Ge(Li) detectors because of their greater handling simplicity at no higher cost or loss of resolution (Choppin et al., 1995).

Two HPGe detectors were used for gamma spectrometry in this study. The first one, is a Reversed-Electrode Coaxial Germanium (REGe) 4.4 cm in diameter by 4.3 cm length, with a thin Be window (0.5 mm), manufactured by Canberra. The detector efficiency is 12.9 % at 1.33 MeV [relative to a 7.62 x 7.62 cm NaI(Tl) scintillation detector, at a source-detector spacing of 25 cm], and its FWHM resolution is 865 eV at 122 keV. The second one (NGC), again in coaxial configuration with Be-Window-Thickness of 0.5 mm, is 4.4 cm in diameter by 3.8 cm length, with a relative efficiency of 11.1 % and a resolution of 810 eV at 122 keV, manufactured by Detector Systems GmbH (DSG).

2.2.1.2 Electronics and data acquisition

Besides the Ge detector, a gamma-ray spectrometer usually consists of a cryostat and preamplifier; detector bias supply; linear amplifier; analog-to-digital converter (ADC); multichannel storage of the spectrum and data-readout devices, or more often nowadays, a micro-processor with display screen, printer and data storage facilities; and finally a background-radiation shield, which surrounds the detector. Figure 2.32 shows a schematic diagram of a typical gamma spectrometer system.

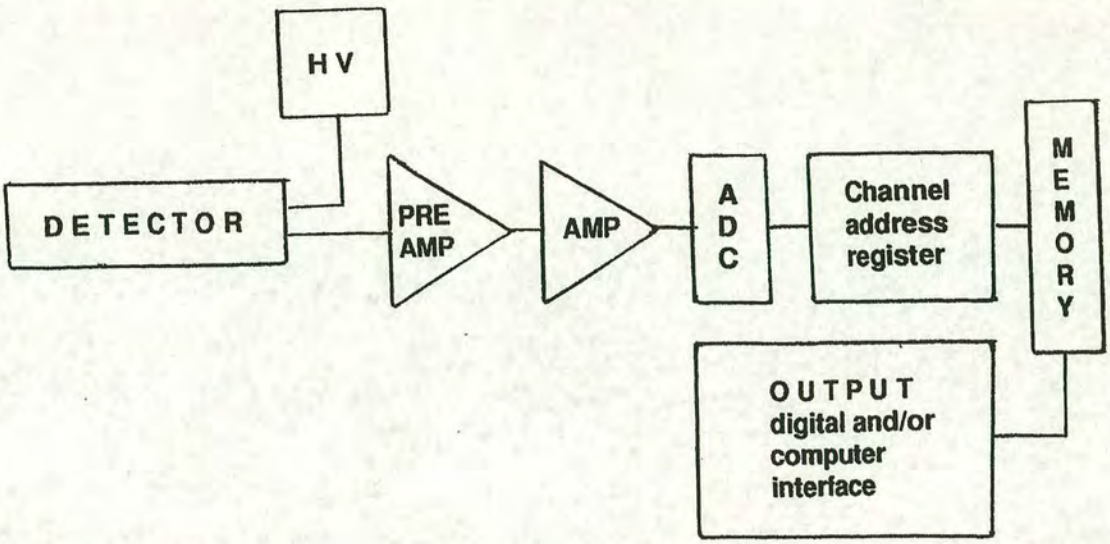

Fig. 2.32: Schematic diagram of a typical γ spectrometer.

The cryostat consists of a reservoir or Dewar containing the cooling medium and a vacuum-chamber housing the detector. Liquid nitrogen (LN_2) is the most common medium for detector cooling. The cryostat used with the REGe detector is a dipstick type. The detector is mounted at the end of a copper cooling-finger, which conducts the LN_2-temperature from the reservoir to the detector. An integral type cryostat has been used in conjunction with the second Ge detector. In this case, the detector chamber is permanently attached to the Dewar.

Commercial cryostats include the preamplifier as a standard component. The preamplifier plays the roles of collecting and integrating the charge deposited in the detector, converting it into an output voltage pulse, and providing an optimized coupling between the output of the detector and the rest of the counting system. The voltage pulse can be then carried by the cable that connects the preamplifier to the main amplifier. This has to be done without significantly degrading the intrinsic signal-to-noise ratio. Therefore, the preamplifier is located as close to the detector as possible to minimise the effect of stray capacitance, and in order to take advantage of the cooling which aids the preamplifier to operate with low noise (IAEA, 1989; Tsoulfanidis, 1989).

The 0-5 kV Ortec *high-voltage power supply* (HVPS) units were used to provide 2 and 3 kV bias supplies required by the NGC and REGe detectors, respectively.

The function of the main amplifier is to amplify the signal from the preamplifier and, to shape it to a convenient form for optimum analog to digital conversion. In this process, a strict proportionality between input and output amplitudes (i.e. linear amplification) must be preserved. Linear amplifiers manufactured by Ortec, were used to set up the two spectrometers. The Gaussian type of shaping was selected with time constants of 4 and 6 μs for the NGC and REGe systems, respectively. The gains were adjusted to 0.17 keV/channel.

Amplified and shaped pulses from the two detectors were analysed by the Canberra AccuSpec PC-based multi-channel analyser (MCA), which contains a computer-controlled, 100 MHz, Wilkinson ADC with 8 K channels of spectral memory. The ADC is the backbone of an MCA which converts the amplitude of a voltage pulse from analog to digital format. In a Wilkinson type ADC the input signal is served to charge a capacitor, which is then discharged at a constant rate. This *run down* is timed by counted pulses from a constant frequency osillator to give a number proportional to the charge on the capacitor. These numbers which correspond to the analog amplitudes at the ADC input, are fed to a dedicated memory and sorted into a histogram to record the number of events counted in each pulse-height interval. The contents of each memory channel can then be displayed on a screen or printed out to give a pulse height spectrum, which is actually a representation of the gamma energy spectrum observed by the detector (Knoll, 1989; Leo, 1987).

The spectra were accumulated in 8192 channels for each detector and covered a typical energy interval of 14-1400 keV. Data acquisition were mostly performed on Dell 486 PCs, using Canberra Genie-PC software.

In the case of samples from Dunslair Heights in the early stage of this work, REGe amplified pulses were fed into a GEC 4090 computer via an ADC, and the analysis of the spectra were carried out using programs developed at the Nuclear Structure Facility at the Daresbury Laboratory (NSFD).

2.2.1.3 Background reduction

Within the normal limitations encountered in environmental radiation studies (i.e. small activities, long counting times and large sample sizes) one must try to decrease as much as possible the contribution of backgrounds under the peaks which are present in all low-level radioactivity measurements. The background under the peaks come mainly from Compton backgrounds of high energy gamma-rays plus accidental occurrence of peaks with the same energies from different radionuclides. A reduction of the gamma background is essential in order to identify the low intensity peaks, which is difficult primarily in the presence of the Compton continuum seen by gammas at lower energies and, the gamma rays not from the sample(see Figure 2.33). The natural radioactive background originates from the uranium and thorium series, from ^{40}K, and from cosmic rays. Natural radionuclides may be present in the system components, the surrounding environment, and within the sample matrix itself.

Both the detector and sample being counted are usually enclosed in a *castle* of high-Z material (normally lead) to reduce the background contribution of the surrounding environment. The cosmic-ray component, however, can be removed only through massive amounts of shielding. An alternative arrangement is the elimination of the highly penetrating cosmic radiation through the use of an *anticoincidance shield* (also called *Compton suppression system*) (Knoll, 1989). This arrangement not only provides a greatly reduced natural background but also removes much of the Compton interference from radionuclides within the sample matrix.

In this technique, a central Ge detector is surrounded by a second large detector which is usually made of NaI(Tl), plastic scintillator, or BGO. A popular and relatively low cost anti-Compton system is the commertialized NaI(Tl) crystal which has cylindrical geometry with a 3 in. hole in the centre (Kiang et al., 1993). Gamma-rays which may undergo Compton scattering and thereby deposit only a portion of their energy in the Ge detector, may be detected in the NaI crystal. Suitable anti-

coincidance circuitry cancels the signal from the Ge detector and only those pulses not accompanied by pulses from the NaI crystal are stored in the spectrum.

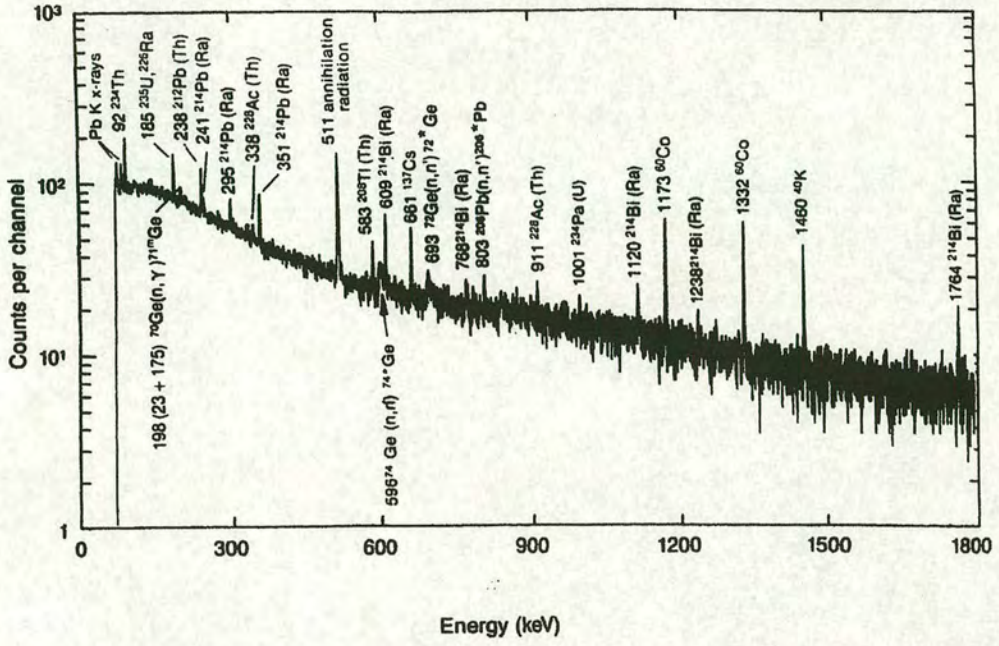

Fig. 2.33: Background γ - ray spectrum obtained with an HPGe detector.

An anticoincidance unit is an electronic device that accepts pulses (events) in two input channels and provides an output signal *only* if the two events *do not* arrive within the time period τ. The logic of an anticoincidence unit is illustrated in Figure 2.34.

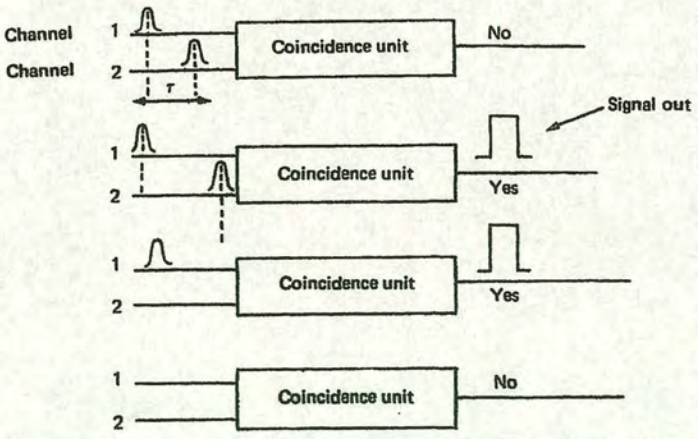

Fig. 2.34: The logic of an anticoincidence unit (Tsoulfanidis, 1989).

With the purpose of achieving adequate background levels, both Ge detectors were surrounded by 10-cm thick lead shields constructed from low-activity lead bricks. This is the optimum thickness of lead shielding for such an application. A greater thickness would result in an increased background due to the buildup of tertiary cosmic-ray particles (Lindstorm et al., 1990).

The REGe detector has been in operation in cojunction with an annular NaI(Tl) scintillation guard detector to reduce the Compton continuum. The NaI(Tl) anticoincidence system has improved the peak to Compton ratio by a factor of 4 for ^{137}Cs peak. Figure 2.35 shows a Compton-suppressed, and unsuppressed spectra for a ^{137}Cs source collected with the REGe detector.

The lead shield for the NGC detector was constructed using brass plate as the support for the ceiling. An inner sleeve of approximately 1 cm thick copper was also mounted to shield the detector from background-^{210}Pb gamma rays and lead-fluorecence K X-rays (ANSI, 1991). This combination has reduced the ^{210}Pb background count-rate by almost 60 %.

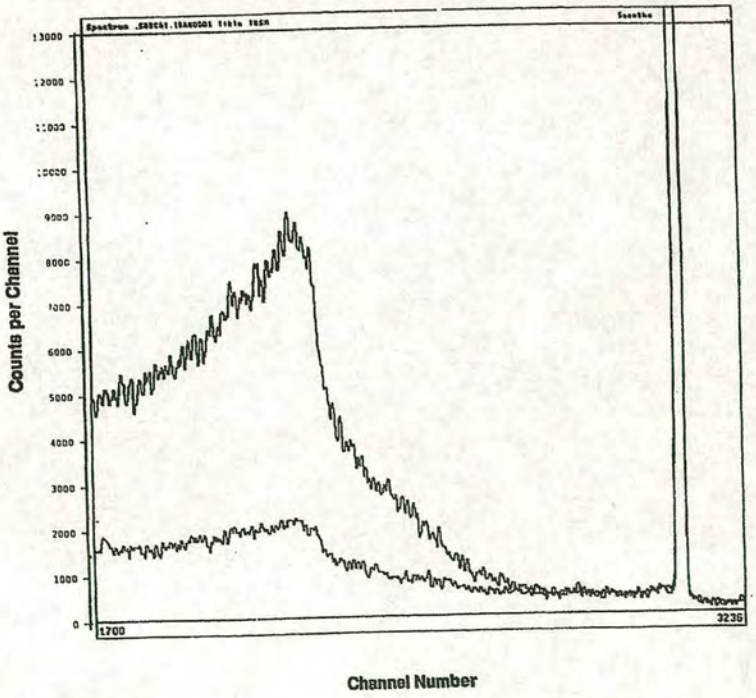

Fig. 2.35: The ^{137}Cs spectrum recorded with and without Compton suppression using the REGe detector system.

2.2.2 Calibration Techniques

The main objectives of gamma-ray spectrometry are: first, to determine the energy spectrum of gamma radiation emitted from a sample in order to identify the corresponding radionuclides, and secondly to dtermine the number of gamma rays emitted. These objectives are achieved by *energy calibration* and *efficiency calibration,* respectively.

2.2.2.1 Energy calibration

The energy calibration is an essential requirement of a gamma-spectrometer system which represents gamma-ray energy as a function of channel number. This is most conveniently achieved using a commercially available mixed source standard. The National Physical Laboratory (NPL) low-level Mixed Radionuclide Standard has been used for this purpose which covers the energy range of interest for environmental radioactivity measurements. The calibration was established by measuring the positions of selected full-enrgy gamma-ray peaks whose energies are known precisely. A typical result of such an energy calibration is shown in Figure 2.36.

2.2.2.2 Efficiency calibration

The basis of all quantitative radioactivity measurements is the direct proportionality between the amount of radioactive substance in the sample and the intensity of the measured radiation. Not all the gamma rays emitted by a specific source
will strike the detector. Moreover, only a fraction of the incident photons will undergo an interaction which will be actually registered by the system. Therefore, an accurate

efficiency calibration of the system is necessary to quantify radionuclides present in a sample.

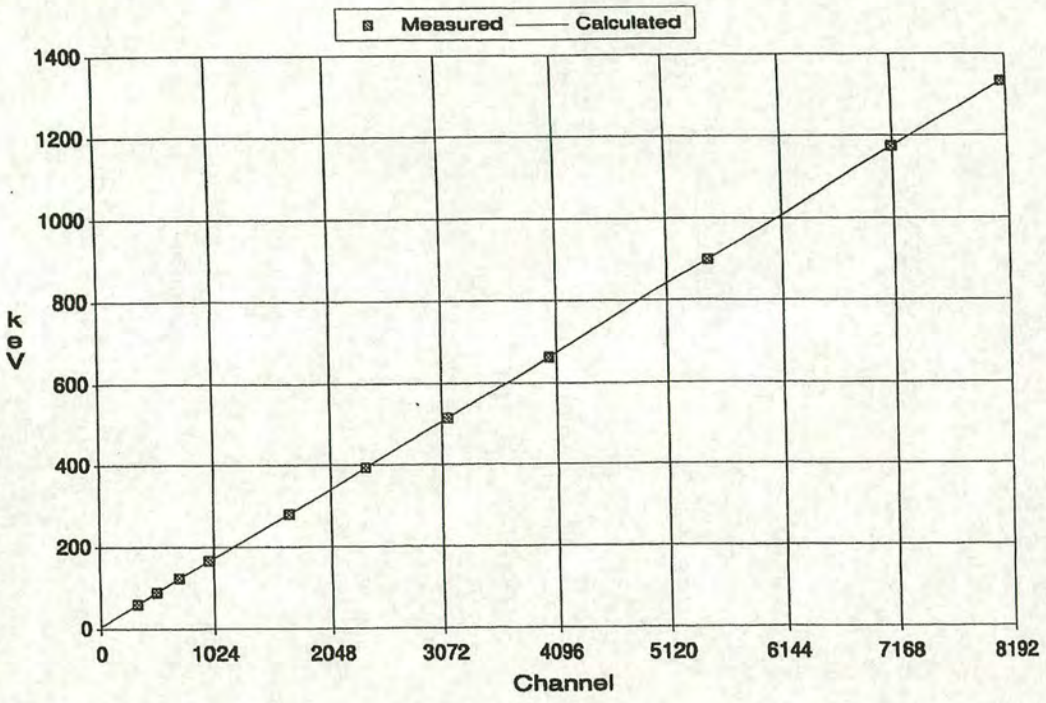

Fig. 2.36: Energy calibration for the NGC spectrometer using NPL mixed source.

Many attempts have been described in the literature to calculate the efficiency of Ge detectors by Monte Carlo methods or to derive it for a particular geometry from measurements of the efficiency for a point-source geometry. However, the method preferred world-wide for determining the efficiency in environmental measurements is the experimental one which involves relative or comparative measurements (IAEA, 1989).

It is a general practice in gamma-ray spectrometry to establish a calibration curve as a function of energy for a defined geometry and energy range. In most cases, it is the *full-energy peak efficiency* (ε_{FEP}), i.e., the efficiency for photoelectric conversion, which is desired. This is given by the total count rate in the photopeak for each gamma-ray devided by the total output of the source (Leo, 1987). It is a function

of both detector geometry and intrinsic efficiency. The intrinsic efficiency depends on $\mu(E)$ (see Figure 2.30), and the size of the Ge crystal. At low energies, it also depends on cross-sectional area as well as window thickness. So, the full-energy peak efficiency of any Ge spectrometer has to be determined for the energy range of interest at each counting configuration. This is usually accomplished by preparing practical calibration standards in an appropriate matrix to the sample under consideration, from appropriate certified radionuclides. A typical result of such an efficiency calibration is shown in Figure 2.37.

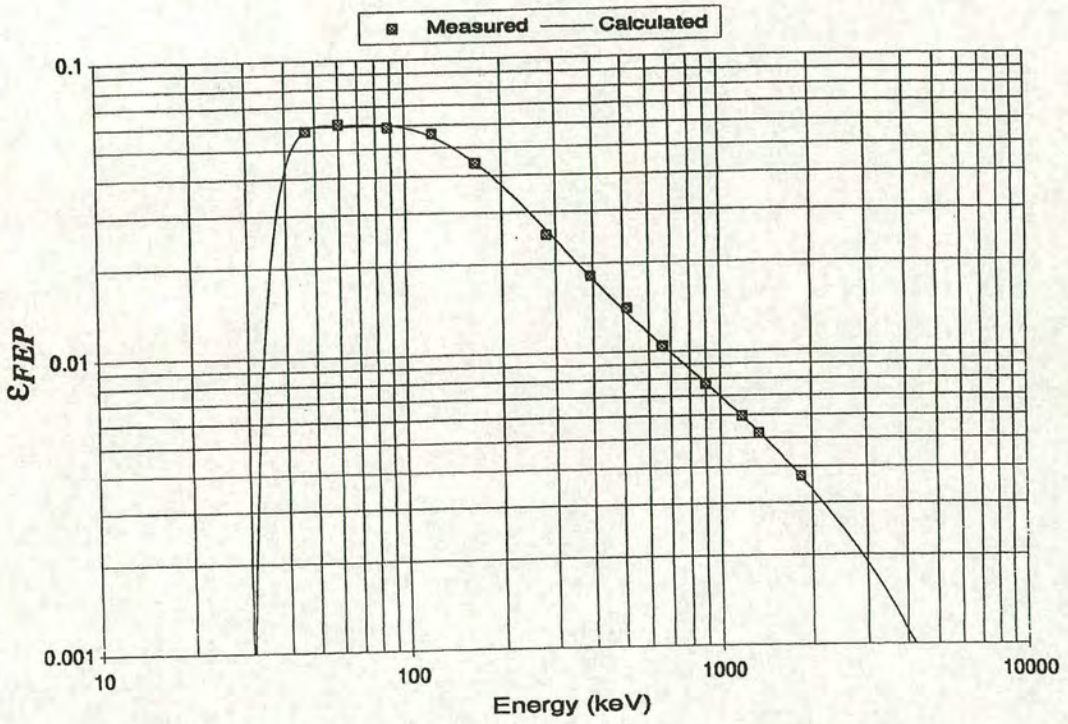

Fig. 2.37: Typical full-energy peak efficiencies for gamma-rays of different energy of the REGe spectrometer.

When the activity or gamma-ray emission rates of a limited number of radionuclides are to be measured, and if there is a calibration source available which contains the same nuclides as the actual source, there is no need to make use of any efficiency calibration curve. Instead, the "radionuclide-related" efficiency method would be the choice which is the most accurate and straightforward. This method

measures a *standardization coefficient* for a selected gamma ray emitted from each specific radionuclide. The coefficient then converts the net peak-area counting rate to the activity of the radionuclide being measured (ANSI, 1991). In the present study, efficiencies for ^{210}Pb and ^{137}Cs gammas were determined by radionuclide-related method, and the efficiency for ^{214}Pb gammas was derived from appropriate efficiency curves.

Calibration of the Ge spectrometers was accomplished by preparing standard soil and vegetation matrices in geometries identical to those used for the soil samples. To achieve a reproducible source-to-detector distance, thin-walled perspex sample holders 70.6 mm in diameter by 26.5 mm deep were precisely machined which mount onto the detectors. The depth of sample holder was chosen on the basis of an optimization study which had been carried out in advance for 46.5 keV gammas.

A further important aspect in the measurement of environmental samples is that of self-attenuating effects within the sample. The attenuation coefficient for gamma rays in the energy range of interest varies significantly from the low to the high end of the region and with sample density. At the early stage of this study, the Cutshall method (Cutshall et al., 1983) was applied for sample self-attenuation correction of the low energy gammas from ^{210}Pb. It relies on calibration of the detector with a standard matrix and the application of a correction factor based on the measured attenuation of a ^{210}Pb source through each sample. The technique relates the attenuated sample output (O) to the sample photon emission rate (A) by the expression

$$A = O\,[\ln(I / I_0) / (I / I_0 - 1)]$$

in which I_0 and I are photon emission rates of a ^{210}Pb disc source through the standard matrix and sample, respectively. For this purpose, a standard matrix was prepared using vegetation standard provided by ITE Merlewood.

Critical examination of the Cutshall method have been performed by Galloway (1990) and Miller (1987). Galloway presents a semi-empirical method which corrects for the effect of self-attenuation as well as the change in effective solid angle for different attenuating material. A more general method for the problem of self-

attenuation and voluminous source efficiency has also been developed by Overwater et al. (1993).

However, due to limited number of detectors and geometries involved, and in order to be as close as possible to the field conditions, the more conventional spiked matrix method has been followed for the rest of the study. The variation in attenuation effects, particularly at low energies, caused by the wide variation of sample densities demand a range of spiked matrices which will allow density corrections to be made. These matrices were prepared by spiking field samples with solutions of known radionulide concentrations including a certified ^{210}Pb solution obtained from the French *Laboratoire de Metrologie des Rayonnements Ionnisants* (LMRI) and a low-level Mixed Radionuclide Standard Solution from NPL, which contained ^{241}Am, ^{109}Cd, ^{57}Co, ^{139}Ce, ^{203}Hg, ^{113}Sn, ^{85} Sr, ^{137}Cs, ^{88}Y and ^{60}Co. The sample spikings were performed according to ANSI N42.14-1991 standard (ANSI, 1991). The derived efficiencies were checked against standard soil and sediment samples (IAEA/SOIL-6 & IAEA 368) obtained from Analytical Quality Control Service of the International Atomic Energy Agency in Vienna. Figure 2.38 shows an example of efficiecy vs density curve of the NGC spectrometer for ^{210}Pb gammas.

2.2.3 Determination of ^{210}Pb and ^{137}Cs soil inventorios

Activities of ^{210}Pb and ^{137}Cs were determined by their gamma emissions at 46.5 and 661.6 keV, respectively. The 351.9 keV gamma of ^{214}Pb was used to measure the in situ decay of ^{222}Rn in order to correct for the supported (non-atmospheric) fraction of ^{210}Pb in soil. To ensure the radioactive equilibrium, samples were sealed in standard holders and left for about two weeks before counting. Spectra were accumulated for periods ranging from several hours to two days depending on the activity concentrations of the samples.

The number of gamma-rays emmited per second, *R(E)*, for each of the full energy peaks is calculated with the following equation:

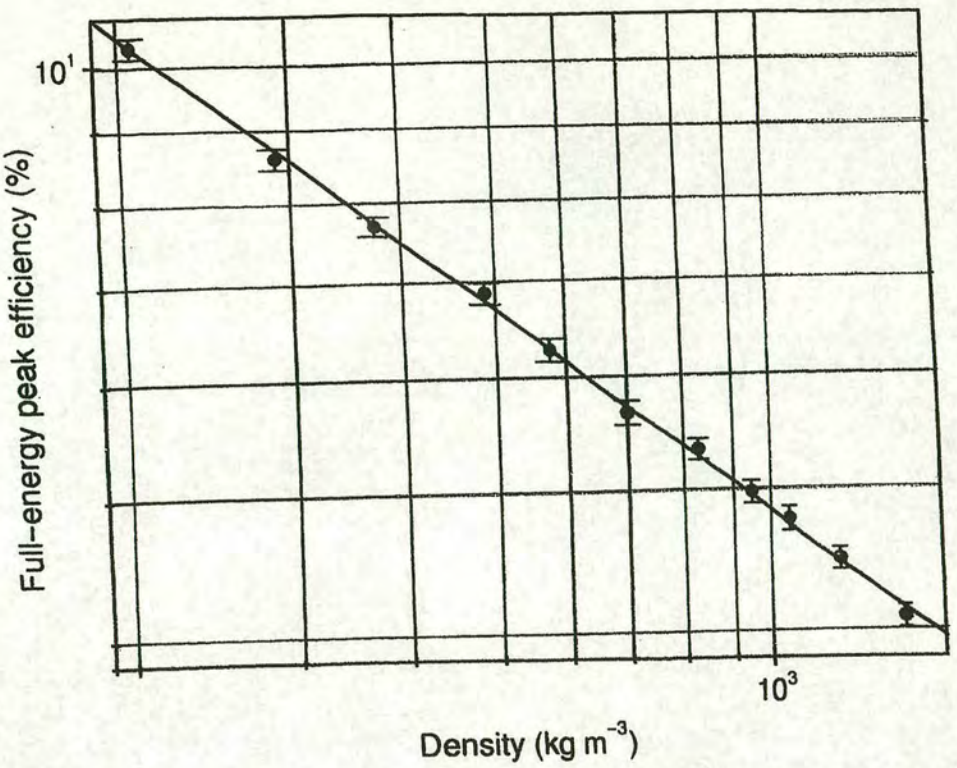

Fig. 2.38: Full-energy peak efficiency, ε_{FEP}, as a function of the matrix density for 46.5 keV gammas.

$$R(E) = [\, n(E) - B(E) \,]\, [\, \Pi C_i / \varepsilon_{FEP}(E) \,]$$

in which $n(E)$ is the counting rate in the net area of the full energy peak at energy E, $n(E) = N(E) / T_l$, where $N(E)$ is the net peak area and T_l is the counting (live) time, $B(E)$ are the net counting rate of the interference peaks in the background, $\varepsilon_{FEP}(E)$ is the full-energy-peak efficiency, and C_i are correction factors including corrections for decay prior to a count, and variation in the attenuation by the sample matrix due to differences in the densities of the sample (if applicable). The radionuclide activity is then calculated by dividing the gamma-ray emission rate by the the appropriate gamma-ray emission probability or *branching ratio*, $b\gamma$

$$A = R(E) / b\gamma$$

Inventories (in Bq m^{-2}) of ^{210}Pb derived from the atmosphere were determined for each of the cores by integrating over the entire core depth the total activity of ^{210}Pb in excess of any ^{210}Pb activity supported by the in situ decay of ^{222}Rn (Moore

& Poet, 1976; Nozaki et al., 1978). Expressing the soil inventory in activity per unit area is advantageous because it would be independent of soil density, which varies considerably between and within sites. The ^{137}Cs inventories were determined by integrating ^{137}Cs activities in each of the cores over the entire core depth.

2.3 Loss-on-ignition Measurement

The weight loss on ignition measurement was carried out on a limited number of soil samples from Dunslair Heights. These were cores taken from sampling points 1A, 2C and 3A, located in the open field, 1st row and 2nd row within the canopy, respectively. Small portions of soil each representing a core sub-division were placed in an oven at 40° C for 24 hours. This treatment was applied to exclude any absorbed moisture since the time they had been air-dried in preparation for gamma-ray analysis. Samples were then weighed and placed in an electric furnace for 15 hours at 450° C. They were re-weighed after removal. The weight loss, which is usually expressed as a percentage of the weight of the original sample, is taken to correspond to the organic matter content of the soil sample.

Chapter 3

Presentation of Results

In this chapter, the results of the γ-ray analyses on the collected vegetation and soil samples are presented. The inventories of atmospherically derived ^{210}Pb and ^{137}Cs are reported , followed by the profiles of specific activities of these radionuclides down soil cores at each site. Finally, loss-on-ignition results are presented for the representative samples from Dunslair Heights.

The activity levels are back-dated to the time of collection, and the soil inventories are reported in units of Bq m^{-2} so that they are independent of soil density, which varies considerably between and within sites. Details of the conversion procedure from γ-counts to activity per unit area have been discussed previously in section 2.2.3. To obtain the ^{210}Pb inventories, activity in each case was integrated over the entire core depth. The ^{210}Pb specific activity profiles generally demonstrate the fact that when no mixing occurs the profile of ^{210}Pb in soil decreases exponentially with depth. Correction for the supported ^{210}Pb due to the in situ decay of ^{222}Rn was performed by subtracting the ^{214}Pb activities for each section of the core. No such correction was needed in the case of solely atmospheric-origin ^{137}Cs. Inventories were simply integrated over the entire core depth to obtain the total activity.

No attempt has been made to estimate the Chernobyl contribution in ^{137}Cs measured activities. Such a practice has been adopted in the early years after the massive release of ^{137}Cs and other fission fragments from the Chernobyl nuclear reactor, based on the activity ratio of $^{134}Cs/^{137}Cs$. The fission yield of ^{134}Cs is much

lower than that of ^{137}Cs, and due to its relatively short half-life (2.06 years) most of deposited ^{134}Cs would have been decayed out, considering the time laps between the accident (April 1986) and the course of these measurements (1993-1996).

The one-sigma percentage counting error for ^{210}Pb activity measurements depended on the activity concentration of each sample and on whether that the Compton shield was used. It was of order 3% for the more active top sections of the cores from Dunslair Heights and Dun Coillich, and up to 8% for the less active lower sections. The range was 4%-14% for Southwest Sweden samples, and 3%-12% for samples from Central Sweden. For the ^{137}Cs measurements, this uncertainty was of order of 2% -10%. The error bars in graphs on radionuclide inventories for individual cores, are due solely to the counting statistics. The error bars in graphs on mean radionuclide inventories represent standard error of the mean as an indication of the inherent variability at each location. From a consideration of the procedure used during field sampling and sample preparation, it is estimated that the systematic errors introduced in these stages are of order of ±10%. It is rather difficult to adapt an exact value to represent uncertainties involved in such procedures.

The results from Dunslair Heights, Dun Coillich, Southwest Sweden and Central Sweden are presented as follows in sections 3.1 - 3.4. In section 3.5 results of a Loss-On-Ignition measurement are presented.

3.1 Dunslair Heights (see section 2.1.1.1, Figures 2.4 & 2.5)

3.1.1 Lead 210 soil inventories

The inventories of atmospherically derived ^{210}Pb for the samples collected from Dunslair Heights are presented in Figures 3.1 and 3.2. Figure 3.1 shows the mean ^{210}Pb inventories for the open field, DH1, at the edge of stand, DH2, 15 m inside the canopy, DH3, and finally 40 m inside the forest canopy, DH4. The error bars in this graph represent standard error of the mean. Under canopy locations show substantially larger inventories with an average increase of approximately 37% with respect to the open grassland. Though it might seem that the inventory in DH3 is

higher than the other canopy locations DH2 and DH4 but, Duncan Multiple Range (DMR) test shows that these values are not significantly different at the 5% level of significance (see Figure 3.7). The levels of ^{210}Pb present in the individual cores are shown in Figure 3.2, where the error bars represent counting statistics. The coefficient of variation for the measured inventories is 5%, 18%, 13%, and 1% for DH1-DH4 locations, respectively. Note that the inherent variability in ^{210}Pb inventories is higher at the edge of canopy relative to the open grassland as well as other canopy locations.

The specific activity variation down soil cores are illustrated in Figures 3.3 to 3.6. These figures show clearly that the activity due to the atmospheric ^{210}Pb was found to be concentrated in the surface organic horizon and no significant amount of ^{210}Pb have leached below 10 cm depth. The deviation from the expected exponential decrease in the activity levels for 10-20 cm depth sections of DH2C, DH3A and DH3E cores (all of which are from the inside canopy sampling points) are rather exceptional considering the whole set of special activity profiles of all sites in this study.

Under the reasonable assumption of a steady state condition between the atmospheric supply of ^{210}Pb and its radioactive decay in soil, the average flux to the Norway spruce(*Picea abies*) canopy and the open grassland in Dunslair Heights would be 99 Bq m^{-2} y^{-1} and 72 Bq m^{-2} y^{-1}, respectively.

3.1.2 Caesium 137 soil inventories

The inventories for this radionuclide are presented in Figures 3.8 and 3.9. Mean ^{137}Cs inventories are shown in Figure 3.8 which follow almost the same trend as with ^{210}Pb results. The error bars in this graph represent standard error of the mean. The average ^{137}Cs inventory inside the forest canopy exceeds that in the adjacent open field by 34% which is very close to the percentage of canopy enhancement for ^{210}Pb deposition at this site. The mean inventories for the sampling locations inside the canopy are not significantly different at the 5% level of significance, according to DMR test (see Figure 3.14). This is the case between

DH1(at the open field) and DH2(at the edge of canopy) locations as well. Figure 3.9 shows the inventories for the individual sampling points, where the error bars are due solely to counting statistics. The coefficient of variation for measured inventories of ^{137}Cs is 17%, 26%, 16%, and 7% for DH1-DH4 locations, respectively. The inherent variability is higher relative to ^{210}Pb inventories, and again higher at the edge of canopy.

Depth profiles for specific activities are illustrated in Figures 3.10 to 3.13. These graphs show that ^{137}Cs is also highly concentrated in the surface horizons of soil at this site. The difference here is that the maximum specific activities was mostly found in the 1-5 cm depth interval rather than in the top most section of the cores. A relatively higher ^{137}Cs specific activity in the lower depth intervals has been observed in DH1D, DH2C, DH3E, DH4A and DH4D sampling points.

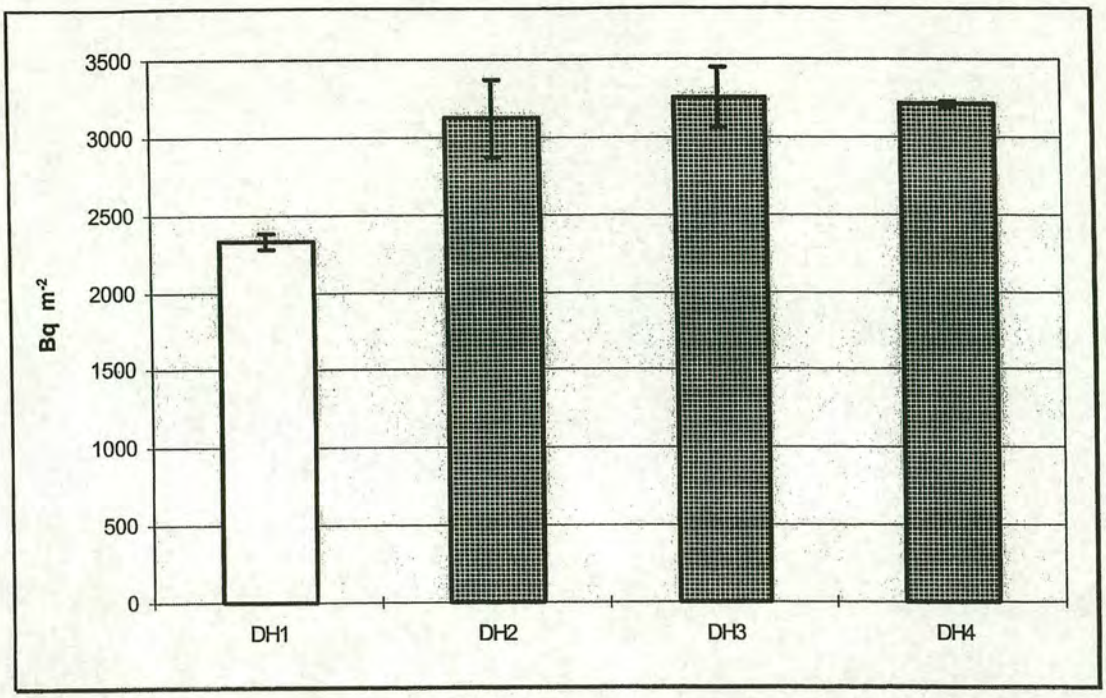

Figure 3.1: Mean atmospheric ^{210}Pb soil inventories in the open field (DH1), edge of the stand (DH2), 15 m from the edge (DH3) and 40 m inside the forest canopy (DH4) at Dunslair Heights.

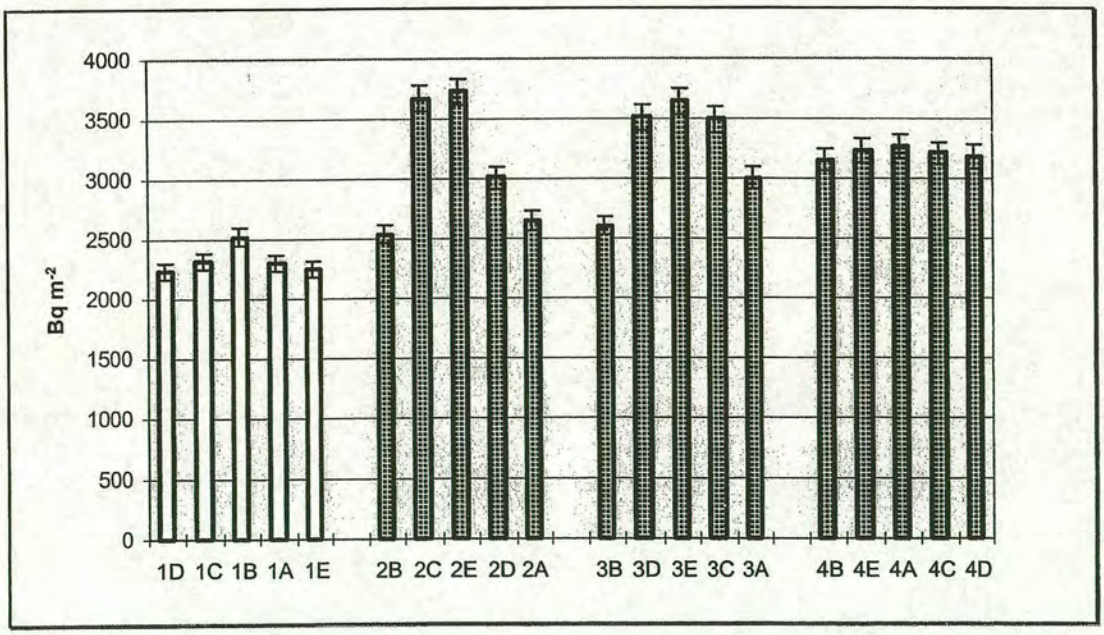

Figure 3.2: Atmospheric ^{210}Pb inventories measured in soil samples from each sampling point at Dunslair Heights.

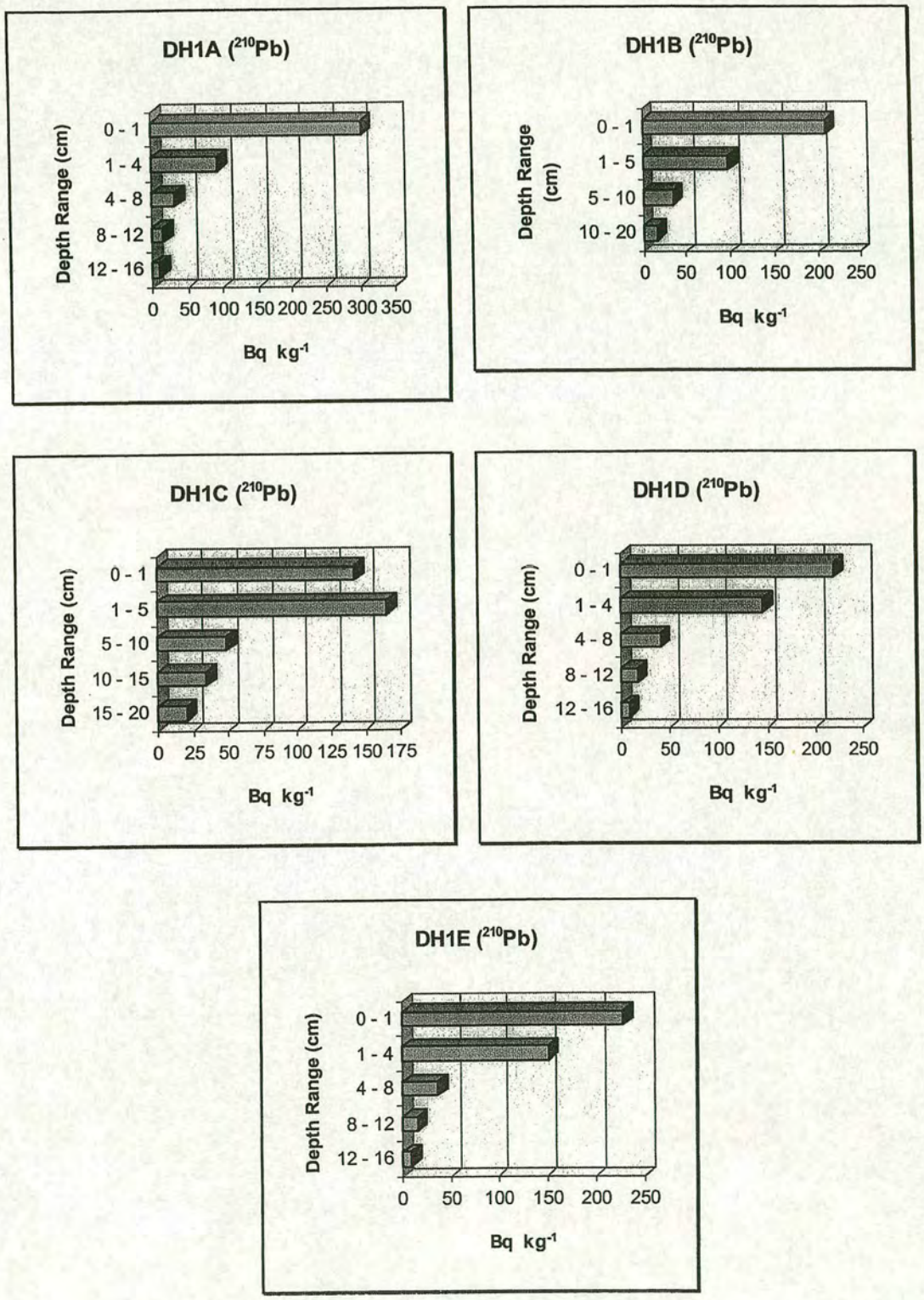

Figure 3.3: Distribution of atmospherically derived ^{210}Pb with depth at Dunslair Heights. Open field locations, DH1A - DH1E.

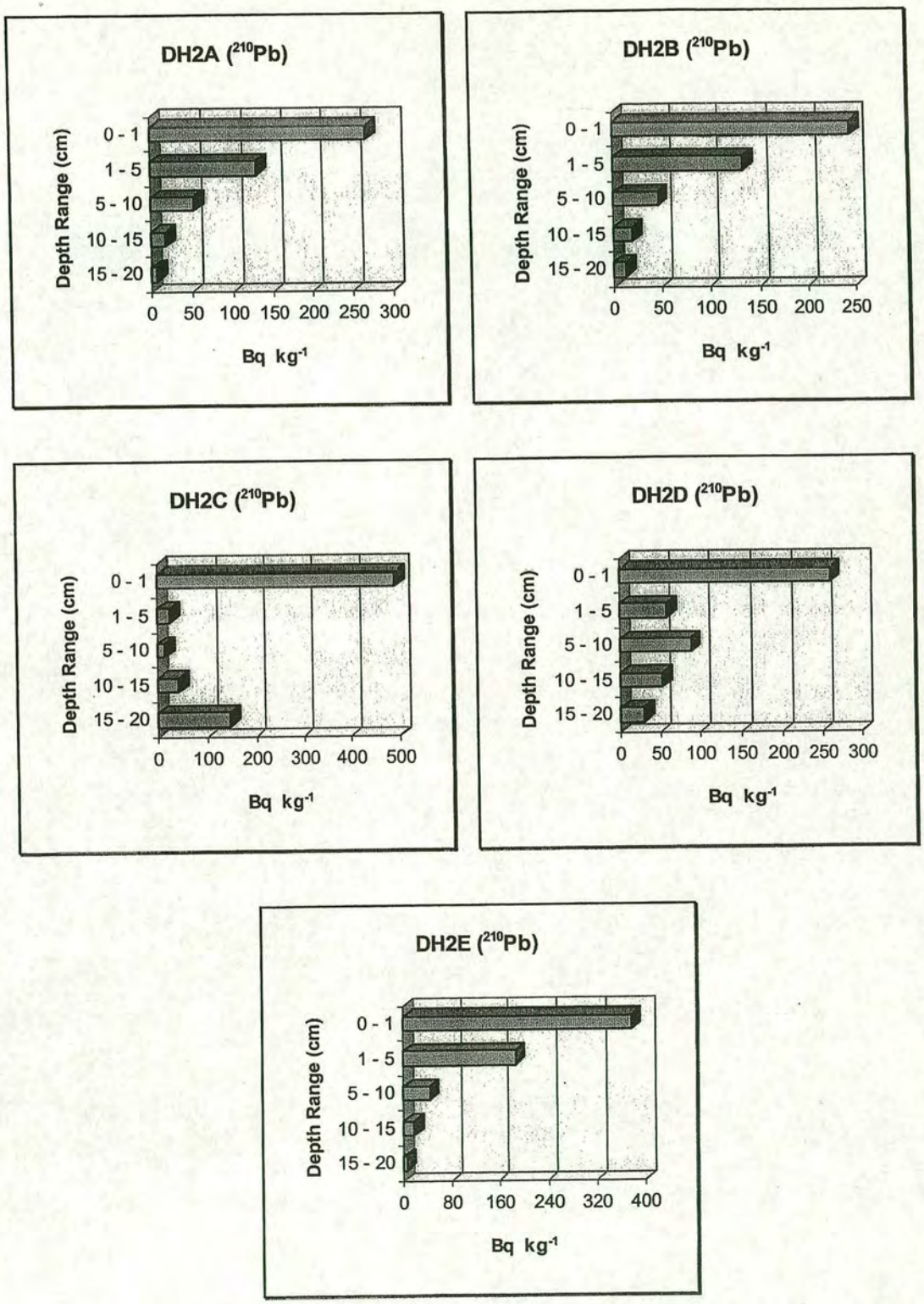

Figure 3.4: Distribution of atmospherically derived ^{210}Pb with depth at Dunslair Heights. Edge of stand locations, DH2A - DH2E.

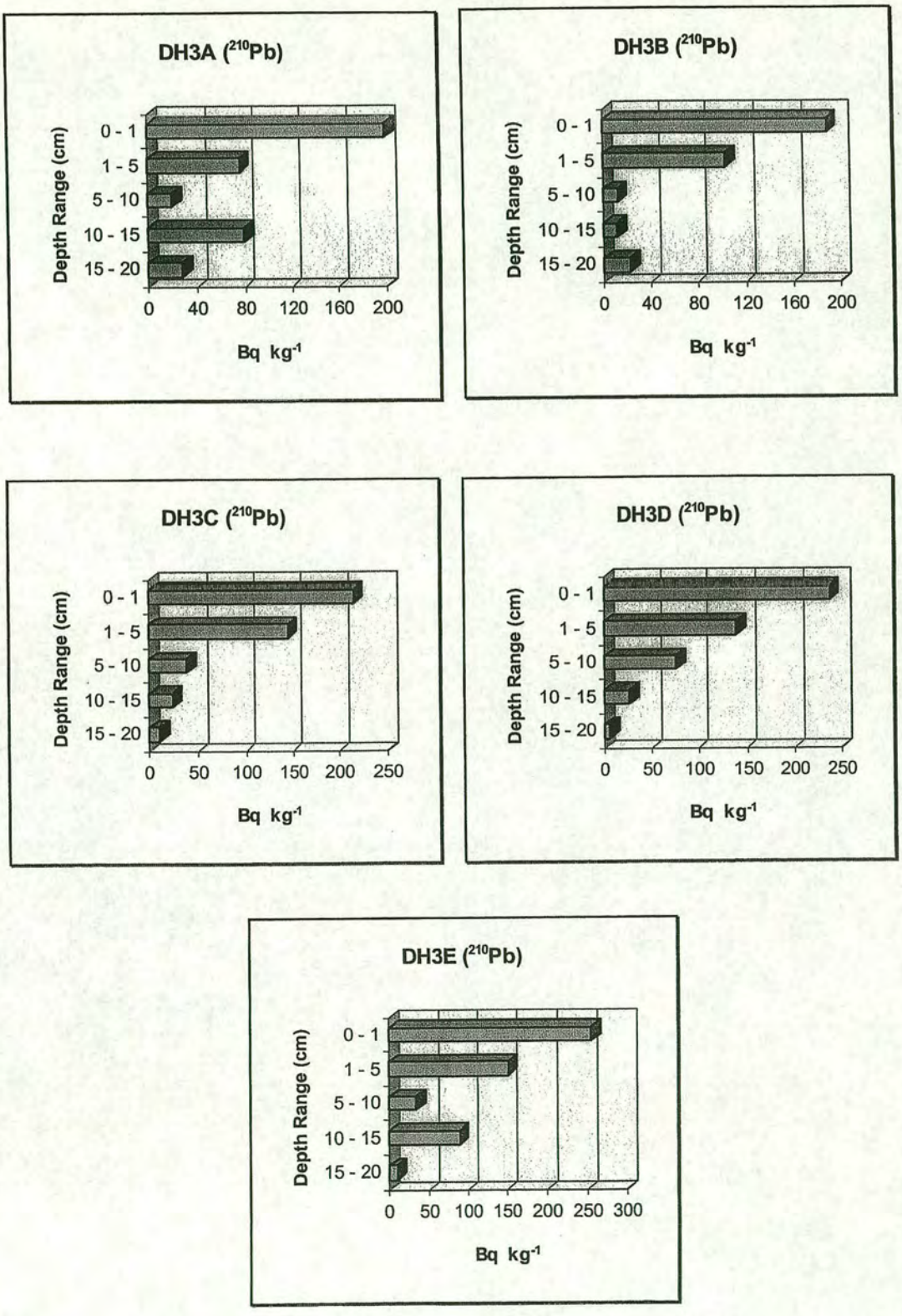

Figure 3.5: Distribution of atmospherically derived ^{210}Pb with depth at Dunslair Heights. Under canopy locations, DH3A - DH3E.

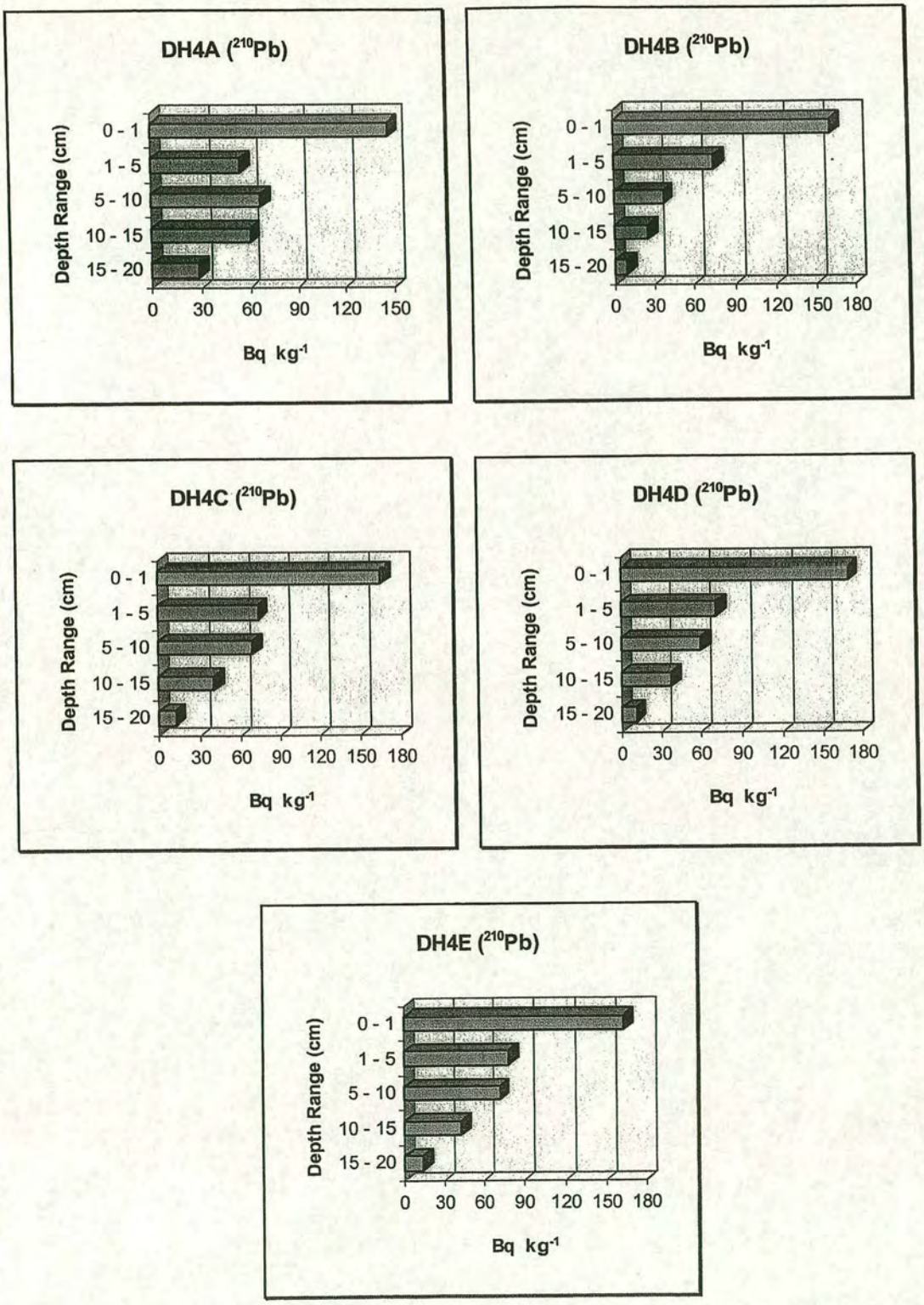

Figure 3.6: Distribution of atmospherically derived ^{210}Pb with depth at Dunslair Heights. Under canopy locations, DH4A - DH4E.

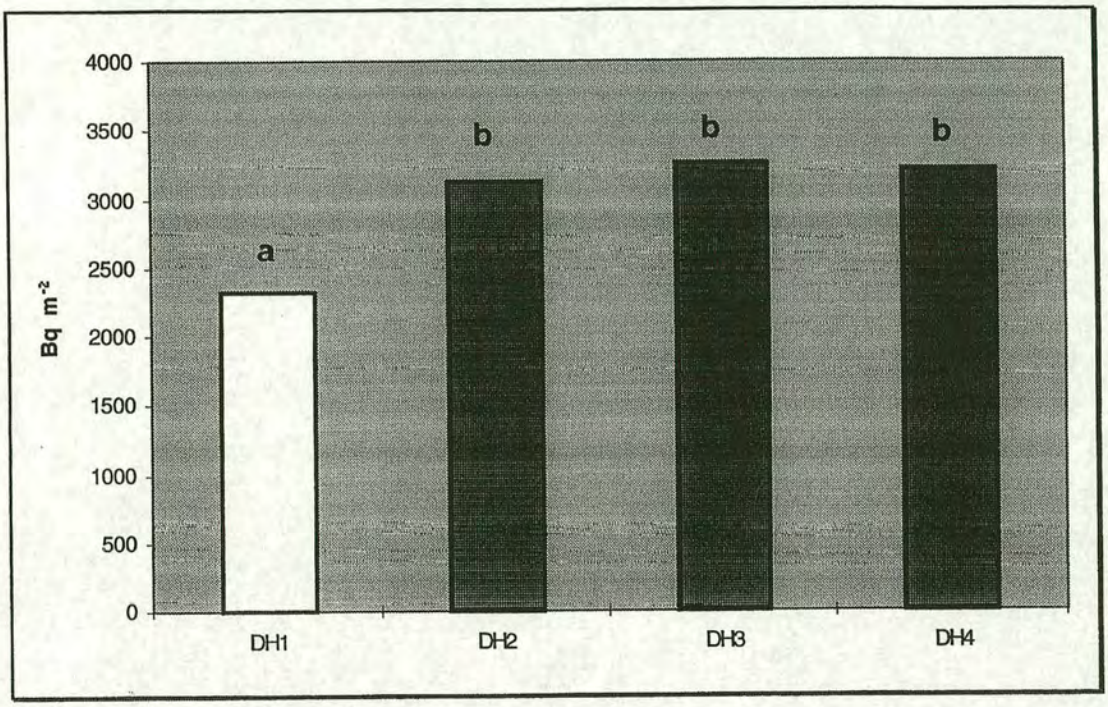

Figure 3.7: Mean atmospheric ^{210}Pb soil inventories in the open field (DH1), edge of the stand(DH2), 15 m from the edge (DH3) and 40 m inside the forest canopy (DH4) at Dunslair Heights.
The letters above each bar denote significant differences as derived from Duncan's multiple range test. Any two means having a common letter are not significantly different at the 5% level of significance .

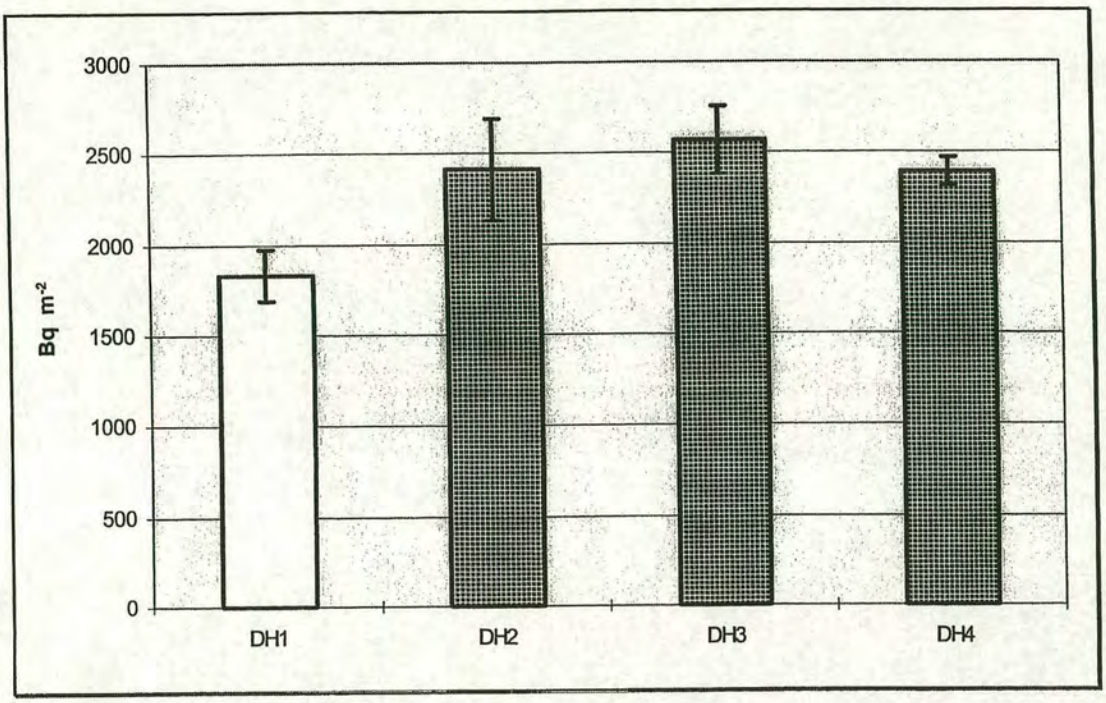

Figure 3.8: Mean ^{137}Cs inventories in the open field (DH1), edge of the stand (DH2), 15 m from the edge (DH3) and 40m inside the forest canopy (DH4) at Dunslair Heights.

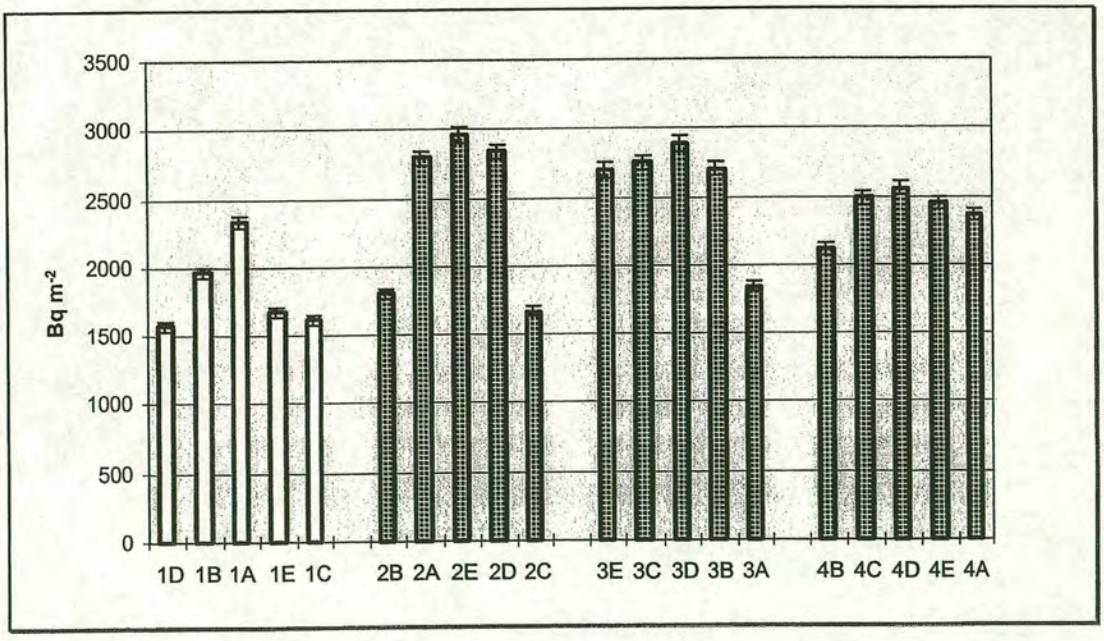

Figure 3.9: ^{137}Cs inventories measured in soil samples from each sampling point at Dunslair Heights.

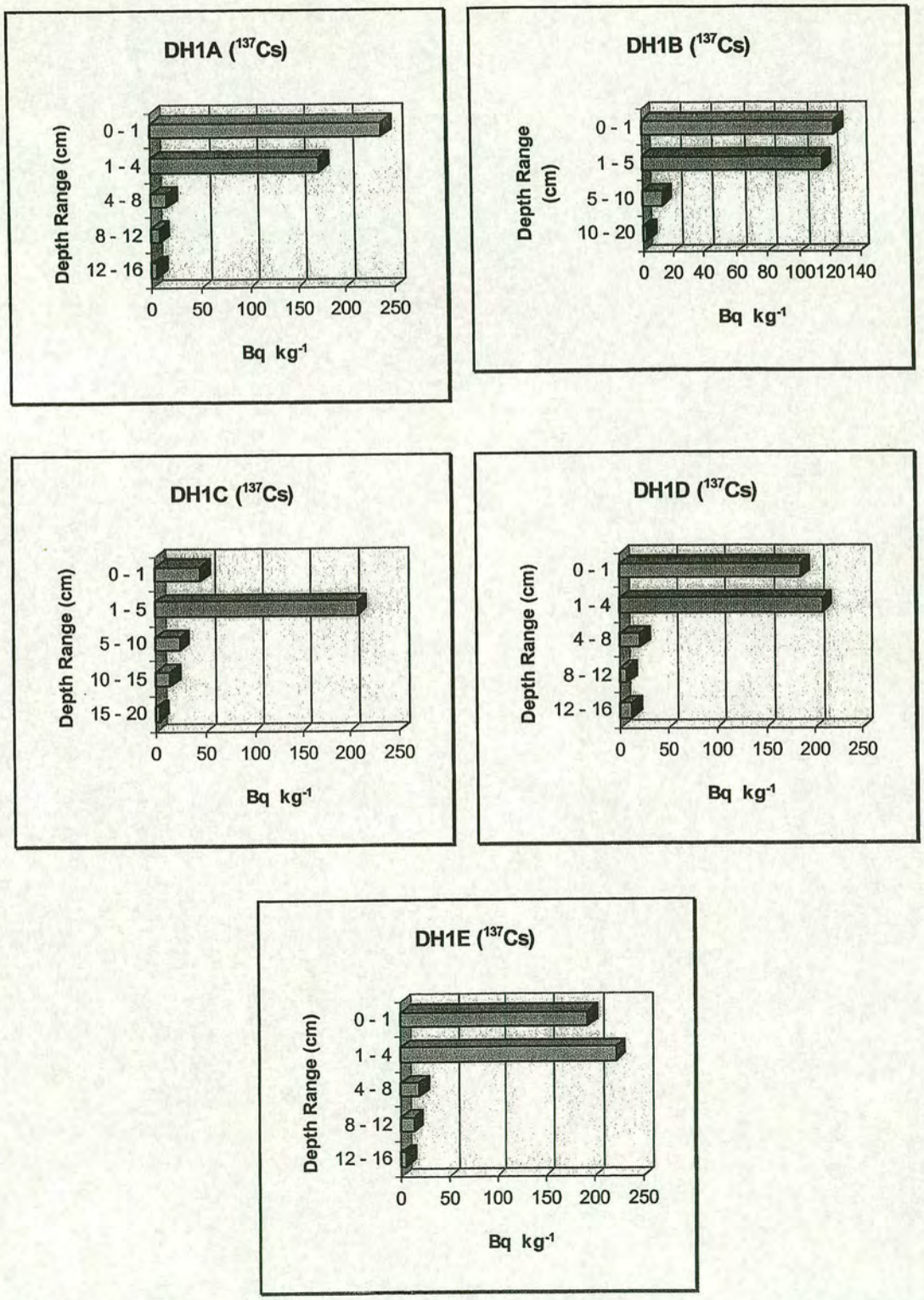

Figure 3.10: Distribution of ^{137}Cs with depth at Dunslair Heights.
Open field locations, DH1A - DH1E.

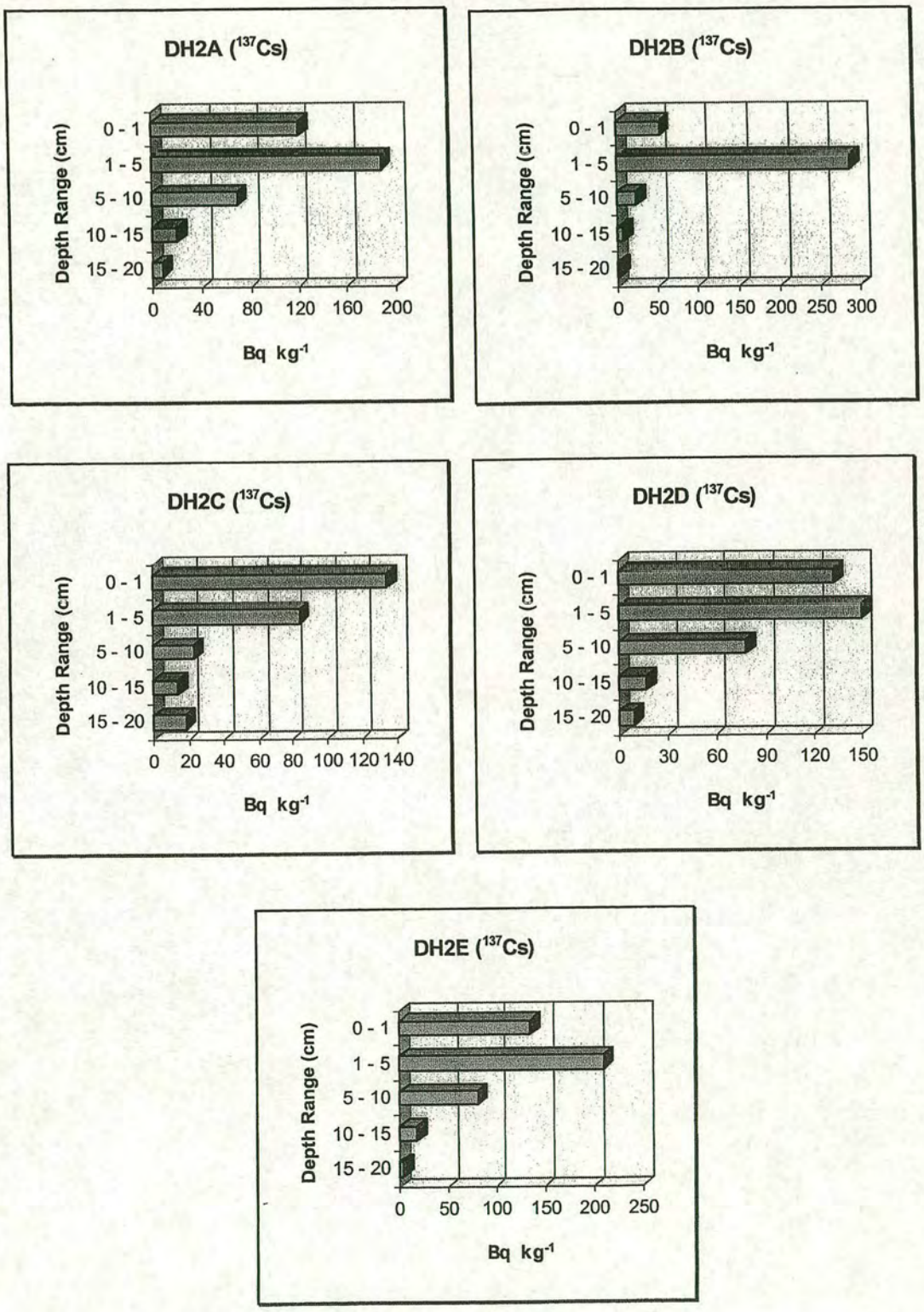

Figure 3.11: Distribution of ^{137}Cs with depth at Dunslair Heights.
Edge of stand locations, DH2A - DH2E.

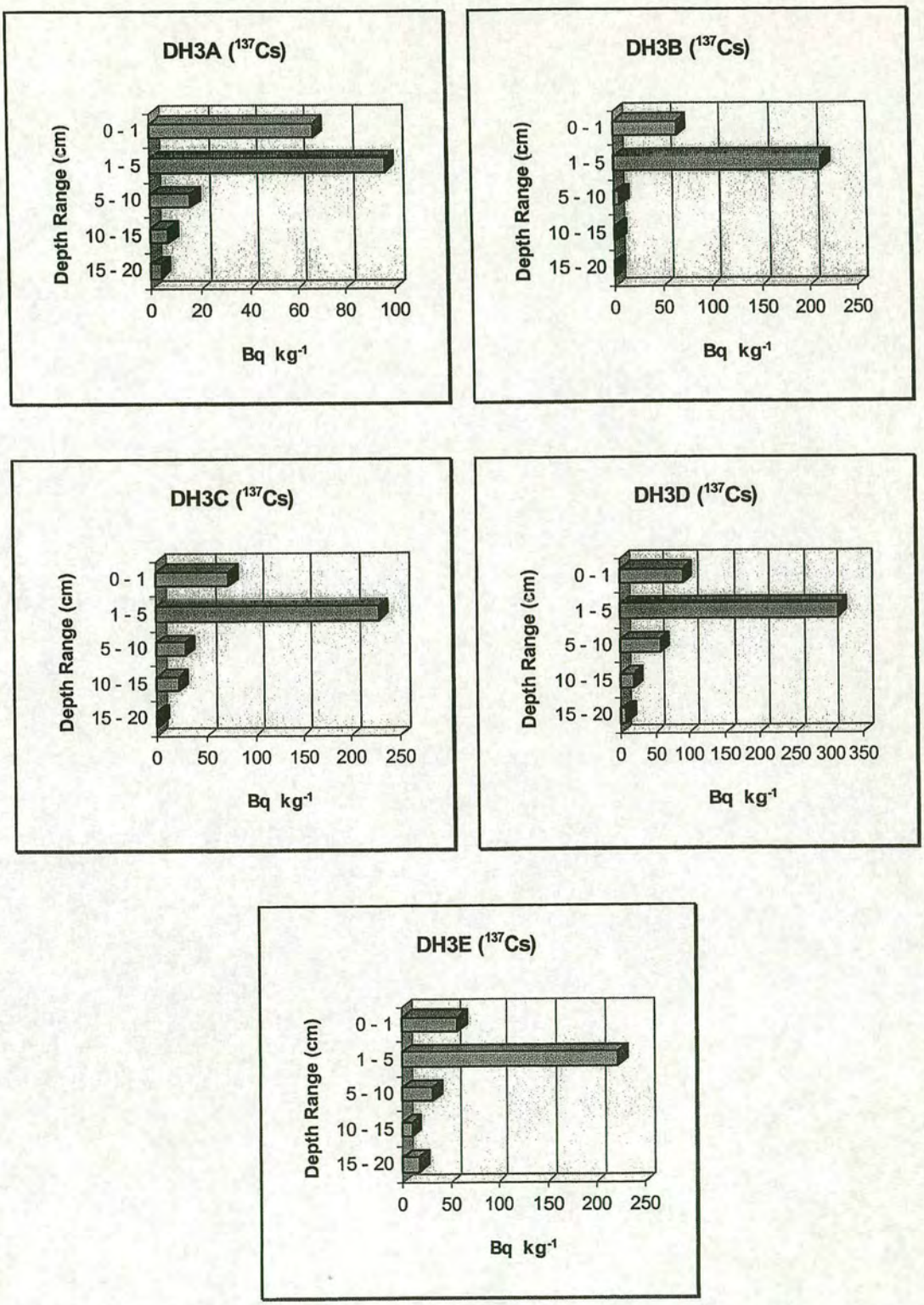

Figure 3.12: Distribution of ^{137}Cs with depth at Dunslair Heights.
Under canopy locations, DH3A - DH3E.

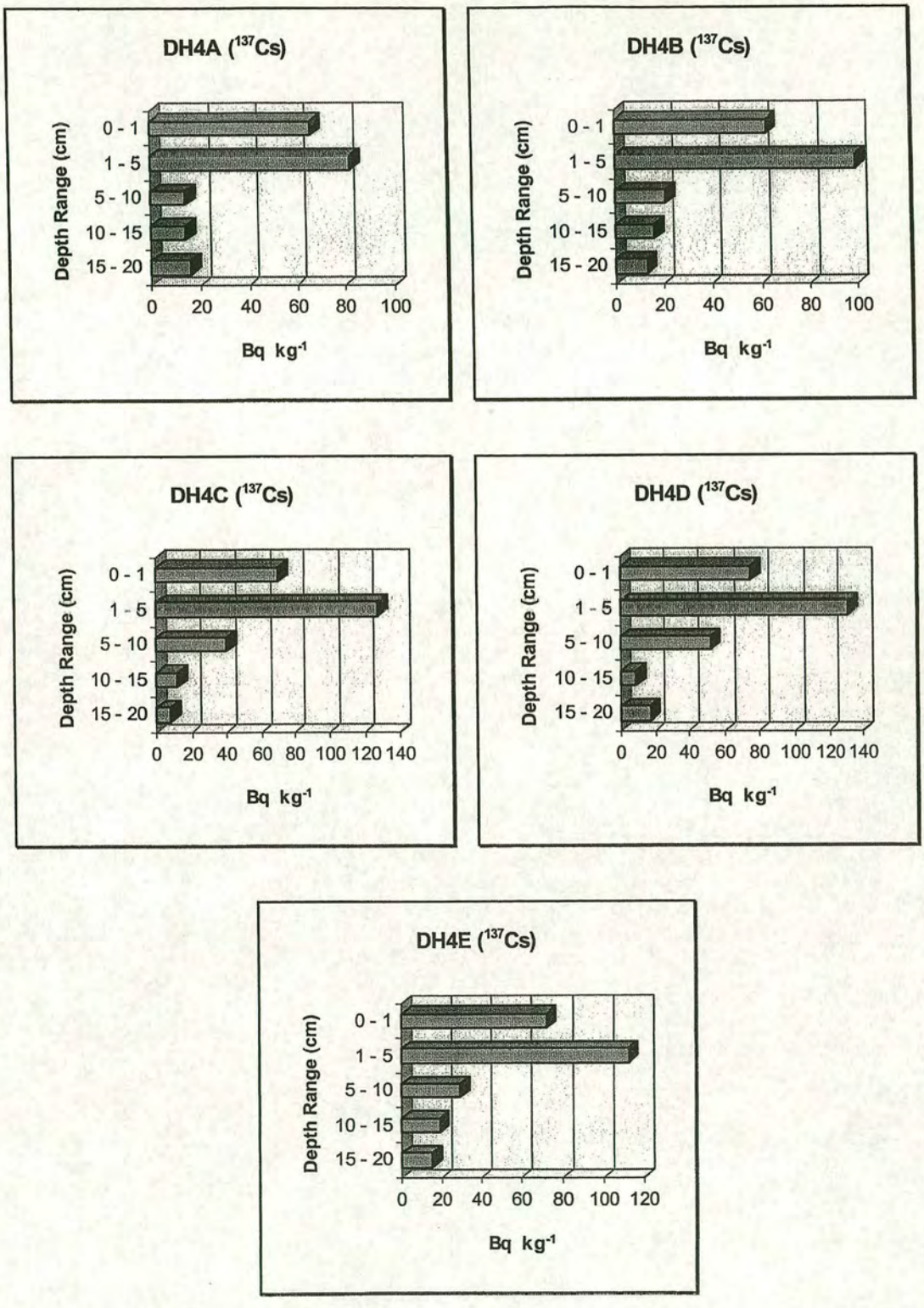

Figure 3.13: Distribution of ^{137}Cs with depth at Dunslair Heights.
Under canopy locations, DH4A - DH4E.

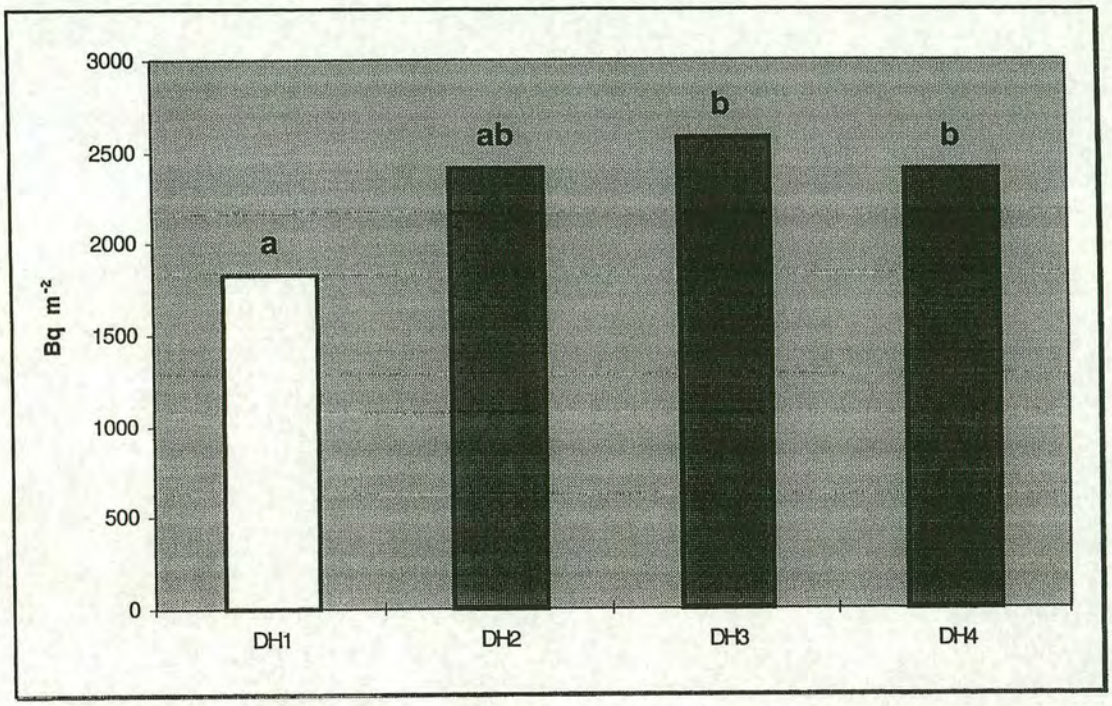

Figure 3.14: Mean ^{137}Cs soil inventories in the open field (DH1), edge of the stand(DH2), 15 m from the edge (DH3) and 40 m inside the forest canopy (DH4) at Dunslair Heights.
The letters above each bar denote significant differences as derived from Duncan's multiple range test. Any two means having a common letter are not significantly different at the 5% level of significance .

3.2 Dun Coillich (see section 2.1.1.1, Figures 2.6 & 2.7)

3.2.1 Lead 210 soil inventories

The inventories of atmospheric ^{210}Pb for the samples collected from Dun Coillich are presented in Figures 3.15 and 3.16. Figure 3.15 shows the mean ^{210}Pb inventories for the open field, DC1, at the edge of canopy, DC2, 25 m inside the canopy, DC3, and finally 50 m inside the forest canopy, DC4. The error bars in this graph represent the standard error of the mean. The canopy enhancement in ^{210}Pb deposition at this site is approximately 36%, on the average, relative to the adjacent open heathland. The enhancement is large at the edge of canopy which exceeds that in the open field by 56%. The DMR test result on the inventory values is illustrated in Figure 3.20. According to the test, there is no significant difference between inventories at DC4 and DC3, neither between DC4 and DC1, at the 5% level of significance. The levels of ^{210}Pb present in the individual cores from Dun Coillich are shown in Figure 3.16, where the error bars are due to counting statistics. The coefficient of variation for measured inventories is 14%, 6%, 10%, and 5% for DC1-DC4 locations, respectively. The inherent variability in ^{210}Pb inventories is higher at the open field relative to under canopy locations at this site.

Depth profiles for specific activities are illustrated in Figures 3.17 to 3.19. The sampling depth at Dun Coillich has been increased by at least 50% compared to Dunslair Heights to be sure of capturing the full profile. Depth intervals are also different. The exceptions are DC4B and DC4C where samples have been collected only to a depth of 20 cm. Note that in the case of one open field point (DC1E) and one under canopy point (DC3B), sampling has been carried out even further down to a depth of 50 cm. At each of the 14 points sampled, no significant amounts of atmospheric ^{210}Pb were detected below 20 cm depth and in 8 points not even below 10 cm depth. The depth profiles show much greater concentration of atmospheric ^{210}Pb in the 0-5 cm depth interval than in the 5-10 cm depth for all the sampling points at this site.

Assuming that the atmospheric supply of ^{210}Pb and its radioactive decay in soil are in equilibrium, which is quite reasonable considering the age of undisturbed canopy (80 years), the average flux to the Scots pine (*Pinus sylvestris*) canopy and the adjacent heatherland in Dun Coillich would be 134 Bq m^{-2} y^{-1} and 98 Bq m^{-2} y^{-1}, respectively. The atmospheric ^{210}Pb inventory values at Dun Coillich exceed those at Dunslair Heights by approximately 35%.

3.2.2 Caesium 137 soil inventories

The soil inventories for ^{137}Cs are presented in Figures 3.21 and 3.22. Figure 3.21 shows a similar pattern of canopy enhancement to the ^{210}Pb inventories for the site. The error bars represent standard error of the mean. The average ^{137}Cs inventory inside the forest canopy exceeds that in the adjacent open field by 36% which is the same as the value of canopy enhancement for ^{210}Pb at Dun Coillich. Caesium 137 inventories for the individual sampling points are given in Figure 3.22, where the error bars are due to counting statistics. The coefficient of variation for measured inventories of ^{137}Cs is 8%, 13%, 9%, and 11% for DC1-DC4 locations, respectively. The inherent variabilities are of the same order of magnitude as with ^{210}Pb inventories. The variation is higher at the edge of canopy relative to the open field as well as other canopy locations. The caesium 137 mean inventories at Dun Coillich are more than a factor of 4 greater than those at Dunslair Heights for both open field and beneath canopy locations.

Depth profiles for specific activities are illustrated in Figures 3.23 to 3.25. The profiles for the open field samples (DC1A-DC1E in Figure 3.23) show that the top 20 cm of soil has retained ^{137}Cs efficiently. However, in the case of under canopy samples there is evidence of deeper penetration of this radionuclide (see DC2A-DC3B profiles in Figure 3.24). In the case of DC4B & DC4C sampling points, taking deeper samples were not possible due to the presence of stones.

According to the DMR test results presented in Figure 3.26, there are no significant difference between ^{137}Cs inventories for the under canopy locations at the 5% level of significance, but all the under canopy values are significantly larger than the open heathland inventory.

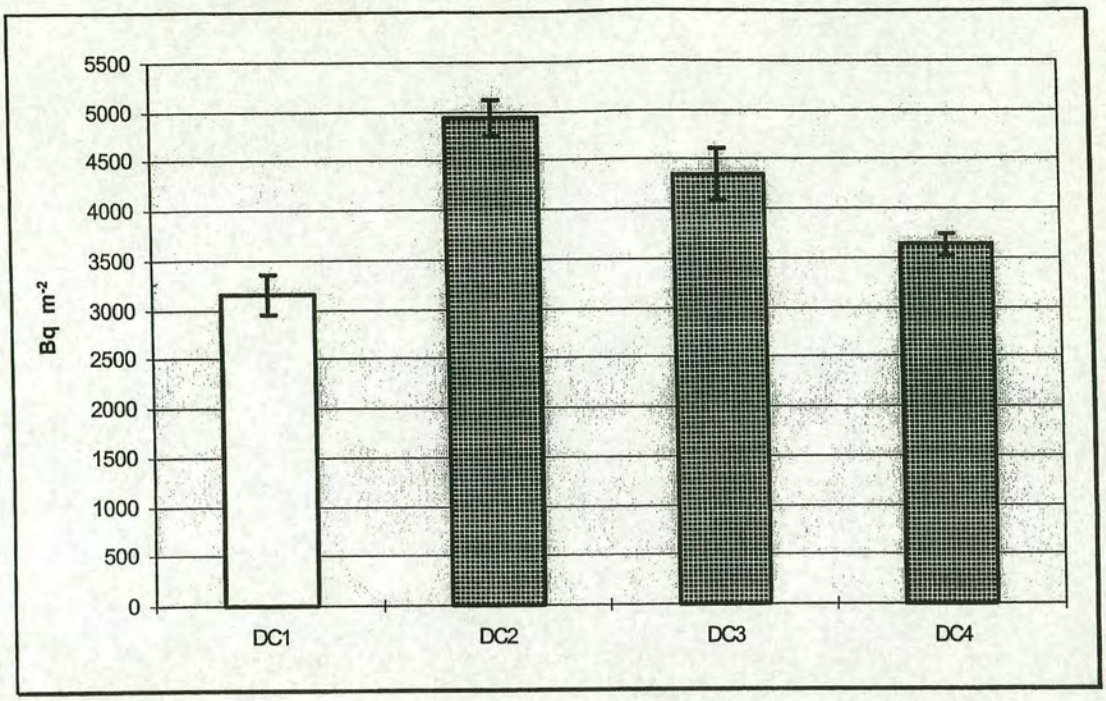

Figure 3.15: Mean atmospheric ^{210}Pb soil inventories in the open field (DC1), edge of the stand (DC2), 25 m from the edge (DC3) and 50 m inside the forest canopy (DC4) at Dun Coillich.

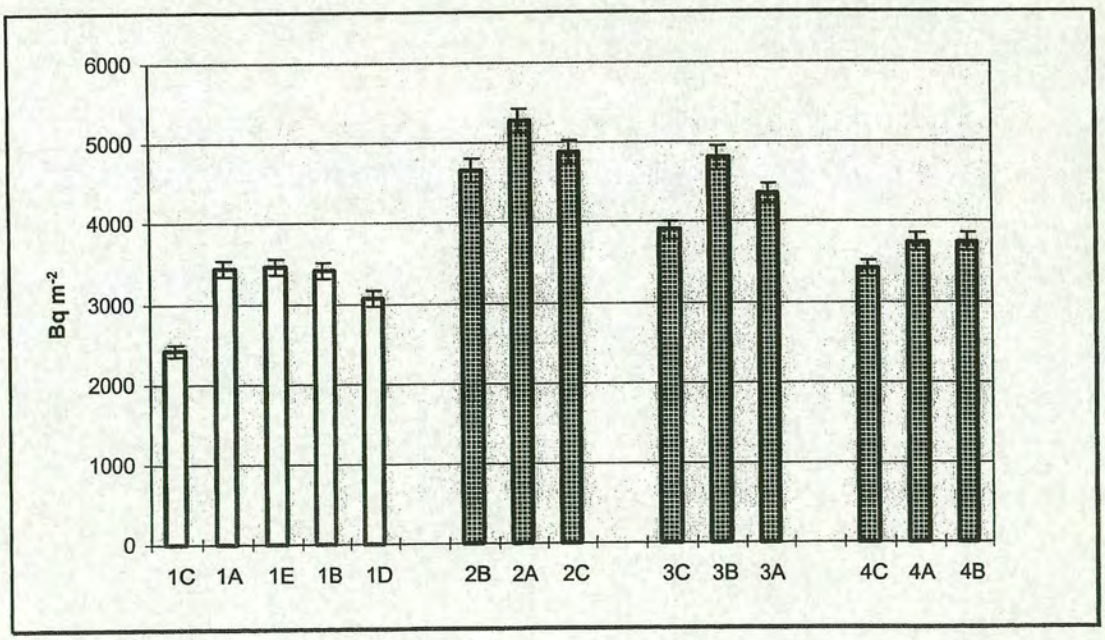

Figure 3.16: Atmospheric ^{210}Pb inventories measured in soil samples from each sampling point at Dun Coillich.

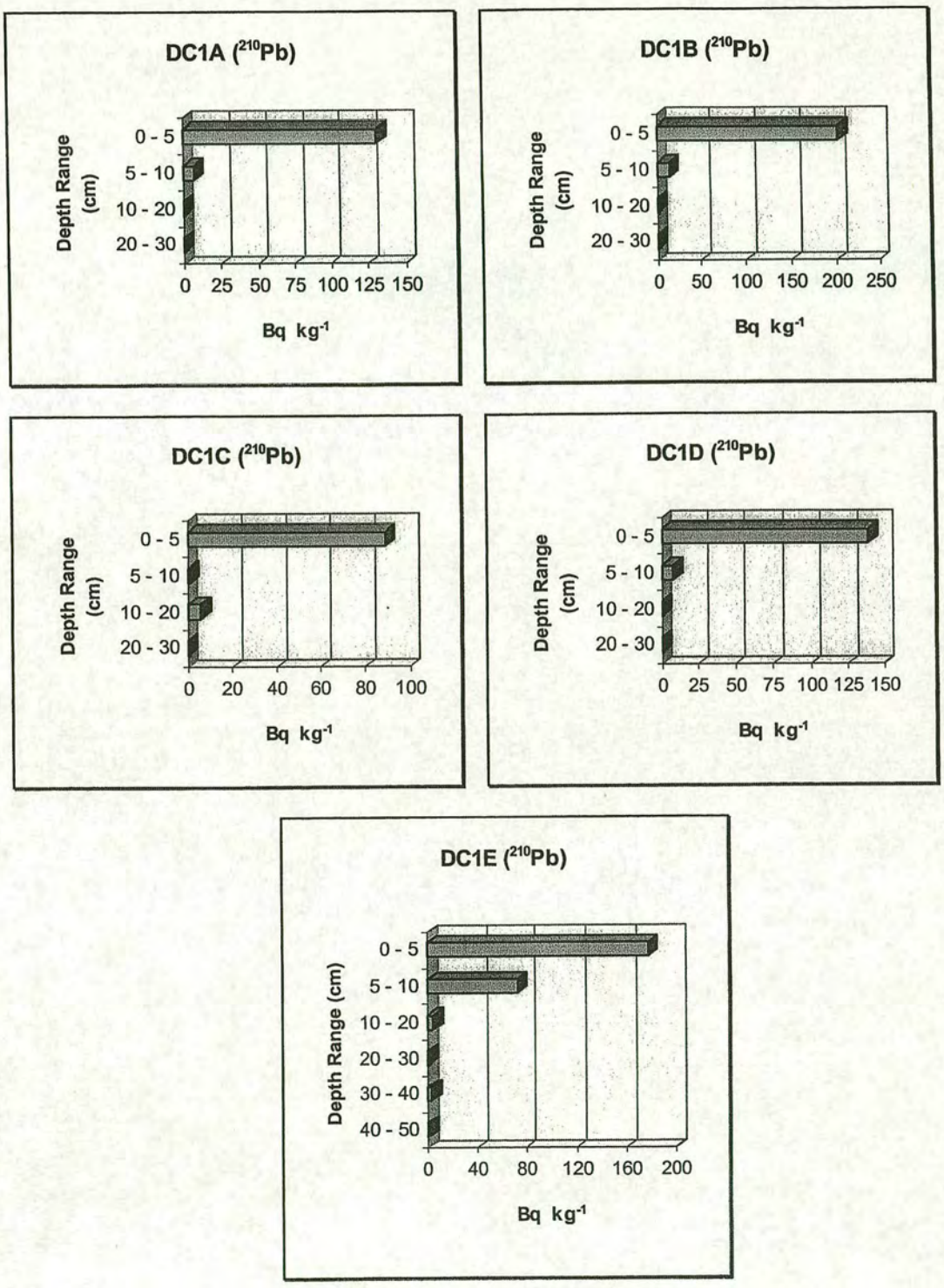

Figure 3.17: Distribution of atmospherically derived ^{210}Pb with depth at Dun Coillich. Open field locations, DC1A - DC1E.

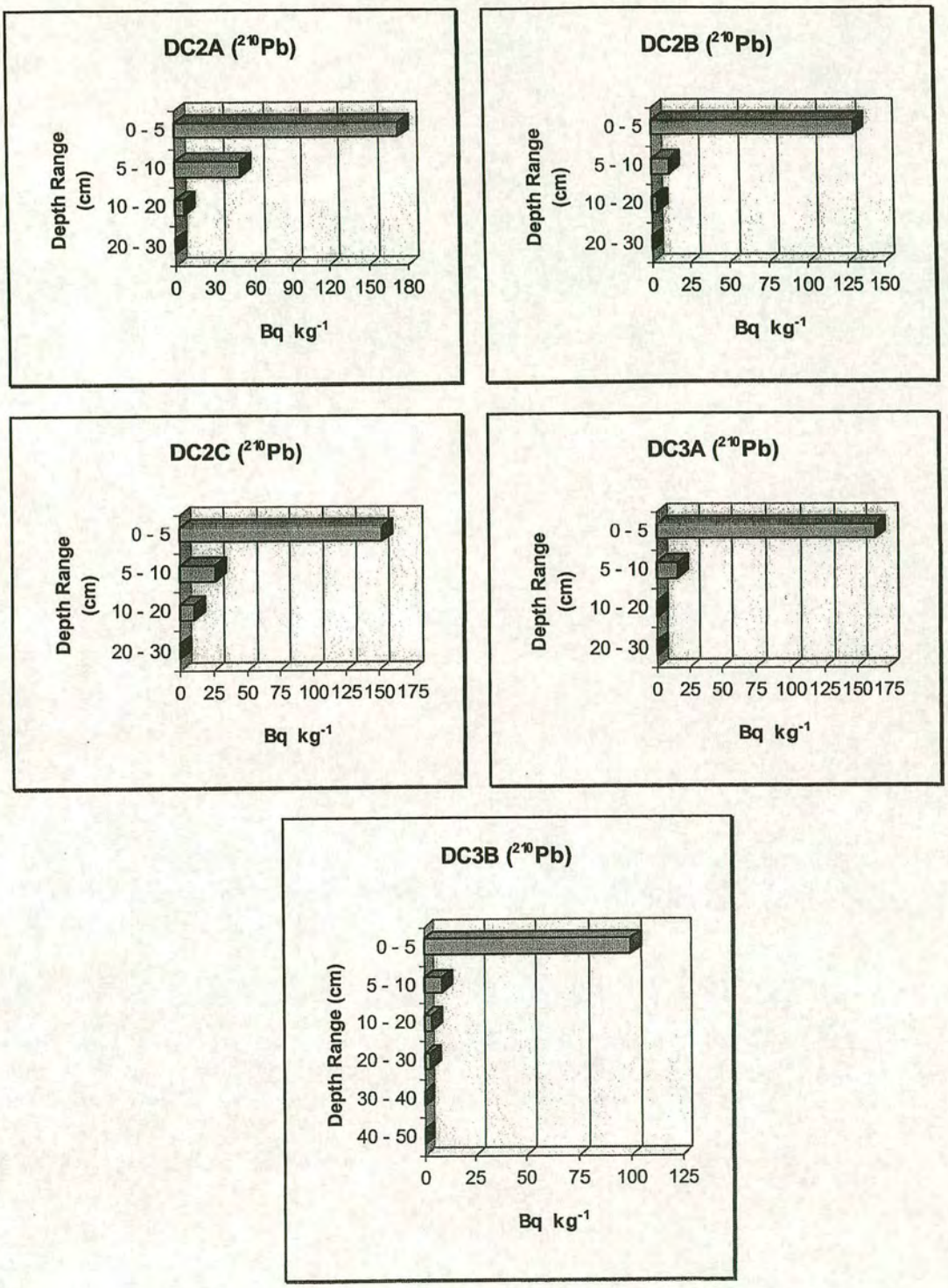

Figure 3.18: Distribution of atmospherically derived ^{210}Pb with depth at Dun Coillich. Edge of stand locations, DC2A - DC2C and inside canopy locations(25 m from the edge), DC3A & DC3B.

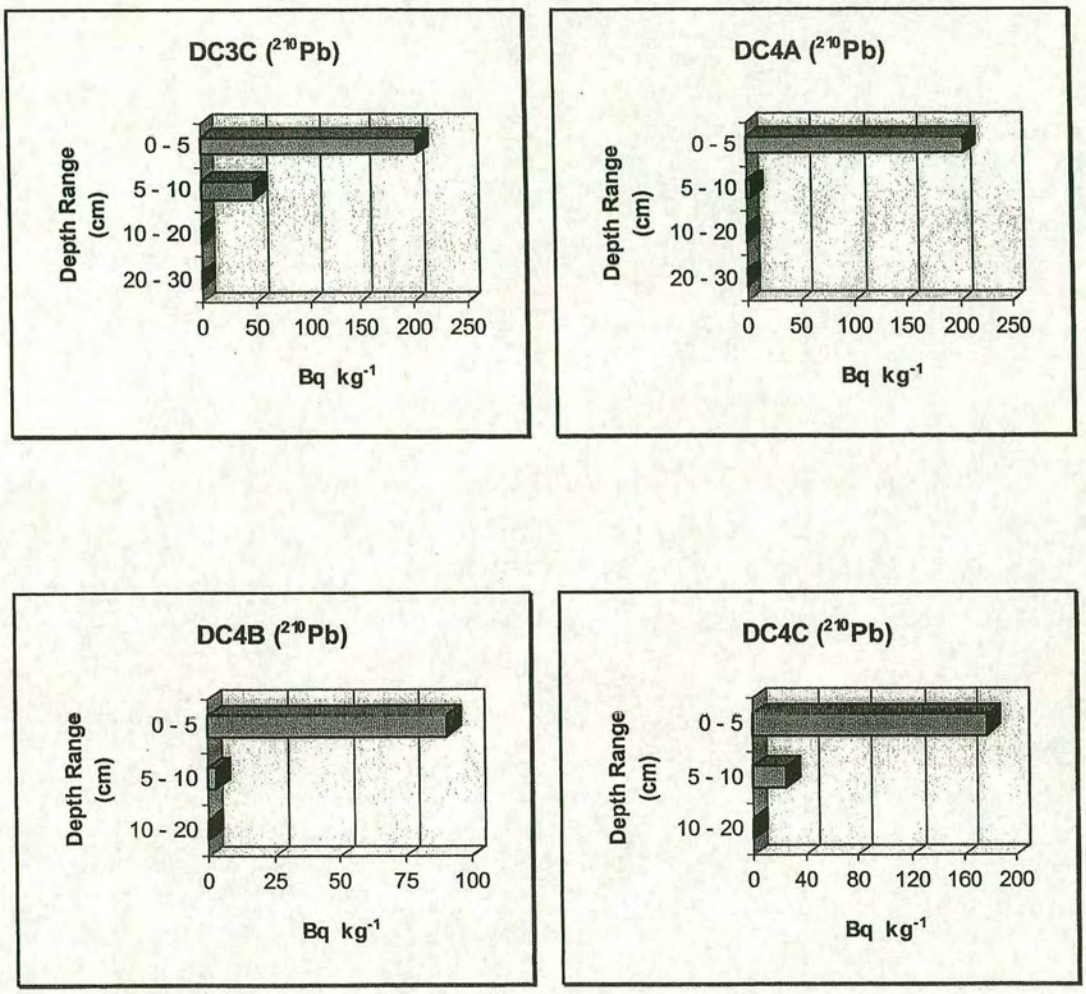

Figure 3.19: Distribution of atmospherically derived ^{210}Pb with depth at Dun Coillich. Inside canopy locations, DC3C(25 m from the edge) and DC4A-DC4C(50 m from the edge).

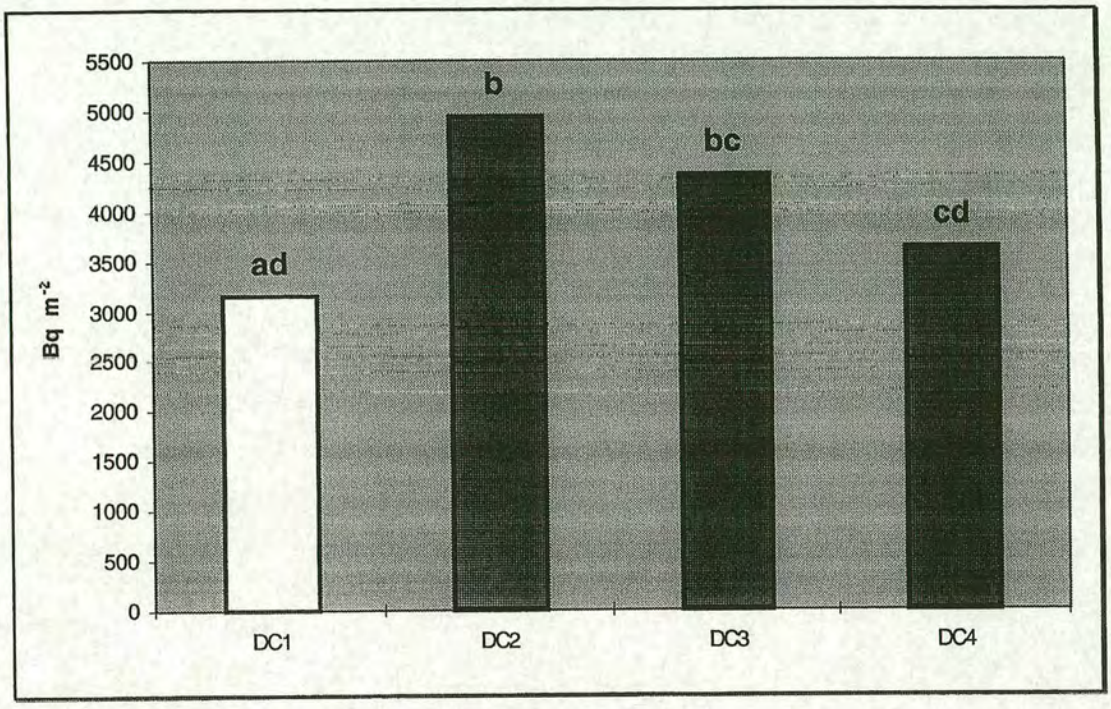

Figure 3.20: Mean atmospheric ^{210}Pb soil inventories in the open field (DC1), edge of the stand(DC2), 25 m from the edge (DC3) and 50 m inside the forest canopy (DC4) at Dun Coillich.

The letters above each bar denote significant differences as derived from Duncan's multiple range test. Any two means having a common letter are not significantly different at the 5% level of significance .

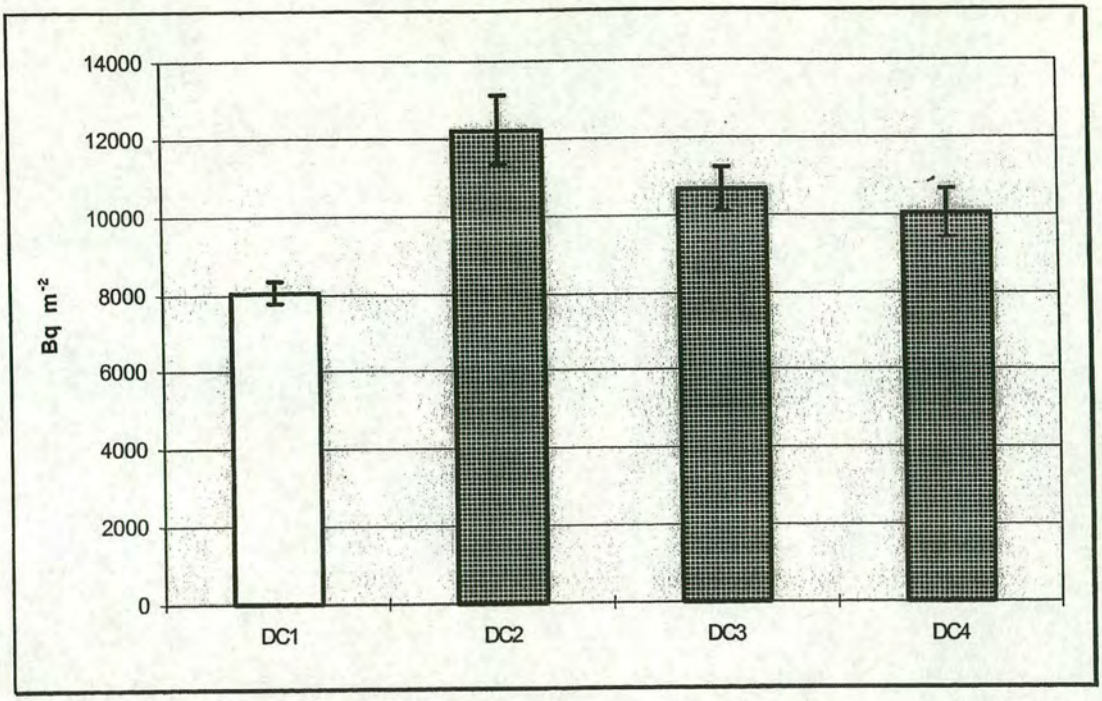

Figure 3.21: Mean ^{137}Cs inventories in the open field (DC1), edge of the stand (DC2), 25 m from the edge (DC3) and 50 m inside the forest canopy (DC4) at Dun Coillich.

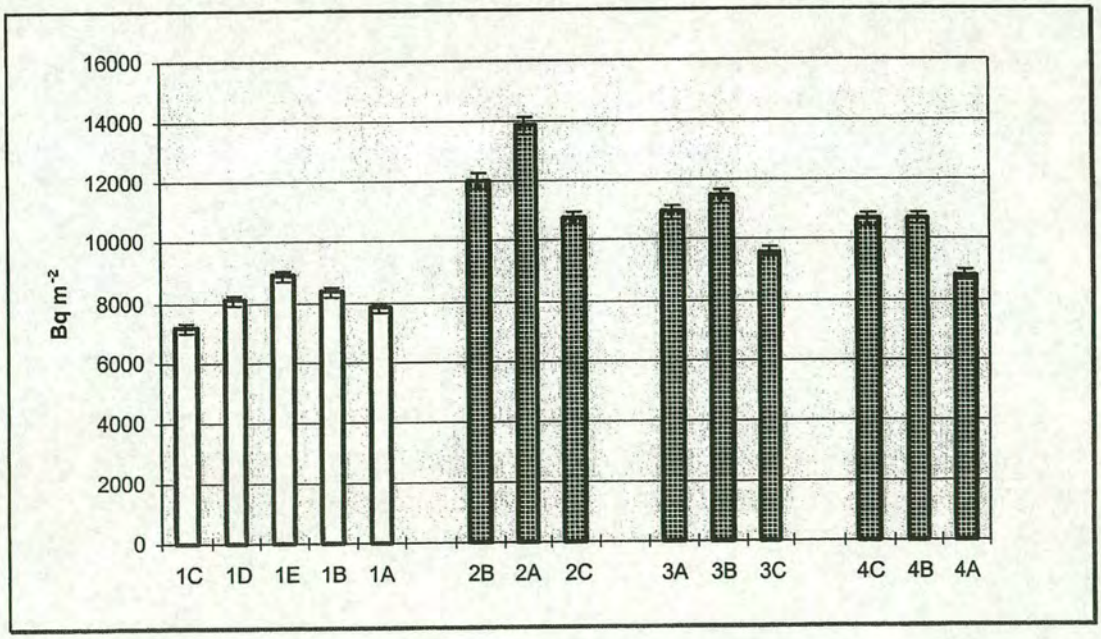

Figure 3.22: ^{137}Cs inventories measured in soil samples from each sampling point at Dun Coillich.

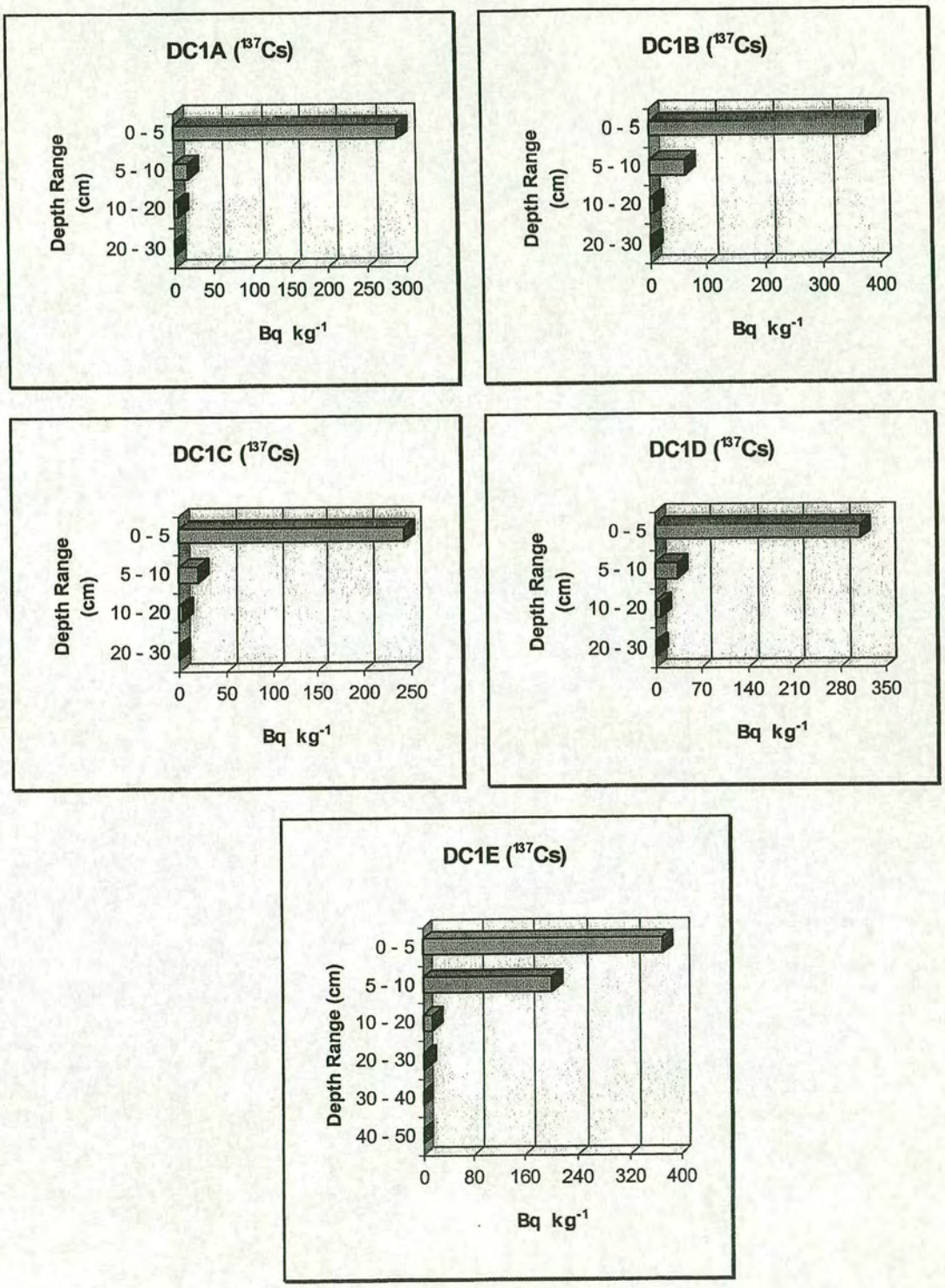

Figure 3.23: Distribution of ^{137}Cs with depth at Dun Coillich.
Open field locations, DC1A - DC1E.

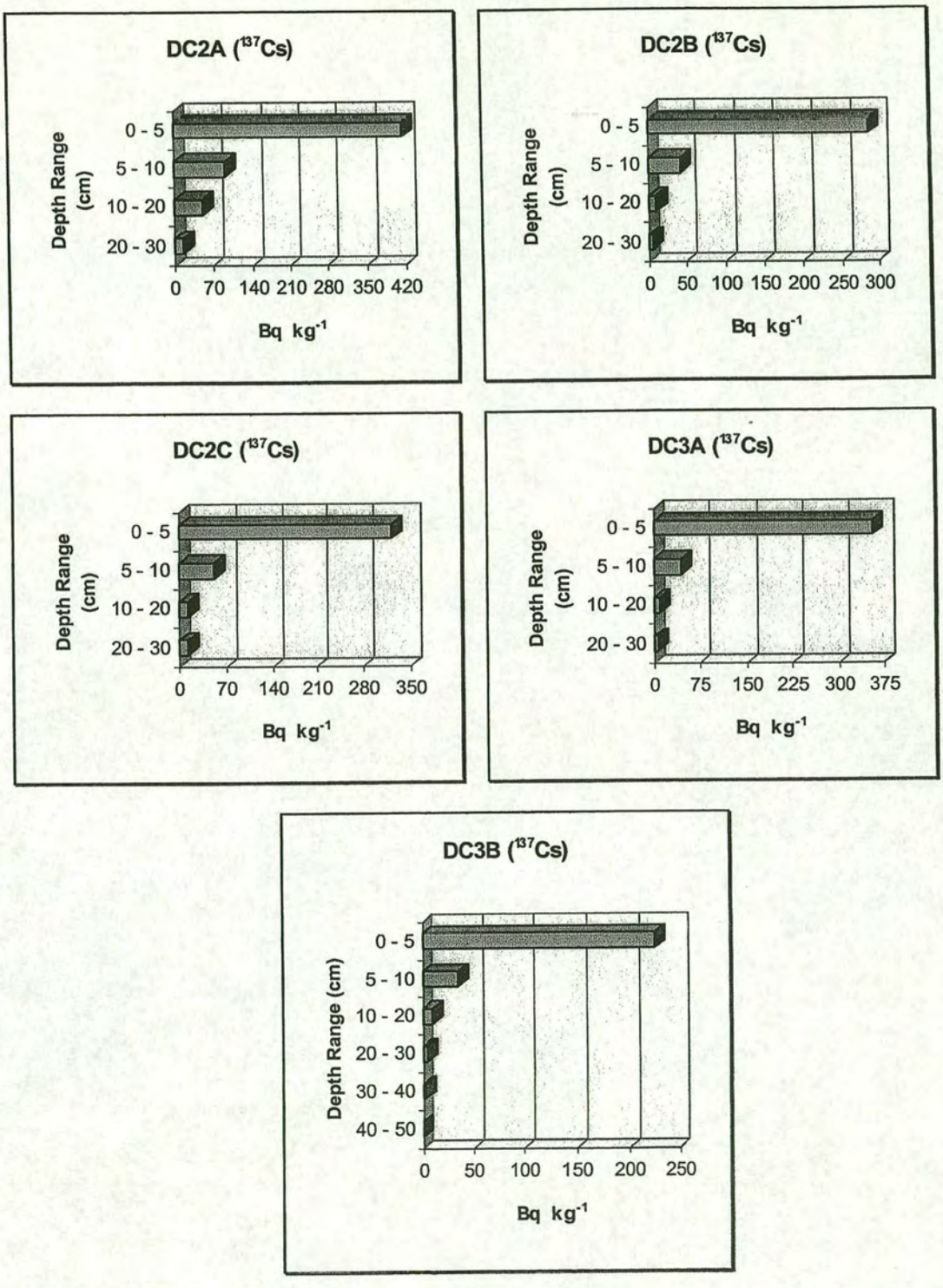

Figure 3.24: Distribution of ^{137}Cs with depth at Dun Coillich. Edge of stand locations, DC2A - DC2C and inside canopy locations(25 m from the edge), DC3A & DC3B.

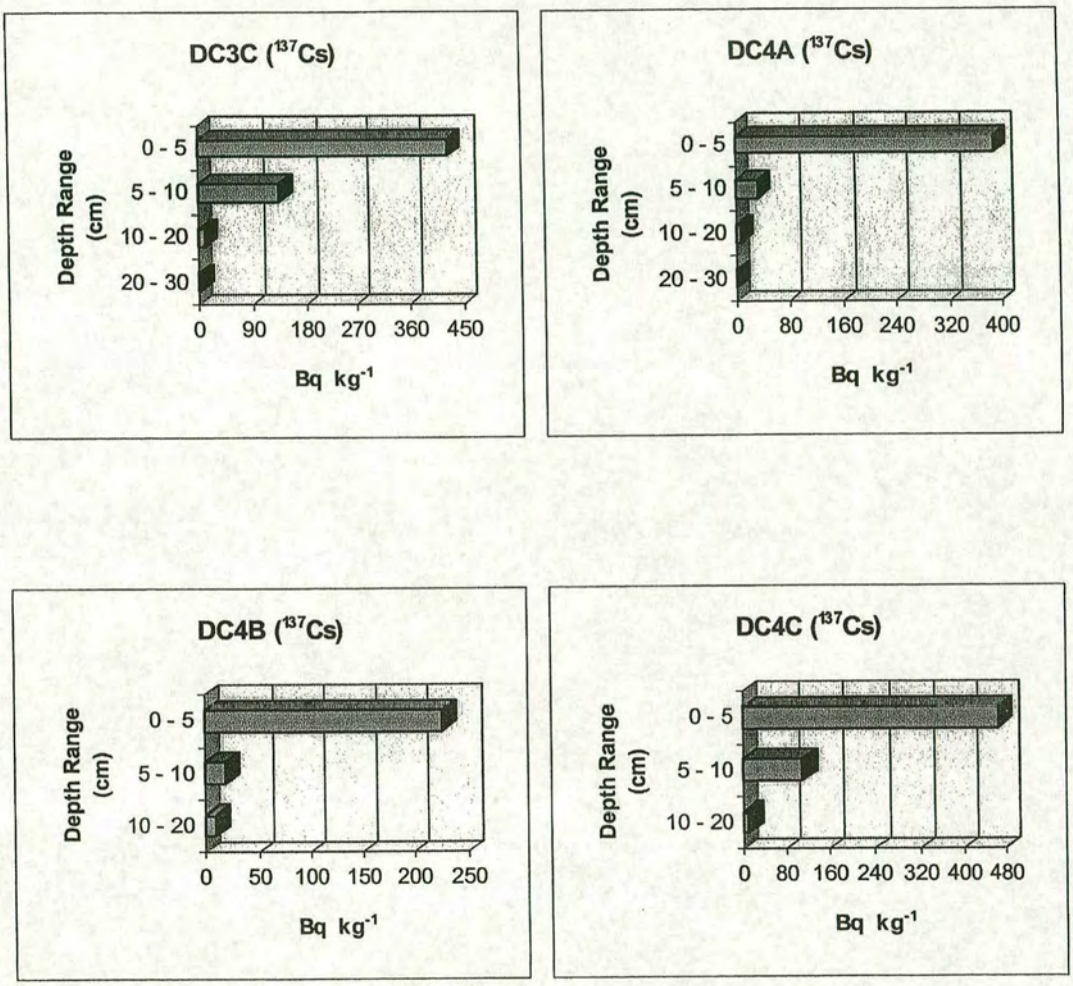

Figure 3.25: Distribution of ^{137}Cs with depth at Dun Coillich. Inside canopy locations, DC3C(25 m from the edge) and DC4A-DC4C(50 m from the edge).

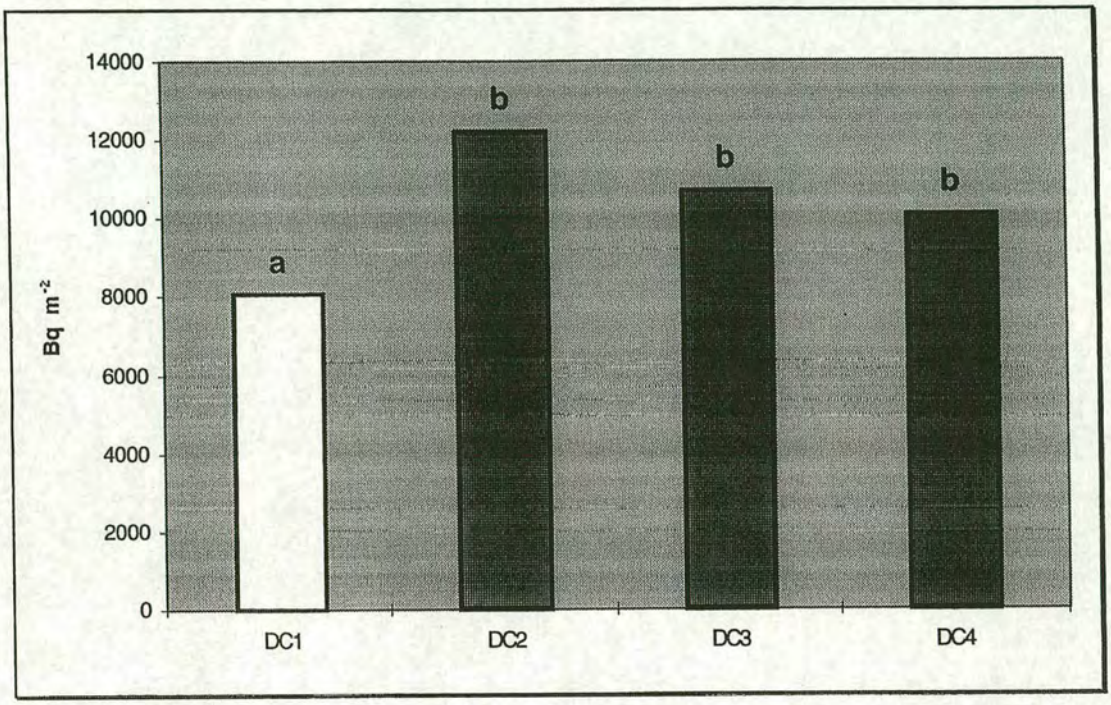

Figure 3.26: Mean ^{137}Cs soil inventories in the open field (DC1), edge of the stand(DC2), 25 m from the edge (DC3) and 50 m inside the forest canopy (DC4) at Dun Coillich.

The letters above each bar denote significant differences as derived from Duncan's multiple range test. Any two means having a common letter are not significantly different at the 5% level of significance .

3.3 Southwest Sweden

The radioanalytical results for soil taken from 10 sites in south-west Sweden are all be presented in this section, site by site, from Hallands Vadero island in the Kattegat Sea to Hassleberg, 61 km inland in the southern Swedish uplands. The pattern of deposition for the whole area is also presented.

3.3.1 Hallands Vadero island (see section 2.1.1.2, Figures 2.9- 2.11)

3.3.1.1 Lead 210 soil inventories

The inventories of atmospheric ^{210}Pb for the samples collected from beneath the Scots pine(*Pinus sylvestris*) canopy as well as the adjacent open field at Hallands Vadero island are presented in Figures 3.27 and 3.28. Mean ^{210}Pb inventories for the open field(A_O) and under canopy(A_C) are shown in Figure 3.27, where the error bars represent standard error of the mean. The coefficient of variation for the measured ^{210}Pb inventories is 11%, for the open field, and 23% for the under canopy locations . This shows that the spatial variability in ^{210}Pb inventories inside the canopy is almost twice that of the open field at this site. The levels of ^{210}Pb present in the individual cores from the open field(A1-A5) and under canopy sampling points(A6-A10) are shown in Figure 3.28, where the error bars are due to counting statistics. There are no statistically significant differences between the mean inventory values for the open field and under canopy samples at this site.

Depth profiles for specific activities are illustrated in Figures 3.29 and 3.30. Figure 3.29 illustrate the fact that top 10 cm soil has retained the atmospheric ^{210}Pb efficiently in the open field. A similar pattern has been observed in the case of under canopy profiles with the exception of SSA9 and SSA10 cores (Figure 3.30). However, even in these two sampling points the contribution from horizons below 10 cm is substantially small.

Under reasonable assumption of a steady state condition between the atmospheric supply of ^{210}Pb and its radioactive decay in soil, the average atmospheric flux at Hallands Vadero island would be 91 Bq m^{-2} y^{-1}.

3.3.1.2 Caesium 137 soil inventories

The soil inventories for ^{137}Cs are presented in Figures 3.31 and 3.32. Mean inventories for the open field(A_O) and under canopy(A_C) are shown in Figure 3.31, where the error bars represent standard error of the mean. The coefficient of variation for the measured ^{137}Cs inventories is 6%, for the open field, and 22% for the under canopy locations . The variability is even larger for the under canopy locations than was observed with ^{210}Pb data. The levels of ^{137}Cs present in the individual cores from the open field(A1-A5) and under canopy sampling points(A6-A10) are shown in Figure 3.32, where the error bars are due to counting statistics. Again there are no significant differences between the mean inventory values for the open field and under canopy samples.

Depth profiles for specific activities are illustrated in Figures 3.33 and 3.34 for the open field and under canopy cores, respectively. Caesium 137 is efficiently retained by the top 10 cm soil in the open field cores (Figure 3.33) whereas in case of under canopy cores (Figure 3.34), there is evidence of deeper penetration of this radionuclide. However, the bulk of caesium 137 is concentrated in the surface horizons of soil.

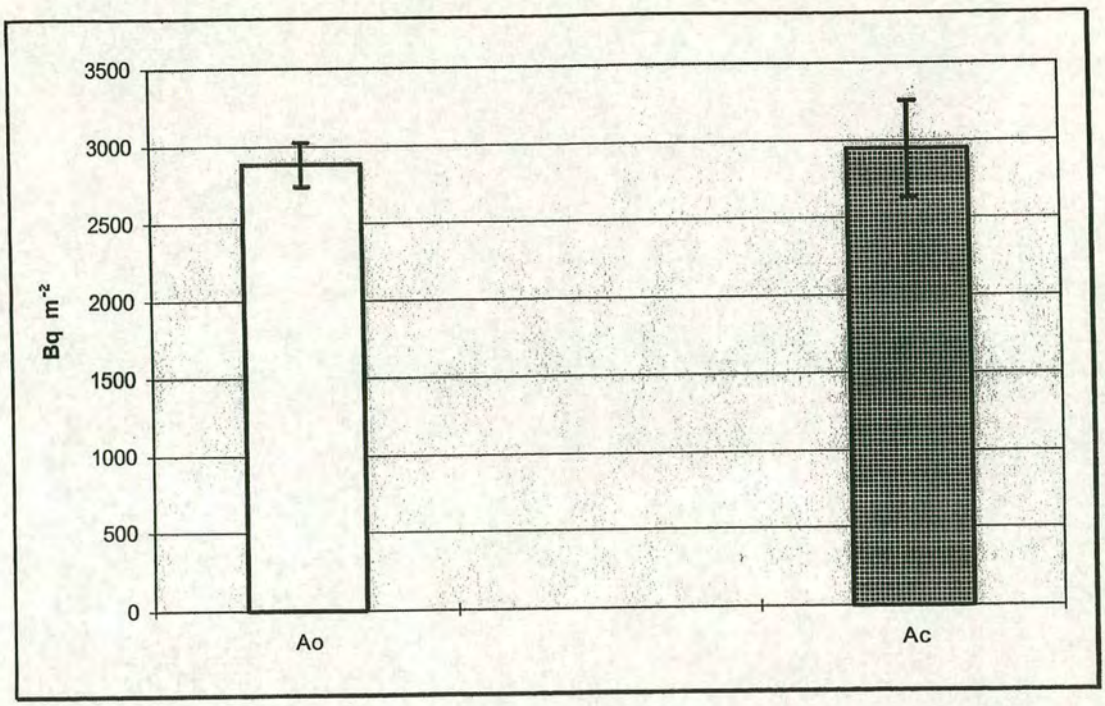

Figure 3.27: Mean atmospheric ^{210}Pb soil inventories in the open field(A_O), and inside the forest canopy(A_C) locations at Hallands Vadero island .

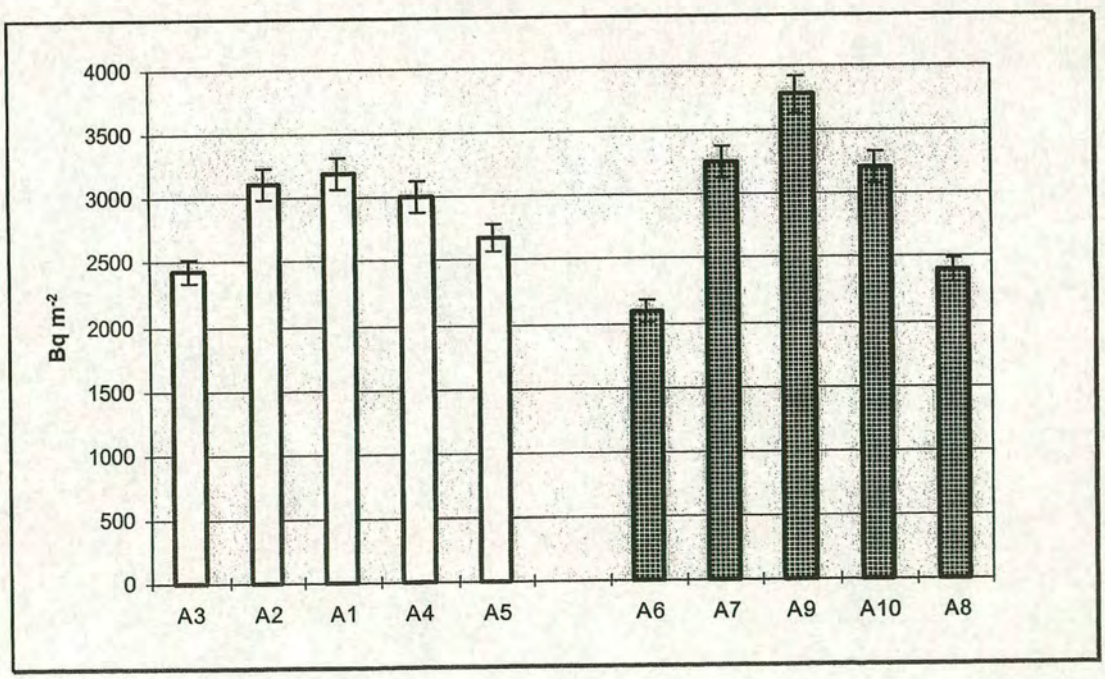

Figure 3.28: Atmospheric ^{210}Pb inventories measured in soil samples from each sampling point at Hallands Vadero island .

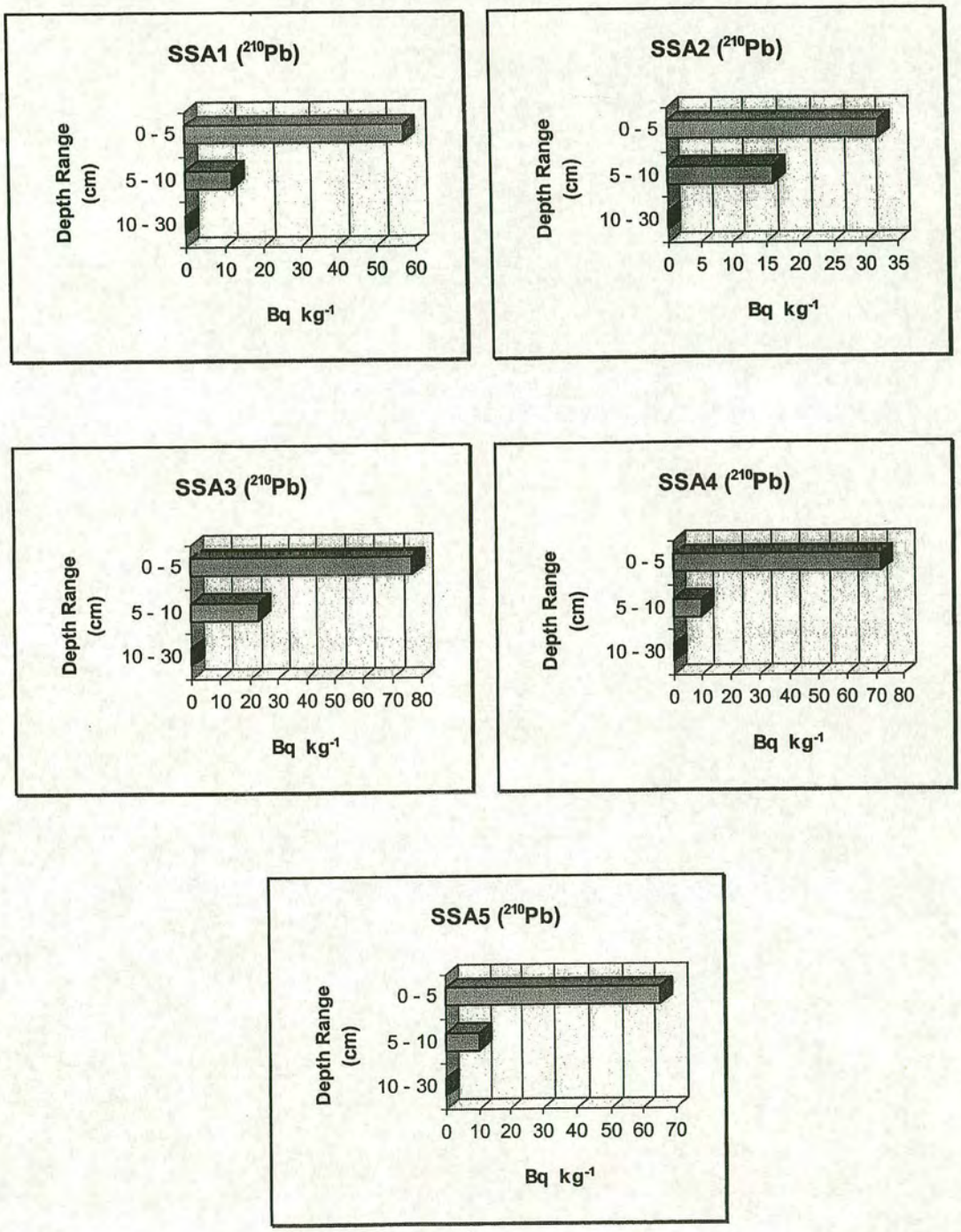

Figure 3.29: Distribution of atmospherically derived ^{210}Pb with depth at Hallands Vadero island. Open field locations, A1 - A5.

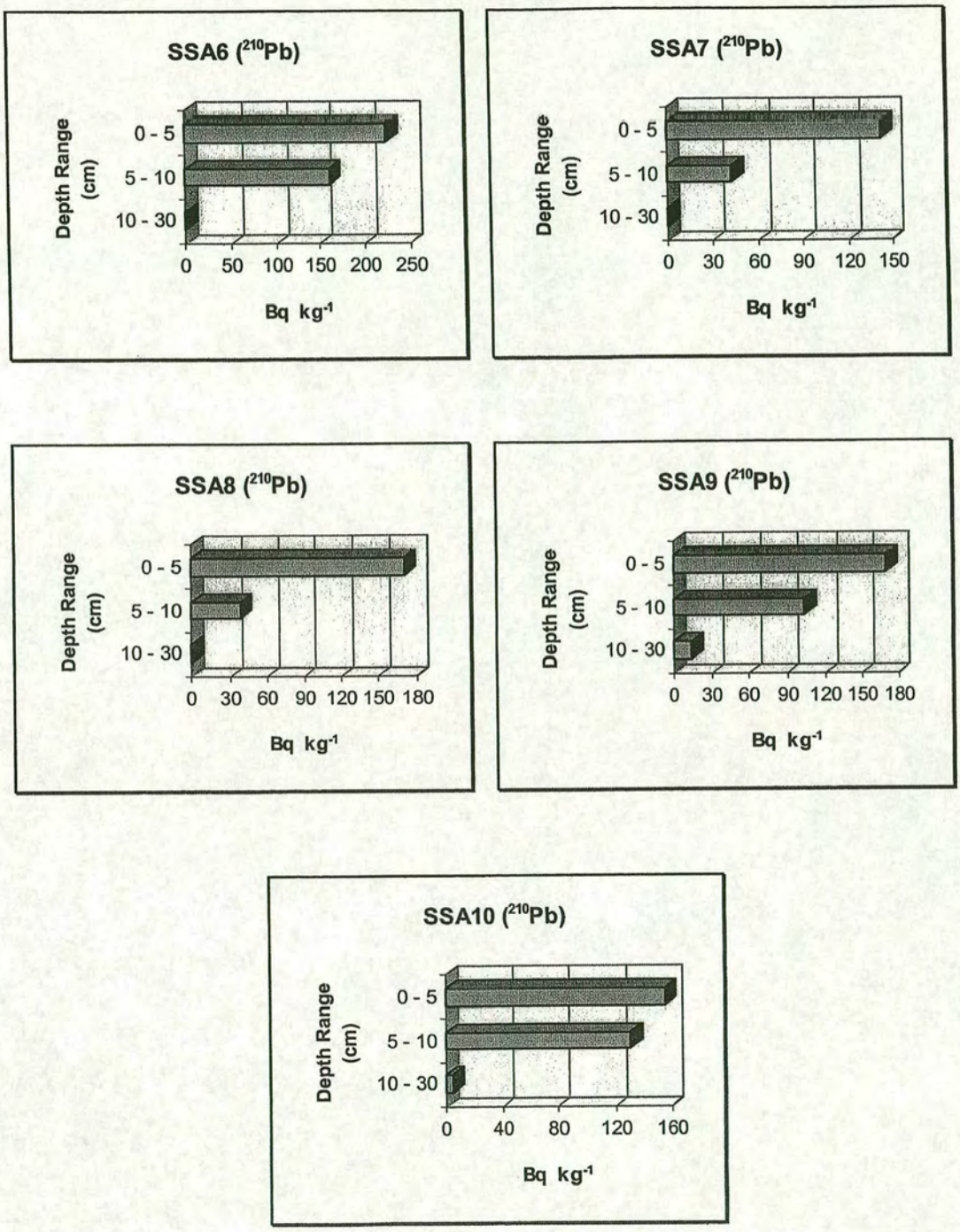

Figure 3.30: Distribution of atmospherically derived ^{210}Pb with depth at Hallands Vadero island. Under canopy locations, A6 - A10.

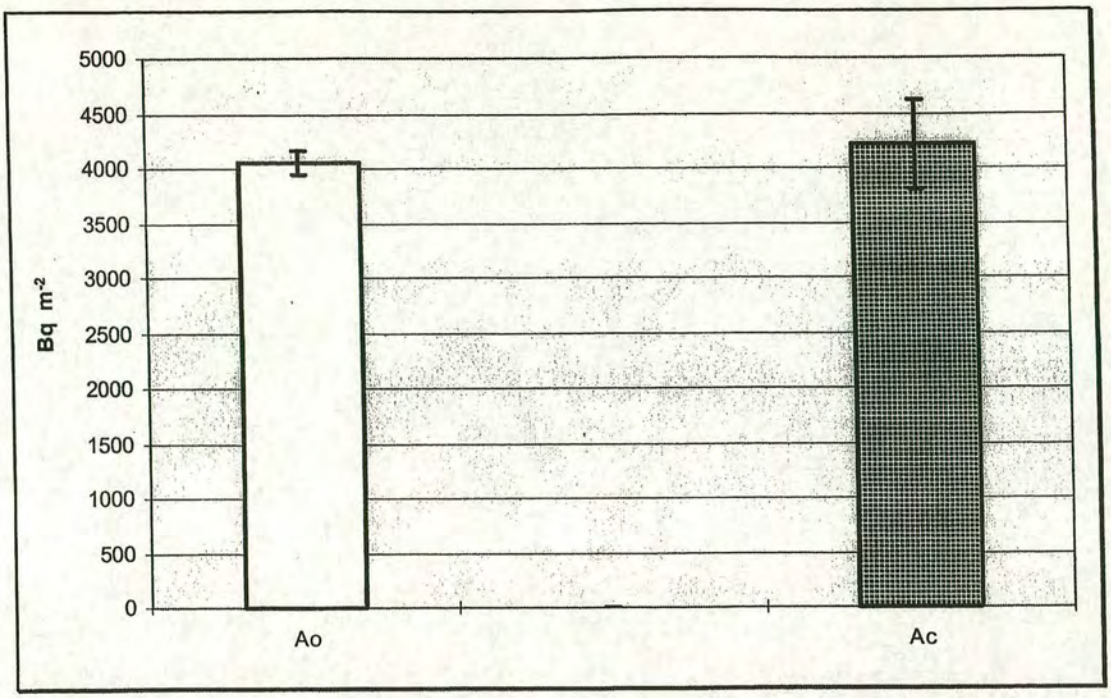

Figure 3.31: Mean ^{137}Cs soil inventories in the open field(A_O), and inside the forest canopy(A_C) locations at Hallands Vadero island .

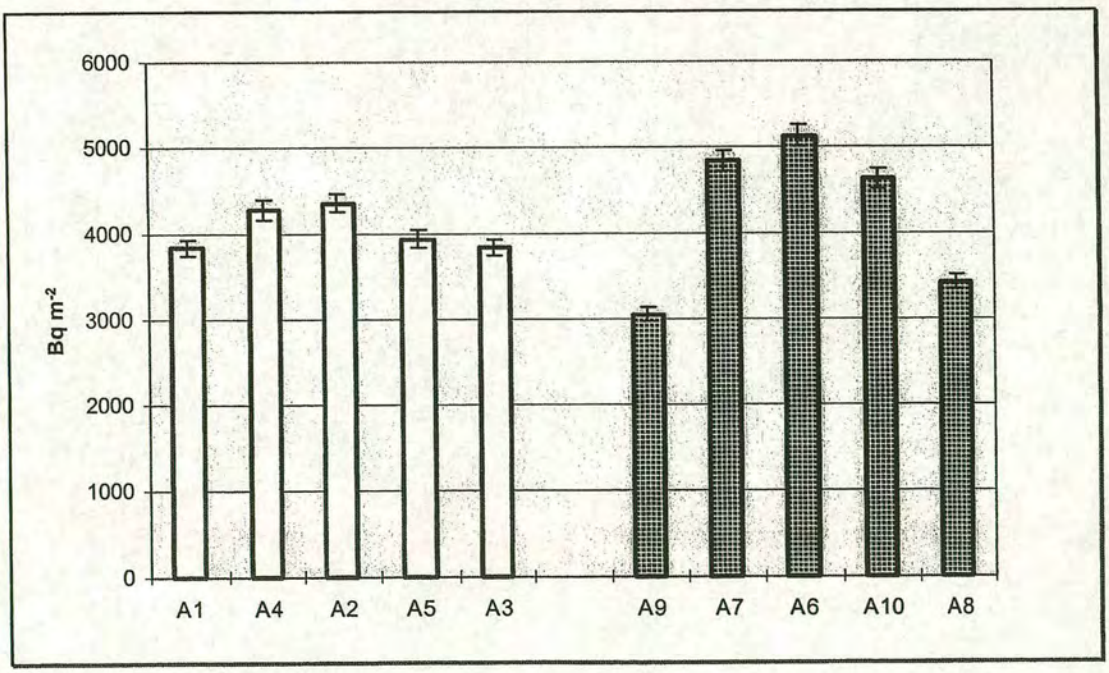

Figure 3.32: ^{137}Cs inventories measured in soil samples from each sampling point at Hallands Vadero island .

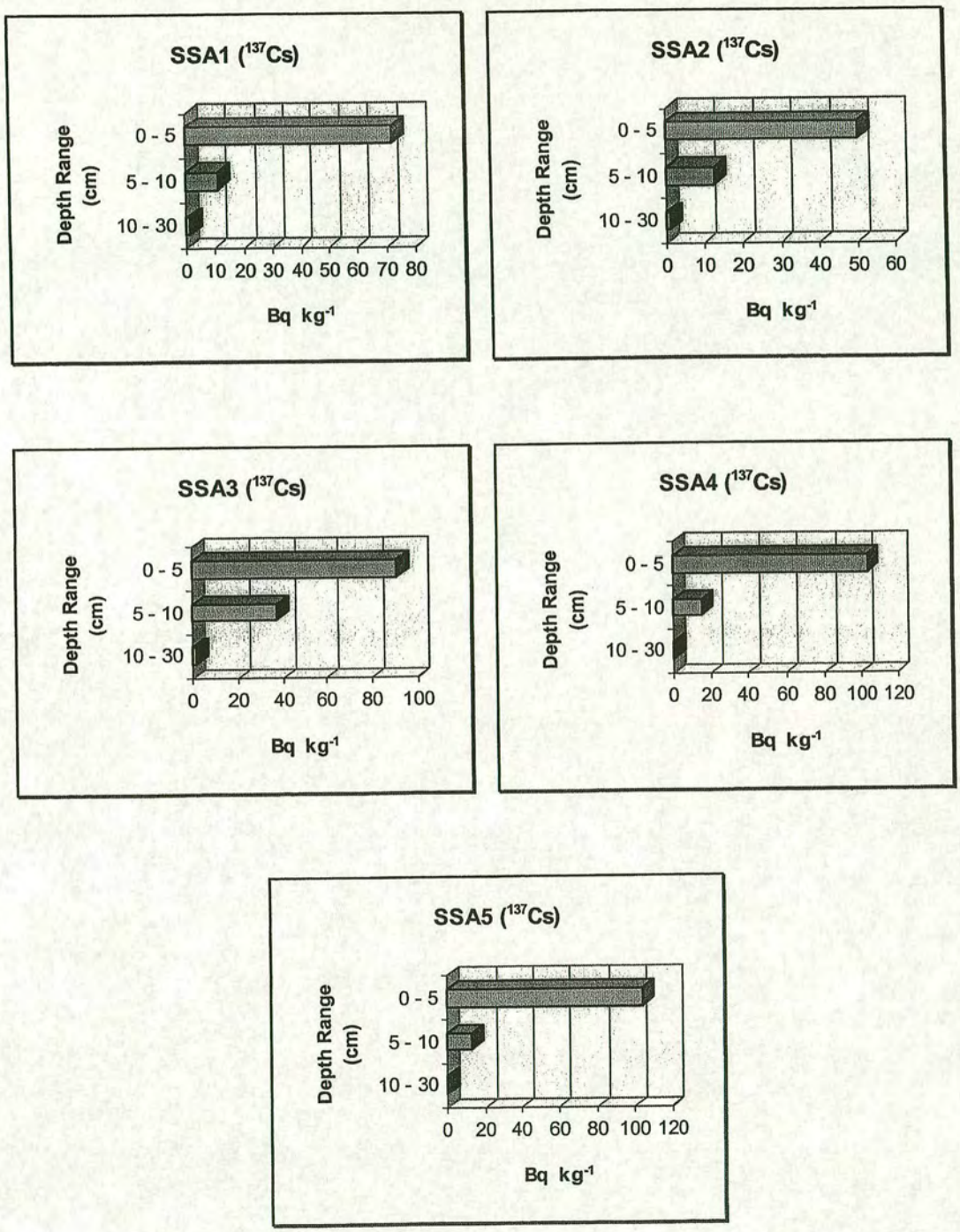

Figure 3.33: Distribution of ^{137}Cs with depth at Hallands Vadero island. Open field locations, A1 - A5.

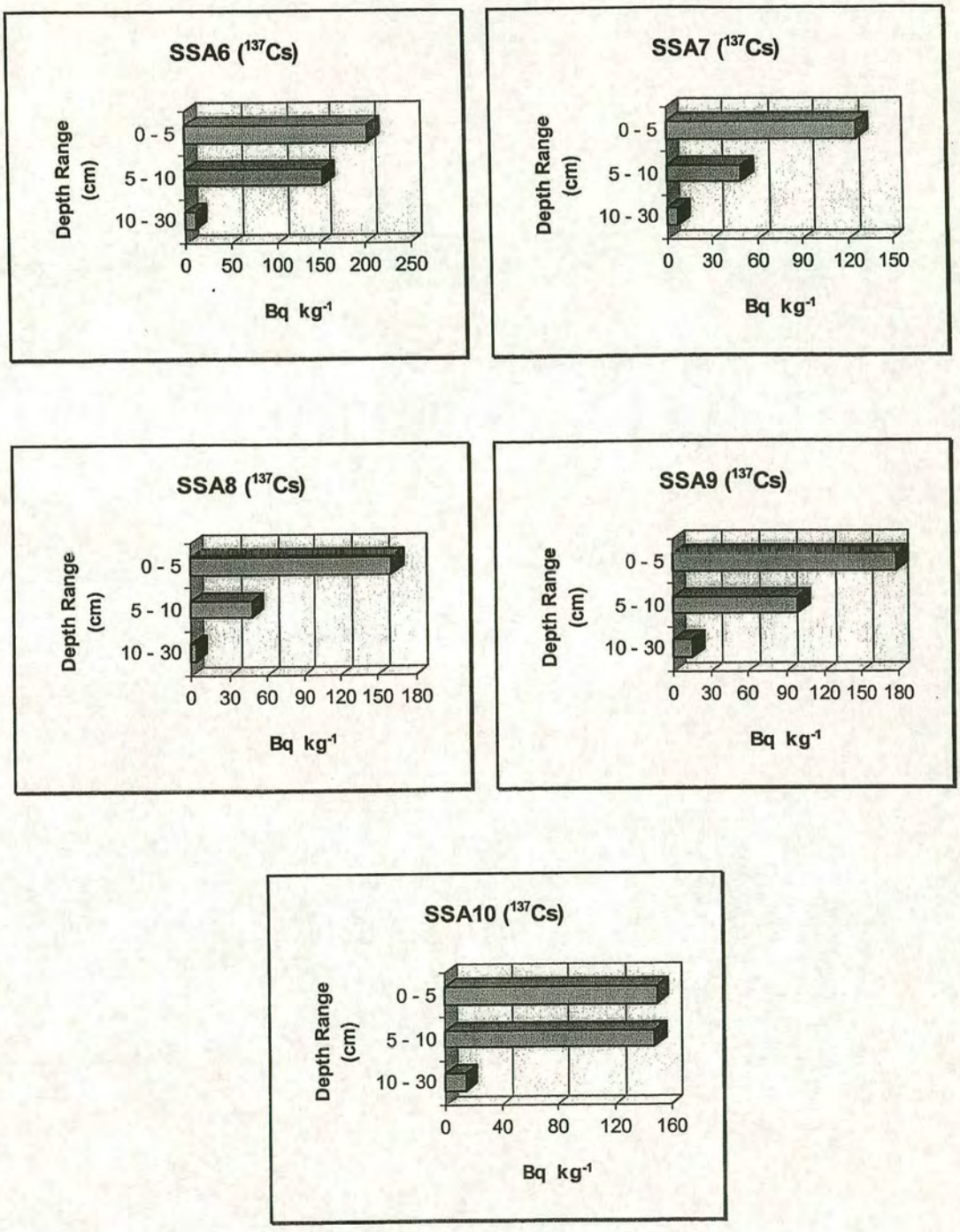

Figure 3.34: Distribution of ^{137}Cs with depth at Hallands Vadero island.
Under canopy locations, A6 - A10.

3.3.2 Haverdals naturreservat (see section 2.1.1.2, Fig.2.10&Table 2.2)

3.3.2.1 Lead 210 soil inventories

The inventories of atmospheric ^{210}Pb for the samples collected from beneath the Scots pine(*Pinus sylvestris*) canopy as well as the adjacent open field at Haverdals naturreservat are presented in Figures 3.35 and 3.36. Mean atmospheric ^{210}Pb inventories for the open field(B_O) and under canopy(B_C) are shown in Figure 3.35, where the error bars represent standard error of the mean. The coefficient of variation for the measured ^{210}Pb inventories is 17%, for the open field, and 14% for the under canopy locations . The variability in inventories for the canopy and open field locations are not significantly different at this site. The levels of ^{210}Pb present in the individual cores from the open field(B1-B5) and under canopy sampling points(B6-B10) are shown in Figure 3.36, where the error bars are due to counting statistics. There are no significant differences between the mean inventory values for the open field and under canopy samples at this site.

Depth profiles for specific activities are illustrated in Figures 3.37 and 3.38. Both figures illustrate the fact that top 10 cm soil has retained the atmospheric ^{210}Pb efficiently. There is no evidence of deeper penetration of this radionuclide in the case of SSB1, SSB6, and SSB8-SSB10 cores. The contribution from horizons below 10 cm, for the atmospheric ^{210}Pb inventory, is substantially smaller for the rest of sampling points at this site.

Under the reasonable assumption of a steady state condition between the atmospheric supply of ^{210}Pb and its radioactive decay in soil, its average flux at Haverdals naturreservat would be 86 Bq m^{-2} y^{-1}, very similar to the estimated value at Hallands Vadero island.

3.3.2.2 Caesium 137 soil inventories

The soil inventories for ^{137}Cs are presented in Figures 3.39 and 3.40. Mean inventories for the open field(B_O) and under canopy(B_C) are shown in Figure 3.39,

where the error bars represent standard error of the mean. The levels of ^{137}Cs present in the individual cores from the open field(B1-B5) and under canopy sampling points(B6-B10) are shown in Figure 3.40, where the error bars are due to counting statistics. The coefficient of variation for the measured ^{137}Cs inventories is 8%, for the open field, and 10% for the under canopy locations . The difference in spatial variability under canopy and in the open is not significant as it was the case with ^{210}Pb atmospheric inventories at this site.

Depth profiles for specific activities are illustrated in Figures 3.41 and 3.42 for the open field and under canopy cores, respectively. Caesium 137 is efficiently retained by the top 10 cm soil in the open field cores (Figure 3.41) whereas in case of under canopy cores (Figure 3.42), there is evidence of deeper penetration of this radionuclide than ^{210}Pb, consistent with other sites sampled in this study (see SSB7, SSB9 and SSB10 profiles). However, the bulk of caesium 137 is concentrated in the surface horizons of soil.

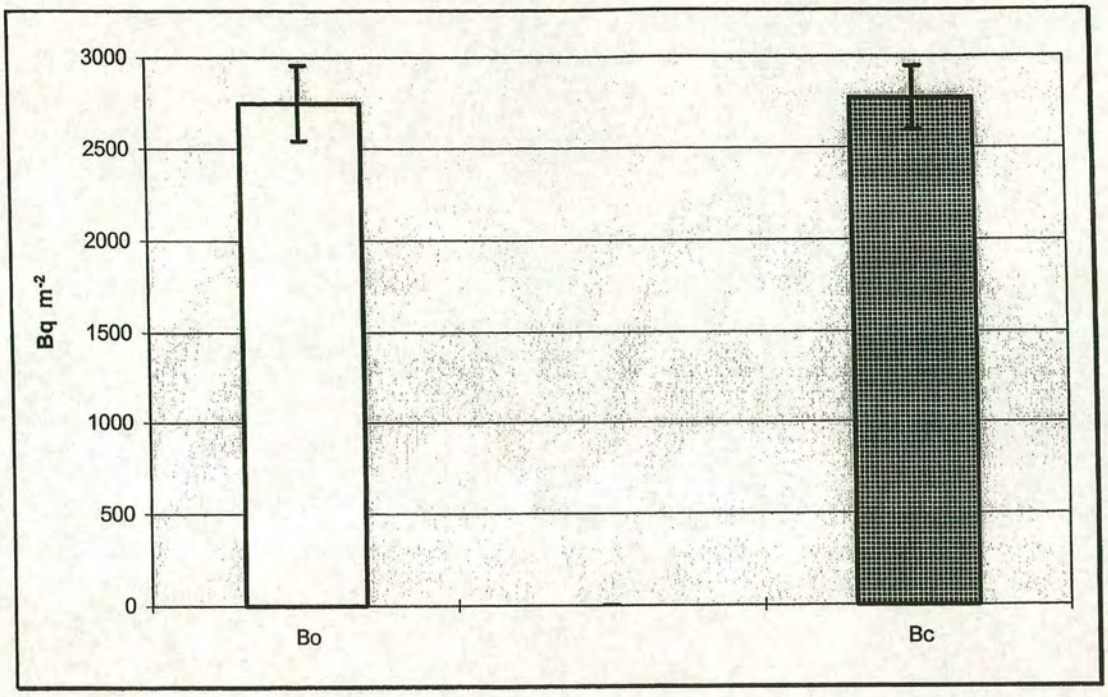

Figure 3.35: Mean atmospheric ^{210}Pb soil inventories in the open field(B_O), and inside the forest canopy(B_C) locations at Haverdals naturreservat.

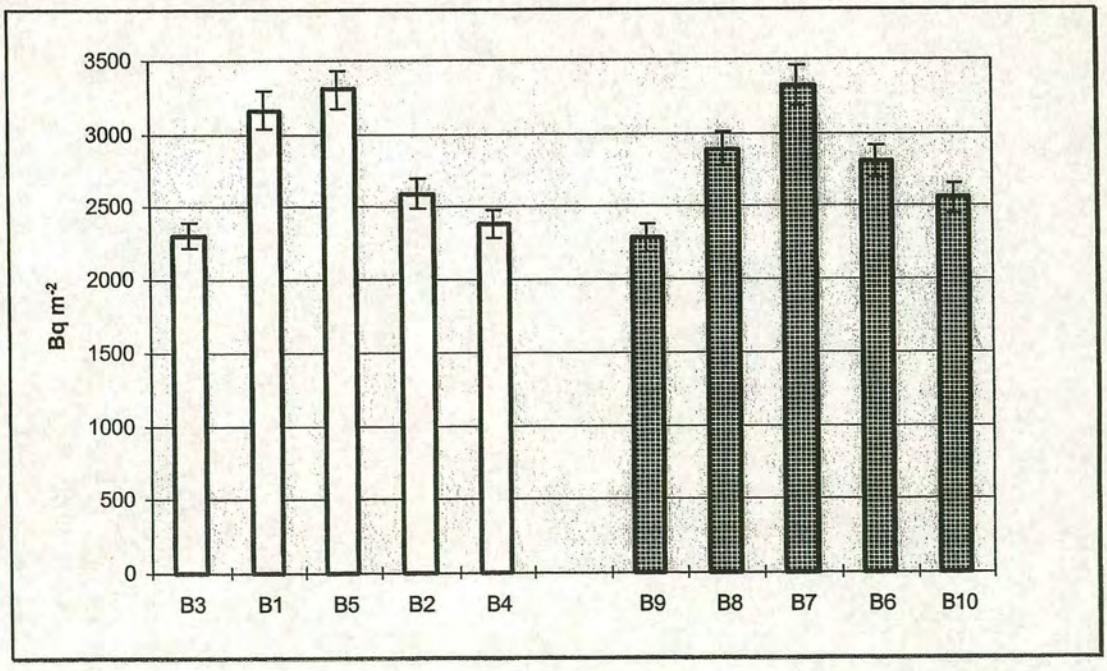

Figure 3.36: Atmospheric ^{210}Pb inventories measured in soil samples from each sampling point at Haverdals naturreservat.

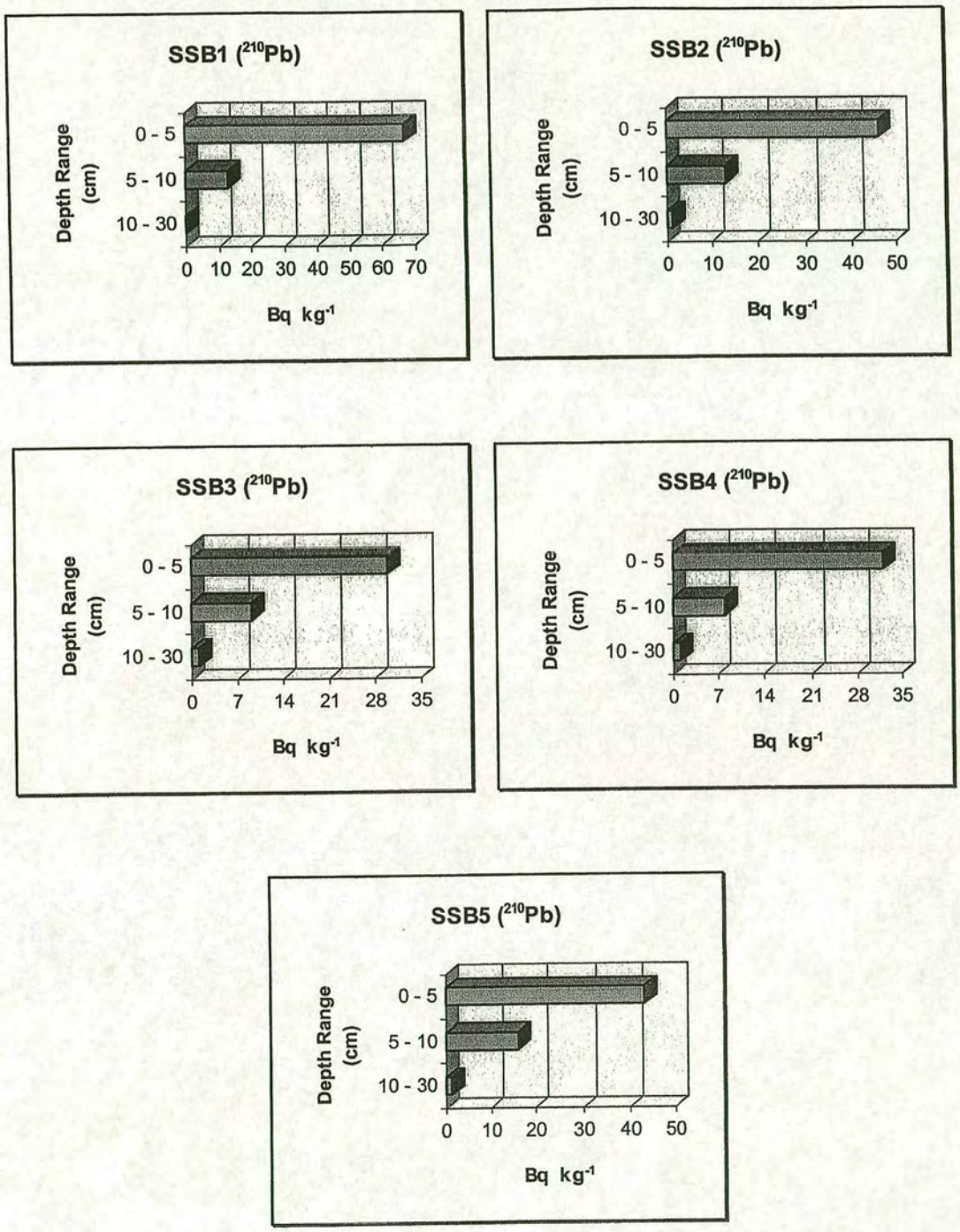

Figure 3.37: Distribution of atmospherically derived ^{210}Pb with depth at Haverdals naturreservat. Open field locations, B1 - B5.

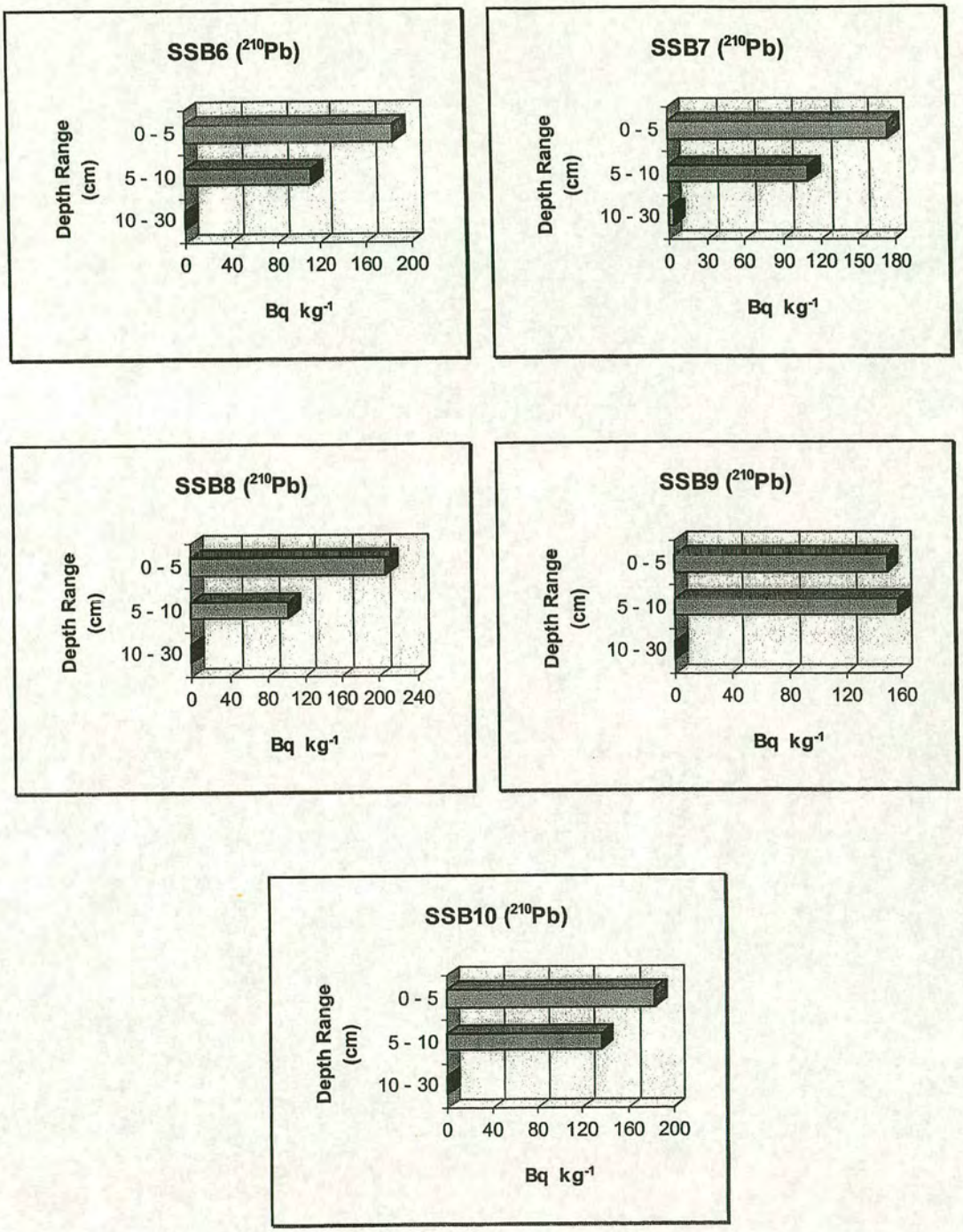

Figure 3.38: Distribution of atmospherically derived ^{210}Pb with depth at Haverdals naturreservat. Under canopy locations, B6 - B10.

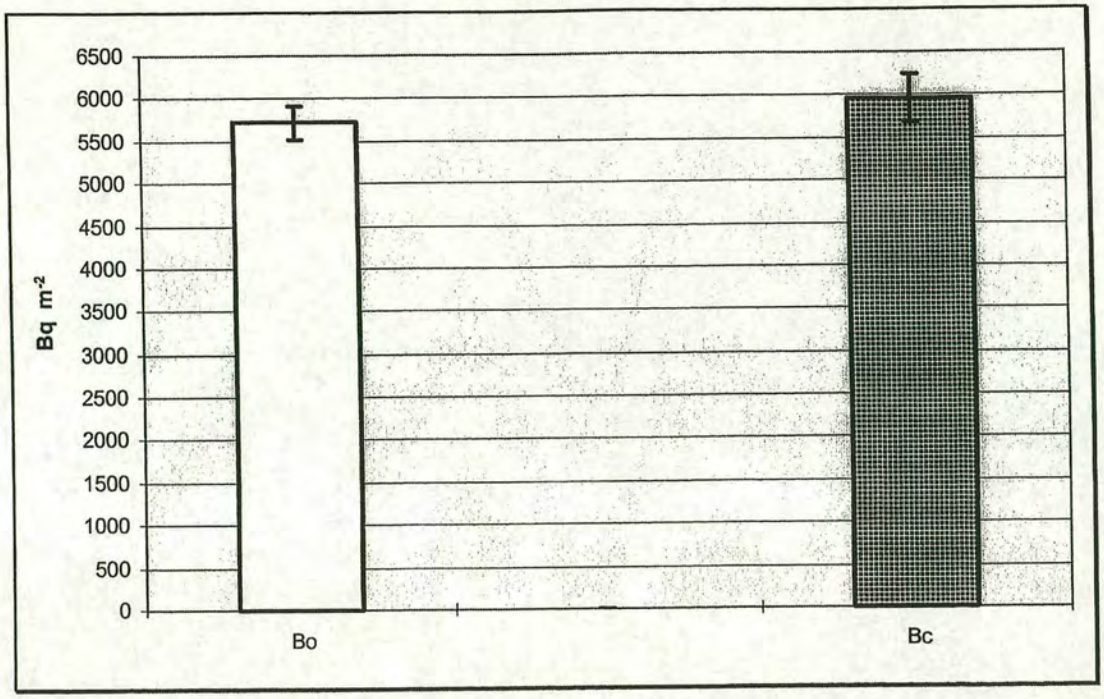

Figure 3.39: Mean ^{137}Cs soil inventories in the open field(B_O), and inside the forest canopy(B_C) locations at Haverdals naturreservat.

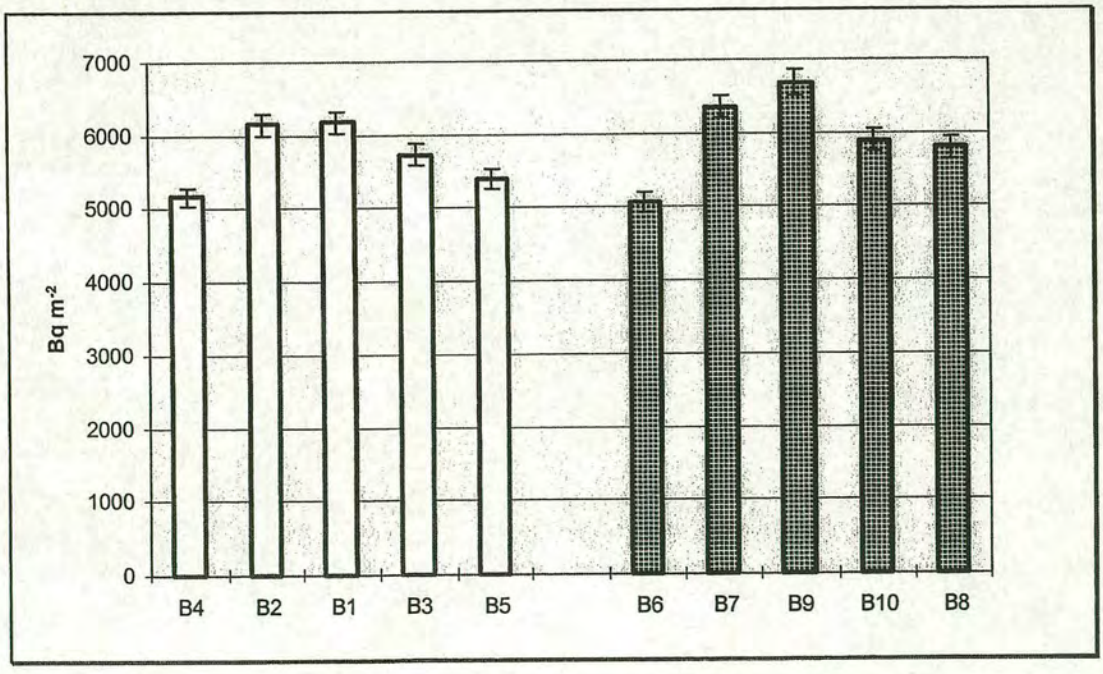

Figure 3.40: ^{137}Cs inventories measured in soil samples from each sampling point at Haverdals naturreservat.

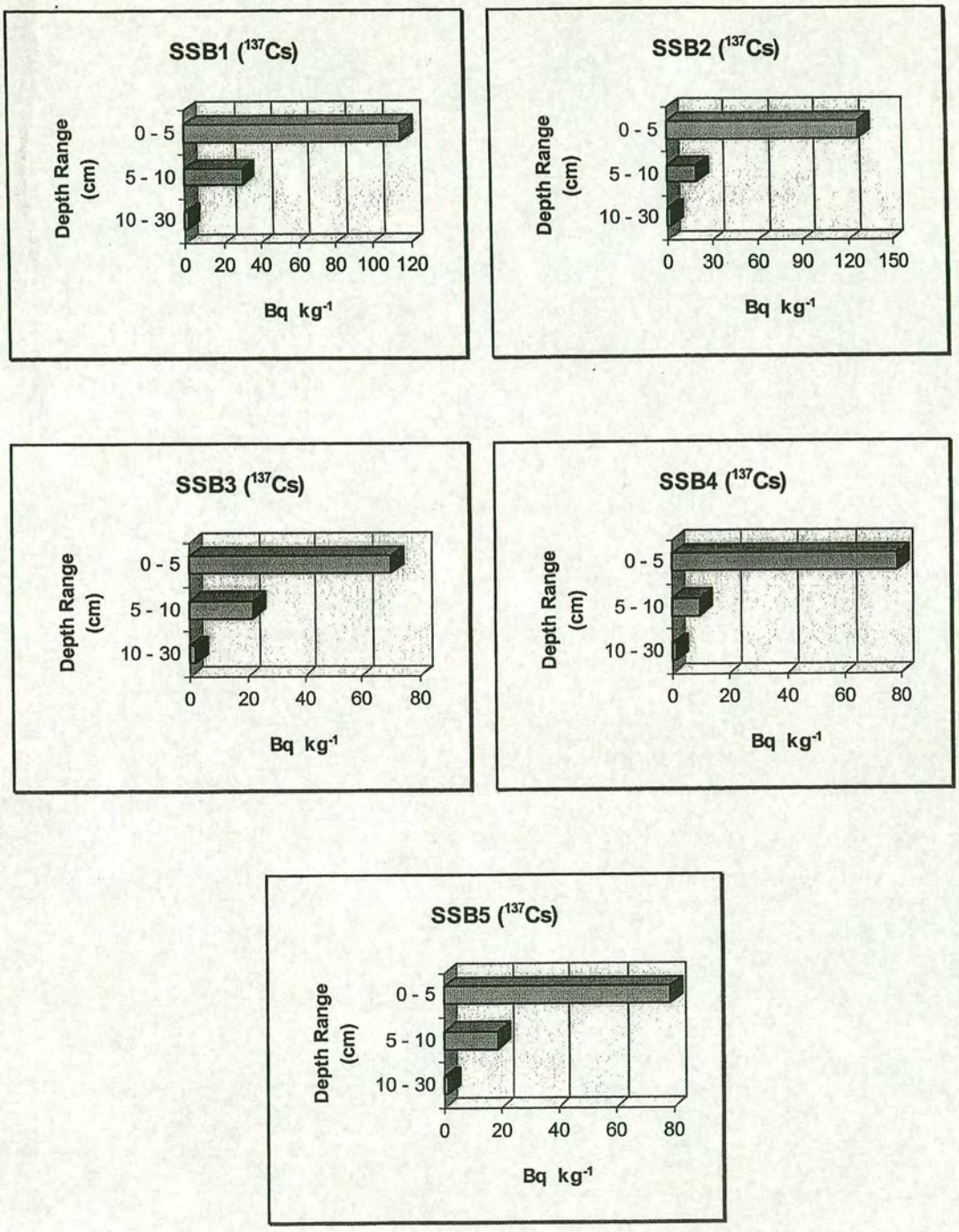

Figure 3.41: Distribution of ^{137}Cs with depth at Haverdals naturreservat. Open field locations, B1 - B5.

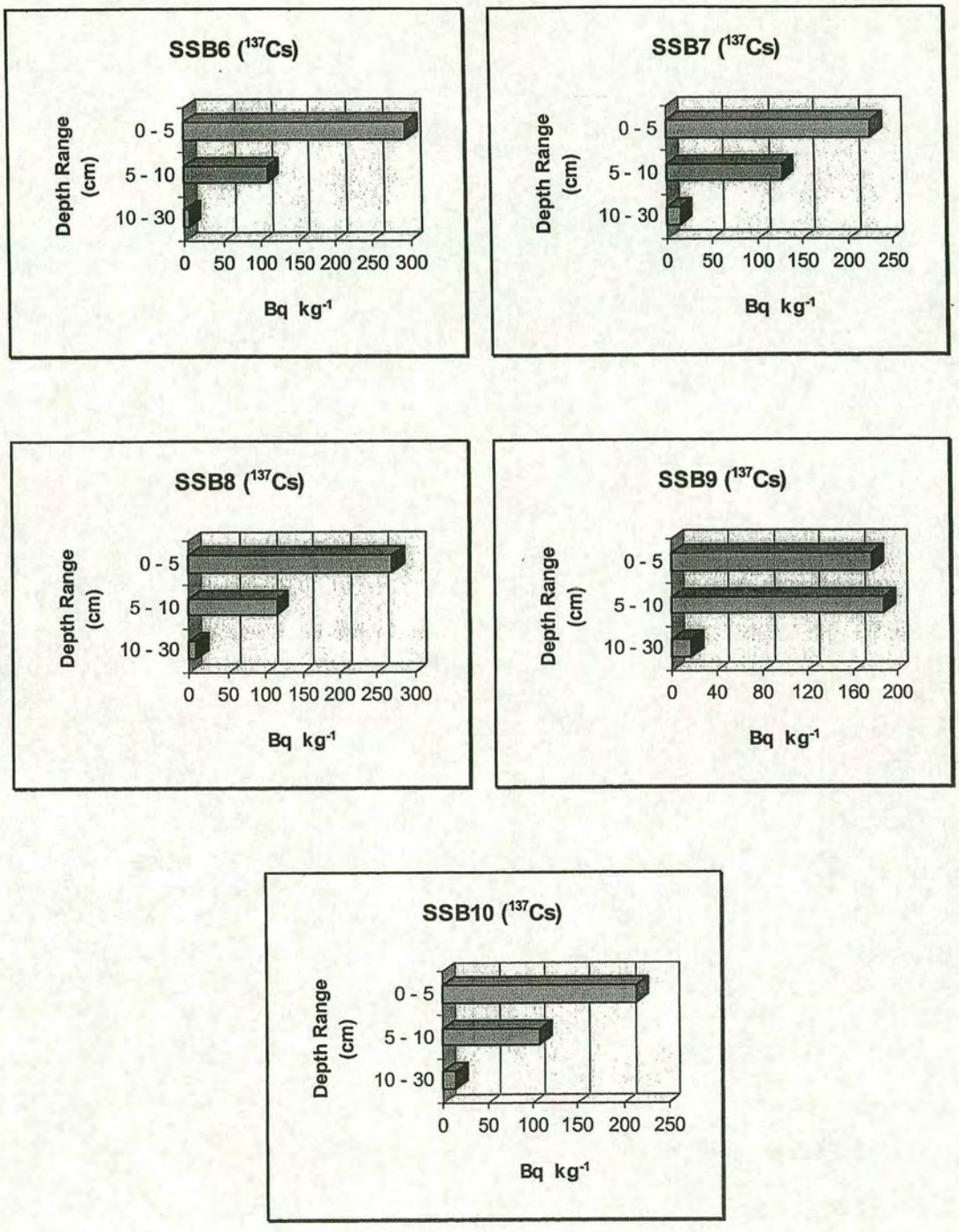

Figure 3.42: Distribution of ^{137}Cs with depth at Haverdals naturreservat. Under canopy locations, B6 - B10.

3.3.3 Bjorketrop (see section 2.1.1.2, Fig. 2.10 & Table 2.2)

3.3.3.1 Lead 210 soil inventories

The inventories of atmospheric ^{210}Pb for the samples collected from the open field at Bjorketrop are presented in Figures 3.43 and 3.44. The mean atmospheric ^{210}Pb inventory for the site(C_O) is shown in Figure 3.43, where the error bar represents standard error of the mean. The coefficient of variation for the measured ^{210}Pb inventories is 9%. The levels of ^{210}Pb present in the individual cores from the open field(C1-C5) are shown in Figure 3.36, where the error bars are due to counting statistics.

Depth profiles for specific activities are illustrated in Figure 3.45. The illustrated profiles indicate the fact that top 10 cm soil has retained the atmospheric ^{210}Pb efficiently, and the contribution from horizons below 10 cm is substantially small in this site.

Under the reasonable assumption of a steady state between the atmospheric supply of ^{210}Pb and its radioactive decay in soil, its average flux at Bjorketrop would be 67 Bq m^{-2} y^{-1}.

3.3.3.2 Caesium 137 soil inventories

The soil inventories for ^{137}Cs are presented in Figures 3.46 and 3.47. The mean ^{137}Cs inventory for the site(C_O) is shown in Figure 3.46, where the error bar represents standard error of the mean. Coefficient of variation for the measured ^{137}Cs inventories is 11%, almost the same variation as with ^{210}Pb inventories for the site. The levels of ^{137}Cs present in the individual cores from the open field(C1-C5) are shown in Figure 3.47, where the error bars are due to counting statistics.

Depth profiles for specific activities are illustrated in Figure 3.48. The illustrated profiles indicate some penetration of this radionuclide to below 10 cm depth interval. However, the bulk of caesium 137 is concentrated in the surface horizons of soil.

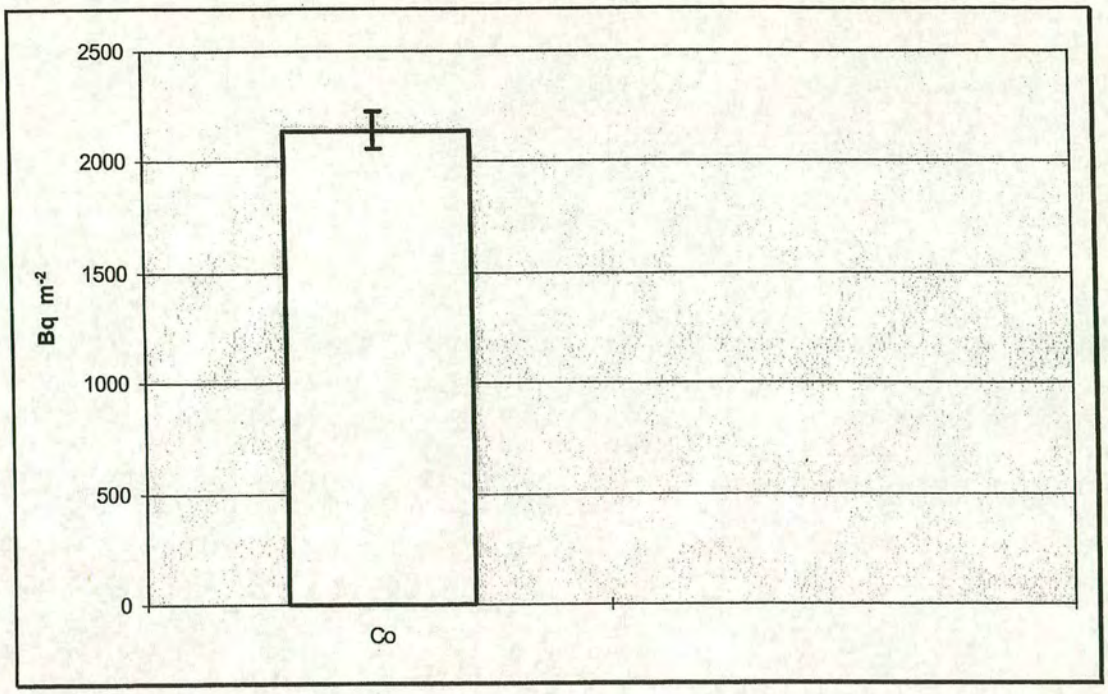

Figure 3.43: Mean atmospheric ^{210}Pb soil inventories in the open field locations at Bjorketrop(C_O).

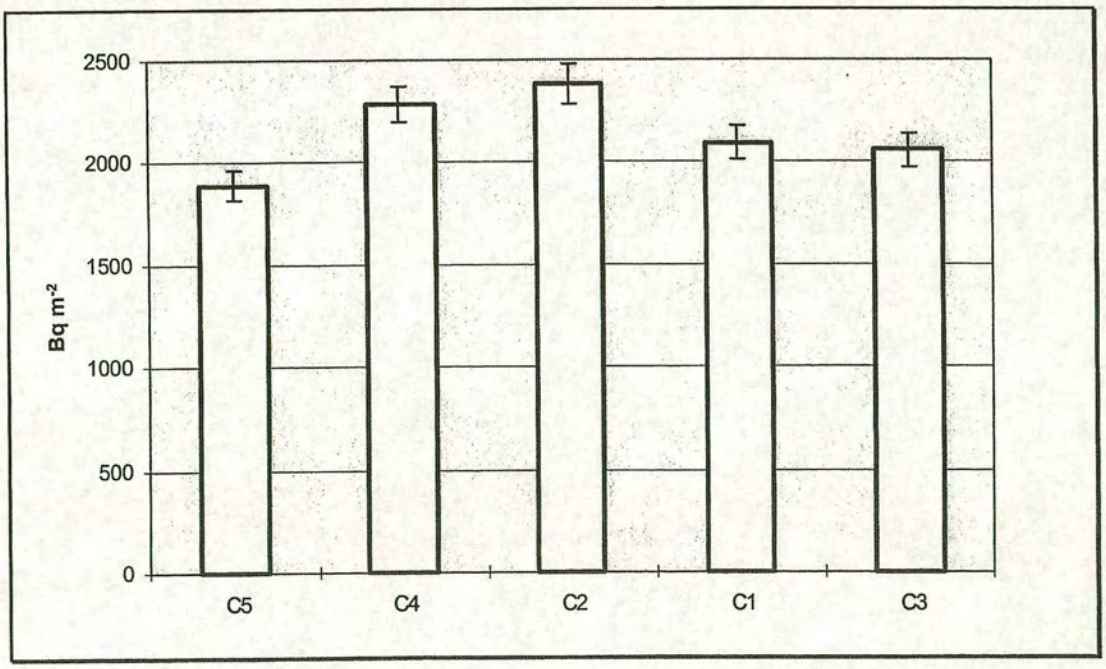

Figure 3.44: Atmospheric ^{210}Pb inventories measured in soil samples from each sampling point at Bjorketrop.

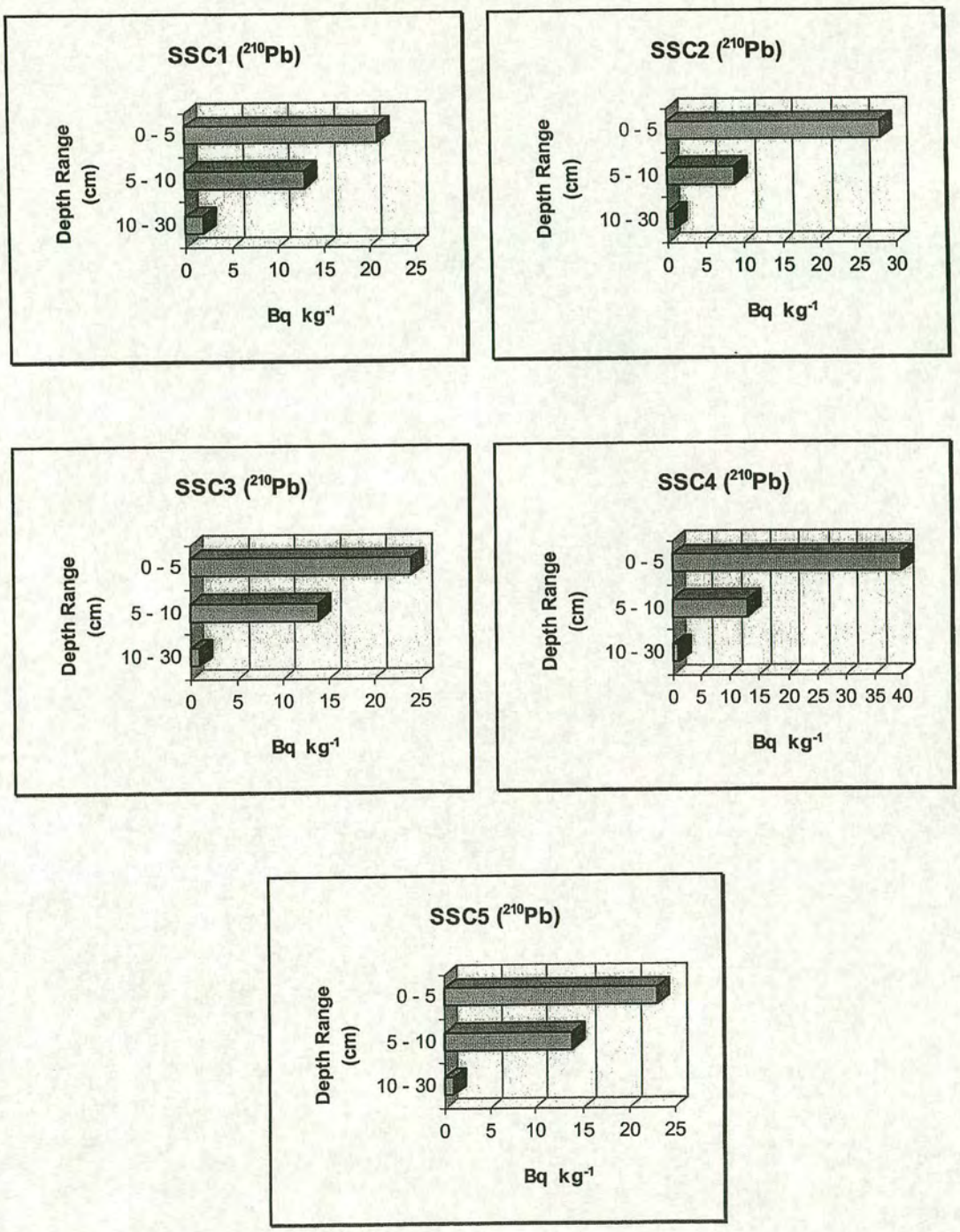

Figure 3.45: Distribution of atmospherically derived ^{210}Pb with depth at Bjorketrop. Open field locations, C1 - C5.

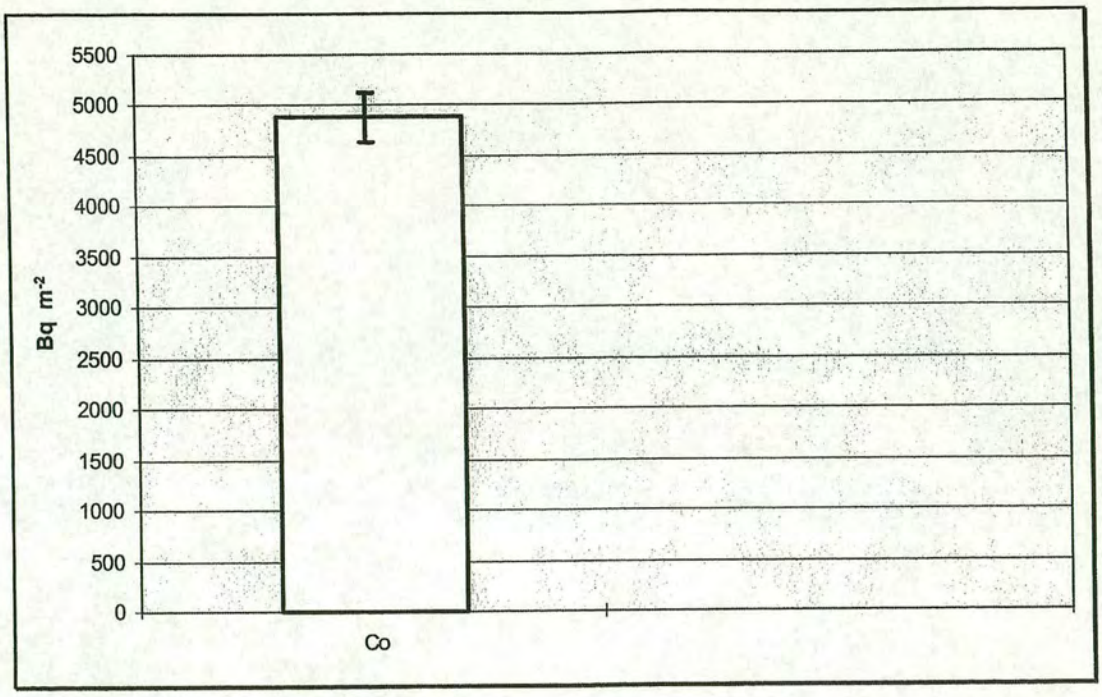

Figure 3.46: Mean ^{137}Cs soil inventories in the open field locations at Bjorketrop(C_O).

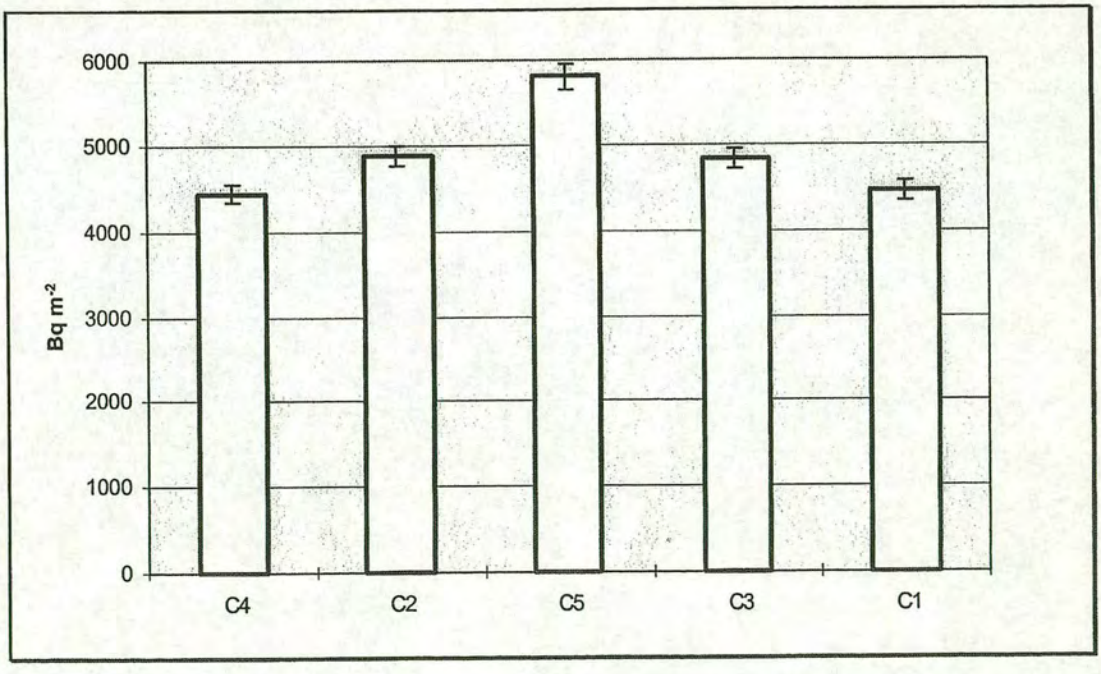

Figure 3.47: ^{137}Cs inventories measured in soil samples from each sampling point at Bjorketrop.

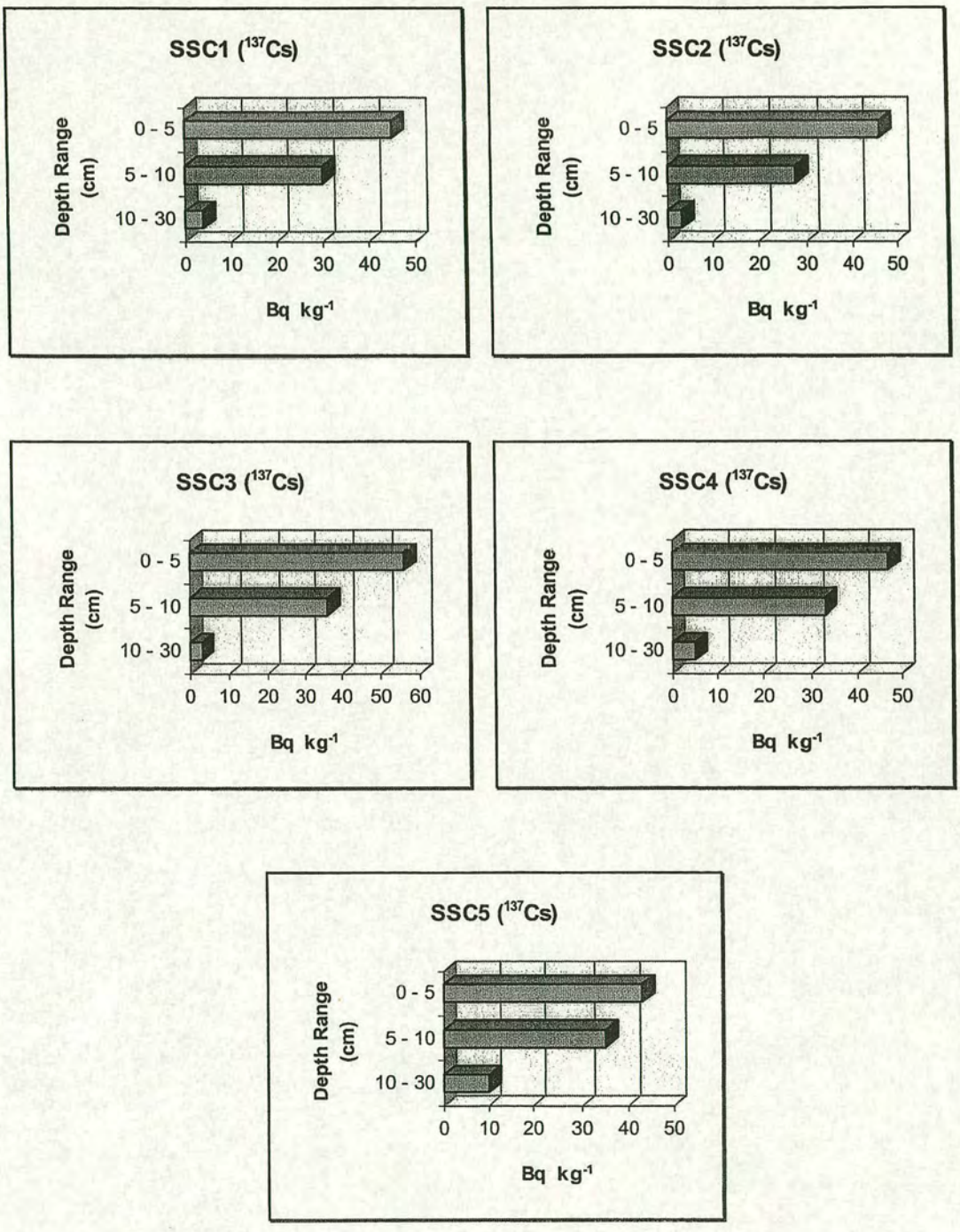

Figure 3.48: Distribution of ^{137}Cs with depth at Bjorketrop.
Open field locations, C1 - C5.

3.3.4 Harplinge (see section 2.1.1.2, Fig. 2.10 & Table 2.2)

3.3.4.1 Lead 210 soil inventories

The inventories of atmospheric ^{210}Pb for the samples collected from beneath the Norway spruce(*Picea abies*) canopy, location D, as well as the adjacent open grassland at Harplinge are presented in Figures 3.49 and 3.50. Mean ^{210}Pb inventories for the open field(D_O) and under canopy(D_C) are shown in Figure 3.49, where the error bars represent the standard error of the mean. Coefficients of variation for the measured ^{210}Pb inventories are almost the same, 14% for the open field, and 15% for the under canopy locations. The levels of ^{210}Pb present in the individual cores from the open field(D1-D5) and under canopy sampling points(D6-D10) are shown in Figure 3.50, where the error bars are due to counting statistics. Considering a calculated t-value of 2.42, there is a significant difference between the mean inventory values for the open field and under canopy samples at 5% level of significance. The canopy enhancement in ^{210}Pb deposition is approximately 26%.

Depth profiles for specific activities are illustrated in Figures 3.51 and 3.52. Though top 10 cm soil has generally retained the atmospheric ^{210}Pb but, The contribution of horizons below 10 cm is relatively higher for the open field cores from this site (note specially SSD2 & SSD5 profiles in Figure 3.51).

Under the reasonable assumption of a steady state condition between the atmospheric supply of ^{210}Pb and its radioactive decay in soil, its average flux would be 99 Bq m^{-2} y^{-1} for the open grassland in Harplinge. Taking into account the other set of samples collected from beneath the canopy at location E(see section 3.3.5),the average ^{210}Pb flux to the spruce canopy in Harplinge is approximately 111 Bq m^{-2} y^{-1}.

3.3.4.2 Caesium 137 soil inventories

The soil inventories for ^{137}Cs are presented in Figures 3.53 and 3.54. Mean inventories for the open field(D_O) and under canopy(D_C) locations are shown in

Figure 3.53, where the error bars represent standard error of the mean. The coefficient of variation for the measured ^{137}Cs inventories is 14%, for the open field, and slightly higher,19% for the under canopy locations. The levels of ^{137}Cs present in the individual cores from the open field(D1-D5) and under canopy sampling points(D6-D10) are shown in Figure 3.54, where the error bars are due to counting statistics. There are no significant differences between the mean inventories for the open field and under canopy samples.

Depth profiles for specific activities are illustrated in Figures 3.55 and 3.56 for the open field and under canopy cores, respectively. Though the bulk of caesium 137 is concentrated in the surface horizons of soil but, these profiles indicate the penetration of this radionuclide to below 10 cm horizons for both open field and canopy locations at Harplinge (note that this is also the case with activity profiles for the other set of beneath canopy samples collected from location E at Harplinge, Figure 3.63).

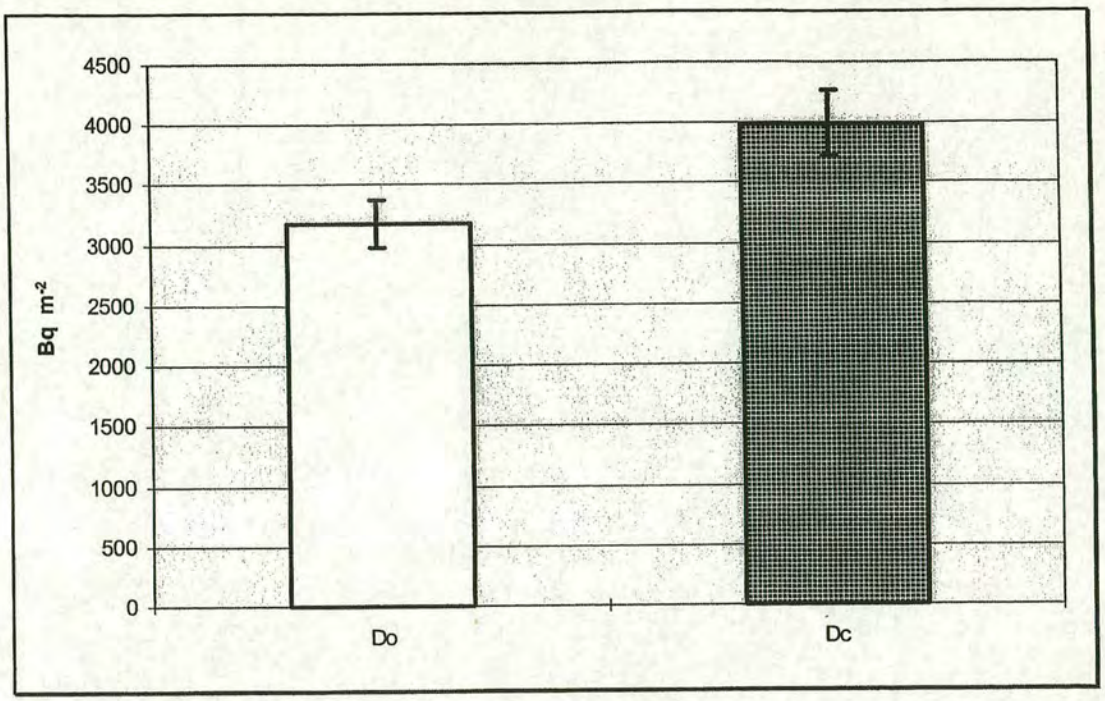

Figure 3.49: Mean atmospheric ^{210}Pb soil inventories in the open field(D_O), and inside the forest canopy(D_C) at Harplinge.

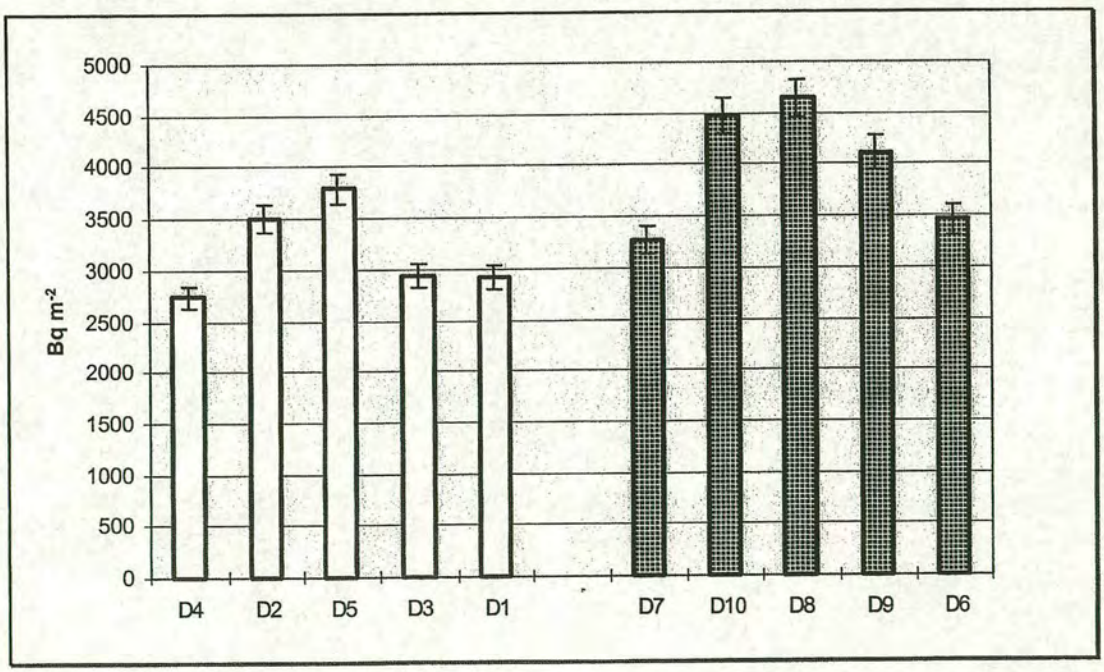

Figure 3.50: Atmospheric ^{210}Pb inventories measured in soil samples from each sampling point at Harplinge.

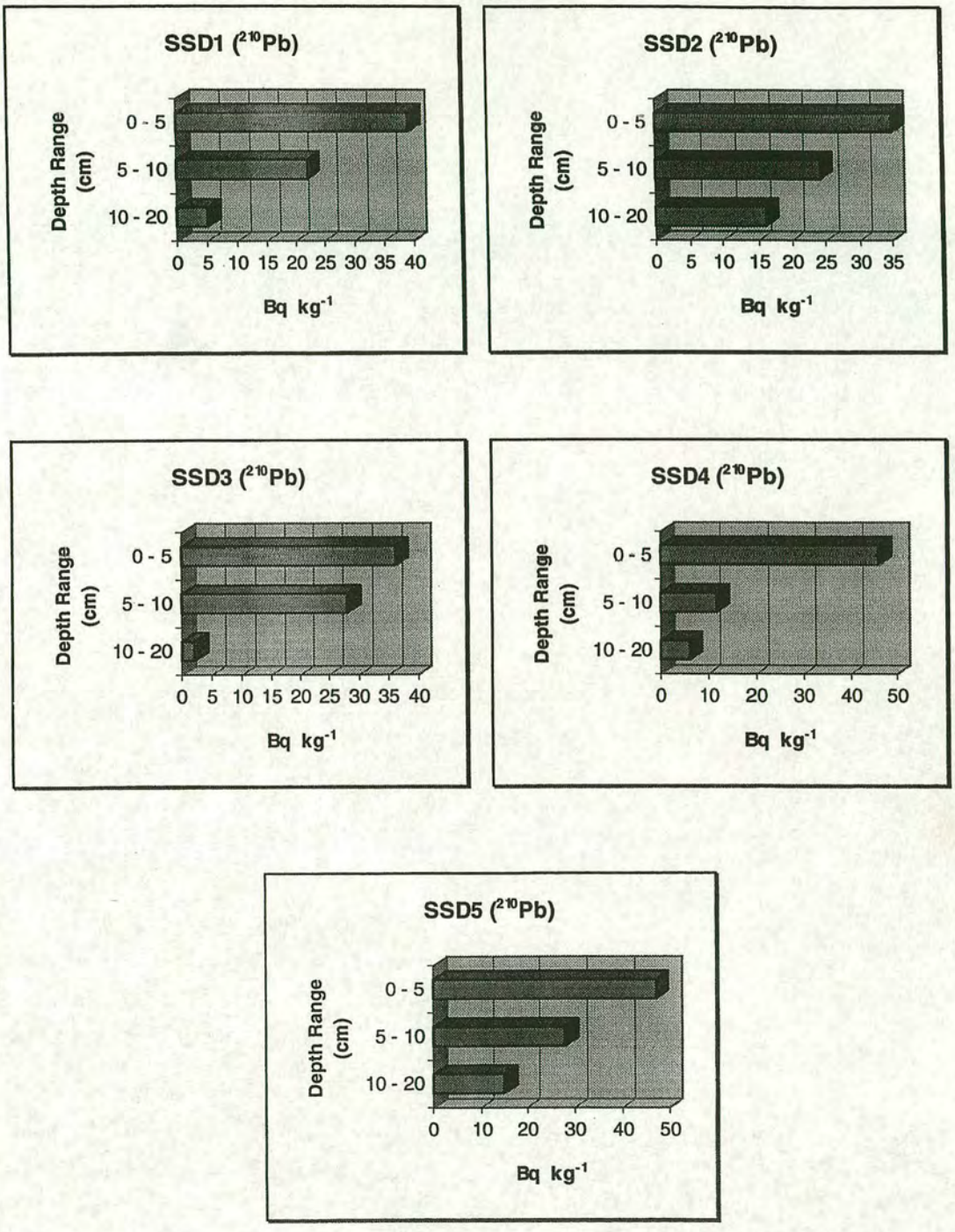

Figure 3.51: Distribution of atmospherically derived ^{210}Pb with depth at Harplinge.
Open field locations, D1 - D5.

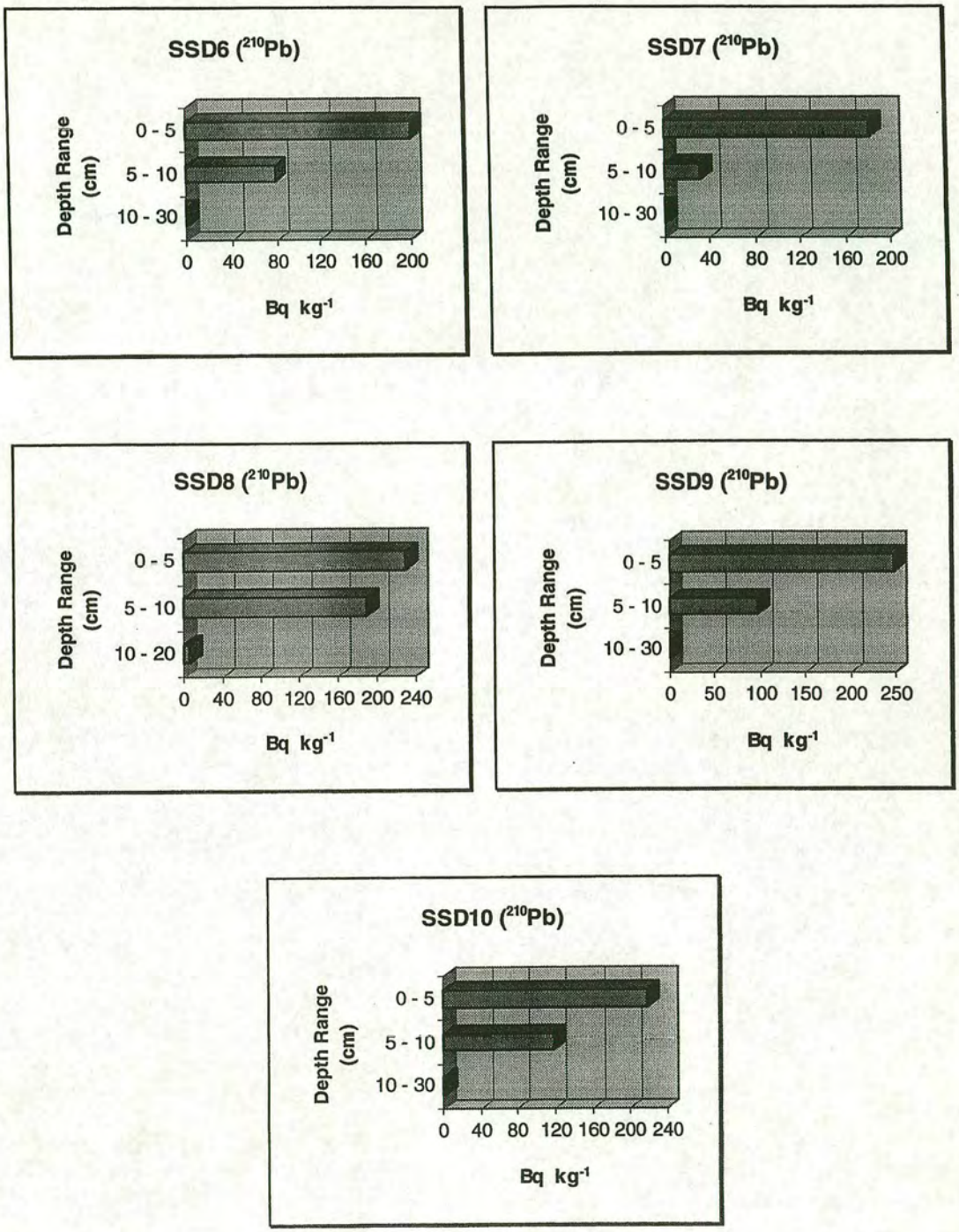

Figure 3.52: Distribution of atmospherically derived ^{210}Pb with depth at Harplinge. Under canopy locations, D6 - D10.

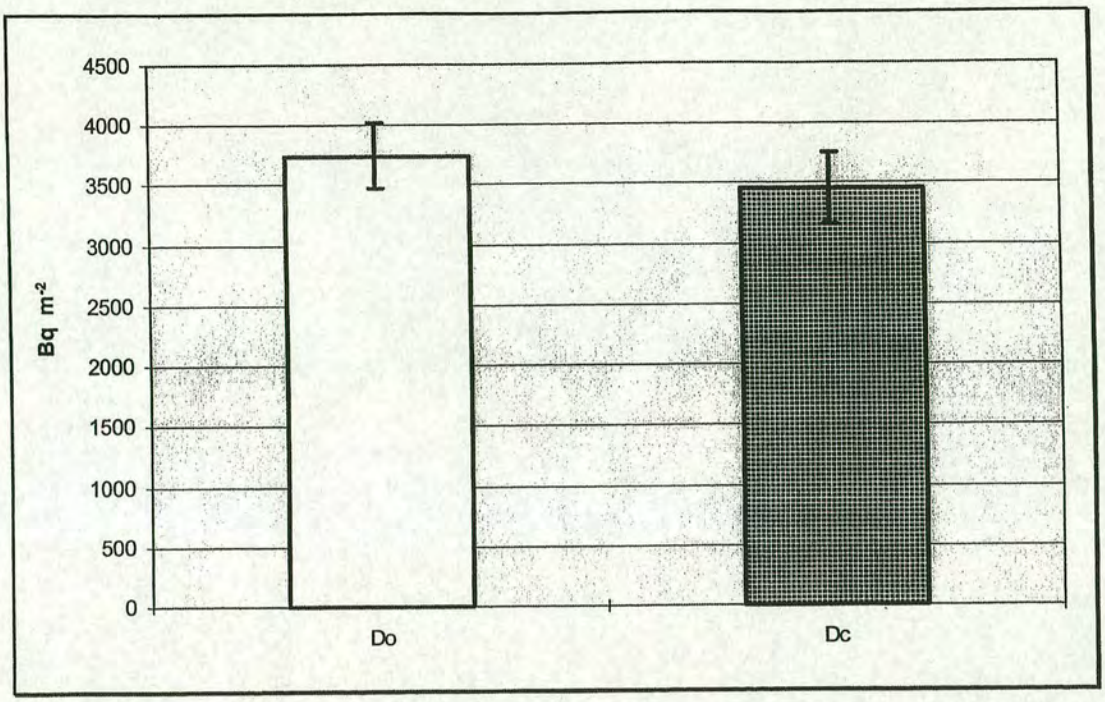

Figure 3.53: Mean ^{137}Cs soil inventories in the open field(D_O), and inside the forest canopy(D_C) at Harplinge.

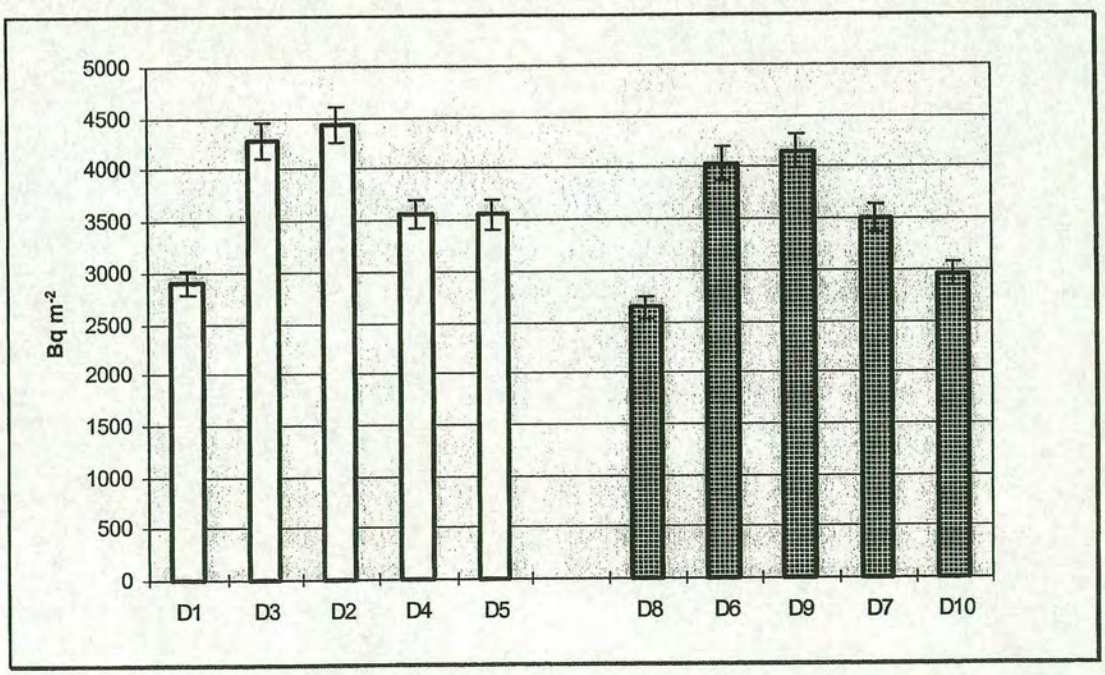

Figure 3.54: ^{137}Cs inventories measured in soil samples from each sampling point at Harplinge.

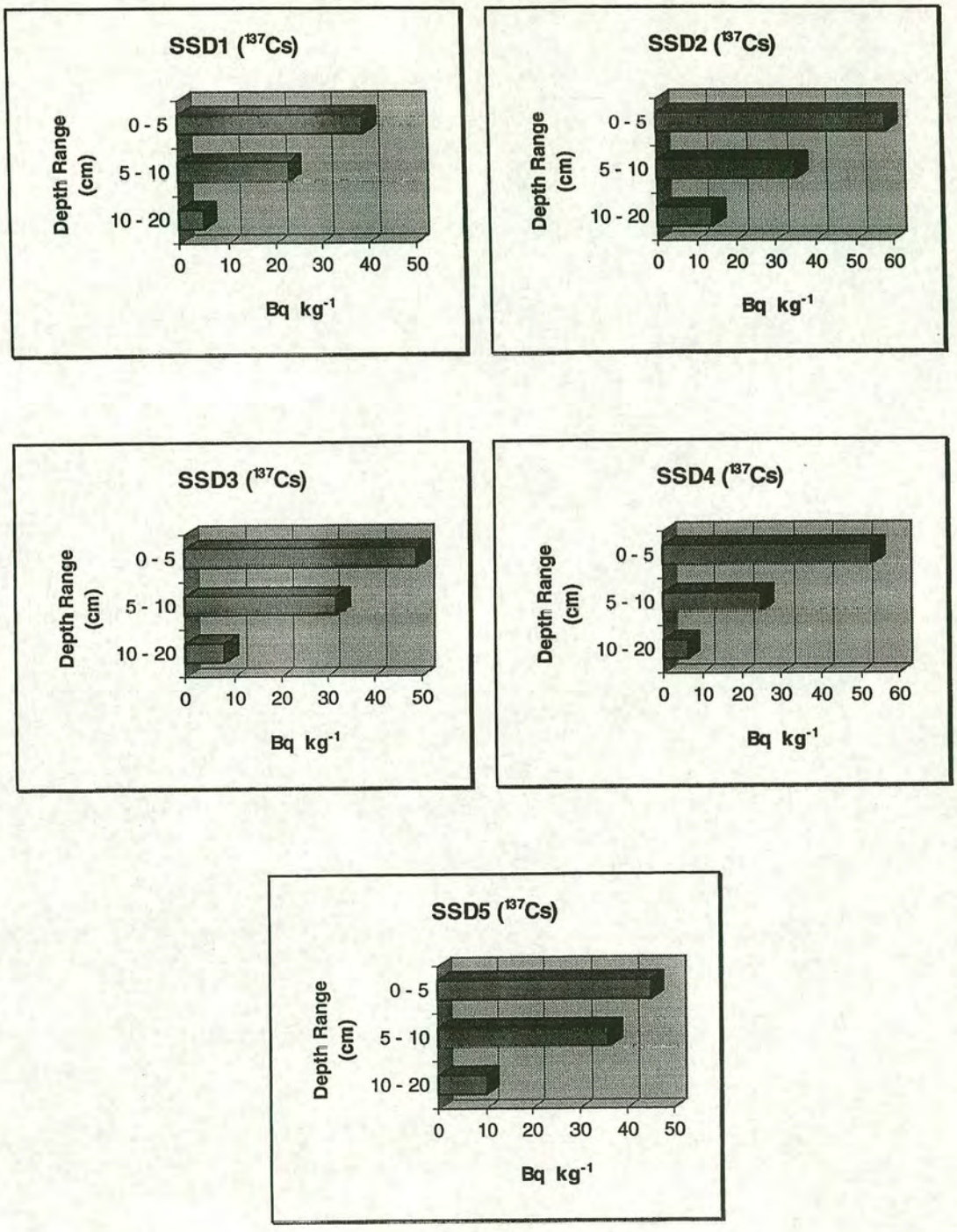

Figure 3.55: Distribution of ^{137}Cs with depth at Harplinge.
Open field locations, D1 - D5.

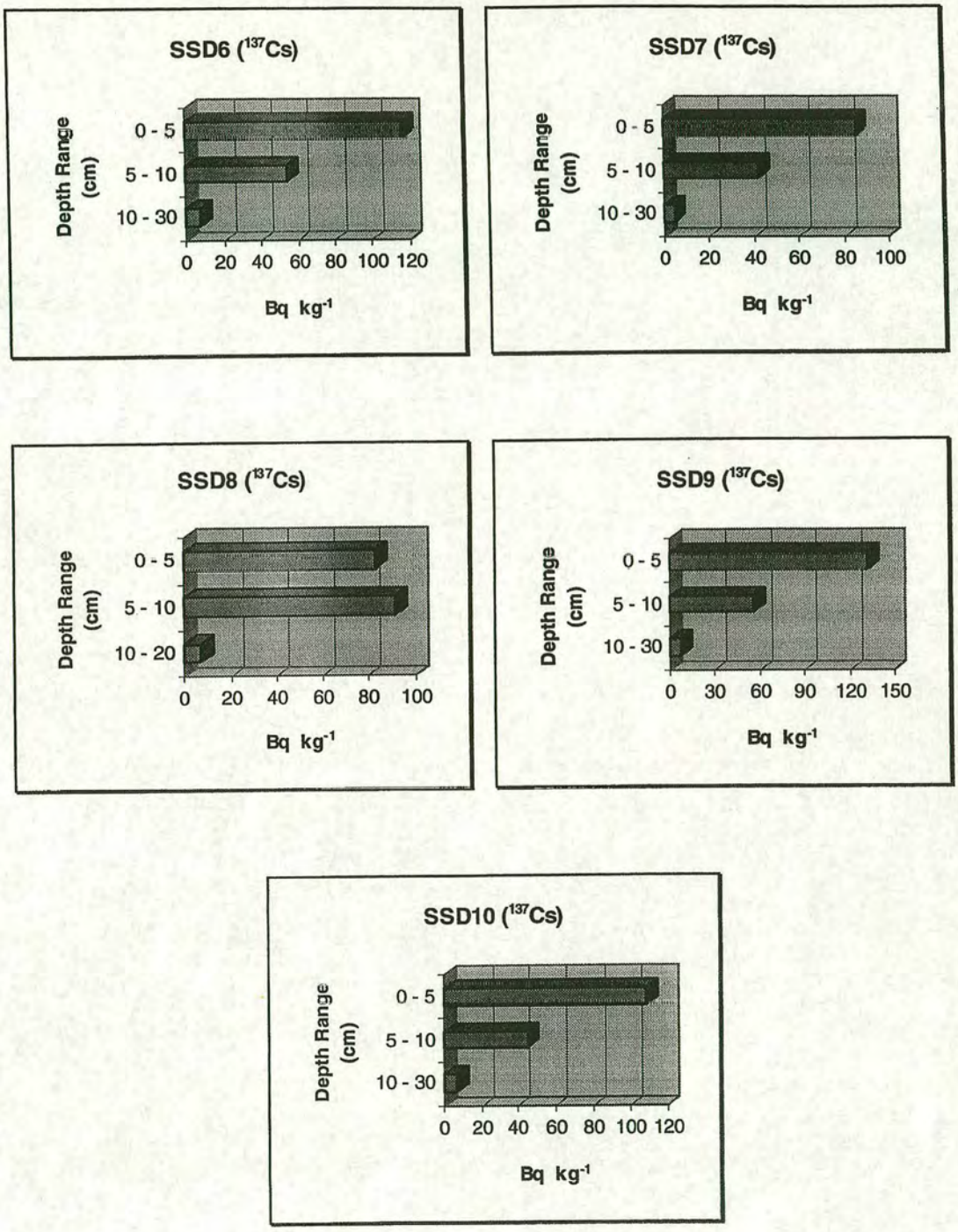

Figure 3.56: Distribution of ^{137}Cs with depth at Harplinge.
Under canopy locations, D6 - D10.

3.3.5 Kvibille & Harplinge (see section 2.1.1.2, Fig. 2.10 & Table 2.2)

3.3.5.1 Lead 210 soil inventories

The inventories of atmospheric ^{210}Pb for the samples collected from beneath the Norway spruce(*Picea abies*) canopies at Harplinge, site E, and Kvibille, site F, are presented in Figures 3.57 and 3.58. Mean ^{210}Pb inventories for Harplinge(E_c) and Kvibille(F_C) are shown in Figure 3.57, where the error bars represent standard error of the mean. Lead 210 deposition to spruce canopy in Kvibille exceeds that of Harplinge(site E) by approximately 34%. The levels of ^{210}Pb present in the individual cores from Harplinge(E6-E10) and Kvibille sampling points(F6-F10) are shown in Figure 3.58, where the error bars are due to counting statistics. The coefficient of variation for measured ^{210}Pb inventories is 13% for Harplinge(site E) and 9% for Kvibille. The observed variation in ^{210}Pb inventories for site E is almost the same as the variation in the other sampling locations in Harplinge, D_O and D_C (see section 3.3.4).

Depth profiles for specific activities are illustrated in Figures 3.59 and 3.560. Top 10 cm soil has generally retained the atmospheric ^{210}Pb efficiently, with the exception of SSF6, SSF8, and SSF9 cores all from Kvibille. However, the contribution of 10-30 cm depth interval is substantially small.

Under the reasonable assumption of a steady state between the atmospheric supply of ^{210}Pb and its radioactive decay in soil, its average flux would be 131 Bq m^{-2} y^{-1} for the canopy in Kvibille. Taking into account the other set of samples collected from beneath the canopy at location D(see section 3.3.4),the average ^{210}Pb flux to the spruce canopy in Harplinge is approximately 111 Bq m^{-2} y^{-1}.

3.3.5.2 Caesium 137 soil inventories

The soil inventories for ^{137}Cs are presented in Figures 3.61 and 3.62. Mean ^{137}Cs inventories for Harplinge(E_c) and Kvibille(F_C) are shown in Figure 3.61, where

the error bars represent standard error of the mean. There are no significant differences between the mean inventory values for these canopies. The levels of ^{137}Cs present in the individual cores from Harplinge(E6-E10) and Kvibille sampling points(F6-F10) are shown in Figure 3.62, where the error bars are due to counting statistics. The coefficient of variation for measured ^{137}Cs inventories is 19% for Harplinge(site E) and 16% for Kvibille. The observed variation in ^{137}Cs inventories for site E is the same as the variation in the other canopy location in Harplinge, D_C (see section 3.3.4).

Depth profiles for specific activities are illustrated in Figures 3.63 and 3.64. Though the bulk of caesium 137 is concentrated in the surface horizons of soil but, these profiles indicate the penetration of this radionuclide to below 10 cm horizons for both canopies at Harplinge and Kvibille.

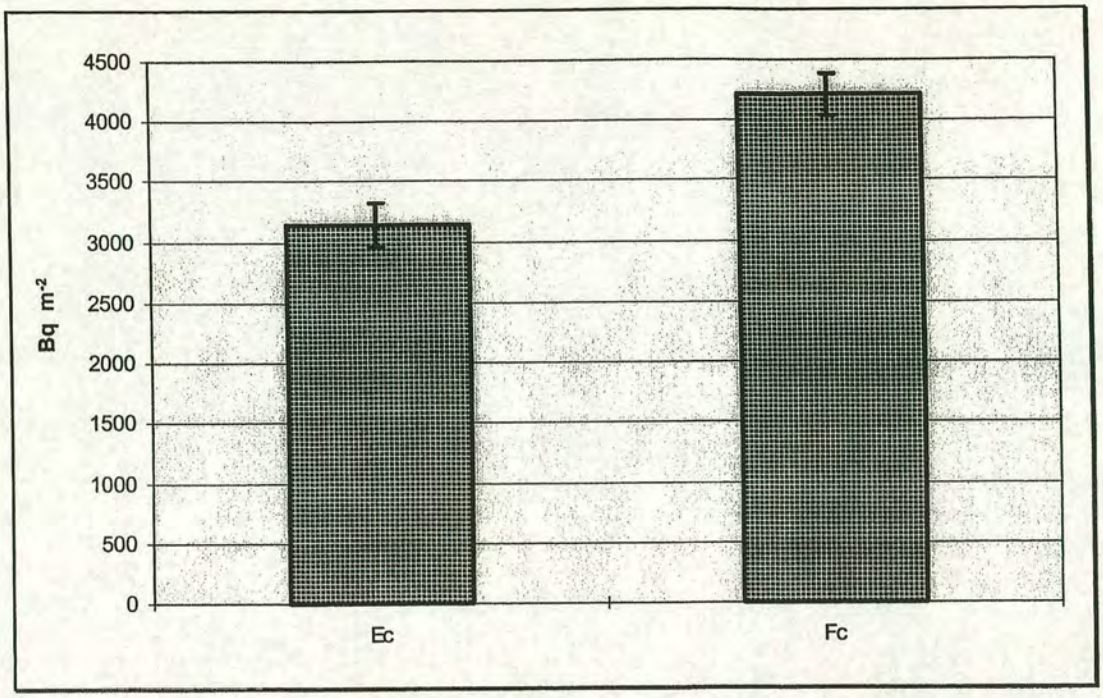

Figure 3.57: Mean atmospheric ^{210}Pb soil inventories inside the forest canopies at Harplinge, site E(E_C) and Kvibille(F_C).

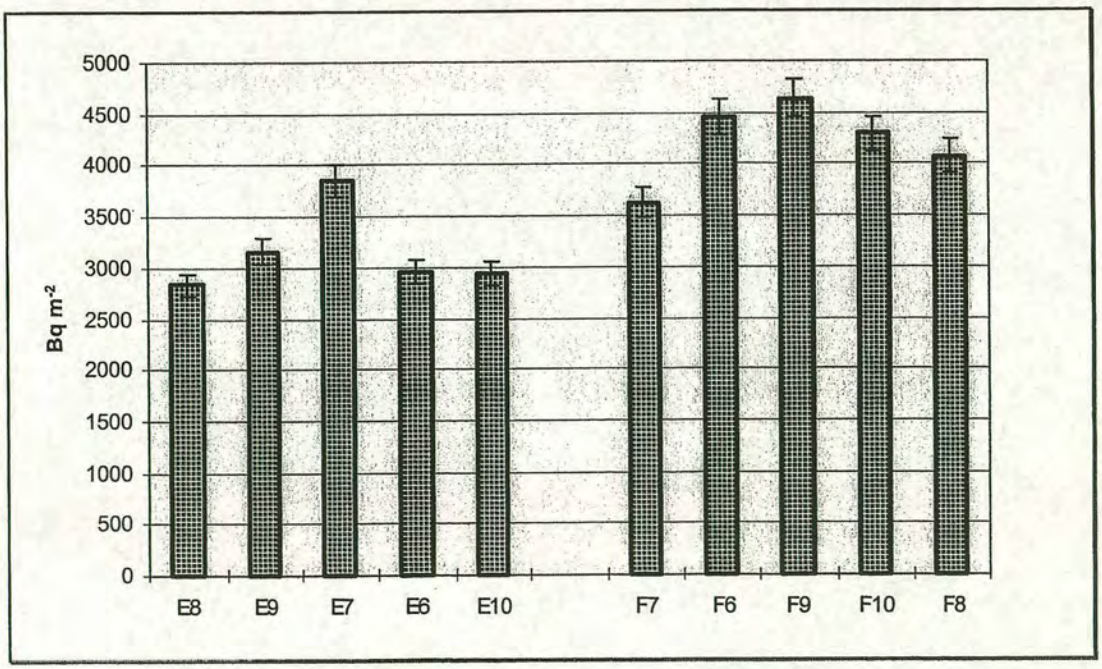

Figure 3.58: Atmospheric ^{210}Pb inventories measured in soil samples from each sampling point at Harplinge(site E) and Kvibille.

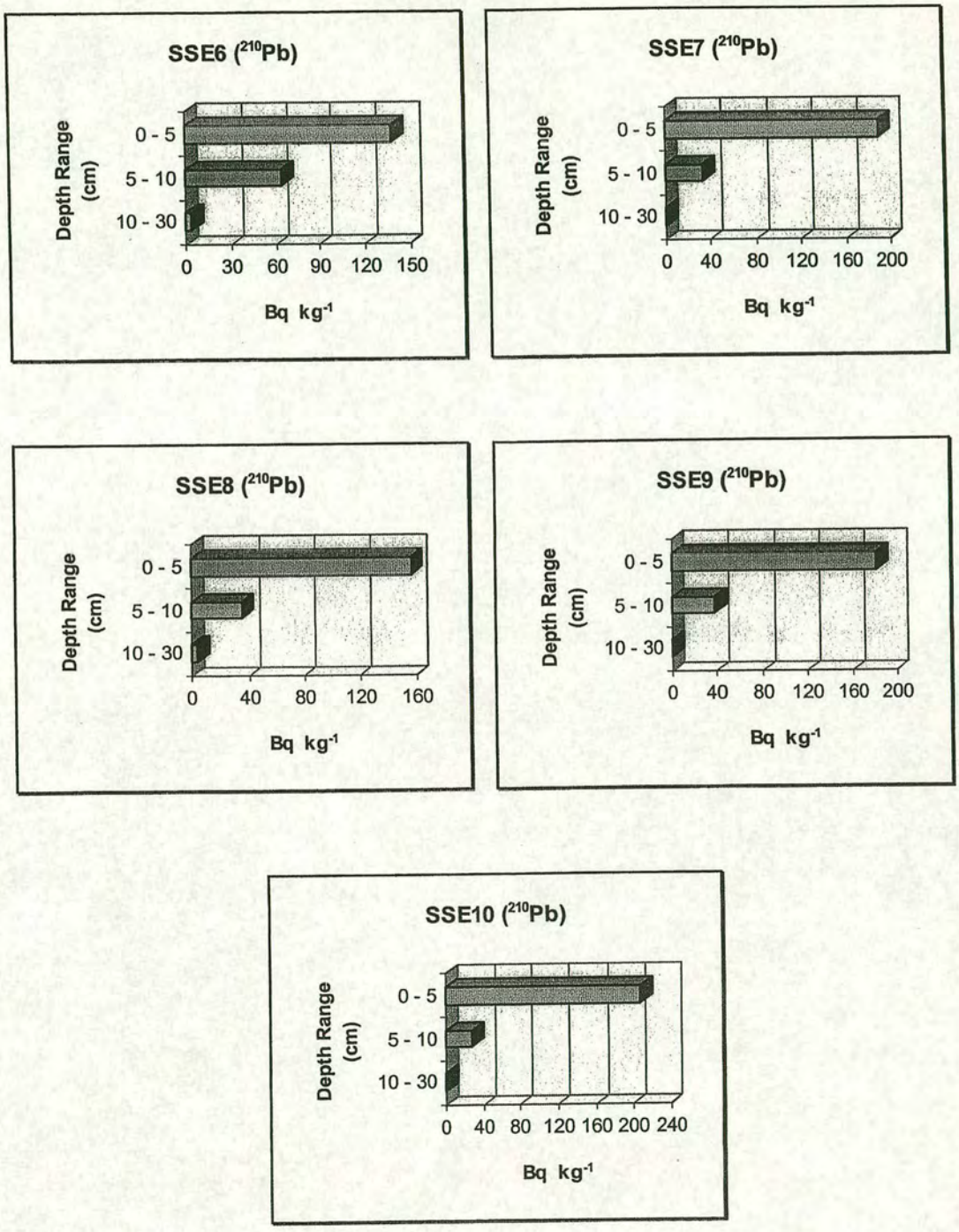

Figure 3.59: Distribution of atmospherically derived ^{210}Pb with depth at Harplinge(site E). Under canopy locations, E6 - E10.

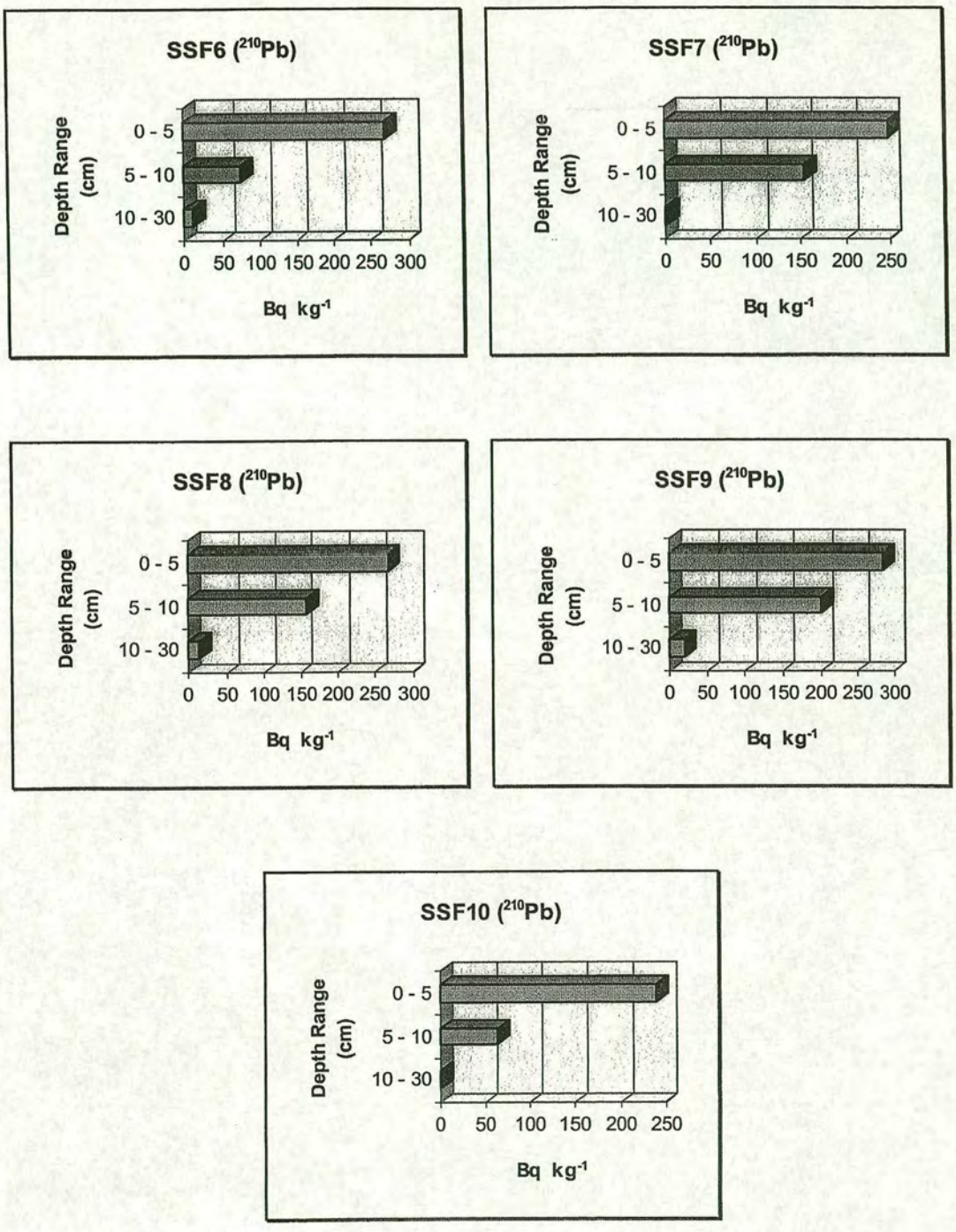

Figure 3.60: Distribution of atmospherically derived ^{210}Pb with depth at Kvibille. Under canopy locations, F6 - F10.

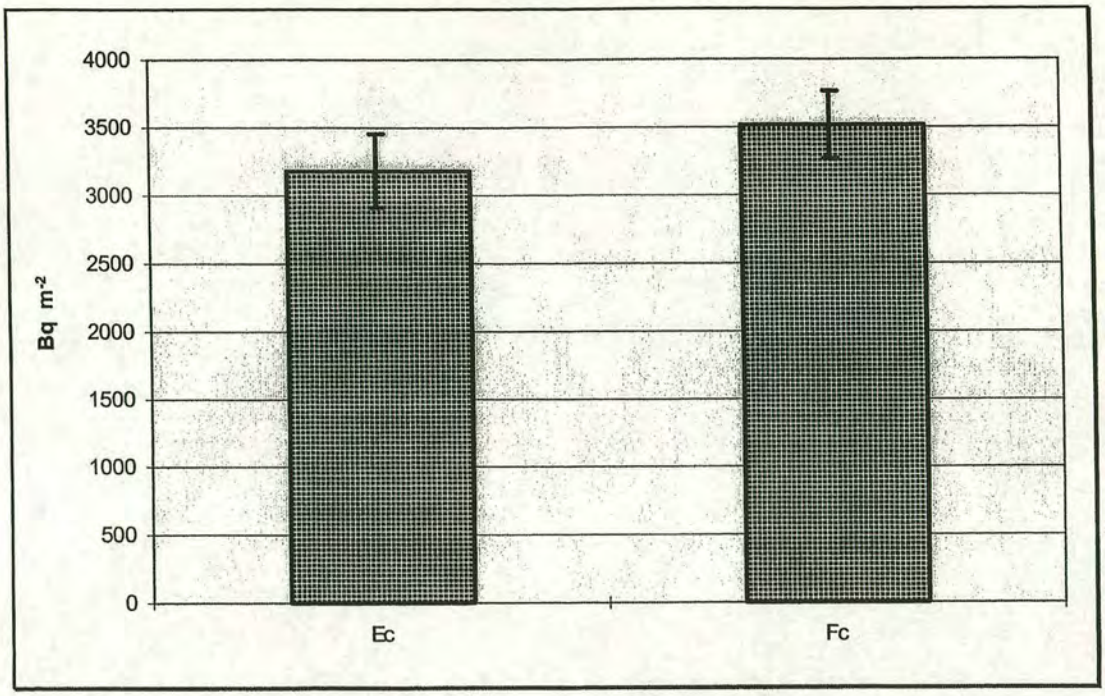

Figure 3.61: Mean ^{137}Cs soil inventories inside the forest canopies at Harplinge, site E(E_C) and Kvibille(F_C).

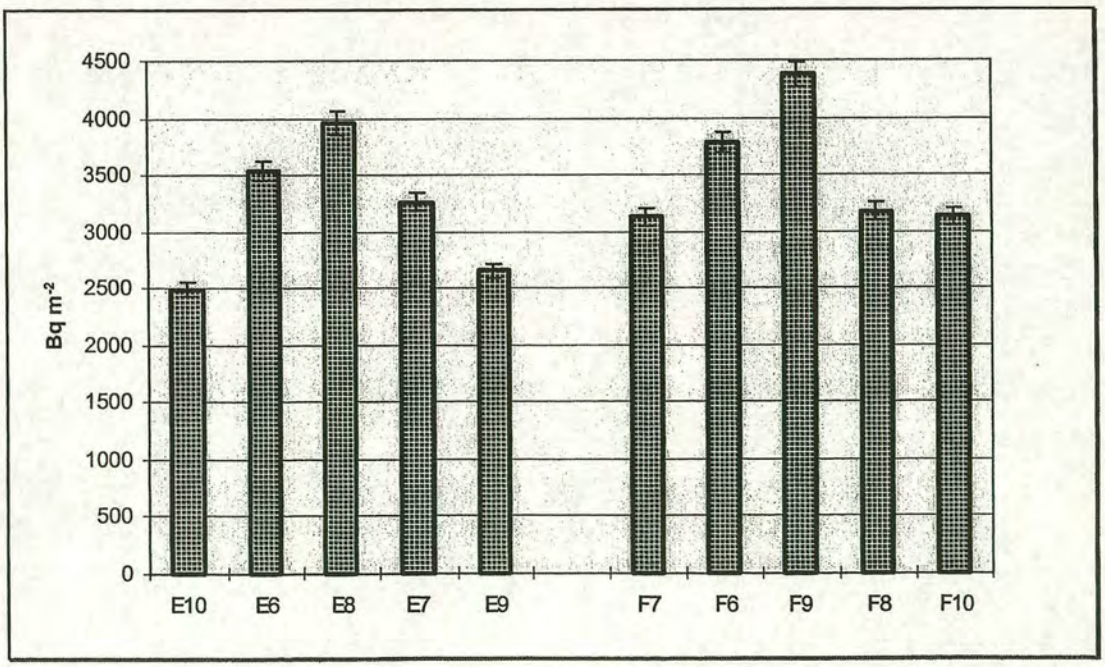

Figure 3.62: ^{137}Cs inventories measured in soil samples from each sampling point at Harplinge(site E) and Kvibille.

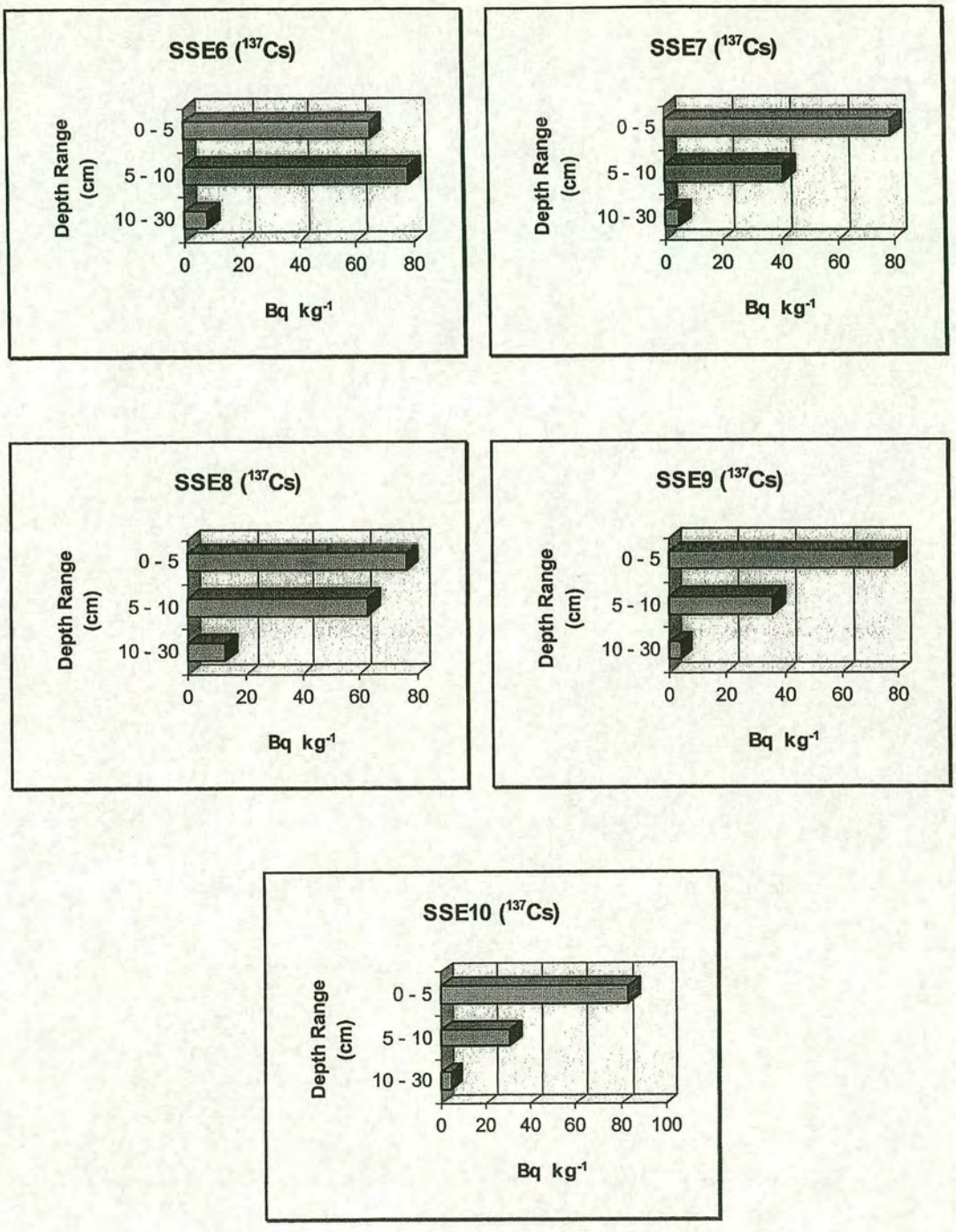

Figure 3.63: Distribution of ^{137}Cs with depth at Harplinge(site E).
Under canopy locations, E6 - E10.

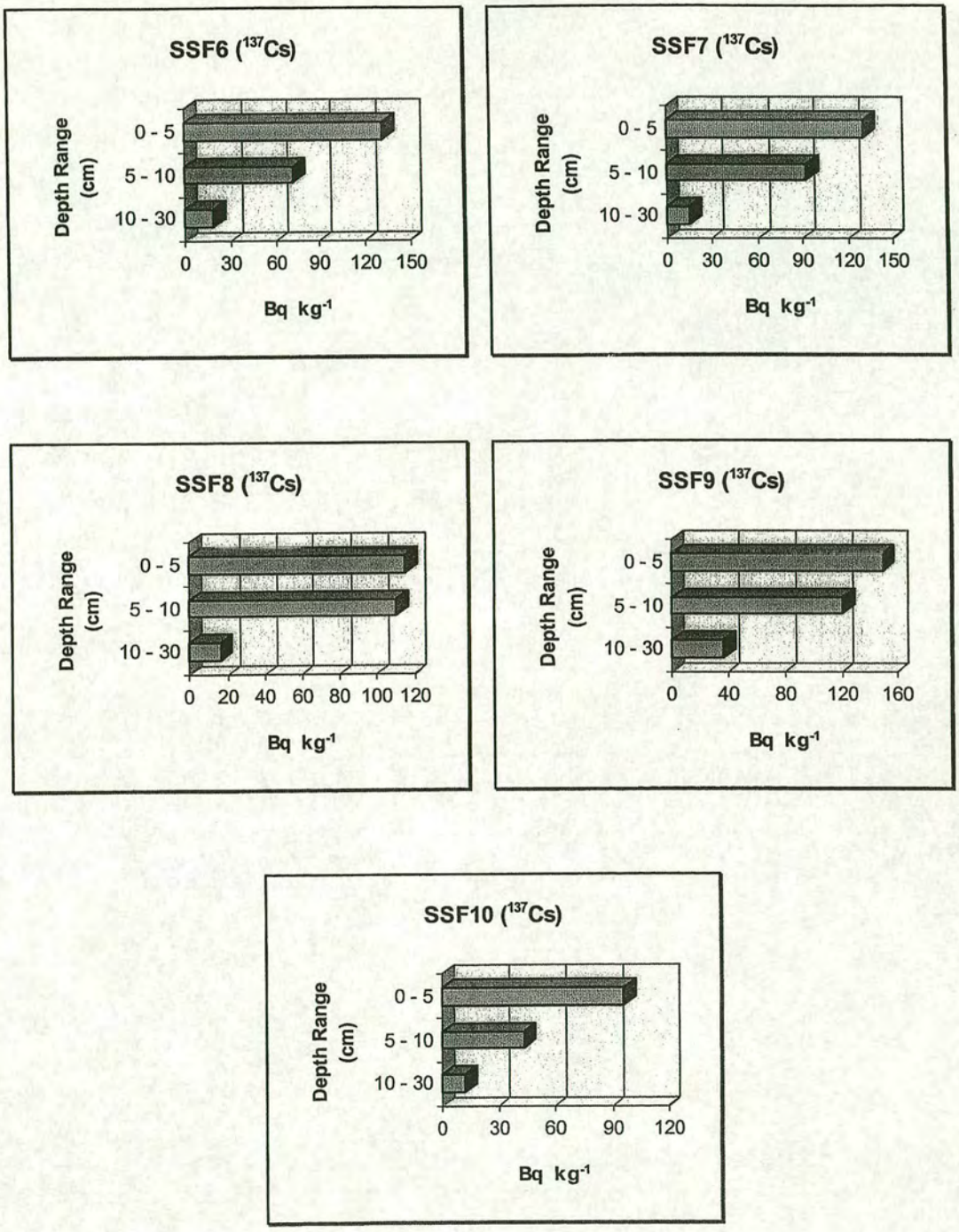

Figure 3.64: Distribution of ^{137}Cs with depth at Kvibille.
Under canopy locations, F6 - F10.

3.3.6 Ovraboke & Stammilt (see section 2.1.1.2, Fig. 2.10 & Table 2.2)

3.3.6.1 Lead 210 soil inventories

The inventories of atmospheric ^{210}Pb for the samples collected from beneath the Norway spruce(*Picea abies*) canopy in Stammilt, as well as the open field in Ovrarboke are presented in Figures 3.65 and 3.66. Mean ^{210}Pb inventories for the open field(G_O) and under canopy(G_C) are shown in Figure 3.65, where the error bars represent standard error of the mean. The coefficient of variation for the measured ^{210}Pb inventories is 12% for the open field, and 7% for the under canopy location. The levels of ^{210}Pb present in the individual cores from the open field(G1-G5) and under canopy sampling points(G6-G10) are shown in Figure 3.66, where the error bars are due to counting statistics. Inside canopy locations at Stammilt show a substantially larger inventory (by approximately 90%) relative to the nearby open field in Ovraboke.

Depth profiles for specific activities are illustrated in Figures 3.67 and 3.68. Under canopy profiles (G6-G10) indicate the fact that top 10 cm soil has efficiently retained the atmospheric ^{210}Pb but, The contribution of horizons below 10 cm is relatively high for the open field cores(G1-G5) from Ovraboke.

Under the reasonable assumption of a steady state between the atmospheric supply of ^{210}Pb and its radioactive decay in soil, its average flux would be 87 Bq m^{-2} y^{-1} for the open field in Ovraboke, and 165 Bq m^{-2} y^{-1} for the spruce canopy in Stammilt.

3.3.6.2 Caesium 137 soil inventories

The soil inventories for ^{137}Cs are presented in Figures 3.69 and 3.70. Mean inventories for the open field(G_O) and under canopy(G_C) locations are shown in Figure 3.69, where the error bars represent standard error of the mean. Though the mean inventories show a canopy enhancement of approximately 26% in ^{137}Cs

deposition but, with a calculated *t-value* of 1.7, the apparent differences between these inventory values are not statistically significant. The levels of ^{137}Cs present in the individual cores from the open field(G1-G5) and under canopy sampling points(G6-G10) are shown in Figure 3.70, where the error bars are due to counting statistics. The coefficient of variation for the measured ^{137}Cs inventories is 16%, for the open field, and 23%, for the under canopy location.

Depth profiles for specific activities are illustrated in Figures 3.71 and 3.72 for the open field and under canopy cores, respectively. Inside canopy profiles(G6-G10) show that the bulk of caesium 137 is concentrated in the surface horizons of soil but, open field profiles(G1-G5) indicate the penetration of this radionuclide to below 10 cm horizons with significant contributions from 10-20 depth intervals.

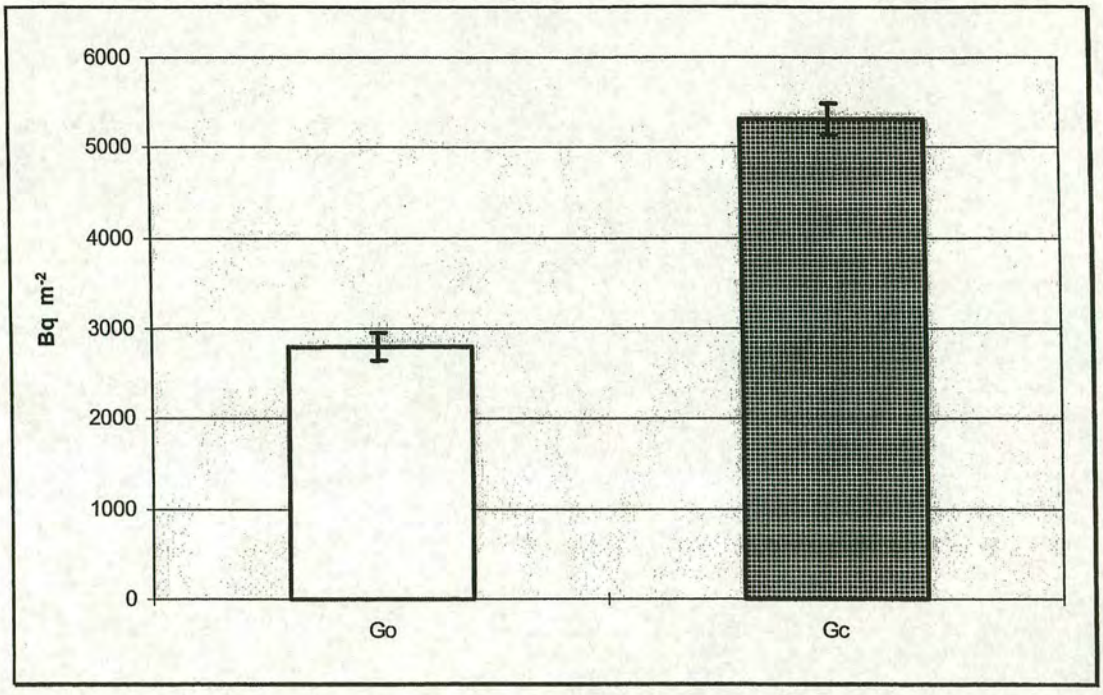

Figure 3.65: Mean atmospheric ^{210}Pb soil inventories in the open field(G_O), and inside the forest canopy(G_C) at Ovraboke and Stammilt, respectively.

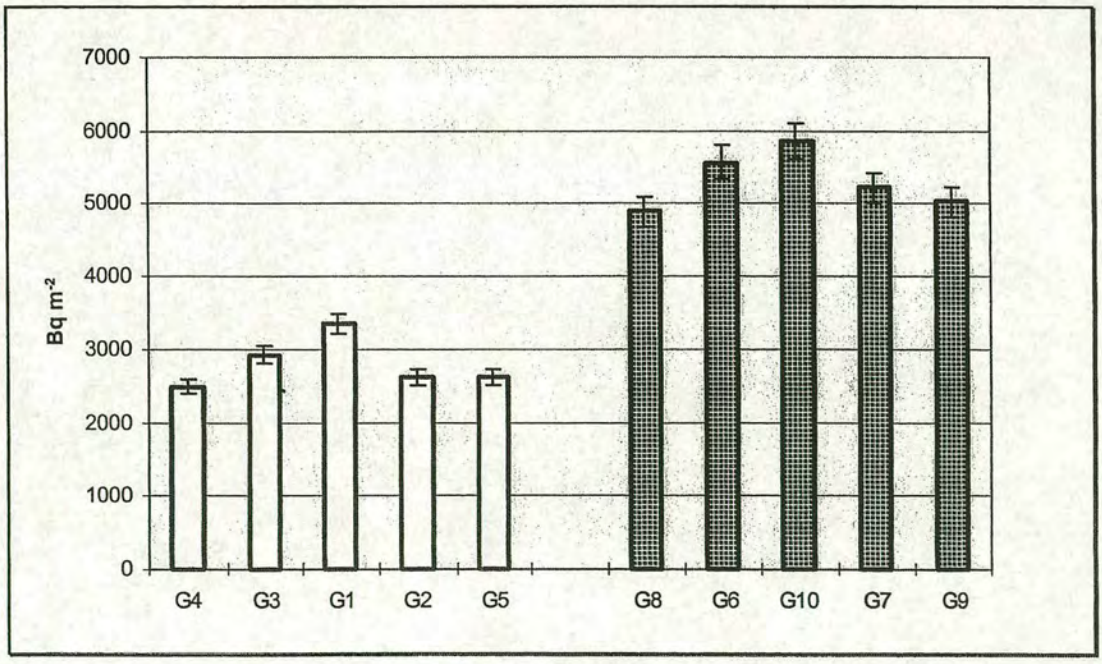

Figure 3.66: Atmospheric ^{210}Pb inventories measured in soil samples from each sampling point at Ovraboke(open field, G1-G5) and Stammilt(under canopy, G7-G10).

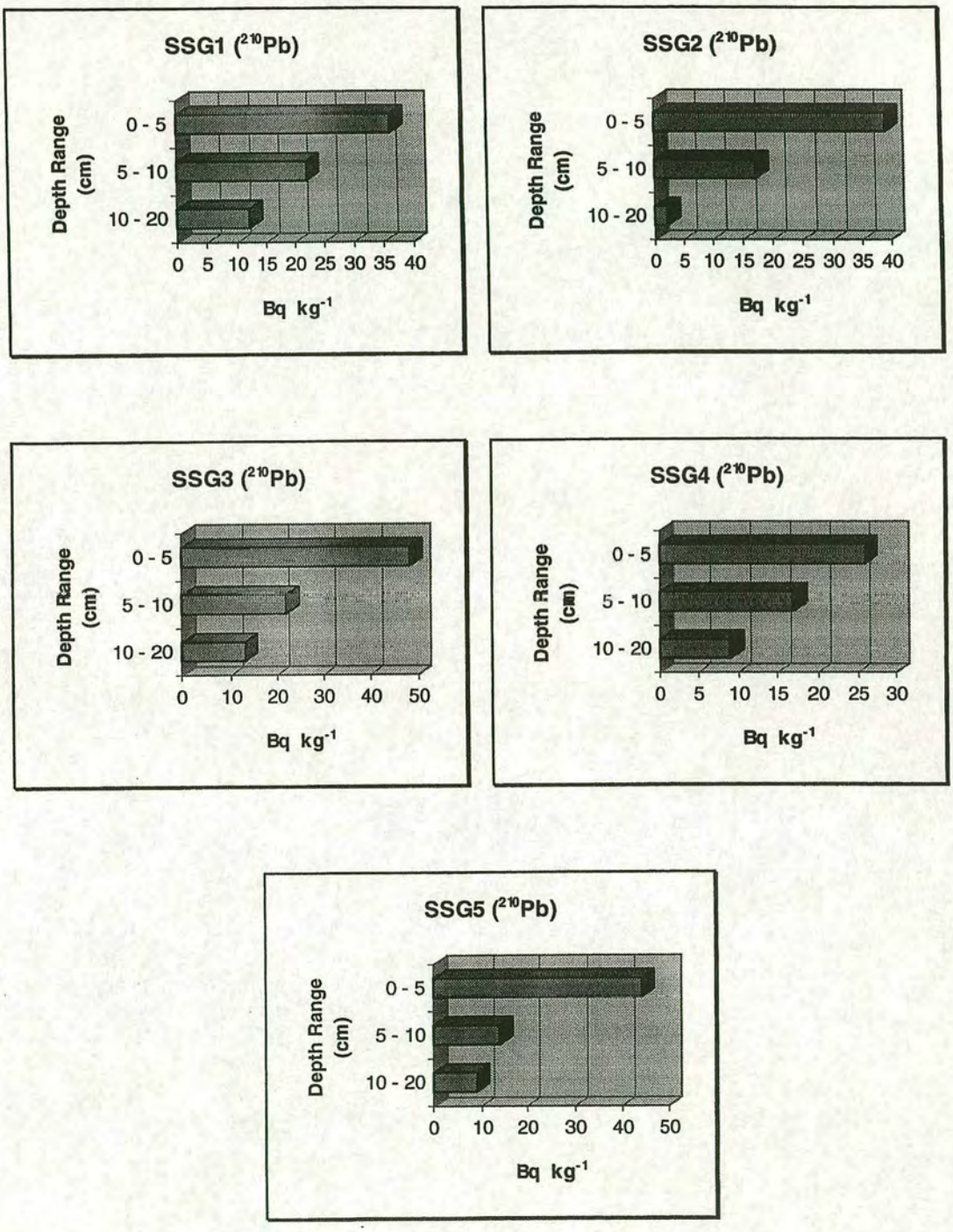

Figure 3.67: Distribution of atmospherically derived ^{210}Pb with depth at Ovraboke. Open field locations, G1 - G5.

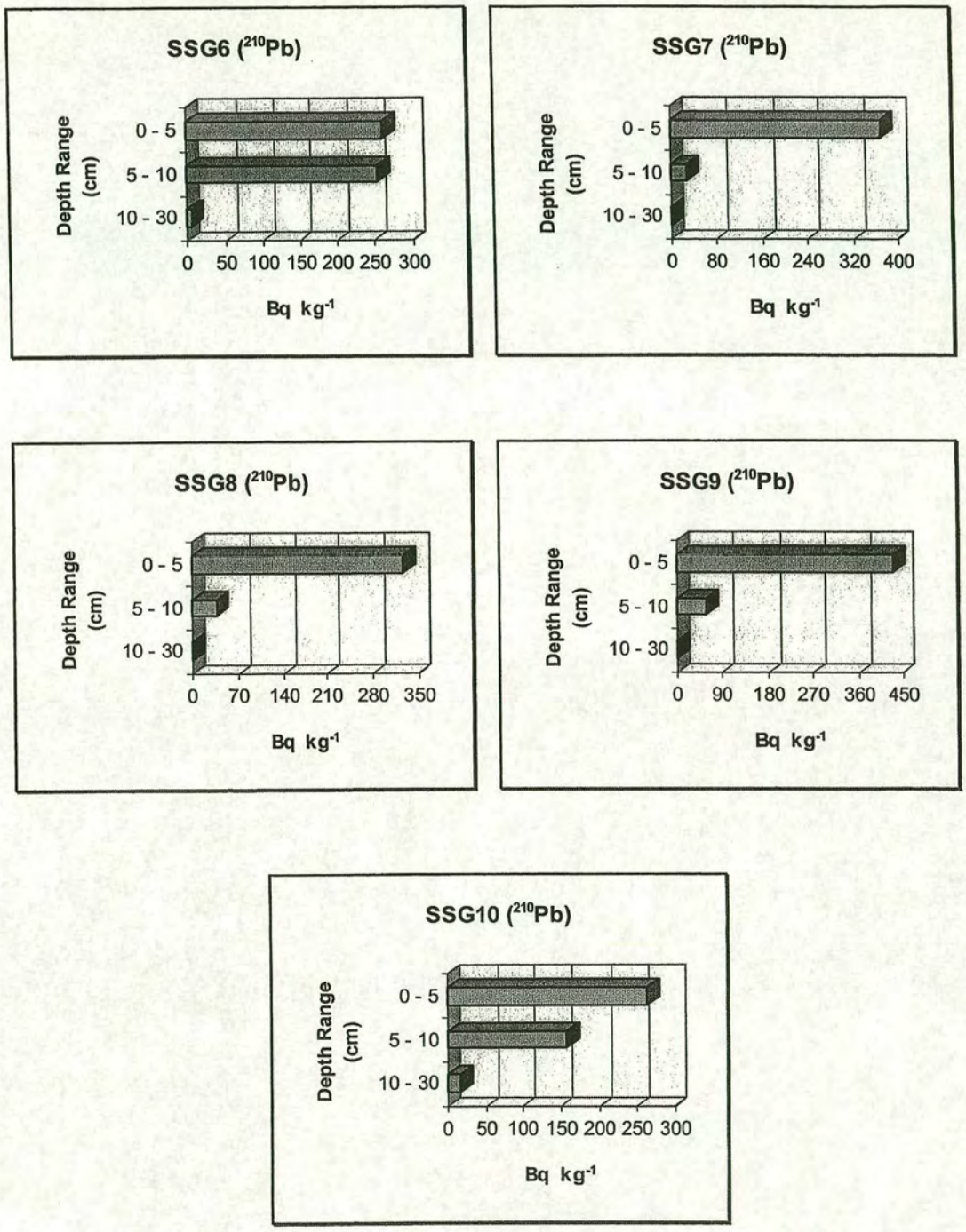

Figure 3.68: Distribution of atmospherically derived ^{210}Pb with depth at Stammilt. Under canopy locations, G6 - G10.

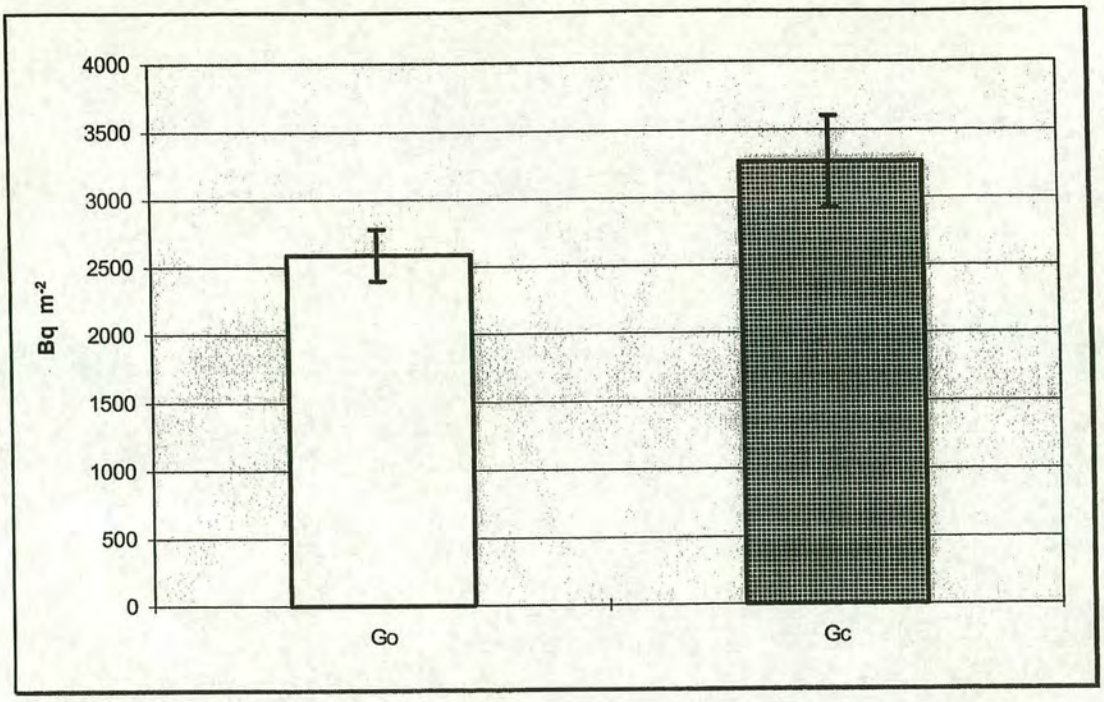

Figure 3.69: Mean ^{137}Cs soil inventories in the open field(G_O), and inside the forest canopy(G_C) at Ovraboke and Stammilt, respectively.

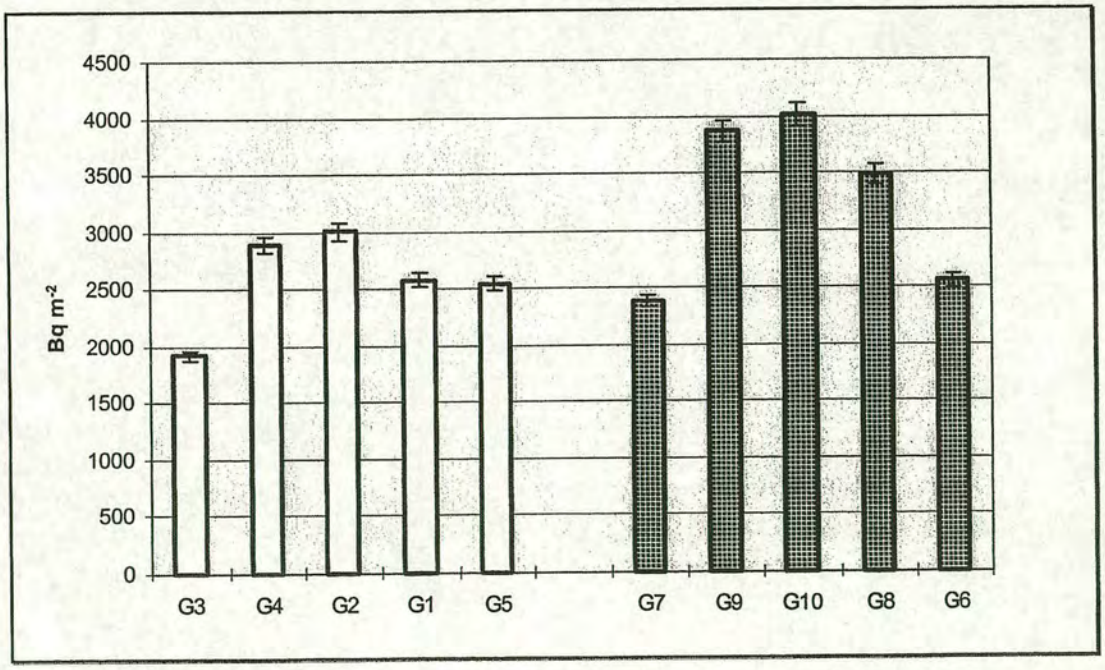

Figure 3.70: ^{137}Cs inventories measured in soil samples from each sampling point at Ovraboke(open field, G1-G5) and Stammilt(under canopy, G7-G10).

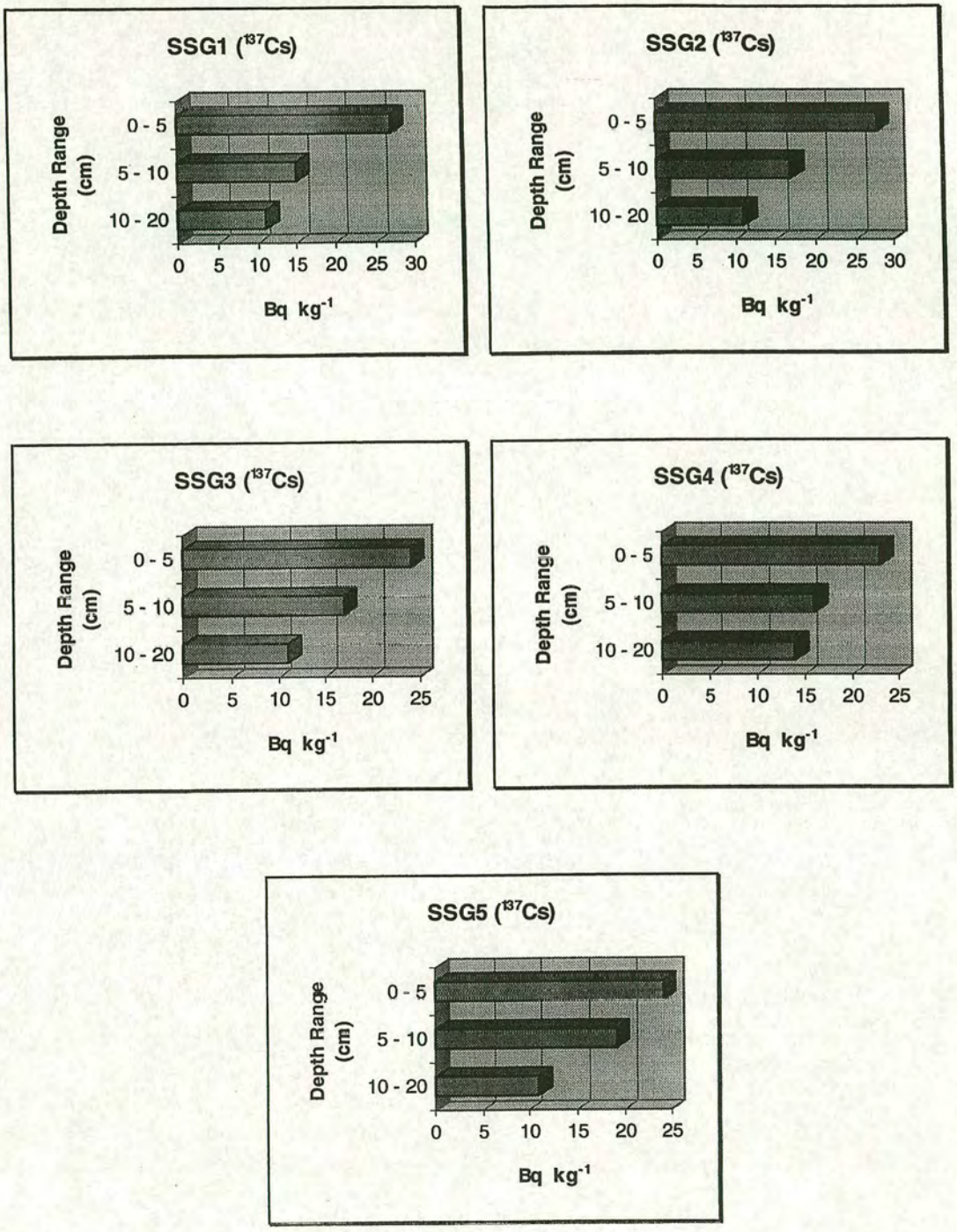

Figure 3.71: Distribution of ^{137}Cs with depth at Ovraboke.
Open field locations, G1 - G5.

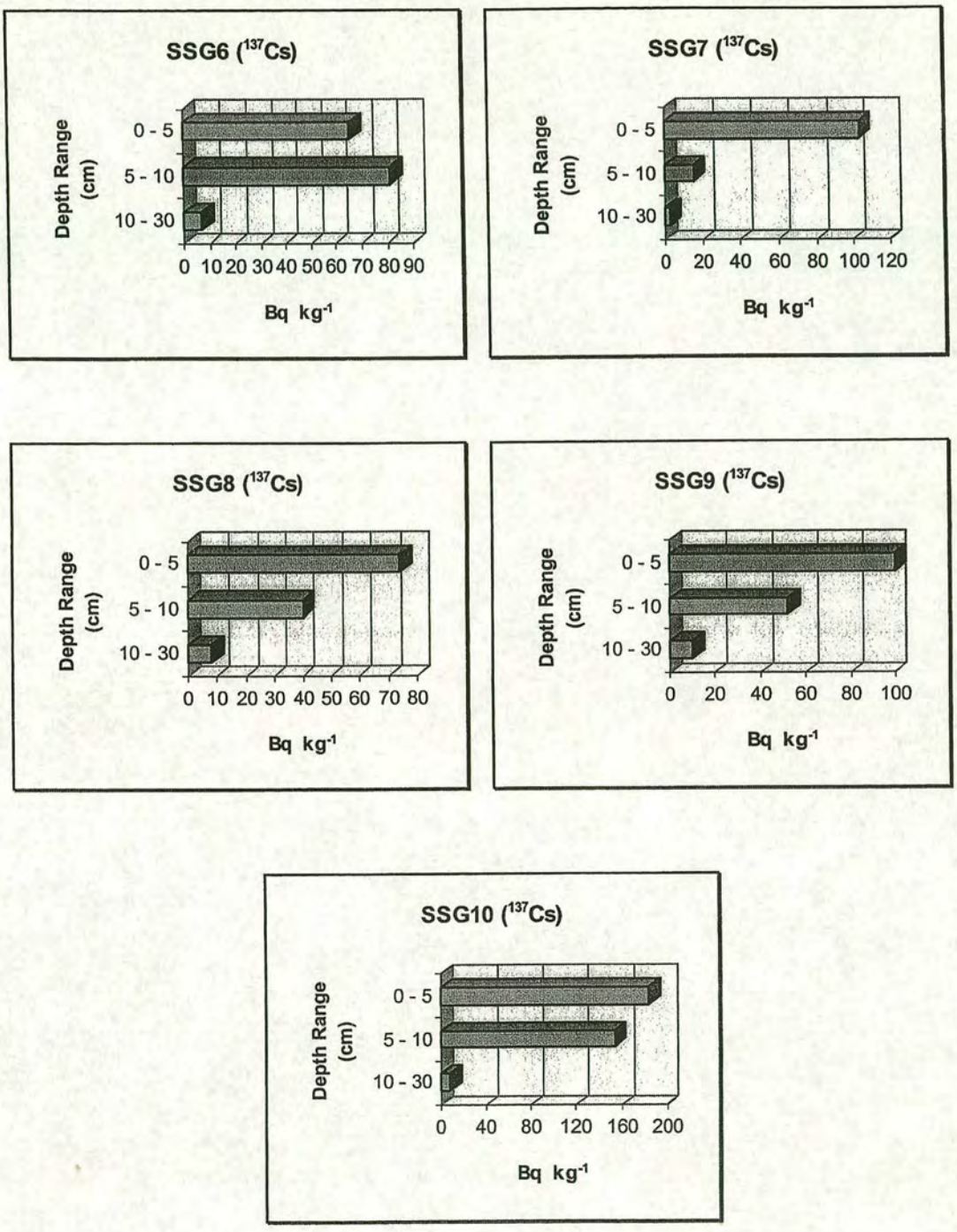

Figure 3.72: Distribution of ^{137}Cs with depth at Ovraboke.
Under canopy locations, G6 - G10.

3.3.7 Normanstorp (see section 2.1.1.2, Fig. 2.10 & Table 2.2)

3.3.7.1 Lead 210 soil inventories

The inventories of atmospheric ^{210}Pb for the samples collected from Normanstorp are presented in Figures 3.73 and 3.74. Figure 3.73 shows the mean ^{210}Pb inventories for the open field, H1, at the edge of canopy, H2, 7 m inside the canopy, H3, and finally 100 m inside the forest canopy, H4. The error bars in this graph represent standard error of the mean. The canopy enhancement in ^{210}Pb deposition at this site is approximately 20%, on the average(excluding H4), relative to the adjacent open field. The enhancement is large at the edge of canopy which exceeds that in the open field by 23%. The DMR test result on the inventory values is illustrated in Figure 3.79. According to the test, there are no significant differences between inventories at H1 and either H3 or H4, neither between H2 and H3, at the 5% level of significance. The levels of ^{210}Pb present in the individual cores from Normanstorp are shown in Figure 3.74, where the error bars are due to counting statistics. The coefficient of variation for measured inventories is 11%, 14%, 8%, and 13% for H1-H4 locations, respectively. The inherent variability in ^{210}Pb inventories is slightly higher at the edge of canopy relative to other locations at this site.

Depth profiles for specific activities are illustrated in Figures 3.75 to 3.78. The sampling depth at SSH16, SSH19, and SSH20 is exceptionally 20 cm. At each of the 20 points sampled, no significant amounts of atmospheric ^{210}Pb were detected below 10 cm depth except for SSH9 core. The depth profiles generally show much greater concentration of atmospheric ^{210}Pb in the 0-5 cm depth interval than in the 5-10 cm depth. Exceptions are SSH12 and SSH17 sampling points.

Assuming that there is a steady state between the atmospheric supply of ^{210}Pb and its radioactive decay in soil, the average flux to the Norway spruce(*Picea abies*) canopy and the adjacent open field in Normanstorp would be 159 Bq m^{-2} y^{-1} and 133 Bq m^{-2} y^{-1}, respectively.

3.3.7.2 Caesium 137 soil inventories

The soil inventories for ^{137}Cs are presented in Figures 3.80 and 3.81. Figure 3.80 shows mean ^{137}Cs inventories for the site, where the error bars represent standard error of the mean. On the average there is no canopy enhancement in ^{137}Cs deposition to the site. The DMR test result on the inventory values is illustrated in Figure 3.86. According to the test, there are no significant differences between inventories at H1 and either H3 or H4 , neither between H1 and H2, at the 5% level of significance. Caesium 137 inventories for the individual sampling points are given in Figure 3.81, where the error bars are due to counting statistics. The coefficient of variation for measured inventories of ^{137}Cs is 10%, 13%,20%, and 15% for H1-H4 locations, respectively. The variation is relatively higher at location H3, 7 m from the edge of canopy.

Depth profiles for specific activities are illustrated in Figures 3.82 to 3.85. Caesium 137 is mostly concentrated in the top 10 cm of soil, and the contribution of 10-30 cm depth interval is rather small except for SSH8, SSH9, SSH11-SSH13, and SSH16.

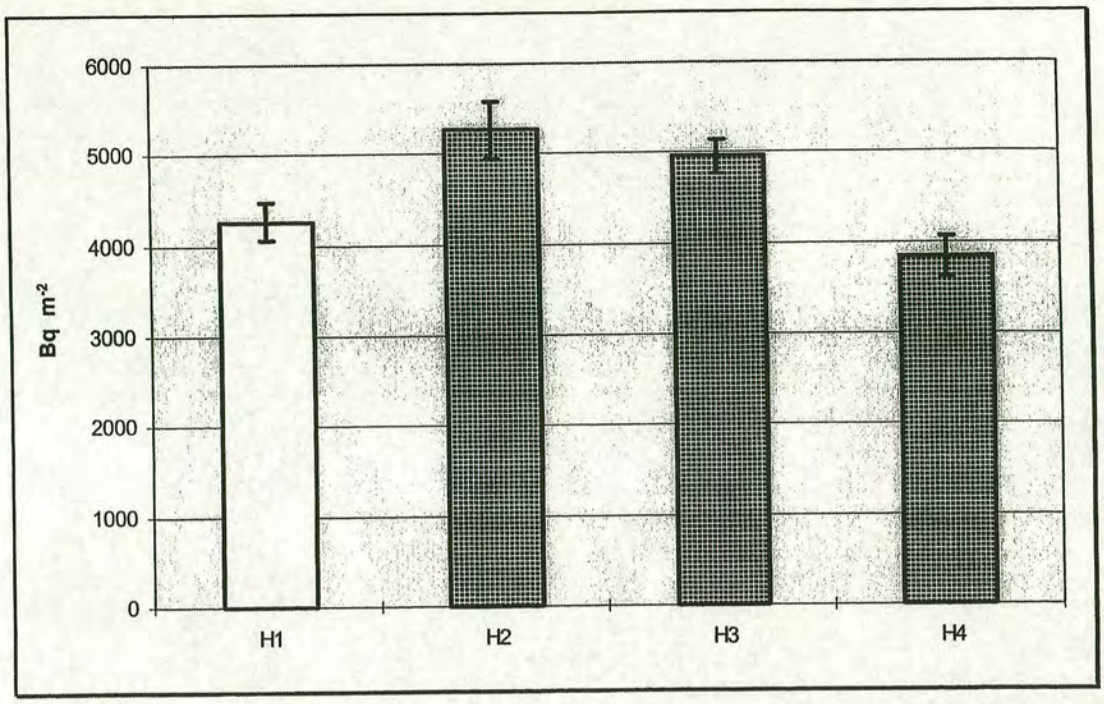

Figure 3.73: Mean atmospheric ^{210}Pb soil inventories in the open field (H1), edge of the stand (H2), 7 m from the edge (H3) and 100 m inside the forest canopy (H4) at Normanstorp.

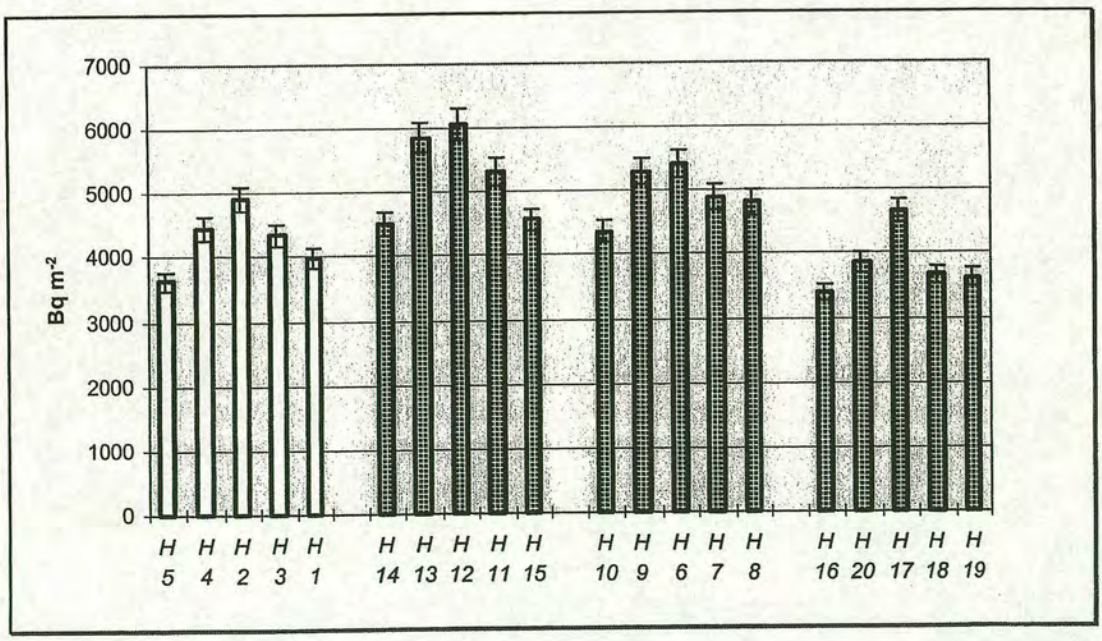

Figure 3.74: Atmospheric ^{210}Pb inventories measured in soil samples from each sampling point at Normanstorp.

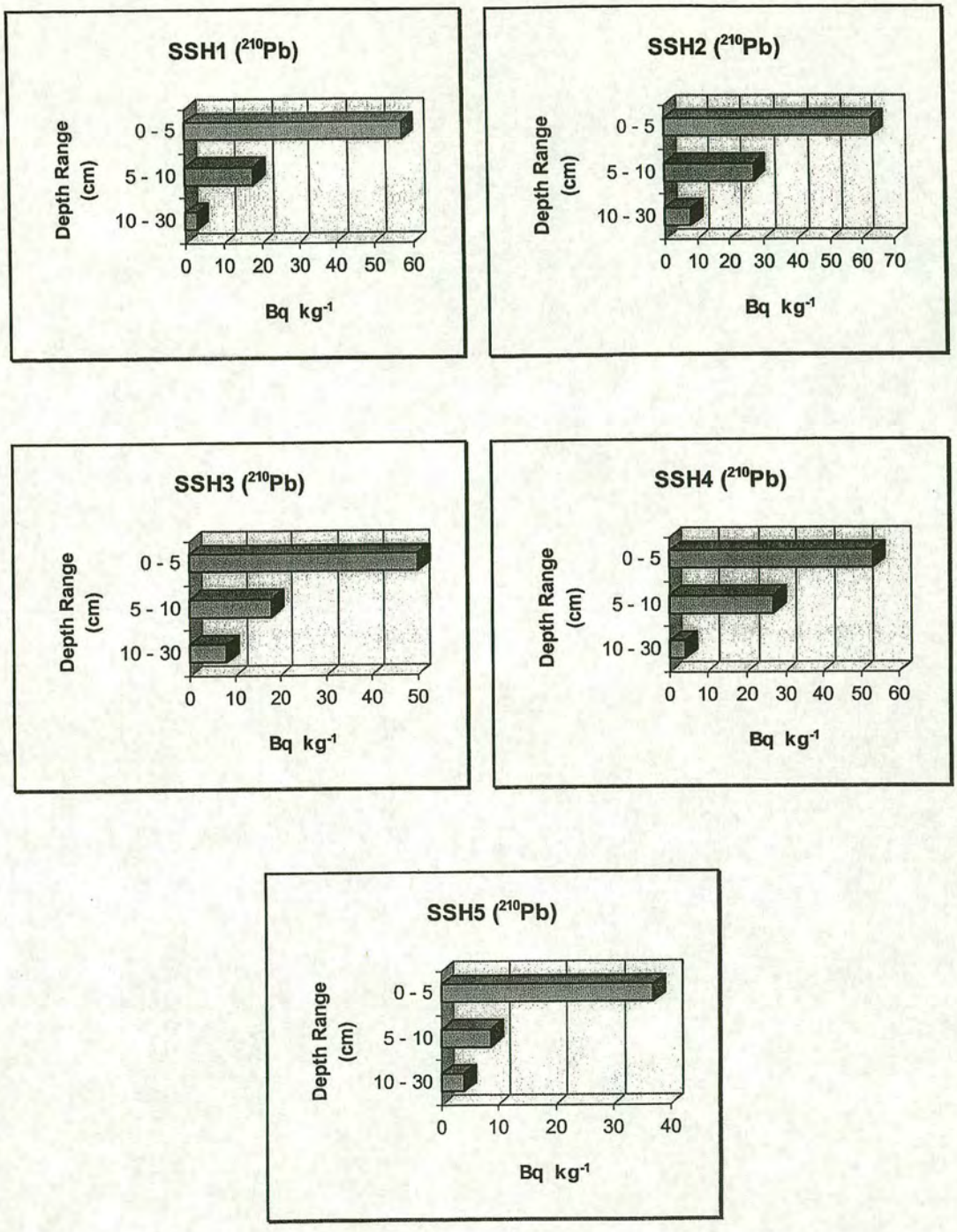

Figure 3.75: Distribution of atmospherically derived ^{210}Pb with depth at Normanstorp. Open field locations, H1 - H5.

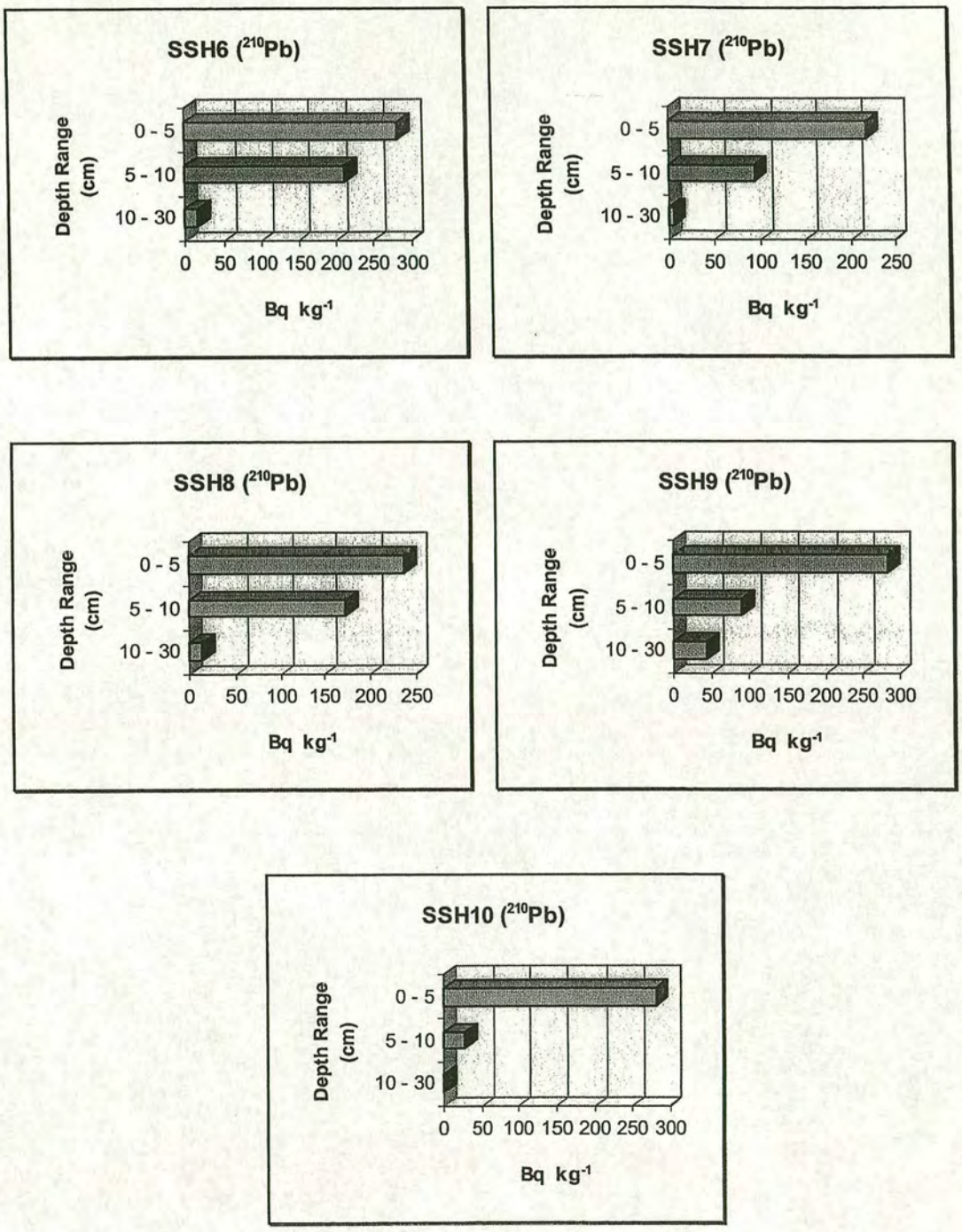

Figure 3.76: Distribution of atmospherically derived ^{210}Pb with depth at Normanstorp. Under canopy locations, H6 - H10.

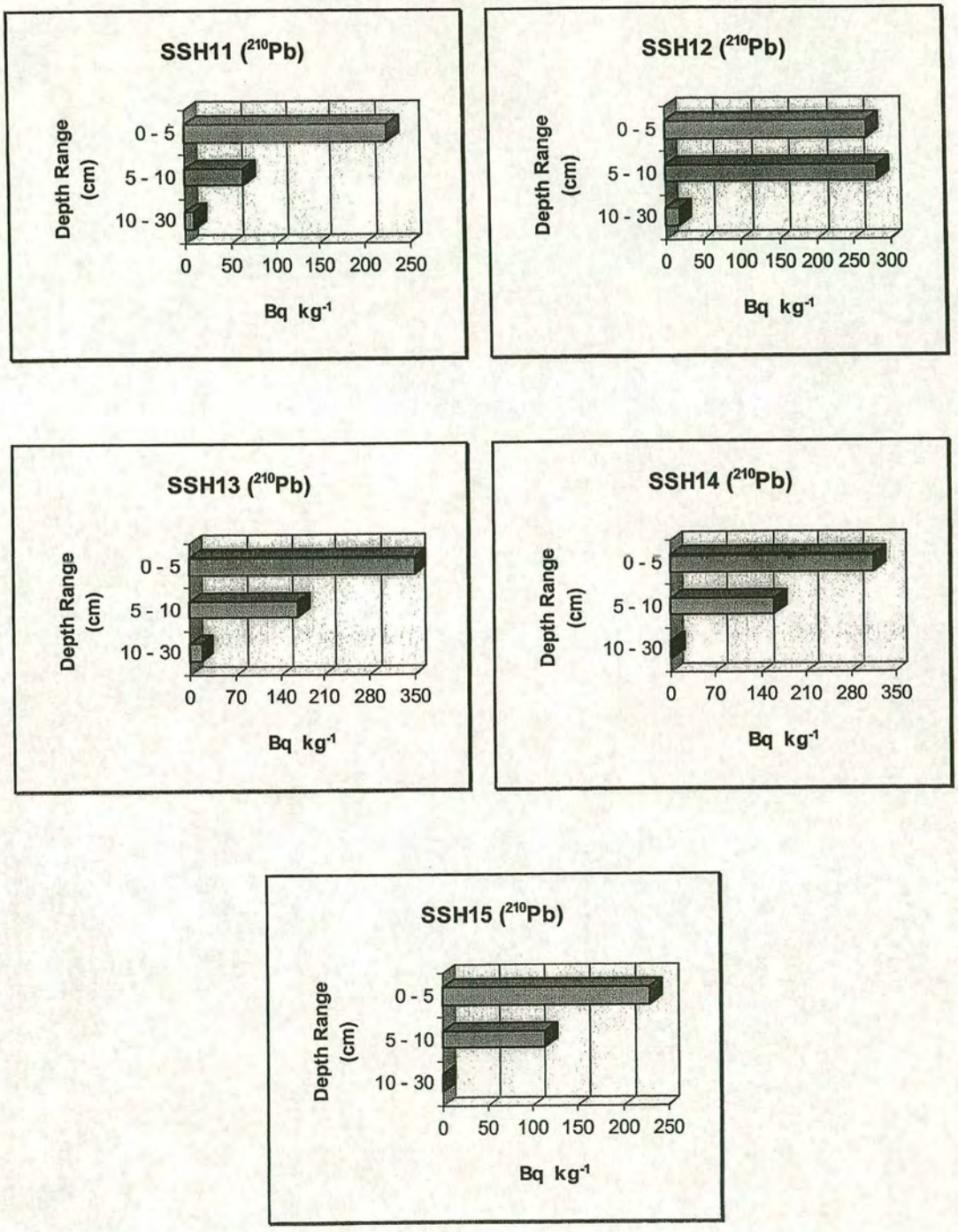

Figure 3.77: Distribution of atmospherically derived ^{210}Pb with depth at Normanstorp. Under canopy locations, H11 - H15.

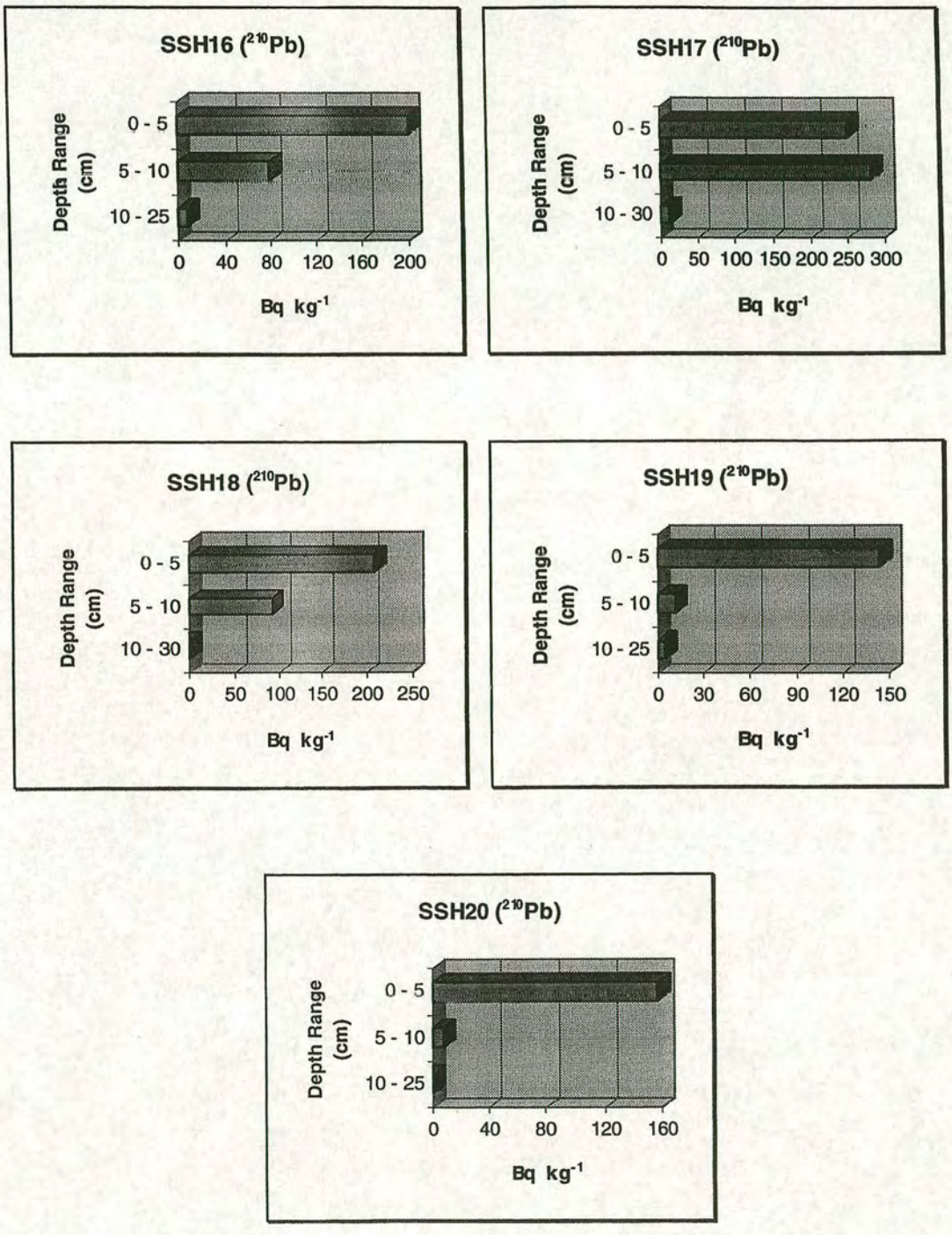

Figure 3.78: Distribution of atmospherically derived ^{210}Pb with depth at Normanstorp. Under canopy locations, H16 - H20.

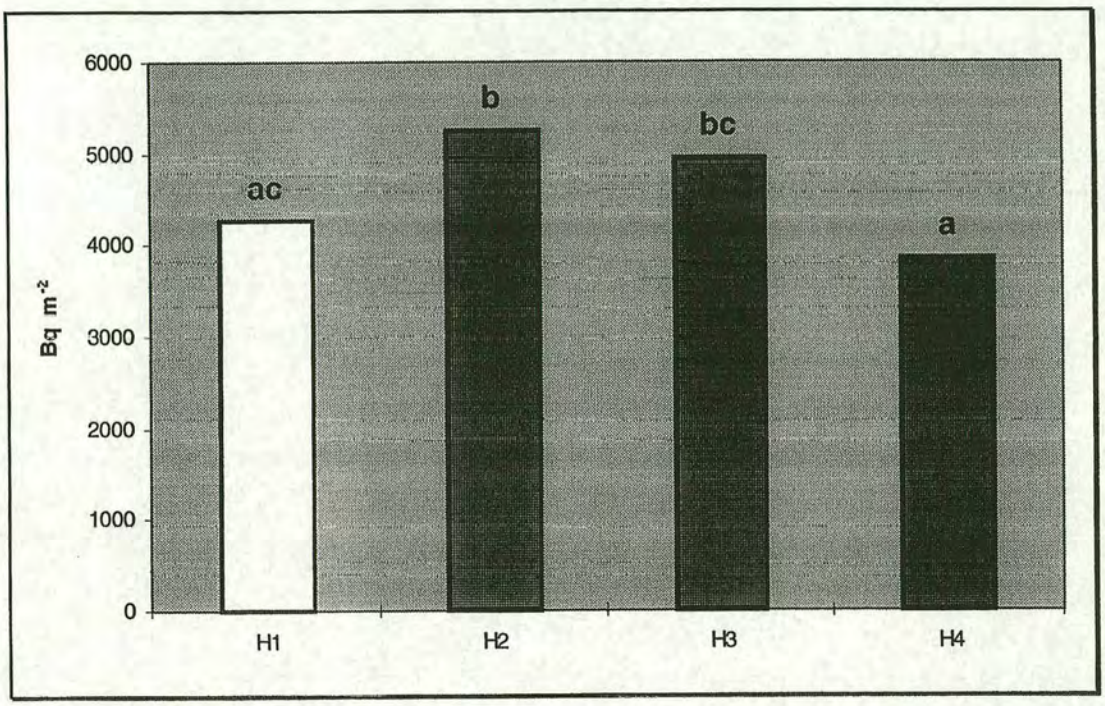

Figure 3.79: Mean atmospheric ^{210}Pb soil inventories in the open field (H1), edge of the stand(H2), 7 m from the edge (H3) and 100 m inside the forest canopy (H4) at Normanstorp.
The letters above each bar denote significant differences as derived from Duncan's multiple range test. Any two means having a common letter are not significantly different at the 5% level of significance .

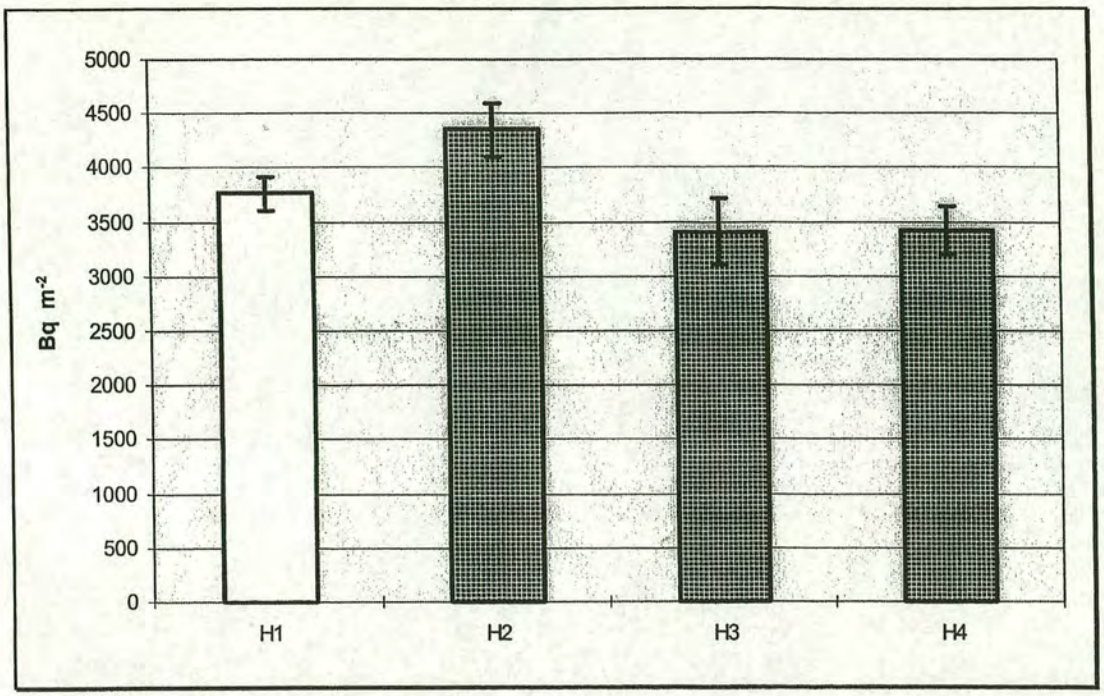

Figure 3.80: Mean ^{137}Cs soil inventories in the open field (H1), edge of the stand (H2), 7 m from the edge (H3) and 100 m inside the forest canopy (H4) at Normanstorp.

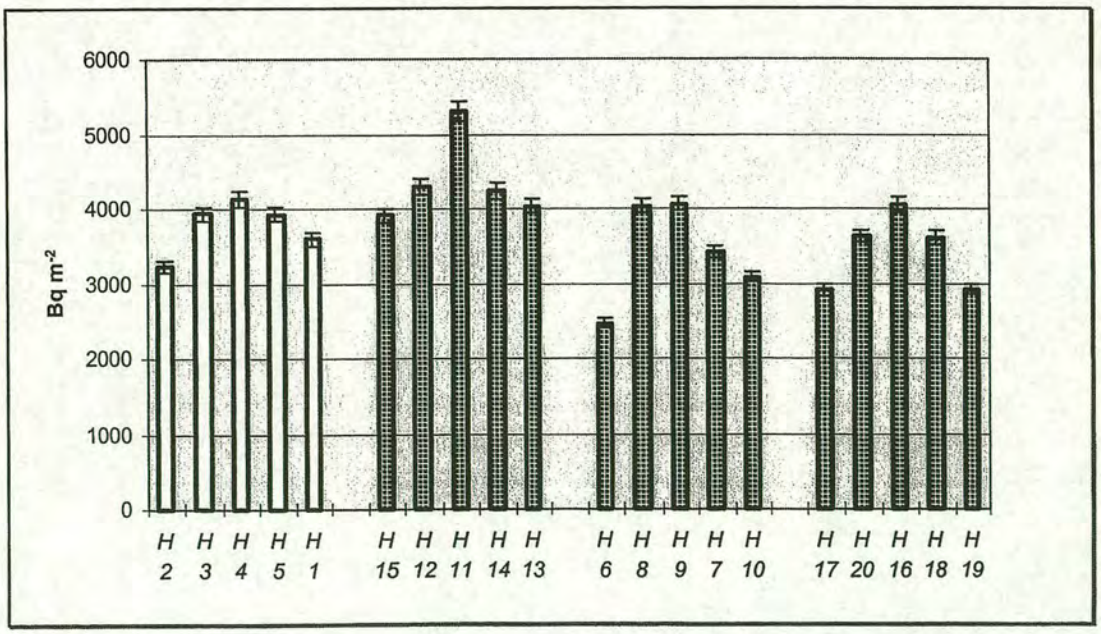

Figure 3.81: ^{137}Cs inventories measured in soil samples from each sampling point at Normanstorp.

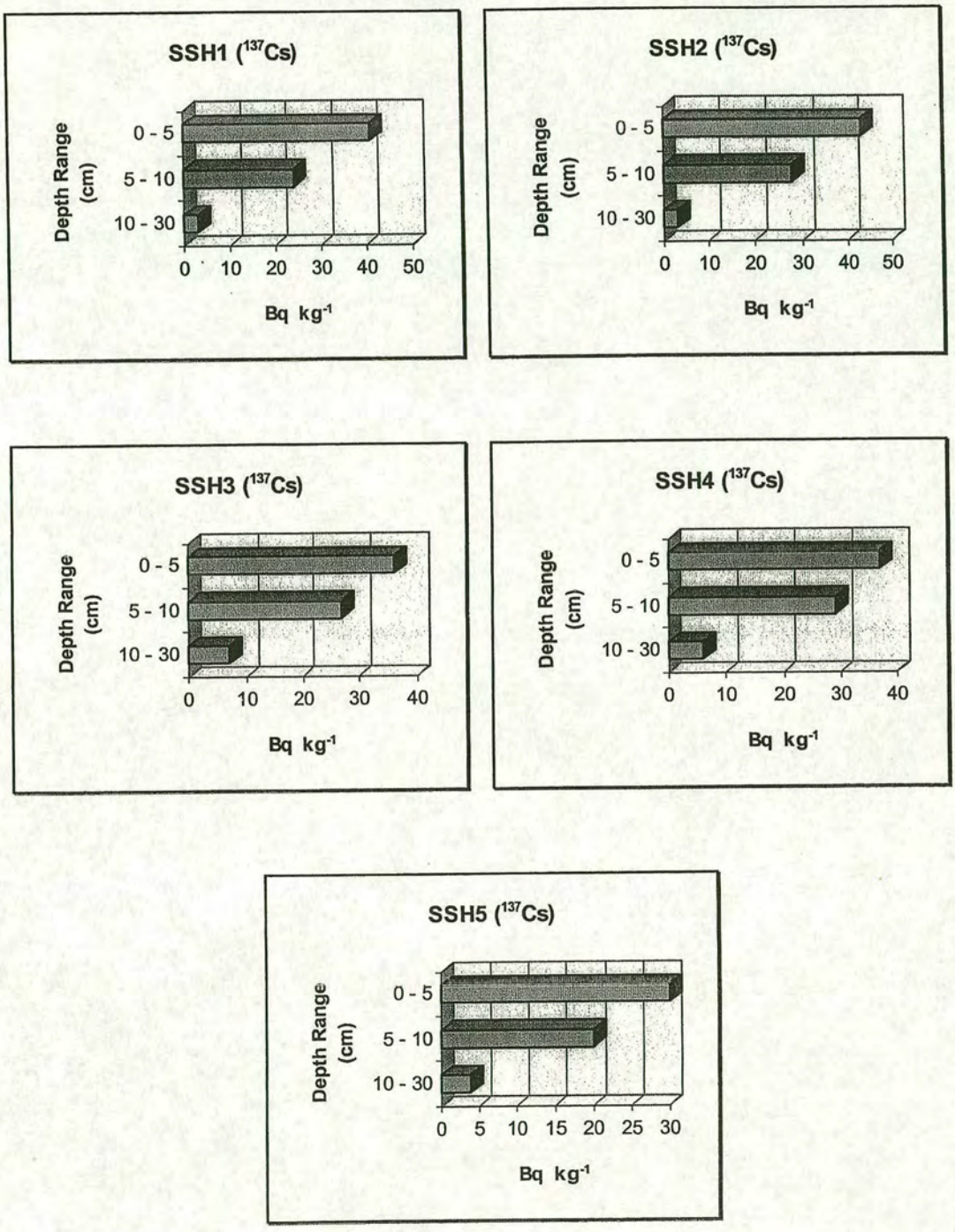

Figure 3.82: Distribution of ^{137}Cs with depth at Normanstorp.
Open field locations, H1 - H5.

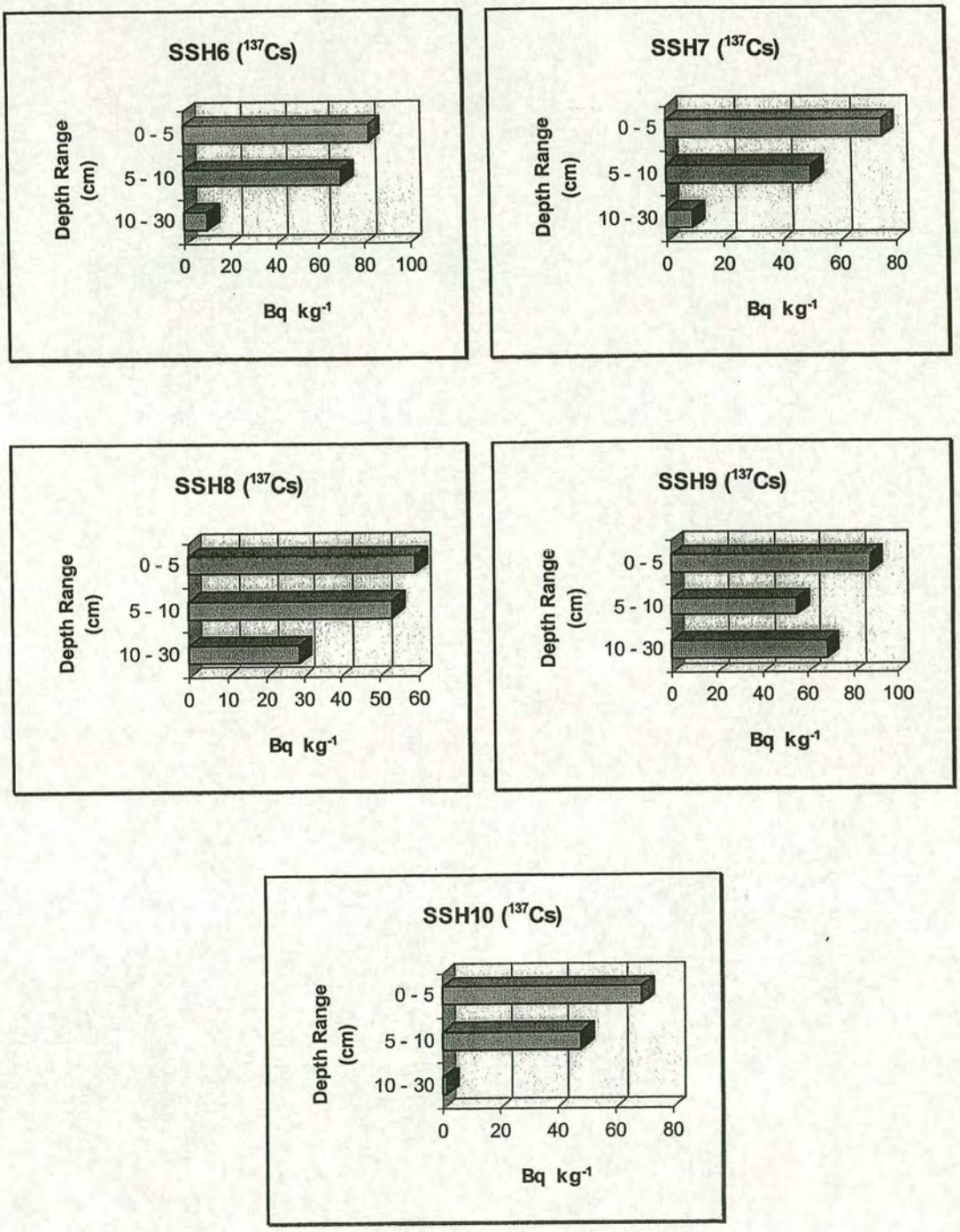

Figure 3.83: Distribution of ^{137}Cs with depth at Normanstorp.
Under canopy locations, H6 - H10.

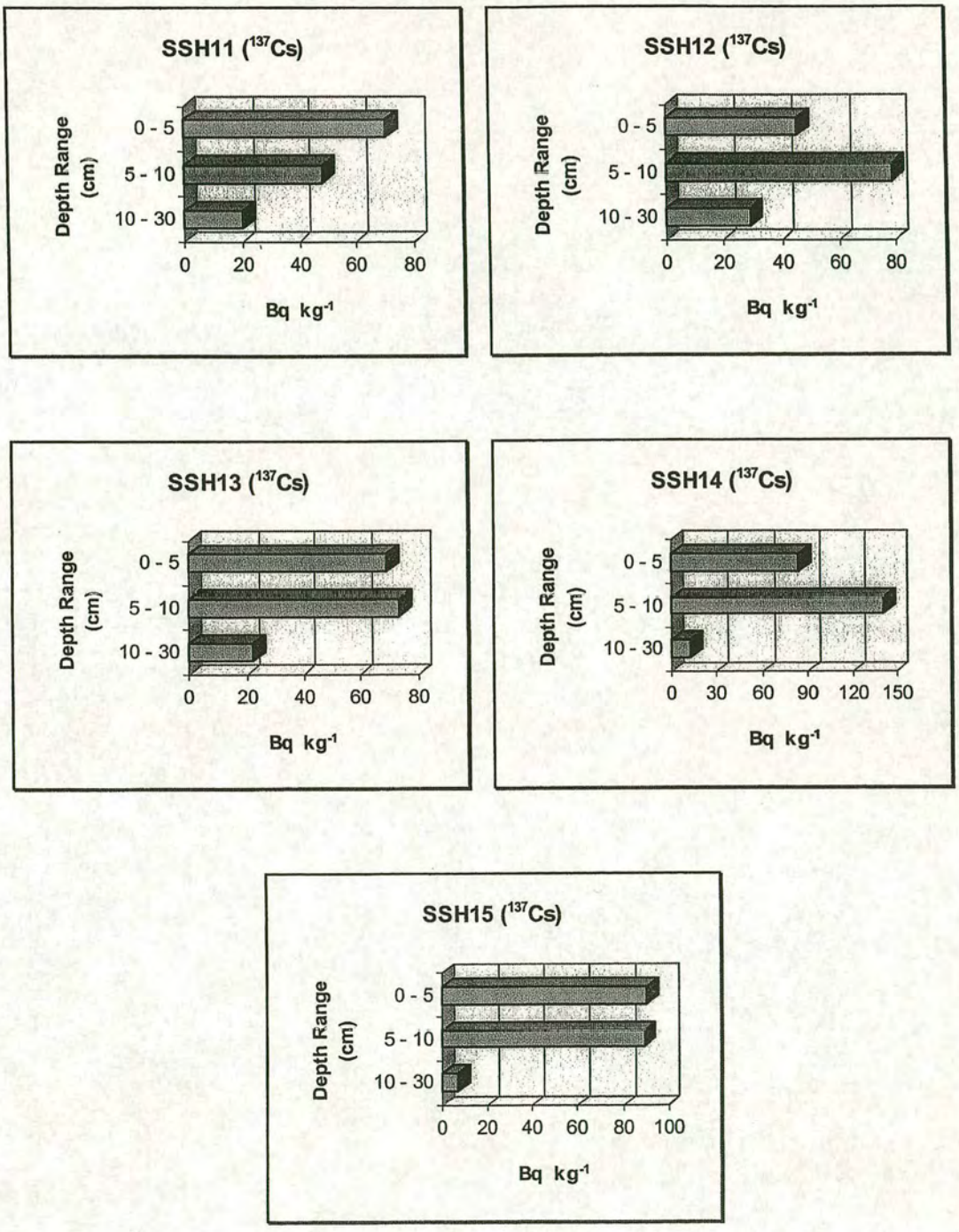

Figure 3.84: Distribution of ^{137}Cs with depth at Normanstorp.
Under canopy locations, H11 - H15.

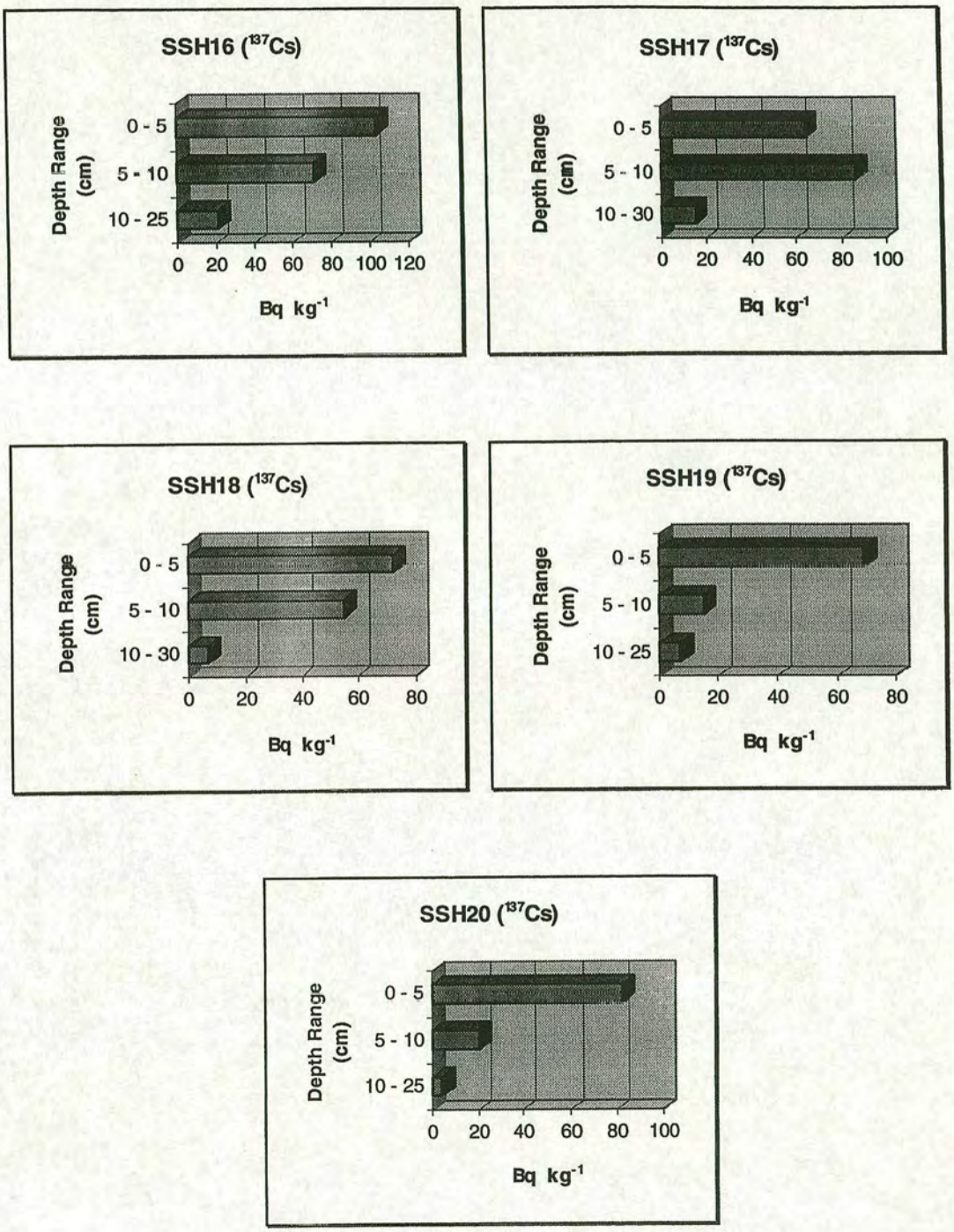

Figure 3.85: Distribution of ^{137}Cs with depth at Normanstorp.
Under canopy locations, H16 - H20.

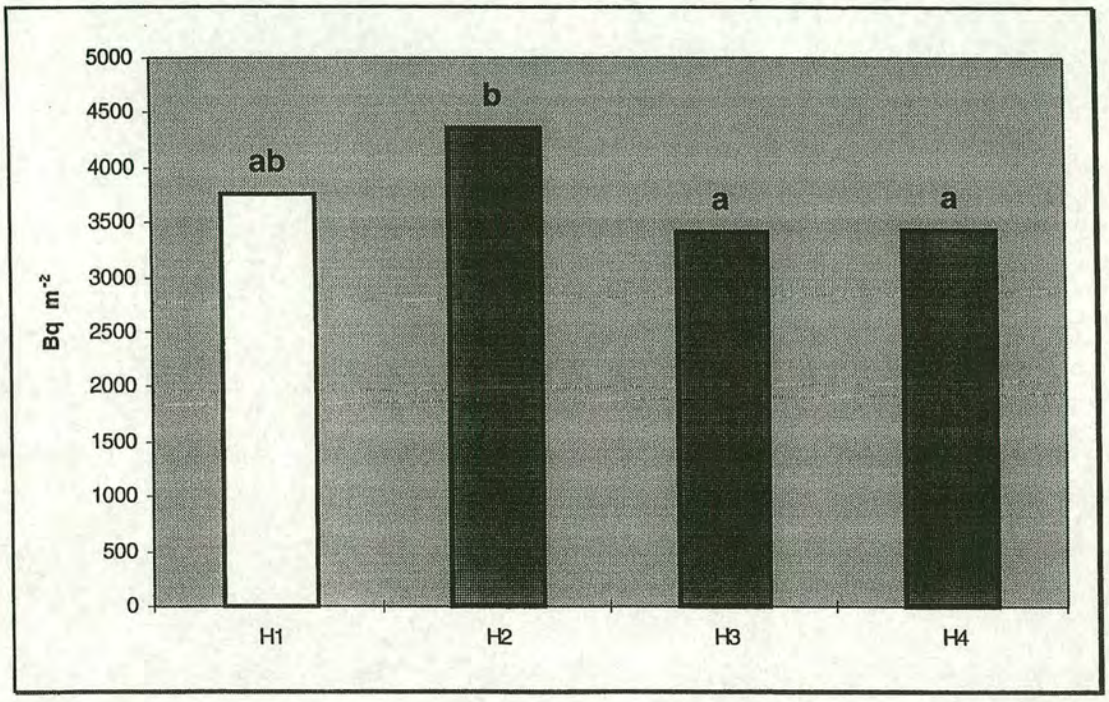

Figure 3.86: Mean ^{137}Cs soil inventories in the open field (H1), edge of the stand(H2), 7 m from the edge (H3) and 100 m inside the forest canopy (H4) at Normanstorp.

The letters above each bar denote significant differences as derived from Duncan's multiple range test. Any two means having a common letter are not significantly different at the 5% level of significance .

3.3.8 Broda (see section 2.1.1.2, Fig. 2.10 & Table 2.2)

3.3.8.1 Lead 210 soil inventories

The inventories of atmospheric ^{210}Pb for the samples collected from beneath the Norway spruce(*Picea abies*) canopy, as well as the nearby open field at Broda are presented in Figures 3.87 and 3.88. Mean ^{210}Pb inventories for the open field(I_O) and under canopy(I_C) are shown in Figure 3.87, where the error bars represent standard error of the mean. The coefficient of variation for the measured ^{210}Pb inventories is 17% for the open field, and 9% for the under canopy location. The levels of ^{210}Pb present in the individual cores from the open field(I1-I5) and under canopy sampling points(I6-I10) are shown in Figure 3.88, where the error bars are due to counting statistics. Considering a calculated *t-value* of 2.50, there are significant differences between the mean inventory values for the open field and under canopy samples at 5% level of significance. The canopy enhancement in ^{210}Pb deposition is approximately 22%.

Depth profiles for specific activities are illustrated in Figures 3.89 and 3.90. Though top 10 cm soil has generally retained the atmospheric ^{210}Pb but, The contribution of 10-30 cm depth interval is relatively higher for the open field cores from this site (note specially SSI2 & SSI4 profiles in Figure 3.89).

Under the reasonable assumption of a steady state between the atmospheric supply of ^{210}Pb and its radioactive decay in soil, its average flux would be approximately 137 Bq m^{-2} y^{-1} for the open field, and 167 Bq m^{-2} y^{-1} for the under canopy locations.

3.3.8.2 Caesium 137 soil inventories

The soil inventories for ^{137}Cs are presented in Figures 3.91 and 3.92. Mean inventories for the open field(I_O) and under canopy(I_C) locations are shown in Figure 3.91, where the error bars represent standard error of the mean. The coefficient of

variation for the measured ^{137}Cs inventories is 13%, for the open field, and 27% for the under canopy locations. The levels of ^{137}Cs present in the individual cores from the open field(I1-I5) and under canopy sampling points(I6-I10) are shown in Figure 3.92, where the error bars are due to counting statistics. Considering a calculated *t-value* of 3.16, thereare significant differences between the mean inventory values for the open field and under canopy samples at 2% level of significance. The mean inventory for the under canopy location is smaller than that of the open field by 32% at this site.

Depth profiles for specific activities are illustrated in Figures 3.93 and 3.94 for the open field and under canopy cores, respectively. Though the bulk of caesium 137 is concentrated in the surface horizons of soil but, these profiles indicate the penetration of this radionuclide to below 10 cm horizons for both open field and canopy locations. The SSI2 & SSI4 cores are rather exceptional as it was the case with ^{210}Pb profiles at this site.

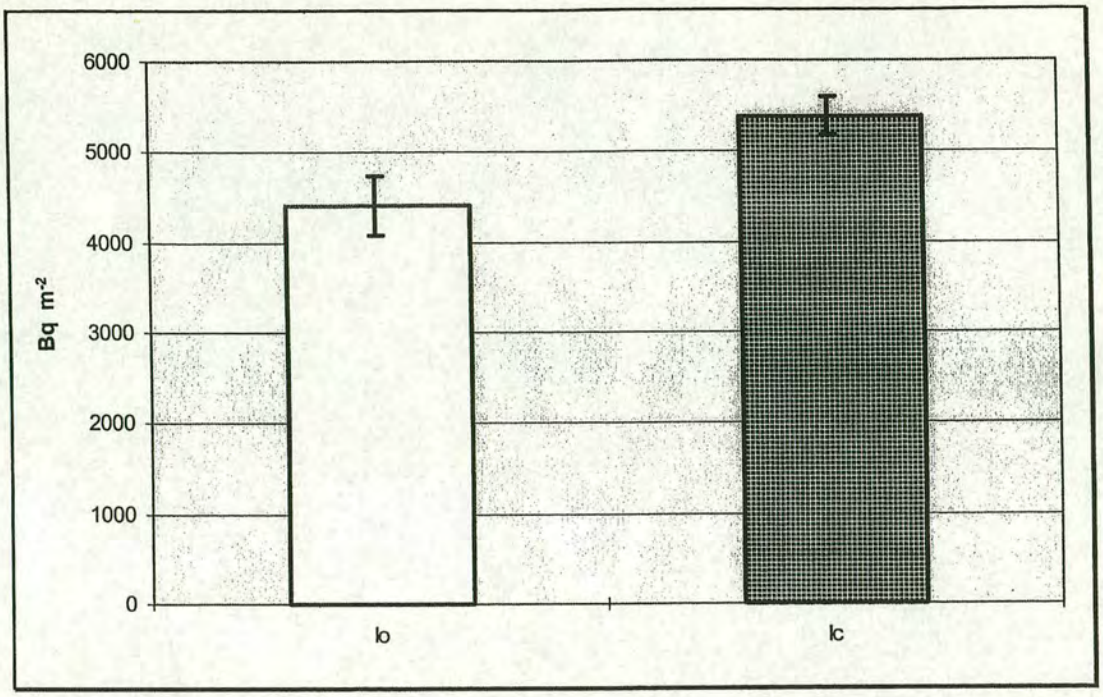

Figure 3.87: Mean atmospheric ^{210}Pb soil inventories in the open field(I_O), and inside the forest canopy(I_C) at Broda.

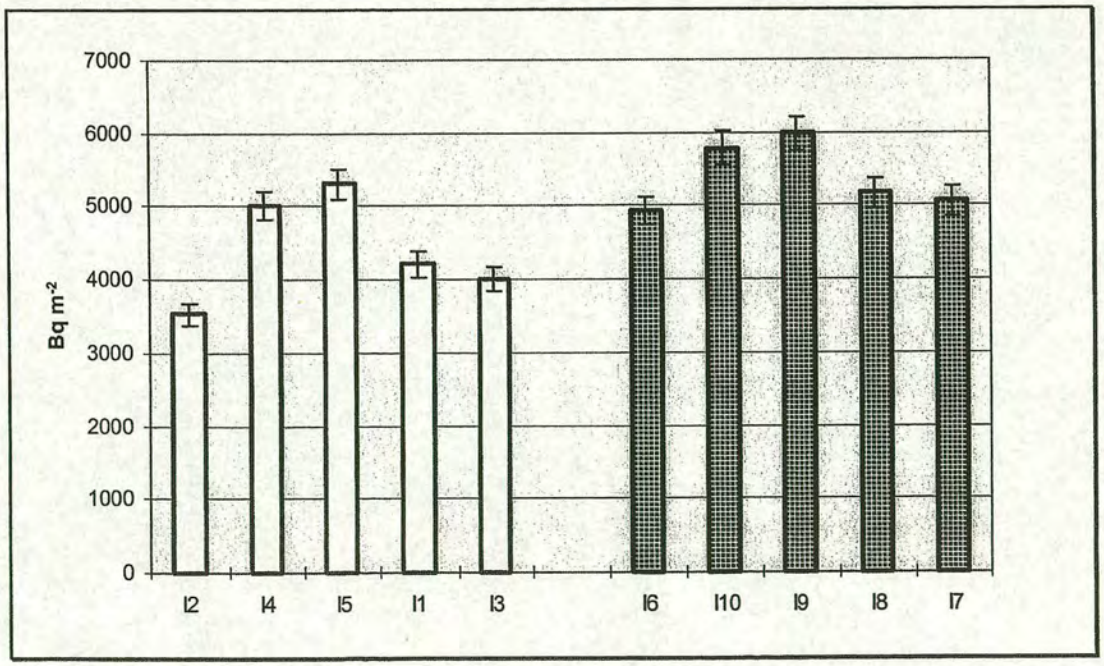

Figure 3.88: Atmospheric ^{210}Pb inventories measured in soil samples from each sampling point at Broda.

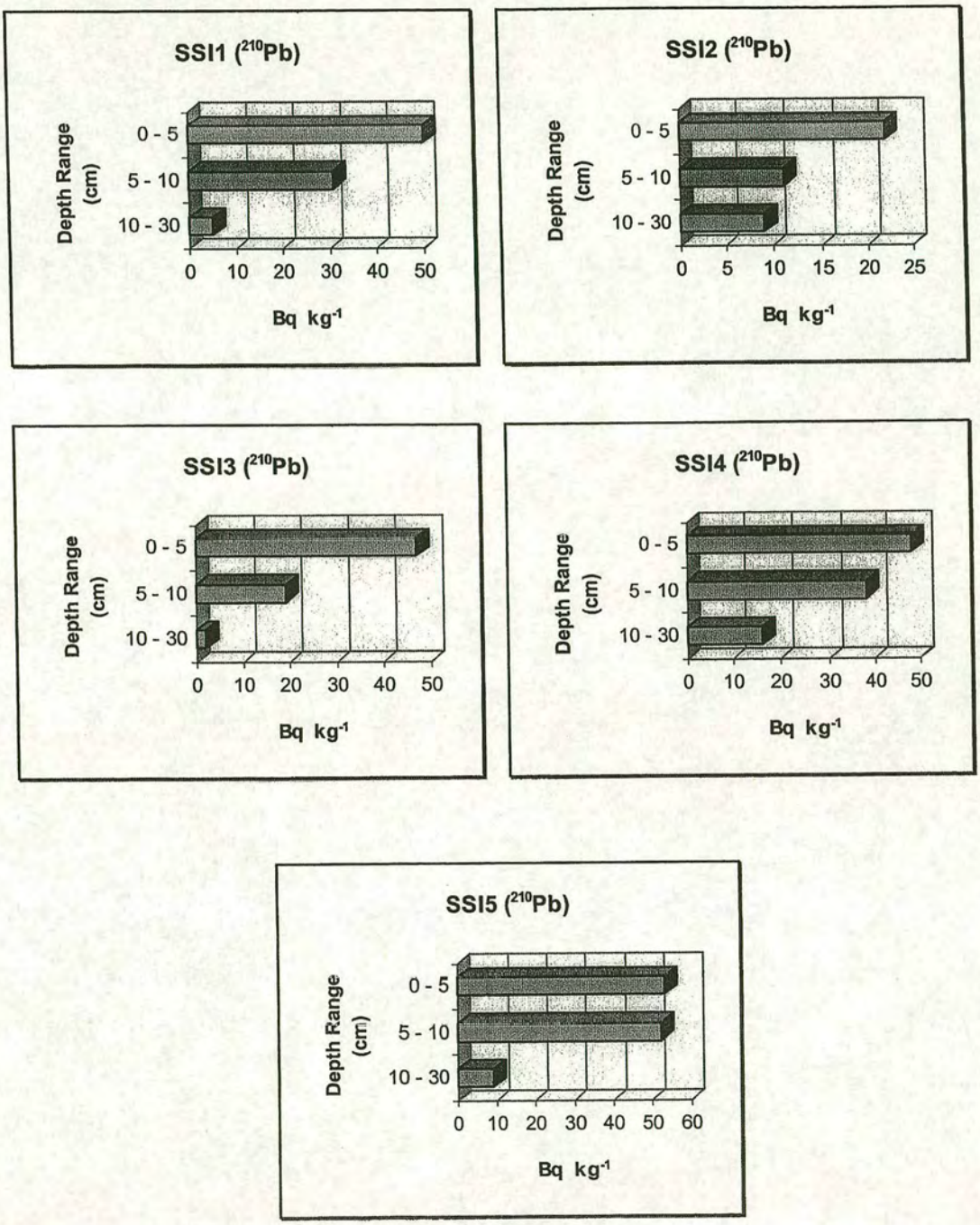

Figure 3.89: Distribution of atmospherically derived ^{210}Pb with depth at Broda. Open field locations, I1 - I5.

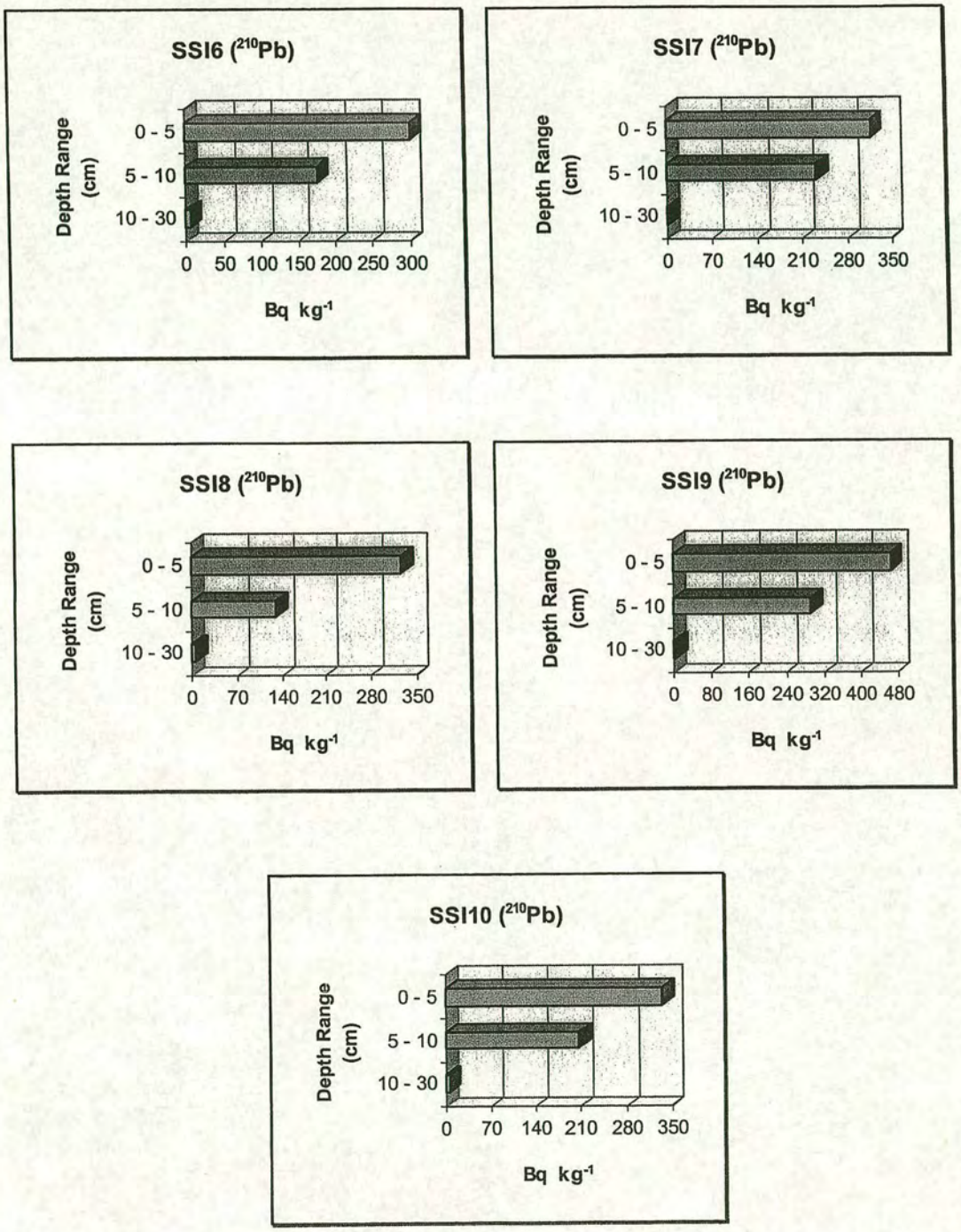

Figure 3.90: Distribution of atmospherically derived ^{210}Pb with depth at Broda. Under canopy locations, I6 - I10.

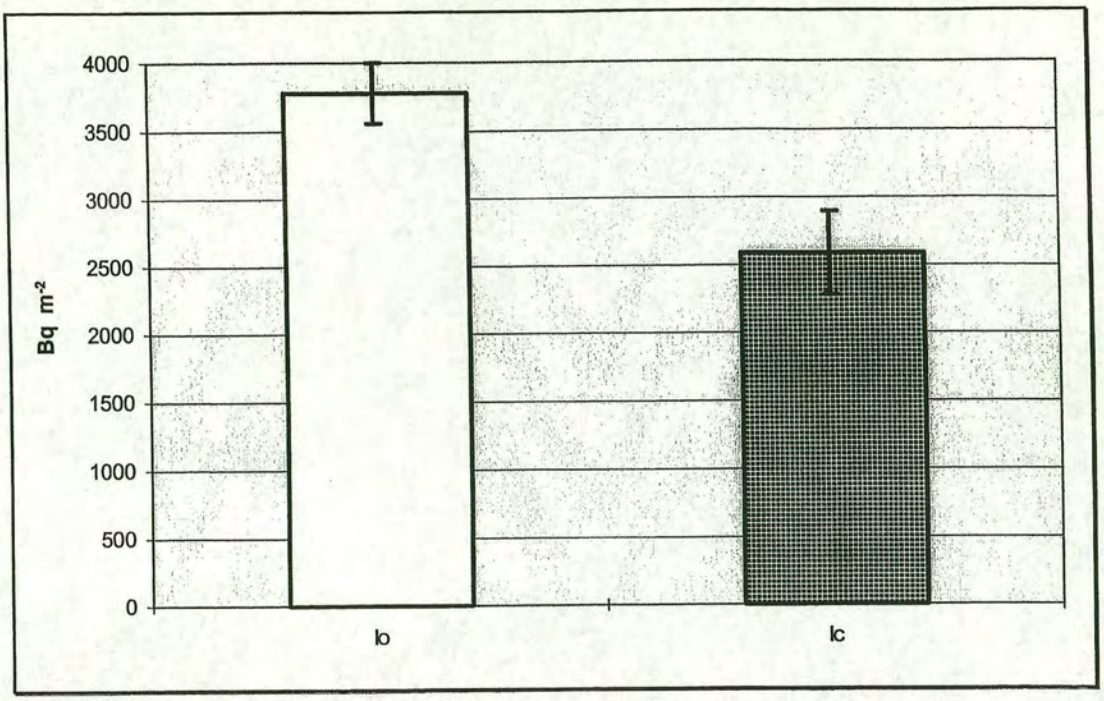

Figure 3.91: Mean ^{137}Cs soil inventories in the open field(I_O), and inside the forest canopy(I_C) at Broda.

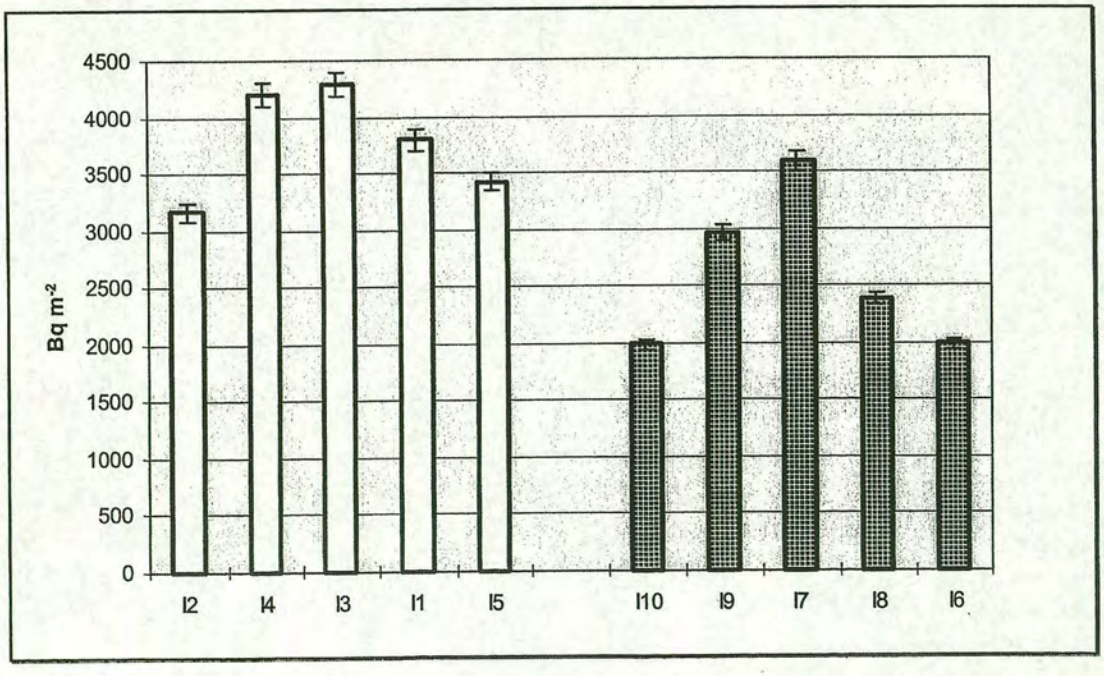

Figure 3.92: ^{137}Cs inventories measured in soil samples from each sampling point at Broda.

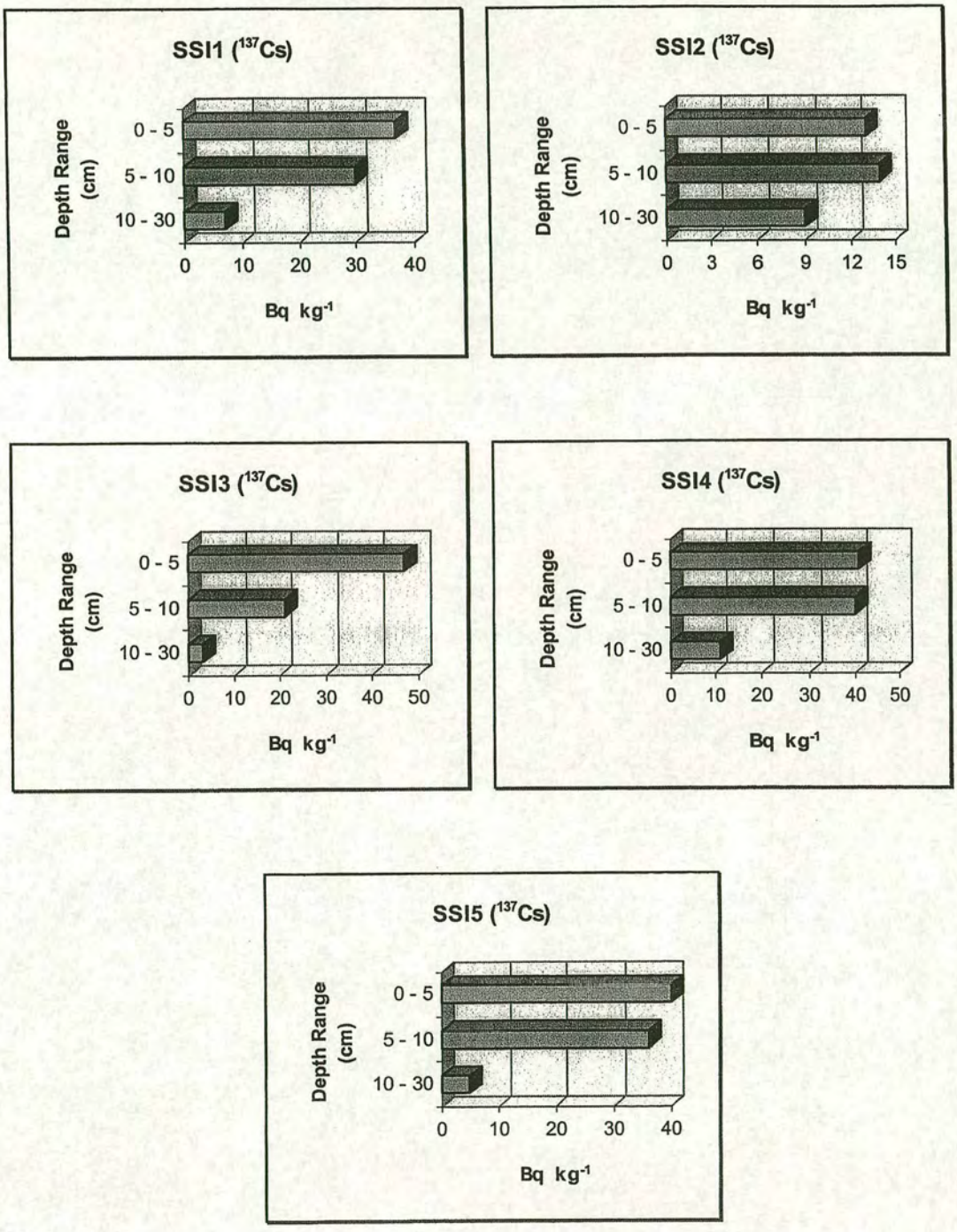

Figure 3.93: Distribution of ^{137}Cs with depth at Broda.
Open field locations, I1 - I5.

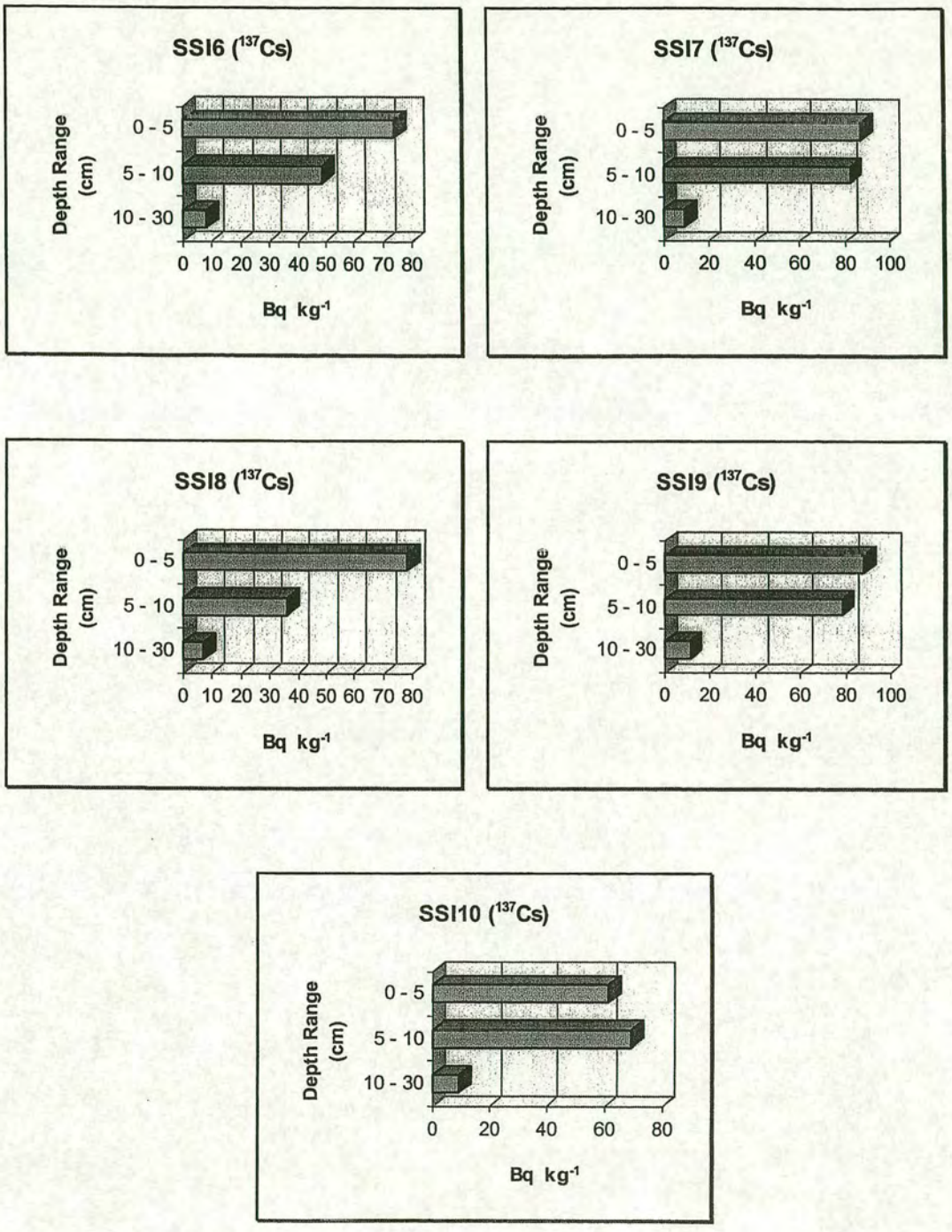

Figure 3.94: Distribution of ^{137}Cs with depth at Broda.
Under canopy locations, I6 - I10.

3.3.9 Hasslehult & Hassleberg (see Fig. 2.10 & Table 2.2)

3.3.9.1 Lead 210 soil inventories

The inventories of atmospheric ^{210}Pb for the samples collected from beneath the Norway spruce(*Picea abies*) canopy in Hassleberg, as well as the open field in Hasslehult are presented in Figures 3.95 and 3.96. Mean ^{210}Pb inventories for the open field(J_O) and under canopy(J_C) are shown in Figure 3.95, where the error bars represent standard error of the mean. The coefficient of variation for the measured ^{210}Pb inventories is 15% for the open field, and 14% for the under canopy location. The levels of ^{210}Pb present in the individual cores from the open field(J1-J5) and under canopy sampling points(J6-J10) are shown in Figure 3.96, where the error bars are due to counting statistics. Considering a calculated *t-value* of 2.26, the significant difference between the mean inventory values for the open field and under canopy samples is only at 10% level. The canopy enhancement in ^{210}Pb deposition is approximately 23%.

Depth profiles for specific activities are illustrated in Figures 3.97 and 3.98. The top 10 cm soil has mostly retained the atmospheric ^{210}Pb in both open field and under canopy locations. The only exception is SSJ10 sampling point, where the contribution of 10-30 cm depth interval is rather significant.

Under the reasonable assumption of a steady state between the atmospheric supply of ^{210}Pb and its radioactive decay in soil, its average flux would be approximately 97 Bq m^{-2} y^{-1} for the open field in Hasslehult, and 119 Bq m^{-2} y^{-1} to the spruce canopy in Hassleberg.

3.3.9.2 Caesium 137 soil inventories

The soil inventories for ^{137}Cs are presented in Figures 3.99 and 3.100. Mean inventories for the open field(J_O) and under canopy(J_C) locations are shown in Figure 3.99, where the error bars represent standard error of the mean. The coefficient of

variation for the measured ^{137}Cs inventories is 21%, for the open field, and 24% for the under canopy locations. The levels of ^{137}Cs present in the individual cores from the open field(J1-J5) and under canopy sampling points(J6-J10) are shown in Figure 3.100, where the error bars are due to counting statistics. Considering a calculated *t-value* of 1.13, there are no significant differences between the mean inventory values for the open field and under canopy samples.

Depth profiles for specific activities are illustrated in Figures 3.101 and 3.102 for the open field and under canopy cores, respectively. The bulk of caesium 137 is mostly concentrated in the surface horizons of soil in the open field. In the case of under canopy profiles, however, the contribution of 10-30 cm depth interval is cosiderably larger.

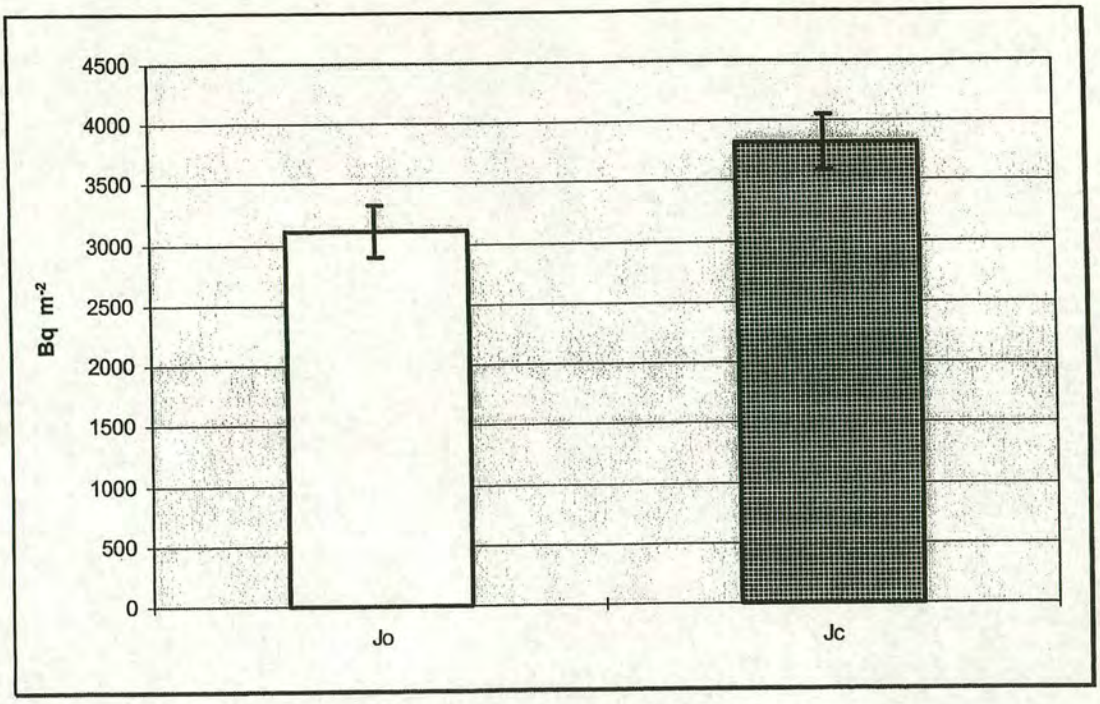

Figure 3.95: Mean atmospheric ^{210}Pb soil inventories in the open field(J_O), and inside the forest canopy(J_C) at Hasslehult and Hassleberg, respectively.

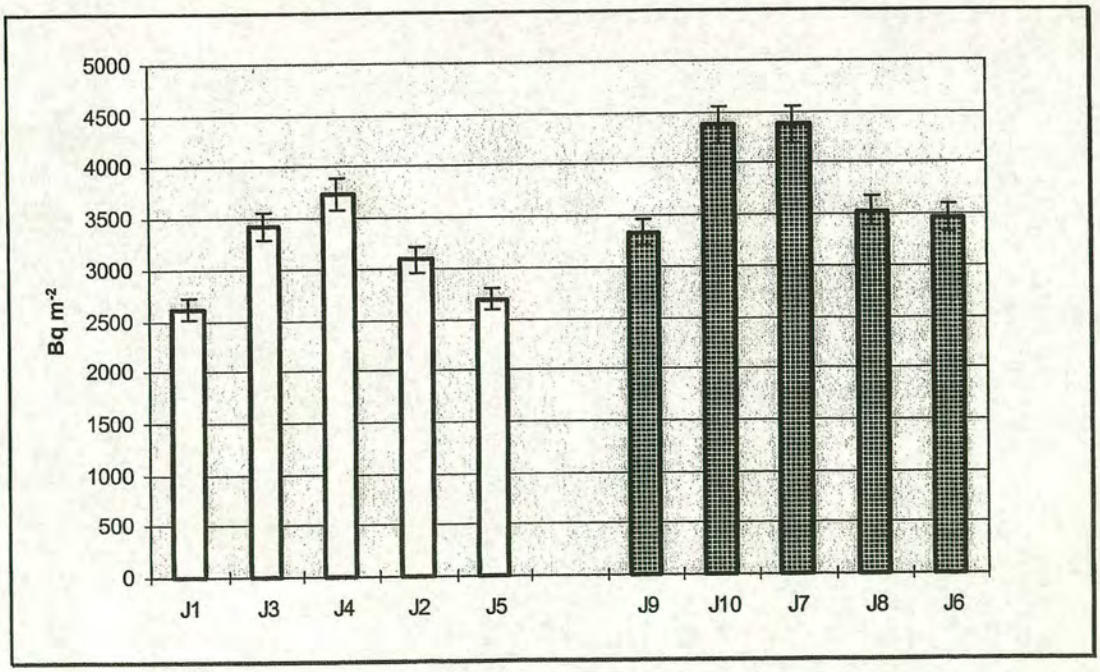

Figure 3.96: Atmospheric ^{210}Pb inventories measured in soil samples from each sampling point at Hasslehult(J1-J5) and Hassleberg(J6-J10).

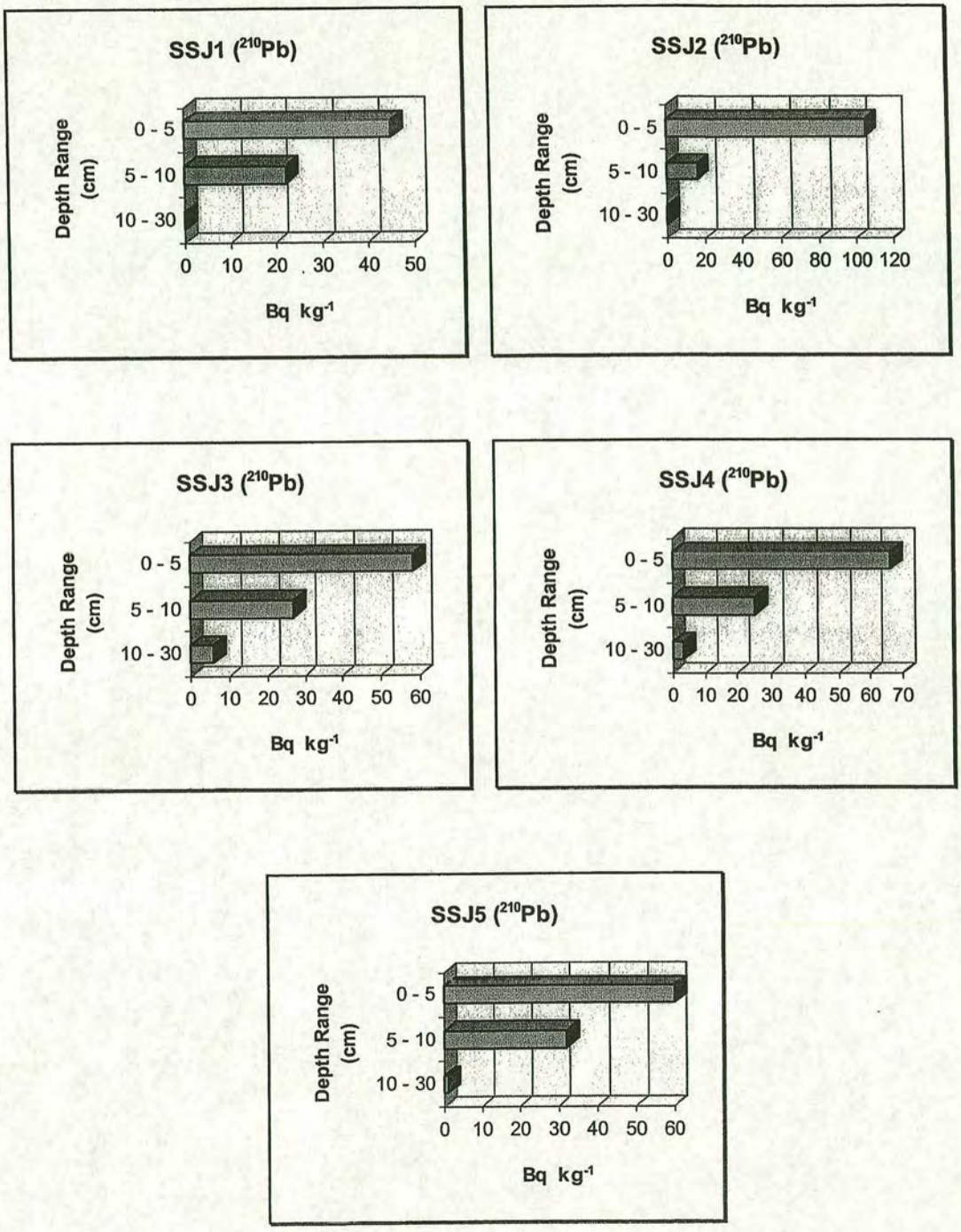

Figure 3.97: Distribution of atmospherically derived ^{210}Pb with depth at Hasslehult. Open field locations, J1 - J5.

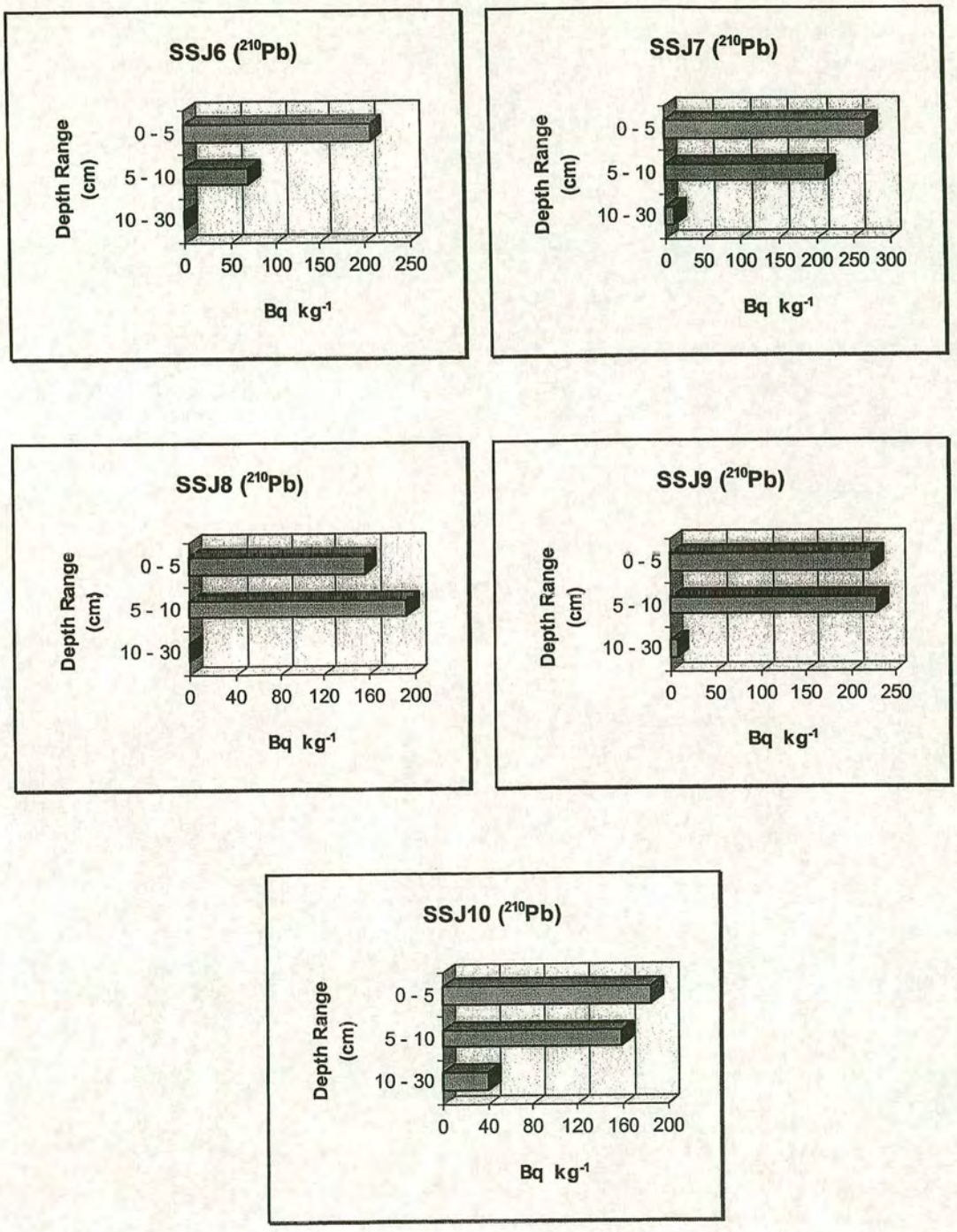

Figure 3.98: Distribution of atmospherically derived ^{210}Pb with depth at Hassleberg. Under canopy locations, J6 - J10.

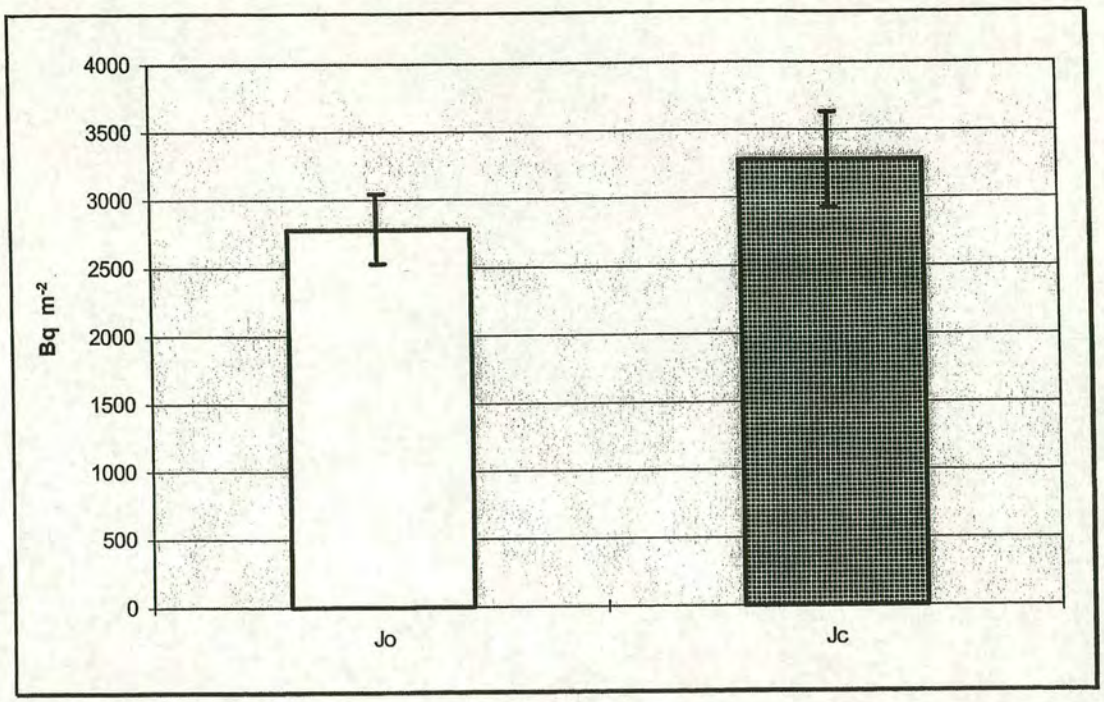

Figure 3.99: Mean ^{137}Cs soil inventories in the open field(J_O), and inside the forest canopy(J_C) at Hasslehult and Hassleberg, respectively.

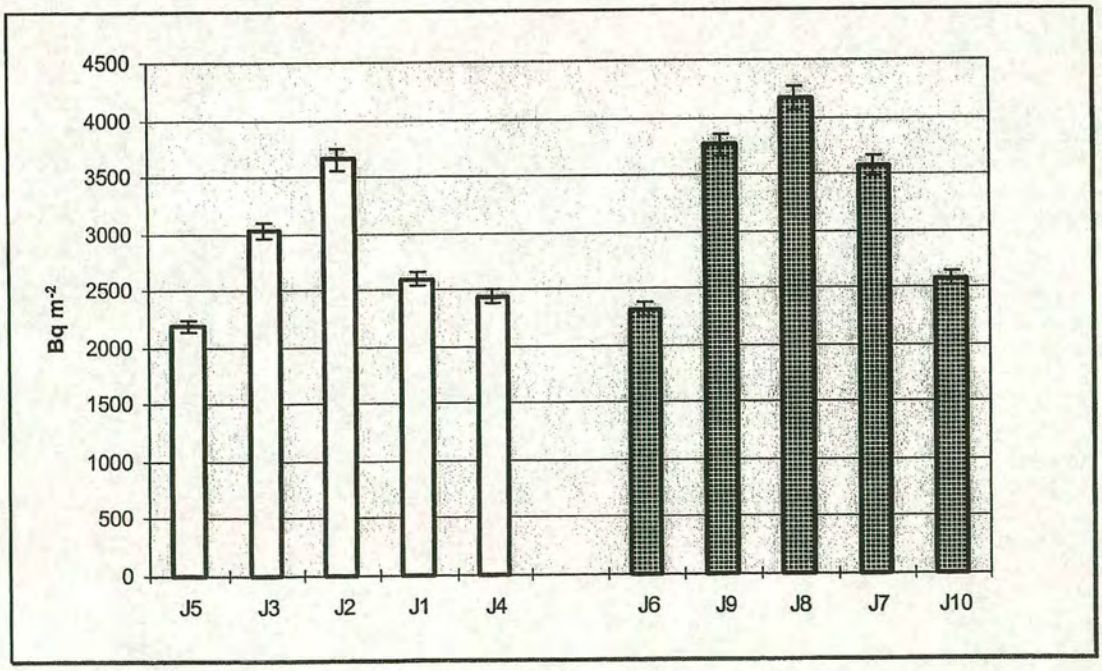

Figure 3.100: ^{137}Cs inventories measured in soil samples from each sampling point at Hasslehult(J1-J5) and Hassleberg(J6-J10).

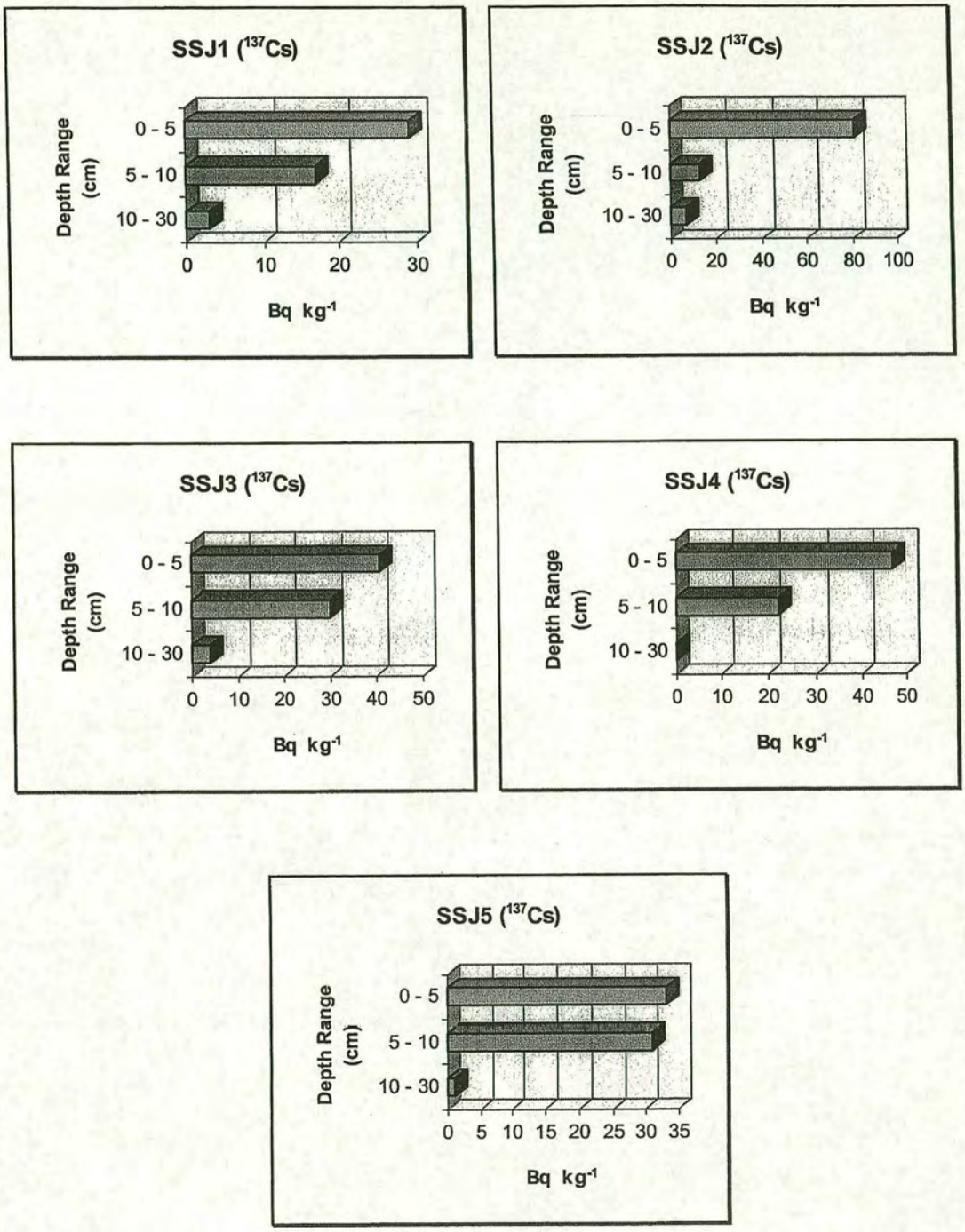

Figure 3.101: Distribution of ^{137}Cs with depth at Hasslehult.
Open field locations, J1 - J5.

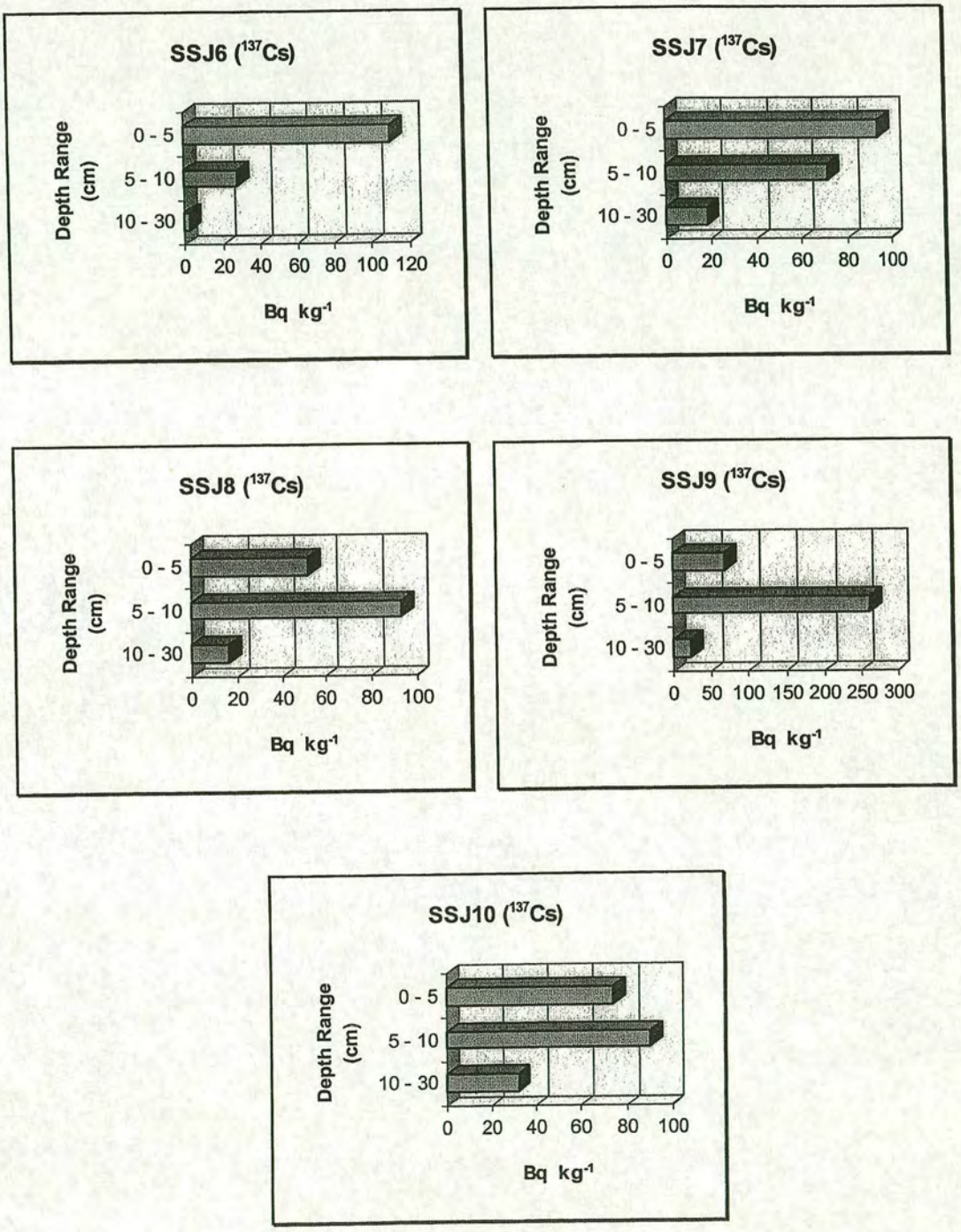

Figure 3.102: Distribution of ^{137}Cs with depth at Hassleberg.
Under canopy locations, J6 - J10.

3.3.10 Deposition pattern in Hallands (see Figs. 2.9, 2.10&Table 2.2)

The mean inventories of atmospheric ^{210}Pb for samples collected from beneath coniferous forest canopies, as well as the adjacent/nearby open fields at 10 sites, situated in the Swedish south-western province of Hallands are presented in Figure 3.103. From these ten sites, eight of them, A-G & J, lie along a transect leading NE to about 60 km inland from the coast. The other two, H & I, form a parallel line to the shoreline which includes site G as well (see section 2.1.1.3 and Figure 2.1.5 for details). Lead 210 soil inventories with respect to geographical distribution are illustrated in Figure 3.104. This figure shows that the ^{210}Pb deposition increases quite markedly with distance inland. The altitude increases in the same direction as well, but to just few hundred meters asl (see section 2.1.1.3 and Table 2.1.2). Deposition values increase to a maximum in sites G, H, and I , roughly 20-30 km from the coast, and decreases by almost 30% relative to the maximum in site J, 61 km from the coast.

The results give no indication of canopy enhancement relative to the adjacent open land covered by short vegetation at the coastal sites A & B. Even taking into account the low value of deposition in nearby open field at site C, the canopy enhancement would be just 10%. On the other hand, at high elevation sites G, H, and I, The canopy enhancement is about 40%, on average, relative to the adjacent/nearby open fields. In between, the canopy enhancement in mid-elevation sites D, E, and F, is almost 20%. At site J, the exposed spruce canopy receives about 23% more atmospheric ^{210}Pb than the nearby open field. A striking feature of these results is that the inputs to exposed forests on elevated hills 20-30 km inland is approximately a factor of 2 larger than that in open land covered by short vegetation in the coastal region.

Under the reasonable assumption of a steady state between the atmospheric supply of ^{210}Pb and its radioactive decay in soil, its average flux would be approximately 81 Bq m^{-2} y^{-1} and 89 Bq m^{-2} y^{-1} for the open field and forest canopies in coastal region, respectively. The average flux to the elevated inland region is

approximately 119 Bq m^{-2} y^{-1} for the open field, and 165 Bq m^{-2} y^{-1} for the upland coniferous forests.

The mean soil inventories of ^{137}Cs for the region are presented in Figure 3.105. In contrast to the ^{210}Pb data, the caesium 137 results give no indication of significant canopy enhancement in deposition. The inventories for the forest canopy in site I, is even 30% less than the nearby open field, on average. Generally, the regional pattern of ^{137}Cs soil inventories is more complicated than that of ^{210}Pb. The main feature of this pattern is that, mean inventory for the coastal sites A-C, are approximately 50% more than that for inland sites G-J.

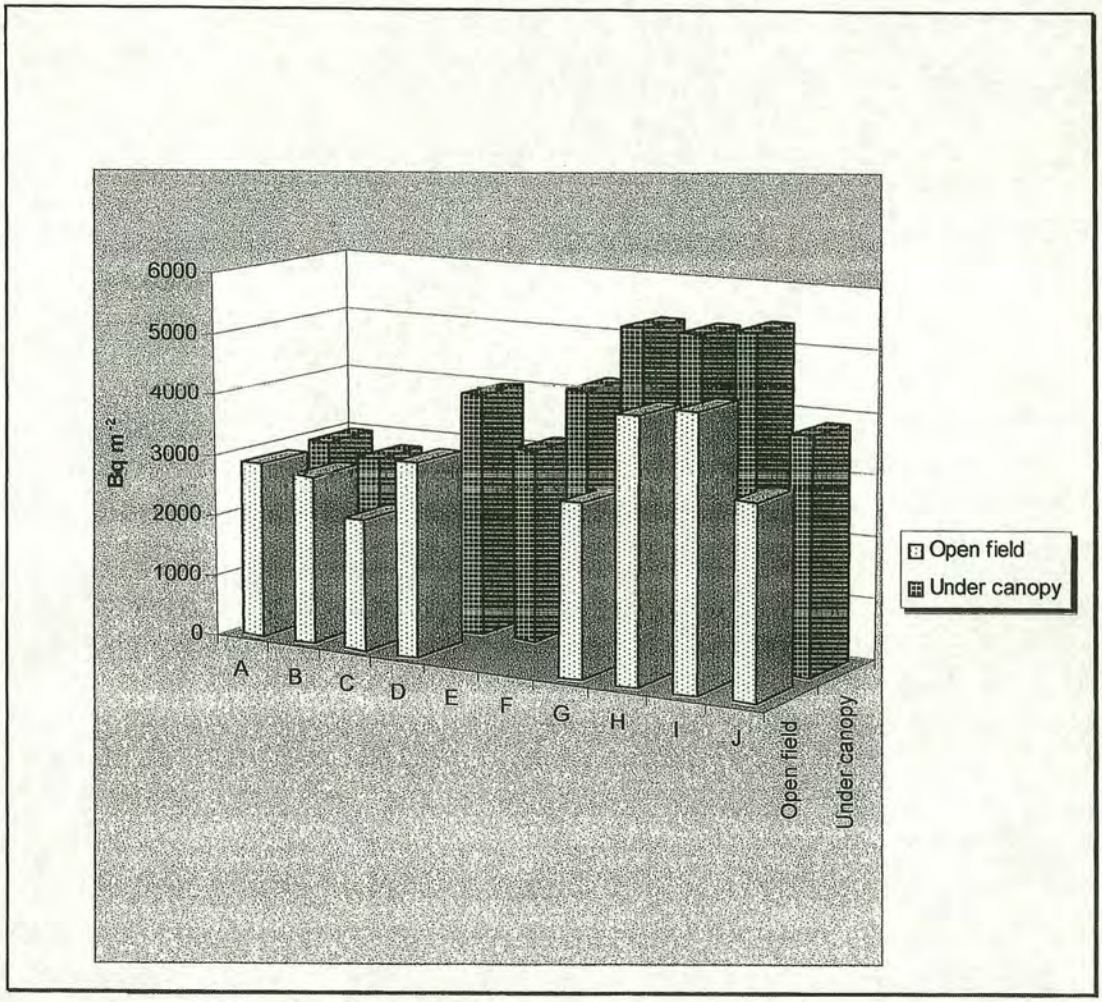

Figure 3.103: Mean atmospheric ^{210}Pb inventories at Southwest Sweden sites A to J.

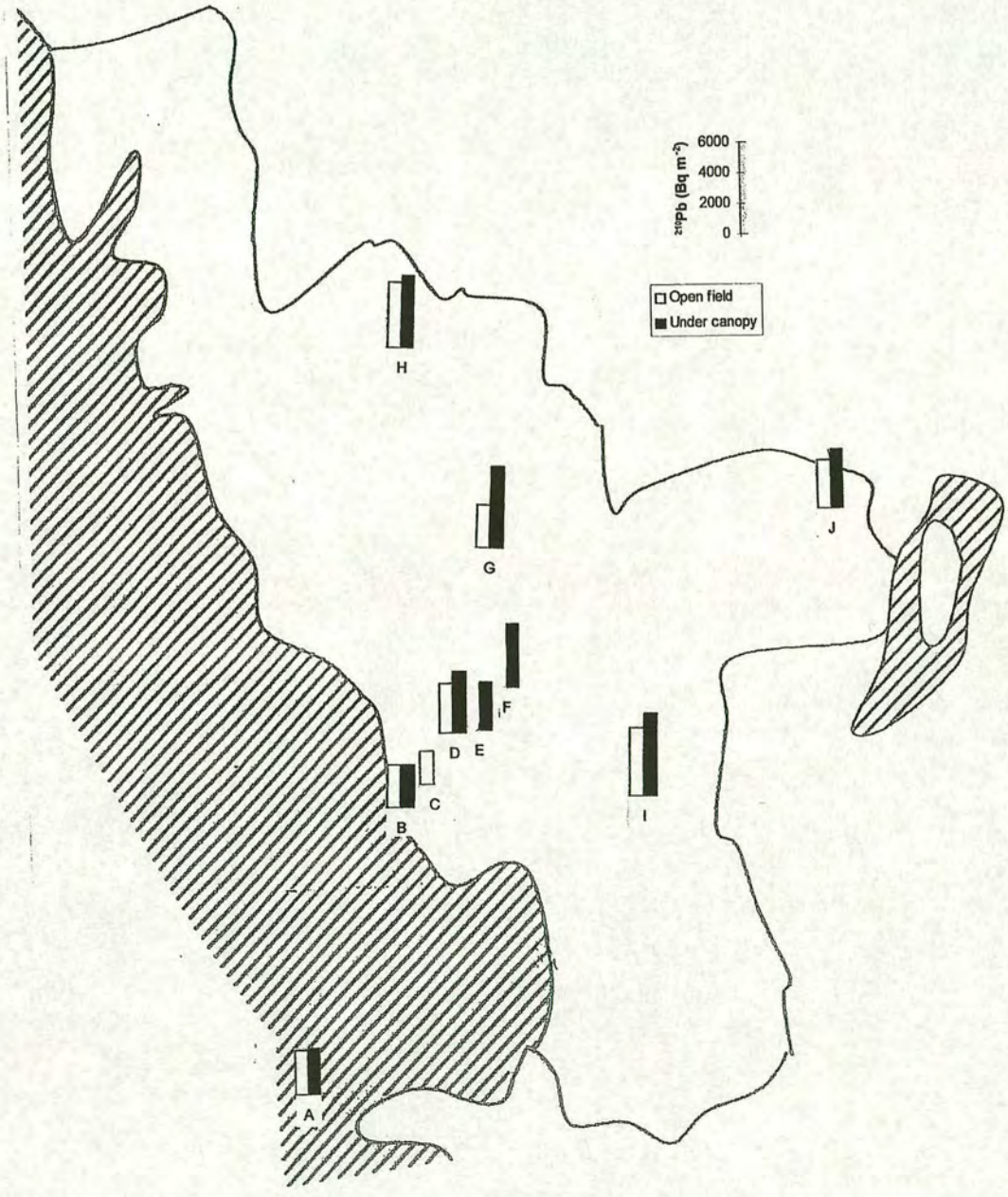

Figure 3.104: Mean atmospheric ^{210}Pb soil inventories at Southwest Sweden sites A to J with respect to their geographical distribution in Hallands province.

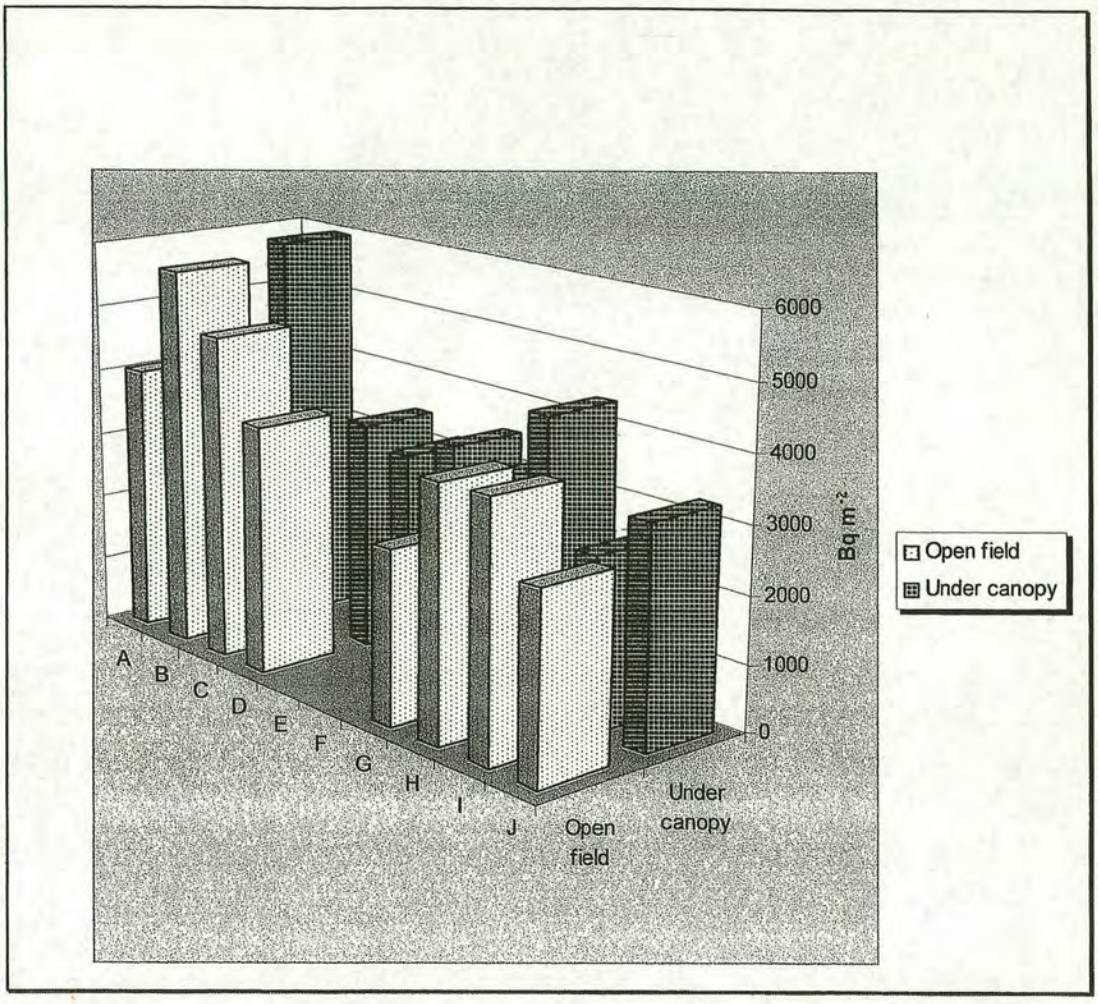

Figure 3.105: Mean ^{137}Cs inventories at Southwest Sweden sites A to J.

3.4 Central Sweden (see section 2.1.1.2, Figs. 2.13, 2.14& 2.15)

Radioanalytical results for soil taken from 4 sites(A-D) in Central Sweden are presented, site by site, in this section. Site A is an open field on top of Gammalsaters Mountain at 870 m asl. Site B includes a spruce canopy and an open heathland on the same mountain at elevations of about 720 and 740 m asl. Site C is situated at the base of Gammalsaters and includes a spruce canopy as well as an open grassland, at 540 and 530 m asl. And finally, site D is at the edge of a mixed spruce/pine canopy besides a lake on an adjacent mountain, Skaftasen, at 620m asl. The pattern of deposition for this regionis then described.

3.4.1 Gammalsaters fjallet, site A

3.4.1.1 Lead 210 soil inventories

The inventories of atmospheric ^{210}Pb for the samples collected from the open field on top of Gammalsaters fjallet are presented in Figures 3.106 and 3.107. Mean ^{210}Pb inventory(A_O) is shown in Figure 3.106, where the error bar represents standard error of the mean. The coefficient of variation for the measured ^{210}Pb inventories is 13%. The levels of ^{210}Pb present in the individual cores from the open field(A1-A5) are shown in Figure 3.107, where the error bars are due to counting statistics.

Depth profiles for specific activities are illustrated in Figure 3.108. The illustrated profiles indicate the fact that top 15 cm soil has retained the atmospheric ^{210}Pb efficiently, and the contribution from horizons below 15 cm is substantially small at this site.

Under the reasonable assumption of a steady state condition between the atmospheric supply of ^{210}Pb and its radioactive decay in soil, its average flux at this site would be 113 Bq m^{-2} y^{-1}.

3.4.1.2 Caesium 137 soil inventories

The soil inventories for ^{137}Cs are presented in Figures 3.109 and 3.110. Mean ^{137}Cs inventory for the site(A_O) is shown in Figure 3.109, where the error bar represents standard error of the mean. The coefficient of variation for the measured ^{137}Cs inventories is 4%. The levels of ^{137}Cs present in the individual cores from the open field(A1-A5) are shown in Figure 3.110, where the error bars are due to counting statistics.

Depth profiles for specific activities are illustrated in Figure 3.111. The illustrated profiles show that the top 15 cm soil has retained ^{137}Cs efficiently, and the contribution from horizons below 15 cm is substantially small as it was the case with ^{210}Pb activity profiles at this site.

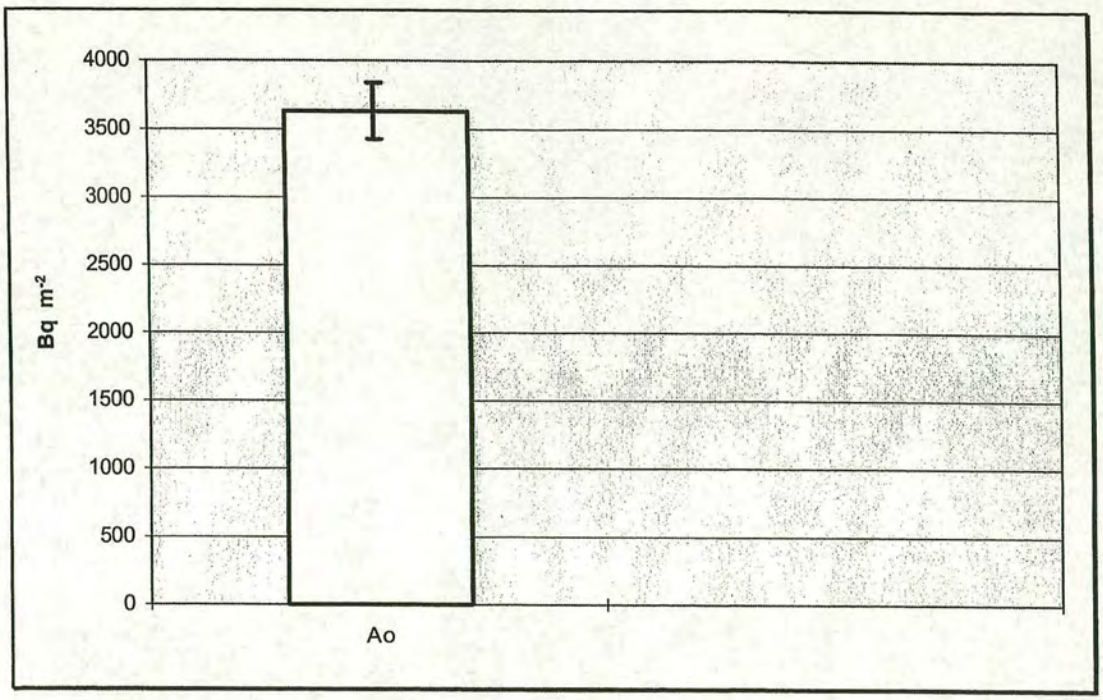

Figure 3.106: Mean atmospheric ^{210}Pb soil inventories in the open field(A_O) at 870 m asl, Gammalsaters fjallet, site A.

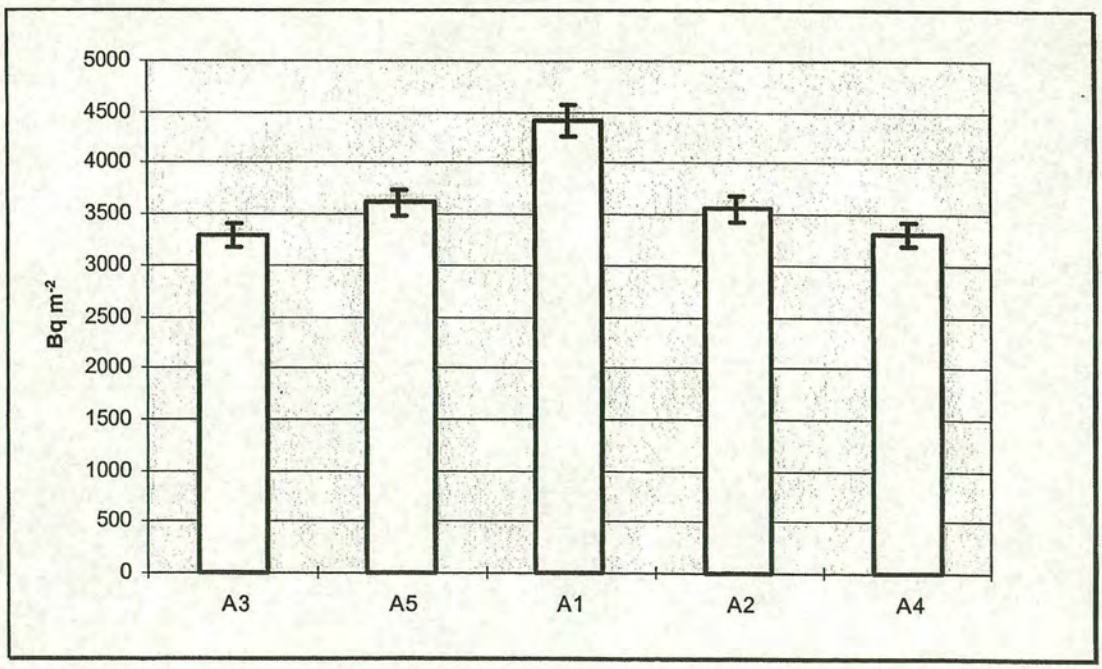

Figure 3.107: Atmospheric ^{210}Pb inventories measured in soil samples from each sampling point at Gammalsaters fjallet, site A.

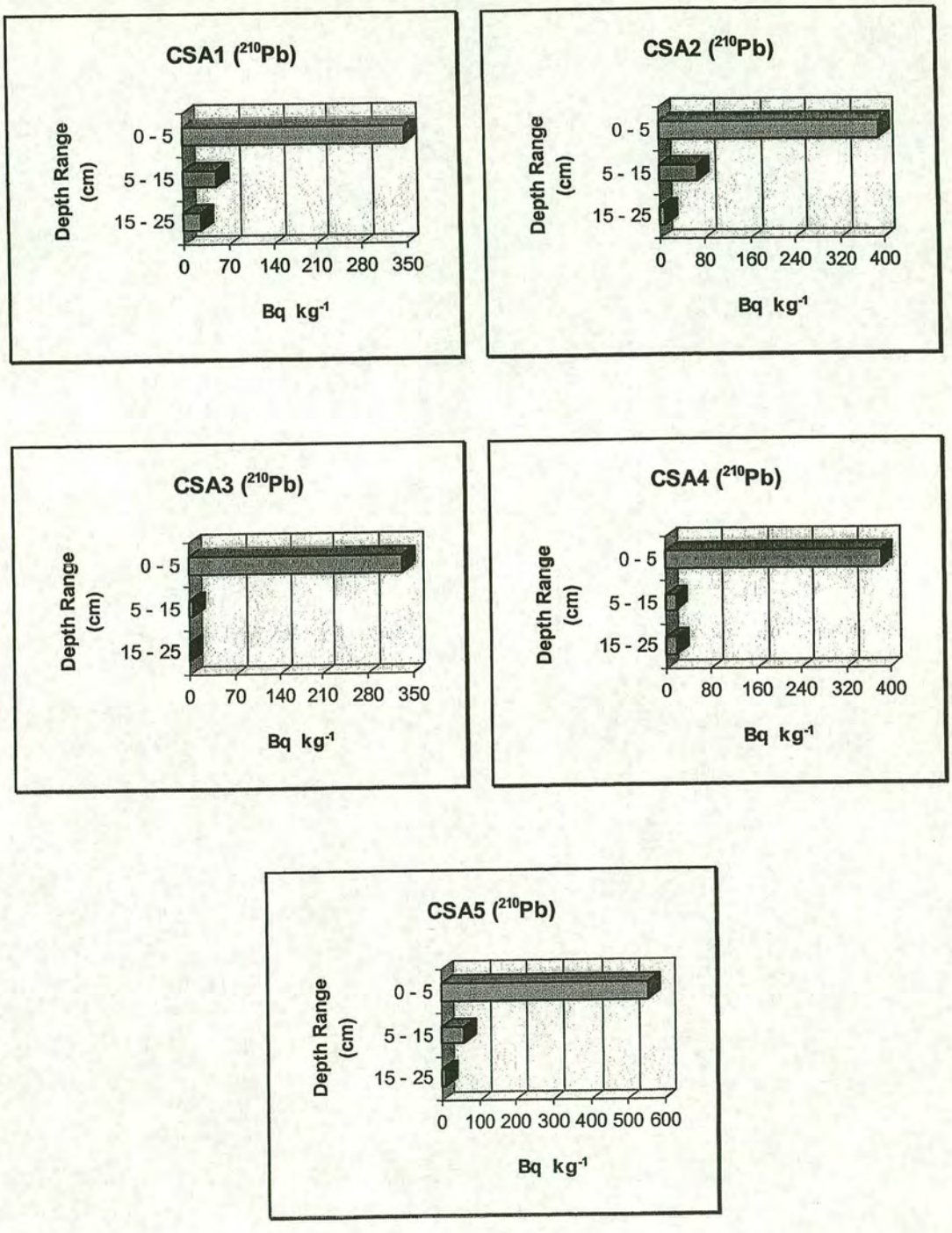

Figure 3.108: Distribution of atmospherically derived ^{210}Pb with depth at Gammalsaters fjallet. Open field locations, A1 - A5.

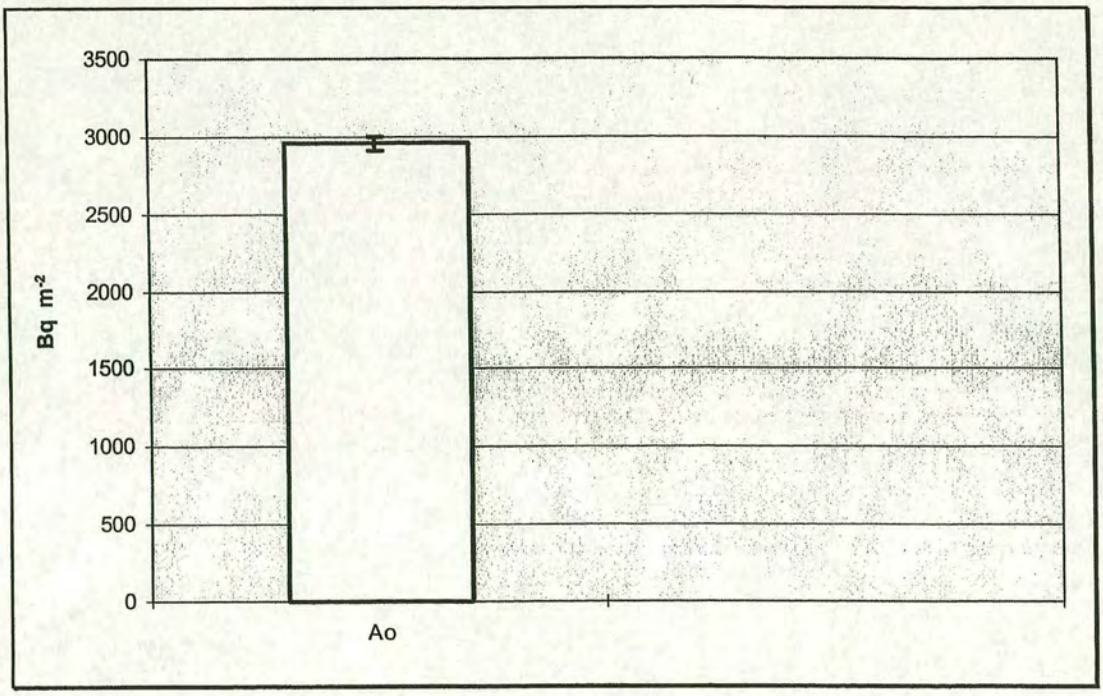

Figure 3.109: Mean ^{137}Cs soil inventories in the open field(A_O) at 870 m asl, Gammalsaters fjallet, site A.

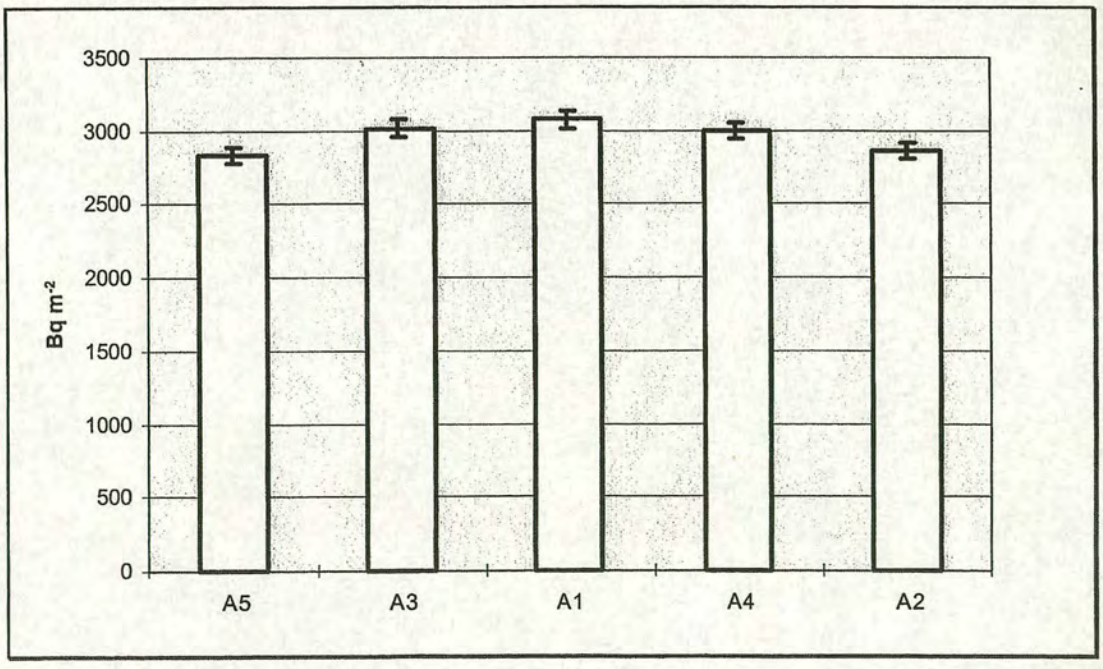

Figure 3.110: ^{137}Cs inventories measured in soil samples from each sampling point at Gammalsaters fjallet, site A.

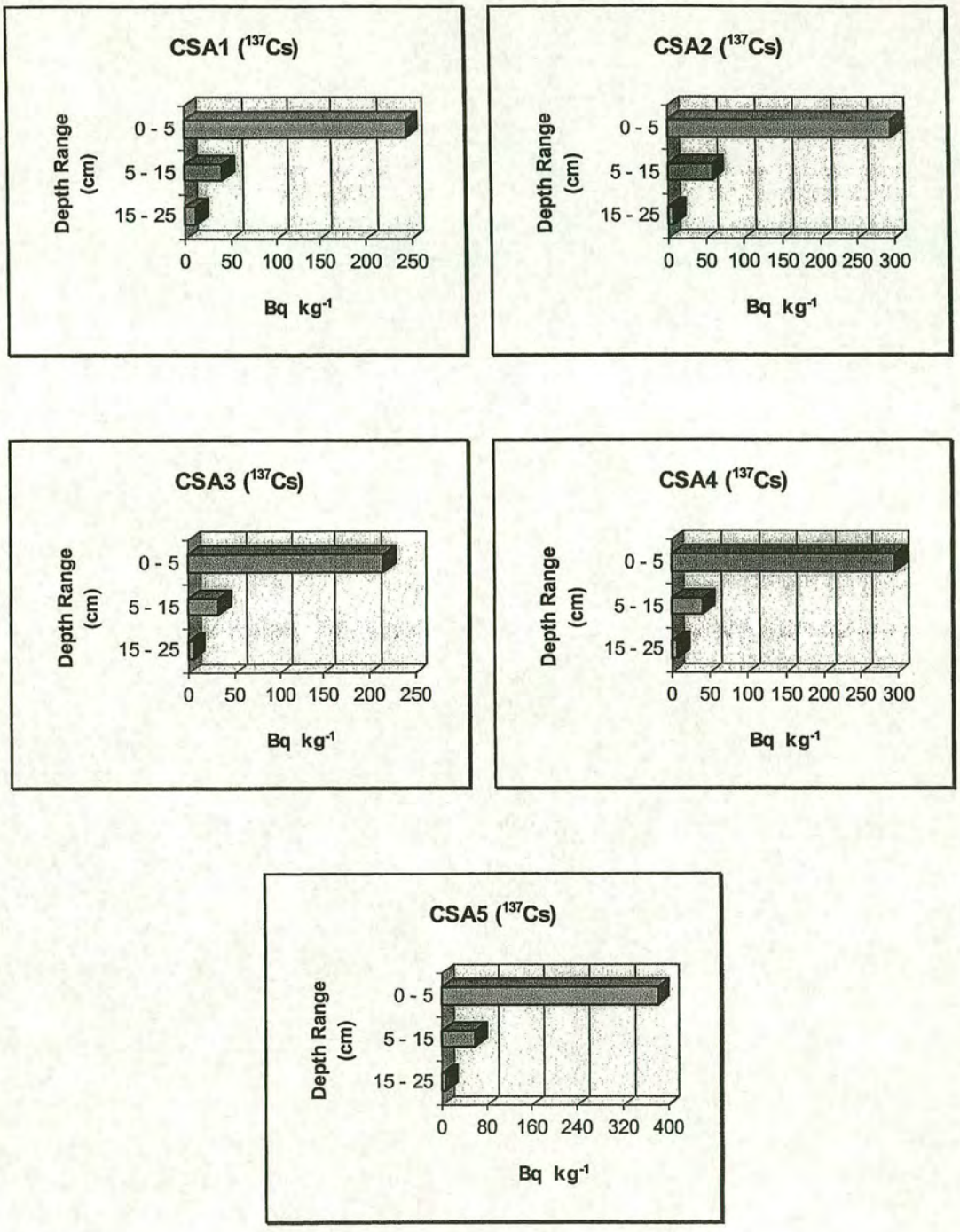

Figure 3.111: Distribution of ^{137}Cs with depth at Gammalsaters fjallet. Open field locations, A1 - A5.

3.4.2 Gammalsaters fjallet, site B (see Figs. 2.13-2.15)

3.4.2.1 Lead 210 soil inventories

The inventories of atmospheric ^{210}Pb for the samples collected from beneath the Norway spruce(*Picea abies*) canopy at 720m asl, as well as the open heathland at 740 m asl are presented in Figures 3.112 and 3.113. The mean ^{210}Pb inventories for the open field(B_O) and under canopy(B_C) are shown in Figure 3.112, where the error bars represent standard error of the mean. The coefficient of variation for the measured ^{210}Pb inventories is 12% for the open field, and 7% for the under canopy location. The levels of ^{210}Pb present in the individual cores from the open field(B1-B5) and under canopy sampling points(B6-B10) are shown in Figure 3.113, where the error bars are due to counting statistics. The canopy enhancement in ^{210}Pb deposition is approximately 36%.

Depth profiles for specific activities are illustrated in Figures 3.114 and 3.115. The top 15 cm soil has mostly retained the atmospheric ^{210}Pb in under canopy location. However, this is not the case with the open field activity profiles, where the contribution of 15-25 cm depth interval is significant.

Under the reasonable assumption of a steady state between the atmospheric supply of ^{210}Pb and its radioactive decay in soil, its average flux would be approximately 100 Bq m^{-2} y^{-1} for the open field, and 136 Bq m^{-2} y^{-1} to the spruce canopy at this site.

3.4.2.2 Caesium 137 soil inventories

The soil inventories for ^{137}Cs are presented in Figures 3.116 and 3.117. Mean inventories for the open field(B_O) and under canopy(B_C) locations are shown in Figure 3.116, where the error bars represent standard error of the mean. The coefficient of variation for the measured ^{137}Cs inventories is 36%, for the open field, and 13% for the under canopy location. The levels of ^{137}Cs present in the individual

cores from the open field(B1-B5) and under canopy sampling points(B6-B10) are shown in Figure 3.117, where the error bars are due to counting statistics. There are no significant differences between the mean inventory values for the open field and under canopy samples.

Depth profiles for specific activities are illustrated in Figures 3.118 and 3.119 for the open field and under canopy cores, respectively. The bulk of caesium 137 is mostly concentrated in the surface horizons of soil in both open field and under canopy locations. However, the contribution from 15-25 cm depth interval is not negligible.

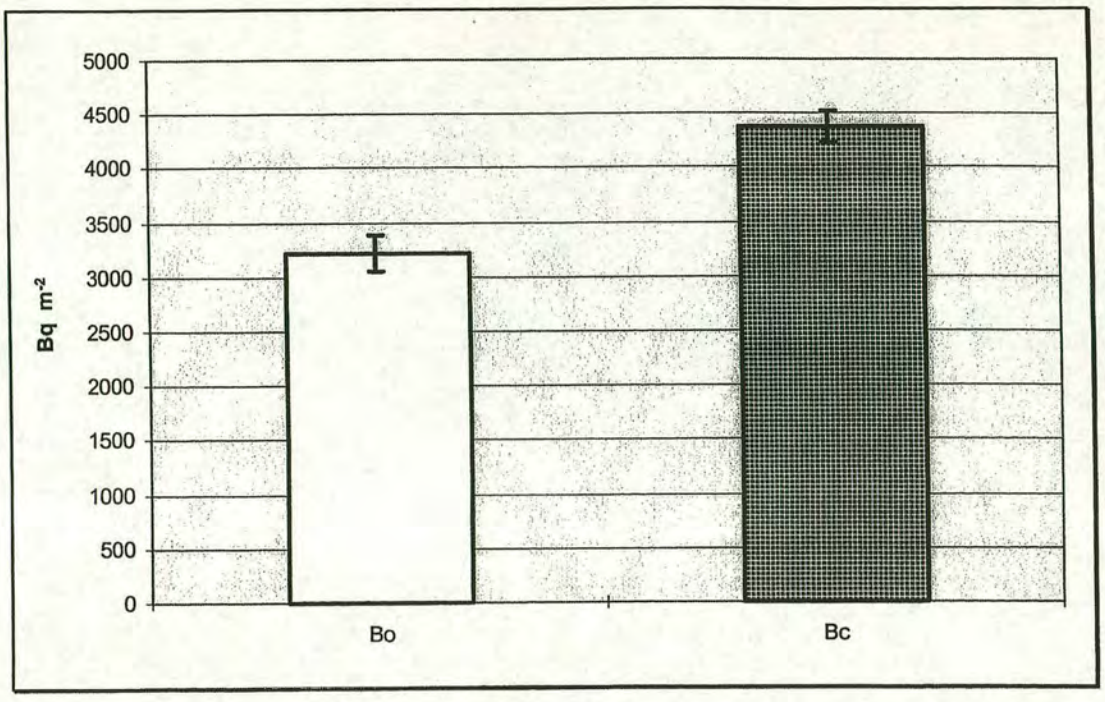

Figure 3.112: Mean atmospheric ^{210}Pb soil inventories in the open field(B_O) at 740 m asl, and inside the forest canopy(B_C) at 720 m asl, Gammalsaters fjallet, site B.

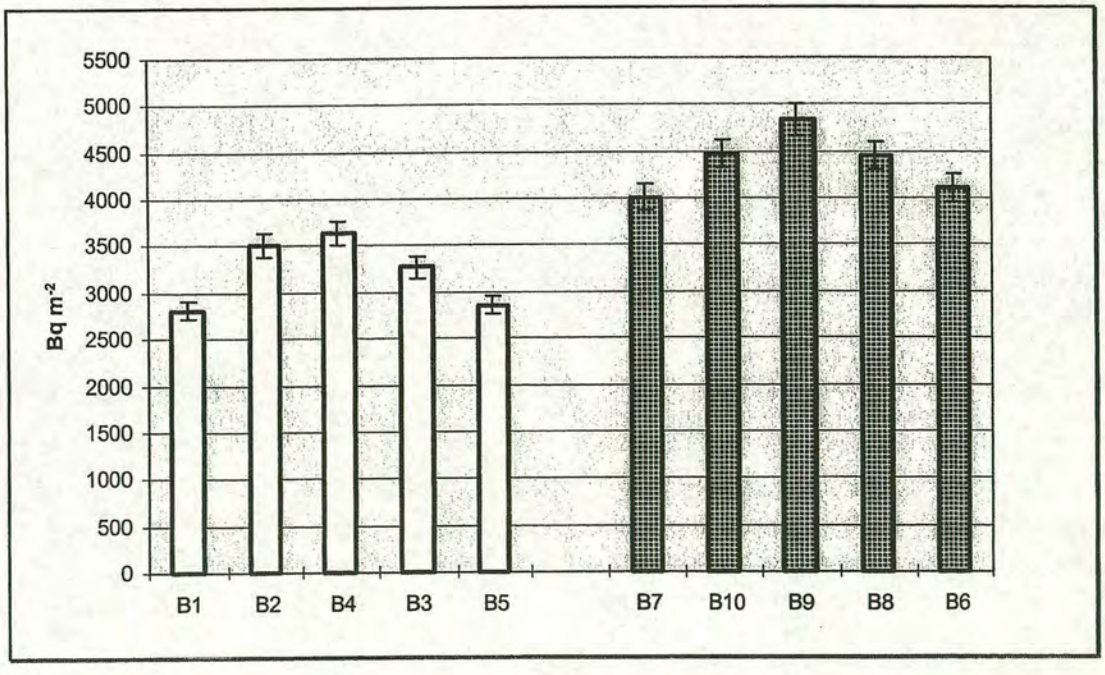

Figure 3.113: Atmospheric ^{210}Pb inventories measured in soil samples from each sampling point at Gammalsaters fjallet, site B.

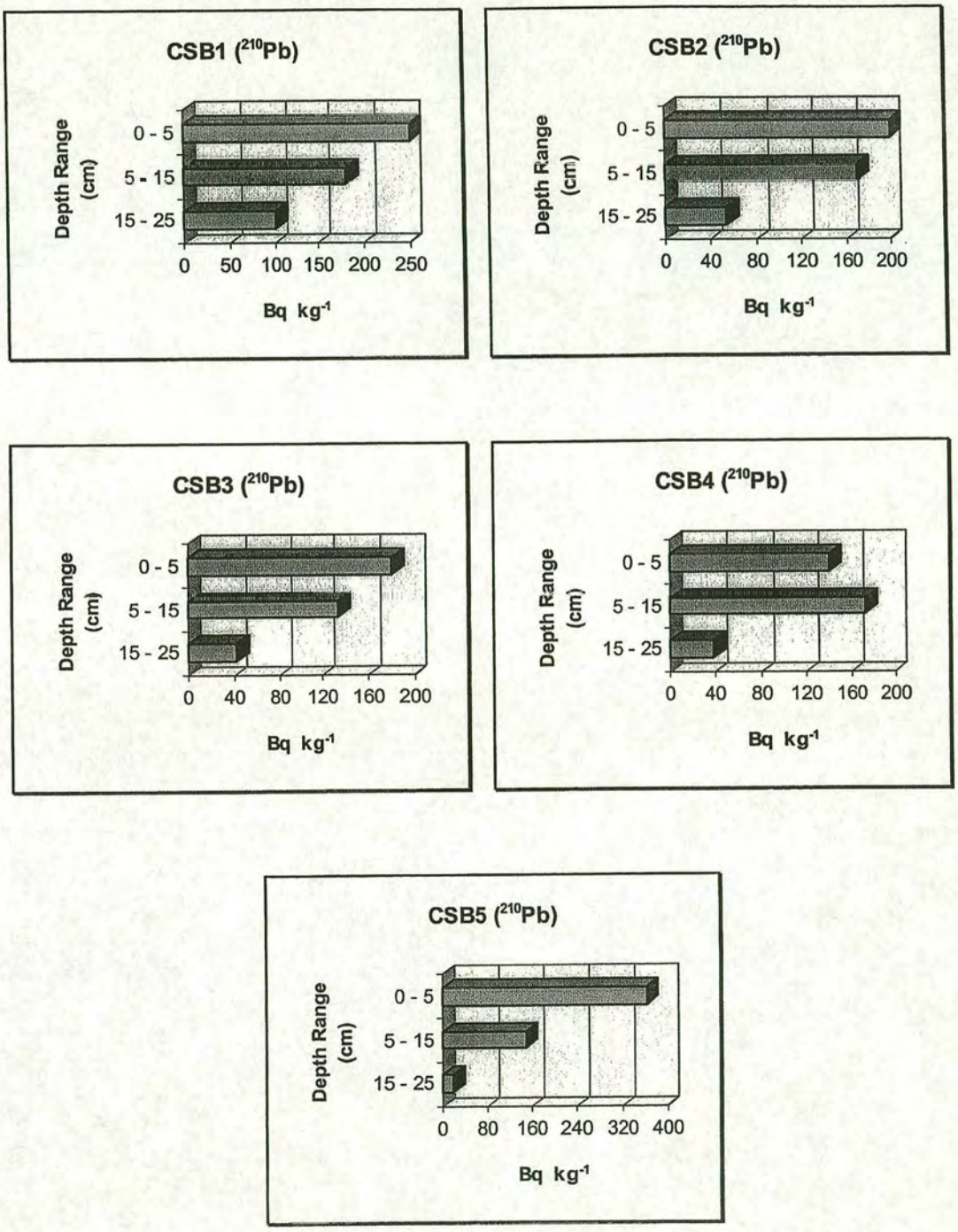

Figure 3.114: Distribution of atmospherically derived ^{210}Pb with depth at Gammalsaters fjallet. Open field locations, B1 - B5.

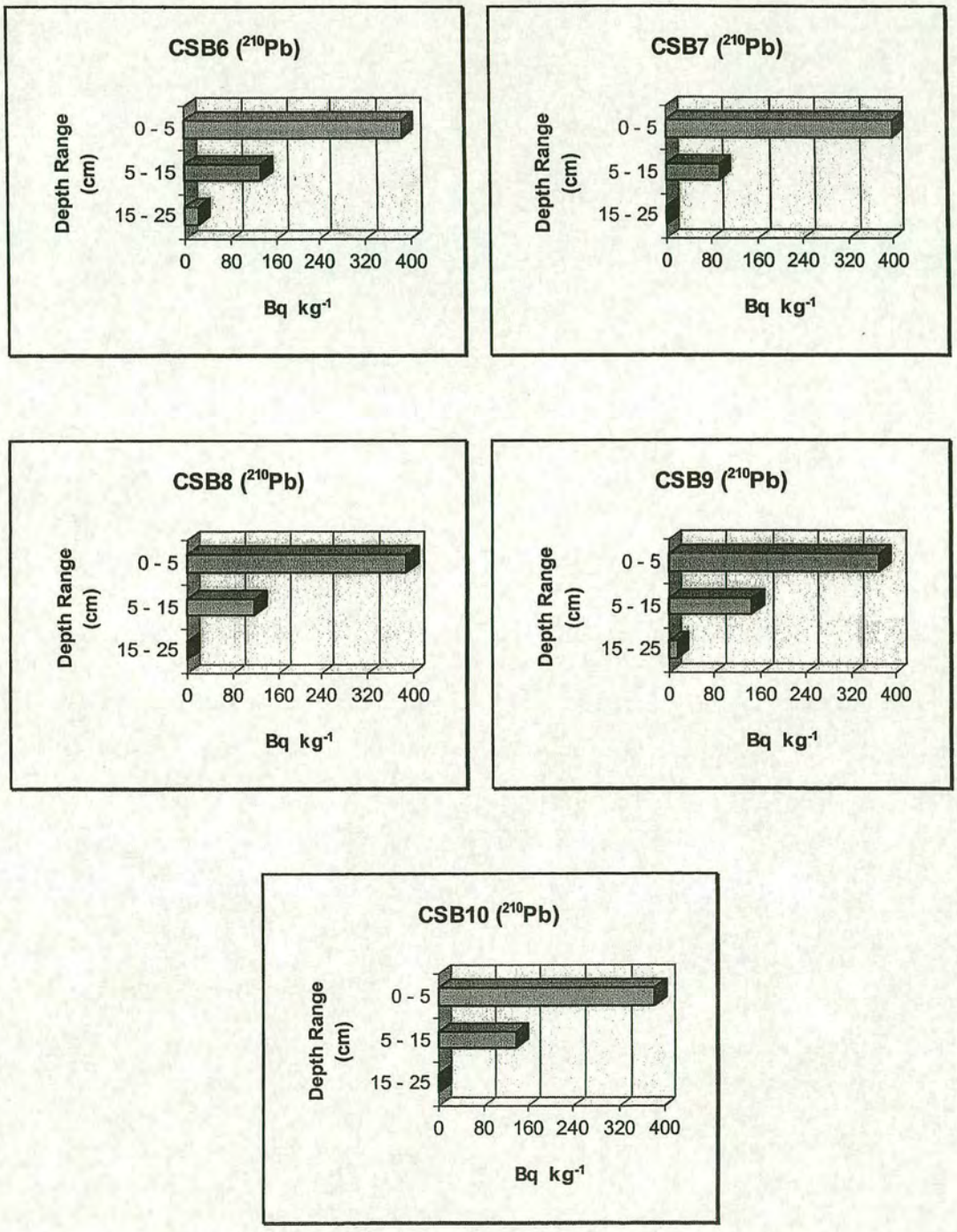

Figure 3.115: Distribution of atmospherically derived ^{210}Pb with depth at Gammalsaters fjallet. Under canopy locations, B6 - B10.

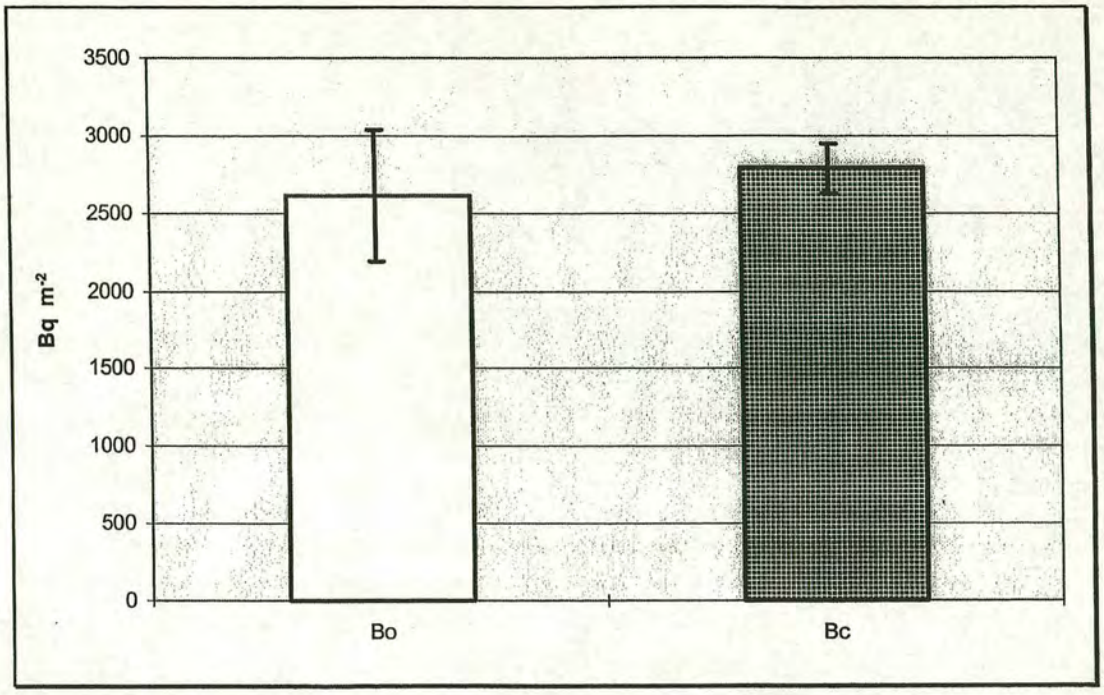

Figure 3.116: Mean ^{137}Cs soil inventories in the open field(B_O) at 740 m asl, and inside the forest canopy(B_C) at 720 m asl, Gammalsaters fjallet, site B.

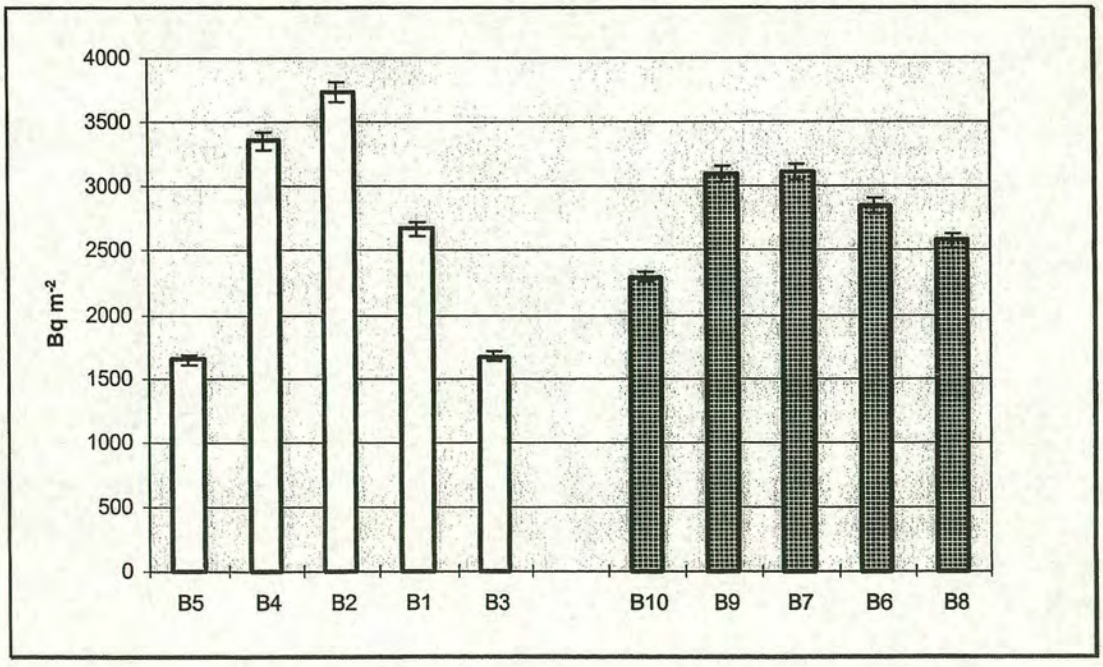

Figure 3.117: ^{137}Cs inventories measured in soil samples from each sampling point at Gammalsaters fjallet, site B.

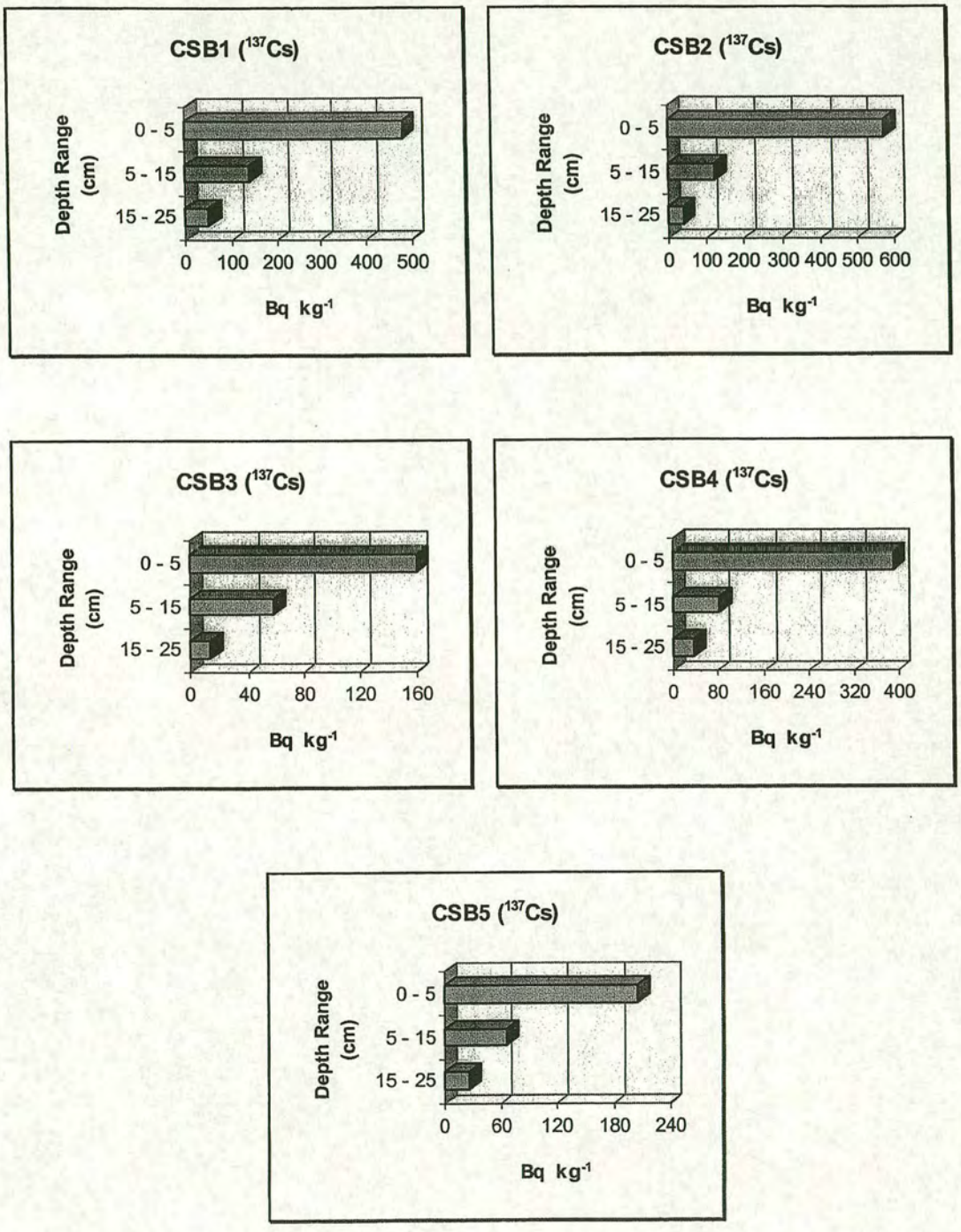

Figure 3.118: Distribution of ^{137}Cs with depth at Gammalsaters fjallet. Open field locations, B1 - B5.

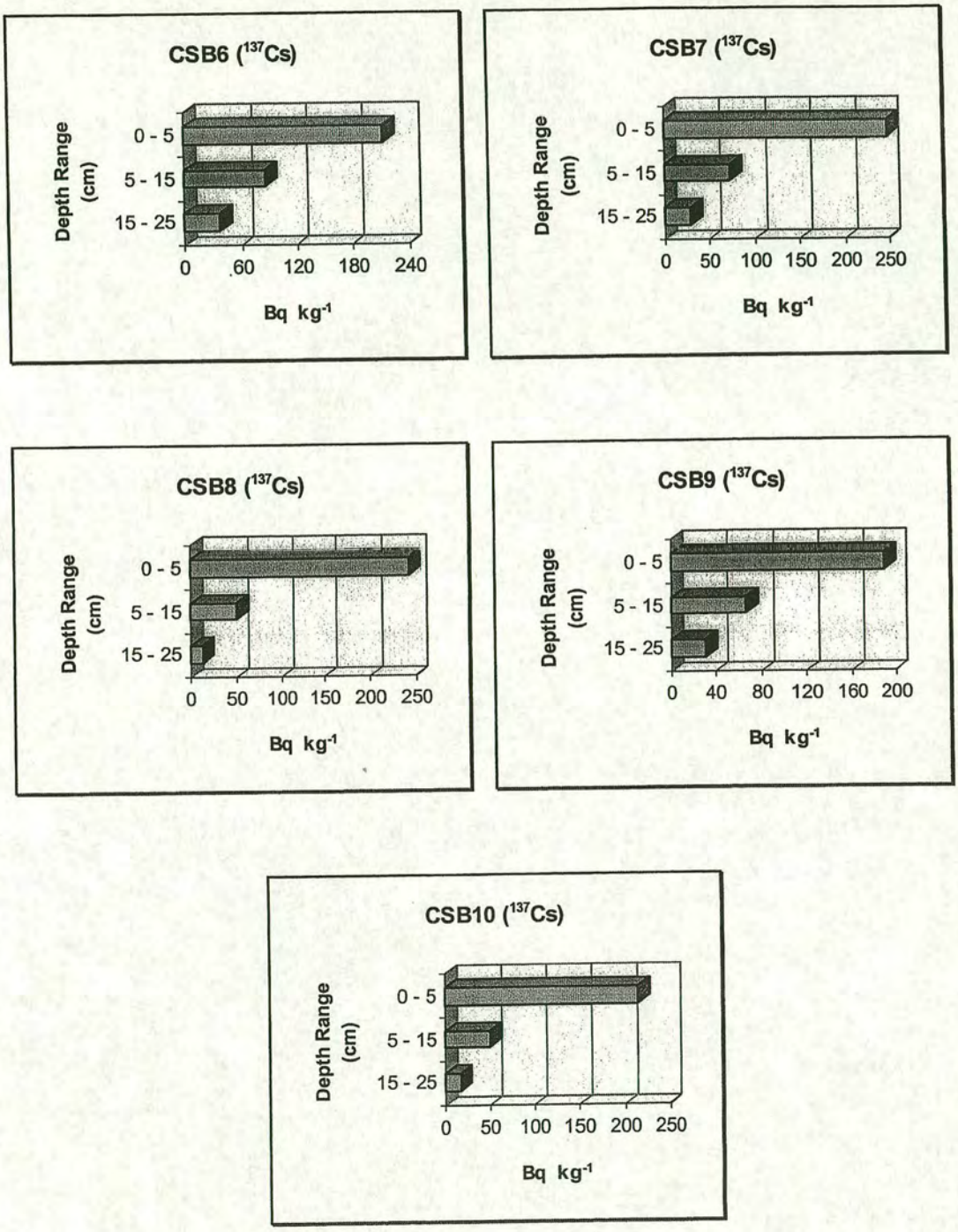

Figure 3.119: Distribution of ^{137}Cs with depth at Gammalsaters fjallet.
Under canopy locations, B6 - B10.

3.4.3 Gammalsatern, site C (see Figs. 2.13 -2.15)

3.4.3.1 Lead 210 soil inventories

The inventories of atmospheric ^{210}Pb for the samples collected from beneath the Norway spruce(*Picea abies*) canopy at 530m asl, as well as the open grassland at 540 m asl in Gammalsatern are presented in Figures 3.120 and 3.121. Mean ^{210}Pb inventories for the open field(C_O) and under canopy(C_C) are shown in Figure 3.120, where the error bars represent standard error of the mean. The coefficient of variation for the measured ^{210}Pb inventories is 8% for the open field, and 11% for the under canopy location. The levels of ^{210}Pb present in the individual cores from the open field(C1-C5) and under canopy sampling points(C6-C10) are shown in Figure 3.121, where the error bars are due to counting statistics. Considering a calculated *t-value* of 4.29, there are significant differences between the mean inventory values for the open field and under canopy samples at 1% level of significance. The canopy enhancement in ^{210}Pb deposition is approximately 32%.

Depth profiles for specific activities are illustrated in Figures 3.122 and 3.123. The top 5 cm soil has mostly retained the atmospheric ^{210}Pb in the open field. However, such a retention has been occurred by the top 12 cm of soil in the case of under canopy sampling points with the exception of CSC9 core, in which the contribution of 12-20 cm depth interval is significant.

Under the reasonable assumption of a steady state between the atmospheric supply of ^{210}Pb and its radioactive decay in soil, its average flux would be approximately 86 Bq m^{-2} y^{-1} for the open grassland, and 114 Bq m^{-2} y^{-1} to the spruce canopy at this site.

3.4.3.2 Caesium 137 soil inventories

The soil inventories for ^{137}Cs are presented in Figures 3.124 and 3.125. Mean inventories for the open field(C_O) and under canopy(C_C) locations are shown in

Figure 3.124, where the error bars represent standard error of the mean. Thecoefficient of variation for the measured ^{137}Cs inventories is 15%, for the open field, and 20% for the under canopy location. The levels of ^{137}Cs present in the individual cores from the open field(C1-C5) and under canopy sampling points(C6-C10) are shown in Figure 3.125, where the error bars are due to counting statistics. Considering a calculated *t-value* of 3.82, there are significant differences between the mean inventory values for the open field and under canopy samples at 1% level of significance. On the average, ^{137}Cs soil inventory under the spruce canopy exceeds that in the open field by approximately 61%.

Depth profiles for specific activities are illustrated in Figures 3.126 and 3.127 for the open field and under canopy cores, respectively. The bulk of caesium 137 is mostly concentrated in the surface horizons of soil in the open field. However, the case is completely different for under canopy profiles at this site. Activity depth profiles in Figure 3.127 show relatively high concentration of ^{137}Cs down to a depth of almost 20 cm.

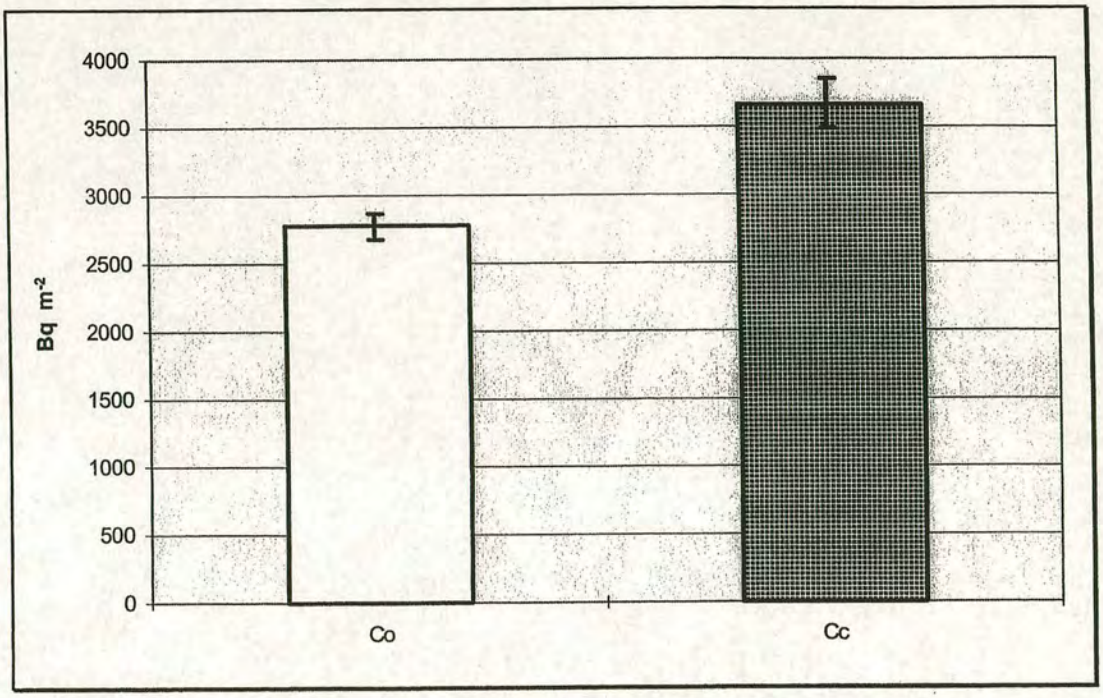

Figure 3.120: Mean atmospheric ^{210}Pb soil inventories in the open field(C_O) at 540 m asl, and inside the forest canopy(C_C) at 530 m asl, Gammalsatern, site C.

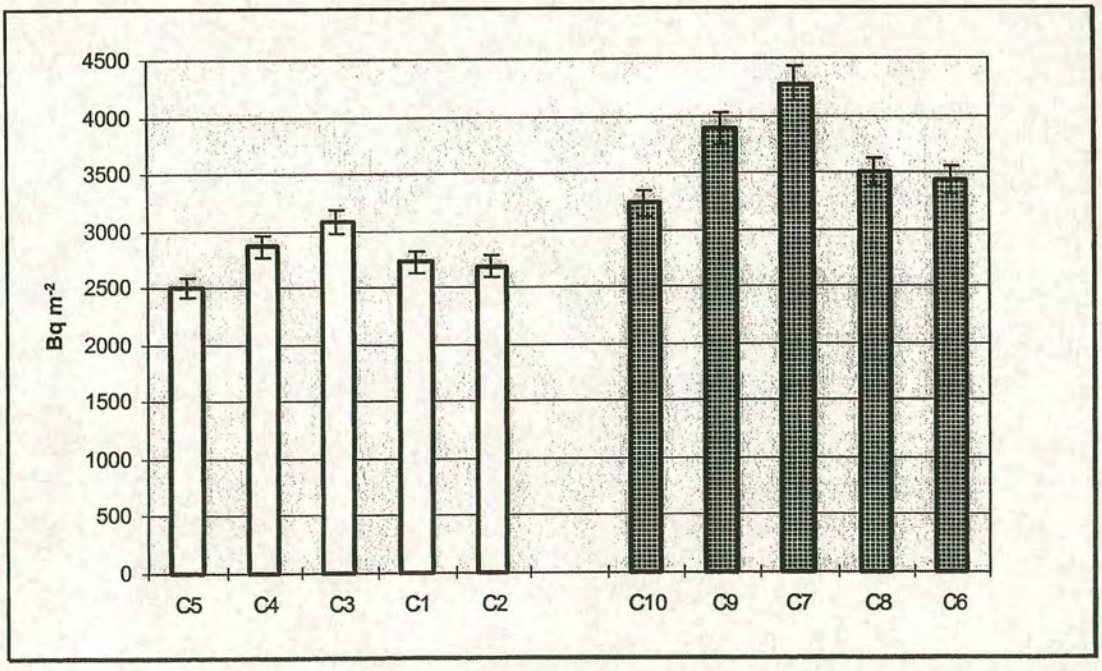

Figure 3.121: Atmospheric ^{210}Pb inventories measured in soil samples from each sampling point at Gammalsatern, site C.

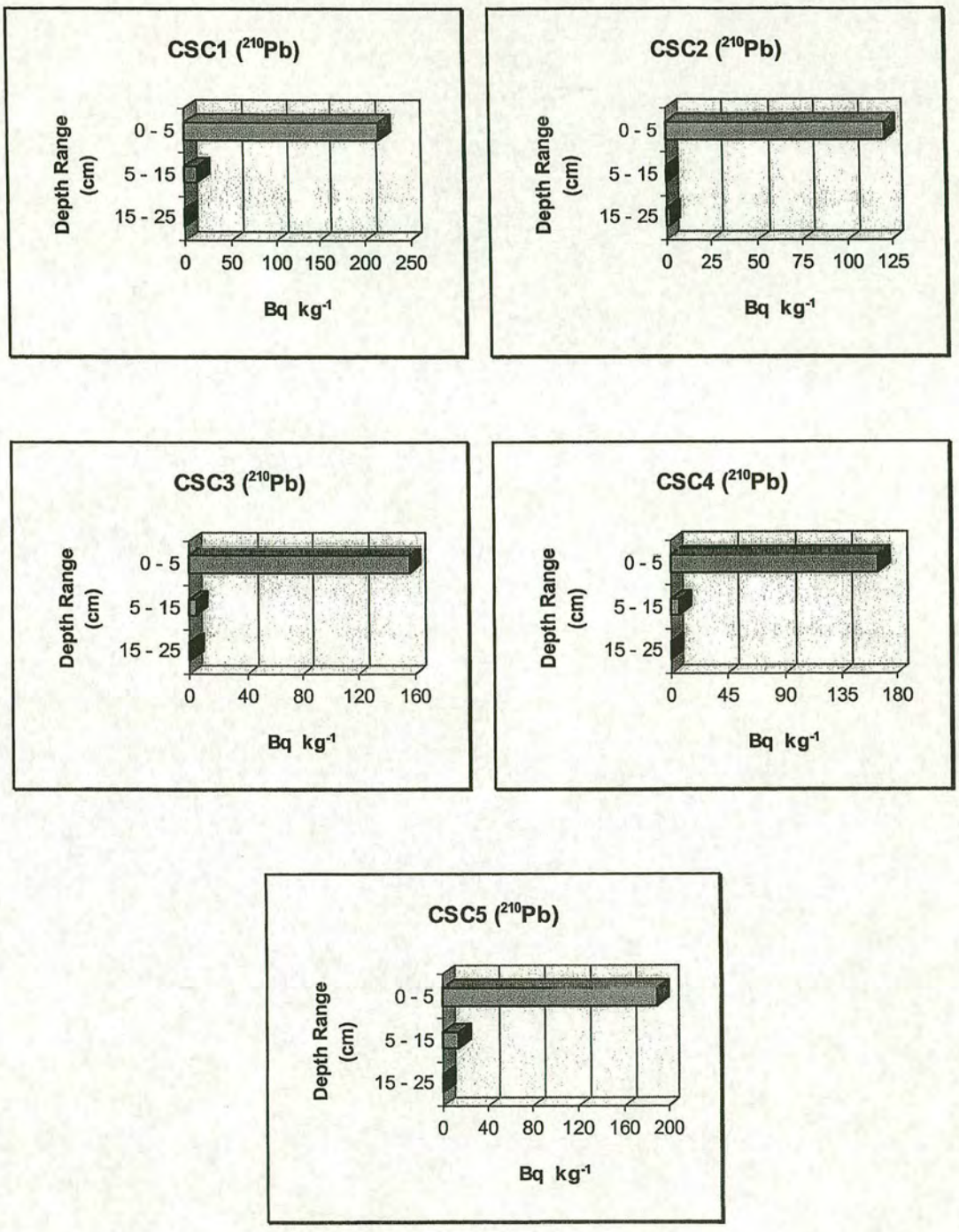

Figure 3.122: Distribution of atmospherically derived ^{210}Pb with depth at Gammalsatern. Open field locations, C1 - C5.

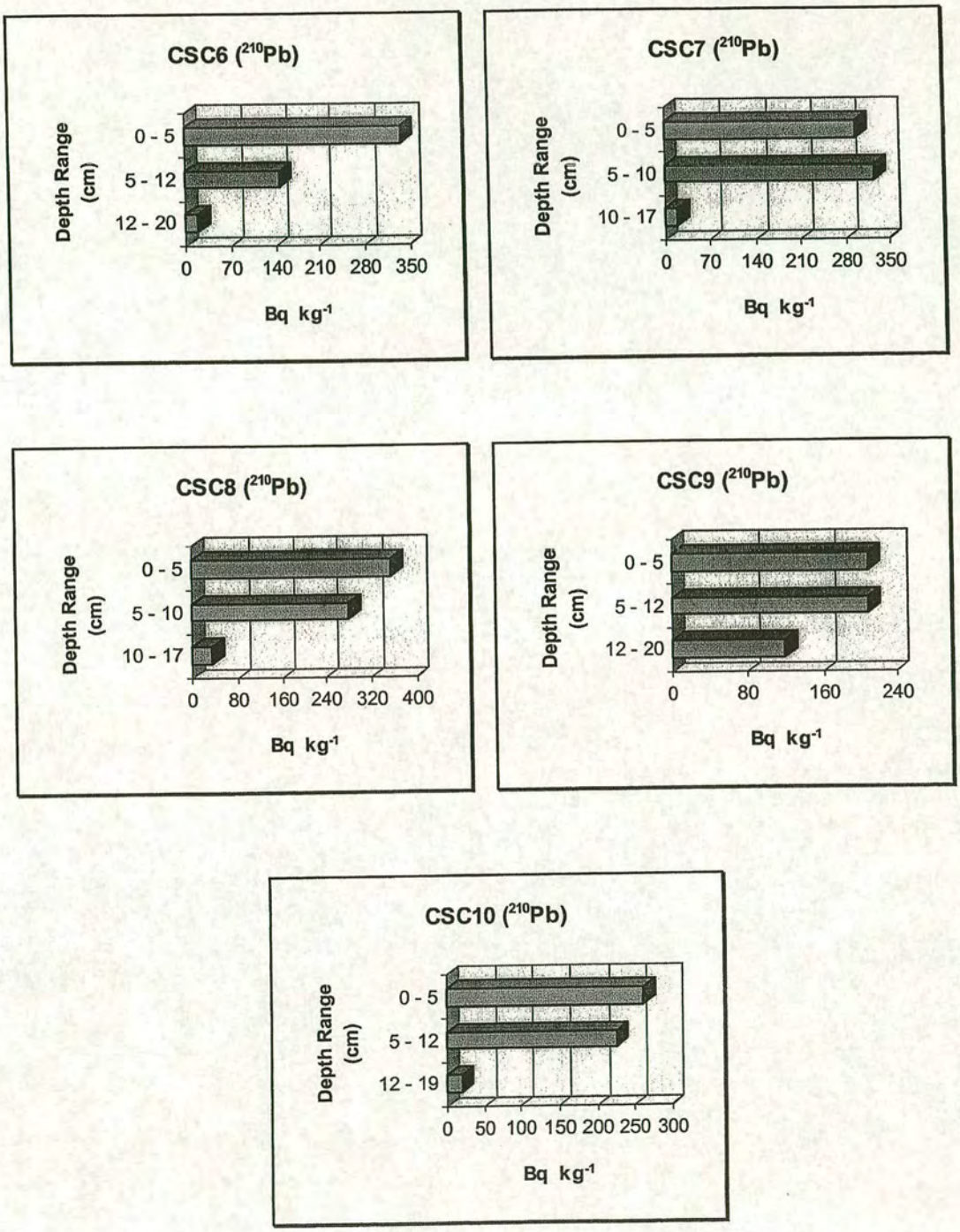

Figure 3.123: Distribution of atmospherically derived ^{210}Pb with depth at Gammalsatern. Under canopy locations, C6 - C10.

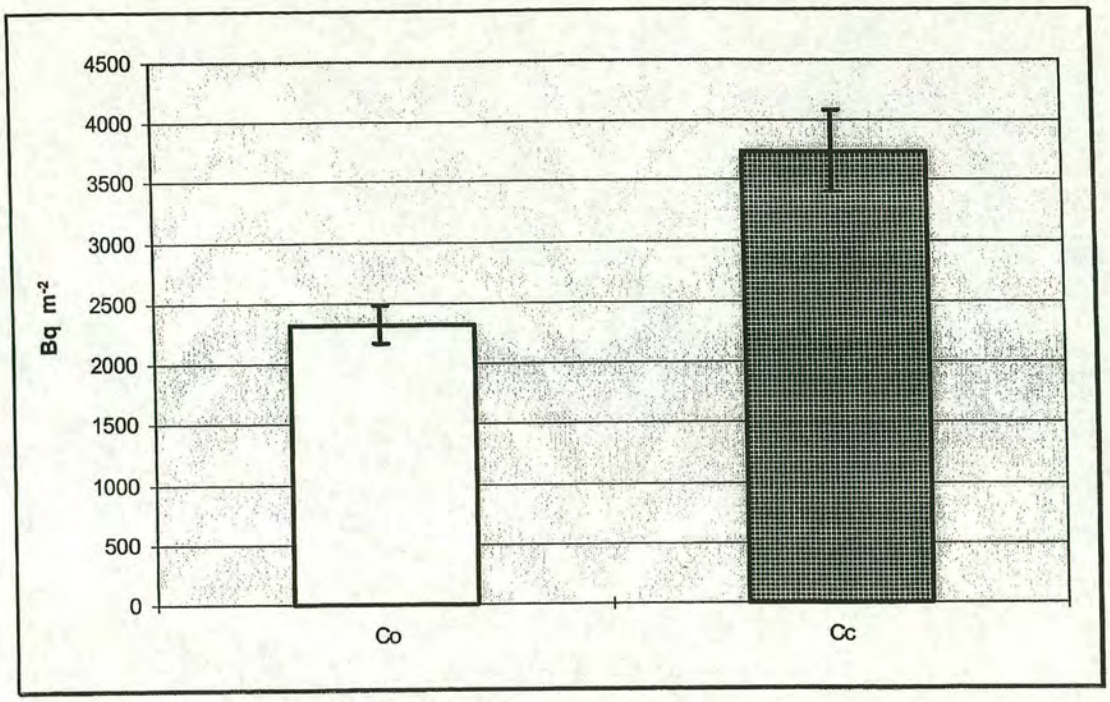

Figure 3.124: Mean ^{137}Cs soil inventories in the open field(C_O) at 540 m asl, and inside the forest canopy(C_C) at 530 m asl, Gammalsatern, site C.

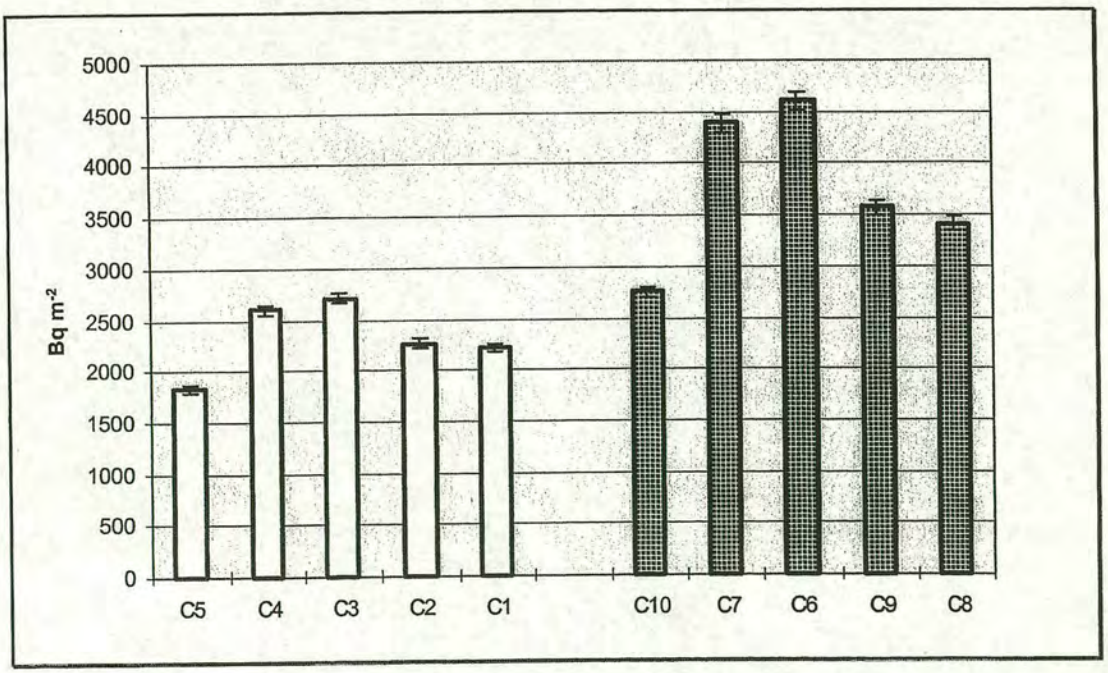

Figure 3.125: ^{137}Cs inventories measured in soil samples from each sampling point at Gammalsatern, site C.

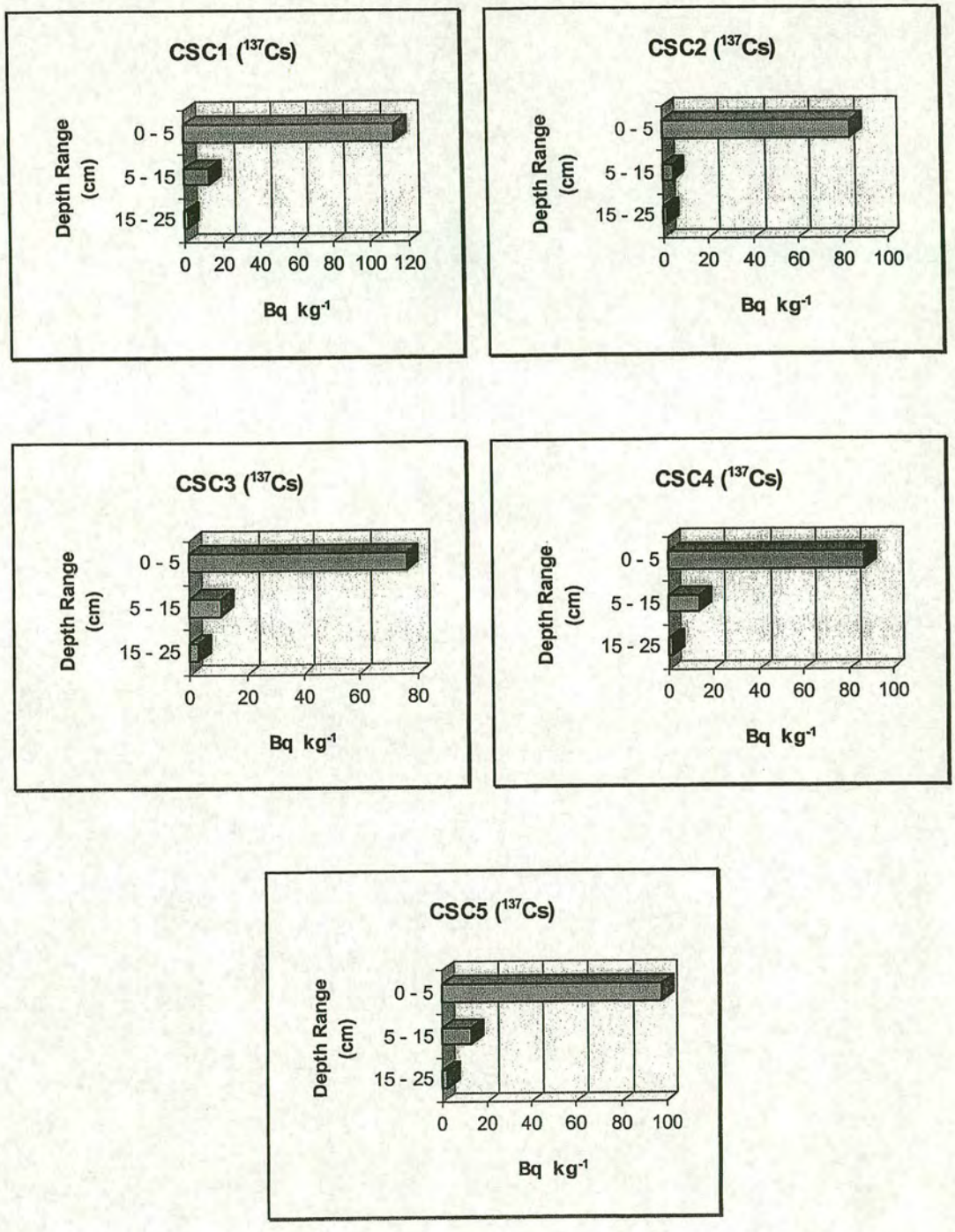

Figure 3.126: Distribution of ^{137}Cs with depth at Gammalsatern.
Open field locations, C1 - C5.

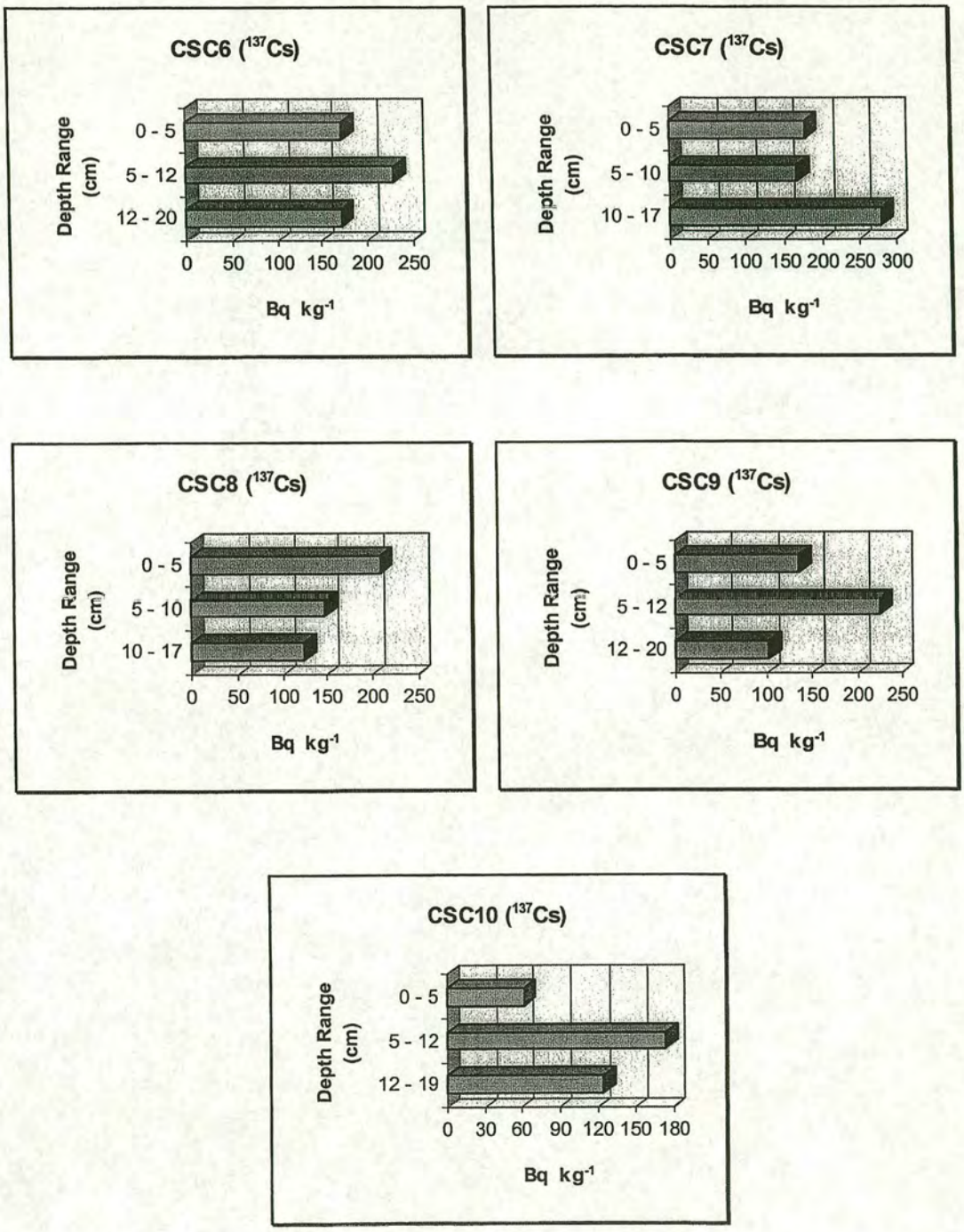

Figure 3.127: Distribution of ^{137}Cs with depth at Gammalsatern.
Under canopy locations, C6 - C10.

3.4.4 Skaftasen, site D (see Figs. 2.13-2.15)

3.4.4.1 Lead 210 soil inventories

The inventories of atmospheric ^{210}Pb for the samples collected from the edge of mixed spruce/pine canopy at 620 m asl on Skaftasen mountain are presented in Figures 3.128 and 3.129. Mean ^{210}Pb inventory(D_C) is shown in Figure 3.128, where the error bar represents standard error of the mean. The coefficient of variation for the measured ^{210}Pb inventories is 11%. The levels of ^{210}Pb present in the individual cores D6-D10 are shown in Figure 3.129, where the error bars are due to counting statistics.

Depth profiles for specific activities are illustrated in Figure 3.130. The illustrated profiles indicate the fact that top 15 cm soil has retained the atmospheric ^{210}Pb efficiently. In the case of CSD9 & CSD10, where some penetration to lower horizons has occurred, the contribution from 15-25 cm depth interval is substantially small.

Under the reasonable assumption of a steady state between the atmospheric supply of ^{210}Pb and its radioactive decay in soil, its average flux to this exposed canopy, at the edge, would be 167 Bq m^{-2} y^{-1}.

3.4.4.2 Caesium 137 soil inventories

The soil inventories for ^{137}Cs are presented in Figures 3.131 and 3.132. Mean ^{137}Cs inventory for the site(D_C) is shown in Figure 3.131, where the error bar represents standard error of the mean. The coefficient of variation for the measured ^{137}Cs inventories is 25%. The levels of ^{137}Cs present in the individual cores from the stand edge(D6-D10) are shown in Figure 3.132, where the error bars are due to counting statistics. Depth profiles for specific activities are illustrated in Figure 3.133. The illustrated profiles indicate that though the bulk of ^{137}Cs is concentrated in top 15 cm of soil but, the contribution of 15-25 depth interval for CSD6, CSD9, and CSD10 is relatively significant.

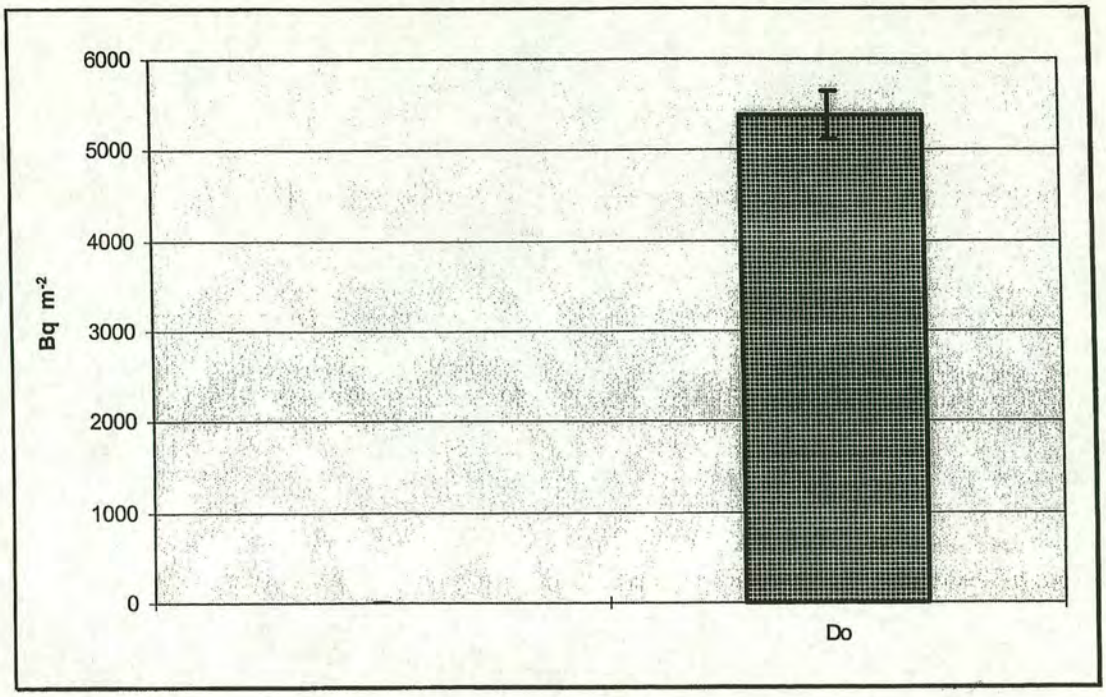

Figure 3.128: Mean atmospheric ^{210}Pb soil inventories at the edge of stand(D_c) at 620 m asl, Skaftasen, site D.

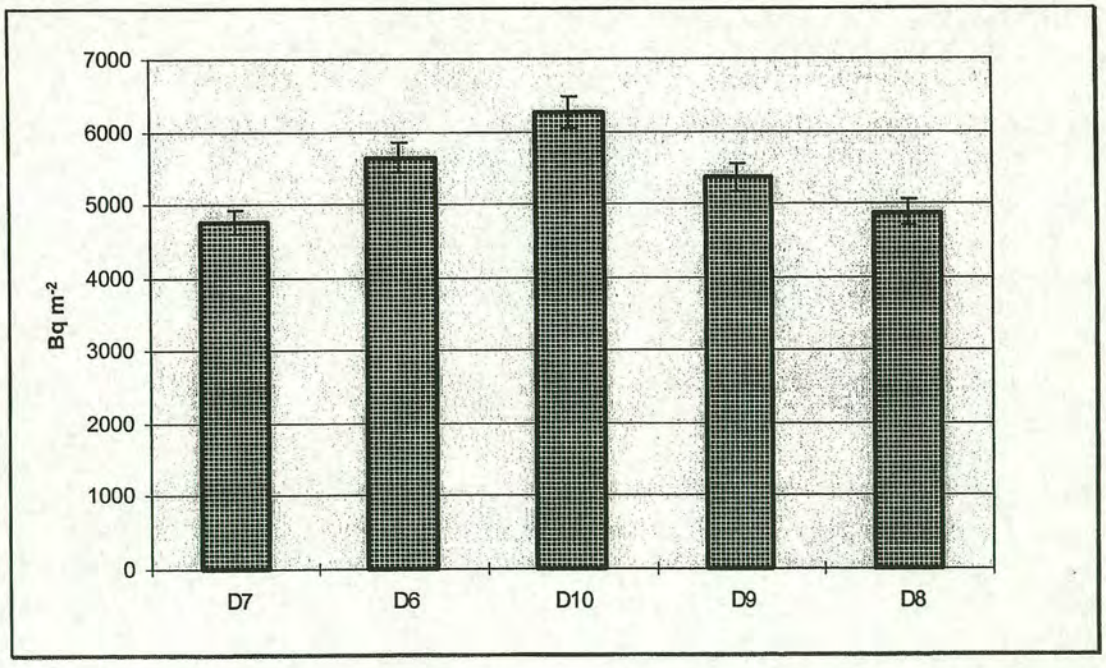

Figure 3.129: Atmospheric ^{210}Pb inventories measured in soil samples from each sampling point at Skaftasen, site D.

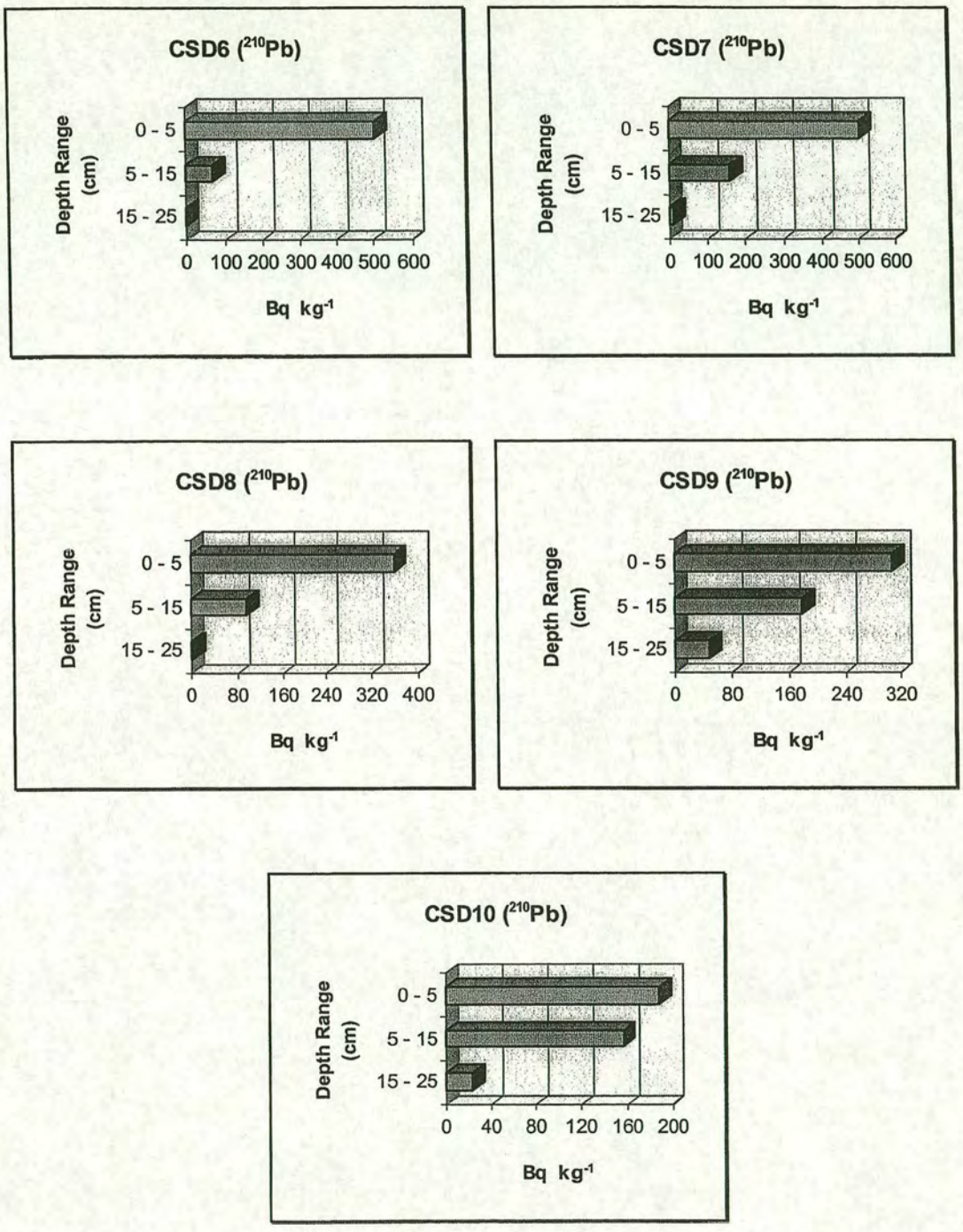

Figure 3.130: Distribution of atmospherically derived ^{210}Pb with depth at Skaftasen. Under canopy locations, D6 - D10.

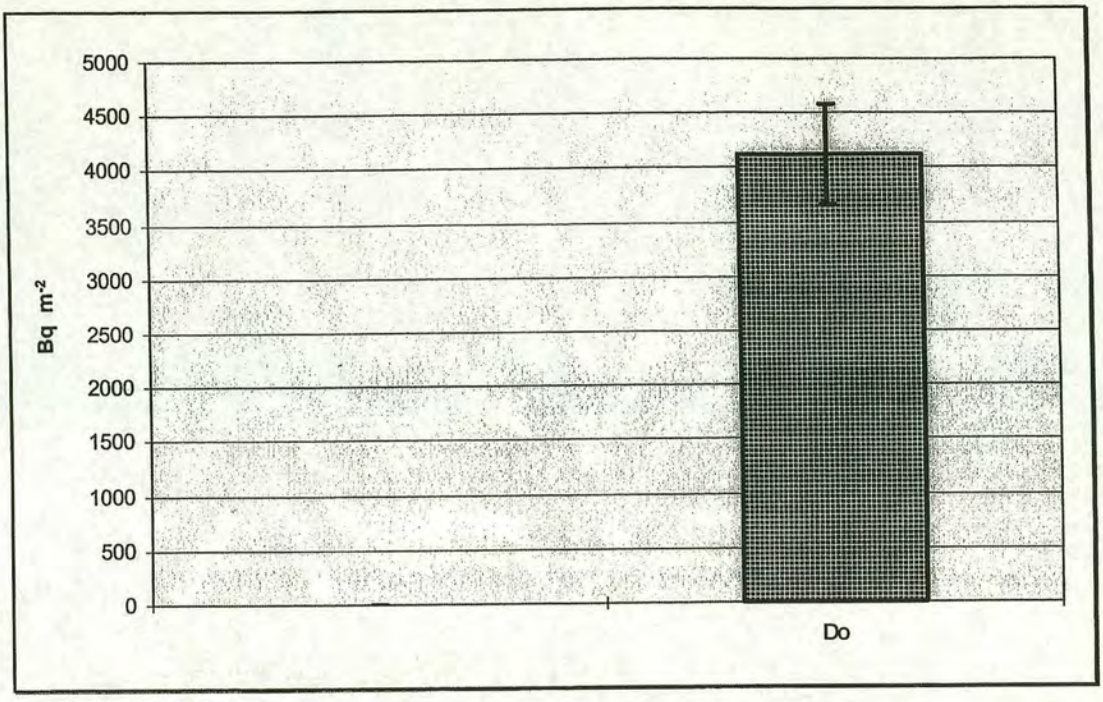

Figure 3.131: Mean ^{137}Cs soil inventories at the edge of stand(D_c) at 620 m asl, Skaftasen, site D.

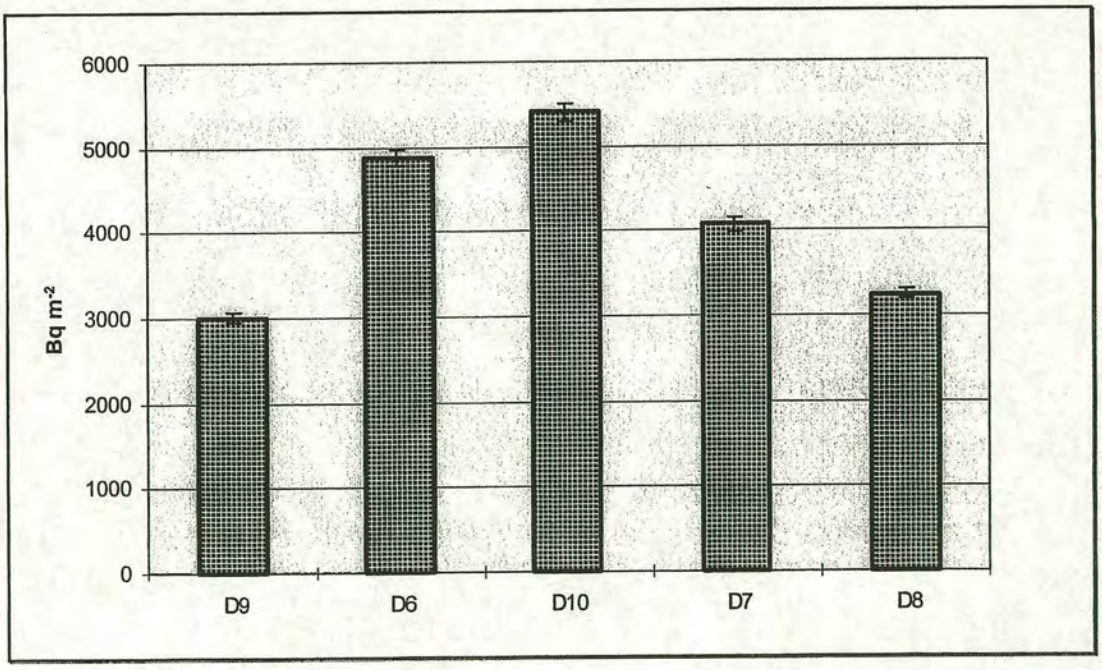

Figure 3.132: ^{137}Cs inventories measured in soil samples from each sampling point at Skaftasen, site D.

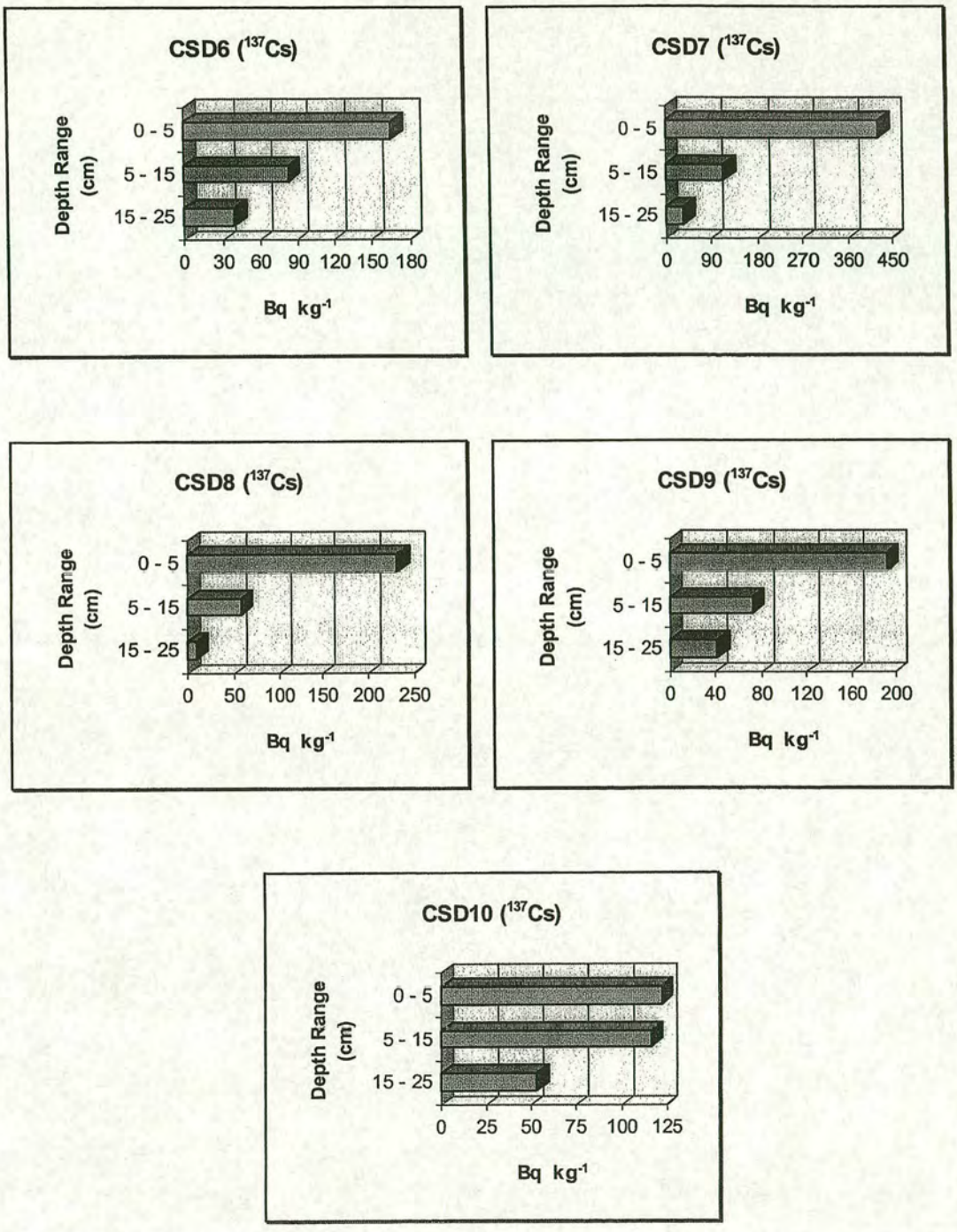

Figure 3.133: Distribution of ^{137}Cs with depth at Skaftasen.
Under canopy locations, D6 - D10.

3.4.5 Deposition pattern in Transtrandsfjallen (Figs. 2.13-2.15)

The mean inventories of atmospheric ^{210}Pb for samples collected from beneath coniferous forest canopies, as well as the adjacent/nearby open fields at 4 sites, situated in the Swedish Central Uplands (Transtrands Mountains) are presented in Figures 3.134 to 3.136. From these 4 sites, three of them, A-C, lie on the southern slope of Gammalsaters, between the valley and summit. The fourth one, D, is situated on the southern slope of a nearby mountain, Skaftasen, besides a small lake, Norra Skaftastjarnen. The mean ^{210}Pb inventories for the open field locations CSA, CSB, and CSC are illustrated in Figure 3.134, where the error bars represent standard error of the mean. The results show that ^{210}Pb inventories increase markedly between valley and summit at Gammalsaters. The increase relative to site C is 16% for site B(at 740 m asl), and 31% for site A(at 870 m asl). Note that the valley itself is at 540 m asl. The mean atmospheric ^{210}Pb inventories for under canopy locations CSB and CSD exceed that of CSC by 19% and 47%, respectively (Figure 3.135). It should be also noted that mean atmospheric ^{210}Pb inventory at the exposed edge of forest canopy at 620 m asl(site D) exceeds that of inside canopy location at 720 m asl(site B) by 23%, and that of open grassland at 550 m asl by 94%. Figure 3.136 shows atmospheric ^{210}Pb inventories for all sampling sites in Transtrands Mountains.

By assuming a steady state between the atmospheric supply of ^{210}Pb and its radioactive decay in soil, its average flux at the lowest elevation open-field sampled in Transtrands(site C) would be 86 Bq m^{-2} y^{-1} which is not significantly larger than the open field mean-flux of 81 Bq m^{-2} y^{-1} for the coastal region in Southwest Sweden. On the other hand, measurements indicate a significant canopy enhancement of approximately 32% in ^{210}Pb flux at site C in Transtrands, whereas no significant canopy enhancement was observed in Hallands coastal region. The average canopy enhancement for the higher elevation sites in central Sweden, of approximately 52%, is larger than that in Swedish southern uplands by almost 30%.

The mean soil inventories of ^{137}Cs for the region are presented in Figures 3.137, 3.138 and 3.139. Mean ^{137}Cs inventories for the open field locations CSA,

CSB, and CSC are illustrated in Figure 3.137, where the error bars represent standard error of the mean. The results indicate an approximately 27% increase in mean inventories between valley and summit at Gammalsaters. Caesium 137 results give no indication of significant differences between mean open field inventories at site B with either site A or site C. In the case of forest canopies, mean inventory at site B is lower than those for sites C and D by approximately 34% and 48%, respectively (Figure 3.138). There are no significant differences between the mean values for sites C and D. Figure 3.139 shows ^{137}Cs inventories for all sampling sites at Transtrands Mountains. Caesium 137 inventories in central Sweden sites are generally lower than those in the south-west.

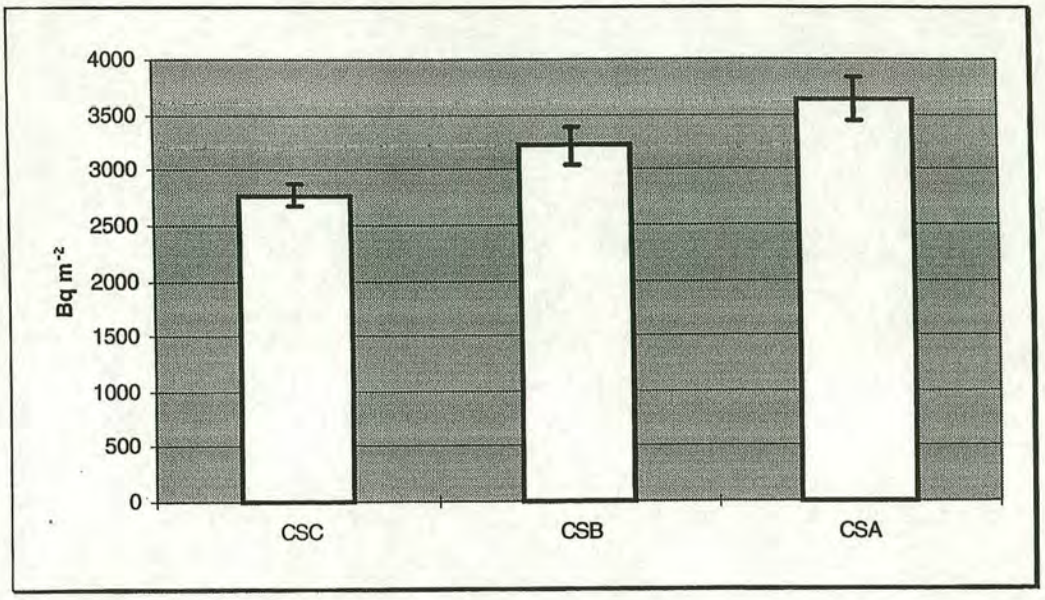

Figure 3.134: Mean atmospheric ^{210}Pb inventories in Central Sweden. Open field sites CSC(540 m asl), CSB(740 m asl) and CSA(870 m asl) at Gammalsaters fjallet.

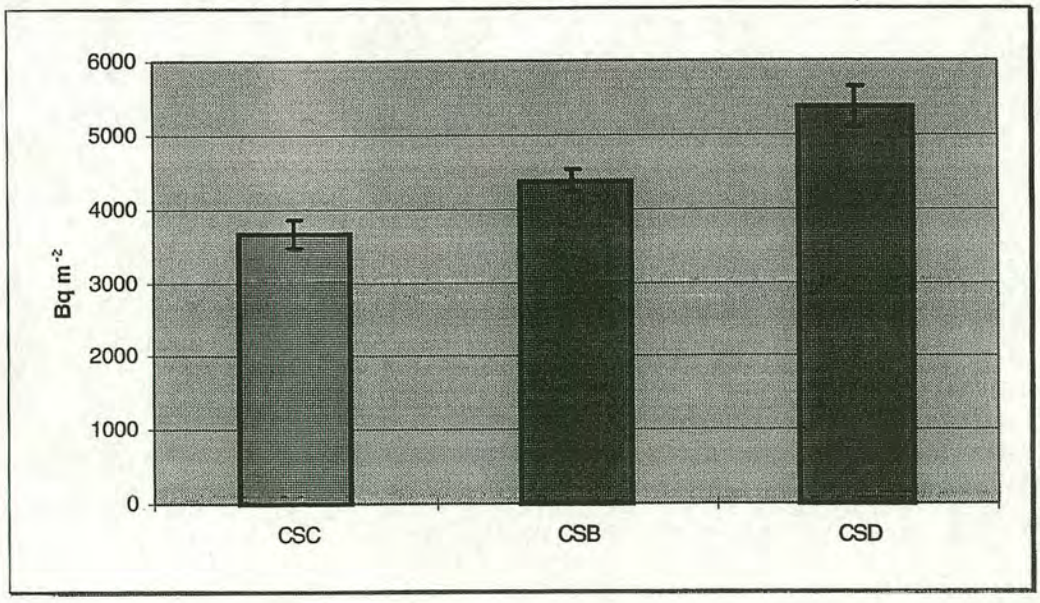

Figure 3.135: Mean atmospheric ^{210}Pb inventories in Central Sweden. Under canopy sites CSC(540 m asl) and CSB(720 m asl) at Gammalsaters fjallet, and CSD(620 m asl) at Skaftasen.

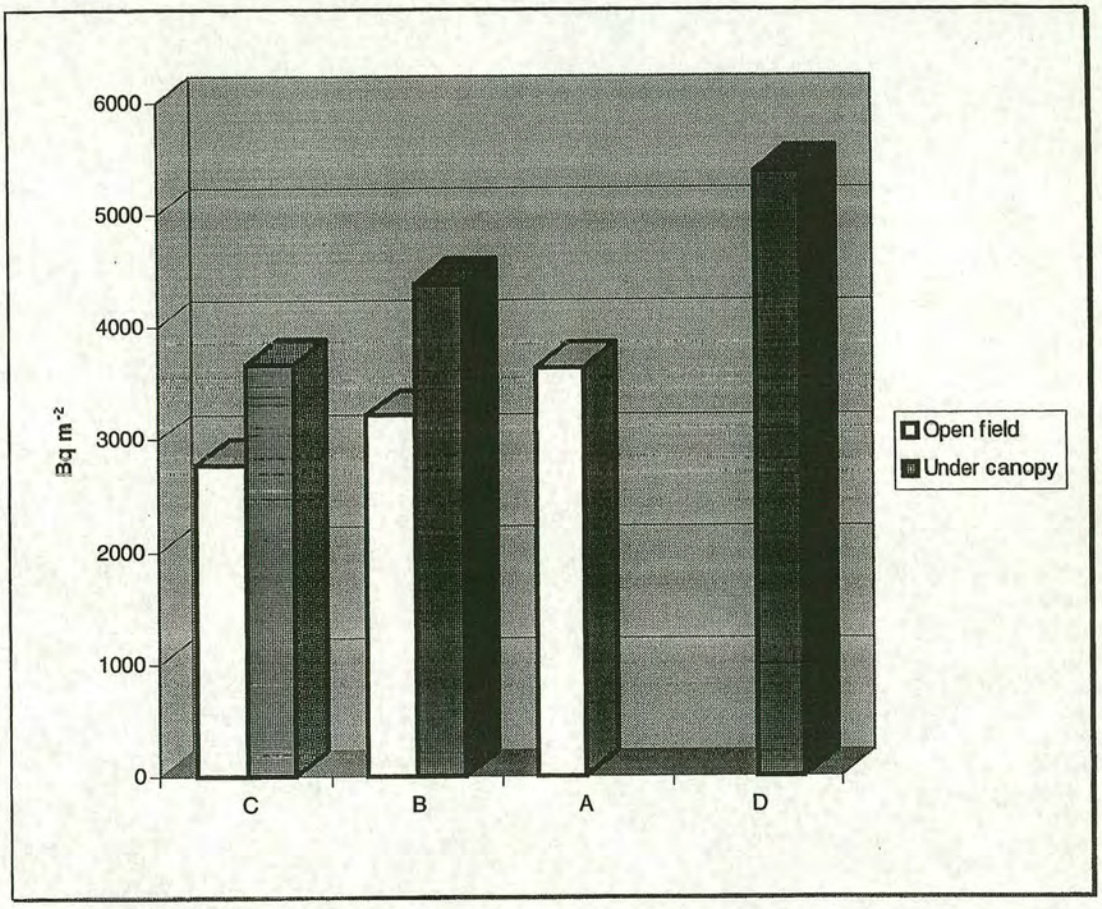

Figure 3.136: Mean atmospheric ^{210}Pb inventories at Gammalsaters fjallet(A-C) and Skaftasen(D) sites in Central Sweden.

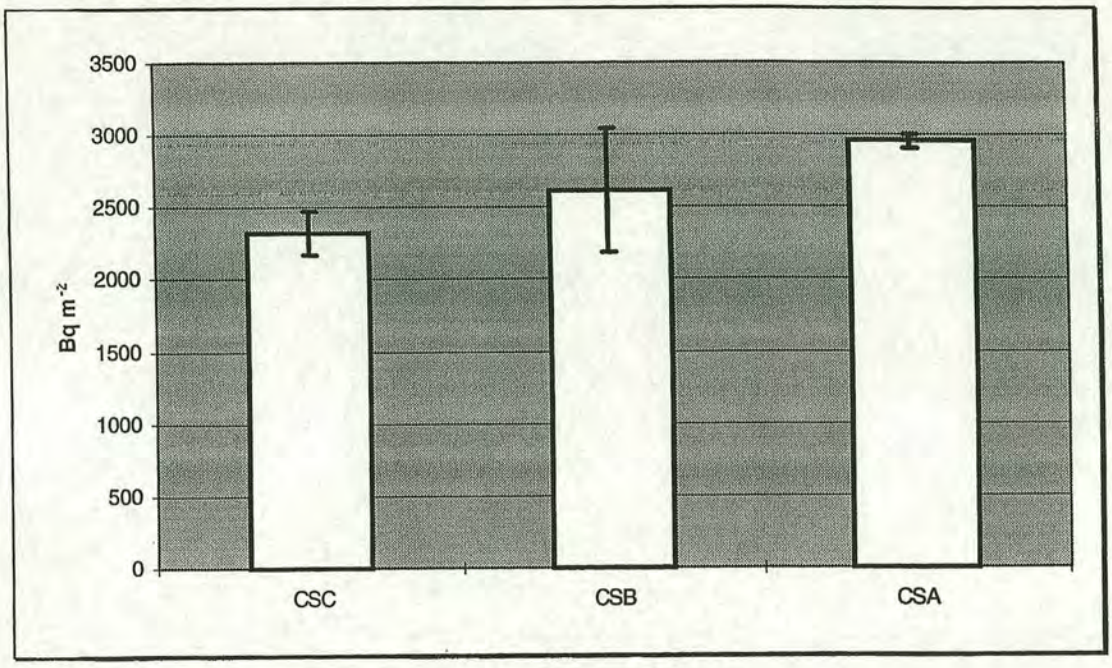

Figure 3.137: Mean ^{137}Cs inventories in Central Sweden.
Open field sites CSC(540 m asl), CSB(740 m asl) and CSA(870 m asl) at Gammalsaters fjallet.

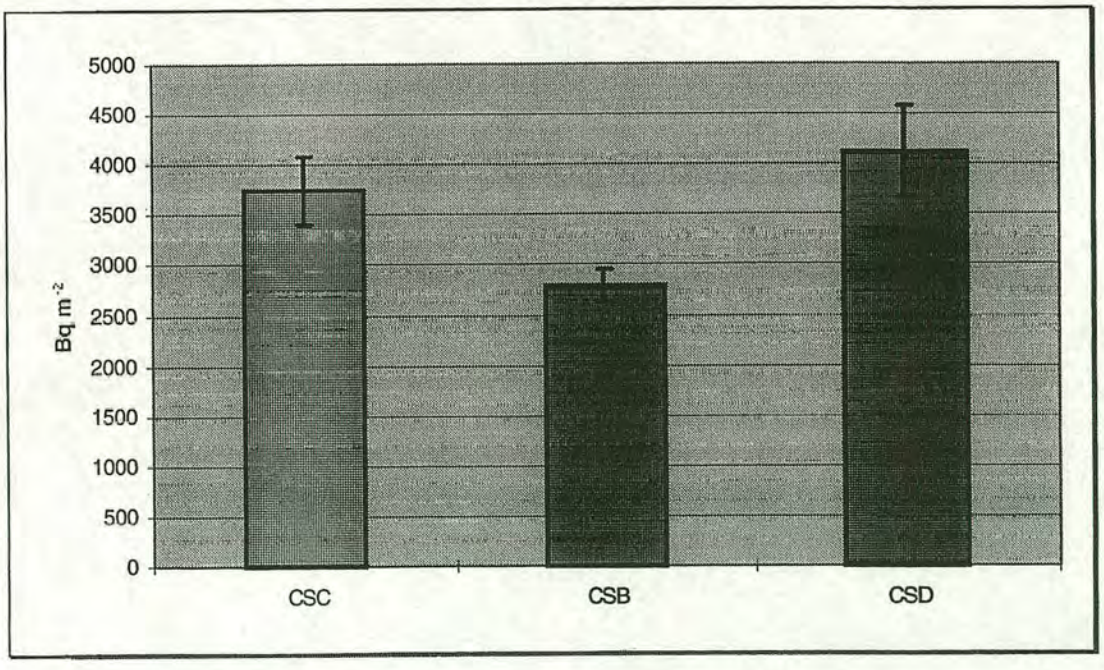

Figure 3.138: Mean ^{137}Cs inventories in Central Sweden.
Under canopy sites CSC(540 m asl) and CSB(720 m asl) at Gammalsaters fjallet, and CSD(620 m asl) at Skaftasen

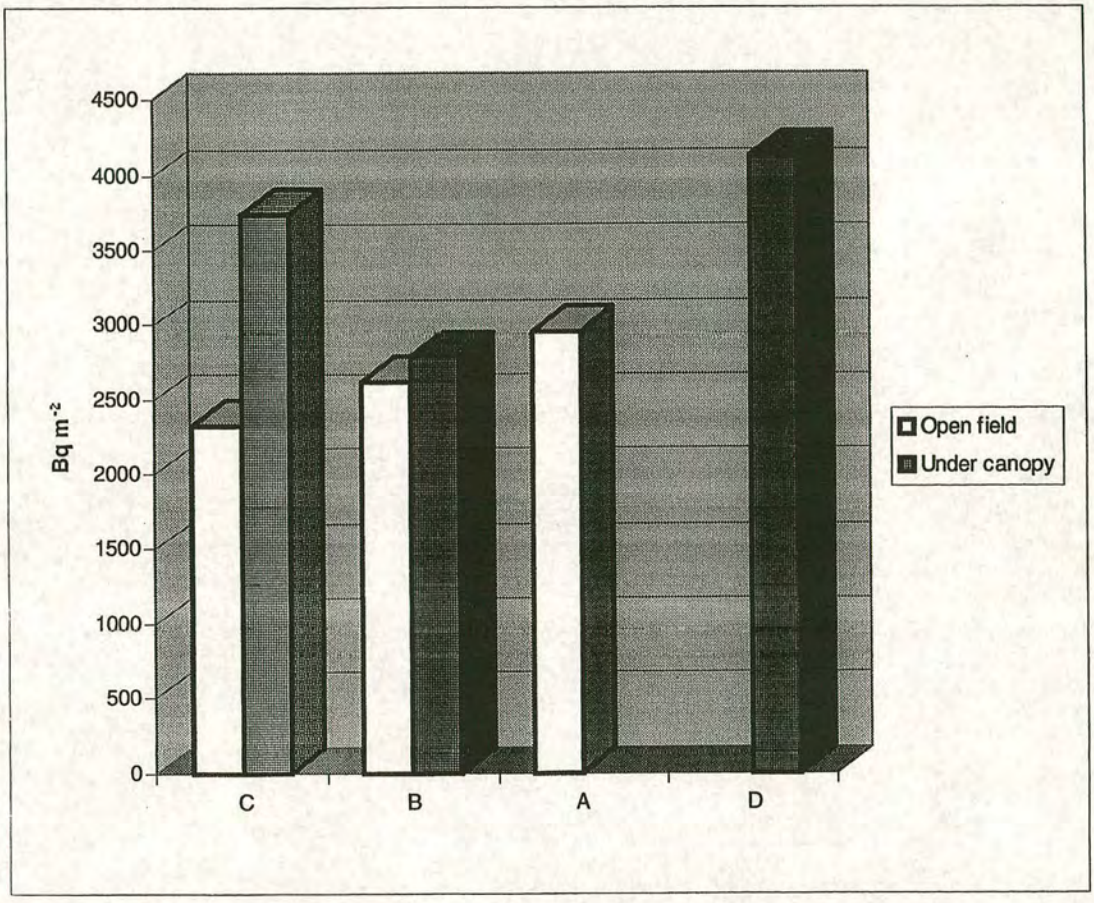

Figure 3.139: Mean ^{137}Cs inventories at Gammalsaters fjallet(A-C) and Skaftasen(D) sites in Central Sweden.

3.5 Loss-On-Ignition Measurement

The results on loss-on-ignition measurement performed on representative samples from Dunslair Heights are presented in Figure 3.140. The distribution of organic matter(OM) down 2C and 3A profiles are rather exceptional and indicate possible dislocation of OM in these sampling points. These data will be compared with the atmospheric ^{210}Pb inventories down soil cores for the same locations in the following chapter.

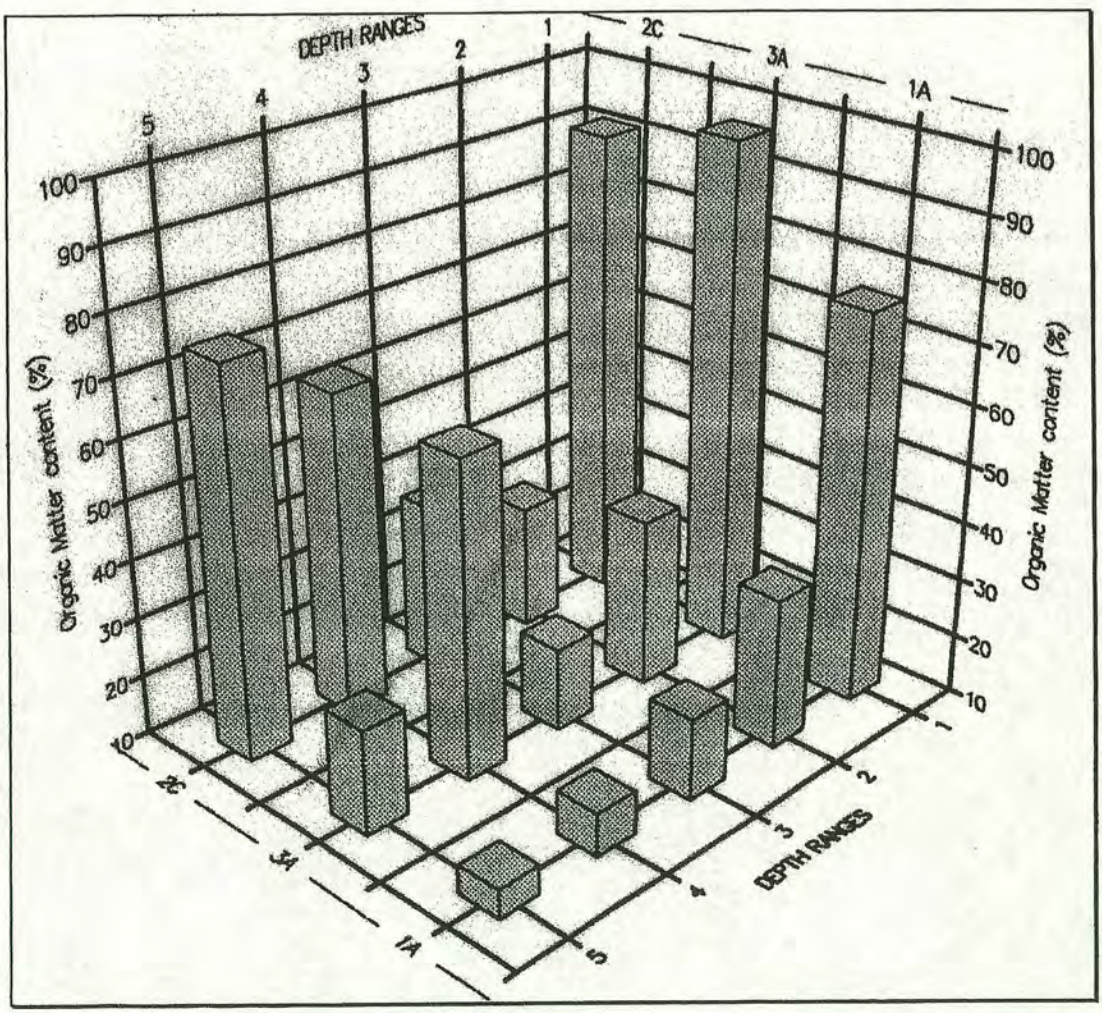

Figure 3.140: Percentage of the organic matter in soil profiles from 3 locations, 1A, 2C and 3A at Dunslair Heights. Depth ranges 1 to 5 represent 0-1, 1-5, 5-10, 10-15 and 15-20 cm depths, respectively.

Chapter 4

Discussion and Conclusion

In this chapter the measured atmospheric ^{210}Pb inventories and annual inputs as well as ^{137}Cs inventories are discussed, interpreted and compared with the published literature. Measurement results for Scottish sites, Dunslair Heights and Dun Coillich, are treated in sections 4.1 and 4.2, respectively. In section 4.3, the spatial pattern of radionuclide inventories in the south-western province of Hallands are considered along with an interpretation of the profile of atmospheric ^{210}Pb inventory in the region. Section 4.4 discusses the measured inventories in the mountains of central Sweden, and finally section 4.5 summarises the concluding remarks.

4.1 Dunslair Heights

4.1.1 Lead 210 results

The estimated ^{210}Pb inventories at four sampling locations lying over a short transect (~ 80 m) across a boundary between open, grass-covered moorland and a Norway spruce forest on Makeness Hill (450 m asl) at Dunslair Heights are

summarised in Table 4.1 and plotted in Figure 4.1 (see sections 2.1.1.1, 2.1.2.1 and 3.1.1 for details).

Table 4.1: Dunslair Heights ^{210}Pb inventories under grass and forest.

	Open moorland	Inside the forest canopy		
Sample location	DH1	DH2	DH3	DH4
^{210}Pb inventory (± σ) Bq m^{-2}	2325 (114)	3121 (557)	3252 (436)	3211 (44)
Increase under forest		34%	40%	38%
Average increase		37%		

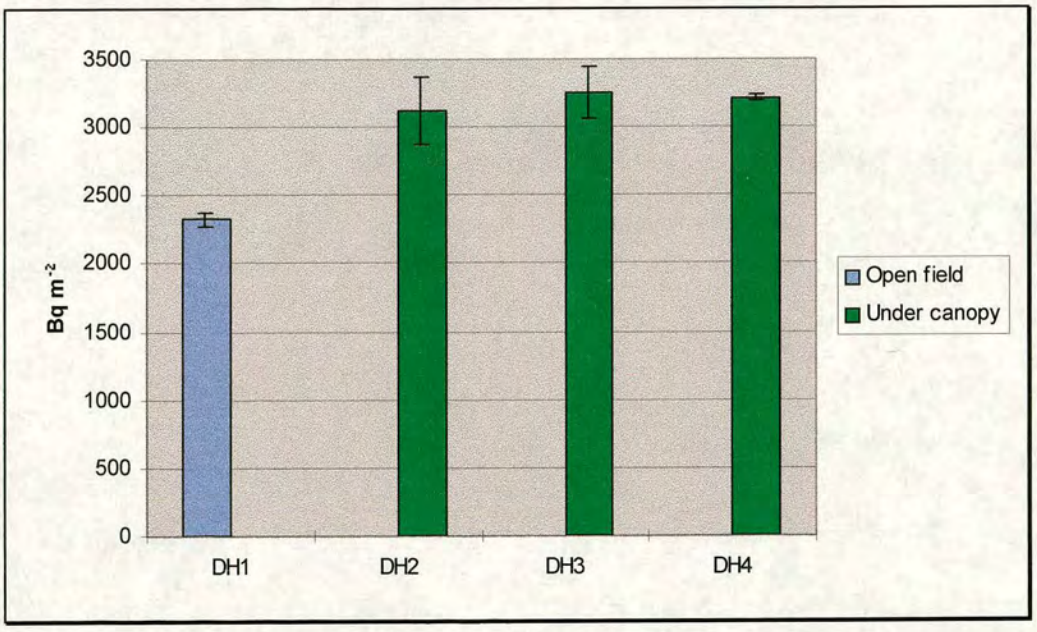

Fig. 4.1: Mean atmospheric ^{210}Pb soil inventories in the open field (DH1) and inside the forest canopy (DH2, DH3 & DH4) at Dunslair Heights. The error bars represent the standard error of the mean for five replicate soil cores at each location.

Under the reasonable assumption of a steady state condition between the atmospheric supply of ^{210}Pb and its radioactive decay in soil, its mean flux to the open moorland is estimated to be 72 Bq m^{-2} y^{-1}. Considering the average annual

rainfall of approximately 1200 mm for the site (Meteorological Office Average Annual Rainfall Map, 1977; Crossley et al. 1988), and using the equation,

$$F_{Pb} = C \times R,$$

$$\text{Bq m}^{-2}\,\text{y}^{-1} \quad \text{mBq l}^{-1} \quad \text{m y}^{-1}$$

this flux corresponds to a mean concentration of ^{210}Pb in rainfall of 60 mBq l^{-1} which compares very closely to the mean UK ^{210}Pb concentrations in rainfall of 77±14 mBq l^{-1} estimated by Smith et al. (1997) and 74 mBq l^{-1} estimated by Eakins and Morrison (1976), and is consistent with the derived concentration of 62 mBq l^{-1} based on measured atmospheric flux at Plymouth by Clifton (1991). The derived concentration in rainfall might be slightly overestimated due to the possibility of dry and cloud droplet deposition of atmospheric ^{210}Pb. However, considering the nature of the surface (short grass of ~ 0.2 m height) and average wind speed of ~5 m s^{-1}, the contribution of these processes would have not been very large. The apparent higher variability observed in ^{210}Pb inventories at the edge of canopy (location DH2 in Figure 4.1; see also Figure 3.2) might be attributed to the disturbances in the vertical wind profile produced by the forest edge. Development of strong turbulences may lead to non-homogeneous distribution of droplets and aerosols (Beier et al., 1993).

Under canopy locations DH2-DH4 show substantially larger inventories, respectively 34%, 40%, and 38% larger than in the open moorland. Assuming that the precipitation input is the same for all sites, the increase may therefore be assumed to result from cloud droplet and aerosol capture by the trees in excess of that by the grassland. The average enhancement in deposition for the three points of the transect inside the forest canopy is 37%, and the DMR test shows that these values are not significantly different (see Figure 3.7). The measured canopy enhancement is consistent with a 30% enhancement in deposition of ^{90}Sr and ^{137}Cs found respectively by Schreiber & Woerner (1979, cited in Bonzl & Kracke, 1988) and Bonzl & Kracke (1988) in soils under spruce canopies relative to the adjacent open grasslands. The coefficient of variation ranges between 1 to 18% which is lower than

the typical range of 15-20%, reported by Graustein & Turekian (1986). The lack of evidence of a pronounced enhancement in deposition at the edge of canopy (the so-called *edge effect*) may be explained partly by the way the edge of stand is oriented at this site. It faces approximately Northwest whereas the prevailing wind direction in the region is south-westerly (Beswick et al., 1991).

Based on the reasonable assumption of the similarity between the rates of cloud droplet deposition and those for momentum (Gallagher et al., 1992), and employing the wind profile equation (see section 1.2.3.3),

$$U_{(z)} = (U*/k)\ ln\{(z-d)/z_o\},$$

it is possible to calculate the droplet deposition velocities to the forest canopy and grassland, and consequently compare the observed enhancement in ^{210}Pb deposition with independent estimate of cloud droplet deposition using on-site measured meteorological parameters. Long-term data on cloud cover and liquid water content, wet deposition and standard meteorological variables are available through a monitoring programme which has been in operation at the site for more than a decade as part of a study on the effects of pollutants on forests (Crossley & Wilson, 1990; Crossley et al., 1992). These data reveal a cloud frequency of 1257 hr y^{-1} (14%) at 600 m asl, a wind speed of 5 m s^{-1} at the canopy height and an annual precipitation rate of 1213 mm, that along with the roughness lengths for the vegetation canopies provide means for the calculation of cloud droplet deposition for the forest and moorland as summarised in Table 4.2. Based on measurements of the concentrations of pollutant ions in rainwater and cloudwater at Dunslair Heights (Crossley et al., in press), an enhancement factor of 5 in concentration of ^{210}Pb in hill cloud over that in rain is adopted.

The calculated magnitude of enhancement in deposition by the forest of 34% appears to be slightly lower than the value estimated by the ^{210}Pb technique. Furthermore, it may be even overestimated because cloud frequency is measured at Dunslair Heights summit (602 m asl) which most likely overestimates the actual exposure of the forest at 450 m asl. The difference, of course, could be attributed to

the contribution of aerosol deposition which is included in the measured values of ^{210}Pb inventories. However, in the absence of any data on ^{210}Pb monitoring in aerosol and cloud at the site and precise estimates of its concentration in air, this cannot be justified.

Table 4.2: Cloud deposition at Dunslair Heights from direct measurements.

	Moorland	Forest
Canopy height	0.2 m	12-15 m
Measured precipitation	1213 mm	1213 mm
Wind speed at the canopy height	5 m s^{-1}	5 m s^{-1}
Cloud deposition	13.6 mm	99.6 mm
Enhancement of ^{210}Pb in cloud	x 5	x 5
Cloud deposition of 210Pb expressed in mm precipitation equivalents	68 mm	498 mm
Total deposition	1281 mm	1711 mm
% increase onto the forest canopy		34%

The measured forest enhancement may also be compared with the outcome of two modelling approaches, namely the UK deposition model (see section 1.2.3.3) and the site-specific model. The modelling has been used to provide national maps at 20 km x 20 km resolution (recently 5 km x 5 km resolution), the procedure of which is fully described in RGAR (1997) and CLAG (1997). These models may also be applied at a specific site using the national data and key site-characteristics such as altitude and land use. Otherwise being the same, the UK model uses the average grid-square height (in this case 341 m) whereas the site-specific model applies the heights and meteorological conditions of the site. Therefore, the latter provides larger forest enhancement due to the larger cloud frequency calculated for the actual height of the forest (450 m) rather than the grid square average.

Applying the UK and site-specific models, results in respectively, 39% and 65% cloud deposition enhancement for the forest canopy relative to the open grassland at Dunslair Heights. The calculated magnitude of enhancement by the UK model is in line with those by direct measurements of ^{210}Pb soil inventories and the direct calculation based on cloud monitoring at the site. However, the site-specific approach produces a larger effect which might be attributed to the uncertainty in the

estimated cloud frequency from the UK cloud base statistics that are provided mainly by airports and are not, therefore, representative of the upland areas.

The depth profile of ^{210}Pb in the soil samples (Figures 3.10 - 3.13) generally show that ^{210}Pb is efficiently immobilised in the surface horizons of soil with more than 70% of the atmospheric inventory concentrated in the top 10 cm. The deviation from the expected exponential decrease in the activity levels for 10-20 cm depth sections of DH2C, DH3A and DH3E cores (all from the inside canopy sampling points) appears to be mainly due to some sort of vertical dislocation of soil layers. The percentage of the organic matter in soil derived from loss-on-ignition measurements for two of these cores (2C & 3A) and a reference, 1A, are compared with the profiles of ^{210}Pb specific activity in Figure 4.2. There is a marked resemblance between specific activity and percentage of organic matter profiles. The unusual presence of relatively high specific activity of ^{210}Pb and high organic soil in deep sections of 2C and 3A cores support the idea that soil at this locations would have undergone vertical mixing.

4.1.2 Caesium 137 results

The measured ^{137}Cs inventories at four sampling locations at Dunslair Heights are summarised in Table 4.3 and plotted in Figure 4.3 (see section 3.1.2 for details). Caesium 137 inventories follow a similar trend to that of atmospheric ^{210}Pb (described in previous section) over the transect across the boundary between open moorland and conifer forest. These data also do not support the presence of a pronounced edge effect for the forest canopy. The range in the values of coefficient of variation between separate cores at the same locations is 7-26% which compares with the reported typical range (15-20%; Graustein & Turekian, 1986).

The increase in under canopy inventories of 32%, 41% and 31% relative to the inventory in the open grass-covered moorland, result in an average canopy enhancement in deposition of 35% which seems to be entirely consistent with the observed enhancement in ^{210}Pb inventories and is in line with the magnitude of

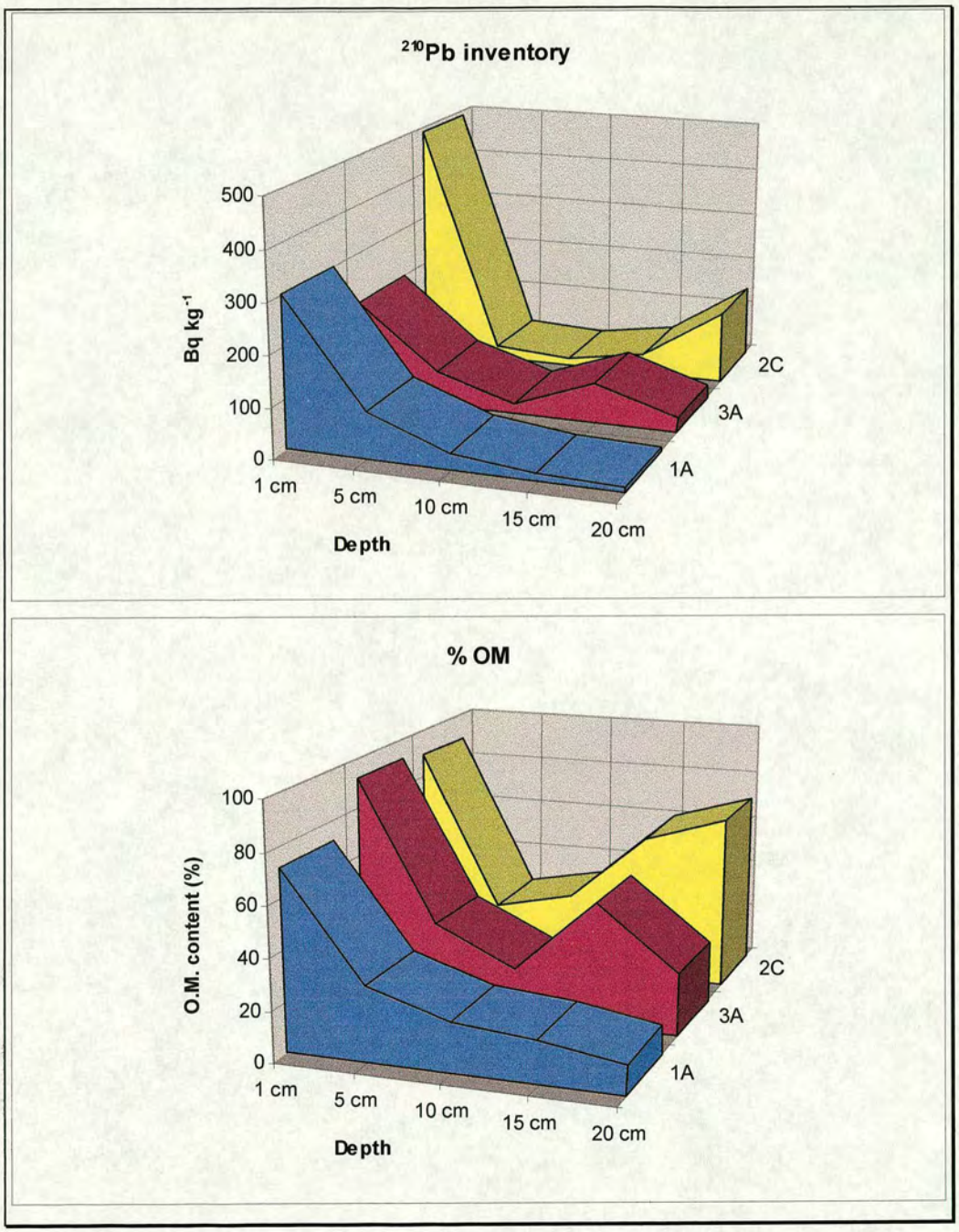

Fig. 4.2: ^{210}Pb specific activity and percentage of organic matter profiles of 1A, 2C, and 3A cores from Dunslair Heights.

enhancement of 34% in ^{210}Pb cloud deposition directly calculated based on site measured meteorological data, and 39% in cloud deposition estimated from the UK deposition model. However, one should be cautious in the interpretation of these average enhancement figures in the case of ^{137}Cs inventories in forest soils. The inherent variability is larger than that for ^{210}Pb inventories especially for locations

Table 4.3: Dunslair Heights ^{137}Cs inventories under grass and forest.

	Open moorland	Inside the forest canopy		
Sample location	DH1	DH2	DH3	DH4
^{137}Cs inventory (± σ) Bq m^{-2}	1830 (320)	2411 (623)	2574 (418)	2395 (170)
Increase under forest		32%	41%	31%
Average increase		35%		

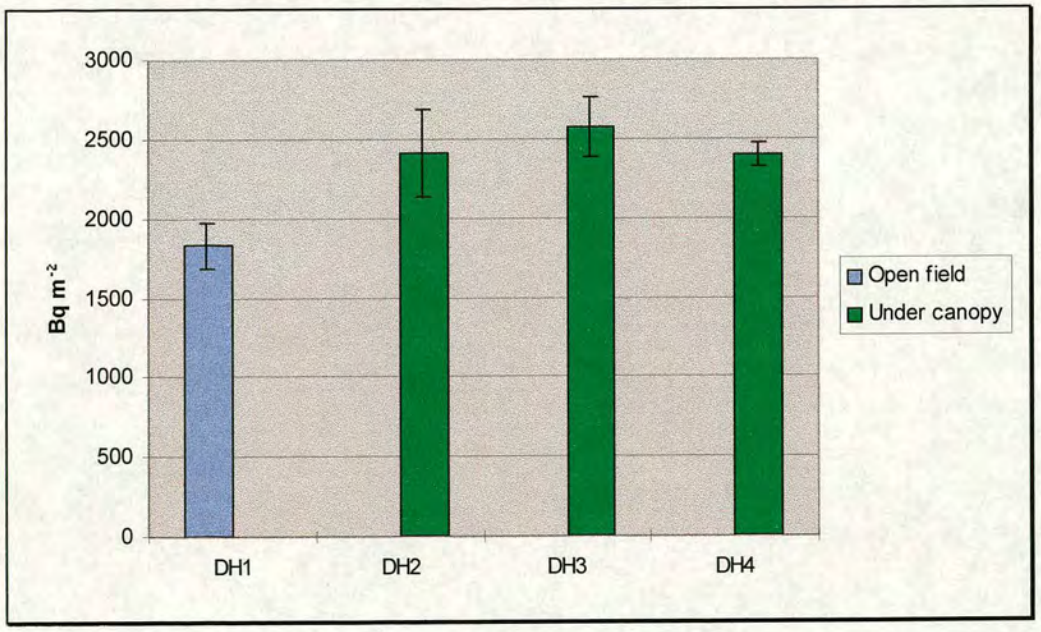

Fig. 4.3: Mean atmospheric ^{137}Cs soil inventories in the open field (DH1) and inside the forest canopy (DH2, DH3 & DH4) at Dunslair Heights. The error bars represent the standard error of the mean for five replicate soil cores at each location.

DH1 (at the open moorland) and DH2 (at the edge of canopy). The DMR test shows that the mean inventories of ^{137}Cs at these two locations are not significantly different at the 5% level of confidence (see Figure 3.14). Though the development of strong turbulences at the edge of stand may lead to greater heterogeneity in deposition as mentioned in the previous section, but there is also a difference between the behaviour of these two radionuclides in upland soils especially under forest canopies. While ^{210}Pb is adsorbed strongly and retained efficiently by the organic matter present in these soils (Lewis, 1977), soil variables contributes to more variation in ^{137}Cs present in woodland than in grassland and they account for more variability than location/climate variables (Cawse & Horril, 1986). In many of these soils, at least in the surface horizons, clays are scarce and the behaviour of the mechanisms controlling caesium availability in soil may be modified by extensive interaction with organic matter as described in section 1.4.2(Livens et al., 1991; Pulford et al., 1995).

The mean inventory value of 1830 Bq m^{-2} in the open moorland is larger than the mean fall-out per unit area of 1429 Bq m^{-2} in the northern hemisphere (decay corrected to 1993 from the value for 1986; Smith et al., 1997), and considerably smaller than the mean UK inventory of 2740 Bq m^{-2} per 1000 mm y^{-1} rainfall, to 30 cm depth (decay corrected to 1993 from the value for 1980; Bonnet & Camberly, 1991). The comprehensive survey of ^{137}Cs soil inventory of the UK by Cawse (1983) gives a value of 904 Bq m^{-2} as the mean inventory for grid square NT (designated letters for the 100 km grid square covering SE Scotland on the UK National Grid). None of these values include the contribution of ^{137}Cs from the Chernobyl Reactor accident in 1986. No attempts has been made to estimate the Chernobyl contribution of the measured ^{137}Cs inventories in the present study as described in Chapter 3. The difference between the measured value in this study and the estimated average value for the grid square NT, however, could not be only justified by the extra inventory in soil that originated from Chernobyl since its contribution in this part of the UK would have been most likely in the order of 100 Bq m^{-2} as demonstrated in Figures 4.4 and 4.5, taken from Clark & Smith (1988) and Scorer (1990), respectively. The upland site at Dunslair Heights might also be receiving higher inputs relative to the sites sampled by Cawse due to enhanced precipitation as well as cloud droplet

deposition. On the other hand, the higher value of the UK mean inventory may be attributed to the contribution of very high deposition values for high rainfall areas of the western England, Wales and north-west of Scotland. There is indeed a significant correlation between total ^{137}Cs deposition in soils and mean annual precipitation as demonstrated by Peirson & Salmon (1959), Cawse & Horril (1986), Cawse et al. (1988) and Bunzl & Kracke (1988).

The measured canopy enhancement of 35% is consistent with a 30% enhancement in deposition of ^{90}Sr and ^{137}Cs found respectively by Schreiber & Woerner (1979, cited in Bonzl & Kracke, 1988) and Bonzl & Kracke (1988) in soils under spruce canopies in the Black Forest and Bavaria, relative to the adjacent open grasslands. Cawse (1983) found no significant canopy enhancement in his study of ^{137}Cs inventories in deciduous forests in the UK, which may be explained being due to the lower efficiency of deciduous forests in capturing aerosols and cloud droplets as well as the lower altitudes of the sites compared to the above mentioned sites in Germany and Dunslair Heights. In the same report, he states that more plutonium is deposited on coniferous woodland than on grassland in a regional survey near Selafield.

The *sub-surface maxima* observed in the depth profiles for specific activities of ^{137}Cs (section 3.2; Figures 3.10-3.13) may be attributed to the shortage of clays essential for the fixation of ^{137}Cs in the top most section of cores (0-1 cm interval). The depth profiles generally show that ^{137}Cs is highly concentrated in the surface horizons of soil. However, in some cases (e.g. DH4A, DH3E, DH4D) there are indications of penetration of activity into deeper sections of the cores due to the mobility of this radionuclide in these upland soils (Liven, 1991).

4.2 Dun Coillich

4.2.1 Lead 210 results

The estimated ^{210}Pb inventories at four sampling locations lying over a short transect (~ 100 m) across a boundary between open heathland and an old plantation

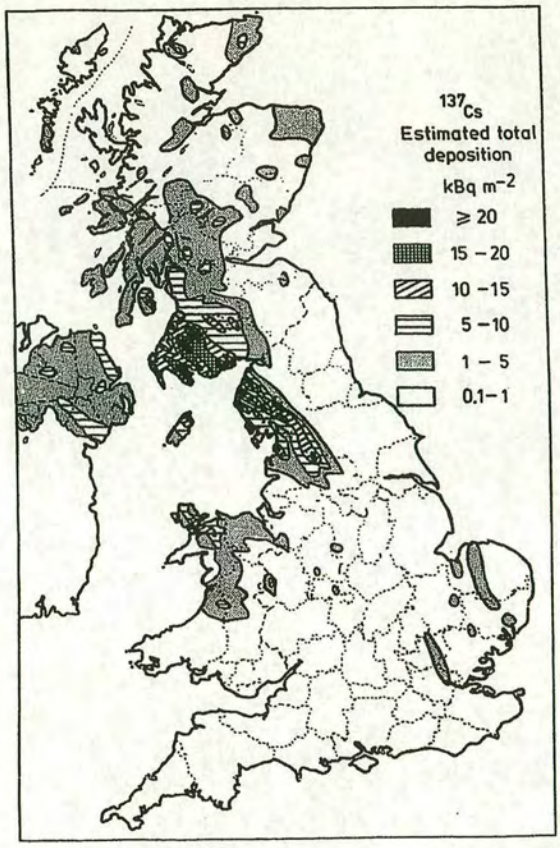

Fig. 4.4: Estimated total deposition of ^{137}Cs (kBq m^{-2}) over the UK due to Chernobyl releases, calculated from the rainfall data and air concentrations (Clark & Smith, 1988).

Fig. 4.5: The contours show the amount of ^{137}Cs (Bq m^{-2}) in vegetation in Britain found after the Chernobyl disaster (Scorer, 1990).

of Scots pine at 420 m asl near the summit of Dun Coillich are summarised in Table 4.4 and plotted in Figure 4.6 (see sections 2.1.1.2, 2.1.2.2 and 3.2.1 for details).

Table 4.4: Dun Coillich ^{210}Pb inventories under heather and forest.

	Open moorland	Inside the forest canopy		
Sample location	DC1	DC2	DC3	DC4
^{210}Pb inventory (± σ) Bq m^{-2}	3175(440)	4939 (313)	4354 (452)	3634 (187)
Increase under forest		56%	38%	15%
Average increase		36%		

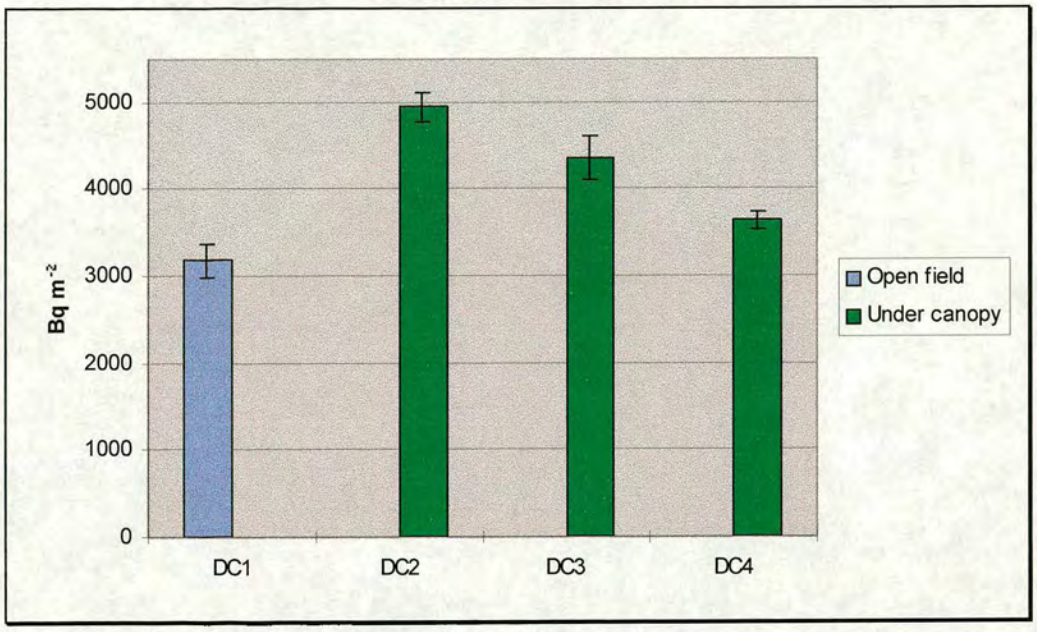

Fig. 4.6: Mean atmospheric ^{210}Pb soil inventories in the open field (DC1) and inside the forest canopy (DC2, DC3 & DC4) at Dun Coillich. The error bars represent the standard error of the mean for five and three replicate soil cores at DC1 and the rest of locations, respectively.

Assuming that the atmospheric supply of ^{210}Pb and its radioactive decay in soil are in equilibrium, its mean flux to the open moorland is estimated to be 98 Bq m^{-2} y^{-1}. Considering the average annual rainfall of approximately 1300 mm for the site (Meteorological Office Average Annual Rainfall Map, 1977), the mean

concentration of ^{210}Pb in rainfall may be deduced from the estimated flux as 75 mBq l^{-1}, using the equation in section 4.1.1. The derived concentration is entirely consistent with the mean UK ^{210}Pb concentrations in rainfall of 77±14 mBq l^{-1} estimated by Smith et al. (1997) and 74 mBq l^{-1} estimated by Eakins and Morrison (1976). However, it should be noted that as a proportion of the atmospheric ^{210}Pb in soil could have been delivered by the processes of dry and cloud droplet deposition, the estimated concentration in rainfall is most likely overestimated. Greater heterogeneity in deposition at locations closer to the edge of stand has led to higher variability in inventories at locations DC2 and DC3 relative to the deep inside canopy location DC4 as it was the case with ^{210}Pb inventories at Dunslair Heights discussed in section 4.1.1.

Inside forest canopy locations DC2-DC4 show substantially larger inventories, respectively 56%, 38%, and 15% larger than in the open heathland. Assuming the same precipitation input for all sites, the increase may then be attributed to cloud droplet and aerosol capture by the trees in excess of that by the heathland. The decrease in inventory at location DC4 might be partly due to a decrease in density of the canopy at the middle. The average enhancement in deposition for the three points of the transect inside the forest canopy is 36%. The DMR test reveals that there is no significant difference between the mean inventories at DC2 & DC3, nor between DC3 & DC4 (see Figure 3.20). The coefficient of variation ranges between 5-14% which is similar to the range observed at Dunslair Heights. However, the variation in inventories in the open field is relatively larger at Dun Coillich. This is the most likely due to a larger average wind speed (8-10 m s^{-1}, Birse & Robertson, 1970) combined with a larger roughness length associated with heathland at Dun Coillich which leads to larger turbulence over vegetative surface.

In contrast to Dunslair Heights, a pronounced *edge effect* in ^{210}Pb deposition is clearly evident at this site, in which the edge of stand is oriented perpendicular to the prevailing SW winds. The ^{210}Pb inventory at the edge of canopy (location DC2) is 56% larger than that in the open heathland, and 36% larger than the inventory deep inside the canopy. The forest canopy is an isolated rectangular plantation quite close to the tree line for Scotland and frequently exposed to orographic cloud (1113 hr y^{-1} ,

12.7%), calculated from the method of Weston (1992). The airflow at the edge presented with a sharp boundary in surface aerodynamic roughness from the heather and moorland to a 15-18 m canopy of Pinus sylvestris. The observed increase may be explained by this sudden change in the surface at the forest edge, which may lead to changes in air turbulence, reduced boundary layer resistance, and consequently increases in interception and impaction of particles and cloud droplets (McNaughton, 1989). Significant edge effects have been observed in wind tunnel studies of particle deposition on artificial canopies (Sehmel & Hodgson, 1980), in model studies (Wiman & Agren, 1985), and in field studies (Lovett & Reiners, 1986; Hasselrot & Grennfelt, 1987; Draaijers et al., 1988; Godt & Mayer, 1988; Ivens et al., 1988; Beier & Gunderson, 1989; Draaijers et al., 1992).

The amount of the canopy enhancement in ^{210}Pb inventories may be compared with an independent estimate of cloud droplet deposition by the procedure described in section 4.1.1. The calculation is summarised in Table 4.5.

Table 4.5: Direct calculation of cloud deposition at Dun Coillich.

	Moorland	Forest
Canopy height	0.2-0.3 m	15-18 m
Measured precipitation	1300 mm	1300 mm
Wind speed at the canopy height	8 m s^{-1}	8 m s^{-1}
Cloud deposition	20mm	108.2 mm
Enhancement of ^{210}Pb in cloud	x 5	x 5
Cloud deposition of 210Pb expressed in mm precipitation equivalents	100 mm	541 mm
Total deposition	1400 mm	1841 mm
% increase onto the forest canopy		32%

The increase in the ^{210}Pb inventory of 36% is very close to the calculated direct estimate of cloud deposition. However, the ^{210}Pb measured data include aerosol deposition as well. One should take account, of course, the fact that the calculation is based on values of average annual precipitation and mean wind speed which are estimated through interpolation from maps with associated systematic errors, or

derivation from the 3-dimensional frequency fields of cloud cover developed by Weston (1992), subject to the uncertainty in application of the UK cloud base statistics provided mainly by airports, to upland areas. Given the uncertainty introduced through these processes, the agreement between the ^{210}Pb and cloud droplet deposition estimates is remarkably good. The 5 km x 5 km UK cloud deposition map developed recently (Smith, 1998), predicts 10% average contribution of cloud deposition in total sulphur deposition for the grid square NN7550 which includes Don Coillich. It should be noted that this is an estimation based on cloud frequency and average wind speed for the grid square average elevation rather than the actual height of the site. The measured canopy enhancement of 36% is also consistent with a 30% enhancement in deposition of ^{90}Sr and ^{137}Cs found by Schreiber & Woerner and Bozl & Kracke, respectively (Bonzl & Kracke, 1988).

The depth profile of ^{210}Pb in the soil samples (Figures 3.17-3.19) demonstrate the efficient immobilisation of ^{210}Pb in the surface horizons of soil. None of the cores showed any evidence of a significant accumulation of atmospheric ^{210}Pb below 10 cm depth. To investigate it more fully, at two sampling points (DC1E, in the open, and DC3B inside the forest canopy) samples were collected to a depth of 50 cm. The apparent change in the pattern of depth profiles with respect to those at Dunslair Heights is mainly due to the fact that at Dun Coillich the sampling has been carried out for a single surface section of 0-5 cm rather than splitting it into 0-1 and 1-5 cm depth ranges.

The mean atmospheric ^{210}Pb inventories at Dun Coillich are approximately 35% larger than that at Dunslair Heights. This increase is most likely because of a greater average annual precipitation (1300 vs 1200 mm) as well as a greater mean wind speed (8 vs 5 m s^{-1}) and, hence, greater deposition.

4.2.2 Caesium 137 results

The measured ^{137}Cs inventories at four sampling locations at Dun Coillich are summarised in Table 4.6 and plotted in Figure 4.7 (see section 3.2.2 for details).

Table 4.6: Dun Coillich ^{137}Cs inventories under heather and forest.

	Open moorland	Inside the forest canopy		
Sample location	DC1	DC2	DC3	DC4
^{210}Pb inventory ($\pm \sigma$) Bq m^{-2}	8050(641)	12206 (1557)	10662(966)	10044 (1085)
Increase under forest		52%	32%	25%
Average increase		36%		

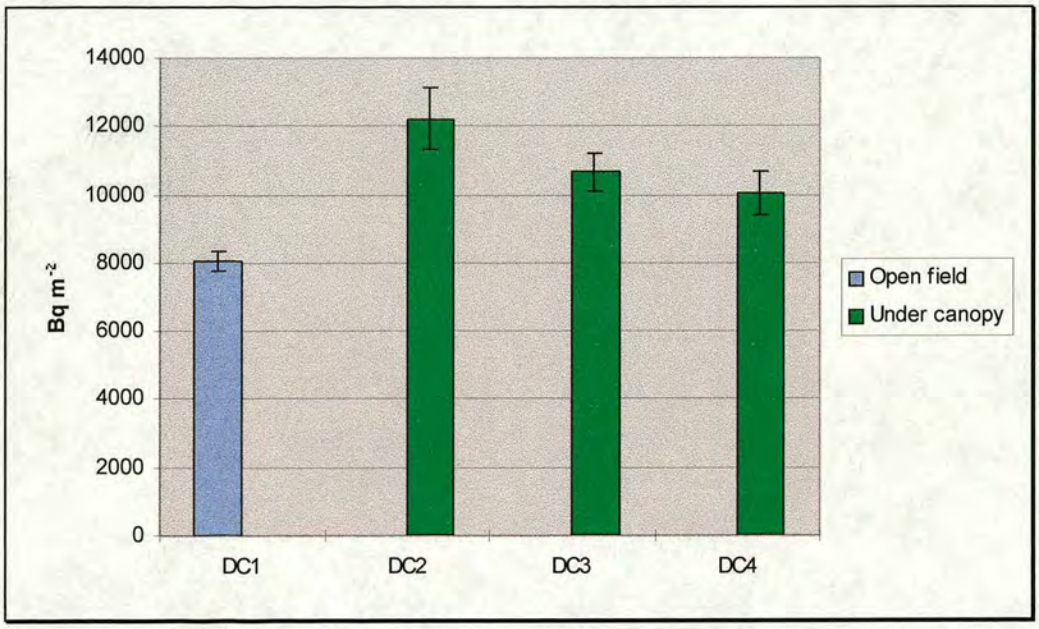

Fig. 4.7: Mean ^{137}Cs soil inventories in the open field (DC1) and inside the forest canopy (DC2, DC3 & DC4) at Dun Coillich. The error bars represent the standard error of the mean for five and three replicate soil cores at DC1 and the rest of locations, respectively.

Caesium 137 inventories follow a similar trend to those of atmospheric ^{210}Pb (described in section 4.2.1) over the transect across the boundary between open heathland and conifer forest. These data also support the presence of a pronounced edge effect at this site. The ^{137}Cs inventory at the edge of canopy (location DC2) is 52% larger than that in the open heathland, and 22% larger than the inventory deep inside the canopy. The range in the values of coefficient of variation between separate cores at the same locations is 8-13% which is smaller than the typical range

of 15-20% reported by Graustein & Turekian (1986). Larger variability is observed for all the under canopy inventory values especially at the edge of stand which may be explained by the development of turbulence at the edge and the behaviour of ^{137}Cs in the highly organic soil inside a canopy of conifers.

The mean inventory value of 8050 Bq m^{-2} is much larger than the mean fall-out per unit area in the northern hemisphere as well as the mean UK inventory mentioned previously in section 4.1.2. The measured value is almost twice the mean inventory for the grid square NN (designated letters for the 100 km grid square covering southern Highlands on the UK National Grid) of 4379 Bq m^{-2} estimated by Cawse (1983) (decay corrected from the value for 1977). The ^{137}Cs mean inventory values of 8050 and 10971 Bq m^{-2} , respectively for the open heathland and inside the forest canopy, are larger than the corresponding values at Dunslair Heights by approximately a factor of 4.4. Such an increase may not be justified by the difference in average annual precipitation and cloud deposition. As the level of increase is the same for both open field and canopy locations, it may be concluded that the excess in inventory would have been accumulated by wet deposition, most likely through rainfall during the passage of the Chernobyl plume in 1986. This hypothesis is supported by the estimated total deposition of 1-5 kBq m^{-2} for the region from Figures 4.4 & 4.5, and the measured mean inventory of ~15 kBq m^{-2} (Chernobyl-origin ^{137}Cs) by Mourne (1993) at Ben Lawers, situated about 15 km SW of Dun Coillich.

The measured canopy enhancement of 36% is entirely consistent with the magnitude of enhancement in ^{210}Pb inventory, and very close to the calculated value of enhancement due to cloud deposition at the site. It is also in line with a 30% enhancement in deposition of ^{90}Sr and ^{137}Cs found in soils under spruce canopies relative to the adjacent open grasslands in Germany (Bonzl & Kracke, 1988).

The depth profiles of ^{137}Cs activity (Figures 3.23-3.25) show that it is highly concentrated in the surface horizons of soil. There is no evidence of the expected sub-surface maxima in the depth profiles because the top sections (0-5 cm) of soil samples were not divided to 0-1 and 1-5 cm sub-sections at this site.

4.3 South-west Sweden

4.3.1 Lead 210 results

The mean soil inventories of atmospheric ^{210}Pb at ten sites A-J lying over the 60 km transect in the south-west province of Hallands, described in section 2.1.1.3, are summarised in Table 4.7 and plotted in Figure 4.8 (see sections 3.3.1-3.3.10 for details).

Table 4.7: South-west Sweden ^{210}Pb inventories in the open fields and under forest canopies.

Site	Site code	^{210}Pb inventory ($\pm \sigma$), Bq m^{-2}		Increase under forest canopy
		Open field	Under canopy	
Hallands Vadero island	A	2883 (320)	2945 (686)	0%[a]
Haverdals naturreservat	B	2772 (456)	2772 (387)	0%[a]
Bjorketrop	C	2143 (193)	-	-
Harplinge	D	3176 (445)	3990 (609)	26%
Harplinge	E	-	3147 (414)	0%[b]
Kvibille	F	-	4216 (389)	33%[c]
Ovraboke & Stammilt	G	2798 (344)	5314 (396)	90%
Normanstrop	H	4264 (483)	5112 (562)	20%
Broda	I	4413 (731)	5386 (469)	22%
Hasslehult & Hassleberg	J	3108 (477)	3817 (516)	23%

a) DMR test shows no significant difference between the inventory values at the 5% level of significance.

b) with respect to the nearby open field at site D.

c) with respect to the open field at site D, 7 km away.

The mean annual precipitation for these sites derived from the long-term (1983-90) average precipitation map of Sweden (Granat, pers. comm.) are presented in Figure 4.9 in order to compare the increase in precipitation with those in ^{210}Pb inventories along the 60 km transect. The ^{210}Pb soil inventory increases quite

markedly with distance inland to a maximum in upland sites G, H, and I, roughly 20-30 km from the coast, and decreases (by almost 30% relative to the

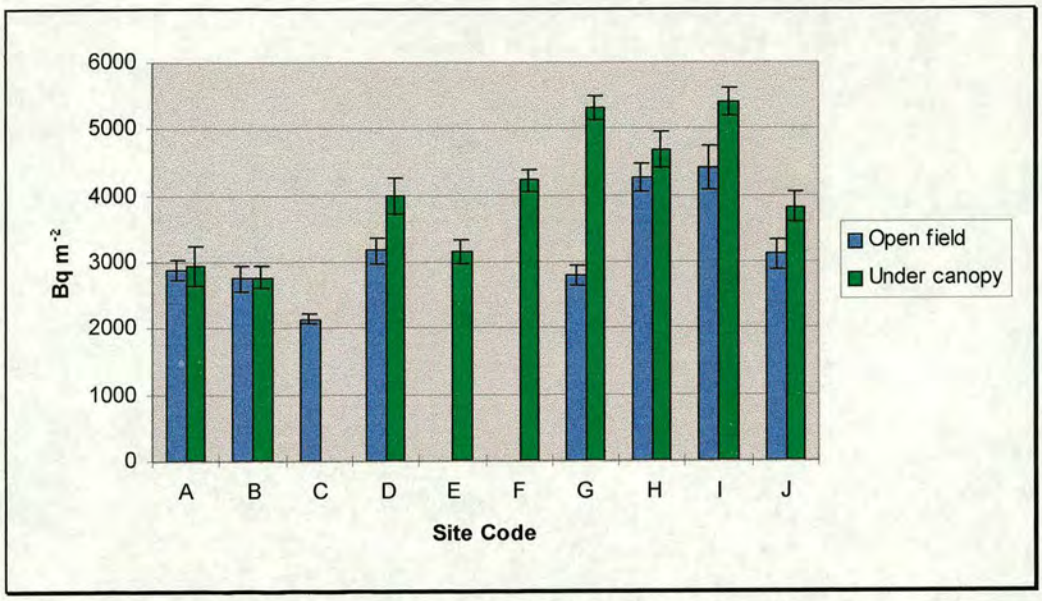

Fig. 4.8: Mean atmospheric ^{210}Pb soil inventories in the open field and inside forest canopies along the south-west Sweden transect. The error bars represent the standard error of the mean for five replicate cores at each location.

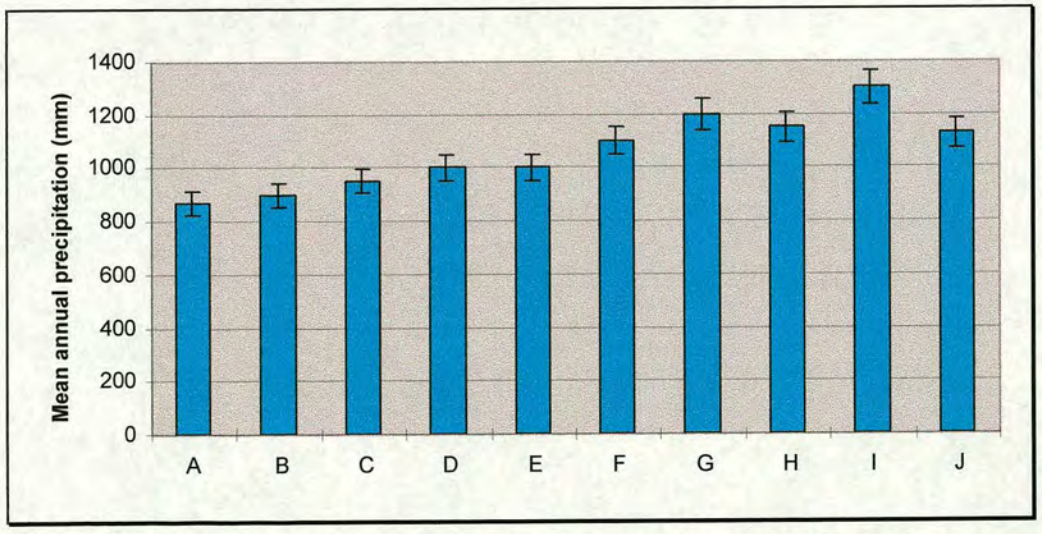

Fig. 4.9: Mean annual precipitation along the south-west Sweden transect derived from precipitation map based on records in the period of 1983-90 (Granat, 1990).

maximum) at site J, about 60 km from the west coast. This follows the trend in long-term precipitation variation along the transect (Figure 4.9). The lower than expected

inventory values are observed in the open fields at sites C & G. The soil samples from site C were sandy and contained very little organic matter which could have seriously impaired the soils capacity to trap deposited ^{210}Pb. It is also possible that disturbances by anthropogenic activity or by soil fauna disturbed the profiles. The open field at site G is situated on a hill slope over looking Ovraboke lake with high proportion of small stones at surface and a dense moss coverage. This might have resulted in enhanced surface run off of ^{210}Pb after deposition, especially in heavy rain or snow melt conditions.

Under the reasonable assumption of a steady state condition between the atmospheric supply of ^{210}Pb and its radioactive decay in soil, its average flux would be approximately 81 and 119 Bq m^{-2} y^{-1} for the open fields in the coastal and upland regions, respectively. These values and the mean value for SW Sweden of 100 Bq m^{-2} y^{-1} compare very well with the published literature on ^{210}Pb deposition fluxes to southern Sweden as follows:

^{210}Pb inventory in cores collected from lakes, marine coasts, and peat bogs in Scandinavia has been measured by Al-Doushy (1986) primarily to evaluate the ^{210}Pb methodology in dating aquatic and peat deposits. His analysis include several sites in southern Sweden as illustrated in Figure 4.10. The average flux of atmospheric ^{210}Pbcalculated from his data for sites No. 1, 2, 8, 9, 11 and 30 is 93 Bq m^{-2} y^{-1} ;

- Preiss et al. (1996b) in a compilation of data on ^{210}Pb deposition fluxes from a database constructed recently by the same authors (1996a) suggest a zonal mean annual ^{210}Pb flux of 85 Bq m^{-2} y^{-1} for the latitude band 50°-60° N, which is based on artificial collector, snow, and soil measurements;
- using the reported fluxes of ^{210}Pb in Europe (Priess & Genthon, 1997), a mean value of 104 Bq m^{-2} y^{-1} is calculated for the latitude band 52.5°-62.5° N;
- model-calculated contours by Lee & Feichter (1995) give an approximate value of 100 Bq m^{-2} y^{-1} for the ^{210}Pb deposition flux in southern and central Sweden.

The trend in deposition fluxes of ^{210}Pb to open fields along the transect may also be compared with the trend in sulphur wet deposition calculated from data on its average concentration in rainfall provided by the local precipitation chemistry

Fig. 4.10: Scandinavian sampling sites for lake sediments and peat bogs.

network (Westling et al., 1992) and national precipitation chemistry network [interpolated from contour maps (Granat, 1990)] as well as mean annual precipitation values based on records of precipitation from the regular meteorological network for the period of 1983 through 1990 (Granat, pers. comm.). It may also be compared with sulphur deposition estimates by a regional atmospheric dispersion model developed by Langner et al. (1995). The comparison is demonstrated in Figure 4.11 which shows a broadly similar overall pattern (relatively low values of ^{210}Pb inventories at sites C & G were explained before). They all show a maximum in deposition on the edge of the uplands. This is due to an increase in precipitation induced by the formation of low level feeder clouds, giving rise to orographic effects, even over small scale terrain features (quite modest elevation hills of few hundred meters) in this part of Sweden (Bergeron, 1965).

The data on ^{210}Pb soil inventories reveal a higher rate of increase with precipitation amount for the under canopy locations relative to those in the open fields as illustrated in Figure 4.12. Assuming that the precipitation input is the same

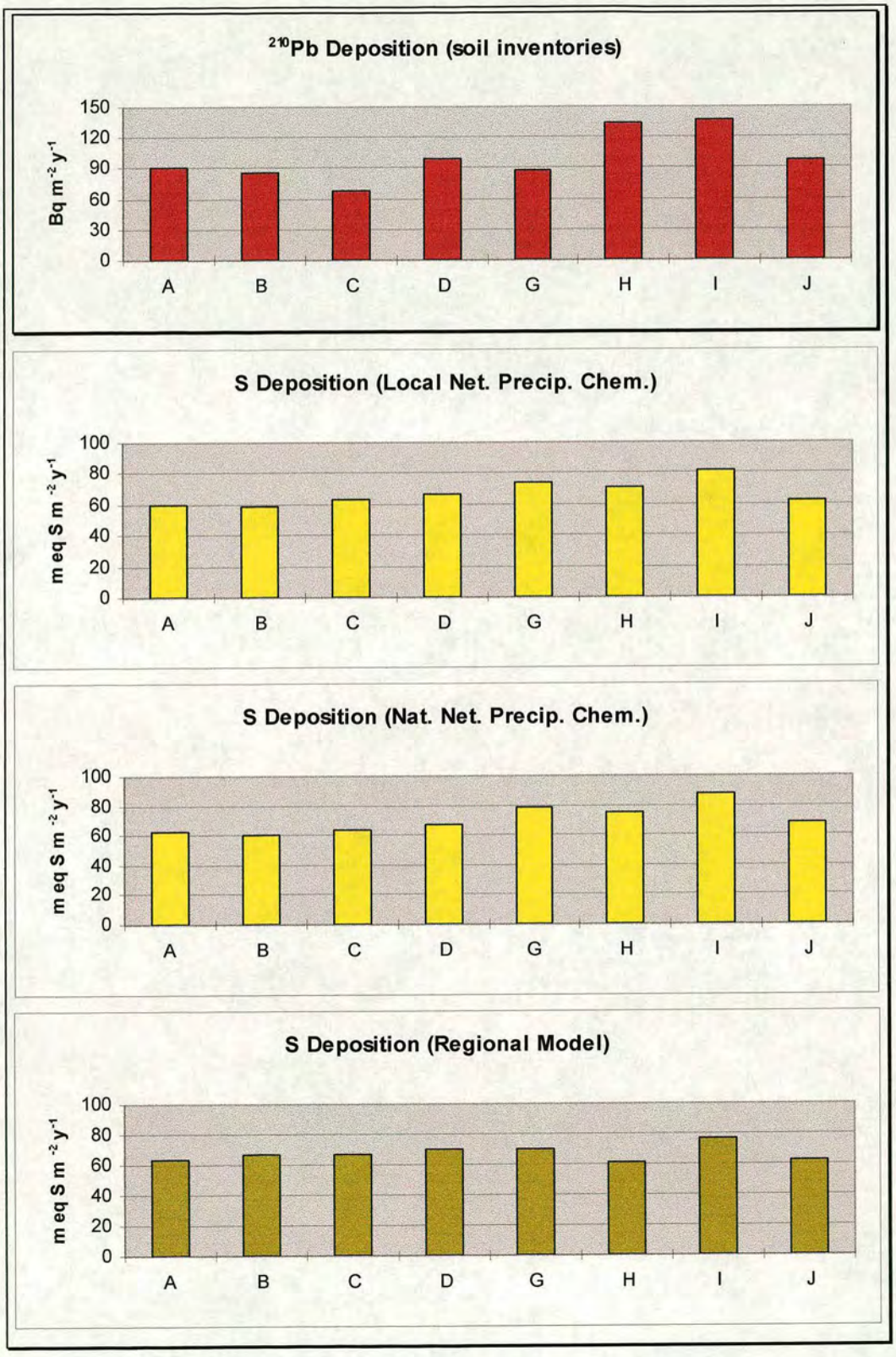

Fig. 4.11: Deposition values for atmospheric ^{210}Pb and anthropogenic sulphur estimated for the open fields at sites along south-west Sweden transect.

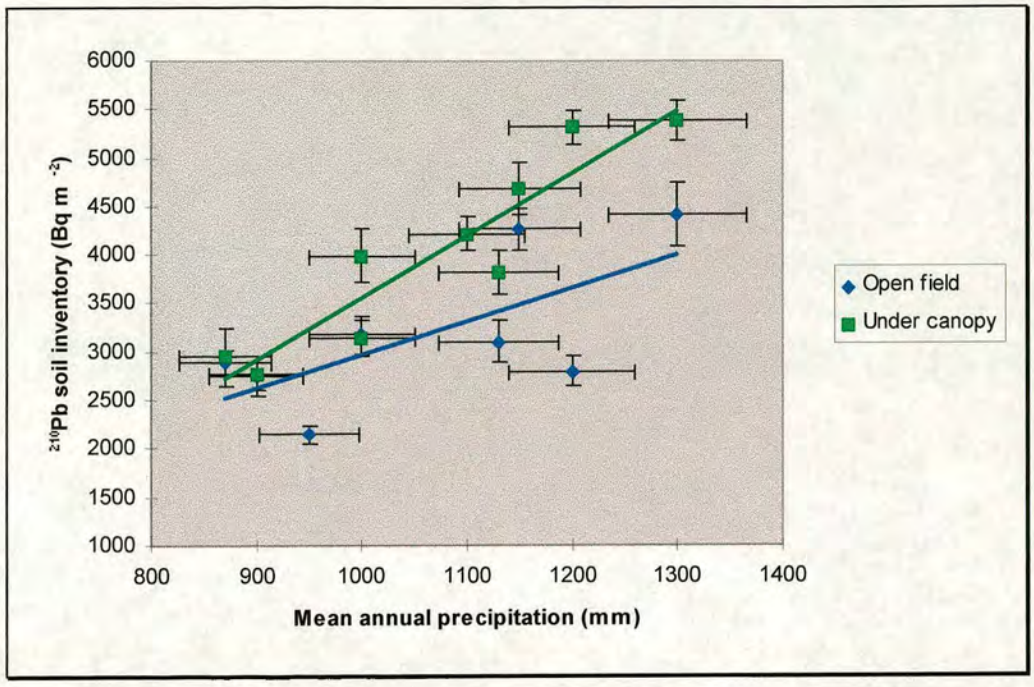

Fig. 4.12: The correlation between atmospheric 210Pb soil inventories in the open field and under canopy locations in SW Sweden

to the open field and over canopy at each site, this increase may therefore be assumed to result from cloud droplet deposition and aerosol capture by the trees in excess of that by the grassland. The average canopy enhancement in deposition for sites G, H, and I situated on the edge of upland is approximately 40%, whereas almost no enhancement is observed at coastal sites A (~ 3 km off-shore) and B (0.5 km inland). The lack of canopy enhancement at these latter sites seems to rule out a major contribution of dry deposition to total deposition in this region. Hultberg & Grennfelt (1991) and Lovblad et al. (1994), however, attribute the relatively large canopy enhancement values found for sulphur deposition in this part of Sweden entirely to dry deposition. Throughfall measurements of sulphur deposition in southern Sweden by Westling (1992) and Hallgren-Larsson et al. (1995) have revealed average enhancement of 100% and 90%, respectively, for spruce canopies in Hallands province. Their data are illustrated in Figures 4.13 and 4.14. Note that the throughfall technique may include the dry deposition of sulphur in gas phase which could be substantial depending on the ambient SO_2 concentration. It should also be noted that the two canopies sampled in the coastal region in ^{210}Pb study (at sites A & B) are

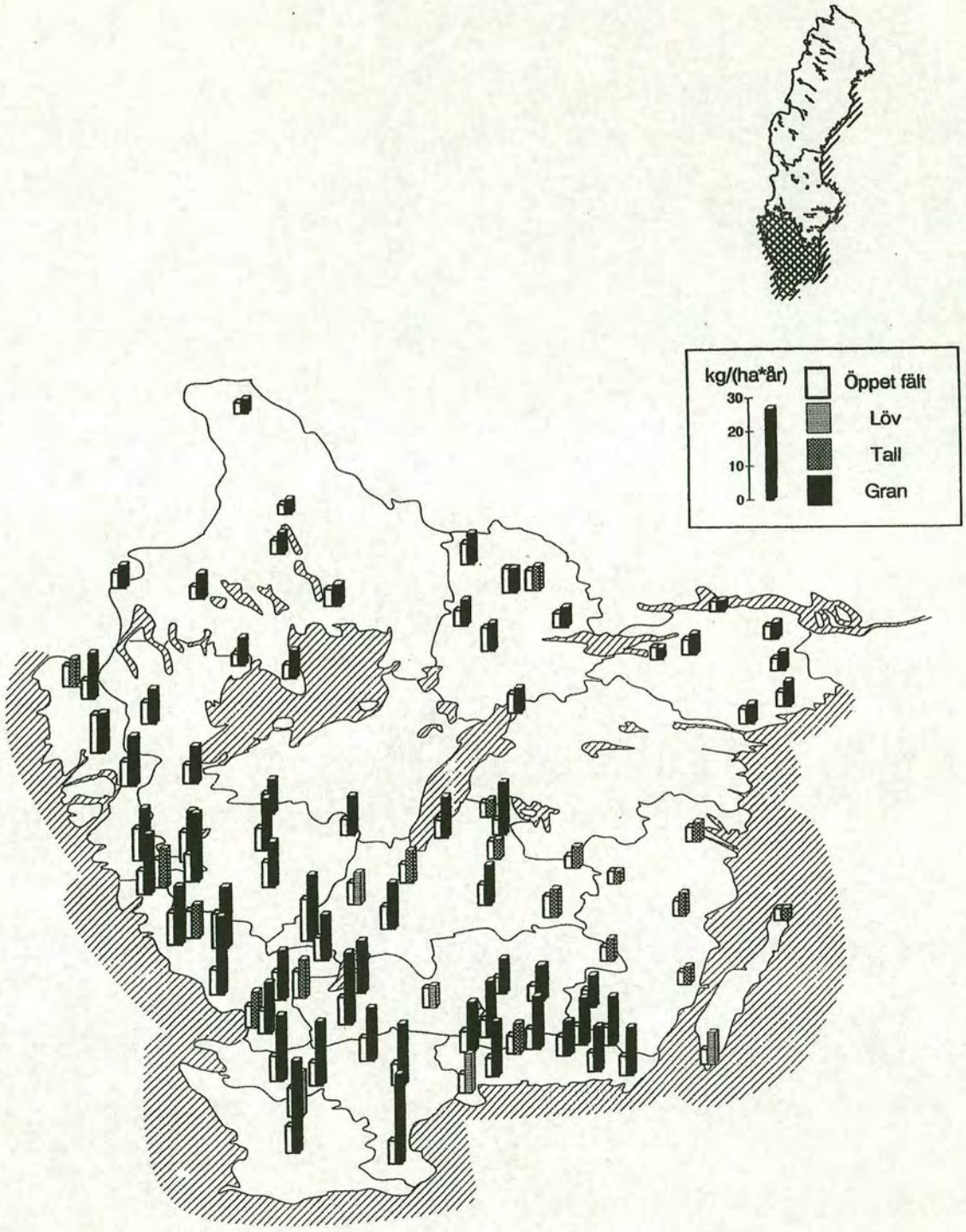

Fig. 4.13: Deposition of anthropogenic sulphur (SO_4-Sex) in the open field and in throughfall; Southern Sweden, during 1991 (Westling et al., 1991). Hallands province is situated in the central west coast(see section 2.1.1.3 for clarification). The map legend reads as follows: Oppet falt: open field; Lov: broad leaf; Tall: pine; Gran: spruce; kg/(ha*ar): kg ha^{-1} y^{-1}.

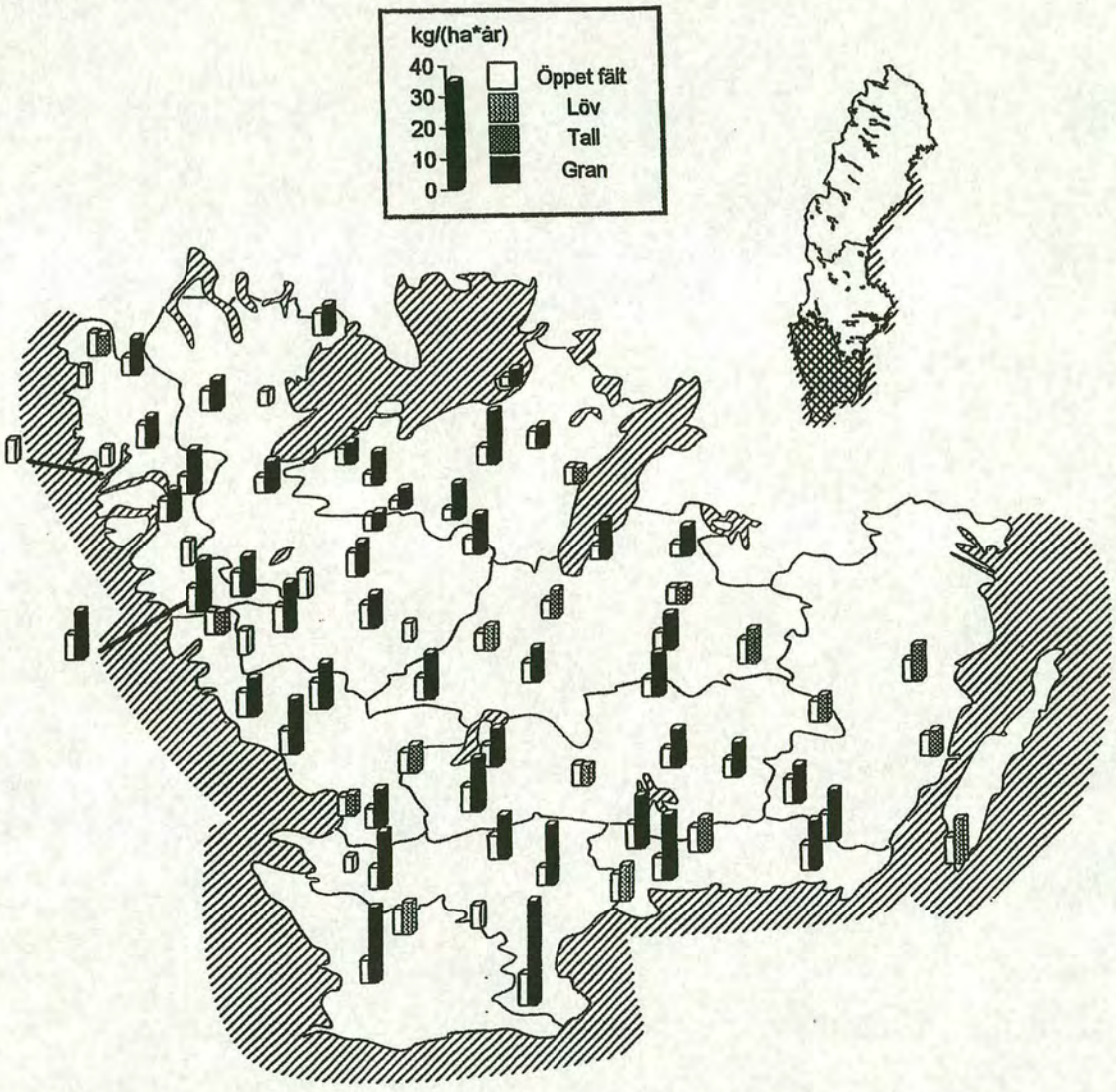

Fig. 4.14: Deposition of anthropogenic sulphur (SO_4-Sex) in the open field and in throughfall; Southern Sweden, in the period of October 1993 to September 1994 (Hallgren-Larsson et al., 1995). Hallands province is situated in the central west coast(see section 2.1.1.3 for clarification).

The map legend reads as follows:

Oppet falt: open field; Lov: broad leaf; Tall: pine; Gran: spruce; kg/(ha*ar): kg ha^{-1} y^{-1}.

relatively thin canopies of pine with much smaller leaf area index than the Norway spruce canopies in-land. Hallgren-Larsson et al. also found no enhancement in sulphur deposition under pine canopies in Hallands as demonstrated in Figure 4.14. On the other hand, the data provided by Westling (Figure 4.13) show an average canopy enhancement of 40% for measurements in Hallands. However, in the absence of site-data on ^{210}Pb concentration in air and cloud , the magnitude of the aerosol component in the deposition to forest canopies could not be quantified. It seems possible that aerosols have not been captured by the pine canopies in the coastal region largely because the canopy leaf area is much smaller than that for the Norway spruce at the inland sites. Thus the relatively large leaf area index of the sampled spruce canopies, and presence of low level orographic clouds in the area, are factors which support the assumption that a substantial contribution from cloud droplet deposition occurs at elevated sites in-land.

The depth profiles of ^{210}Pb in all collected soil samples (section 3.3) demonstrate the efficient immobilisation of the radionuclide in the surface horizons of soil, and none of them show any evidence of a significant accumulation of atmospheric ^{210}Pb below 10 cm depth.

4.3.2 Caesium 137 results

The mean soil inventories of atmospheric ^{137}Cs at ten sites A-J lying over the 60 km transect in the south-west province of Hallands, described in section 2.1.1.3, are summarised in Table 4.8 and plotted in Figure 4.15 (see sections 3.3.1-3.3.10 for details).

The coast to in-land pattern of ^{137}Cs soil inventories does not follow the trend in mean annual precipitation along the transect, and is not consistent with the corresponding pattern of ^{210}Pb soil inventories. Comparison of the inventories in the soils reveals marked variations which are larger for all under canopy locations than those in the open fields. Depth profiles show penetration of activity into deeper sections of the cores in more than ten cases. These effects are more pronounced

under old spruce canopies in-land and may be attributed to an increased mobility of ^{137}Cs in the highly organic and acidic soil in this part of Sweden. Most likely due to the same reason, there is no indication of a significant canopy enhancement in

Table 4.8: South-west Sweden ^{137}Cs inventories in the open fields and under forest canopies.

Site	Site code	^{137}Cs inventory (± σ), Bq m^{-2}		Increase under forest canopy
		Open field	Under canopy	
Hallands Vadero island	A	4051 (249)	4216 (915)	0%
Haverdals naturreservat	B	5724 (447)	5959 (615)	0%
Bjorketrop	C	4885 (552)	-	-
Harplinge	D	3746 (616)	3457 (661)	0%
Harplinge	E	-	3180 (611)	-
Kvibille	F	-	3518 (555)	-
Ovraboke & Stammilt	G	2588 (422)	3260 (751)	26%
Normanstrop	H	3762 (358)	3362 (588)	0%
Broda	I	3775 (487)	2582 (688)	-32%
Hasslehult & Hassleberg	J	2781 (577)	3279 (794)	0%

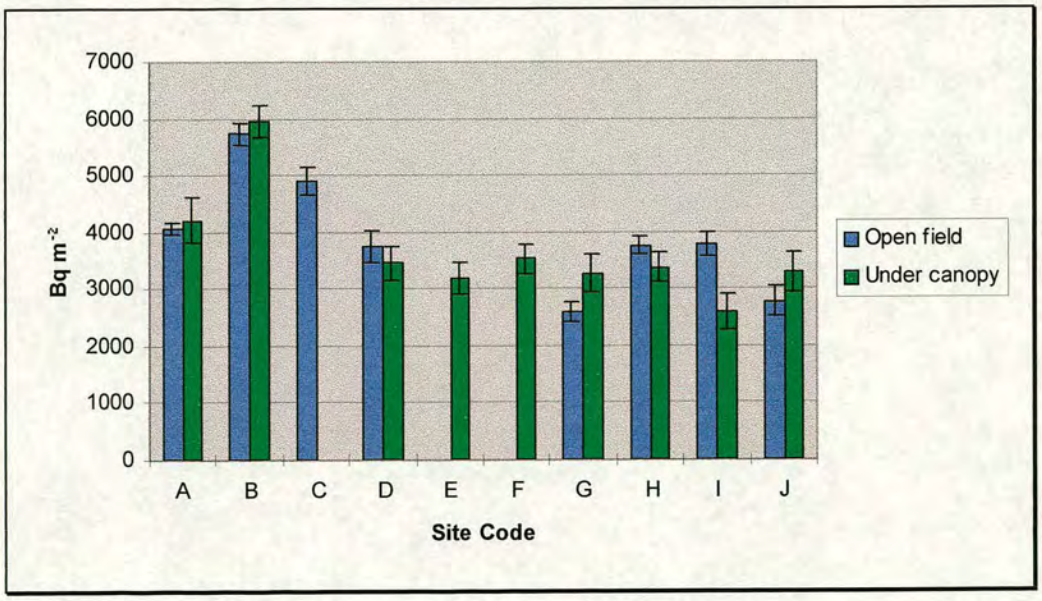

Fig. 4.15: Mean ^{137}Cs soil inventories in the open field and inside forest canopies along the south-west Sweden transect. The error bars represent the standard error of the mean for five replicate cores at each location.

deposition. The mean inventory for the forest canopy in site I is even 32% less than the inventory in the nearby grassland. The soil inventories at coastal sites A-C, on the average, are approximately 50% more than those at in-land sites G-J. This may be explained by either a possible patchy deposition of Chernobyl origin ^{137}Cs in the coastal region (see section 1.4.2) or substantial losses due to the increased mobility in more organic and more acidic peaty soil in-land.

4.4 Central Sweden

4.4.1 Lead 210 results

The mean soil inventories of atmospheric ^{210}Pb at four sites sampled on the two close by mountains, Gammalsaters and Skaftasen, from the Transtrands range in central Sweden are presented in Table 4.9 and Figure 4.16 (see sections 2.1.1.4 & 3.4 for details). Hill profile featuring the locations of sampling sites and plot of the results versus distance along the transect at Gammalsaters are shown in Figures 4.17 and 4.18, respectively.

Table 4.9: Central Sweden ^{210}Pb inventories in the open fields and under forest canopies.

Site	Site code	^{210}Pb inventory ($\pm \sigma$), Bq m^{-2}		Increase under forest canopy
		Open field	Under canopy	
Gammalsaters fiallet	A	3636 (460)	-	-
Gammalsaters fiallet	B	3214 (374)	4376 (328)	36%
Gammalsatern	C	2773 (214)	3668 (415)	32%
Skaftasen	D	-	5381 (612)	-

Under the reasonable assumption of a steady state condition between the atmospheric supply of ^{210}Pb and its radioactive decay in soil, its average flux would be approximately 113, 100 and 86 Bq m^{-2} y^{-1} for the open fields at sites A, B and C,

respectively. The value of ^{210}Pb flux calculated from Al-Doushy's data for his sites No. 3, 14 and 15 in central Sweden (see Figure 4.10 in the previous section) is 83 Bq m^{-2} y^{-1}. Attributing the increase in inventories at higher elevation sites B and A to most likely orographic effect and cloud droplet deposition, the measured flux of 86 Bq m^{-2} y^{-1} at the lower elevation site C is in good agreement with the above value

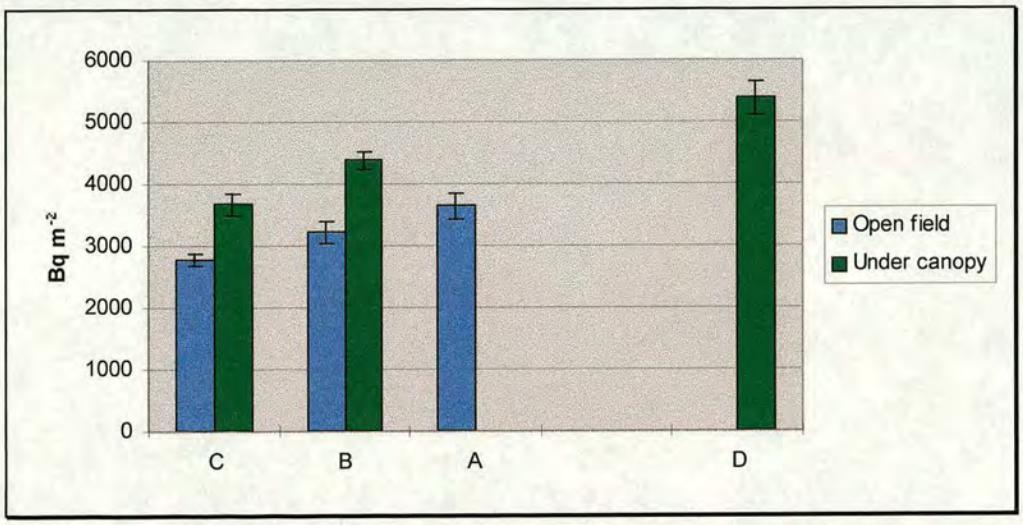

Fig. 4.16: Mean atmospheric ^{210}Pb inventories in the open fields and inside the forest canopies at Gammalsaters sites, A (870 m asl), B (740 & 720 m asl), C (540 & 530 m asl) and at Skaftasen site D (620 m asl). The error bars represent the standard error of the mean for five replicate cores at each location.

based on Al-Doushy's work. The average flux at Gammalsaters is approximately 100 Bq m^{-2} y^{-1} which is consistent with the calculated mean value of 104 Bq m^{-2} y^{-1} for the latitude band 52.5°-62.5° N using the reported fluxes of ^{210}Pb in Europe by Priess & Genthon (1997), and the approximate value of 100 Bq m^{-2} y^{-1} derived from model-calculated contours by Lee & Feichter (1995). The mean flux for the sites in central Sweden is entirely consistent with that of the sites sampled in the south-west. It seems that the *cleansing* of the boundary layer air (depletion of ^{210}Pb carrier aerosols in air parcels as they are transported over land) is compensated at the more continental nature of Transtrands mountains by the effects most likely related to a substantial difference in elevation (e.g. larger cloud frequency and wind speed). The annual average precipitation of 1100-1200 mm (Granat, 1990) is slightly larger at

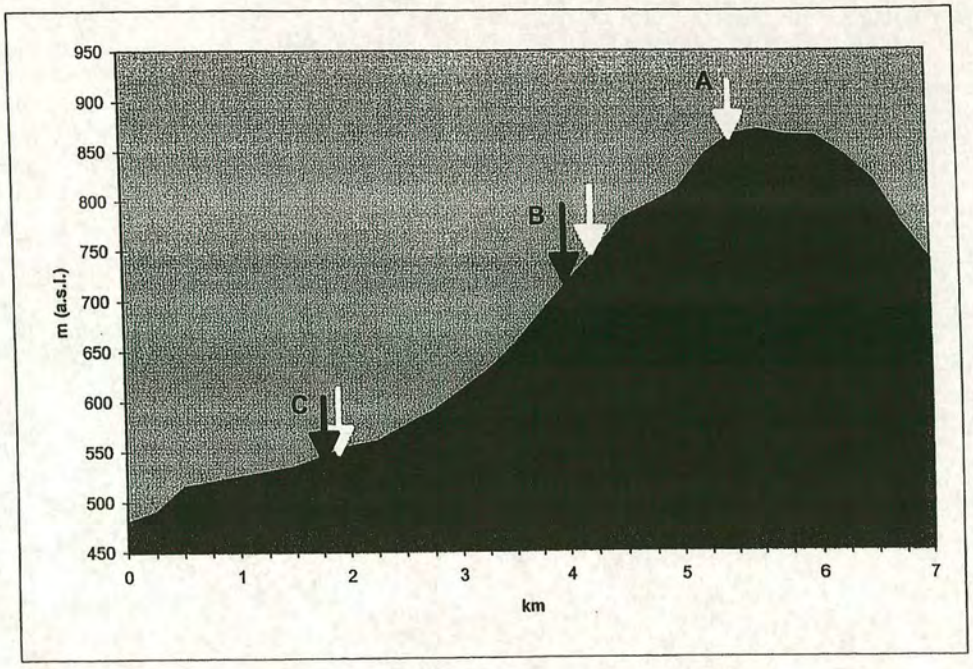

Fig. 4.17: Hill profile and the locations of open field (white arrows) and under canopy (black arrows) sampling sites at Gammalsaters.

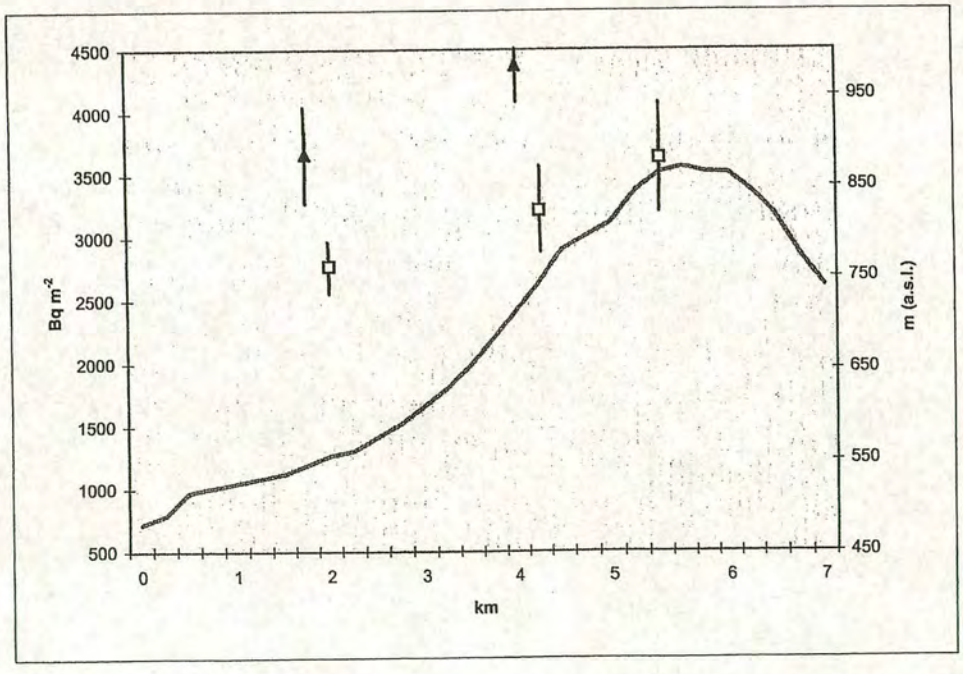

Fig. 4.18: Measured atmospheric ^{210}Pb inventories in the open fields (white squares) and under canopy locations (black triangles) at Gammalsaters. Solid line is the hill profile (height in m, right-hand scale). The error bars represent the standard deviation of the mean for five replicate cores at each location.

Transtrands compared to an average value of 1060 mm for sites in SW Sweden which might attribute as part of the compensation.

The atmospheric ^{210}Pb inventory at Gammalsaters increases quite moderately with elevation as illustrated in Figures 4.16 and 4.18. The inventory at the summit (A) is significantly larger than that at the valley (C, open field) by approximately 30%. It is not, however, comparable with the magnitude of increase in inventory over the same range of difference in altitude in areas under the influence of substantial orographic effect. Branford et al. (1998), for instance, report an increase in ^{210}Pb inventory by a factor of 2.2 over the same range of altitude difference at Ben Cruachan in W Scotland. It should be noted, of course, that Ben Cruachan is a much steeper mountain in a coastal region and its full altitude range is approximately 100-1000 m asl.

The canopy enhancement in deposition at 540 m asl (site C) is 32% whereas its magnitude at the altitude range of 620-720 m increases to 52% (average of under canopy inventories at sites B & D over open heathland at site B). These enhancements may be attributed to enhanced cloud droplet and aerosol deposition where greater proportions are encountered over forest due to enhanced turbulence, and greater incidence of surface cloud cover at higher elevations combined with greater wind speed (Gallagher et al. 1992). The same reasoning also applies to the larger canopy enhancement in deposition (approximately 30%) measured at the Transtrands mountains relative to that in the southern uplands. The magnitude of the observed increase with elevation is larger for forest canopies than the open fields (33% versus 16%, between site C and sites B & D) due to the enhanced turbulent deposition of cloud and aerosol to forests.

Transtrands is a ski resort area where snowfall is frequent and open fields as well as forest canopies are covered by snow for a substantial proportion of winter time. This is an important characteristic of the site to be considered. Hasselrot & Grennfelt (1987), suggest that the precipitation amount at the edge of canopies might be substantial during snowfall when the wind is blowing towards the edge. The high amount arises because of the low settling velocity of snowflakes and the increase in turbulent deposition. The mean inventories observed at the edge of an exposed stand

of conifers facing Norra Skaftastjarnen lake at 620 m asl (site D) were, respectively, 67%, 23% and 94% larger than the mean inventories at the open heathland at 740 m asl (site B_O), the forest canopy at 720 m asl (site B_C), and the open grassland at 540 m asl (site C_O). It seems, therefore, that the observed edge effect is partly due to the enhancement in capturing snow at the forest edge in addition to the main processes involved (i.e. enhanced cloud droplet and aerosol deposition due to the enhancement in turbulence at the edge). The effects of snow on deposition to a forest are however more complex, as shown by Gallagher et al. (1992) who on the basis of their measurements and a modelling study of cloudwater deposition to a snow-covered forest canopy, conclude that the combination of an increase in effective target diameter for the droplets impacting on the tree and a reduction in the surface roughness of the canopy may considerably reduce the deposition of chemical species to forests at high altitude where snow cover and low cloud are common in winter. The reduction of surface roughness due to snow coverage (see Table 1.2) might also have a weakening effect on the elevation related enhancement in deposition at the summit of Gammalsaters.

In a parallel study at Gammalsaters, samples of *Calluna vulgaris* were taken at the same locations and during the same sampling period. These samples were then analysed for their nitrogen contents at the Edinburgh Station of Institute of Terrestrial Ecology. These data show similar increase in N concentration in *C. vulgaris* to those reported for ^{210}Pb measurements. The nitrogen content (as an indication of the magnitude of N deposition) is found to be 11% and 24% larger for samples taken from under canopy locations relative to those from open fields at sites C and B, respectively. Samples collected from under canopy locations at elevated site B show a 15% increase in nitrogen content relative to that of under canopy location in the valley (site C). No significant difference is observed between the open field samples from these two sites (Skiba, pers. comm.). The grass meadow in the valley is used for grazing cattle in summer, which might be the cause for an increase in nitrogen input.

The depth profile of ^{210}Pb in the soil samples demonstrate its efficient immobilisation in the surface horizons of soil, mostly in the top 10 cm section. In the case of extremely peaty and very wet soils of few sampling points in the open

heathland at site B (CSB1-B4), and one sampling point under the canopy at site C (CSC9), however, a relatively larger proportion is found down to 15-25 and 12-20 cm depth sections, respectively.

4.4.2 Caesium 137 results

The mean soil inventories of ^{137}Cs at four sites sampled on Transtrands mountains are summarised in Table 4.10 and plotted in Figure 4.19 (see sections 2.1.1.4 & 3.4 for details).

Table 4.10: Central Sweden ^{137}Cs inventories in the open fields and under forest canopies.

Site	Site code	^{210}Pb inventory (± σ), Bq m^{-2}		Increase under forest canopy
		Open field	Under canopy	
Gammalsaters fiallet	A	2954 (105)	-	-
Gammalsaters fiallet	B	2616 (954)	2787 (351)	0%
Gammalsatern	C	2324 (351)	3746 (755)	61%
Skaftasen	D	-	4122 (1029)	-

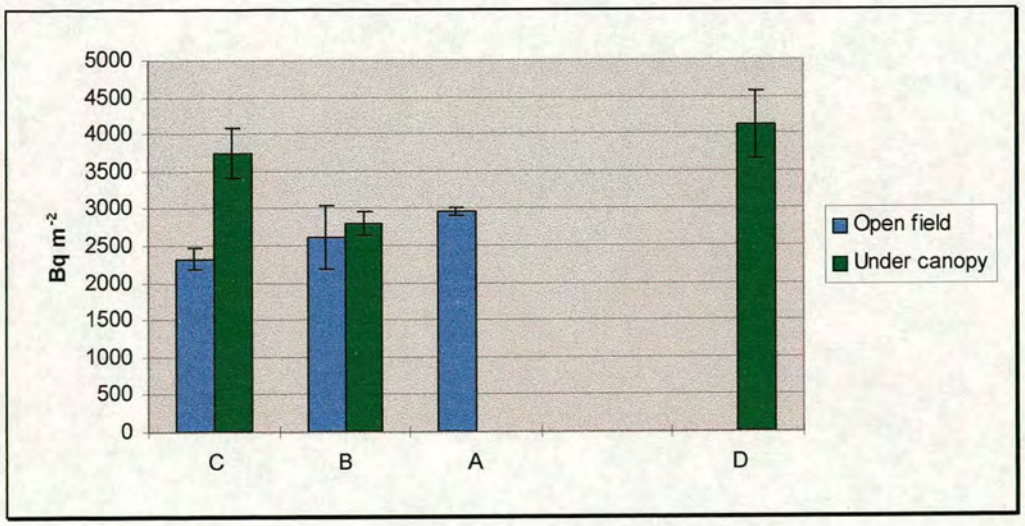

Fig. 4.19: Mean ^{137}Cs inventories in the open fields and inside the forest canopies at Gammalsaters sites, A (870 m asl), B (720 & 740 m asl), C (540 & 530 m asl) and at Skaftasen site D (620 m asl). The error bars represent the standard error of the mean for five replicate cores at each location.

Comparison of ^{137}Cs inventories in the sampled soils reveals marked variation especially in the open field location at site B and under canopy locations at sites D & C, most likely due to the mobility of this radionuclide in these highly organic and peaty soils. The depth profiles for the under canopy location of site C (Figure 3.127) is another evidence for this mobility.

There is an indication of elevation related enhancement by approximately 27% between open fields at the valley and summit of Gammalsaters but the variations at site B is too large to make any reliable judgement in this regard. In the case of forest canopies, the mean inventory at site B is lower than those for sites C & D, but the depth profiles do not provide any indication for loss of inventory. In contrast to ^{210}Pb results, ^{137}Cs inventories are generally lower than those in the south-west Sweden. Considering the similar inconsistency between sites in SW Sweden as well as in Scotland, it may be concluded that ^{137}Cs has the potential for comparisons within an individual site, but definitely not in-between sites largely as a consequence of the patchy deposition of the ^{137}Cs in convective precipitation associated with the Chernobyl ^{137}Cs deposited in 1986. Moreover, it was found that it has a high mobility in highly organic and acidic soils. The value of ^{137}Cs as a confirmatory tracer, is therefore, diminished by these findings.

4.5 Summary and Conclusion

- The overall aim of this experimental study has been to use the soil inventory of atmospherically derived ^{210}Pb in soil to determine deposition patterns of atmospheric aerosols averaged over decades (physical half-life of ^{210}Pb is 22.3 years). The method has been applied to quantify the long-term average enhancement in aerosol and cloud water deposition as a consequence of aerodynamic roughness effects of forest canopies in Scotland and Sweden.

- Acid deposition remains an important environmental issue, now with a global perspective. Considering the large variation in pollutant deposition to various

ecosystems, receptor specific estimates are required to quantify the relationship between effects and deposition. The present knowledge of cloud droplet deposition and dry deposition of aerosols to forests is still insufficient and there is a need for the clarification of the present large gap between measured values in field experiments and results from model and wind tunnel work. However, collection of more reliable field data using conventional methods, especially over extended period of time, requires extensive field and/or laboratory work which are both expensive and for which suitable instrumentation for the long-term measurements are not readily available.

- Natural and artificial radionuclides present in the atmosphere (e.g. radon and its daughters, cosmogenic radionuclides, fission products) are associated with nonradioactive aerosols and hence can serve to trace the fluxes of aerosols to various surfaces. Lead-210 and ^{137}Cs have been shown (Moore et al., 1973; Graustein and Turekian, 1986) to be particularly useful because they are associated mainly with submicron-sized aerosols which contain the bulk of the pollutant sulphur and nitrogen. When scavenged from the atmosphere along with carrier aerosols, ^{210}Pb is retained by the organic-rich surface horizons of soil which acts as an efficient integrating collector (Lewis, 1977). The ^{210}Pb isotope is the decay product of ^{222}Rn, a water-insoluble inert gas which belongs to the natural uranium ^{238}U decay series and readily diffuses from soil into the atmosphere. Its total inventory (less the supported fraction by the in situ decay of ^{222}Rn) in undisturbed soils may be used as a measure of total aerosol deposition (dry plus wet deposition and cloud droplet interception) averaged over about 30 years, approximately the mean nuclear lifetime.

- The measurements reported in this thesis, were performed by collecting samples of soil to a depth of 20-30 cm at selected locations from within the canopy as well as the adjacent open land at each site. Split-level sampling technique were applied to determine the depth profiles of ^{210}Pb, ^{137}Cs and ^{214}Pb. Measurement of ^{214}Pb inventories were also conducted for each sub-section of a core, in order to make

corrections for *supported* ^{210}Pb due to in situ decay of ^{222}Rn. The specific activities of ^{210}Pb in dried soil samples were determined by non-destructive γ-spectrometry using high resolution HPGe detectors, one of which fitted with a Compton suppression system. The Compton shield proved to be very useful especially in counting low energy (46.5 keV) gamma rdiation from ^{210}Pb in samples of low-activity content from lower sections of cores in the presence of a relatively large natural background. For the sample self-attenuation correction of 46.5 keV gammas from ^{210}Pb, the conventional spiked matrix method as well as the method developed by Cutshall et al. (1983) have been applied in this study.

- Initial sampling was conducted at Dunslair Heights beneath a Norway spruce (Picea abies) canopy and in the adjacent open grassland at an elevation of 450 m asl in the Scottish Southern Uplands. The average enhancement in the ^{210}Pb inventory under the forest canopy of 37% is found to be consistent with deposition estimates obtained from a continuous record of cloud frequency and meteorological variables, and is also in good agreement with the UK model deposition estimates for the site. The magnitude of enhancement also compares very well with the canopy enhancement found in ^{137}Cs inventories at the site and those measured by Schreiber & Woerner (1979, cited in Bonzl & Kracke, 1988) and Bonzl & Kracke (1988) in deposition of ^{90}Sr and ^{137}Cs in soils under spruce canopies relative to the adjacent open grasslands in Germany. The mean flux to the open moorland is estimated to be 72 Bq m^{-2} y^{-1}. This flux corresponds to a mean concentration of ^{210}Pb in rainfall of 60 mBq l^{-1} which compares closely to the mean UK ^{210}Pb concentrations in rainfall of 77±14 mBq l^{-1} estimated by Smith et al. (1997) and 74 mBq l^{-1} estimated by Eakins and Morrison (1976), and is consistent with the derived concentrations of 62 & 66 mBq l^{-1} based on measured atmospheric fluxes by Clifton (1991) and Mourne (1993), respectively (see section 4.1).

- Measurement of radionuclide inventories at the second site, an old plantation of Scots pine (Pinus sylvestris) at 420 m asl near the summit of Dun Coillich in the

Scottish Highlands, revealed an average canopy enhancement in deposition of approximately 36% relative to the open heathland in close correspondence with independent estimates of cloud droplet deposition at the site and is supported by the prediction of the average contribution of cloud deposition in total sulphur deposition for the relevant National Grid square, derived from the 5 km x 5 km cloud deposition map developed recently (Smith, 1998). Deposition at the exposed edge of stand, however, is 56% larger than that in the open heathland, and 36% larger than the inventory deep inside the canopy which shows a pronounced *edge effect* in ^{210}Pb deposition. The measured value of canopy enhancement is entirely consistent with the one found for ^{137}Cs inventories at the site and also in close agreement with values reported for the canopy enhancement in deposition of ^{90}Sr and ^{137}Cs (Bonzl & Kracke, 1988). The mean ^{210}Pb flux to the open heathland is estimated to be 98 Bq m^{-2} y^{-1} which corresponds to a mean concentration of ^{210}Pb in rain of 75 mBq l^{-1}. The derived concentration is consistent with the mean UK ^{210}Pb concentrations in rainfall of 77±14 mBq l^{-1} estimated by Smith et al. (1997) and 74 mBq l^{-1} estimated by Eakins and Morrison (1976) and compares closely to the derived cocentrations of 66 & 62 mBq l^{-1} based on fluxes measured by Mourne (1993) and Clifton (1991), respectively (see section 4.2).

- A mean ^{210}Pb flux of 72 ± 10 Bq m^{-2} y^{-1} per meter of annual rainfall may be calculated from all UK data as presented in Table 4.11.

- The method was then applied to measure the pattern of total aerosol deposition at ten sites in south-west Sweden, along a transect from Hallands Vadero Island at the coast to the southern Swedish uplands. The soil inventory of ^{210}Pb increases quite markedly with distance inland to a maximum in upland sites, roughly 20-30 km from the coast and decreases by almost 30% relative to the maximum at a site about 60 km from the west coast. This follows the trend in long-term precipitation variation along the transect. The trend in sulphur wet deposition calculated from data on its average concentration in rainfall (Granat, 1990; Westling et al., 1992) and sulphur deposition estimates by a regional atmospheric dispersion model

developed by Langner et al. (1995) show a broadly similar overall pattern. The mean ^{210}Pb flux would be approximately 81 and 119 Bq m^{-2} y^{-1} for the open fields in the coastal and upland regions, respectively. These values and their average of 100 Bq m^{-2} y^{-1} compare very well with measurements reported by Al-Doushy (1986), Preiss et al. (1996b), Priess & Genthon (1997), and the estimated value from model-calculated contours by Lee & Feichter (1995). The canopy enhancement in deposition was found to be relatively high for quite modest elevations of few hundred meters at 20-30 km from the coast, with no enhancement in the coastal region, suggesting that the significant enhancements is due to cloud/fog deposition at elevated sites in-land. The increased input to exposed forests on elevated hills in-land is up to 100% relative to that in open fields covered by short vegetation in the coastal area (see section 4.3).

Table 4.11: ^{210}Pb atmospheric flux in the United Kingdom.

Location	^{210}Pb flux (Bq m^{-2} y^{-1}) per meter rainfall	Reference
Cumbria[a]	74	Smith et al. (1997)
NW England & Scotland[a]	66	Mourne (1993)
Cumbria[a]	68	Eakins et al. (1984)
Southern Upland, Scotland[a]	60	This study
Highlands, Scotland[a]	75	This study
Cumbria[b]	70	Eakins et al. (1984)
Milford Haven[b]	93	Peirson et al. (1966)
Harwell[b]	83	Burton & Stewart (1966)
Plymouth[c]	62	Clifton (1991)
Mean ($\pm \sigma$)	72 ($\pm$10)	

a) soil core measurements

b) rainwater measurements

c) sediment core measurements

- Four sites on the two adjacent mountains, Gammalsaters and Skaftasen, from the Transtrands range in central Sweden were the last sites sampled in this study.

Measurements revealed a significant increase in ^{210}Pb inventory on the summit of Gammalsaters, 870 m asl, relative to the valley at 540 m asl. A higher rate of increase with elevation was observed for atmospheric ^{210}Pb inventories under forest canopies sampled in these mountains relative to the open fields, due to enhanced cloud droplet and aerosol deposition over forest due to enhanced turbulence and greater cloud frequency combined with greater wind speed. The mean inventory at the exposed edge of a forest canopy at 620 m asl exceeds that of open grassland at an elevation of 540 m asl by approximately 90%. The mean flux to the open fields situated at 540, 740, and 870 m asl are approximately 86, 100 and 113 Bq m^{-2} y^{-1}, respectively. Attributing the increase in inventories at higher elevation sites to most likely orographic effect and cloud deposition, the measured flux of 86 Bq m^{-2} y^{-1} at the lower elevation site is in good agreement with measurements reported by Al-Doushy (1986). The average flux at Gammalsaters is approximately 100 Bq m^{-2} y^{-1} which is consistent with the calculated mean value for the latitude band 52.5°-62.5° N based on the reported fluxes of ^{210}Pb in Europe by Priess & Genthon (1997), and the value derived from model-calculated contours by Lee & Feichter (1995) (see section 4.4).

- The depth profiles of ^{210}Pb in more than 500 collected soil samples demonstrate the efficient immobilisation of the radionuclide in the surface horizons of soil and show no evidence of a significant accumulation of atmospheric ^{210}Pb below 10 cm depth.

- Based on measurements carried out in this study, it may be concluded that ^{137}Cs has the potential for comparisons within an individual site, but definitely not in-between sites largely as a consequence of the patchy deposition of the ^{137}Cs in convective precipitation associated with the Chernobyl ^{137}Cs deposited in 1986. Moreover, it is found that it has a high mobility in highly organic and acidic soils. The value of ^{137}Cs as a confirmatory tracer, is therefore diminished by these findings.

- As the bulk of atmospheric ^{210}Pb has been shown to be concentrated in the top 10 cm of soil profiles, taking sample to a depth of 20 cm devided to 0-5, 5-10, and 10-20 depth intervals seems to be quite sufficient and no further sub-division is needed. The soil sampling technique is relatively easy to implement, requires no expensive equipment and is well suited for monitoring at a large number of sites. However, care should be taken in the selection of suitable sites. Field sampling may be conducted in a reasonable time duration but γ-ray analysis of low activity environmental samples is a very time consuming process.

- The direct γ-spectrometry technique allows measurements on the same sample for numerous radionuclides. As a non-destrutive technique, it also allows repeated γ-measurements on the same sample, and/or other analyses following the γ–assay.

- The method may be also applied to provide further insight into aerosol deposition study by performing comparative measurements on forest canopies and adjacent open fields at low level non-marine environments. Such studies would benefit from complementary measurements of ^{210}Pb concentration in rain and air at the site.

- The soil inventories of ^{210}Pb provide a measure of long-term variation in deposition rate of atmospheric aerosols as particles and/or droplets that is operationally easier to carry out than the direct measurement by artificial collectors over extended period of time. It appears to be particularly valuable in quantifying aerosol and wet deposition processes at sites where conventional methods are not applicable.

Bibliography

Aamlid, D. et al. (1992). Forest decline in Europe. In: D.W. Johnson and S.E. Lindberg (eds), Atmospferic Deposition and Forest Nutrient Cycling. Springer-Verlag, New York: 543-570.

Alcamo, J. et al. (1990). The RAINS Model of Acidification. Kluwer Academic, Dordrecht, The Netherlands.

Al-Doushy, F. (1986). The value of 210Pb in dating Scandinavian aquatic and peat deposits. Radiocarbon, 28: 1031-1040.

Allard, B. et al. (1994). Acidifying substances and tropospheric ozone: Effects and critical loads. Report 4352, Swedish Environmental Protection Agency.

Amann, M. (1990). Energy use, emissions, and abatement costs. In: J. Alcamo et al. (eds), The RAINS model of acidification. Kluwer Academic, Dordrecht:61-113.

ANSI (1991). American National Standard Calibration and Use of Germanium Spectrometers for the Measurement of Gamma-Ray Emission Rates of Radionuclides. IEEE, New York.

Asman, W.A.H. (1992). Ammonia emission in Europe: updated emission and emission variations. National Institute of Public Health and Environmental Protection, Bilthoven, The Netherlands.

AWRG (1986). Acidity in United Kingdom fresh waters. UK Acid Water Review Group report, Department of the Environment.

Baltakmens, T. (1974). Profiles of lead-210 and rdium-226 in four New Zeland soils. New Zeland J. of Science, 17: 435-439

Barretto, R.M.C. et al. (1972). Physical characteristics of radon-222 emanation from rocks, soils and minerals. In: J.A.S. Adams et al. (eds.), The Natural Radiation Environment, II; USERDA, Rept. CONF-720805-P2: 731-740.

Battarbee, R.W. et al. (1985). Lake acidification in Galloway: A palaeoecological test of competing hypotheses. Nature, 314: 350-352.

Beier, C. et al. (1992). A new method for estimation of dry deposition of particles based on throughfall measurements in a forest edge. Atmos. Environ.,26A: 1553-1559.

Beilke, S. (1982). Acid deposition: The present situation in Europe. In: S. Beilke and A.J. Elshout (eds), Acid deposition. CEC Environmental Research Programme, Berlin: 5-32.

Beir, C. and Gundersen P. (1989). Atmospheric deposition to the edge of a spruce forest in Denmark. Environ. Pollut., 60: 257-271.

Beir, C. et al. (1993). Spatial variability of throughfall fluxes in a spruce forest. Environ. Poll., 81: 257-267.

Benkovitz et al. (1996). Global gridded inventories of anthropogenic emissions of sulphur and nitrogen. J. of Geophys. Res., 101:29239-292545.

Benninger, L.K. et al. (1975). The use of natural Pb-210 as a heavy metal tracer in river-estuarine systems. In: T.M. Church (ed), Marine Chemistry in the Coastal Environment, ACS Symp. Ser. vol. 18. American Chemical Society, New York: 201-210.

Berge, F. et al. (1991). Palaeolimnological changes relayed to acid deposition and land-use in the catchment of two Norwegian softwater lakes. Phil. Trans. R. Soc. London, B327: 385-389.

Bergeron, T. (1965). On the low-level redistribution of atmospheric water caused by orography. Proc. Int. Conf. on Cloud Physics, Tokyo and Sapparo: 96-100.

Bernes, C. (1987). Sulphur and Nitrogen. In: C. Bernes and C. Grundsten (eds), The Environment. The National Environmental Protection Agency:18-23.

Beswick, K.M. et al. (1991). Size resolved measurements of cloud droplet deposition velocity to a forest using an eddy correlation technique. Qurt. J. Roy. Met. Soc., 117: 623-645.

Bhandari, N. et al. (1970). Vertical structure of the troposphere as revealed by radioactive racer studies. J. Geophys. Res., 75, No. 15: 2974-2980.

Birse, E.L. and Robertson, L. (1970). Assessment of climatic conditions in Scotland: Based on Exposure and accumulation frost. The Macauley Institute for Soil Research: Aberdeen.

Blifford, I.H. et al. (1952). On the natural radioactivity in the air. J. Geophys. Res., 57: 499-509.

Bobbink, R. (1992). Atmospheric deposition and canopy exchange processes in heathland ecosystems. Environ. Pollut., 75: 29-37.

Bonnet, P.J.P. and Cambroy, R.S. (1991). The record of deposition of radionuclides in the sediments of Ponsonby Tarn, Cumbria. Hydrobiologia, 214:63-70.

Bonnyman, J. et al. (1972). Lead-210 in the Australian environment. In: J.A.S. Adams et al. (eds.), The Natural Radiation Environment, II; USERDA, Rept. CONF-720805-P2: 819-931.

Bown, C.J. and Shipley, B.M. (1982). South-East Scotland. Soil Survey of Scotland, Sheet 7. The Macaulay Institute for Soil Research, Aberdeen.

Branford,D., Mourne, R.W. and Fowler, D. (1998). Spatial variation of wet deposition rates in an extended region of complex topography deduced from measurements of ^{210}Pb soil inventories. J. Environ. Radioactivity, 41, No. 2: 111-125.

Bredemeier, E. et al. (1988). A simple and appropriate method for the assessment of total atmospheric deposition in forest ecosystem monitoring. In: M.H. Unsworth and D. Fowler (eds.), Acid Deposition at the High Elevation Sites. Kluwer Academic, Dordrecht: 607-614.

Brimblecombe, P. (1996). Air composition & chemistry (2nd ed.): Cambridge Environmental Chemistry series No. 6. Cambridge Univ., Cambridge, England.

Brodin, Y. and Kuylenstierna, J. (1992). Acidification and critical loads in Nordic countries: A background. Ambio, 21, No. 5: 332-338.

Bunzl, K. and Kracke, W. (1988). Cumulative deposition of ^{137}Cs, ^{238}Pu, $^{239+240}$ Pu and ^{241}Am from global fallout in soils from forest, grassland and arable land in Bavaria (FRG). J. Environ. Radioactivity, 8:1-14.

Bunzl, K. (1991). The migration of radionuclides in the soil. In: M. Garcia-Leon and G. Madurga (eds.), Low-Level Measurements of Man-made radionuclides in the environment. World Scientific: 328-353.

Burton, W.M. and Stewart, N.G. (1960). Use of long-lived natural radioactivity as an atmospheric tracer. Nature, 186: 584-589.

Cambray, R.S. et al. (1970). Radioactive fallout in air and rain. AERE, R-6556, HMSO, London.

Cambray, R.S. et al. (1987). Observations on radioactivity from the Chernobyl accident. Nucl. Energy, 26: 77-110.

Cape, J.N. et al. (1997). The budget of oxidised nitrogen species in orographic clouds. Atmos. Environ., 31: 2625-2636.

Carruthers, D.J. and Chpularton, T.W. (1984). Acid deposition in rain over hills. Atmos. Environ., 18: 1905-1908.

Cawse, P.A. (1983). The accumulation of caesium and plutonium-239+240 in soils of Great Britain, and transfer to vegetation. In: P.J. Coughtrey et al. (eds.), Ecological Aspects of Radionuclide Release. Blackwell Scientific, Oxford, England.

Cawse, P.A. and Horril, A.D. (1986). A survey of caesium-137 and plutonium in British soils in 1977. AERE, R-10155, HMSO: London.

Cawse, P.A. et al. (1988). A survey of background levels of environmental radioactivity in Wales, 1984-86(Pre-Chernobyl). AERE, R-12535, HMSO: London.

Cerny, J. and Paces, T. (eds) (1995). Acidification in the Black Triabgle Region. Czech Geological Survey, Prgue.

Chamberlain, A.C. (1960). Aspects of the deposition of radioactive and other gases and particles. Int. J. of Air Pollut., 3: 63-88.

Chamberlain, A.C. (1991). Radioactive Aerosols. Cambridge Univ. Press: Cambridge, England.

Charles, D.F. (1991). Effects of acidic deposition on North American lakes: Palaeolimnological evidence from diatoms and chryophtes. Phil. Trans. R. Soc. London, B327: 403-412.

Charlson, R.J. et al. (1978). Chemical properties of tropospheric sulfur aerosols. Atmos. Environ., 12: 39-53.

Choppin, G.R. et al. (1995). Radiochemistry and Nuclear Chemistry.Butterworth-Heinemann, Oxford, England.

Choularton, T.W. et al. (1988). The influence of altitude on wet deposition: Comparison between field measurement at Great Dun Fell and the preditions of a seeder feeder model. Atmos. Environ., 22, No. 7: 1363-1371.

Choularton, T.W. et al. (1997). The Great Dun Fell cloud experiment 1993: An overview. Atmos. Environ., 31: 2393-2405.

CLAG (1994). Critical loads of acidity in the United Kingdom. Critical Loads Advisory Group, Summary Report, Department of Environment.

Clark, M.J. and Smith, F.B. (1988). Wet and dry deposition of Chernobyl releases. Nature, 332: 245-249.

Clarke, J.F. et al. (1992). Routine estimation and reporting of dry deposition for the USA Dry Deposition Network. In: S.E. Schartz and W.G.N. Slinn (eds.), Proc. 5th IPSASEP Conf. Hemisphere, Washington: 1481-1472.

Clements W.E. and Wilkening, M.H. (1974). Atmospheric pressure effects on Rn-222 transport across the earth-air interface. J. Geophys. Res., 79: 5025-5029.

Clifton, R.J. (1991). The use of radionuclides (unsupported ^{210}Pb, ^{7}Be and ^{137}Cs) in describing the mixing characteristics of estuarine sediments. In: P.J. Kershaw and D.S. Woodhead (eds.), Radionuclides in the tudy of Marine Processes. Elsevier Applied Science, Essex, England: 255-264.

Collett, J.L. et al. (1991). Spatial and temporal variations in precipitation and cloud deposition in the Sierra Nevada of central California. Tellus, 43B: 390-400.

Cothern, C.R. and Smith, J.E.(eds.) (1987). Environmental Radon. Plenum: New York.

Cowling, E.B. (1982). A historical resume of progress in scientific and public understanding of acid precipitation and its consequences. Environ. Sci.Tech.,16: 110A-123A.

Cowling, E. and Nilsson, J. (1995). Acidification research: Lessons from history and visions of environmental future. Water, Air and Soil Pollution, 85: 279-292.

Cox, R.A. and Penkett, S.A. (1983). Formation of atmospheric acidity. In: S. Beilke & A.J Elshout (eds), Acid Deposition. Proceedings of the CEC workshop, Berlin: 58-83.

Cremers, A. et al. (1988). Quantitative analysis of radiocaesium retention in soils. Nature, 335: 247-249.

Crossley, A. (1988). Particles in orographic cloud and the implication of their transfer to plant surfaces. In: M.H. Unsworth and D. Fowler (eds), Acid Deposition at High Elevation Sites, Kluwer, Dordrecht: 553-664.

Crossley, A. and Wilson, D.B. (1990). Pollution in the upland environment. Int. Conf. on Acidic Deposition, Gasgow, 16-21 September 1990. Roy. Soc. Ed.: 071.

Crossley, A. et al. (1992). Pollution in the upland environment. Environ. Pollut., 75: 81-87.

Crossley, A. et al. (in press). Long-term measurements of cloud frequency and chemical composition in an upland forest in Scotland.

Cutshall, N.H., Larsen, I.L. and Olsen, C.R. (1983). Direct analysis of ^{210}Pb in sediment samples: Self-absorption corrections. Nucl. Instr. Methods, 206: 309-312.

Davidson, C.I. and Wu, Y.L. (1990). Dry deposition of particles and vapours. In: S.E. Lindberg et al. (eds): Acidic precipitation (vol.3), Springer Verlag, New York: 103-216.

Dentener, F and Crutzen, P. (1993). J. Geophys. Res., 98:7149-7163.

Dibb, J.E. (1992). The accumulation of ^{210}Pb at Summit, Greenland since 1855. Tellus, 44B: 72-79.

Dibb, J.E. et al. (1992). Beryllium-7 and lead-210 in the western hemisphere arctic atmosphere. J. Geophys. Res., 97: 16709-16715.

Dollard, G.J. et al. (1983). Pollutant transfer in upland regions by occult precipitation. Nature, 302: 241-243.

Dollard, G.J. et al. (1988). Measurements of ambient SO_2 and H_2O_2 at Great Dun Fell and evidence of their eaction in cloud. In: M.H. Unsworth and D. Fowler (eds.), Acid Deposition at the High Elevation Sites. Kluwer Academic, Dordrecht: 607-614.

Dore, A.J., Choularton, T.W. and Fowler, D. (1992). An improved wet deposition map of the United Kingdom incorporating the seeder-feeder effect over mountainous terrain. Atmos. Environ., 26A, No. 8: 1375-1381.

Draaijers, G.P.J. et al. (1988). Atmospheric deposition in forest edges measured by monitoring canopy throughfall. Water, Air and Soil Pollut., 42: 129-136.

Draaijers, G.P.J. et al. (1992). Research on the impact of forest stand structure on atmospheric deposition. Environ. Pollut., 75: 243-249.

Eakins, J.D. and Morrison, R.T. (1976). A new procedure for the dtermination of lead-210 in lake and marine sediments. AERE, R-8475. HMSO, London.

Eakins, J.D. et al. (1984). The transfer of natural and artificial radionuclides to Brotherwater from its catchment. In: Haworth and J.W.G. Lund (eds.), Lake Sediments and Environmental History. Leicester Univ. Press, Leicester: 125-144.

Eder, B.K. et al. (1990). On the use of scavenging ratios for the influence of surfac-elevel concentrations and subsequent dry deposition of Ca, Mg, Na and K. Water, Air and Soil Pollution, 52: 197-216.

Eisenbud, M. (1987). Environmental Radioactivity (3rd ed.). Academic Press: San Diego, California.

Elsom, D. (1987). Atmospheric pollution: Causes, effects and control policies. Basi Blackwell, Oxford.

Elvingson, P. (1996). Evidence of continued decline. Acid News, 5: 6-7.

EMEP (1997). Transboundary air pollution in Europe. MSC-W Report 1/1997. Norwegian Meteorological Institute, Oslo.

Erisman, J.W. (1993). Acid deposition onto nature areas in the Netherlands; Part I. Methods and results. Water, Air and Soil Pollution: 51-81

Erisman, J.W. et al. (1994a). A generalised description of the deposition acidifying pollutants on a small scale in Europe. In: P.M. Borrel et al. (eds), The proceedings of EUROTRC symposium '94. Academic, The Hague: 588- 596.

Erisman, J.W. et al. (1994b). Review of deposition monitoring methods. Tellus, 46B: 79-93.

Erisman, J.W. et al. (1995). Particle deposition to forests. In: G.J. Heij and J.W. Erisman (eds), Acid Rain Research: Do we have enough answers? Elsevier Science, Amsterdam: 115-126.

Erisman, J.W. and Draaijers, G.P.J. (1995). Atmospheric deposition in relation to acidification and eutrophication. Elsevier, Amsterdam.

Evans, C.G. (1972). The Quantitative Analysis of Plant Growth. Blackwell Scientific: Oxford, England.

Evans, R.D. (1982). The Atomic Nucleus. Krieger, New York.

Feichter, J. et al. (1991). Three-dimesional modelling of the concentration and deposition of ^{210}Pb aerosols. J. Geophys. Res., 96: 22447-22460.

Fisenne, I.M. (1968). Distributions of lead-210 and radium-226 in soil. Rep. UCRL-18140, US Department of Energy, Washington, D.C.: 145-158.

Foell, W.K. and Green, C.W. (1990). Acid rain in Asia: An economic, energy and emission overview. Second workshop on acid rain in Asia, Asian Institute of Technology, Bankok, 19-22 November, 1990.

Fowler, D. (1978). Dry deposition of SO_2 on agricultural crops. Atmos. Environ., 12: 369-373.

Fowler, D. (1984). Transfer to terrestrial surfaces. Phil. Trans. R. Soc. London, B30: 281-297.

Fowler, D. (1986). The transfer of air pollutants to the ground by wet and dry deposition. In: S. Sandroni (ed), Regional and long-range transport of air pollution, Elsevier, Amsterdam: 95-126.

Fowler, D. (1988). The influence of altitude on rainfall composition at Great Dun Fell. Atmos. Environ., 22: 1355-1362.

Fowler, D. et al. (1989). Deposition of atmospheric pollutants on forests. Phil. Trans. R. Soc. London, B324: 247-265.

Fowler, D. et al. (1991). Inputs of trace gases, particles and cloud droplets to terrestrial surfaces. Proceed. R. Soc. Edinburgh, 97B: 35-59.

Fowler, D. et al. (1992). Deposition of acidifying compounds. In: T. Schneider (ed), Acidification research: Evaluation and policy applications. Elsevier, Amsterdam: 553-572.

Fowler, D., Mourne, R. and Branford, D. (1995a). The application of ^{210}Pb inventories in soil to measure long-term average wet deposition of pollutants in complex terrain. Water, Air and Soil Pollution, 85: 2113- 2118.

Fowler, D. (1995b). Atmospheric inputs of nitrogen. In: M. Hornung et al. (eds.), Mapping and Modelling of Critical Loads for Nitrogen- a workshop report. Institute of Terrestrial Ecology, Edinburg: 128-141.

Fowler, D. et al. (1998). Quantifying fine-scale variability in pollutant deposition in complex terrain using 210Pb inventories in soil. Water , Air and Soil Pollution, 105: 459-470.

Fredriksson, L. et al. (1966). Caesium-137. In: R.S. Russell (ed.), Radioactivity and Human Diet. Pergamon, Oxford: 319-353.

Friedmann, H. (1997). Radon: the Fleeting Daughter of Radium. Nucl. Phys. News, 7: 14-20.

Fukuda, K. and Tsunogai, S. (1975). Pb-210 in precipitation in Japan and its implication for the transport of continental aerosols across the ocean. Tellus, 27: 514-521.

Gaggeler, H.et al. (1976). Determination of ^{210}Pb in lake sediments and in air samples by direct gamma-ray measurement. Earth and Planetary Science Letters 33: 119-121.

Gallagher, M.W. et al. (1988). Measurements of the size dependence of cloud droplet deposition at a hill site. Quart. J. Roy. Met. Soc., 114: 1291-1303.

Gallagher, M.W., Beswick, K.M. and Choularton, T.W. (1992). Measurement and modelling of cloudwater deposition to a snow-covered forest canopy. Atmos. Environ., 26A: 2893-2903.

Gallagher, M.W. et al.(1992). Measurements and modelling of cloudwater deposition to moorland and forests. Environ. Pollut., 75: 97-107.

Galloway, J.N. (1995). Acid deposition: Perspectives in time and space. Water, Airand Soil Pollution, 85: 15-24.

Galloway,R.B. (1990). Correction for sample self-absorption in activity determination by gamma spectrometry. Nucl. Instr. Meth. Phys.Res., A 300: 367-373.

Garland, J.A. (1977). The dry deposition of sulphur dioxide to land and water surfaces. Proc. R. Soc. Lond., A354: 245-268.

Gervat, P.A. et al. (1988). Controlled chemical kinetic experiments in cloud: A view on the CERL/UMIST Great Dun Fell project. In: M.H. Unsworth and D. Fowler (eds.), Acid Deposition at the High Elevation Sites. Kluwer Academic, Dordrecht: 607-614.

Godt, J.M. et al. (1986). Processes in the canopy of trees: Internal and external turnover of elements. In: H.W. Georgii (ed.), Atmospheric Pollutants in Forest Areas. Reidel: 263-276.

Godt, J. and Mayer, R. (1988). Deposition rayes of airborne substances to forest canopies in relation to surface structure. In: M.H. Unsworth and D. Fowler (eds), Acid Deposition at High Elevation Sites, Kluwer, Dordrecht: 593-606.

Goldsmith, P. et al. (1984). Atmospheric transport and tranformation. Phil. Trans. R. Soc. Lond. B305: 259-279.

Gorham, E (1989). Scientific understanding of ecosystem acidification: A historical review. Ambio, 18, No. 3: 150-154.

Graedel, T.E. et al. (1995). Global emissions inventories of acid related compounds. Water, Air and Soil Pollution, 85:25-36.

Granat, L. (1990). Luft-Och Nederbordskemiska Stationsnatet inom PMK. Naturvardsverket Rapport 3942, Naturvardsverket: Solna, Sweden.

Granat, L. (pers. comm., 1995). Arrhenius Laboratory, University of Stockholm, Sweden.

Graustein, W.C. and Turekian, D.D. (1982). ^{210}Pb as a tracer of the deposition of sub-micrometer aerosols. In: H.R. Prupacher et al. (eds), *Precipitation Scavenging, Dry Deposition, and Resuspension*. Elsevier Science: 1315-1324.

Graustein, W.C. and Turekian, K.K. (1986). ^{210}Pb and ^{137}Cs in air and soils measure the rate and vertical profile of aerosol scavenging. J. Geophys. Res., 91, No. D13: 14355-14366.

Graustein, W.C. and Turekian, K.K. (1989). The effects of forests and topography on the deposition of sub-micrometer aerosols measured by lead-210 and caesium-137 in soils. Agricultural and Forest Meteorology, 47: 199-220.

Graustein, W.C. and Turekian, K.K. (1996). ^{7}Be and ^{210}Pb indicate on upper troposphere source for elevated ozone in the summertime subtropical free troposphere of the eastern North Atlantic. J. Geophys. Res., 23,: 539-542.

Grundsten, C. (1992). Geographical Regions. In: C. Bernes and C Grundsten (eds.), The Environment, The National Atlas of Sweden. The National Protection Agency: 10-13.

Guelle, Y.J. et al. (1998). Wet deposition in a global size-dependent aerosol transport model. J. Geophys. Res., 103, No. D10: 11429-11445.

Hallgren-Larsson, E. et al. (1995a). Air pollution in southern and central Sweden: Deposition and Effects, October 1993-September 1994. IVL Report B-1192, Swedish Environmental Research Institute, Aneboda, Sweden.

Hallgren-Larsson, E. et al. (1995b). Deposition of acidifying compounds in Sweden. Water , Air and Soil Pollut., 85: 2271-2276.

Hasselrot, B. and Grennfelt, P. (1987). Deposition of air pollutants in a wind-exposed forest edge. Water, Air and Soil Pollut., 34: 135-143.

Havas, M. and Rosseland, B.O. (1995). Response of zooplankton, benthos and fish to acidification: An overview. Water, Air and Soil Pollution, 85: 51-62.

Henrikson, A. et al. (1992). Critical loads of acidity: Nordic surface waters. Ambio, 21, No. 5: 356-363.

Hicks, B.B. et al. (1987). A preliminary multiple resistance routine for deriving dry deposition velocities from measured quantities. Water, Air and Soil Pollution, 36: 311-330.

Hicks, B.B. et al. (1989). Atmospheric processes research and processes model development. State of science/technology, report No. 2, National Acid Precipitation Assesssment Program.

Hicks, B.B. (1995). On the determination of total deposition to remote areas. In: G.J. Heij and J.W. Erisman (eds), Acid Rain Research: Do we have enough answers? Elsevier Science, Amsterdam: 163-173.

Hov, O. (1987). Transport and acid deposition. In: O. Hov et al. (eds), Evaluation of atmospheric processes leading to acid deposition in Europe. CEC Report: EUR 11441, Lillestrom, Norway: 69-85.

Hov, O. et al. (1987). Evaluation of atmospheric processes leading to acid deposition in Europe. Rep. 10, EUR 11441, CEC, Brussels.

Howells, G. (1990). Acid rain and acid waters. Ellis Horwood, Chichester, England.

Hultberg, H. and Grennfelt, P. (1991). Sulphur and saesalt deposition as reflected by throughfall and runoff chemistry in forested catchments. IVL, B-1009, Swedish Environmental Resaerch Institute, Goteborg, Sweden.

IAEA (1989). Measurement of Radionuclides in Food and the Environment. Technical Report No. 295. International Atomic Energy Agency, Vienna.

IPCC (1992). Climate change 1992- The supplementary report to IPCC Scientific Assessment. Cambridge University Press., Cambridge, UK.

Ivens, W.P. et al. (1988). Dutch forests as air pollution sinks in agricultural areas. Dutch priority Prog. on Acidification. Rep. 37-09. Univ. of Utrecht, the Netherlands.

Jaworowski, Z. (1969). Radioactive lead in the environment and in the human body. Atomic Energy Review, 7: 3-45.

Jaworowski, Z. et al. (1978). Lead-210 from nuclear explosions in the environment. Nucl. Tech., 37: 156-166.

Joshi, S.R. (1987). Nondestructive determination of Lead-210 and Radium-226 in sediments by direct photon analysis. J. Radioanal. Nucl. Chem., 116: 169-182.

Joshi, S.R. and Mudroch, A. (1988). Direct determination of geochronologically useful radionuclides in sediments by low-energy photon analysis. Nucl.Instr. Meth. , A263: 529-536.

Jung, C.E. (1963). Air Chemistry and Radioactivity. Academic Press: New York.

Kamari, J. (1986). Linkage between atmospheric inputs and soil and water acidification. In: J. Alcamo and J. Bartnicki (eds), Atmospheric computations for

assessment of acidification in Europe, RR-86-5, International Institute for Applied Systems Analysis, Laxenberg, Austria.

Kauranen, P. and Miettinen, J.K. (1974). Specific activity of ^{210}Pb in the environment. Int. J. of Environ. Anal. Chem., 3: 307-316.

Kerfoot, O. (1968). Mist precipitation on vegetation. Forest Abstract, 29: 8-20.

Kiang, L.L. et al. (1993). A study on T-shape Compton suppression spectrometer by Monte Carlo simulation. Nucl. Instr. Methods Phys. Res.,A 327: 427-432.

Killham, K. (1994). Soil Ecology. Cambridge Univ. Press: Cambridge, England.

Knoll, G.F. (1989). Radiation Detection and Measurement. 2nd ed. John Wiley , New York.

Knuth, R.H. et al. (1983). Size distribution of atmospheric Pb and Pb-210 in rural New Jersy. In: H.R. Pruppacher et al. (eds.), Precipitation Scavenging, Dry Deposition and Resuspension. Elsevier, New York: 1325-1334.

Koide, M. et al. (1972). Marine geochronology with Pb-210. Earth Planet. Sci. Lett., 23: 199-205.

Krahl-Urban, B. et al. (1990). Forest decline. Assessment Group for Biology, Ecology and Energy, Julich Nuclear Research Centre, German Ministry of Research and Technology.

Krishnaswamy, S. et al. (1971). Geochronology of lake sediments, Earth Planet. Sci. Lett., 11: 407-414.

Kroll, G. and Winkler, P. (1989). Trace substance input to coniferous forests via cloud interception. In: H.W. Georgii (ed.), Mechanisms and Effects of Pollutant-Transfer into Forests. Kluwer, Dordrecht: 205-211.

Kurata, T and Tsunogai, S. (1986). Exhalation rates of ^{222}Rn and deposition of ^{210}Pb at the earth's surface estimated from ^{226}Ra and ^{210}Pb profiles in soils. Geochem. J., 20: 81-90.

Langner J., Persson, C. and Robertson, L. (1995). Concentration and deposition of acidifying air pollutants over Sweden: Estimates for 1991 based on the MATCH model and observations (and supplement). Water, Air and Soil Pollution, 85: 2021-2026.

Lee, D.S. et al. (1997). Estimations of global NO_X emissions and their uncertainties. Atmos. Environ., 31: 1735-1749.

Lee, H.N. and Feichter, J. (1995). An intercomparison of wet precipitation scavenging schemes and the emission rates of ^{222}Rn for the simulation of global transport and deposition of ^{210}Pb. J. Geophys. Res., 100, No. D11: 23253-23270.

Leo, W.R. (1987). Techniques for Nuclear and Particle Physics Experiments. Springer-Verlag, Germany.

Lewis, D.M. (1977). The use of ^{210}Pb as a heavy metal tracer in the Susquehanna River system. Geochem. Cosmo. Acta, 41: 1557-1564.

Lindberg, S.E. (1992). Atmospheric deposition and canopy interations of sulfur. In: D.W. Johnson and S.E. Lindberg (eds.), Atmospheric Deposition and Forest Nutrient Cycling. Springer-Verlag, New York: 74-90.

Lindstrom, R.M. et al. (1990). A low-background gamma-ray assay laboratory for activation analysis. Nucl. Instr. Methods Phys. Res., A 299: 425-429.

Liu, S. et al. (1992). The nutrient cycling model (NuCM): Overview and application. In: D.W. Johnson and S.E. Lindberg (eds), Atmospheric deposition and forest nutrient cycling. Springer-Verlag, New York: 583-609.

Liven, F.R. and Loveland, P.J. (1988). The influence of soil properties on the environmental mobility of caesium in Cumbria. Soil Use and Management, 4: 69-75.

Liven, F.R. et al. (1991). Distribution of radiocesium in soil-plant systems of upland areas of Europe. Health Phys., 60, No. 4: 539-545.

Lockhart, L.B. et al. (1965). Distribution of air-borne activity with particle size. In: A.W. Klement (ed.), Radioactive Fallout from Nuclear Weapons Tests. CONF 765, NTIS, Springfield, Va.

Lovblad, G. et al. (1992). Deposition of sulphur and nitrogen in the Nordic countries: Present and future. Ambio, 21, No. 5: 339-347.

Lovblad, G. et al. (1994). Thoughfall monitoring in the Nordic countries. IVL report B-1132, Swedish Environmental Research Institute, Goteborg, Sweden.

Lovett, G.M. et al. (1982). Cloud droplet deposition in sub-alpine balsm fir forests. Science, 218: 1303-1304.

Lovett, G.M. and Lindberg, S.E. (1984). Dry deposition and canopy exchange in a mixed oak forest as determined by analysis of throughfall. J. Appl. Ecol., 21: 1013-1027.

Lovett, G.M. and Reiners, W.A. (1986). Canopy structure and cloud water deposition in subalpine coniferous forests. Tellus, 38B: 319-327.

Mannion, A.M. and Bowlby, S.R. (1992). Environmental Issues in the 1990's. John Wiley; Chichester, UK.

Mason, B.J. (1992). Acid rain. Claredon, Oxford.

Matzner, E. and Murach, D. (1995). Soil changes induced by air pollutant deposition and their implication for forests in Centra Europe. Water, Air and Soil Pollution, 85: 63-76.

Meteorological Office. (1977). Average Annual Rainfall Map, International Standard Period 1941-1970. Met. O. 866(NB).

Miller, K.M. (1987). Self-absorption correction for gamma ray spectral measurements of ^{210}Pb in environmental samples. Nucl. Instr. Meth. Phys. Res., A 258: 281-285.

Monaghan, M.C. (1989). Lead-210 in surface air and soils from California: Implications for the behavior of trace constituents in the planetary boundary layer. J. Geophys. Res., 94: 6449-6456.

Monteith, J.L. and Unsworth, M.H. (1991). Principles of Environmental Physics (2nd ed.). Edward Arnold: London.

Moore, H.E. et al. (1973). ^{222}Rn, ^{210}Pb, ^{210}Bi, and ^{210}Po profiles and aerosol residence times versus altitude. J. Geophys. Res., 78: 7065-7075.

Moore, H.E. and Poet, S.E. (1976). ^{210}Pb fluxes determined from ^{210}Pb and ^{226}Ra soil profiles. J. Geophys. Res., 81: 1056-1058.

Mourne, R. (1993). Lead-210 as a tracer for acidic deposition in areas of complex topograghy. PhD thesis, University of Edinburgh.

MSC-W (1997). Transboundary Air Pollution in Europe. MSC-W Report 1/1997. Norwegian Meteorological Institute, Blindern, Norway.

Muggleton, A.H.F. (1972). Semiconductor devices for gamma-ray, x-ray and nuclear radiation detection. Journal of Physics E: Scientific Instruments, 5: 390-404.

Murray, W.H. (1993). Scotland's Mountains. Scottish Mountaineers Trust, Pillans & Wilson, Edinburgh.

Myrick, T.E. et al. (1983). Determination of concentrations of selected radionucles in surface soils in the US. Health Phys., 45: 631-639.

Neal, C. et al. (1986). Modelling the effects of acidic deposition and conifer afforestation on stream acidity in the British uplands. J. Hyrol., 86: 15-26.

Nijampurkar, V.N. and Clauson, H.B. (1990). A century old record of lead-210 fallout on the Greenland ice sheet. Tellus, 42B: 29-38.

Nozaki, Y.D. et al. (1978). Atmospheric ^{210}Pb fluxes determined from soil profiles. J. Geophys. Res. 83, 4047-4051.

Oden, S. (1968). The acidification of air and precipitation and its consequences in the natural environment. Ecological Committee Bulletin 1, Swedish Natural Science Research Council, Stockholm. Translations Consultants, Ltd. Arlington, Va, USA.

OECD (Organizattion for Economic Co-operation and Development) (1979). The OECD programme on long range transport of air pollutants: Measurements and findings. OECD, Paris.

Office of Technology Assessment (OTE). (1984). Acid rain and transported air pollutants: Implications for public policy. Washington, DC.

Olsen, C.R. etal. (1985). Atmospheric fluxes and marsh-soil inventories of ^{7}Be and ^{210}Pb. J. of Geophys. Res., 90: 10487-10495.

Overrein, L.N. et al. (1980). Acid precipitation: Effects on forest and fish. Final report of the SNSF project 1972-1980. Oslo, Norway.

Overwater, M.W. et al. (1993). Gamma-ray spectroscopy of voluminous sources: Corrections for source geometry and self-attenuation. Nucl. Inst. Methods Phys.Res., A 324: 209-218.

Peirson, D.H. and Salmon, L. (1959). Gamma-radiation from deposited fallout. Nature, 184: 1678-1679.

Peirson, D.H. et al. (1966). ^{210}Pb and ^{210}Po in the atmosphere. Tellus, 18: 427-433.

Peirson, J.E. and Jones, G.E. (1965). Emanation of radon-222 from soils and its use as a tracer. J. of Geophys. Res., 70: 5279-5290.

Pfeiff, M. (1977). Harvesters of the clouds. Reader's Digest, April 1997: 84-88.

Poet, S.E. et al. (1972). Lead-210, Bismuth-210, and Polonium-210 in the atmosphere: Accurate ratio measurement and application to aerosol residence time determination. J. Geophys. Res., 77, No. 20: 6515-6527.

Postendorfer, J. (1994). J. Aerosol Sci., 25: 219-263.

Preiss, N. et al. (1996a). *http://glaciog.ujf-grenoble.fr/equipes/glaciers/*

Preiss, N. et al. (1996b). A compilation of data on lead-210 concentration in surface air and fluxes at the air-surface and water-sediment interfaces. J. Gepphys. Res., 101: 28847-28862.

Preiss, N. and Genthon, C. (1997). Use of a new database of lead-210 for global aerosol model validation. J. Geophys. Res., 102, No. D21: 25347-25357.

Prinz, B. (1989). Air pollution and forest ecosystem research. In: A.H.M. Bresser and P. Mathy(eds.), Monitoring Air Pollution and Forest Ecosystem Research. Report No. 21, CEC, Brussels, Belgium: 7-28.

Pulford, I.D. et al. (1995). Mobility of 137Cs and 210Pb in organic soils. In: R.D. Wilken et al. (eds.), Heavy Metals in the Environment; Int. Conf. held in Humburg, Sep. 1995: 137-140.

Rama (1963). Atmospheric circulation from observations of natural radioactivity. J. Geophys. Res., 68, No. 13: 3861-3866.

Rasmussen, L. et al. (1995). Experimental studies and modelling of enhanced acidification and recovery. Water, Air and Soil Pollution, 85: 77-88.

Rehfeld, S. and Heimann, M. (1995). Three dimentional atmospheric transport simulation of the radioactive tracers ^{210}Pb, ^{7}Be, ^{10}B, and ^{90}Sr. J. Geophys. Res., 100, No. : 26141-16161.

Renberg, I. and Hellberg, T. (1982). The pH history of lakes in SW Sweden, as calculated from the subfossil diatom flora of the sediments. Ambio, 11: 30-33.

Renberg, I. et al. (1991). Recent acidification and biological changes in Lilla Oresjon, southwest Sweden, and the relation to atmospheric pollution and land-use history. Phil. Trans. R. Soc. London, B327: 391-396.

RGAR (1997). Acid deposition in the United Kingdom, 1992-1994. Fourth report of the Review Group on Acid Rain, Department on Environment.

Roberts, T.M. et al. (1989). Causes of type-1 spuce decline in Europe. Forestry, 62, No. 3: 179-222.

Robins, J.A. (1978). Geochemical geophysical applicatios of radioactive lead. In: J.O. Nriagu (ed.), The biogeochemistry of lead in the environment. Elsevier: 286-393.

Rodhe, H. et al. (1995a). Acid Reign '95? Summary Statement from the 5th International Conference on Acidic Deposition Science and Policy.Goteborg, Sweden, 26-30 June 1995: Kluwer Academic.

Rodhe, H. et al. (1995b). Global scale transport of acidifying pollutants. Water, Air and Soil Pollution, 85: 37-50.

Ruijgrok, W. (1995). Dry deposition of acidifying and alkaline particles to forests: Model and experimental results compared. In: G.J. Heij and J.W. Erisman (eds), Acid Rain Research: Do we have enough answers? Elsevier Science, Amsterdam: 431-438.

Ruijgrok, W. et al. (1995). Dry deposition of particles: Implications and recommendation for mapping of deposition over Europe. Tellus, 47B: 587-601.

Schmitt, G. (1989). Comparison of wet deposition inputs via rain and fog interception at a high elevated forest site. In: H.W. Georgii (ed.), Mechanisms and Effects of Pollutant-Transfer into Forests. Kluwer, Dordrecht: 213-220.

Scorer, R.S. (1990). Meteorology of Air Pollution. Ellis Horwood: Chichester, England.

Sehmel, G.A. and Hodgson, W.H. (1980). A model for predicting dry deposition of particles and gases to environmental surfaces. AIChE Symp. Series 76: 218-230.

Seinfeld, J.H. (1986). Atmospheric Chemistry and Physics of Air Pollution. John Wiley: New York.

Skiba, U. (pers. comm., 1998). Institute of Terrestrial Ecology, Edinburgh Station, EH26 0QB, UK.

Slinn, W.G.N. (1982). Predictions for particle deposition to vegetation surfaces. Atmos. Environ., 16: 1785-1794.

Smith, F.B. (1991). An overview of the acid rain problem. Meteorological Magazine, 120, No. 1426: 77-91.

Smith, F.B. and Clark, M.J. (1986). Radionuclide deposition from the Chernobyl cloud. Nature, 322: 690-691.

Smith, J.T. et al. (1997). Inventories and fluxes of ^{210}Pb, ^{137}Cs and ^{241}Am determined from the soils of three small catchments in Cumbria, UK. J. Environ. Radioactivity, 37: 127-142.

Smith, R.I. (pers. comm., 1998). Institute of Terrestrial Ecology, Edinburgh Station, UK.

Spiro P.P. et al. (1992). Global inventory of sulfur emissions with $1^{\circ}x1^{\circ}$ resolution. J. Geophys. Res., 97:6023-6036.

Stull, R.B. (1988). An Introduction to Boundary Layer Meteorology. Kluwer Academic: Dordrecht.

Sutton, G.A. (1993). The analysis of environmental materials using gamma spectrometry. Aquat. Environ. Prot.: Analyt. Meth., MAFF Direct. Fish. Res., Lowestoft, (10).

Sverdrup, H. et al. (1990). Mapping critical loads. Guidance to criteria, methods and examples for mapping critical loads and areas where they have been exeeded. Report 1990:14, Nord 1990:98, Nordic Council of Ministers,Copenhagen.

Sverdrup, H. et al. (1992). Critical loads for forest soils in the Nordic countries. Ambio, 21, No. 5: 348-355.

Tamm, C.O. (1989). Comparative and experimental approaches to the study of acid deposition effects on soil as substrate for forest growth. Ambio, 18, No. 3: 184-191.

Thom, A.S. (1975). Momentum, mass and heat exchange of plant communities. In : J.L. Monteith (ed.), Vegetation and Atmosphere. Academic Press, London: 58-109.

Todd, J.F. et al. (1989). Atmospheric depositional characteristics of Be-7 and Pb-210 along the southeastern Virginia Coast. J. of Geophys. Res., 94: 11106-11116.

Tolgyessy, J. and Klehr, E.H. (1987). Nuclear Environmental Chemical Analysis. Ellis Horwood, Chichester, England.

Tsoulfanidis, N. (1989). Measurement and Detection of Radiation. McGraw-Hill series in Nuclear Engineering. Hemisphere, Washington.

Turekian, K.K. et al. (1977). Geochemistry of atmospheric radon and radon products. Annual Review of Earth Planetary Science, 5: 227-255.

Twomey, S. (1977). Atmospheric aerosols. Elsevier Scientific, Amsterdam.

UN ECE (1997). Forest condition in Europe. Results of the 1996 crown condition survey, 1997 Technical Report. Brussels, Belgium.

United Nations Economic Commission for Europe (1988). Conclusions and draft recommendations of the workshops on critical levels for forests, crops and materials and on critical loads for sulphur and nitrogen, EB.AIR/R.30, UN ECE, Geneva.

Unsworth, M.H. and Wilshaw, J.C. (1989). Wet, occult and dry deposition of pollutants on forests. Agricultural and Forest Meteorology, 47: 221-238.

Urban, N.R. et al. (1990). Mobility and diagenesis of Pb and ^{210}Pb in peat. Geochimica et Cosmochimica Acta, 54: 3329-3346.

Vermeulen, A.T. et al. (1994). Fog deposition on Douglas fir forest, ECN Report RX-94-100, Petten, The Netherlands.

Vermeulen, A.T. et al. (1995). Fog deposition on Douglas fir forest. In: G.J. Heij and J.W. Erisman (eds), Acid Rain Research: Do we have enough answers? Elsevier Science, Amsterdam:453-454.

Visser, H. (1995). Forest condition in Europe and North America: What have we learnt over the past ten years? In: G.J. Heij and J.W. Erisman (eds), Acid Rain Research: Do we have enough answers? Elsevier Science, Amsterdam:465-472.

Volchok, H.L. (1980). Atmospheric deposition of man-made radioactivity. In: T.Y. Torbara et al. (eds), Polluted Rain. Plenum, New York: 435-448.

Walker, A.D. et al. (1982). Eastern Scotland. Soil Survey of Scotland, Sheet 5. The Macaulay Institute for Soil Research, Aberdeen.

Wellburn, A. (1988). Air Pollution and Acid Rain. Longman, Essex, UK.

Westling, O. et al. (1992). Air pollution in southern and central Sweden: Deposition and Effects. IVL Report B-1079, Swedish Environmental Research Institute, Aneboda, Sweden.

Weston, K.J. (1992). Objectively analysed cloud immersion frequencies for the United Kingdom. Meteor. Magazine, 121: 108-111.

Whelpdale, D.M. (1987). Atmospheric deposition of acidic pollutants. In: Int.Symp. on acidification and water pathways. Bolkesjo, Norway, 4-8 May,1987.

Whithy, K.T. (1978). The physical characteristics of sulfur aerosols. Atmos. Environ., 12: 135-160.

Wild, A. (1993). Soils and the Environment. Cambridge Univ. Press: Cambridge, England.

Wilkening, M.H. et al. (1975). Radon-222 flux measurements in widely separated regions. In: J.A.S. Adams et al. (eds.), The Natural Radiation Environment, II. USERDA Rep., CONF-720805-P2: 717-730.

Wiman, B.L.B. and Agren, G.I. (1985). Aerosol deposition and deposition in forests, a model analysis. Atmos. Environ., 19: 335-362.

WMO (1989). Workshop on Precipitation Measurement (1989: St. Moritz, Switzerland),World Meteorological Organization.

Zhao, D. and Sun, B. (1986). Air pollution and acid rain in China. Ambio, 15, No. 1: 2-5.